ANNALS OF THE NEW YORK ACADEMY OF SCIENCES

VOLUME 94, ART. 2 PAGES 337–654

CURRENT PROBLEMS IN ELECTROBIOLOGY

Conference Editor:
DOMINICK P. PURPURA

LIST OF AUTHORS

DOMINICK P. PURPURA (*Conference Chairman*), T. ARAKI, M. V. L. BENNETT, G. H. BISHOP, H. GRUNDFEST, E. R. KANDEL, W. R. LOEWENSTEIN, L. J. MULLINS, J. D. ROBERTSON, W. A. SPENCER, C. A. TERZUOLO, AND S. THESLEFF

Editor
FRANKLIN N. FURNESS

Managing Editor
EDGAR W. WHITE

Associate Editor
THOMAS SIMPSON

NEW YORK
PUBLISHED BY THE ACADEMY
September 6, 1961

THE NEW YORK ACADEMY OF SCIENCES

(Founded in 1817)

BOARD OF TRUSTEES

BORIS PREGEL, *Chairman of the Board*

Class of 1960–1961
HARDEN F. TAYLOR
HENRY C. BRECK

Class of 1960–1962
W. STUART THOMPSON
LOWELL C. WADMOND

Class of 1960–1963
DEAN RUSK

Class of 1961–1964
GORDON Y. BILLARD **BORIS PREGEL**

FREDERICK Y. WISELOGLE, *President of The Academy*
M. J. KOPAC, *Past President* **HILARY KOPROWSKI**, *Past President*
EUNICE THOMAS MINER, *Executive Director*

SCIENTIFIC COUNCIL, 1961

President, **FREDERICK Y. WISELOGLE**
President-Elect, **JAMES B. ALLISON**
EMERSON DAY, *Vice-President* **CHARLES W. MUSHETT**, *Vice-President*
Recording Secretary **KARL MARAMOROSCH**
Corresponding Secretary **ROSS F. NIGRELLI**

Elected Councilors

1959–1961
JOHN E. DEITRICK **CHARLES W. MUSHETT**
ROBERT S. MORISON **E. L. TATUM**

1960–1962
JOHN JOSEPH LYNCH, S.J. **MORRIS SCHAEFFER**

1961–1963
JACOB FELD **ANDRES FERRARI**

Executive Director, **EUNICE THOMAS MINER**

SECTION OF BIOLOGICAL AND MEDICAL SCIENCES
CHARLES R. NOBACK, *Chairman* **PRESTON L. PERLMAN**, *Vice-Chairman*

DIVISION OF ANTHROPOLOGY
ETHEL BOISSEVAIN, *Chairman* **ROBERT HECKEL**, *Vice-Chairman*

DIVISION OF INSTRUMENTATION
ANDRES FERRARI, *Chairman* **WALTER E. TOLLES**, *Vice-Chairman*

DIVISION OF MICROBIOLOGY
EMANUEL GRUNBERG, *Chairman* **H. CHRISTINE REILLY**, *Vice-Chairman*

DIVISION OF PSYCHOLOGY
LOUIS W. MAX, *Chairman* **GEORGE K. BENNETT**, *Vice-Chairman*

SECTION OF CHEMICAL SCIENCES
FREDERICK R. EIRICH, *Chairman* **A. D. SHABICA, JR.**, *Vice-Chairman*

DIVISION OF BIOCHEMISTRY
RAYMOND L. GARNER, *Chairman* **J. J. BURNS**, *Vice-Chairman*

SECTION OF GEOLOGICAL SCIENCES
R. W. FAIRBRIDGE, *Chairman* **BARTHOLOMEW NAGY**, *Vice-Chairman*

DIVISION OF OCEANOGRAPHY AND METEOROLOGY
CHARLES KNUDSEN, *Chairman* **JAMES K. McGUIRE**, *Vice-Chairman*

SECTION OF PHYSICAL SCIENCES
HIRAM HART, *Chairman* **ROBERT D. HATCHER**, *Vice-Chairman*

DIVISION OF ENGINEERING
JACOB FELD, *Chairman* **JOSEPH F. SKELLY**, *Vice-Chairman*

DIVISION OF MATHEMATICS
BRADFORD F. HADNOT, *Chairman* **MARY P. DOLCIANI**, *Vice-Chairman*

Past Presidents
M. J. KOPAC **HILARY KOPROWSKI**

The Sections and the Divisions hold meetings regularly, one evening each month, during the academic year, October to May, inclusive. All meetings are held at the building of The New York Academy of Sciences, 2 East Sixty-third Street, New York 21, New York.

Conferences are also held at irregular intervals at times announced by special programs.

ANNALS OF THE NEW YORK ACADEMY OF SCIENCES

VOLUME 94, ART. 2 PAGES 337–654

September 6, 1961

CURRENT PROBLEMS IN ELECTROBIOLOGY*

Conference Editor and Conference Chairman

DOMINICK P. PURPURA

Editor

FRANKLIN N. FURNESS

Managing Editor

EDGAR W. WHITE

Associate Editor

THOMAS SIMPSON

CONTENTS

Ultrastructure of Excitable Membranes and the Crayfish Median-Giant Synapse. *By* J. DAVID ROBERTSON 339
The Macromolecular Properties of Excitable Membranes. *By* L. J. MULLINS 390
Ionic Mechanisms in Electrogenesis. *By* HARRY GRUNDFEST 405
Modes of Operation of Electric Organs. *By* MICHAEL V. L. BENNETT 458
Excitation and Inactivation in a Receptor Membrane. *By* WERNER R. LOEWENSTEIN. 510
Nervous Control of Chemosensitivity in Muscle. *By* S. THESLEFF 535
An Analysis of Intra- Versus Extracellular Potential Changes Associated with Activity of Single Spinal Motoneurons. *By* CARLO A. TERZUOLO AND T. ARAKI 547
The Organization of Cortex with Respect to Its Afferent Supply. *By* GEORGE H. BISHOP 559
Electrophysiological Properties of an Archicortical Neuron. *By* E. R. KANDEL AND W. A. SPENCER 570
Analysis of Axodendritic Synaptic Organizations in Immature Cerebral Cortex. *By* DOMINICK P. PURPURA 604

---

* This series of papers is the result of a conference on *Current Problems in Electrobiology* held and supported conjointly by The New York Academy of Sciences, New York, N.Y., and Section F, American Association for the Advancement of Science, Washington, D.C., on December 30, 1960.

Copyright, 1961, by The New York Academy of Sciences

ULTRASTRUCTURE OF EXCITABLE MEMBRANES AND THE CRAYFISH MEDIAN-GIANT SYNAPSE

J. David Robertson*

Department of Anatomy, University College, London, England and Department of Neuropathology, Harvard Medical School, Boston, Mass.

In this article I shall first review the evidence that has led me to advance the unit membrane theory. This requires a treatment in some detail of certain aspects of peripheral nerve fiber structure. Finally, I shall include a reinterpretation of some of my older findings on invertebrate synapses now made possible by the unit membrane concept.† I shall begin by reviewing the background information on membrane structure leading to the unit membrane concept.

FIGURE 1 is a segment of nerve myelin fixed with potassium permanganate. In this micrograph one can see the satellite cell membrane (u.) at the top. This is a structure consisting of a pair of dense lines each about 20 Å thick bordering a light central zone about 35 Å wide making a unit about 75 Å thick. Below the satellite cell membrane there is a thin layer of cytoplasm (cyt.). Below this there is the compact myelin structure. This consists of a repeating pattern of so-called major dense lines (MDL) repeating at a period of 120 Å. In between the major dense lines there is an intraperiod line (IPL) that is just as regular and complete as the major dense line but somewhat less dense. Below the compact myelin is a very thin layer of satellite cell cytoplasm (cyt.). Below this there is the inner satellite cell membrane (u.) next to the axon. Bordering this there is a second gap (not at all clear in this micrograph). We then come to the axon membrane which is for the most part broken up or obliquely sectioned here. There is a layer of axoplasm (ax.) visible below.

I propose now to show how this compact myelin structure comes about. In order to do so I shall deal first with the structure of unmyelinated nerve fibers drawing largely on the work of Gasser,[12,13] who showed that unmyelinated nerve fibers consist of axons running in troughs in the surfaces of Schwann cells. Some of the axons are pushed down into the Schwann cell, as shown in FIGURE 2, and the overhanging lips of Schwann cytoplasm come together to make a paired membrane structure, measuring 250 to 300 Å across. The area marked by the rectangle and enlarged to the right shows two ~75 Å-unit membrane structures bounding a gap of matrix material. This material is present in a layer about 100 to 150 Å thick, and is continuous with a layer at the surface of the cell that is condensed in the layer called the basement membrane or, to use a term proposed by B. Katz,[20] the "ectolemma." This material is PAS positive, has a certain rigidity, and should be regarded as an important cell boundary layer. In my view, nevertheless, it represents simply a condensation of the intercellular ground substance. I think the gap between the membranes in these paired membrane structures contains the same kind of material but in very much lower concentration.

---

* Present address: McLean Hospital, Research Laboratory, Belmont, Mass.

† Parts of this article represent condensations or abstractions from material published[41,43,44] elsewhere or now in preparation for publication in more complete form.

FIGURE 3 is an electron micrograph of an adult unmyelinated nerve fiber. It demonstrates some of the structures shown diagrammatically in FIGURE 2. The enlarged region below is a portion of an axon bounded by its satellite Schwann cell (dotted area). Each of these is bounded by typical ~75-Å unit membranes, as in FIGURE 2. The unit membranes are separated here by a gap ~100 Å wide.

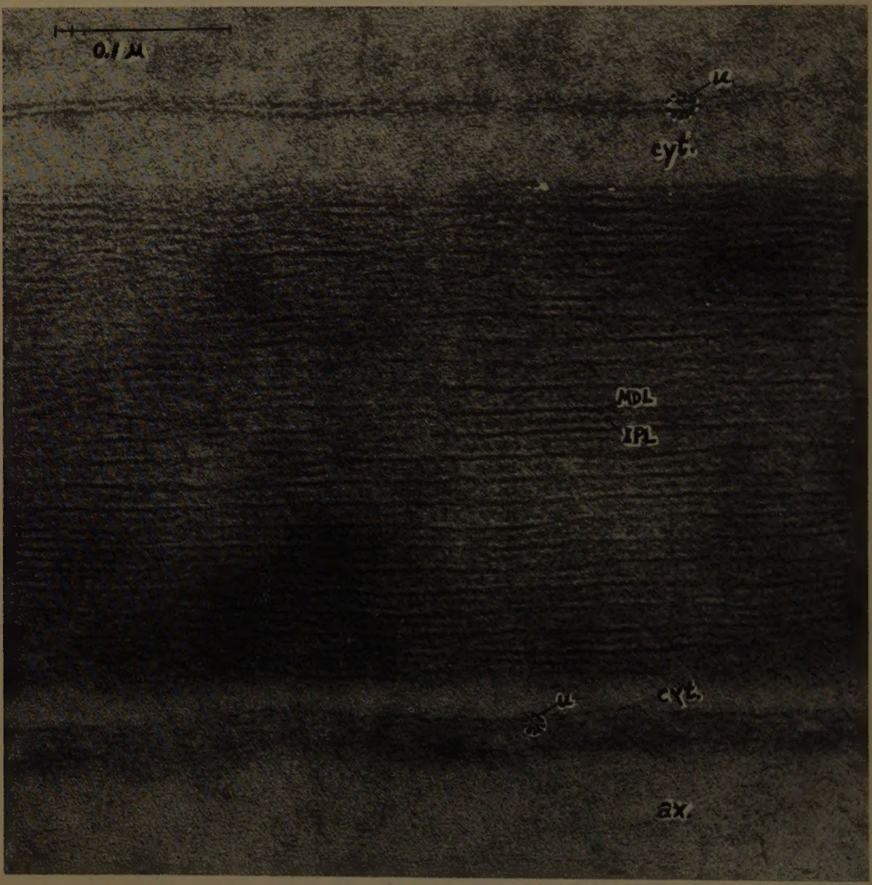

FIGURE 1. Segment of myelin, fixed with potassium permanganate and embedded in araldite. ×370,000.

I have begun by illustrating the organization of unmyelinated nerve fibers because myelinated nerve fibers originate from a type of unmyelinated fiber such as the one in FIGURE 4*a*. Such fibers are very similar in their basic structural plan to the unmyelinated fiber shown in FIGURE 2 but there is generally only one axon per Schwann cell. This kind of nonmyelinated fiber was first noted by Geren,[14] who observed in developing chick nerves fibers such as those in FIGURES 4*a* and *b* and postulated that myelin was, in fact, formed simply by close packing of a spirally wrapped mesaxon. During development, myelination typically begins with an axon embedded in a single Schwann cell with a short mesaxon as in FIGURE 4*a*; in fact, even earlier stages may be recognized in which there is no mesaxon and the Schwann cell and axon are simply in contact. As development proceeds the mesaxon elongates in a perfect spiral around the axon as shown in FIGURE 4*b*. However, first something happens that is a bit more subtle. This is an obliteration throughout most of the length of the mesaxon, of the gap that is normally present between these membranes. I think this is a very fascinating feature of the development of myelin and it is readily demonstrable in permanganate fixed preparations. The gap between the unit membranes is simply obliterated, and the membranes come together to make a structure that measures, instead of 250 to 300 Å across, about 150 Å across. As the process evolves further the mesaxon elongates spirally several times around the axon and its loops come together along their cytoplasmic surfaces. The layer of Schwann cytoplasm present between the mesaxon loops is then obliterated, and one ends up with the compact myelin structure as in FIGURE 4*c*. Two features of the diagram that should be emphasized are: first,

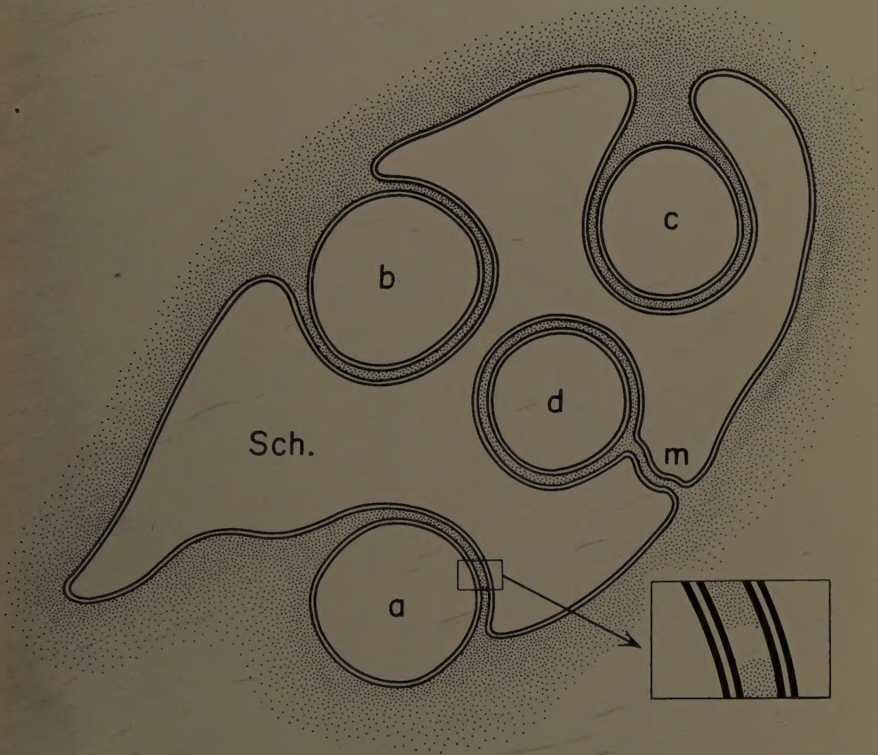

FIGURE 2. Diagram of an unmyelinated peripheral nerve fiber. Key: a–d, axons; Sch., Schwann cell; m, mesaxon.

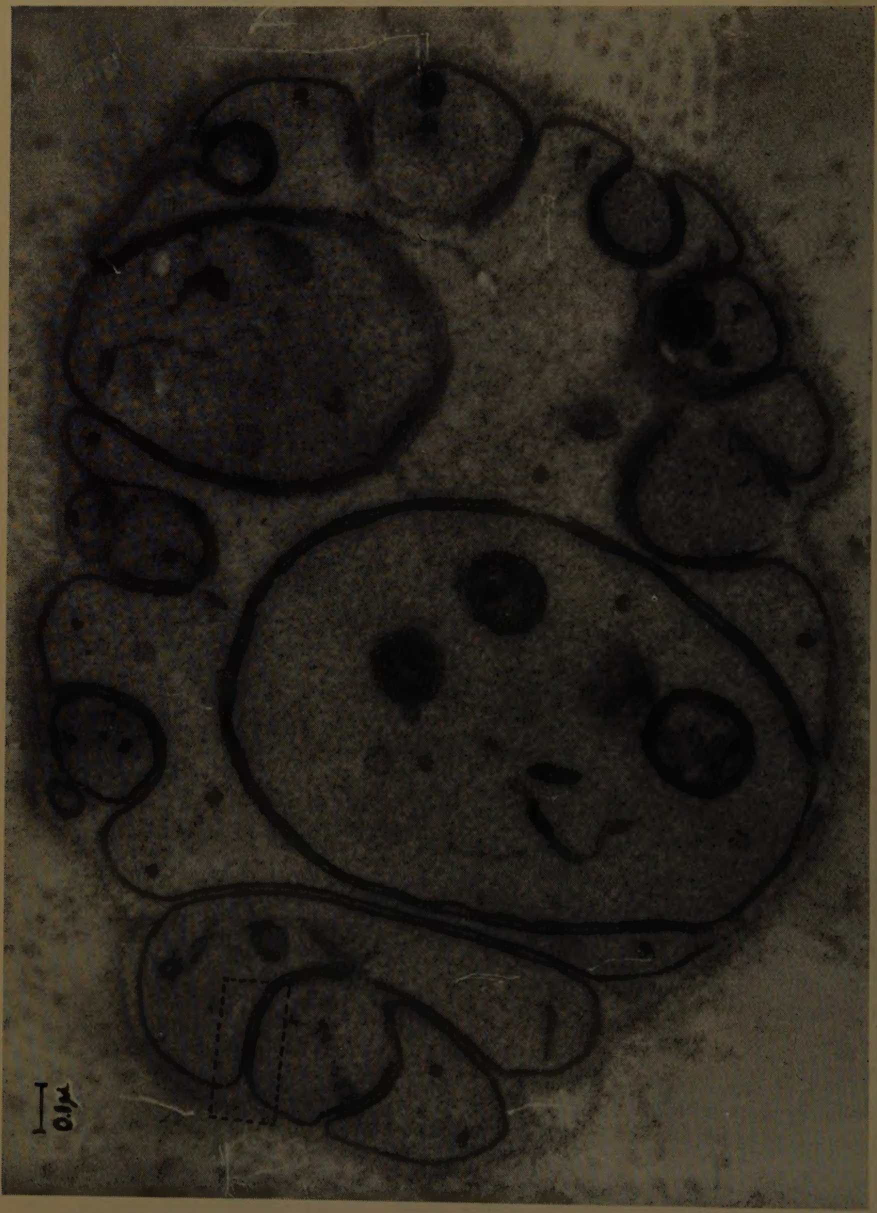

FIGURE 3a.

the intraperiod line of compact myelin originates by the apposition of the *outside* surfaces of the Schwann cell membrane; second, the major dense line that bounds the repeating unit is formed by apposition of the *inside* (cytoplasmic) surfaces of the mesaxon. These two repeating dense strata in myelin thus represent fundamentally different surfaces: one bounding the material outside the cell and the other the material inside the cell.

FIGURES 5 to 8 illustrate these points with examples from permanganate-fixed developing mouse sciatic nerves. In FIGURE 5 the earliest stages of myelination are represented by protofibers (p.) in which there are short mesaxons. One intermediate fiber (I) is shown. Here the mesaxon is elongated in 2½ loops around the axon. Numerous myelinated fibers (myl.) are present in various stages of development. FIGURE 6 shows a protofiber at somewhat higher magnification. The section passes through the Schwann cell nucleus here. Note how small the axon is in relation to the Schwann cell. The intimate contact of the unit membranes of the mesaxon with obliteration of the intermembranous gap may be seen in the enlargement below. FIGURE 7 illustrates a later stage of development. Three mesaxon loops have come together to make compact myelin (enlargement to the right). There is also in this fiber a transverse shearing defect similar to that of Schmidt-Lanterman clefts.[40] The thin layer of Schwann cytoplasm between the separated myelin lamellae contains a membrane-bounded profile of the endoplasmic reticulum (ER—inset enlargement). In passing I call attention to the fact that in these preparations the axon filaments often show up with unusual clarity, as in this fiber, which is from a permanganate-fixed preparation stained with uranyl acetate. Sometimes the axon filaments that usually measure less than 100 Å in diameter appear larger and seem to have a light center giving them a hollow tubular appearance (arrows). This is interesting in view of the current ideas of Davison and Taylor,[2] derived from physical chemical studies of axoplasmic proteins. Gray has demonstrated[16] a more definite tubular component more than 200 Å

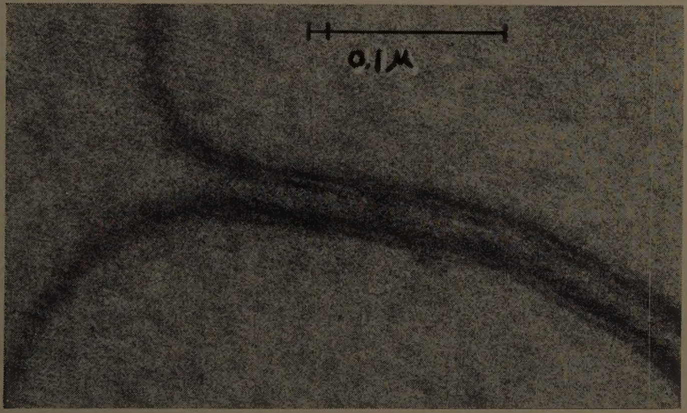

FIGURE 3. (*a*, opposite page.) Adult unmyelinated peripheral nerve fiber fixed with potassium permanganate and embedded in araldite. ×56,000. (*b*, above.) Enlargement of dotted area, ×260,000.

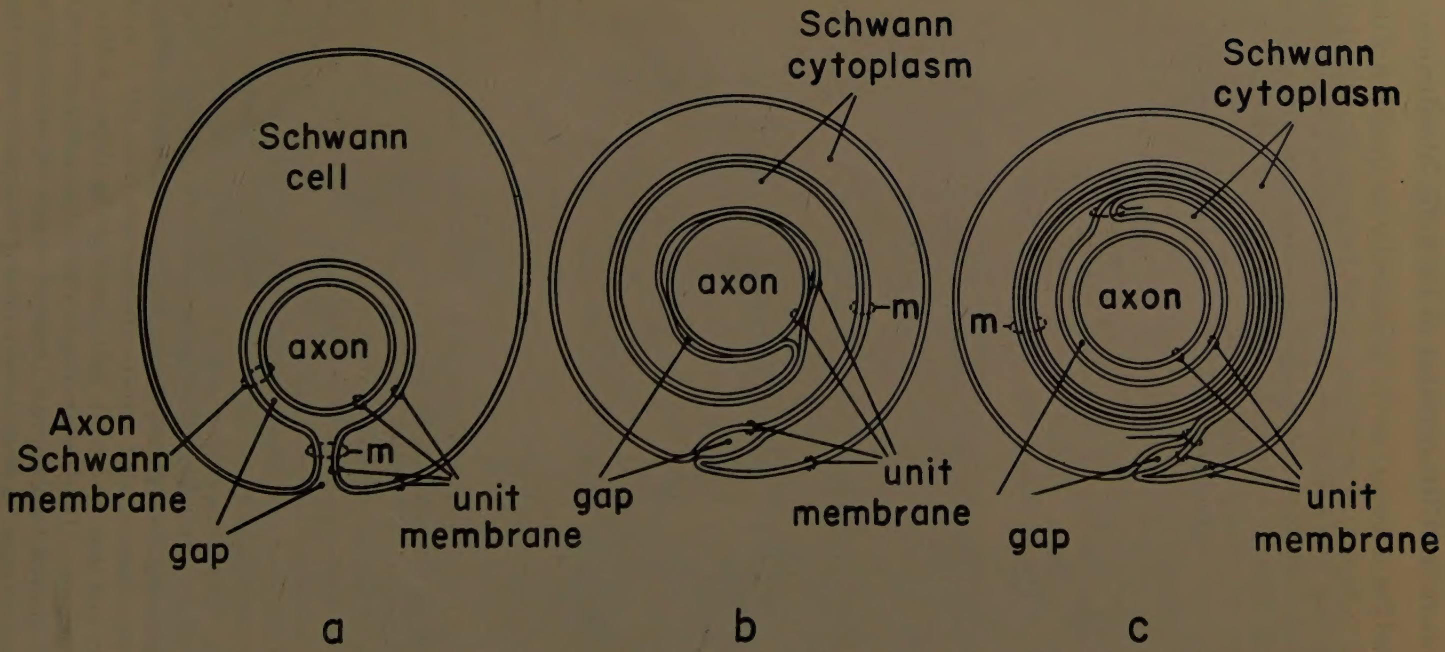

FIGURE 4. Diagrams illustrating the evolution of nerve myelin. (*a*) A protofiber; (*b*) an intermediate fiber; (*c*) a myelinated fiber.

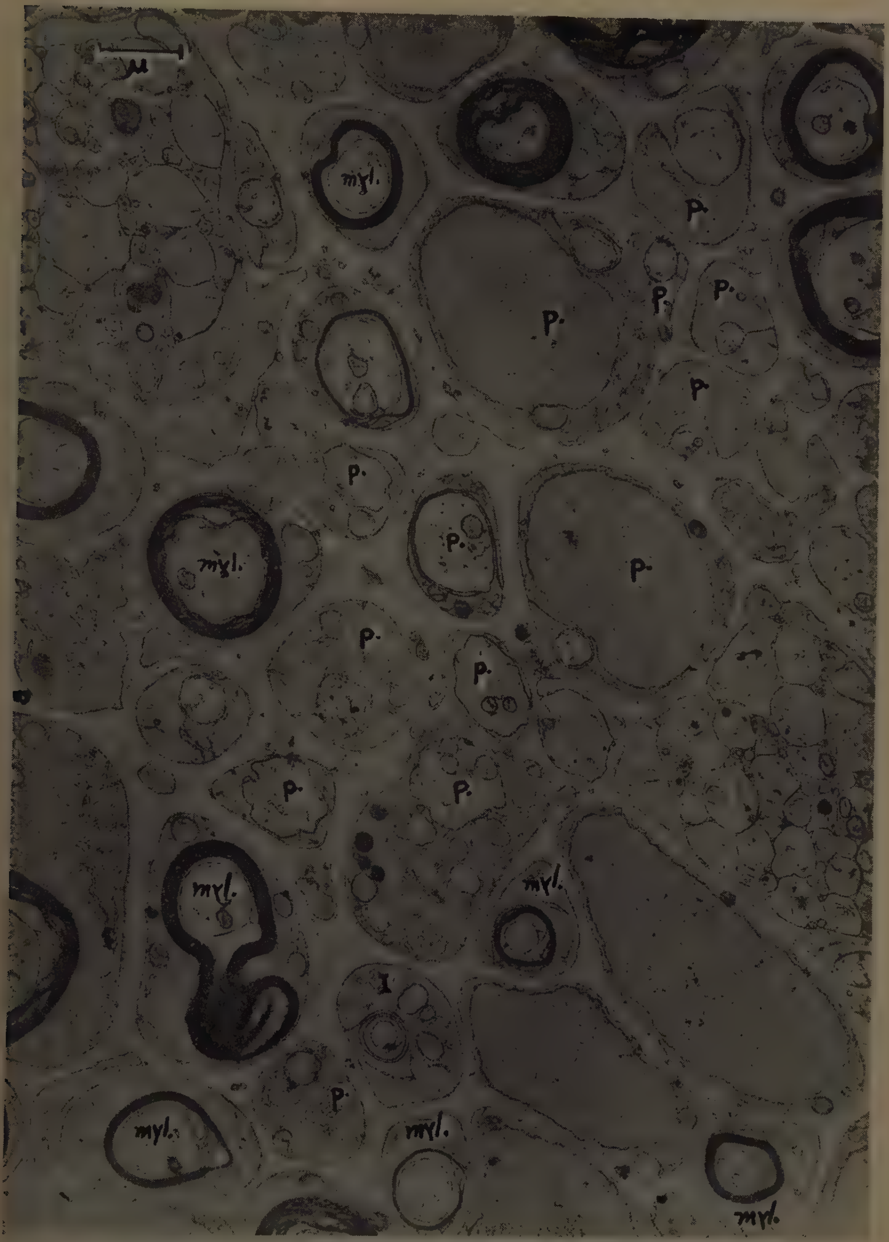

FIGURE 5. Transection of a four-day-old mouse sciatic nerve fixed with potassium permanganate, embedded in araldite, and stained with uranyl acetate. ×11,500.

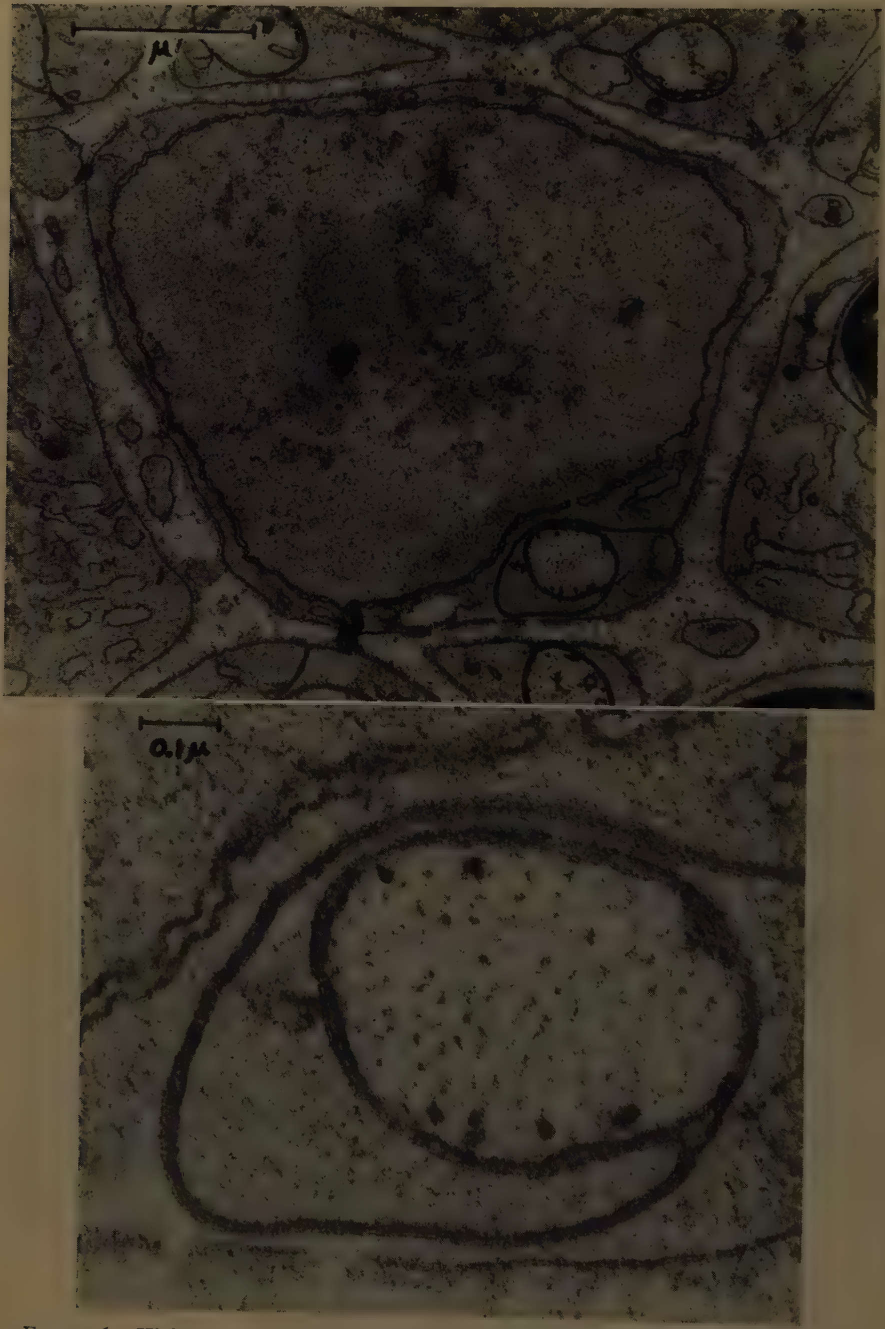

Figure 6. Higher magnification micrograph from the same specimen as shown in figure 5. ×24,000. Enlargement below, ×105,000.

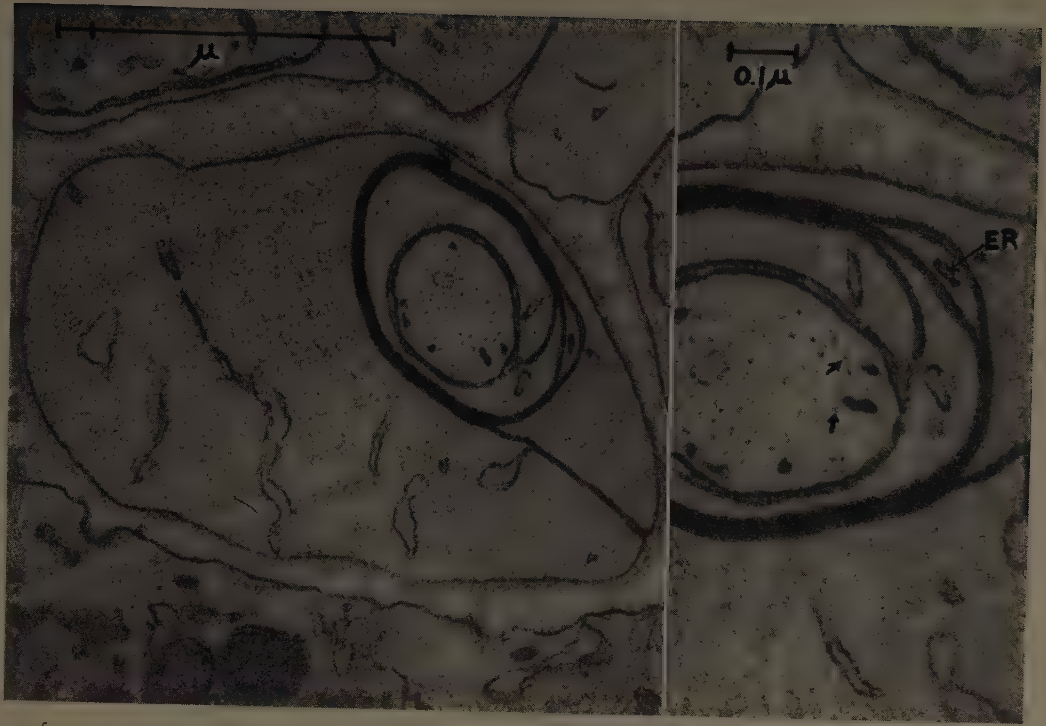

FIGURE 7. Section of a young myelinating fiber in mouse sciatic nerve, fixed with permanganate and embedded in araldite. ×44,000. Inset to the right, ×88,000.

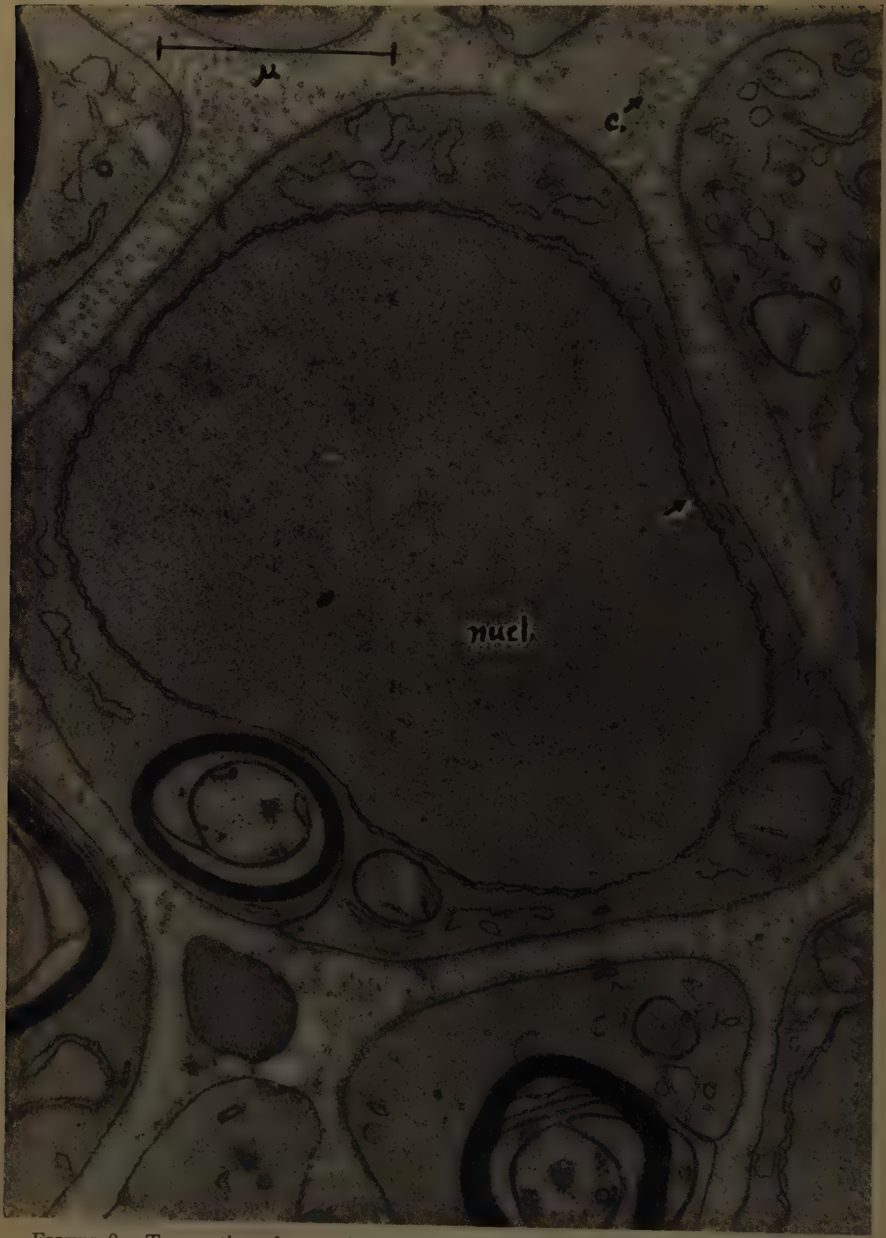

FIGURE 8. Transection of a myelinating fiber in young mouse sciatic nerve. The section passes through the Schwann cell nucleus (nucl.). Note the nuclear pore at the arrow. The collagen fibrils (c.) around the Schwann cell show up with unusual clarity. Permanganate fixed, araldite embedded and uranyl acetate stained. ×31,000.

in diameter in vertebrate central nervous system dendrites. These findings are of particular interest to me because on several occasions I have noted continuity between axon filaments and tubular or vesicular components of the endoplasmic reticulum. In 1955[34] I published a micrograph showing such continuity between a neural filament and a vesicle in the crayfish median-giant synapse. In 1956[35] in my paper on motor end plates (p. 391) I discussed at some length the possibility that synaptic vesicles represent beadlike swellings of neural filaments. Recently it has been established[44] that the vesicles in motor end plates are in fact primarily isolated spherical bodies bounded by a unit membrane. However they may nevertheless be connected with one another via neurofilament strands, somewhat like beads on a string. One wonders whether or not the protein of axon filaments may act as a framework along which lipid and other molecules can be organized or perhaps directly synthesized in patches to make unit membranes. If such is the case then one would expect to see a mixture of tubular or vesicular unit membrane bounded forms in motor endings, just as one observes. A very interesting problem is whether the neural filaments are continuous with the nonlipid monolayer of the unit membrane bounding the neuron and, further, whether there are concentrations of such connections in synaptic regions. There is no doubt[26] that neurofilaments run for considerable distances as discrete continuous unbranched structures in neurons. It is perhaps not too far fetched to suggest that some may run all the way from the unit membrane at an afferent synapse to the region of the membrane of the same neuron at an effector ending. This speculative idea should be tested further since it has obvious functional implications.

FIGURE 8 shows a later stage in myelin evolution. I call your attention in the higher magnification micrograph of this fiber (FIGURE 9) to the fact that you can trace into this myelin sheath with unusual clarity all of the strata of the unit membranes of the mesaxon to show that the major dense line does indeed originate from the apposition of the cytoplasmic surfaces of the mesaxon loops as indicated in FIGURE 4 and the intraperiod line by apposition of the outside surfaces of the mesaxon loops. In this instance we can almost trace the spiral mesaxon around completely throughout seven myelin lamellae.

Three different myelin segments from peripheral nerve fibers fixed in different ways are shown in FIGURE 10. The top one (*a*) is fixed with OsO_4, the middle one (*b*) with potassium permanganate, and the lowest one (*c*) with a technique old to histology but new to electron microscopy. The technique is the one used in classical cytology by Baker[22] and recently applied to electron microscopy by Lasansky and deRobertis.[21] Fixation with formalin is followed by treatment with potassium dichromate. In these three kinds of preparations one gets essentially similar pictures, although there are very significant variations. In the OsO_4 fixed preparation the major dense line (MDL) is just as regular as it is in the permanganate fixed preparation. On the other hand the intraperiod line (IPL), which is very regular in the permanganate preparation, here is broken up into dots or granules or short very thin lines. Quite often it is not seen. The most important point, however, is that the repeating period in most instances is essentially the same (100 to 120 Å) whether OsO_4 or $KMnO_4$ is used as the fixative. The formalin-chrome fixed preparation is rather dif-

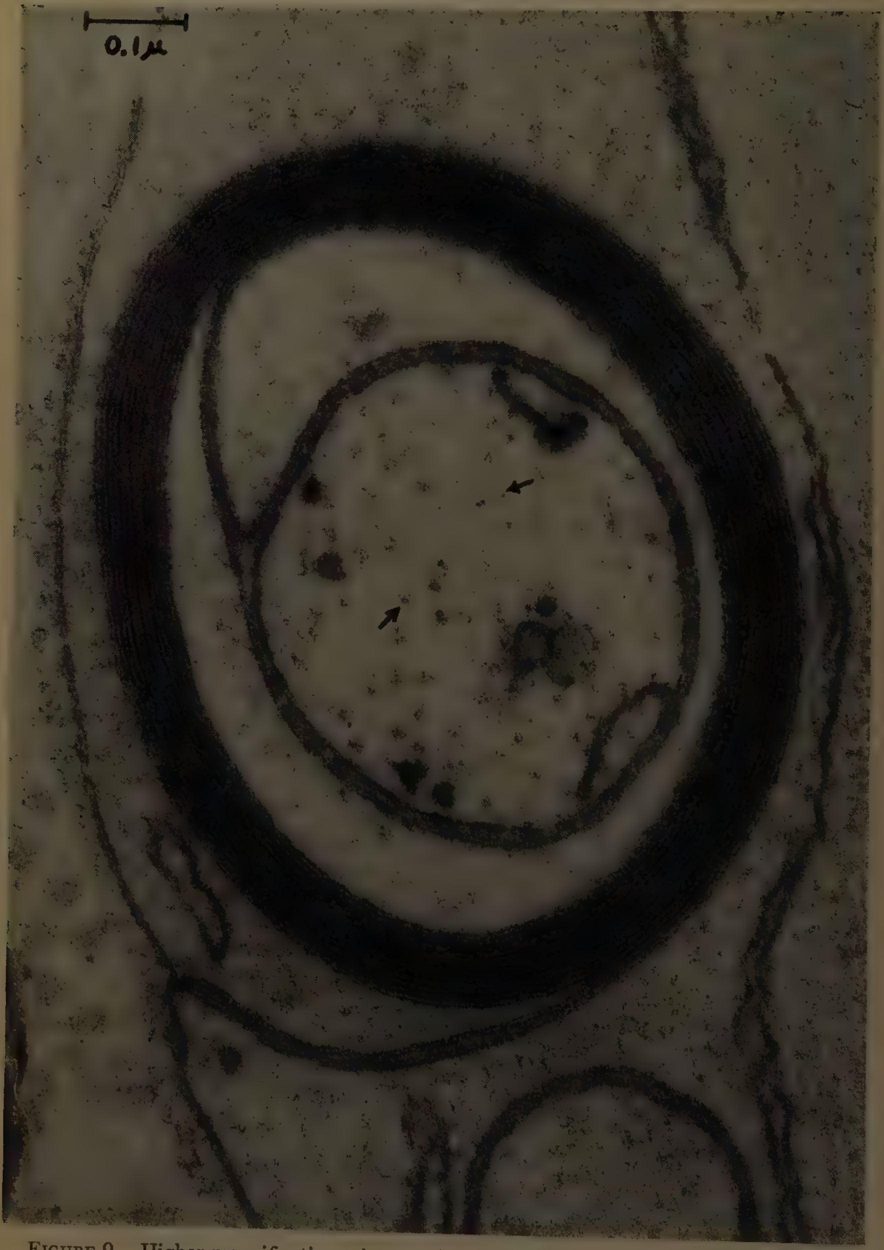

FIGURE 9. Higher magnification micrograph of the same fiber shown in FIGURE 8. Note the suggestion of a tubular nature of the axon filaments (*arrow*). The origin of the major dense line by apposition of the cytoplasmic surfaces of the mesaxon loop is clearly shown here. ×140,000.

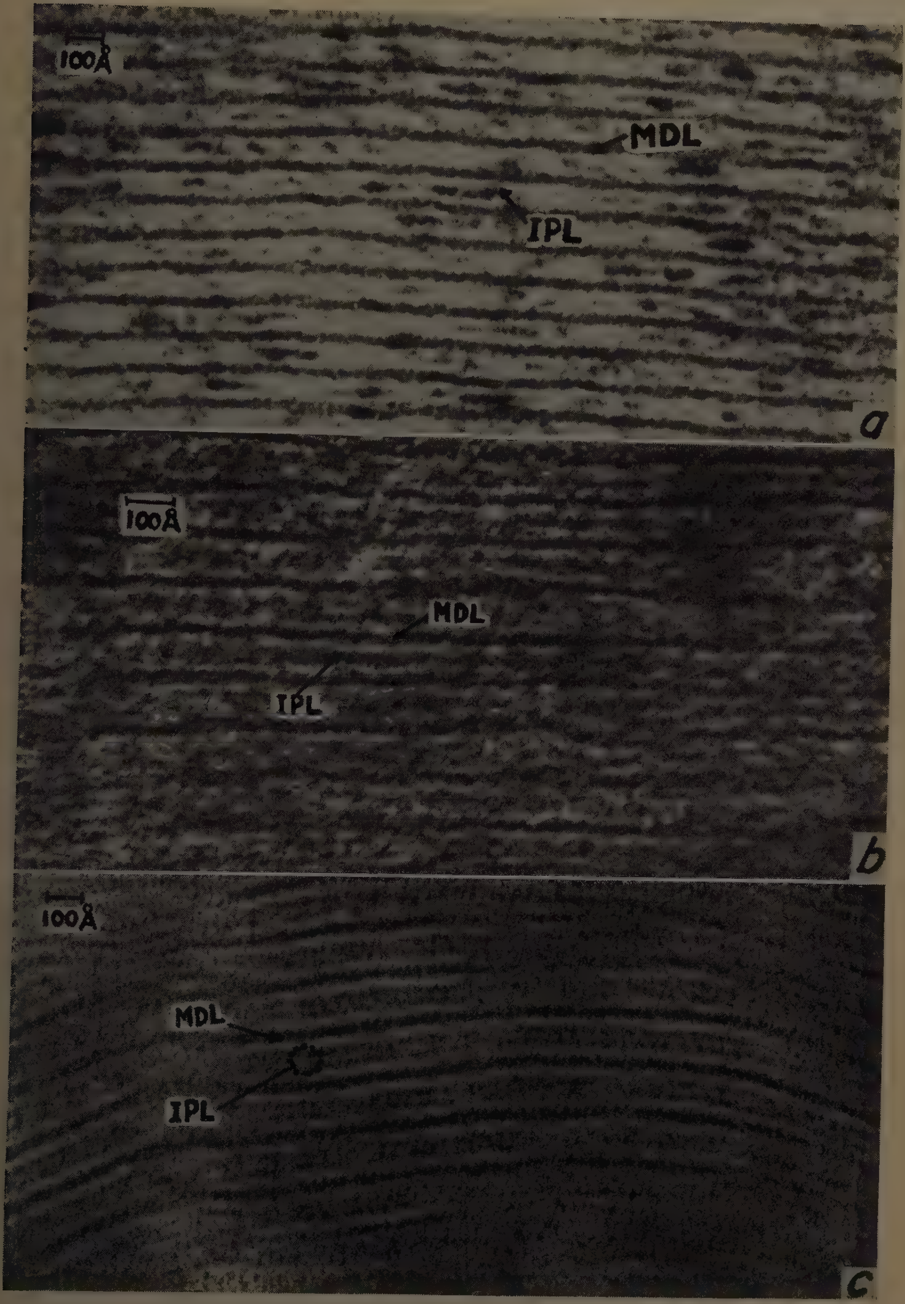

FIGURE 10. These three micrographs show segments of peripheral nerve myelin fixed in three different ways; (*a*) fixed with OsO_4 and embedded in methacrylate, ×450,000; (*b*) fixed with potassium epermanganate and embedded in araldite, ×600,000; (*c*) fixed with Baker's formalin-chrome technique and embedded in araldite. ×450,000.

ferent in that the repeating period is increased to about 140 Å, and we see here a splitting apart of the intraperiod line into 2 dense lines ~20 Å thick separated by a gap ~20 Å wide. This I interpret to mean that the unit membranes of the myelin during fixation (or perhaps they had this characteristic before fixation) have become separated slightly along their outside surfaces. The gap between the separated membranes is ~20 Å thick and accounts for the increase in the repeating period.

FIGURE 11 shows for comparison preparations fixed in permanganate on the left and osmium tetroxide on the right. Each micrograph shows the outer mesaxon of a myelinating fiber, and I direct attention to regions where the membranes of the Schwann cell come into most intimate apposition. These are indicated by the arrows in each preparation. Here the two apposed membranes make a compound membrane that measures in each instance ~130 Å across in the regions of most intimate contact (arrows). In the permanganate fixed preparation (*a*) this compound membrane shows five distinct light and dark strata. When we consider the preparation fixed with OsO_4 (*b*) we see a structure of the same thickness, but we do not see the line down the middle. Here there are only three strata (two dark and one light). If we look at the surface of the Schwann cell in the OsO_4 fixed preparation we do not see the outer strata of the unit membrane; these are very clear in the permanganate

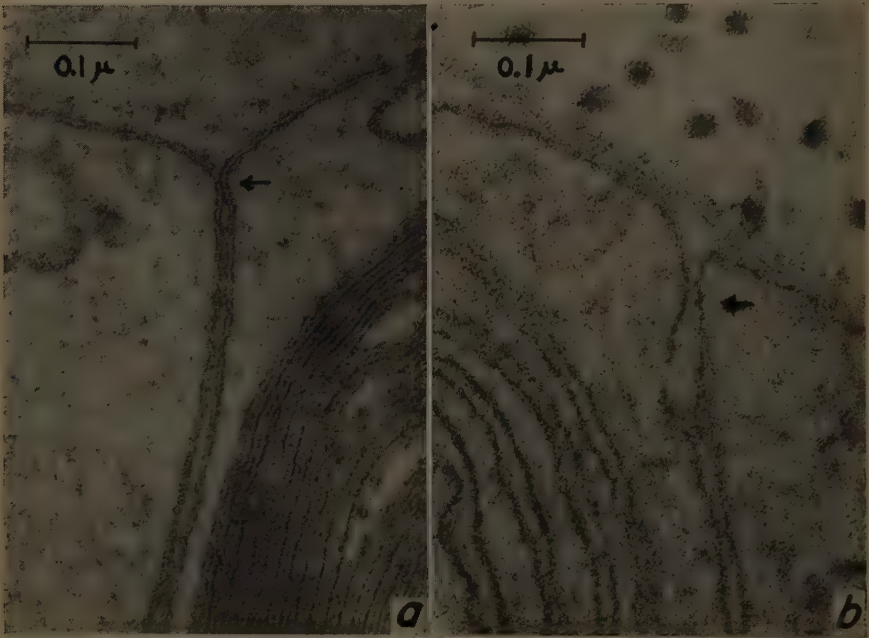

FIGURE 11. Portion of an outer mesaxon in (*a*) a myelinating peripheral nerve fiber fixed with potassium permanganate and embedded in araldite, ×145,000; and (*b*) in a myelinating mouse sciatic nerve fiber fixed with OsO_4 and embedded in araldite. ×145,000.

fixed preparation. I believe that the outer half of the unit membrane structure in the osmic fixed preparation is there, but you cannot see it as you obviously can in the permanganate fixed preparation. Why do I believe it is there in the osmic fixed preparation if we cannot see it? We cannot be positive about this but we can infer its presence because the membranes do not get any closer together in the osmic preparations than they do in the permanganate fixed ones. The over-all thickness of the compound membranes is in each instance about the same. It may be inferred that the outer half of the membrane structure, although it does not show up regularly in the osmic fixed preparations, is present, and this inference is supported further by the fact that in the compact myelin structure the intraperiod line after osmic fixation, sometimes is not seen. Nevertheless it is sometimes demonstrable, and whether it is seen, the spacing of the major dense lines is the same. The conclusion that I am leading to is that OsO_4 is not a good fixative for the whole cell membrane structure. Permanganate displays the whole structure consistently; osmium tetroxide usually displays only the cytoplasmic half of it. Sometimes OsO_4 shows up the whole or part of the outer half, but not regularly. OsO_4 fixed membranes sometimes appear as a thin dense stratum ~20 Å thick, sometimes as a wider dense stratum and sometimes as triple layered typical ~75-Å unit membrane. This variability in the action of OsO_4 has led some to believe that differences in the thickness of OsO_4 fixed membranes in different regions indicate differences in the underlying structure. I think it is more likely that such differences merely reflect the fact that OsO_4 is not a good fixative for displaying the whole membrane structure.

I reinforce this point by showing two adult myelinated nerve fibers in FIGURES 12*a* and *b*. These are printed at slightly different magnifications. In *a* is seen an outer mesaxon after permanganate fixation; in *b* both outer and inner mesaxons are shown after OsO_4 fixation. The repeating period in the compact myelin is about the same in each case. Below in *b* the intraperiod line in the osmic preparation at the label (IPL) may be discernible, but generally it is not visible. Above in *a* it is quite clear. At the surface of the cell in *a* (upper arrow) one sees clearly all of the strata of the unit membrane. Below in the osmic preparation one sees in comparable locations a fuzzy dense line that is very difficult to measure but is certainly well under 75 Å in thickness. My interpretation of these findings is that OsO_4 simply does not show up all of the cell membrane structure at the free surfaces of the Schwann cell despite the fact that these undisplayed strata manifest themselves in the compact myelin structure. Permanganate shows up all the components at the free cell surface that are manifested in compact myeline. The fact that OsO_4 fixation fails to reveal them should then not be taken as an indication that they are not there. The deficiency is in the fixative, not the membranes.

I now return to some concepts that originated in the 1930s from the works of W. J. Schmidt,[45] Schmitt *et al.*,[46] Schmitt *et al.*[47] and, more recently Finean,[7,8] which have led to certain concepts of the molecular structure of myelin. These studies have indicated that myelin consists of regularly arranged lipid molecules with the polar surfaces of the lipid bimolecular leaflets covered by monolayers of protein. Fresh myelin was found to have a radial repeating unit

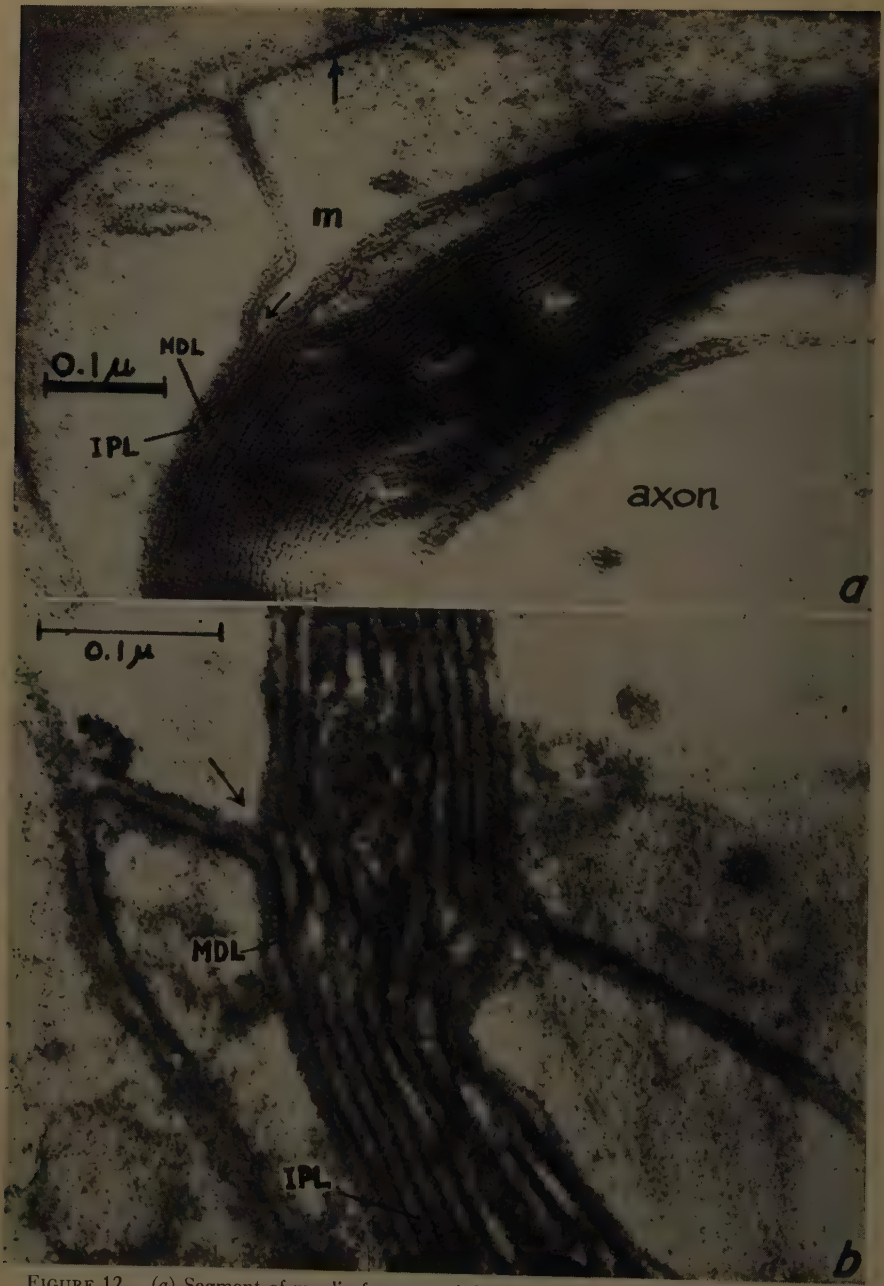

FIGURE 12. (*a*) Segment of myelin from an adult frog sciatic nerve fiber showing an outer mesaxon (m.), the major dense line (MDL) and the intraperiod line (IPL). Fixed in potassium permanganate, embedded in araldite, ×160,000; (*b*) similar segment fixed with OsO_4 and embedded in araldite, the major dense line (MDL) and intraperiod line (IPL) being indicated. ×250,000.

~170 to 185 Å thick by X-ray diffraction studies. I shall not dwell on these earlier findings; instead I call attention to a diagram (FIGURE 13) taken from the recent X-ray diffraction studies of Finean.[7] This gives Finean's conception of the molecular organization of the radial repeating unit in myelin. Finean

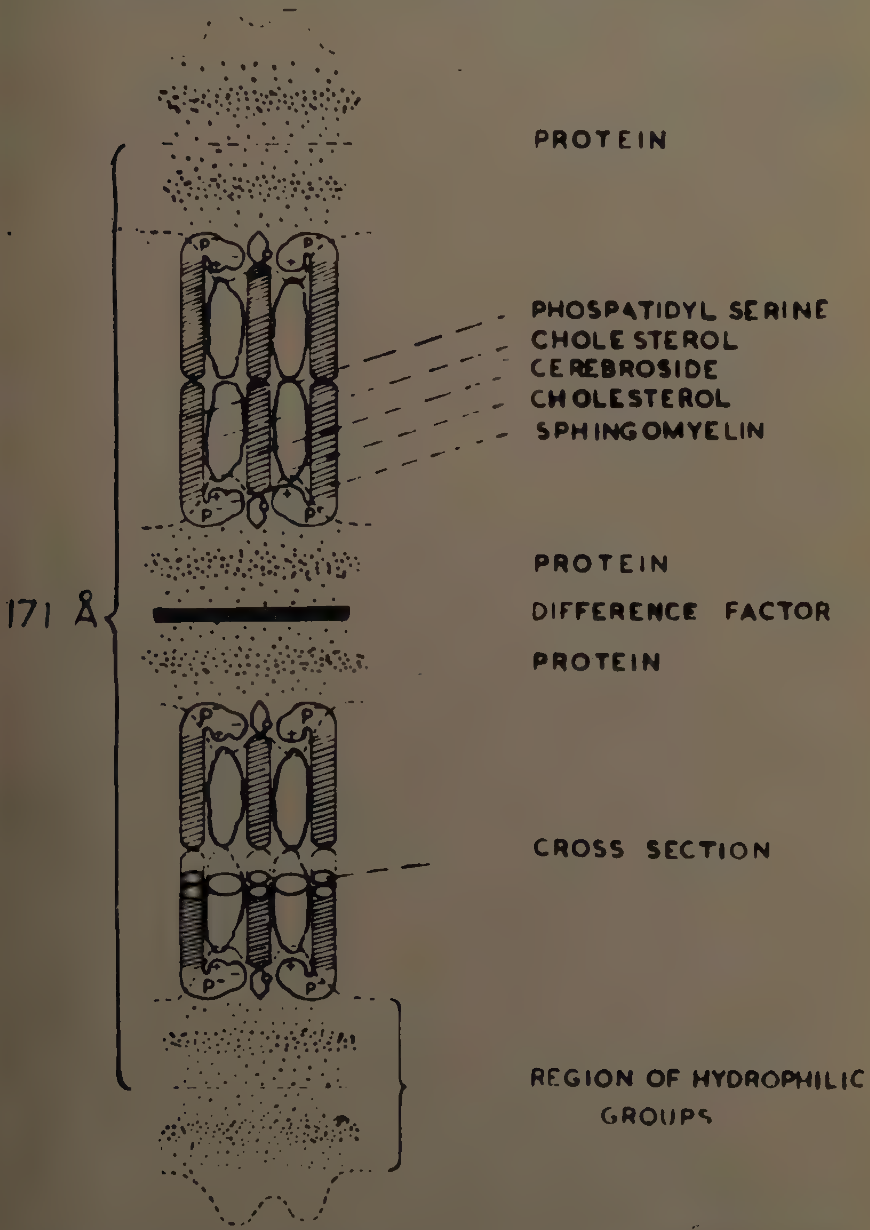

FIGURE 13. Diagram from Finean (7), showing his conception of the molecular organization of the repeating unit in nerve myelin.

proposes to insert lipids and proteins into the radially repeating structure as indicated in the diagram.

Finean[6] and Fernandez-Moran and Finean[4] showed that during fixation with OsO_4 the ~170 to 185 Å repeating period in myelin is reduced to 150 Å or less during the specimen preparation procedures leading to sectioning for electron microscopy. It is well known that sections shrink in the electron beam, and I think we can say that the radial repeating period seen in myelin by electron microscopy is identical with the repeating period detected in fresh myelin by X-ray diffraction.[36] Furthermore, on symmetry grounds alone it is quite obvious that the repeating structure in myelin is simply the mesaxon. I think, therefore, that it is quite justifiable to superimpose the X-ray diffraction diagram for myelin on the pattern seen by electron microscopy as indicated in FIGURE 14.[37]

I believe I have now presented ample evidence to justify the statement that an identity has been established between every stratum in myelin and corresponding strata in the Schwann cell membrane down to a resolution of about 20 Å or less. This allows us to extrapolate out to the surface of the Schwann cell and make statements about its molecular structure. If we assume that the X-ray analysis is, in broad terms, correct, we may say that the Schwann cell surface membrane must consist of a single bimolecular leaflet of lipid, the polar surfaces of which are covered by monolayers of nonlipid material. One cannot say, however, that this is a unique determination of the structure. The X-ray analysis is far from complete, and the model is useful only in giving a general pattern of structure for the Schwann cell membrane and, perhaps most importantly, for indicating how the problem can be uniquely solved. We now have a way to arrive at a definitive solution of the problem of cell membrane structure if the X-ray diffraction analysis of myelin structure can be made to yield a definitive solution.

There is one other point that I would like to make here. There is a distinct difference in the reactivity of the outside surface of the Schwann cell membrane as compared with that of the inside surface. This is indicated by the differences between the intraperiod line and the major dense line in compact myelin after OsO_4 and $KMnO_4$ fixation. The findings suggest that this evident chemical difference between the outside and inside surfaces is a fairly subtle one and I have suggested,[41,43] that the difference may result from the presence on the outside of a monolayer of mucopolysaccharide or possibly mucoprotein instead of the monolayer of protein that probably forms the inside surface. In fact, however, all one can be reasonably certain of is that the outside and inside surfaces contain single fully spread monolayers of two distinctly different types of nonlipid material.

I now turn briefly to another approach to the problem of determining the structure of the unit membrane. I have indicated that I believe the molecular model derived in FIGURE 14 to be in a broad sense correct. According to this model the nonlipid monolayers in combination with the polar ends of the lipid molecules interact with the fixing agents to produce thin dense strata well within the dimensions of these groups. One might have supposed, however, from the well known reactions of OsO_4 with the unsaturated bonds in lipid carbon chains[52] that such a thin dense stratum would be produced instead along the hydrophobic carbon chains. Since this was not seen some have questioned the interpretation proposed here, and alternative models have been proposed in the past to account for this apparent discrepancy.[18,51] Therefore, it was important to decide whether lipid polar groups in isolated bimolecular leaflets of lipid would in fact show up as dense strata after OsO_4 or $KMnO_4$ fixation.

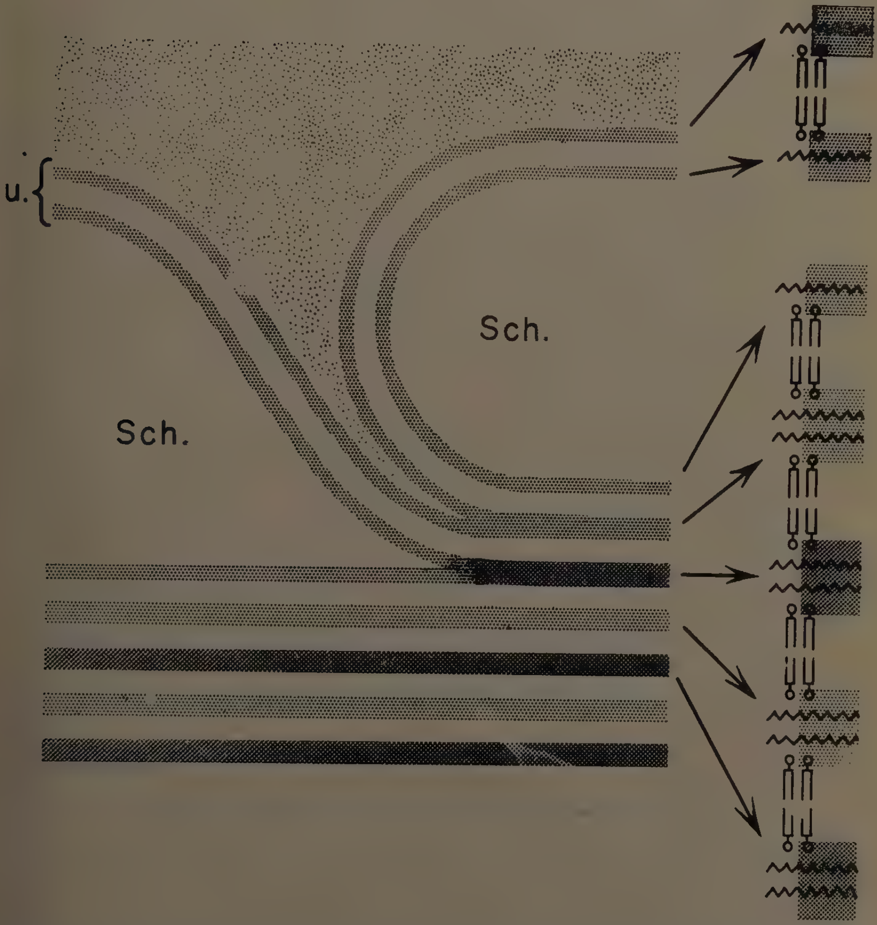

FIGURE 14. Diagram showing a way in which the molecular interpretation of the X-ray diffraction given in FIGURE 13 can be superimposed on the electron microscope pictures of myelin to allow a deduction to be made about the molecular structure of the unit membrane.

From the work of Schmitt *et al.*[47] it was known that emulsified lipids under some conditions arrange themselves roughly as in FIGURE 15*a* to give an X-ray diffraction period of ~64 Å. As water is added to such systems the period can be made to increase by almost 100 per cent by the addition of water between the polar groups as in FIGURE 15*b*. Geren and Schmitt,[15] Stoeckenius,[51] Ito, Revel *et al.*[29] and I[38,43,44] have independently demonstrated that various lipids can be fixed with OsO_4 or $KMnO_4$ and treated in the same way as a specimen of a tissue. FIGURE 16 is an electron micrograph of a section of egg kephalin dried from ethyl alcohol, fixed with OsO_4, embedded in araldite, and sectioned for electron microscopy. Here we see a very regular lattice of dense lines less than 20 Å thick repeating at a period of ~40 Å. This presumably represents the kind of molecular arrangement seen in FIGURE 15*a*.* However do the dense layers represent the polar ends of the lipid molecules or the nonpolar ends? Insofar as the picture goes it could be either. The solution to this problem comes partly from a study of regions in which the micelles of lipid are partially hydrated, as in FIGURE 15*b*, before they are stabilized by the fixative.

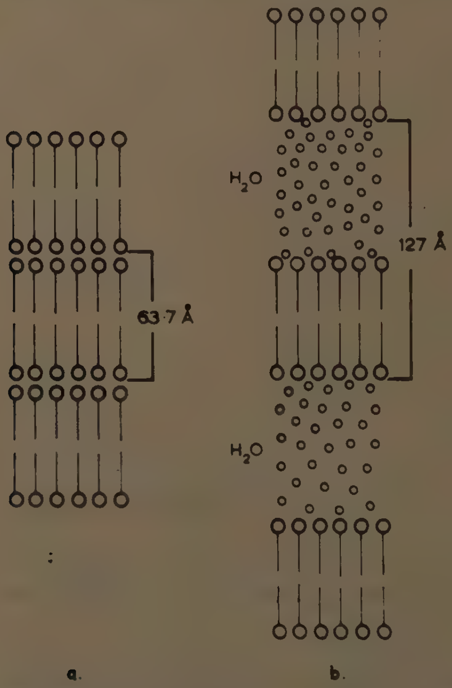

FIGURE 15. Diagram taken from Schmitt *et al.*[47] showing a molecular interpretation of the effects of hydration on a lipid system organized as smectic bimolecular leaflets as indicated in *a*. After hydration of the system, water enters along the polar groups of the bimolecular leaflets and expands the structure as indicated in *b*.

There is one point which must be made clear before proceeding. $KMnO_4$ fixation sometimes gives in egg kephalin preparations exactly the same sort of compact regions showing ~20 Å thick dense and light strata repeating regularly at a period of 40 Å, as does OsO_4.[38] Therefore each fixative must produce dense strata selectively at either the polar or nonpolar ends of kephalin mole-

---

* The period is different here partly because a different lipid is being considered, partly because the lipid is in a different polymorphic state,[5] and partly because of changes occurring during the preparatory procedures.

FIGURE 16. Portion of a section of a specimen of purified egg kethalin (supplied by M. MacFarlane) fixed with OsO_4, embedded in araldite, and sectioned. Dense and light strata each measuring about 20 Å in thickness are seen repeating at a period at approximately 40 Å. ×1,206,000.

cules. In myelin, OsO_4, and $KMnO_4$ each produces dense strata in precisely the same places, as brought out earlier. It follows that each of these fixatives acts in the same way in the sense that if one produces dense strata at the polar groups of kephalin the other most probably also does this.

In FIGURE 17 is seen a region in a kephalin preparation fixed this time in $KMnO_4$. Here the individual lipid bimolecular leaflets are shown separated by ~100 to 200 Å from one another presumably because of the entrance of water during fixation. Each of the separate similar membrane elements in isolation measures ~75 Å in thickness and looks very much like the unit membrane structure. If the dense strata of the compact lamellae in FIGURE 16 were produced by the nonpolar groups of the lipid molecules one should see single dense lines instead of the pairs of dense strata seen here in the isolated units. This is very good evidence that the dense strata represent the polar ends of the lipid molecules in $KMnO_4$ fixed preparations and, by analogy, in OsO_4 fixed preparations.

FIGURE 17. Segment of the same preparation of egg kethalin shown in FIGURE 17, but this time fixed with $KMnO_4$. In this case the single bimolecular leaflets of lipid are separated, presumably by the entrance of water during fixation. ×265,000.

It is not yet clear how this can be reconciled with known reactions of OsO_4 with double bonds in lipid carbon chains. Stoeckenius (personal communication) in some recent elegant experiments as yet unpublished has provided quite strong evidence of another kind that the polar groups show up as denser layers than the nonpolar ones after fixation. He has therefore altered his earlier interpretations[51] in which he assumed the reverse. Although we do not understand exactly the chemical mechanism leading to the observed distribution of densities we must accept the facts and seek further for a chemical explanation. The mechanism of chemical fixation remains very poorly understood, and we have here a manifestation of this poor understanding. Nevertheless, the evidence is very strong that the dense strata observed in lipids after either OsO_4 or $KMnO_4$ fixation represent the polar ends of the lipid molecules. It is well known that OsO_4 reacts with proteins to produce a dense deposit.[28,1,51] For example, protein filaments such as collagen or myofilaments are well displayed by OsO_4 fixation. Thus it seems quite reasonable to say that the dense strata in the unit membrane probably represent metallic layers at lipid polar groups combined with a protein monolayer on one side and with some other nonlipid monolayer on the other.

I suggested above that the outside monolayer of nonlipid might represent mucopolysaccharide rather than protein. While this is chiefly speculation there is some reason to believe it to be true. I have indicated above that there is ample reason to believe there is a chemical difference between the outside and inside surfaces of the unit membrane simply because of the ways in which these two surfaces react to fixing agents. The X-ray diffraction studies of Finean[8] suggest that the differences are fairly subtle since there is a distinct tendency for the myelin period to be halved under certain conditions. Therefore the nonlipid constituents bordering the bimolecular leaflet of lipid on either side must be very similar in composition to the extent that their composition might affect their scattering of X rays. The difference between these two strata could be readily accounted for by the presence in the one case of monolayers of protein and in the other by monolayers of mucopolysaccharide. There are two additional bits of information which bear on this problem.

A direct morphological continuity exists between the mucopolysaccharide ground substance condensed in the basement membrane material about Schwann cells and the gap between the unit membranes of the mesaxon. Compare FIGURES 2 and 3. Note the amorphous basement membrane substance around the whole nerve fiber in FIGURE 2 and its indefinite shading off externally and into the paired membrane gaps. Perhaps FIGURE 18 may further substantiate this point. Here the basement membrane substance bordering an unmyelinated fiber is almost continuous with that bordering a myelinated fiber. This amorphous diffuse material extends right up to the external dense stratum of the unit membrane of the Schwann cell (arrow 1); the same sort of material seems to occupy the gap between the Schwann cell and the axon membrane (arrow 2). This material is what I call the "gap substance."

During the formation of myelin the gap between the paired mesaxon membranes is reduced to less than 20 Å in thickness and, presumably, only two monolayers of the gap substance would be left after this reduction. There is considerable evidence to support a contention that the basement membrane material and the intercellular ground substance is high in its content of mucopolysaccharide (see Robertson[43] for references). I believe that the gap substance is the same kind of material. It seems reasonable to suggest that the remaining monolayers after the collapse of the gap during myelin development also represent in large measure mucopolysaccharides though this is clearly quite speculative.

There is in fact no direct conclusive evidence on the chemical nature of either of the nonlipid monolayers in the unit membrane. All that can be said with any degree of certainty is the following: the unit membrane theory holds that all normal cellular membranes not fused with another membrane are chemically asymmetric and that they consist of a single bimolecular leaflet of lipid of unspecified composition bounded on one side by a fully spread monolayer of one kind of nonlipid and, on the other, by a monolayer of a different kind of nonlipid. One of the monolayers of nonlipid always borders cytoplasmic matrix or a direct derivative thereof. This may be called the X layer. The other nonlipid monolayer always borders extracellular matrix material or a direct derivative of it. This may be called the Y layer. These features are indicated in very schematic form in FIGURE 19.

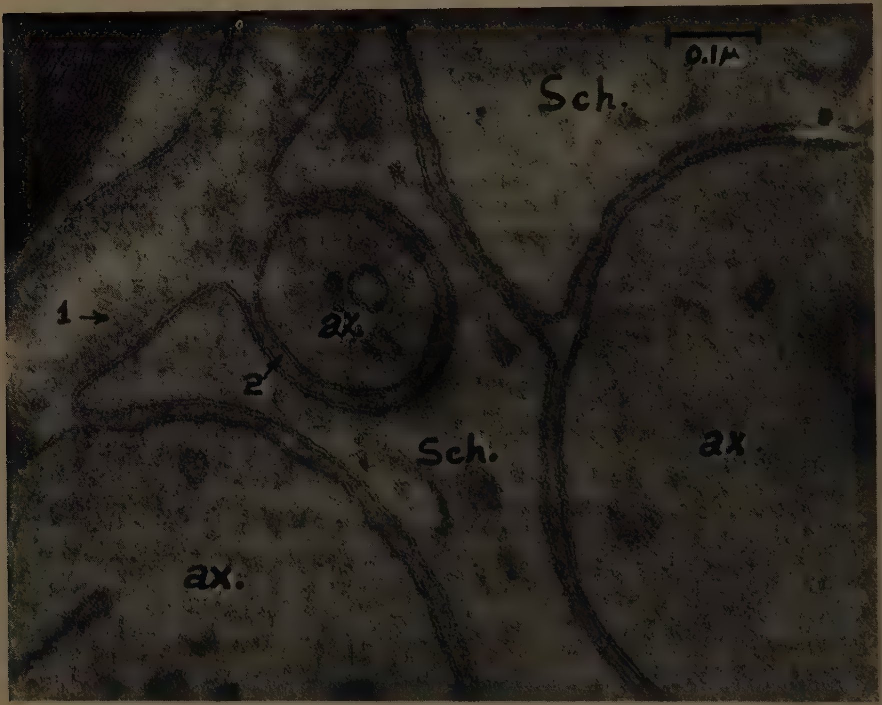

FIGURE 18. Segment of a mouse unmyelinated nerve fiber showing portions of three axons (ax.) and a Schwann cell (Sch.). A portion of a myelinated fiber is shown to the upper left. The basement membrane material designated by the arrow 1 seems to extend up to the unit membrane. A similar type of material appears to occupy the gaps between the unit membranes as at arrow 2. ×120,000.

I propose now to review briefly some experiments on the effects of hypotonic and hypertonic solutions on myelinated and unmyelinated nerve fibers. Finean and Millington[9] showed in 1958 that the nerve myelin period is increased if fresh nerve fibers are soaked in hypotonic solutions for a few hours. Their studies were done by X-ray diffraction, and the nature of the increase could not be determined. I then showed that it is possible, after soaking nerve fibers in distilled water for two hours, to fix them with permanganate and demonstrate by electron microscopy the increase in the myelin period.[39] It was shown that the increase was due to a splitting apart of the myelin lamellae selectively along the outside surfaces of the unit membranes united at the intraperiod line, as indicated in FIGURE 20. The inside cell surfaces united at the major dense line do not separate under these conditions. FIGURE 21 shows a micrograph of a myelinated fiber soaked in distilled water before fixation in permanganate to illustrate this phenomenon. FIGURE 22 shows the separated lamellae at higher magnification in a through-focus series. This experiment has been repeated a number of times, and it is quite clear, since the separation of the lamellae always occurs along the outside cell surfaces, that a different kind of chemical bonding must be set up between the outside surfaces as compared with that set up between the inside cell surfaces. This experiment provides important evidence indicating that unit membranes are chemically asymmetric.

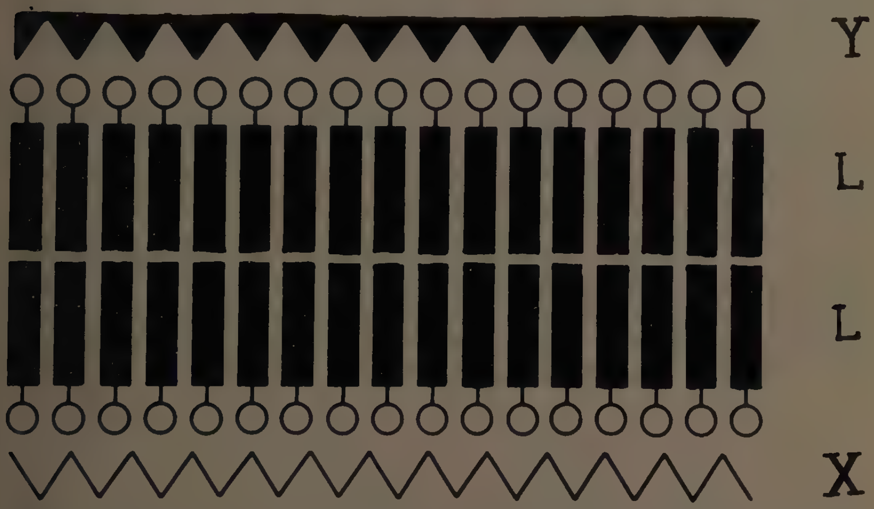

FIGURE 19. A highly schematic diagram of a unit membrane showing two monolayers of lipid molecules (L.) and two fully spread monolayers of nonlipid designated by the letters X and Y. Different letters are used for the nonlipid monolayers to indicate that they are chemically different, even though their exact nature is as yet unknown. X borders cytoplasm.

In these studies of the effects of hypotonic solutions on nerve fibers I also studied the effects of hypertonic solutions. Here the most interesting findings occurred in the unmyelinated nerve fibers. FIGURES 23*a* and *b* show unmyelinated nerve fibers soaked in hypotonic Ringer solution (*a*) or distilled water (*b*) before fixation. Note that the gap (g.) between the unit membranes in

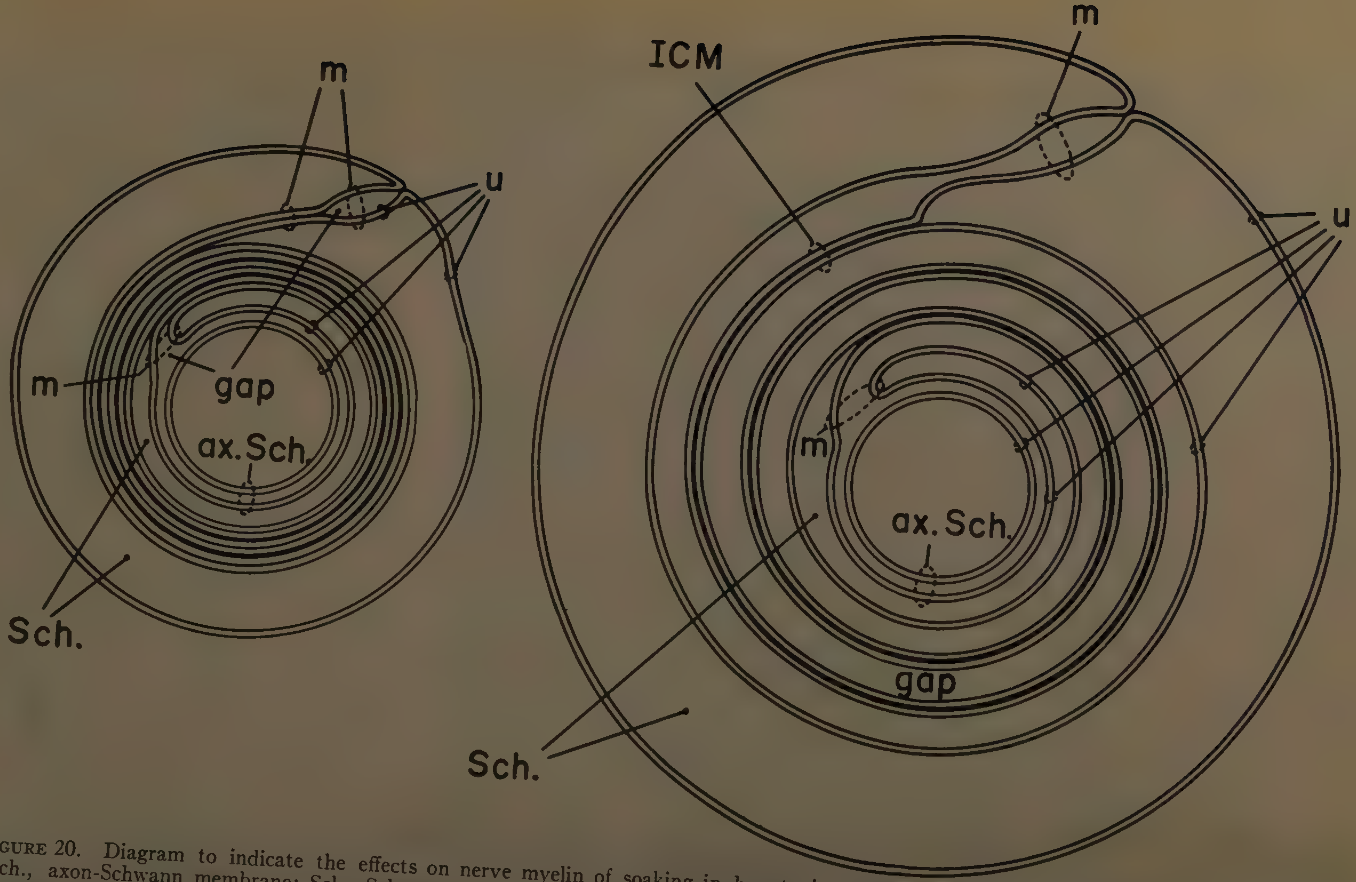

FIGURE 20. Diagram to indicate the effects on nerve myelin of soaking in hypotonic solutions. Symbols: m, mesaxon; g, unit membrane; ax. Sch., axon-Schwann membrane; Sch., Schwann cytoplasm; ICM, internal compound membrane. The normal fiber is shown to the left and the appearance of such a structure after soaking in a hypotonic solution before fixation is shown to the right. Note that the outside cell surfaces united at the intraperiod line split apart whereas the inside surfaces united at the major dense line do not.

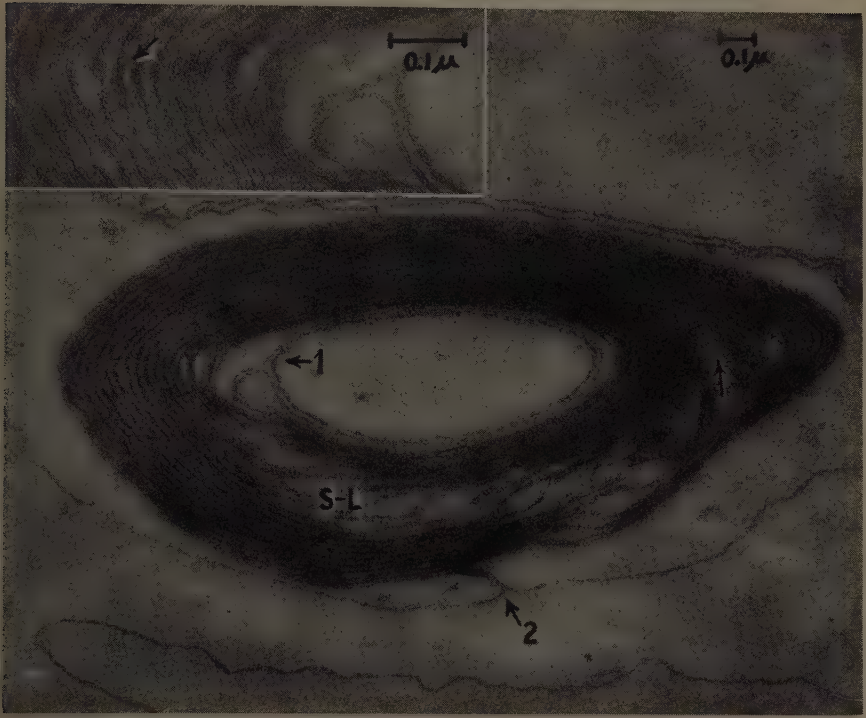

FIGURE 21. Electron micrograph of a myelinated nerve fiber soaked in distilled water about two hours before fixation with potassium permanganate and embedding in araldite. Note that the inner and outer mesaxons (1 and 2) are still visible. The myelin lamellae are kinked at the unlabeled arrow, and a Schmidt-Lanterman type transverse shearing defect (S-L) is seen below. In the upper left corner a portion of the myelin is enlarged to show that the separation of the lamellae occurs along the intraperiod line. ×51,000; inset, ×110,000.

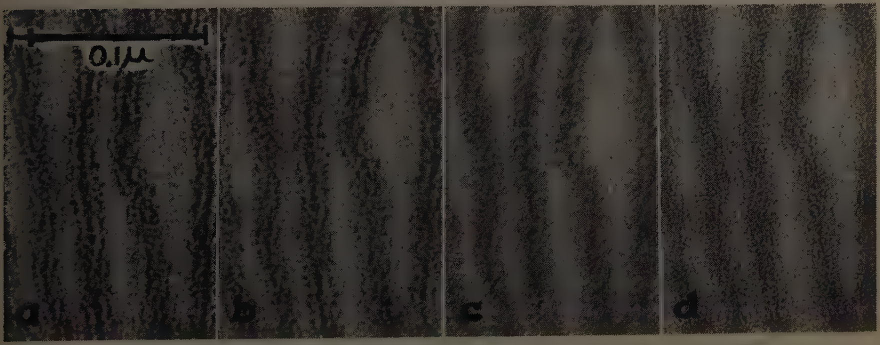

FIGURE 22. A segment of myelin lamellae separated by soaking in distilled water for two hours before fixation in potassium permanganate and embedding in araldite. This is a through focus series: (*c*) very nearly focused; (*a* and *b*) underfocused; (*d*) overfocused. ×250,000.

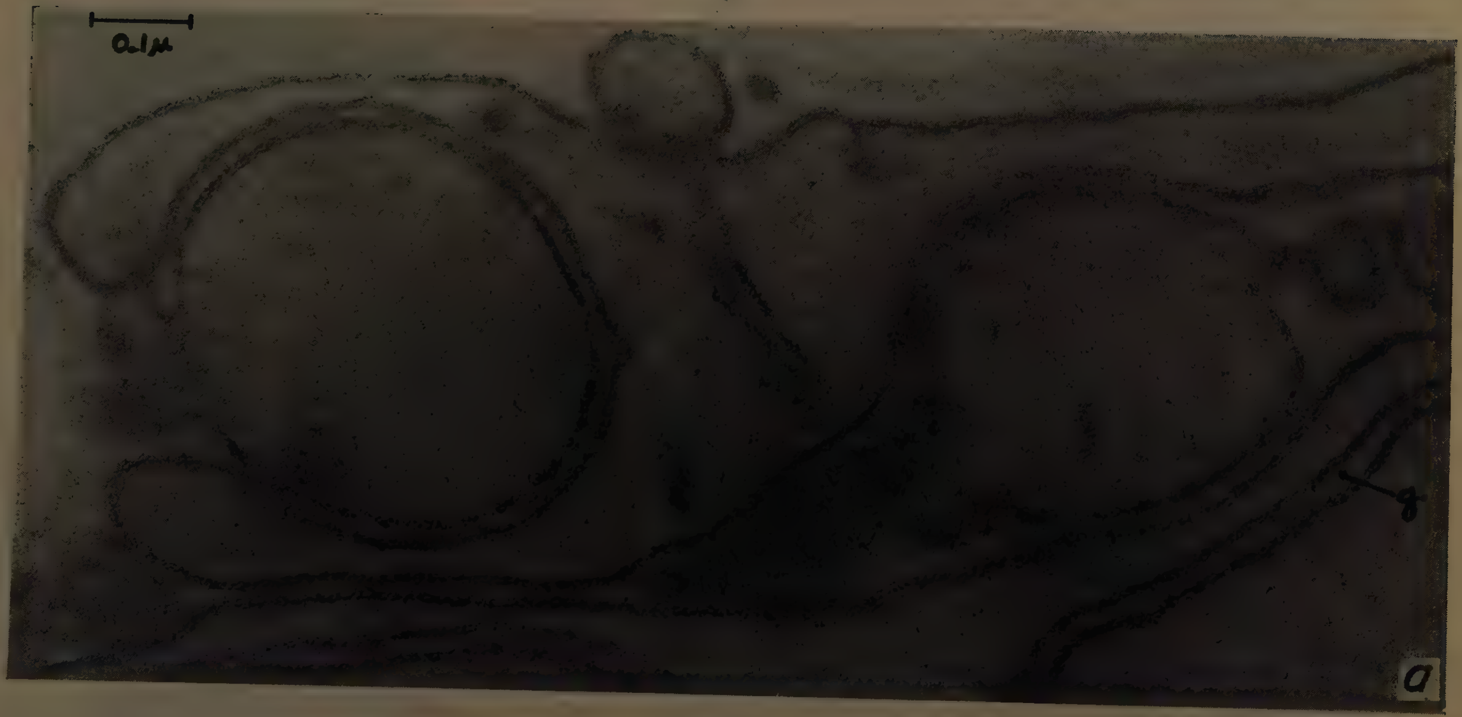

FIGURE 23*a*.

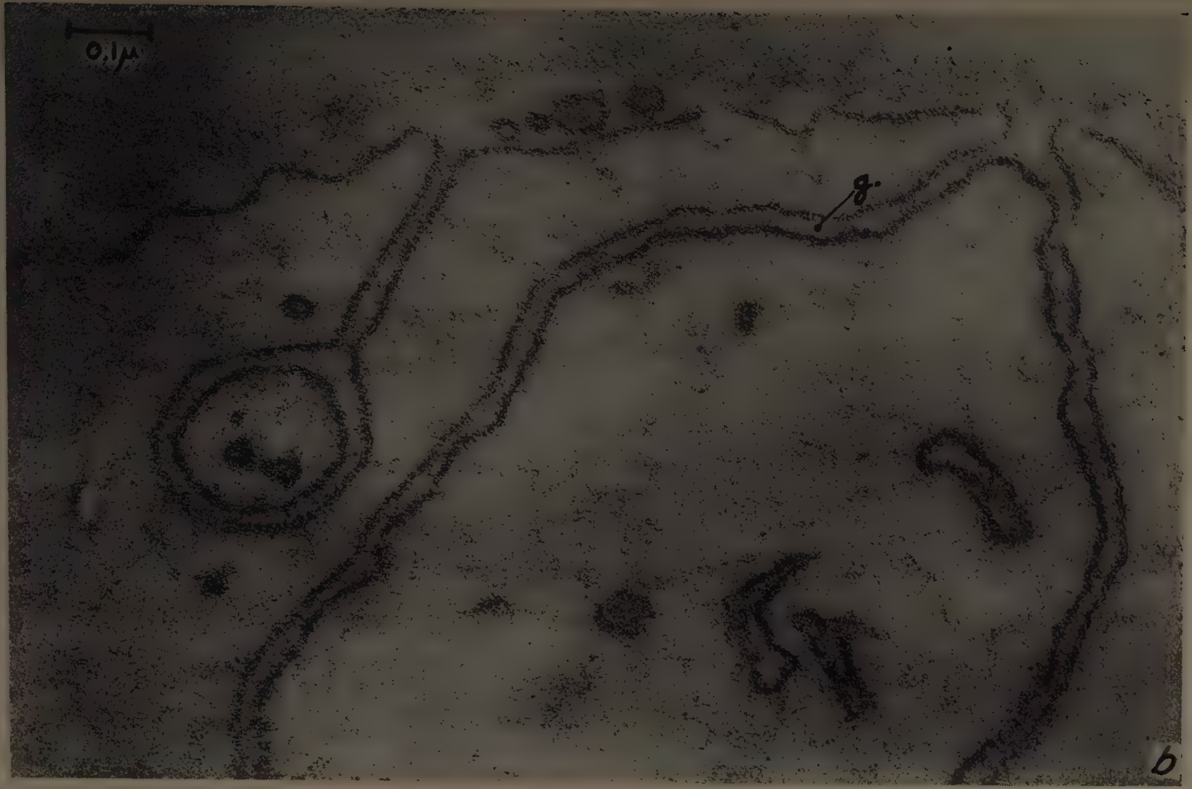

FIGURE 23. (*a*) Unmyelinated nerve fiber soaked in hypotonic Ringer solution before fixation in permanganate and embedding in araldite, ×130,000; (*b*) unmyelinated nerve fiber soaked in distilled water before fixation with potassium permanganate and embedding in araldite. Note the widening of the gap (g.) between the unit membranes of the paired membrane structures. The gaps at the marked regions measure over 200 Å in thickness as compared with the usual 100 to 150 Å seen in the controls. ×110,000.

all the paired membrane structures are greatly widened by this treatment. On the other hand treatment with hypertonic solutions resulted in a closure of the gaps as indicated in FIGURES 24*a* and *b*. Here the over-all width of the paired membrane structures has been reduced to about 150 Å and the gap between the unit membranes to less than 20 Å. This finding indicates that the gap substance between the paired membranes that is usually ~100 to 150 Å thick is very highly hydrated. FIGURE 25 is a diagram summarizing these findings in an unmyelinated nerve fiber. The findings are compatible with the assumption that the gap substance is a highly hydrated mucopolysaccharide gel, but they do not prove this point. It is possible that the membranes are stabilized in their usual relationship of ~100 to 150 Å separation only by some kind of electric interactions that are sensitive to ion concentrations.

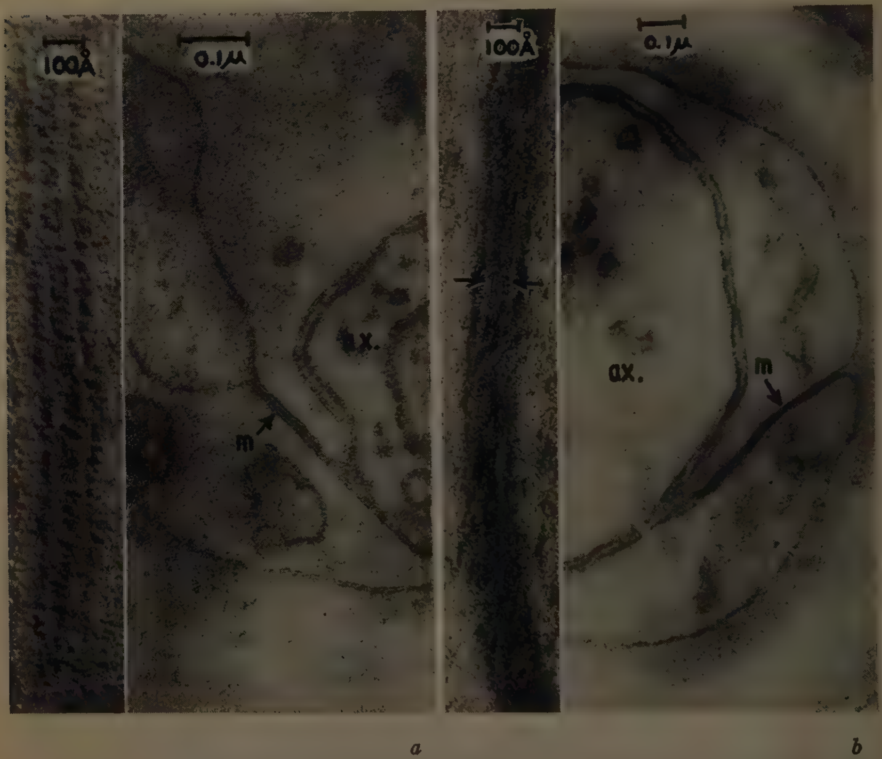

FIGURE 24. (*a*) Unmyelinated nerve fiber soaked in four times isotonic Ringer solution for one hour before fixation. Note the closed mesaxon gap (m.) connecting with the axon (ax.). A segment of this is enlarged to the left. Note that the central dense line is about twice as thick as the other two and consists of two closely apposed dense lines. ×92,000; inset, ×600,000. (*b*) Unmyelinated fiber similar to that in *a* but soaked in 10 times isotonic sucrose-Ringer solution for 1 hour before fixation. Note the closed mesaxon gap (m.) leading to the axon (ax.). This is enlarged in the inset to the left. The two apposed dense layers of the membranes in contact forming the central dense layer in the enlargement seem to show some fine structure. They are separated by ~15 Å. Each appears to be ~20 Å across and composed of 2 dense layers less than 10 Å wide separated by light zones. These images must not be interpreted too literally, however, since no through focus series was obtained in this instance. ×60,000; inset, ×450,000.

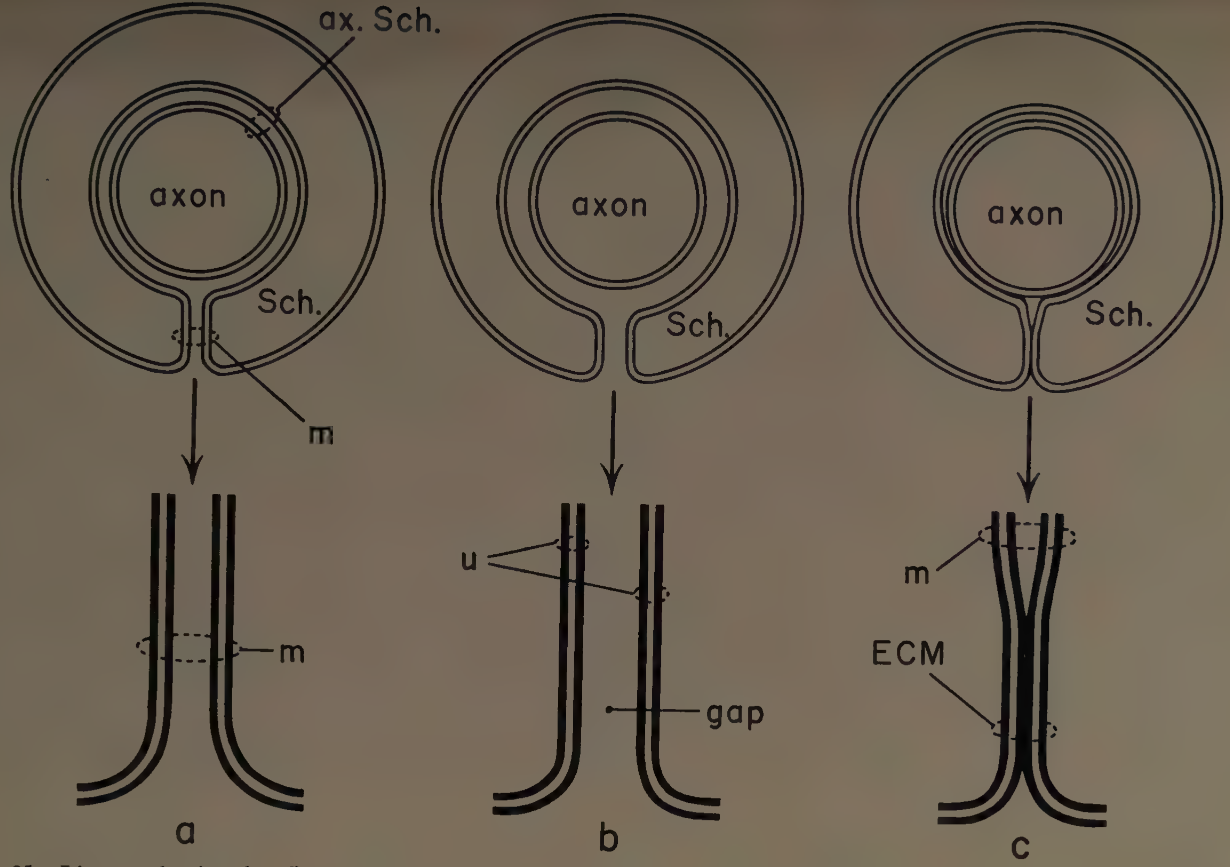

FIGURE 25. Diagram showing the effects of hypotonic and hypertonic solutions on an unmyelinated nerve fiber. (*a*) Fiber soaked in normal Ringer solution before fixation; (*b*) one soaked in hypotonic Ringer solution or distilled water before fixation; (*c*) one soaked in hypertonic Ringer solution before fixation. Key: Sch., Schwann cytoplasm; m, mesaxon; u, unit membrane; ECM, external compound membrane.

There is one additional point that may be considered in relation to the hypothesis that the outer stratum of the unit membrane represents mucopolysaccharide and the inner stratum protein. As already mentioned OsO_4 is preferred as a fixative for protein filaments, such as the myofilaments of muscle. It also fixes collagen fibrils very well. Potassium permanganate, on the other hand, is a much less effective fixative of protein structures, although the myofilaments of muscle and collagen fibrils are in fact detectable after treatment with this fixative. Recently Revel *et al.*[30] have shown that while OsO_4 is a relatively poor fixative for glycogen, permanganate is a very good one. Both permanganate and OsO_4 are quite good fixatives for phospholipids. If the unit membrane structure is organized, as I have postulated, with a bimolecular leaflet of lipid bounded on one side by a monolayer of protein and on the other by a monolayer of mucopolysaccharide, then one would expect the structure to react with OsO_4 and $KMnO_4$ in precisely the way that has been observed. One would expect the cytoplasmic surface, if it is lipid and protein, to react equally well with OsO_4 and $KMnO_4$ to produce a dense stratum that stands the embedding and sectioning procedures. If the outside surface is lipid and mucopolysaccharide then one would expect this to be well fixed by permanganate and to be inadequately preserved by OsO_4, as observed with the unit membrane structure. These findings I regard as support for my hypothesis that the X layer of the unit membrane is primarily protein and that the Y layer is primarily some kind of polysaccharide.

May I point out here that the unit membrane structure is not confined to nerve fibers. It has been demonstrated at the surfaces of many different kinds of cells and in membranous cell organelles such as mitochondria. In fact, it appears to be demonstrable in all cells and membranous organelles so far studied, and it has been suggested that the pattern of molecular organization of the cell membrane represented by the unit membrane pattern is constantly present in all normal animal or plant cells. The reader is referred to others of my publications for elaborations of this point.[41,43,44]

In FIGURES 3 and 18 I showed the paired membrane structures called the axon-Schwann membrane formed by the apposed axon and Schwann cell membranes in unmyelinated nerve fibers. In these examples the gap between the unit membranes is about the same as that seen generally in adult nonmyelinated nerve fibers and in nonnervous tissues. Frankenhaeuser and Hodgkin[10] and Ritchie and Straub[31] have each independently presented electrophysiological evidence that suggests that important electrical properties of nerve fibers can be explained by the assumption that potassium ions leaving the axoplasm during impulse propagation are momentarily trapped in the axon-Schwann membrane or mesaxon gaps before leaking slowly away into the extracellular spaces. It seems reasonable to assume that the presence or absence of the gap between unit membranes might be very important in determining the electrical properties of all nerve fibers. Evidence has been presented elsewhere[37,42] to show that in nodes of Ranvier the axon-Schwann membrane gap is obliterated in the juxtaterminal myelinated regions of the nodes but present over the major part of the internode and the unmyelinated portions of the nodes. It is believed that these membrane relations in nodes of Ranvier may be of considerable importance in mediating saltatory conduction since the gap substance, because of its high degree of hydration, may be utilized as a pathway for ionic current flow. I now turn to the invertebrate synapse alluded to above. There are special membrane contact relationships in the crayfish median-to-motor giant fiber synapse that may in a similar way be of importance in determining the peculiar electrical properties of this synapse noted by Furshpan and Potter.[11] Since the work of these investigators there has been a great deal of interest in crayfish giant synapses, and I therefore present here some findings bearing on their work. The accompanying micrographs, with the exception of FIGURE 29, have not been previously published. They are included and discussed here because the unit membrane concept now makes possible some interpretations that could not previously be made.

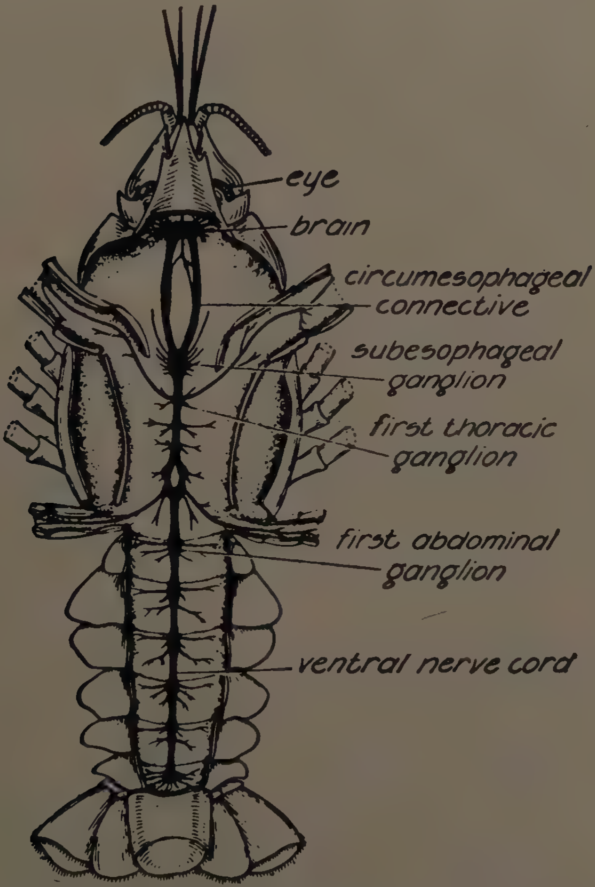

FIGURE 26. Diagram of a crayfish showing the ventral nerve cord. Reproduced by permission of John Wiley & Sons, Inc., New York, N.Y.[54]

The crayfish median-to-motor giant synapse was first described by Johnson in 1924.[19] It was studied in terms of physiological connectivity by Wiersma.[52] I carried out the first studies of it by electron microscopy from 1950 to 1953.[32,33,34,36] This earlier work will be summarized before going on to more recent findings and interpretations.

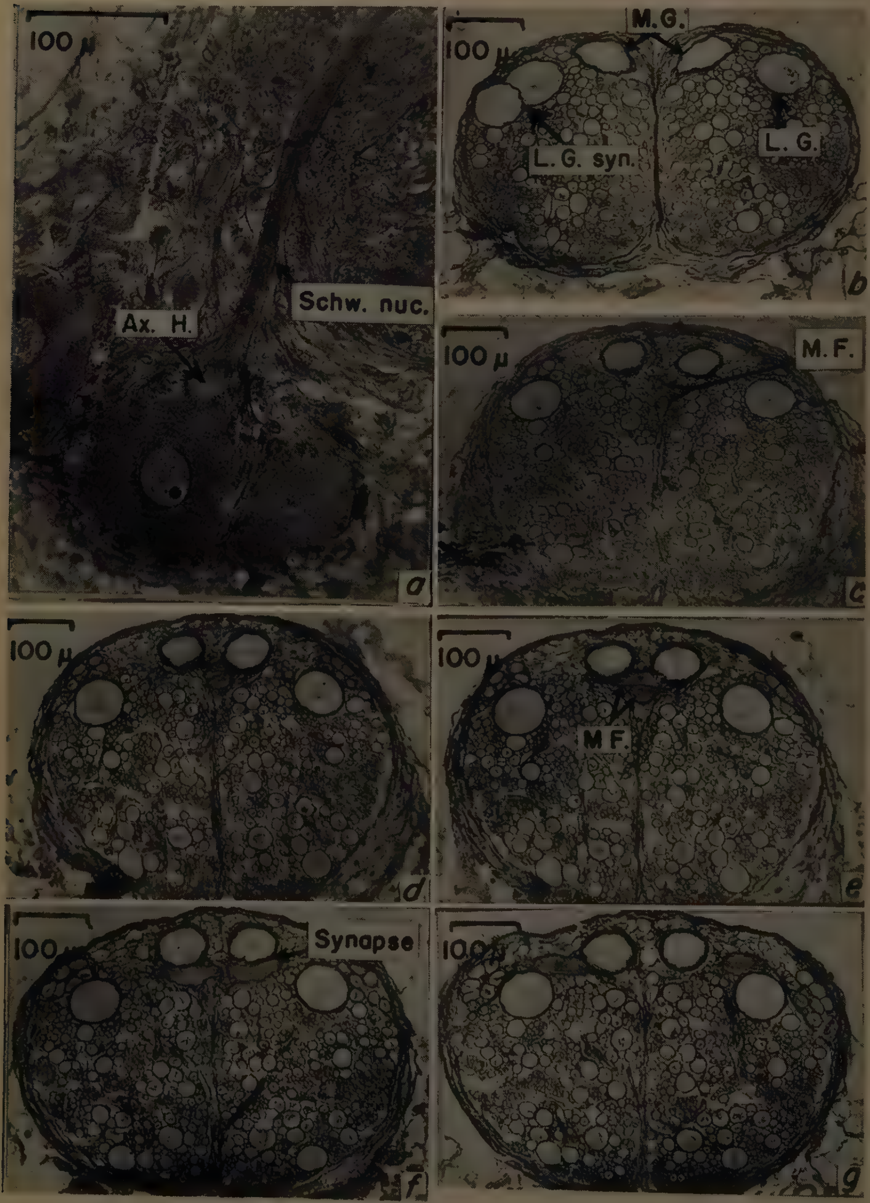

Figure 27.

FIGURE 26 is a diagram of a crayfish showing the ventral nerve cord. From each abdominal ganglion there emerge three symmetrical motor nerve roots, the most caudal of which carry motor fibers innervating the muscle fibers of the tail. In the nerve cord there is a giant fiber system extending the entire length of the animals. This consists of two median giant fibers and two lateral giant

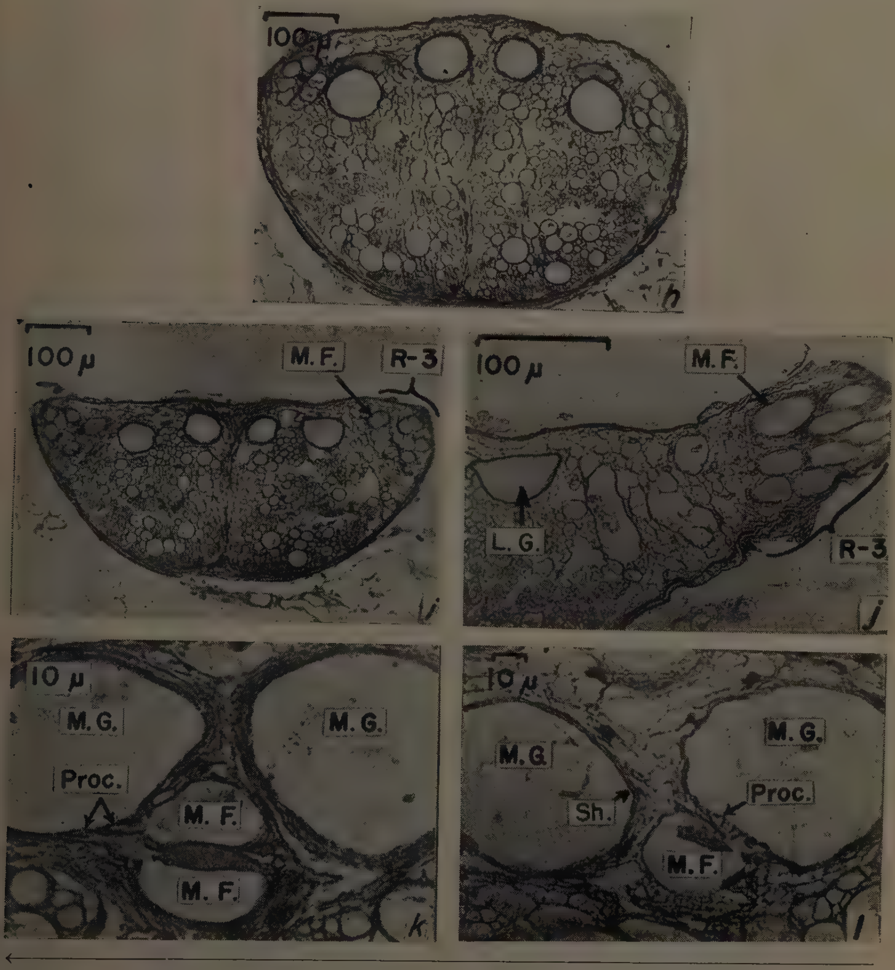

FIGURE 27. Light micrographs (*a* to *l*) of paraffin sections of a crayfish abdominal ganglia fixed by the method of Vom Rath. (*a*) A unipolar neuron in the cell mass of an abdominal ganglion. (*b* to *j*) Serially arranged transverse sections proceeding through a ganglion from the cranial to the caudal end. Numerous sections are left out between the levels shown but micrographs are consecutively arranged to show the formation of the median giant and lateral giant to motor synapses. In (*b*) the lateral-giant-to-lateral-giant synapse is shown (L.G.Syn.). (*k* and *l*) show the median-giant-to-motor synapse at higher magnification by light microscopy. Key: Sch. nuc., Schwann cell nucleus; Ax. H., axon hillock; L.G., lateral giant fiber; M.G., median giant fiber; M.F., motor fiber; R-3, third root of a ganglion; Proc., synaptic process of the motor fiber; Sh., sheath of the median giant fiber. Magnifications are given by the markers.

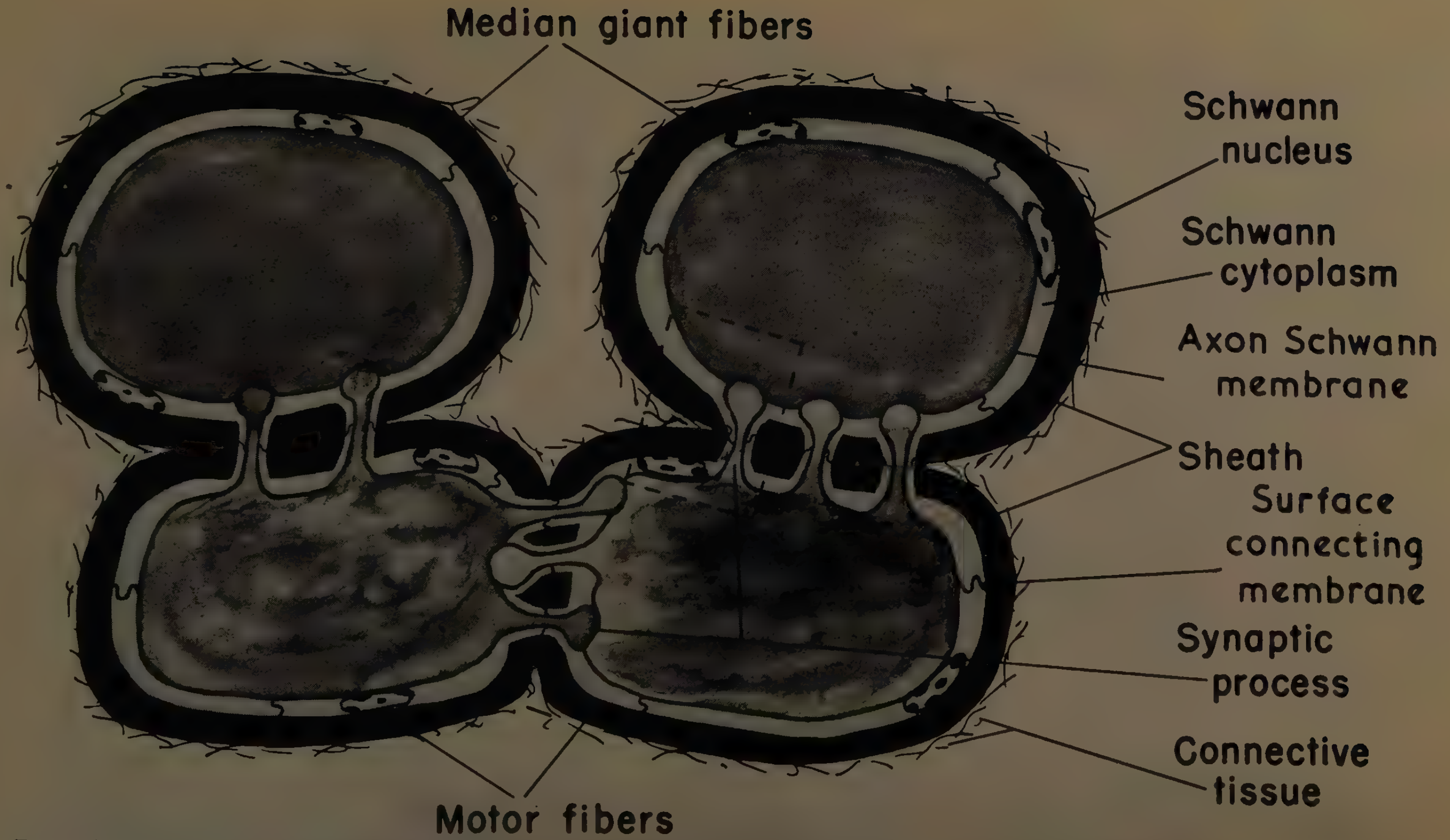

FIGURE 28. Diagram of the crayfish median-to-motor giant synapse showing the synaptic processes of the motor fibers extending toward one another and toward the median giant fibers. The term surface connecting membrane is used here in place of mesaxon.

fibers, each of which forms synaptic relationships with the motor fibers in each ganglion before they pass out through the third roots to the abdominal muscles. The two median giant fibers originate as the axons of unipolar neurons in the brain and extend uninterrupted throughout the length of the animal. In each abdominal ganglion two motor fibers originate as axons of unipolar neurons like the one shown in FIGURE 27*a* in the ventral cell mass of the ganglion. These axons pass dorsocaudally and decussate just beneath the median giant fibers. Here they set up synaptic relationships with one another. They then each form synaptic contacts with each of the median giant fibers and finally each motor fiber synapses with the contralateral lateral

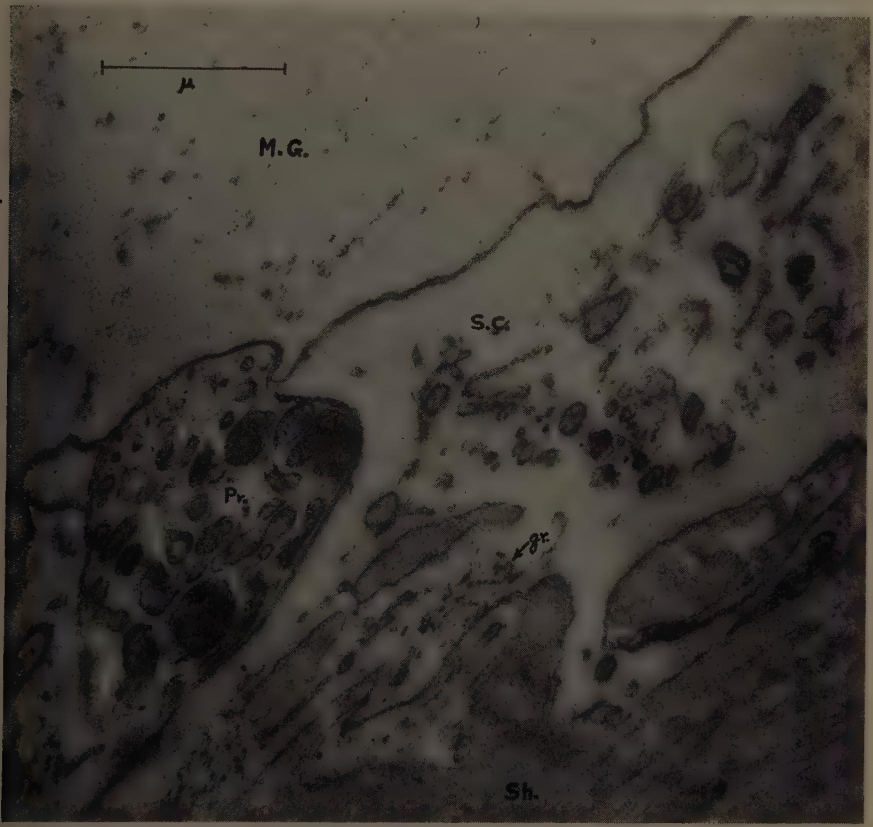

FIGURE 29. Electron micrograph of portion of crayfish median-to-motor giant synapse showing the median giant fiber above (M.G.) portion of a Schwann cell (S.C.) and a sheath (Sh.) and a synaptic process (Pr.) extended by the motor fiber which is not shown in this micrograph. Note the irregular granular component (gr.) of the Schwann cell shown in the lower center of the micrograph. This component is sometimes quite regularly arranged and may represent a tubular component of the endoplasmic reticulum. The tubules measure, however, less than 250 Å in diameter which is quite unusual for elements of the ER, and these components may, therefore, represent a different kind of structure. ×44,000.

giant fiber before passing out through the third roots to innervate the tail muscle fibers. These relationships are shown at the light microscope level in the serial transverse sections of a Vom Rath fixed paraffin embedded abdominal ganglion in FIGURES 27*b* to *j*. The serial sections proceed caudally through the ganglion. The sections are each about 10 μ thick and are not true serials. A number of sections were omitted between each one illustrated.* The median giant fibers and lateral giant fibers are labeled M.G. and L.G. respectively, and the motor fibers M.F.

FIGURES 27*k* and *l* show the median-to-motor giant synapse in a light microscope preparation at a higher magnification. Here it may be seen that in the synaptic region the motor fiber extends numerous small pseudopodium-like synaptic processes (Proc.) toward the median giant fiber. These processes penetrate successively the sheath of the motor fiber and the sheath of the median giant fiber and come to lie in very intimate apposition with the axoplasm of the median giant fiber. No synaptic processes are extended toward the motor fiber by the median giant fibers. A very similar kind of synaptic relationship is set up between the two motor fibers as they decussate just cranial to the synapse with the median giant fiber. Again synaptic processes penetrate the Schwann cell of adjacent fibers and contact the axon membrane. The main difference between the median-giant-to-motor synapse and the motor-to-motor synapse morphologically seems to be that whereas in the case of the median giant synapse processes are extended only by the motor fiber, in the motor-to-motor synapse each giant axon extends synaptic processes toward the other. These relationships are shown in diagrammatic fashion in FIGURE 28. The diagram shows the relationships designated "synapse" in FIGURE 27*f*. The fact that synaptic processes are not extended by the median giant fibers but only by the motor fibers correlates well with Wiersma's elctrophysiological experiments,[52] which showed that impulses set up in either median giant fiber are transmitted to both motor fibers while impulses set up in either motor fiber by stimulation of the third root of the ganglia, while crossing to the opposite motor fiber, do not stimulate the median giant fibers. Thus the synaptic processes would seem to be organelles specialized for picking up an impulse, and their small size relative to that of the giant axons they contact may be enough by itself to account for electrical transmission.

FIGURE 29 is an electron micrograph showing a portion of the Schwann cell of the median giant fiber (MG) with a synaptic process (Pr) of a motor fiber like the ones indicated by the arrows in FIGURE 27*k*. The synaptic process is in intimate contact with the median giant axon. This contact is brought about by the penetration of the motor fiber process through the Schwann cell of the median giant fiber. The pseudopodiumlike extension of motor fiber axoplasm pushes first through a mesaxon gap in the motor fiber and then through a mesaxon gap in the median giant fiber Schwann cell. It then enlarges and expands next to the axon membrane.

There are several features illustrated in FIGURE 29 that warrant discussion but I shall confine myself here chiefly to the membrane contact relationships. However, in passing I will re-emphasize one or two points made in earlier papers.[34,36] First, unlike vertebrate synapses as described by Palade and Palay,[23] Palay[24,25,27] and others,[17] postsynaptic rather than presynaptic axoplasm contains the most striking concentrations of organelles. Numerous mitochondria are seen in the synaptic processes and accumulations of vesicles are noted. The latter point is better made by FIGURE 30. This shows a motor fiber synaptic process penetrating the presynaptic Schwann cell just before contacting the presynaptic membrane. Here many 300 to 500 Å vesicular-appearing profiles are seen with a few interspersed tubular profiles and mitochondria. This is the kind of appearance considered in vertebrate central nervous system synapses to characterize presynaptic axoplasm. A similar appearance characterizes terminal axons in motor end plates. The peculiarity of the crayfish synapse whereby the vesicular accumulation occurs in post- rather than presynaptic axoplasm is most interesting. I have pointed out before that it may be that this differentiation of axoplasm is more charac-

---

* These micrographs are taken from my thesis submitted in partial requirement for the Ph.D. degree at the Massachusetts Institute of Technology in 1952,[32] and have not been published elsewhere.

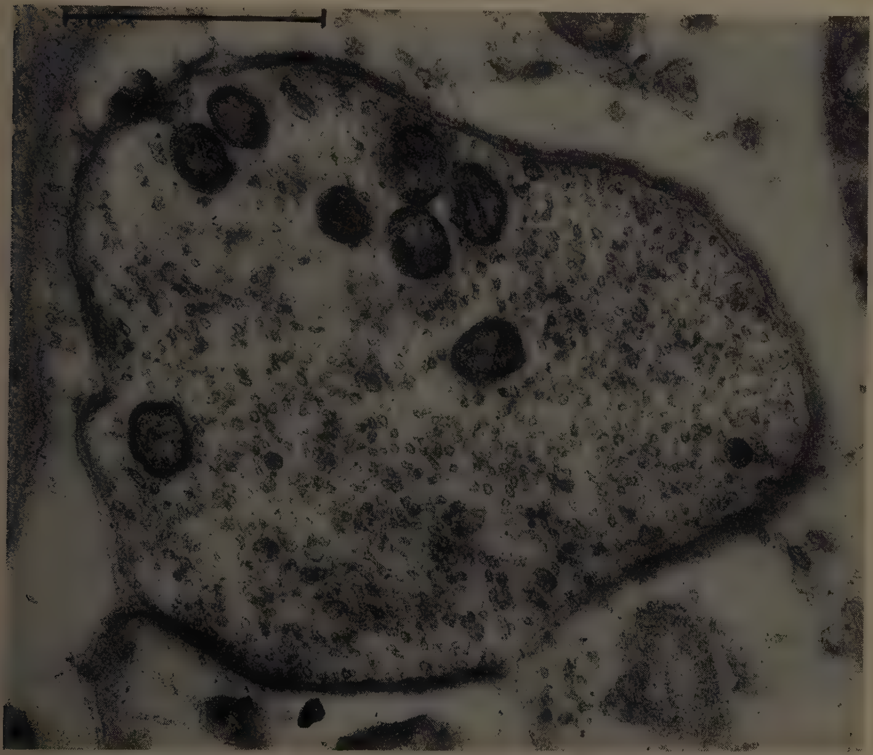

FIGURE 30. Section of a motor fiber synaptic process penetrating the Schwann cell layer of a presynaptic fiber in the crayfish giant fiber synapse. Ca. × 50,000.

teristic of terminal branches of axons than of synapses,* for this is the most obvious structural feature common to the three regions of vesicle accumulation mentioned.

There are two other points about the crayfish synapse I shall make in passing. It appears from some micrographs that in some regions small round profiles like the vesicular bodies concentrated in postsynaptic axoplasm accumulate in the gap between the pre- and postsynaptic axon membrane. These are shown in FIGURES 31 and 32. Some of these bodies are dense, as if they contained material similar to that in the round profile designated by the arrow in postsynaptic axoplasm to the right and below in the enlargement. This ~300 Å body contains a very dense amorphous material not unlike that often identified in some situations as a secretory product. This kind of body is more common in squid giant fiber synapses as reported earlier.[36]

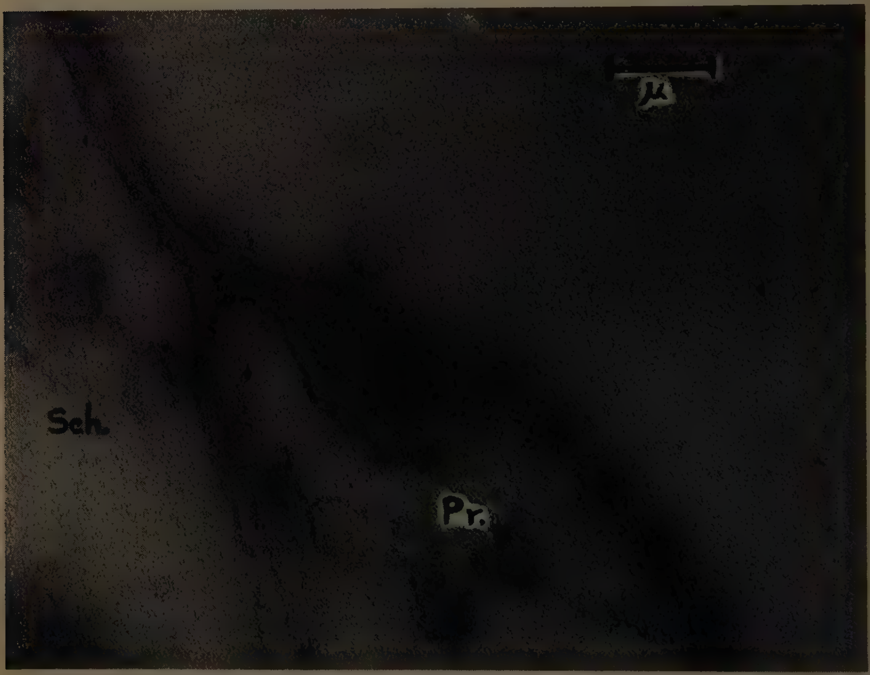

FIGURE 31. A synaptic process (Pr.) is shown in contact with the pre-synaptic axon membrane in the crayfish giant fiber synapse. Schwann cytoplasm (Sch.) appears to the left. Note the round bodies containing dense material present between the pre- and postsynaptic membranes. These measure between 800 and 1000 Å in diameter. Fixed with OsO_4, embedded in methacrylate and unstained. ×140,000.

The last point I shall make in passing is concerned with the presence in FIGURE 29 of a peculiar tubular or granular structure labeled gr. I have noticed this component on numerous occasions in Schwann cells at the crayfish median giant synapse and, on occasion, it has had a rather remarkable regularity. In such regions of regularity it appears as an interlaced lattice of tubular profiles about 200 Å in diameter. It may represent a component of the endoplasmic reticulum but some of my micrographs suggest that it may represent a separate component. This structure will be considered in detail elsewhere.

---

* In discussion on page 49 of paper by S. L. Palay.[37]

I now return to the contact relationships of the pre- and postsynaptic membranes. Since, in 1955, when the micrograph in FIGURE 29 was first published,[34] the unit membrane concept had not yet been evolved, the views of Sjöstrand and his collaborators[48-50] on so-called "double membrane" structure were accepted and used in interpreting the membrane relationships observed in the crayfish synapse. Accordingly the axon-Schwann membranes of the afferent median giant fiber and the motor fiber synaptic processes were each considered as separate complete entities. Since the synaptic membrane complex displayed most of the features of either of these separate entities it was supposed that the two axon-Schwann membranes fused to make another entity, the synaptic membrane. The unit membrane concept, however, requires that we treat each axon-Schwann membrane as consisting of three distinctly separate entities: the unit membrane of the axon, the gap substance, and the unit membrane of the Schwann cell. The synaptic membrane complex accordingly must be considered as three entities: the presynaptic unit membrane, the gap substance, and the post synaptic unit membrane. Considered in this way the only elements that would have been fused on the older interpretation were the layers of gap substance between the unit membranes involved. The gap substance is regarded in the unit membrane interpretation as extracellular, extramembranous material. Fusion involving only this substance thus does not mean true membrane fusion. The two unit membranes might remain as separate complete entities each bounded on their apposed surfaces by extracellular material. We must, then, in using the unit membrane concept reconsider the possibility of the existence of a true fusion of the unit membranes in this synapse.

In my 1955 paper[34] on this synapse a figure of 200 to 300 Å was given for the over-all thickness of the synaptic membrane complex including the dense strata next to pre- and postsynaptic axoplasm. Similar dimensions have been found recently by de Lorenzo[3] in the closely related lateral giant-to-motor synapse. These figures of 200 to 300 Å did not represent statistical averages, since extreme values of as little as 140 Å and as much as 400 Å were found. However, these extremes were considered due to artifacts introduced partly by the stresses of sectioning and partly by fixation and disregarded. It was considered better to delay further interpretation of the meaning of the features of the synaptic membrane complex until a better understanding of the general structure of axon and Schwann cell membranes could be achieved. Hence this problem was laid aside in favor of the problem of myelin structure and development, for this seemed to offer the possibility of acquiring an understanding of membrane structure that would make a more complete interpretation of the synaptic membrane complex possible. During the period 1955 to 1960 this related but separate topic was, therefore, pursued and led eventually to the understanding of cell membrane structure expressed in the unit-membrane concept. A re-examination of the membranes at the crayfish synapse then seemed worthwhile and was begun.

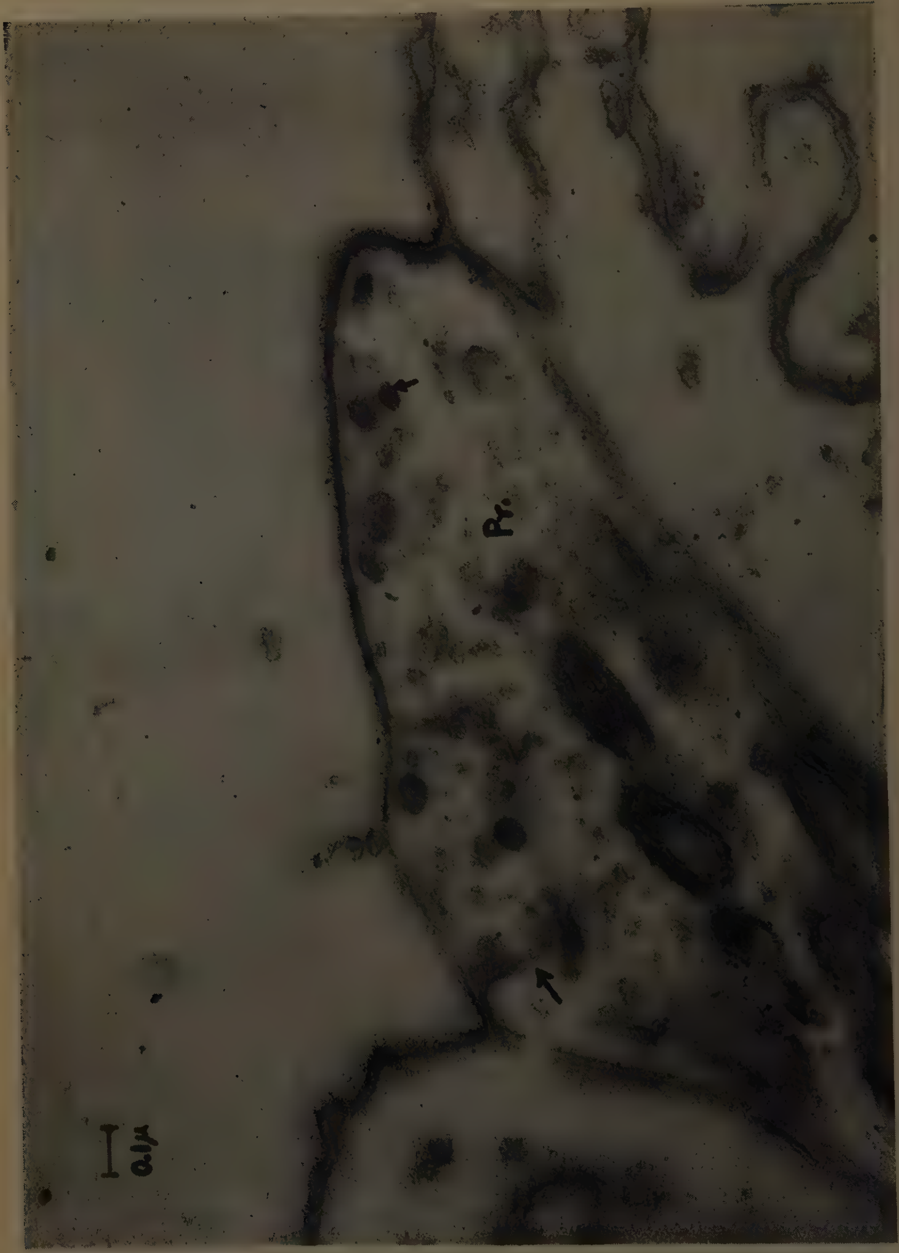

FIGURE 32.

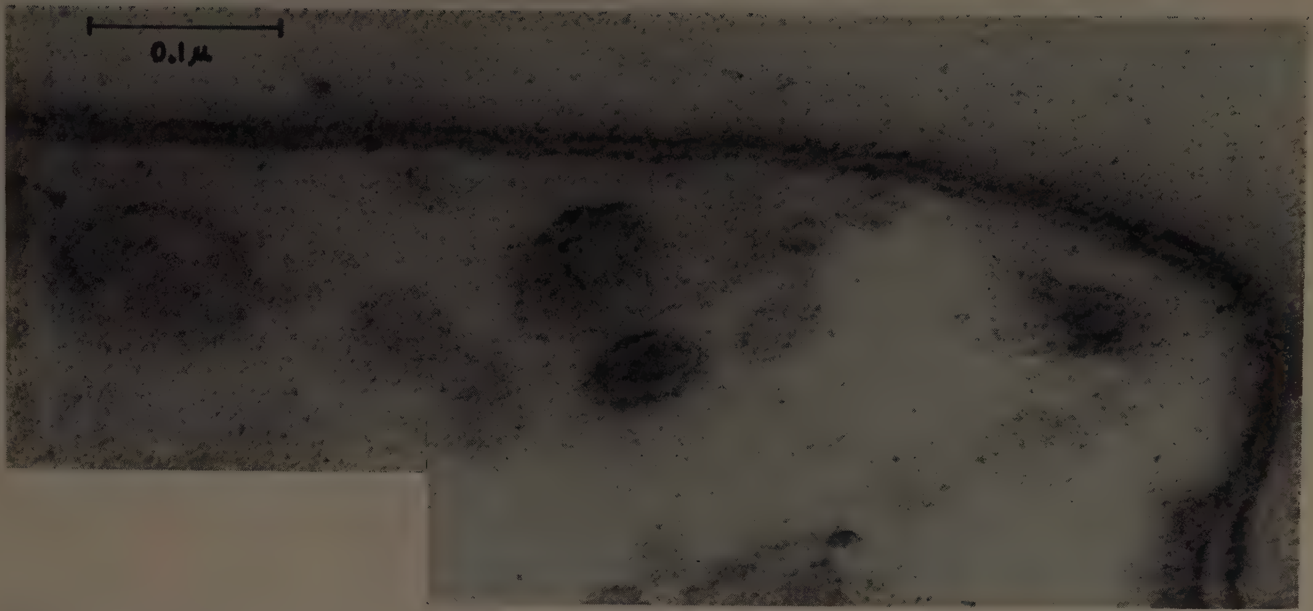

FIGURE 32. Above: a synaptic process (Pr.) in a crayfish giant fiber synapse showing very close apposition of the presynaptic and postsynaptic membranes as indicated in the enlargement below. The over-all thickness of the synaptic membrane complex in the enlarged regions is 110 Å. In the left part of the figure (*arrow*) the pre- and postsynaptic membranes are split apart and accumulations of granular or vesicular bodies are seen in the intervening space. Both membranes in this region are rather obliquely sectioned, but can be traced out. ×66,000, inset (below), ×250,000.

The preliminary evidence reported here, however, involves mainly a re-evaluation of older micrographs.

Although not always found, many instances were noted in which the over-all thickness of the synaptic membrane complex over most of the extent of contact

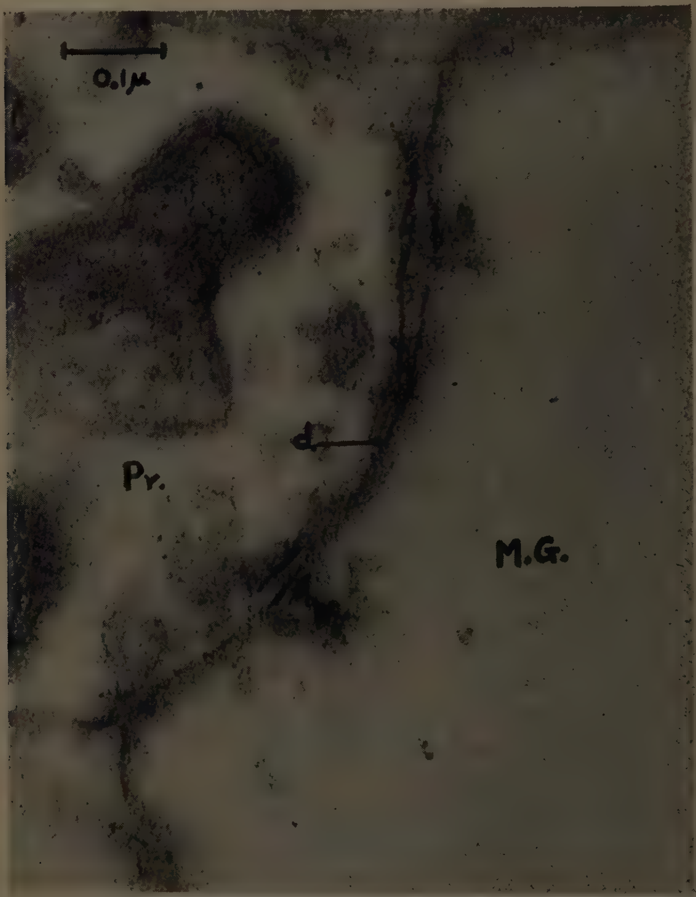

FIGURE 33. Enlargement of a portion of a median giant-to-motor synapse showing a synaptic process (Pr.) of the motor fiber to the left and a portion of median giant fiber axoplasm (M.G.) to the right. Note the dense stratum (d.) bisecting the light zone between the dense strata bounding the axoplasm of the process and the axoplasm of the median giant fiber. ×135,000.

of a synaptic process with the median giant axon fell as low as ~150 Å, and this now appears to have more significance. Furthermore, upon cutting new sections of the older methacrylate-embedded material and examining them at higher resolution with the Siemens electron microscope in some instances I found a delicate dense stratum ~30 to 40 Å thick bisecting the light zone of the synaptic membrane complex. This is illustrated in FIGURE 33. The synaptic membrane complex in this instance measures less than 200 Å in over-all thickness. There is a broken delicate dense line ~30 Å thick not unlike an intraperiod line in myelin bisecting the gap between the paired membrane structures. Although the over-all thickness of this paired membrane structure was somewhat high, being closer to 200 Å than 150 Å, the appearance was very similar to that which one would expect to see in an "external compound membrane" as defined in my paper of 1958.[39] External compound membranes result whenever the ~100 to 150 Å gap between paired ~75 Å unit membranes is obliterated and the two membranes come together with very intimate apposition of their outside dense strata as occurs in myelin at the intraperiod line. A number of examples were found in the crayfish synapse in which the synaptic membrane complex measured ~150 Å in thickness. This finding may be quite significant since such intimate membrane contacts as this have not been seen at all in other types of synapses[23,24,25,16] where a definite gap between the apposed membranes has been found.

External compound membranes as noted above occur normally in the axon-Schwann membranes of the juxtaterminal myelinated regions of nodes of Ranvier in a relationship suggesting that they may have some function in saltatory conduction. It seemed thus that this kind of unusually intimate membrane contact relationship in this excitatory crayfish synapse might be in some important way related to the evidence of Furshpan and Potter[11] suggesting that this synapse is characterized by electrical rather than neurohumoral transmission. While the findings suggest strongly that numerous external compound membranes exist in this crayfish synapse, it is intriguing to go further and consider the possibility that even more intimate contacts might exist involving true membrane fusion. Before taking up this matter we must decide exactly what we mean by "fusion," for one may think of membrane fusion in several different ways.

For our purposes we may define the minimum requirement for fusion as that condition in which the structural integrity of one or both of the apposed membranes is broken to such an extent that one or more of the essential monomolecular strata of one of the unit membranes is replaced by a single monolayer where two existed before. Whether this new monolayer is formed from a mixing together of the constituent molecules of the two previously separate monolayers or represents only one or the other need not be specified. We shall exclude from this definition even the most intimate and purely physical contacts of the two membranes. For example, we shall not speak of fusion even if two apposed membrane monolayers are so close together that interpenetration of side-chain groups occurs, as long as the integrity of the backbone chains of each monolayer is retained. Thus very intimate membrane contacts such as those found in nerve myelin or in the most tightly bound together external compound membranes will not be considered to represent fusion in this paper.

Some external compound membranes such as those shown in FIGURES 11*a* and *b* are so intimately associated that their over-all thickness is less than the sum of the over-all thicknesses of two ~75 Å unit membranes. Instead of measuring ~150 Å in thickness they may measure ~120 Å. The mesaxon loops packed in myelin are an example of a similar phenomenon. Here the isolated mesaxon before compact myelin is formed may measure ~150 Å in thickness but, when included within compact myelin, it may measure only 100 to 120 Å in thickness. It would be expected to measure ~150 Å if each of its component unit membranes simply added its thickness to the compact structure. I do not consider this kind of reduction of thickness to be necessarily due to membrane fusion in the sense defined above. The differences can be explained in several ways, even leaving out optical artifacts. This reduction, in my opinion, does not involve true membrane fusion although it is conceivable that it involves some degree of interpenetration of side chains of the nonlipid monolayers bounding the unit membranes. This latter possibility might be entertained more seriously in considering the major dense line constituents but there is very little evidence to support it. At any rate, no fusion in the sense defined above seems to occur in myelin.

There is nevertheless one kind of structure seen in mesaxons in which there seems definitely to be a partial membrane fusion in the sense defined here. I have already described this structure,[44] but since it is of such pertinence to the present discussion I think it should be mentioned again. In developing nerve fibers there are regions of evident partial membrane fusion in very restricted loci in mesaxons. These occur quite regularly in young myelinating fibers and are also seen in mesaxons of adult nerve fibers. FIGURE 34 is a transection of a developing mouse sciatic nerve fiber in which such a partial fusion of the unit membranes of the mesaxon may be seen in three restricted local regions (arrows). The enlargement shows these regions in more detail. At the arrow in the enlargement to the right the two outer dense strata of the unit membranes of the mesaxon, which in some places are combined to make the central dense stratum of the usual external compound membrane, are eliminated locally. In such regions the over-all thickness of the compound membranes is reduced to less than 120 Å. There is no doubt about the significance here of the reduction locally of the compound membrane thickness, for the region of reduction is small and the compound membrane to the upper right may be used as a control to eliminate sectioning and optical artifacts. It is possible to explain this evident partial membrane fusion as being produced by a retraction locally of both the outside nonlipid monolayers bounding each of the two combined unit membranes externally with some degree of interpenetration of the remaining lipid polar groups roughly as indicated in the molecular diagram in FIGURE 35*c*. Complete fusion of the unit membranes in such regions has not yet been observed. This would involve the complete merging together of the two lipid bimolecular leaflets to make a structure ~75 Å thick like a single unit membrane as shown in FIGURE 35*d*. Note, however, that if such a structure is found, despite a similar appearance and thickness, it will be different from the ordinary unit membrane in a most important way. The unit membrane is thought to be chemically asymmetric in the sense that the nonlipid monolayer bounding cytoplasm is significantly different from the one bounding extracellular material. In the fusion membrane of FIGURE 35*d* each of the nonlipid monolayers bordering the single bimolecular leaflet of lipid is alike in the sense that it borders cytoplasm. Such a membrane would then be chemically symmetrical and quite different from the asymmetric unit membrane hitherto referred to.

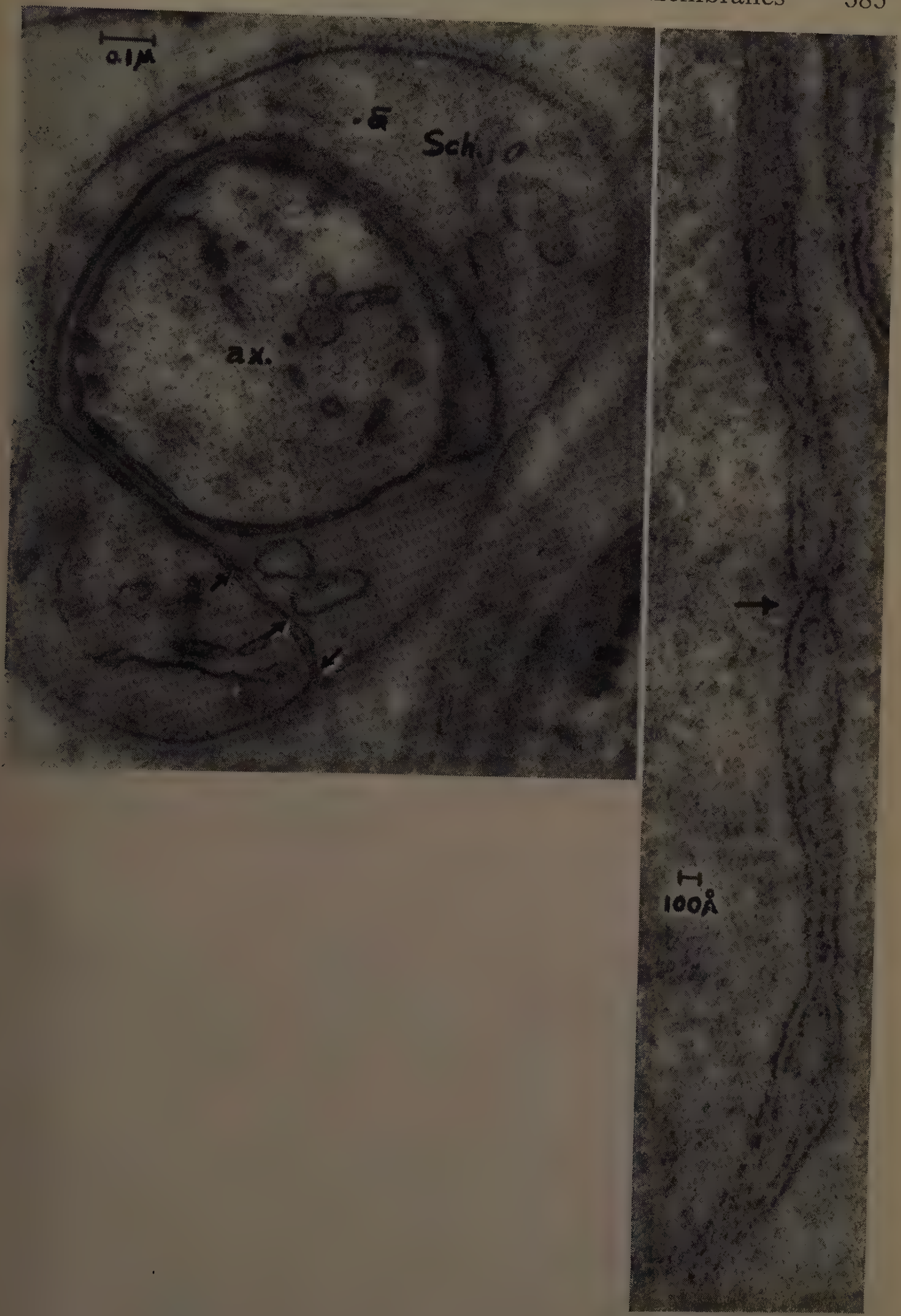

FIGURE 34. Micrograph of transected protofiber in young mouse sciatic nerve fixed with $KMnO_4$ and embedded in araldite (Ax., axon; Sch., Schwann cytoplasm). The mesaxon at the 3 arrows shows regions of unusually close apposition or partial fusion. One such region is indicated by the arrow in the enlargement to the right. ×70,000; enlargement, ×265,000.

We must now ask whether true unit membrane fusion occurs in the crayfish synapse. In fact there is a certain amount of evidence that might be interpreted as suggesting this. Unfortunately the evidence is at present, in my experience, confined to OsO_4-fixed material embedded in methacrylate, and hence the details of unit membrane structure are not visible as they would be in $KMnO_4$ fixed preparations embedded in epoxy resins. An examination of this kind of material will be essential before a final decision is made. To be sure there are some instances in which the over-all thickness of the synaptic membrane complex is reduced well below 150 Å. For example, in FIGURE 32 the over-all thickness is only 100 to 120 Å. This reduction in thickness might very well be explained in the same way as that used to explain the reduced thickness of the external compound membranes in FIGURES 11*a* and 11*b* or the reduction of the apparent thickness of the mesaxon in compact myelin as outlined above without invoking true membrane fusion. A partial membrane fusion like that in FIGURE 35*c*, might very well be responsible. It is also pos-

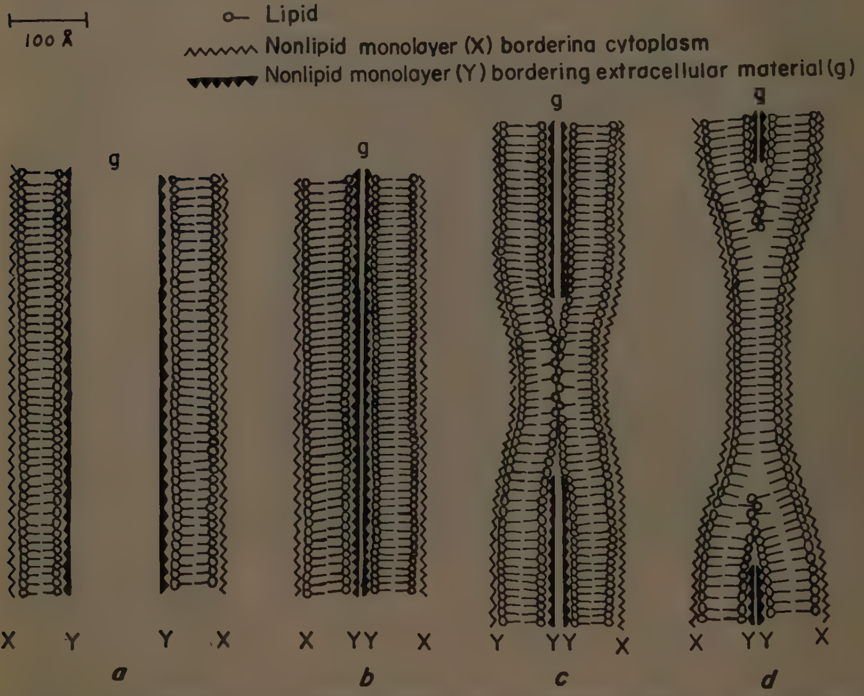
100 Å
Lipid
Nonlipid monolayer (X) bordering cytoplasm
Nonlipid monolayer (Y) bordering extracellular material (g)
g
g
g
g
X Y
Y X
X YY X
Y YY X
X YY X
a
b
c
d

FIGURE 35. Diagram of an ordinary paired membrane structure like that seen generally between cells. (*b*) Diagram of an external compound membrane with very great reduction of the gap between the two paired membranes. (*c*) Diagram of an external compound membrane with regions of partial fusion of the kind seen in FIGURE 34. (*d*) Diagram illustrating a hypothetical complete unit membrane fusion. Note that the unit membrane resulting from such a fusion would consist of a bimolecular leaflet of lipid bounded by two 'X' layers. Other kinds of unit membranes are characterized by a bimolecular leaflet bounded by an 'X' layer on one side and a 'Y' layer of nonlipid on the other. These molecular interpretations are highly schematic and hypothetical.

sible that a complete membrane fusion like that in FIGURE 35*d*, is responsible. The evidence presented here does not allow a final decision on these alternatives.

From the findings reported here it appears highly probable that external compound membranes occur in the crayfish giant synapse, but whether a complete or even partial unit membrane fusion occurs is unsettled. In any event, the elimination of the gap between the paired axon membranes at some regions in this synapse may be expected to have a profound effect on synaptic transmission and may conceivably be sufficient of itself to account for the apparently pure electrical transmission properties of this synapse.

It is not as yet clear whether such intimate membrane contacts with the formation of external compound membranes and possibly partial or complete fusion is present to a significant degree in vertebrate central nervous systems. However, it seems important to seek these structures since, if they are present, they may be of great importance in excitatory synaptic transmission in vertebrate nervous systems, as well as in the special case of the excitatory crayfish synapse dealt with here in preliminary fashion.

References

1. BAHR, G. F. 1954. Osmium tetroxide and ruthenium tetroxide and their reactions with biologically important substances. Electron stains III. Exptl. Cell Research. **7:** 457–479.
2. DAVISON, P. F. & E. W. TAYLOR. 1960. Chemical studies of proteins of Squid nerve axoplasm with special reference to the axon fibrous protein. J. Gen. Physiol. **43:** 801–823.
3. DE LORENZO, A. J. 1959. Electron microscopy of electrical synapses in the crayfish. Biol. Bull. **117:** 390.
4. FERNANDEZ-MORAN, H. & J. B. FINEAN. 1957. Electron microscope and low angle X-ray diffraction studies of the nerve myelin sheath. J. Biophys. Biochem. Cytol. **3:** 725–748.
5. FINEAN, J. B. 1953. X-ray diffraction studies on the polymorphism of phospholipids. Biochim. Biophys. Acta. **12:** 371–384.
6. FINEAN, J. B. 1954. The effects of osmium tetroxide fixation on the structure of myelin and sciatic nerve. Exptl. Cell Research. **6:** 283–293.
7. FINEAN, J. B. 1955. Recent ideas on the structure of myelin. Biochem. Prob. Lipids, Proc. 2nd Int. Conf. Univ. Ghent. 27–30 July. : 127–131. Butterworths. London, England.
8. FINEAN, J. B. 1958. X-ray diffraction studies on the myelin sheath in peripheral and central nerve fibers. Exptl. Cell Research. Suppl. **5:** 18–32.
9. FINEAN, J. B. & T. F. MILLINGTON. 1957. The effects of ionic strength of immersion medium on the structure of peripheral nerve myelin. J. Biophys. Biochem. Cytol. **3:** 89–94.
10. FRANKENHAEUSER, B. & A. HODGKIN. 1956. The after-effects of impulses in the giant nerve fibers of *Loligo*. J. Physiol. (London). **131:** 341–376.
11. FURSHPAN, E. J. & D. D. POTTER. 1959. Transmission of the giant motor synapses of the crayfish. J. Physiol. (London). **145:** 289–325.
12. GASSER, H. S. 1952. Discussion in the hypothesis of saltatory conduction by B. Frankenhaeuser. Cold Spring Harbor Symposium Quant. Biol. **17:** 32–36.
13. GASSER, H. S. 1955. Properties of dorsal root unmedullated fibers on the two sides of the ganglion. J. Gen. Physiol. **38:** 709–728.
14. GEREN, B. B. 1954. The formation from the Schwann cell surface of myelin in the peripheral nerves of chick embryos. Exptl. Cell Research. **7:** 558–562.
15. GEREN, B. B. & F. O. SCHMITT. 1953. The structure of the nerve sheath in relation to lipid and lipid-protein layers. J. Appl. Phys. **24:** 1421.
16. GRAY, E. G. 1958. Electron microscopy of dendrites and axons of the cerebral cortex. J. Physiol. (London). **145:** 25–26.
17. GRAY, E. G. 1959. Axo-somatic and axo-dendritic synapses of the cerebral cortex: an electron microscope study. J. Anat. **93:** 420–432.
18. JENSEN, L. 1959. Membrane structure. Anat. Record. **133:** 294.

19. Johnson, G. E. 1924. Giant nerve fibers in crustaceans with special reference to cambarus and palaemonetes. J. Comp. Neurol. **36:** 323–373.
20. Katz, B. E. 1961. Dunham Lectures. Harvard Medical School. Harvard Univ. Press. Cambridge, Mass.
21. Lasanky, A. & DeRobertis, E. 1960. Electron microscopy of retinal photoreceptors. J. Biophys. Biochem. Cytol. **7:** 493–497.
22. Lillie, R. D. 1948. Baker's technique. *In* Histopathologic Technic. Blakeston. Philadelphia, Pa.
23. Palade, G. E. & S. L. Palay. 1954. Electron microscope observations of interneuronal and neuromuscular synapses. Anat. Record. **118:** 335–336.
24. Palay, S. L. 1956. Synapses in the central nervous system. J. Biophys. Biochem. Cytol. Suppl. **2:** 193–206.
25. Palay, S. L. 1958. The morphology of synapses of the central nervous system. Exptl. Cell Research. Suppl. **5:** 275–293.
26. Palay, S. L. 1961. Structural peculiarities of the neurosecretory cells in the preoptic nucleus of the goldfish, *Carassius auratus*. Anat. Record. **139:** 262.
27. Palay, S. L. 1957. The fine structure of the neurohypothesis. *In* Ultrastructure and Cellular Chemistry of Neural Tissue. Progr. in Neurobiol. II. H. Waelsch, Ed. : 31–49. Hoeber-Harper. New York, N.Y.
28. Porter, K. R. & F. Kallman. 1953. The properties and effects of osmium tetroxide as a tissue fixative with special reference to its use for electron microscopy. Exptl. Cell Research. **4:** 127–141.
29. Revel, J. P., S. Ito & D. W. Fawcett. 1958. Electron micrographs of myelin figures of phospholipids simulating intracellular membranes. J. Biophys. Biochem. Cytol. **4:** 495–498.
30. Revel, J. P., L. Napolitano & D. W. Fawcett. 1960. Identification of glycogen in electron micrographs of thin tissue sections. J. Biophys. Biochem. Cytol. **8:** 575–590.
31. Ritchie, J. M. & R. W. Straub. 1957. The hyperpolarization which follows activity in mammalian non-medullated fibers. J. Physiol. (London). **136:** 80–97.
32. Robertson, J. D. 1952. The ultrastructure of an invertebrate synapse. Ph.D. Thesis. Massachusetts Institute of Technology. Cambridge, Mass.
33. Robertson, J. D. 1953. The ultrastructure of two invertebrate synapses. Proc. Soc. Exptl. Biol. Med. **82:** 219–223.
34. Robertson, J. D. 1955. Recent electron microscope observations on the ultrastructure of the crayfish median-to-motor giant synapse. Exptl. Cell Research. **8:** 226–229.
35. Robertson, J. D. 1956. The ultrastructure of a reptilian myoneural junction. J. Biophys. Biochem. Cytol. **2:** 381–394.
36. Robertson, J. D. 1957. Some aspects of the ultrastructure of double membranes. *In* Ultrastructure and Cellular Chemistry of Neural Tissue. Progr. in Neurobiol. II. H. Waelsch, Ed. : 1–30. Hoeber-Harper. New York, N.Y.
37. Robertson, J. D. 1957. New observations on the ultrastructure of the membranes of frog peripheral nerve fibers. J. Biophys. Biochem. Cytol. **3:** 1043–1048.
38. Robertson, J. D. 1958. A molecular theory of cell membrane structure. Proc. IVth Int. Congr. for Electron Microscopy. : 159–171. Springer. Berlin, Germany.
39. Robertson, J. D. 1958. Structural alterations in nerve fibers produced by hypotonic and hypertonic solutions. J. Biophys. Biochem. Cytol. **4:** 349–364.
40. Robertson, J. D. 1958. The ultrastructure of Schmidt-Lanterman clefts and related shearing defects of the myelin sheath. J. Biophys. Biochem. Cytol. **4:** 39–46.
41. Robertson, J. D. 1959. The ultrastructure of cell membranes and their derivatives. Biochem. Soc. Symposium. **16:** 3–43.
42. Robertson, J. D. 1959. Preliminary observations on the ultrastructure of nodes of Ranvier. Z. Zellforsch. Mikroscop. Anat. **50:** 553–560.
43. Robertson, J. D. 1960. The molecular structure and contact relationships of cell membranes. Progr. in Biophys. **10:** 343–418.
44. Robertson, J. D. 1961. Cell membranes and the origin of mitochondria, Proc. IVth Neurochem. Symposium. Seymour Kety, Ed. : 497-530. Pergamon Press. London, England. In press.
45. Schmidt, W. J. 1936. Doppellbrechung und Feinbau der Markscheide der Nervenfasern. Z. Zellforsch. Mikroscop. Anat. **23:** 657–676.
46. Schmitt, F. O., R. S. Bear & G. L. Clark. 1935. X-ray diffraction studies on nerve. Radiology. **25:** 131–151.
47. Schmitt, F. O., R. S. Bear & K. J. Palmer. 1941. X-ray diffraction studies on the structure of the nerve myelin sheath. J. Cell Comp. Physiol. **18:** 31–41.
48. Sjöstrand, F. S. 1953. Electron microscopy of mitochondria and cytoplasmic double membranes. Nature. **171:** 30–31.

49. Sjöstrand, F. S. 1960. Electron microscopy of myelin and of nerve cells and tissue. *In* Modern Scientific Aspects of Neurology. J. N. Cumings, Ed. : 188–231. Arnold. London, England.
50. Sjöstrand, F. S. & J. Rhodin. 1953. The ultrastructure of the proximal convoluted tubules of the mouse kidney as revealed by high resolution electron microscopy. Exptl. Cell Research. **4:** 426–456.
51. Stoeckenius, W. 1959. An electron microscope study of myelin figures. J. Biophys. Biochem. Cytol. **5:** 491–500.
52. Wiersma, C. A. G. 1947. Giant nerve fiber system of the crayfish. A contribution to comparative physiology of synapse. J. Neurophysiol. **10:** 23–38.
53. Wigglesworth, U. B. 1957. The use of osmium in fixation and staining of tissues. Proc. Roy. Soc., **B147:** 185–199.
54. Curtis, W. C. & M. J. Guthrie. 1938. The Textbook of General Zoology. Third edition. John Wiley & Sons, Inc. New York, N. Y.

THE MACROMOLECULAR PROPERTIES OF EXCITABLE MEMBRANES*

L. J. Mullins

Department of Biophysics, University of Maryland School of Medicine, Baltimore, Md.

Our notions about the structure of cell membranes in general and excitable membranes in particular have undergone considerable revision over the past 15 years; I hope to touch on these changes and the reasons for them. My task is made somewhat difficult because I am expected to serve as a bridge, connecting the findings of J. D. Robertson, who tells us what excitable membranes look like, and those of Harry Grundfest, who discusses what an excitable membrane does and how it does what it does.

The classic membrane model is that of Danielli: a bimolecular lipid layer with an outer protein coat. With the assumption that it is the lipid layer that is the barrier to solute diffusion, many experimental measurements of membrane permeability have been reconciled. Nevertheless, in spite of these reassuring features, it must in fairness be noted that the proposition that large, lipid-soluble molecules penetrate more rapidly than water-soluble molecules of equal size has never been subjected to an adequate experimental test. The apparent ease of penetration of relatively small molecules of high partition coefficient may have another explanation along the following lines. Consider 2 molecules: 2 methyl butanol and glycerol; they are both about the same size because the sum of C and O atoms is 6 in both cases. They differ in that the butanol forms only 1 H-bond with water, while glycerol forms 3. If the energy of such bonds is considered to be 6 kcal./mole, then glycerol with 18 kcal. differs from butanol by 12 kcal., and the result to be expected is that glycerol will have a negligible vapor pressure in equilibrium with aqueous solutions while that of butanol is easily measurable. With respect to the cell membrane, 2 possibilities emerge from this analysis: either glycerol must penetrate in the hydrated state, which means that the molecule is much larger than one would judge from model measurements, or the molecule penetrates in an unhydrated state. We must then consider, however, that very few molecules exist in such a state, so that the use of aqueous concentration for estimating driving force grossly overestimates the available concentration of penetrating molecules. Notice that these conclusions are reached without introducing any role for lipids. Partition coefficients can be expected to correlate well with penetration rates in so far as they reflect the activity coefficients of a molecule in water (relative to the pure liquid as a standard state). If pore size is the limiting factor for penetration, large lipid molecules would be excluded. From the fact that a large lipid-soluble molecule such as ouabain appears to act only on the outside of the membrane, it is possible that this molecule cannot penetrate.

Nonhomogeneous Membranes

The attractiveness of the Danielli membrane, from the standpoint of mathematical analysis, is that it is approximately homogeneous. When the pene-

---

* The work described in this paper was supported in part by Research Grant B-2075 from the National Institute for Neurological Diseases and Blindness, Public Health Service, Bethesda, Md.

tration process is considered to take place through channels or pores in the membrane the situation becomes more complex. The analysis of this complexity and the development of another model of the membrane is the subject of this paper.

Capacitance. The classic studies of Cole and Curtis (1936) and of Fricke (1925) showed that a membrane capacitance of 1 μF/cm.^{2} was an almost universal biological constant and, furthermore, that this value was unaltered by electrical excitation. The reasonable inferences drawn from such measurements were two: the membrane is a thin structure (about 50 Å), and there is no drastic structural alteration during electrical conduction. Furthermore, the measurements appeared to fit well with a bimolecular lipid layer of 37 Å and a dielectric constant of 3.5. A membrane resistance of 1KΩ cm.^{2} also gives a specific resistivity of the lipid layer of about $10^9\Omega$ cm., that, although several orders of magnitude lower than the usual values for oils, still appears reasonable.

If the pathways through which ion penetration takes place are nonhomogeneous, it is possible that the structure responsible for the capacitance is also not a simple one. The two general cases are shown in FIGURE 1, wherein (*b*) the dielectric constant varies in the direction across the membrane while in (*c*) the dielectric constant varies from point to point on the membrane surface. The diagram of FIGURE 1*a* is the homogeneous dielectric constant membrane that gives a constant electric field across the membrane, and is the case for which general flux equations have been worked out. In the 'dielectric sandwich' membrane *b*, the electric field is variable across the membrane thickness, while in *c* it is the surface charge density that is variable. The conclusion comes from considering that such a capacitor can be divided into two capacitors in parallel with different dielectric constants. If both had the same charge density on the plates, then the potential difference across them would be different; as they are connected together, however, charge will be redistributed until potentials are equal and charge densities different. The effect of both arrangements (*b* and *c*) is to permit a thicker membrane for the same capacitance than would be the case for a homogeneous, low dielectric constant structure. Arrangement *b* would appear to have the advantage that, if one considers that the structure seen as a double line in the electron microscope is lipid, its thickness approximates the spacing that is actually observed.

At this point it seems worthwhile to interject a note of protest against the use of myelin as a model for the structure of excitable membranes. This excretion of the Schwann cells appears to have as its principal physiological role that of an insulator. While it is true that one wants an axon reasonably insulated at rest, it is equally true that one wants a high conductance during activity, and it is difficult to see how such a structure could be rearranged to manage this. To the argument that Schwann cells are always found in intimate contact with axons one can reply that muscle fibers give action potentials in very many ways similar to those of axons and yet have no Schwann cells.

Ion flux. As we turn from the ion impermeable part of the membrane to the part that allows the passage of ions, we face the problem of developing a structure that will (1) discriminate between ions of various sorts, (2) exhibit marked permeability changes in response to altered membrane potentials, and

(3) show some relationship between ion flux and electrochemical potential difference that can be derived from first principles.

The usual equations for ion flux as a function of potential and concentration are two, one derived from a simple statement of Ohm's law (Equation **1**) and the second from the integration of the general equation for flux along

$$\bar{m} = g(E - E_e)/F \tag{1}$$

$$\bar{m} = \frac{P\,EF(C_o e^{EF/RT} - C_i)}{RT(1 - e^{-EF/RT})} \tag{2}$$

a concentration gradient with constant field. The symbols are: $\bar{m}$, the net flux of an ion, g its conductance, F the Faraday, E the membrane potential, E_e is the equilibrium potential of the ion defined as $E_e = RT(F)^{-1} \ln C_o/C_i$, P is ion permeability, C_o and C_i are outside and inside concentrations. The

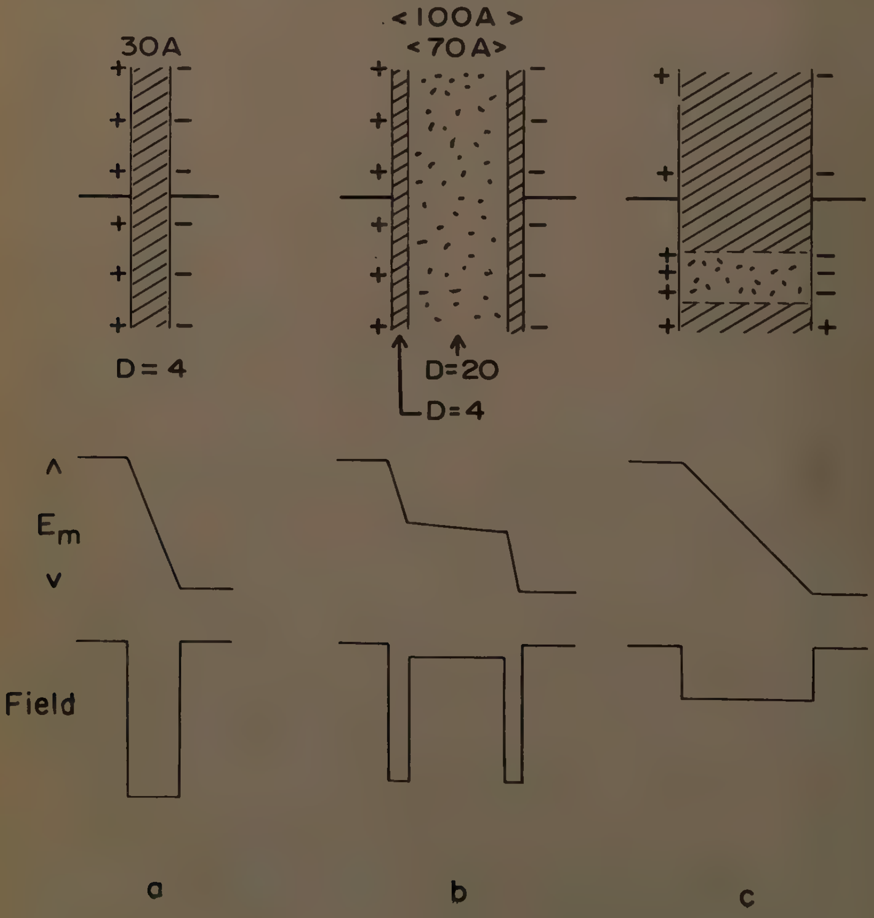

two equations are not equivalent, but have been found convenient to apply to different sorts of experimental measurements. Thus Equation **1** has been used for the analysis of the squid axon currents during voltage clamps by Hodgkin and Huxley (1952). Similar voltage clamp data for the nodal membrane of frog nerve fibers (Dodge and Frankenhaeuser, 1959) have required Equation **2**. The fact that either of these equations are used for the experimental data does not represent a very exacting test because of the presence of an adjustable parameter, g in **1** and P in **2**. In the total absence of information as to how permeability ought to change with potential, no real test is possible. When we come to the analysis of unidirectional fluxes with isotopes, **2** has the desirable feature that it can be divided into an influx and efflux term. Such measurements of influx and efflux of an ion using tracers provide a further check on the validity of relations between current and unidirectional fluxes. Note, however, that **1**, which has been found to be valid over times of the order of those experienced in voltage clamp measurements, is a more general equation. It does not require a constant field assumption and by combining it with the Behn (1897) equation for flux ratios as given by **3**, unidirectional fluxes can be obtained when E is far from E_e.

$$m_i/m_o = e^{(E-E_e)F/RT} \qquad (3)$$

Such a transformation is shown in **4**. When the exponential becomes

$$\bar{m} = m_i - m_o = m_o(e^{(E-E_e)F/RT} - 1) \qquad (4)$$

quite small as it does for $(E - E_e)$ greater than 75 mv., the current $\bar{m}$ approaches $-m_o$, the outflux.

There are some advantages that derive from considering that the electric field of the membrane is distributed discontinuously across its thickness, as in FIGURE 1*b*, and that such field as exists acts to set boundary conditions of concentration on the two sides of the membrane. The difference between such a variable field membrane and the constant field membrane of Goldman (1943) is that ions are not driven by an electric field acting continuously on them as they cross the membranes; the field acts on ions as they enter or leave the membrane. If we suppose that the region of high field has a thickness of the order of ion size, the distribution of ions between bulk solution and surface phase is given by the usual relationship $C_m = BC_o e^{z\phi F/RT}$ where C_m is the membrane surface concentration, C_o is the concentration in the bulk solution, ϕ is the fraction of the membrane potential acting on the outside surface, B is a partition coefficient, and the other symbols have their usual significance. A similar equation can be written for the inside of the membrane:

$$C'_m = B'C_i e^{-z\phi' F/RT}.$$

FIGURE 1. Three different arrangements of the membrane condenser are shown. In *a* is the conventional parallel plate condenser with a material of homogeneous dielectric constant (D = 4) between the plates. The potential falls linearly across such a condenser and the electric field is constant. In *b* the dielectric is a sandwich type of structure with 2 thin sections of low dielectric constant and a thicker region of high dielectric constant. Both the potential drop and therefore the electric field vary discontinuously with distance across such a condenser. In *c* there are regions of high and low dielectric constant but these extend across the thickness of the condenser. The field is approximately constant, but the charge density, shown by + and — is variable.

Now the net movement of ions across the membrane in the absence of an electric field should be given by the relatively simple equation $\bar{m} = P(C_m - C'_m)$ where $\bar{m}$ is the net flux and P is ion permeability and includes the constants B, B'. The relationship developed can therefore be written as in Equation **5**, where a is the fraction of the total membrane potential

$$\bar{m} = P[C_o e^{zaEF/RT} - C_i e^{-z(1-a)EF/RT}] \tag{5}$$

acting on the outside. For the symmetrical variable field case shown in FIGURE 1*b*, a is 0.5 and with the substitution $\beta = zEF/2RT$, Equation **5** can be rewritten as Equation **6**.

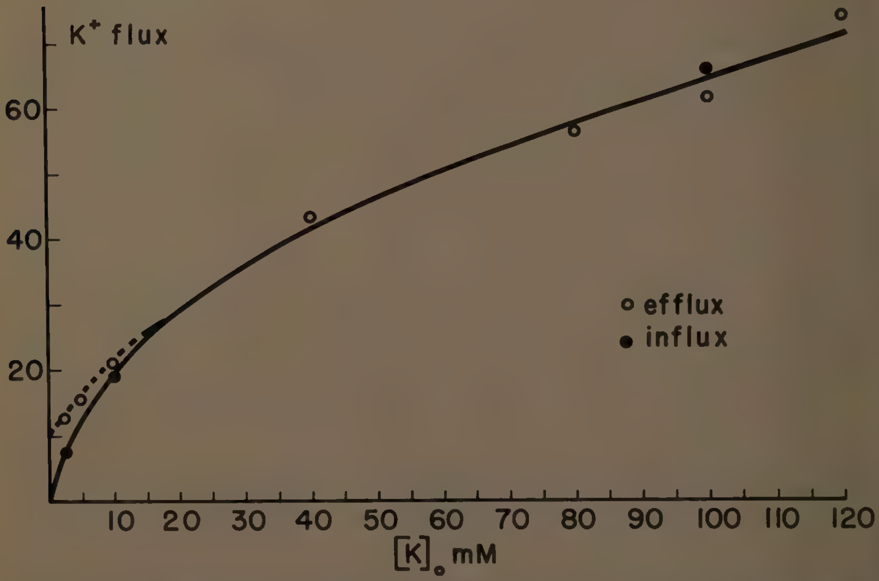

FIGURE 2. This is a plot of K⁺ influx and efflux (in *p*mole/cm.² sec.) for a muscle in sulfate ringer solution as a function of external K⁺ concentration. Osmotic pressure is maintained at the normal value of ringer solution and the curve is calculated from Equation **6**. Points for both influx and efflux are from some unpublished data from this laboratory, except for the value for influx in 100 mM K⁺, which has been supplied by R. A. Sjodin.

$$\bar{m} = P(C_o e^{\beta} - C_i e^{-\beta}) \tag{6}$$

For reasons discussed below, some reservations must be made regarding the applicability of **6** to cases where $\bar{m}$ is not equal to zero. For the zero net flux case, however, the equation should be strictly applicable and can be tested by comparing its predictions with measured fluxes of frog sartorius muscle in sulfate ringer with varying K^+ concentrations. Such a comparison is shown in FIGURE 2 where the solid line is Equation **6** with $P_K = 55$ Å/sec., $[K]_i = 140$ mM and E_m taken from best values for membrane potential. It should be pointed out that the equation reduces to the flux ratio Equation **3** whatever the value of a in **5**, but not all values of a give the experimentally measured values for unidirectional K^+ flux. No great effort has been made to adjust a for best fit, as a value of 0.5 appears quite satisfactory. At low values of $[K]_0$, influx and efflux diverge, and at 2.5 mM K, $\bar{m}_K$ is 4 pmole/cm.^{2} sec. which is precisely equal to the computed Na$^+$ influx where this is given as $m_i = P_{Na}C_oe^{\beta}$ with P_{Na} taken as 1 per cent of P_K or 0.55 Å/sec. This is satisfactory agreement, but it must be noted that Sjodin (1959) has found that the constant field equation, with a constant P_K also represents K$^+$ influx quite well.

Another situation where the variable field model may be of help is in the analysis of the rate of membrane potential change when a muscle fiber in sulfate ringer is subjected to a sudden step change in $[K]_0$. Neglecting the possible leak of any other ions, the only change in K$^+$ is that ionic current necessary to change the charge on the membrane capacitor to a value representing a new potential. Assuming that at zero time the net K$^+$ flux is zero, the capacitative current Cdv/dt should equal the ionic current density I_i as given by Equation **7**, where R_m is

$$Cdv/dt = \bar{m}F = I_i = (E - E_K)/R_m \qquad (7)$$

the membrane resistance. A step change in $[K]_0$ changes E_K to a new value and if the difference $(E - E_K)$ is denoted by v, then $dv/dt = v/R_mC$, where R_mC has the dimensions of time and is the time constant for the change in v. Such an equation predicts a symmetrical rate of response of the membrane potential to displacements of E_K while experimentally (Hodgkin and Horowicz, 1960) an asymmetry is found.

The variable field model gives a somewhat different result in that the initial value of dv/dt is several fold greater for depolarization as compared with repolarization. For the step change from 2.5 — 140 mM K$^+$, a P_K cf 55 Å/sec. and an initial value of E_m of 100 mv, the initial value of dv/dt is about 10 v/sec., while for the return from 140 to 2.5 mM K$^+$ with $E_m = 0$ at $t = 0$, dv/dt is 1.4 v/sec. The net flux has been computed at 10 mv intervals using Equation **6** and this used to compute v vs. t for the step change in K$^+$ indicated above. The result is shown in FIGURE 3.

The objection may reasonably be raised that Equation **6** predicts an exponential relationship between current and potential because for large displacements of membrane potential the net flux or current will be given almost entirely by one of the exponentials, while the other will have a value close to zero. This is so because no allowance has been made for the change of membrane surface concentrations that must be expected whenever there is a net flux. Such a change has the effect of diminishing the difference in surface concentration and thereby making the net flux less. A proper modification of the equation would be to introduce permeability coefficients for the movement of ions from membrane surface into internal and external phases but such a treatment would make the equation an arbitrary one and it appears better at present not to attempt to deal with the effects of current flow. For small (ca. 25 mv) displacements of the membrane potential, Equation **6** gives a reasonably linear relationship between current and voltage, and indeed it is doubtful if displacements as large as 50 mv show up as deviations from such a linear relationship. Potassium ion conductances can be calculated for the muscle fiber in 2.5 and 140 mM K$^+$ using Equation **1** for g_K and **6** for $\bar{m}_K$.

When this is done for the condition: $E_m = 110$ mv, $[K]_0 = 2.63$, $E_K = 100$ mv, $[K]_i = 140$, g_K is 45 μmho/cm.[2] For $E_m = 10$ mv, $[K]_0 = 140$, $E_K = 0$, $[K]_i = 140$, g_K is 290 μmho/cm.[2] These values, at a constant P_K of 55 Å/sec., are within the range of those measured experimentally.

Flux interactions. Another difference between homogeneous and pore membranes is that in the latter the movement of ions of various sorts may not be independent. The nonindependence of K^+, Rb^+, and Cs^+ influxes from mixtures of these ions has been clearly demonstrated by Sjodin (1961), who finds that in frog sartorius muscle the influx of K^+ or Cs^+ is depressed several fold by the presence of Rb^+ in ringer solution. In a homogeneous membrane the expectation would be that, for reasonably dilute solutions each ion would set up its own gradient in electrochemical potential and that each would move independently. A pore membrane differs from the homogeneous case in that it has a limited number of sites where transfer of ions can take place. The result is that phenomena such as transfer rate saturation and competition for sites may be expected to take place.

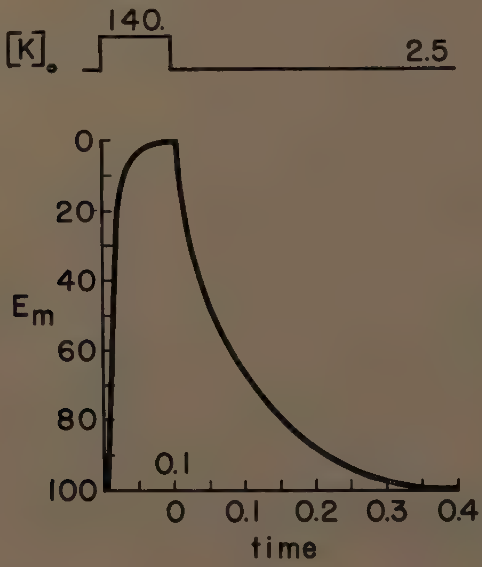

FIGURE 3. The change of membrane potential as a function of time after a muscle has been subjected to a step change in K_0 from 2.5 to 140 mM has been computed as described in the text and is shown on the left of this diagram. The repolarization on returning to 2.5 mM K^+ is shown on right. Time is in seconds and has been computed using a membrane capacity of 5.5 μF/cm.[2]

The implications of these findings are two: the apparent permeability of the membrane for, for example, K^+ is a function of $[Rb]_0$, (competition) and the influx of Rb^+ versus $[Rb]_0$ curve shows a continuous decline in P_{Rb} as concentration increases. Using the constant field equation, P_{Rb} declines five fold in going from 2.5 – 100 m*M*. With the variable field assumption, P_{Rb} need only decline by a factor of two but it is still clear that there is some sort of interaction between Rb influx and K efflux such that both fluxes are decreased from values to be expected on the basis of a constant ion permeability.

The Nature of Ions in Solution

Because electrophysiological phenomena depend upon the ability of the excitable membrane to undergo relatively specific permeability changes favoring a particular ion species, it is of considerable importance that we understand how such changes may be brought about. Such an understanding can come only when more is known about the nature of ions in solution.

The conventional view is that the size of ions in aqueous solution can be derived by applying Stokes' law to conductance data. For a homogeneous, lipid film membrane one might expect that ions would pass by their ability to dissolve in the low dielectric constant lipid material. On the basis that LiCl can be almost quantitatively extracted from a mixture of Li, Na, K, Rb, and Cs by shaking with amyl alcohol, one infers that a lipid membrane ought to have a high permeability for Li^+ while precisely the opposite is true; Li^+ is the least permeable of the alkali metal ions. For a pore membrane, the large size of Li^+ as deduced from conductance data would appear to offer good grounds for supposing that Li^+ was kept out on a size basis. The fact that Cs^+ is also a poorly penetrating ion, although from conductance data it is smaller than K^+, would appear to offer considerable difficulty in accepting the validity of conductance data in predicting ion size. A somewhat different method of estimating ion size for penetration through cell membranes has been described by Mullins (1959); this supposes that the radius of an ion is given by the crystal radius of the ion plus one water molecular diameter.

These two methods of estimating ion size are compared in FIGURE 4, which shows both the 'hydrated ion radii', the singly hydrated ion radii, the relative permeabilities of the ions, and a pore size that has been measured in the squid axon by Villegas (1961) using a method developed by Solomon (1960) and is based on considerations of molecular sieving. The advantage of this method appears to be that it offers some prospect of making possible the estimation of pore size of the membrane by measuring ion permeability for a variety of monovalent cations. The general reasoning in connection with the penetration of an ion through a membrane pore is that the hydration energy binding the ion into the water structure will not permit an ion to escape from solution to membrane unless there is a rather precise fit between the pore and the hydrated ion. Ion size, itself, must be quantized in units of water molecules. An ion can therefore have a size equal to crystal radius plus one complete shell of water molecules, or any integral number of such shells. The energetics involved in the passage of ions through a membrane with large (10 Å) and small (4 Å) pores is shown in FIGURE 5 where movement through a large pore is similar to that involved in diffusion in the sense that a close fit between the ion and the pore wall is not required, while for the 4-Å pore a close fit makes the difference between an activation energy of about 60 kcal. and perhaps 10 kcal. The binding energy for shells beyond the first is small and for other reasons this appears to be the proper size for physiological membranes. Thus the rate of permeation, at constant driving force, must be expected to be proportional to the number of pores that fit an ion of a particular size.

Crystal radius. It is important to realize that the crystal radii of ions have been derived on a semiempirical basis. While it is true that interatomic distances in crystals can be measured by X-ray diffraction with great precision, the assignment of radii for the constituent atoms depends on assumptions. The great confidence that one has in such values, however, derives from the fact that the radii obtained are additive in the sense that correct distances are obtained for a variety of crystals with different combinations of cation and anion. When we come to substances such as tetraethylammonium ions, however, it seems reasonable to measure crystal radii from models for C, H, and N. Such model measurements may not have the same scale factor as that used for crystal radii of inorganic substances and a small difference in scale may suffice to make the wrong conclusions about ion size. Some points of interest about the "onium" ions are that in a structure such as $^+N(C_2H_5)_4$ the C_2H_5 groups make the charge on N^+ sufficiently remote from the surround-

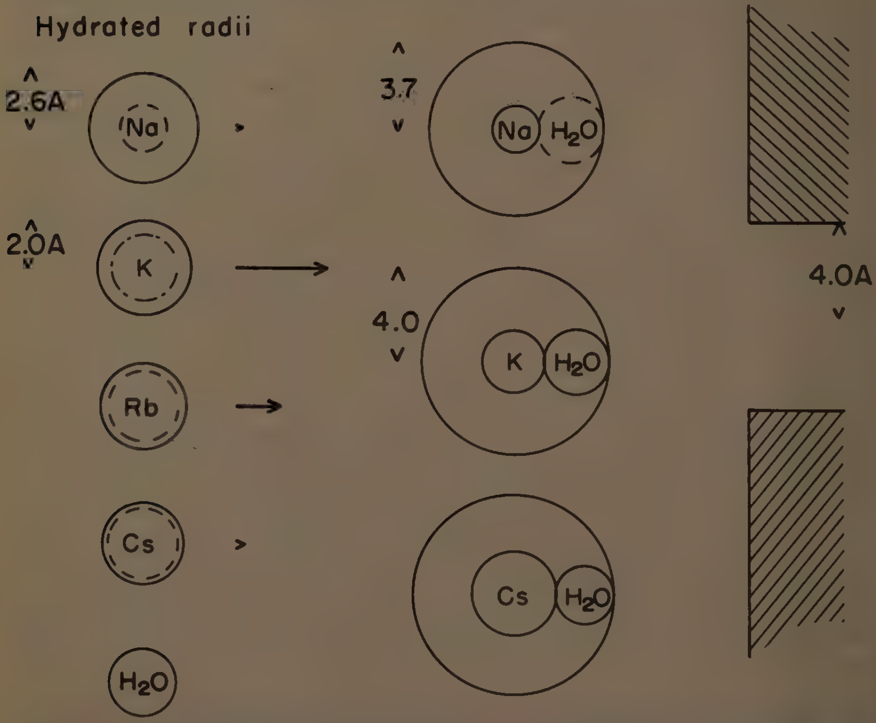

FIGURE 4. The hydrated ion radii derived from conductance data are compared with the singly hydrated radii. On the left is shown the conventional hydrated radii of ions Na-Cs together with the size of a water molecule. The dashed circles are crystal radii. Arrows immediately to the right of the first column denote the relative permeability of the muscle fiber membrane for these ions. In the next column the singly hydrated radii are shown, the center solid line is the crystal radius, while the outer solid line is the singly hydrated radius. On the right is a membrane pore of 4-Å radius that is far larger than the conventional hydrated radii but of the same order of size as the singly hydrated ions.

ing water so that such ions can be considered as unhydrated. From model considerations ${}^{+}N(CH_3)_4$ would appear too small for penetration while ions beyond tetrabutylammonium would appear too large.

Cations. Provided that the crystal radius of an ion is within the range of sizes 0.9 to 1.7 Å the packing of water molecules around the ion to form a first shell offers relatively little difficulty, although there may not be the same number of molecules in the shell for ions at the large end of size scale. When an ion has a crystal radius as small as Li^+ or Mg^{++} (ca. 0.6 Å), however, it appears that the water molecule shell that is to comprise the first layer cannot contract sufficiently to fit such ions. The minimum size would appear to be about 3.55 Å (from model measurements) while computations using Li^+ crystal radius (0.65 + 2.72) would give 3.37. This situation with Li^+ is similar to that encountered in the analysis of interatomic distance in Li-containing crystals. FIGURE 6 shows a scale drawing of the packing in KF and LiI. The

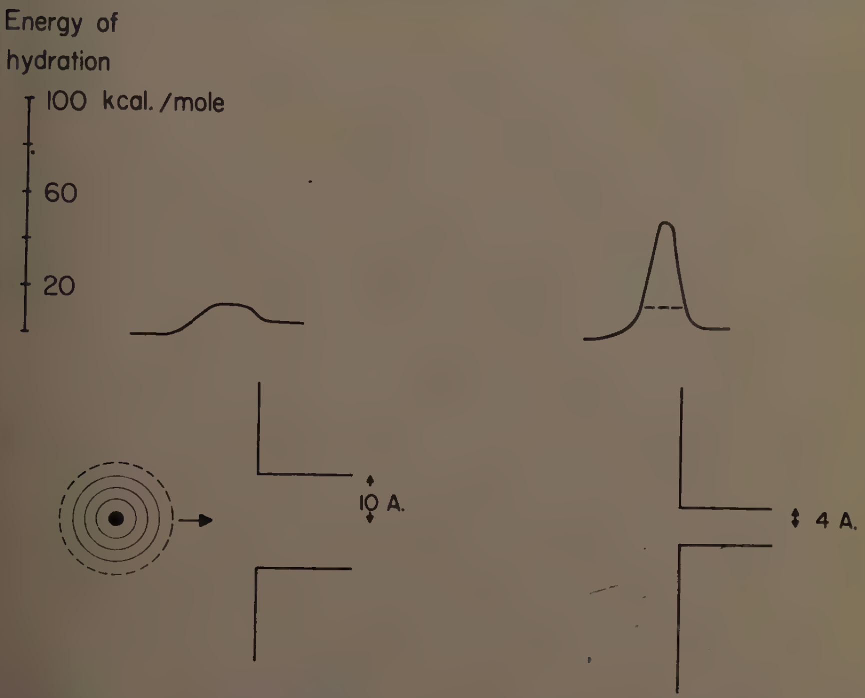

FIGURE 5. On the lower left is shown an ion with 3 complete layers of hydration (solid lines) while the dashed line represents any further hydration. Such a triply hydrated ion requires only about 9 kcal. of energy to escape from any further hydration, and has a radius of about 9 Å. If therefore, a membrane has pore radius of 10 Å it should be able to pass such ions in a manner similar to that involved in aqueous diffusion. The energy profile for such an ion is shown above. By contrast, on the right is shown a pore of 4-A radius that will accommodate an ion only in the singly hydrated state. To enter such a pore by a diffusion mechanism would require that the ion have an energy of about 60 kcal. It is supposed that there is a tunnel in the potential energy diagram, shown by the dashed line above, and that the conditions for entry via this pathway are that the ion and pore fit each other closely.

crystal radii of K and F are virtually identical, while the crystal radii of Li and I differ greatly. It has been shown that the interatomic distance between I^- is fixed by the repulsive forces set up as two adjacent I^- approach each other and the Li^+ are not packed tightly into the crystal. The situation for hydrated Li^+ would appear to be similar to that in LiI crystals. It seems necessary therefore to correct the sizes of Li^+ and Mg^{++} for this effect but such corrections will not be necessary for other cations.

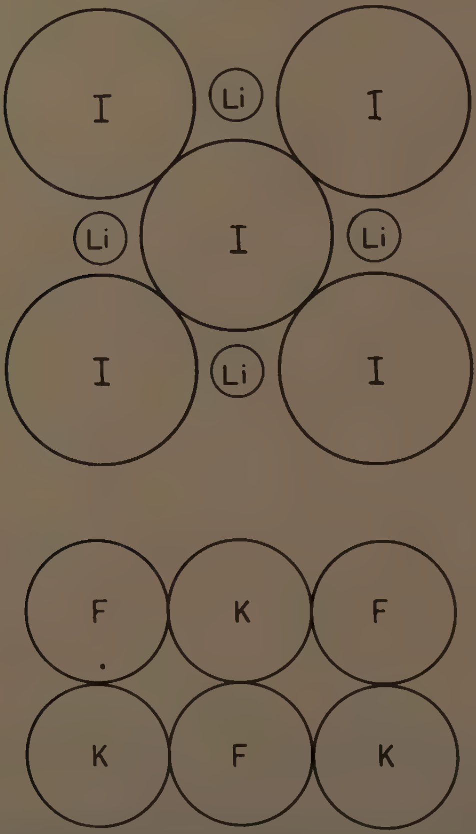

FIGURE 6. The arrangement of K and F ions in a crystal of KF is compared with the arrangement of Li and I in a crystal of LiI. Note that the dimensions of I^- determine the spacing.

Anions. In applying the same considerations to obtain the size of anions, it must be noted that as water molecules are oppositely oriented, the effective size of the water molecule is different from that when it surrounds a cation. This is so because water is a V-shaped structure and can therefore fit more closely around an anion than a cation as shown in FIGURE 7. Model measurements suggest that there is close to an 18 per cent contraction, hence anion sizes have been calculated as crystal radius +0.82 (2.72). The results of these calculations are shown in FIGURE 8 where the singly hydrated radii of a large number of ions are given.

The physiological properties of ions. Penetration rates into frog sartorius muscle have been determined for a number of ions; from such measurements it is possible to infer something about a pore size distribution curve. This is shown in FIGURE 9, where the rates for the alkali cation series Na, K, Rb, and Cs are from Mullins (1959). The rate for Li^+ is not shown but is similar to that for Na^+ (Keynes and Swan, 1960). The values for I^- are some unpublished ones from this laboratory, while the values for P_{Cl} is taken from Hodgkin and Horowicz (1959). Together these values for permeability describe a curve which should be related to pore size of the membrane. The possibility that anions and cations may pass the membrane of the muscle fiber via different pathways does not disturb this analysis; it is also consistent with the idea that the permeability data can be accommodated within a single range of pore sizes.

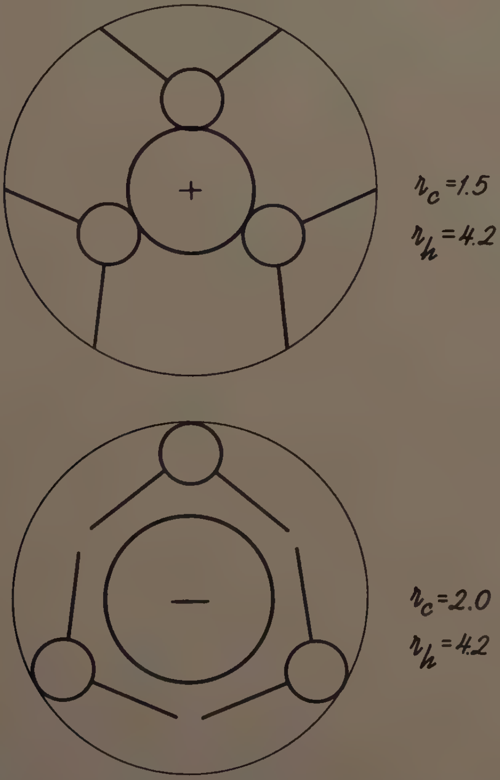

FIGURE 7. The orientation of water molecules of hydration around a cation (*above*) and an anion (*below*) is shown for 2 hypothetical ions of crystal radius r_c 1.5 for the cation and 2.0 for the anion. The singly hydrated radii, r_h, are identical in both cases (4.2).

It is to be emphasized that there is no clear-cut experimental information on the precision of fit demanded by the membrane-ion interaction but, from the marked interference between K^+ and Rb^+, it may be assumed that they both have a fairly high probability of dividing between them the pores that are available. The fact that a high discrimination between Na and K can be maintained is probably not so much a reflection of a lack of competition between these ions as it is a competition between Ca^{++} and K^+ since Ca^{++}, with the same size as Na^+, may be expected to be a much stronger competitor.

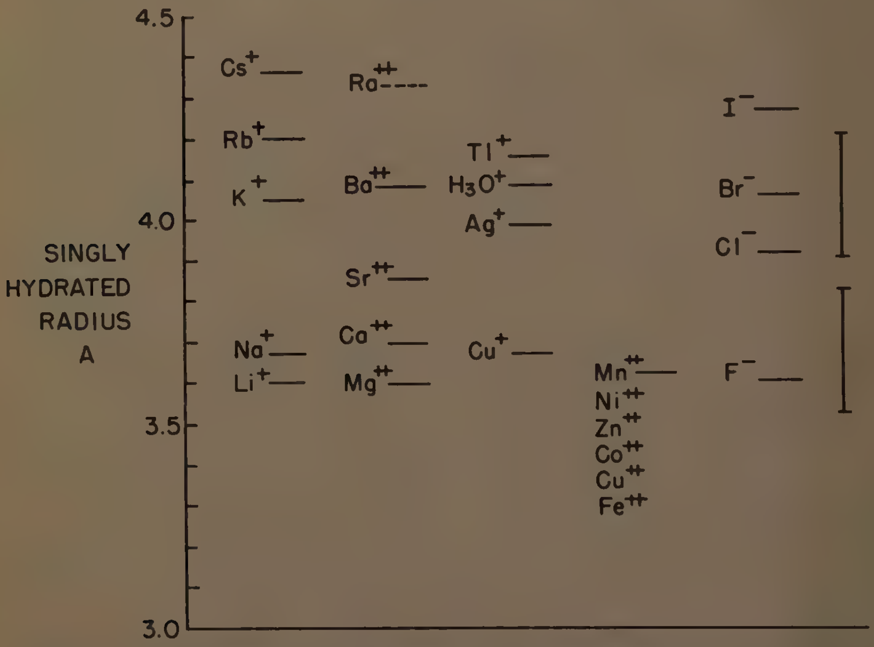

FIGURE 8. This diagram shows the computed singly hydrated radii of a variety of ions. Values for Li^+ and Mg^{++} have been adjusted as explained in the text, as have the values for the anions. Their vertical bars on the right indicate the limits, within 1 standard deviation ± of a pore size with a mode at K^+ size (*upper bar*) and Na^+ (*lower bar*).

Summary

A suggested model of the excitable membrane is that of a nonhomogeneous structure containing ion permeable areas, or pores, and ion-impermeable areas that are responsible for the condenserlike properties of the membrane. If the dielectric constant of the membrane is considered to be nonhomogeneous, the equations for ion fluxes are altered from those obtaining for the constant field case. An analysis of the rate of penetration of ions of differing size leads to the suggestion that the ion-permeable parts of the membrane have pores of the order of 4 Å in radius. The discrimination shown by the membrane for Na^+, K^+, and other ions appears to be on the basis of ion size.

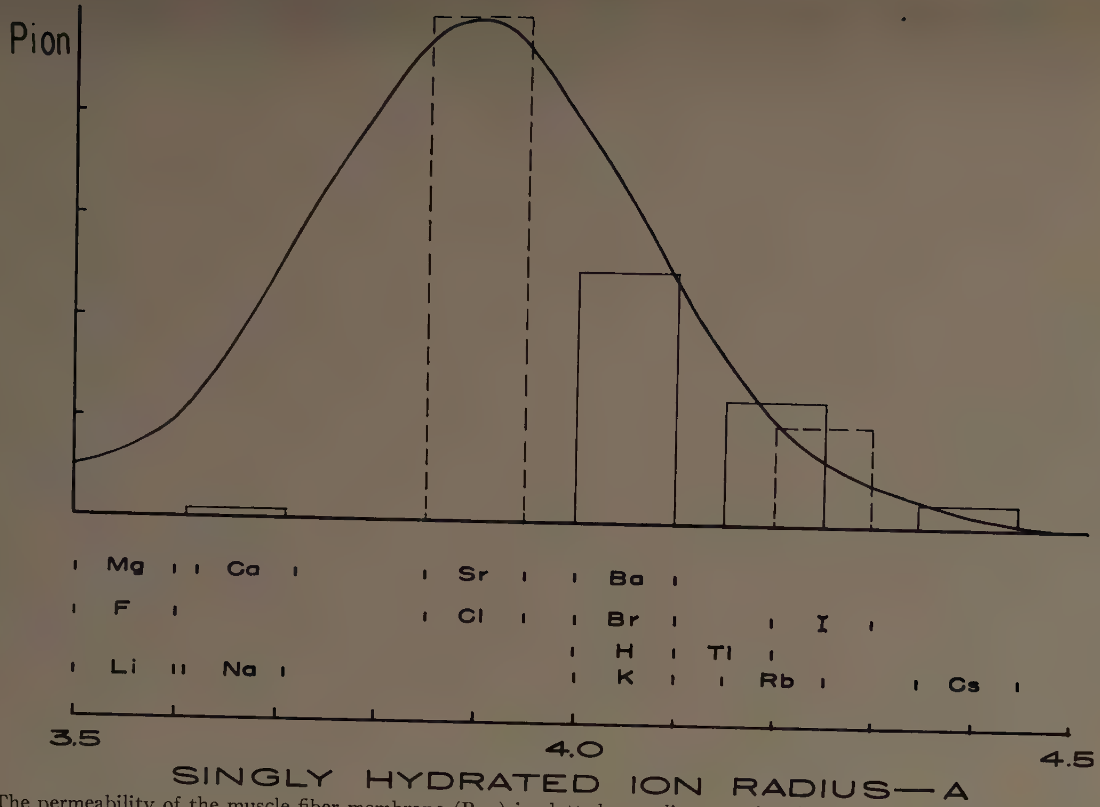

FIGURE 9. The permeability of the muscle fiber membrane (P_{ion}) is plotted as ordinate against ion radius as abscissa. The curve indicates the distribution of membrane pore sizes.

References

Behn, U. 1897. Ann. phys. **62:** 54.
Cole, K. S. & H. J. Curtis. 1936. Cold Spring Harbor Symposium. **4:** 73.
Dodge, F. A. & B. Frankenhaeuser. 1959. J. Physiol. **148:** 188.
Fricke, H. 1925. Physiol. Rev. **26:** 678.
Goldman, D. E. 1943. J. Gen. Physiol. **27:** 37.
Hodgkin, A. L. & P. Horowicz. 1959. J. Physiol. **148:** 127.
Hodgkin, A. L. & P. Horowicz. 1960. J. Physiol. **153:** 370.
Hodgkin, A. L. & A. F. Huxley. 1952. J. Physiol. **117:** 500.
Keynes, R. D. & R. C. Swan. 1959. J. Physiol. **147:** 626.
Mullins, L. J. 1959. J. Gen. Physiol. **42:** 817.
Sjodin, R. A. 1959. J. Gen. Physiol. **42:** 983.
Sjodin, R. A. 1961. J. Gen. Physiol. **44:** 929.
Solomon, A. K. 1960. J. Gen. Physiol. **43**(5): Suppl. 1.
Villegas, R. 1961. Abstr. Comm. Biophys. Soc.

IONIC MECHANISMS IN ELECTROGENESIS*

Harry Grundfest
Department of Neurology, College of Physicians and Surgeons,
Columbia University, New York, N.Y.

Electrogenic Cells

Varieties of excitable cells. Since the classical objects of electrophysiological study have been peripheral nerves and a few kinds of muscles, excitable cells have come to be identified with responsiveness to electrical stimuli. This meaning, which still persists in textbooks (cf. Ruch and Fulton, 1960, p. 37), is wrong, however, since gland and sensory cells, some muscle fibers and electroplaques and, indeed, the receptor portions of nearly every "excitable" cell are electrically inexcitable, although they do respond to various specific stimulating agents (Grundfest, 1957*b*, 1959*a*; Grundfest and Bennett, 1961). The excitable cells of the electrophysiologist would be more properly called "electrogenic cells," for when they are excited to activity by some stimulus they tend to respond with a change in their membrane potential.†

However, the occurrence of electrically inexcitable electrogenesis is not the only fact that falsifies the common tendency to regard frog and squid axons and vertebrate muscle fibers as the exemplars of electrogenic cells. Recent microelectrophysiological studies on many kinds of cells, carried out with sufficient attention to the details of their electrogenic activities, have also shown that the responses of electrically excitable membrane exhibit many variations.

Thus, differences in effects of chemical agents on different tissues indicate distinctive membrane structures, although their electrogenic activities may be fundamentally the same. The kinetics of the different processes involved in electrogenesis may also differ, so that some cells produce brief spikes; in others the spikes are prolonged, while in still other cells the responses are graded rather than all-or-none. Graded responsiveness may be converted to all-or-none activity, and spikes may also be converted to graded responses. The durations and shapes of spikes may be modified by various agents and, in some cells, these changes can occur spontaneously. Spikes may occur in the absence of Na^+ by appropriate change of the extracellular or intracellular milieu. Hyperpolarizing responses can be elicited under different conditions in various cells, while other excitable cells do not produce such responses.

Accumulating at a rapid rate in recent years, these data have been regarded

---

* The work described in this article is supported in part by grants from the Muscular Dystrophy Associations of America, Inc., New York, N.Y.; by Grant B-389 (C5) from the National Institute of Neurological Diseases and Blindness, Public Health Service, Bethesda, Md.; by Grant NSF G-5665 from The National Science Foundation, Washington, D.C.; and by the United Cerebral Palsy Research and Educational Foundation, New York, N.Y.

† The change should not be identified (cf. Ruch and Fulton, 1960) exclusively with the spike that is the all-or-none response produced by axons and by some muscle fibers (TABLE 1). The action potentials of these tissues may include after potentials as well as spikes (Grundfest, 1940). In many types of invertebrate muscle fibers the electrically evoked action potential is a graded response (Altamirano and Grundfest, 1954; Altamirano *et al.*, 1955*a*). Their neurally evoked activity may be a combination of an electrically inexcitable postsynaptic potential (p.s.p.) and of an electrically excitable graded response. The combination frequently results in a potential that resembles a spike (Cerf *et al.*, 1959, and FIGURE 2).

(Spyropoulos and Tasaki, 1960; Koketsu, 1961) as a challenge to and refutation of the currently accepted ionic hypothesis that was initially designed to account specifically for responses of squid axons (Hodgkin and Huxley, 1952) but which has also shown remarkable versatility in its application to account for the activity of other electrically excitable cells (Hodgkin, 1957). Nevertheless, many of these seemingly discordant data may be explained in terms of the ionic hypothesis, on the basis, however, of including a number of additional membrane processes. Evidence will be presented to show that the events of electrogenic activity are more varied and complex than was envisaged in the original hypothesis.*

Role of the cell membrane. The intimate nature of the various electrogenic processes, or *transducer actions* (Grundfest, 1957*a*) is still unknown, but their seat is very probably in the cell membrane that separates the interior of the cell from the surrounding fluid. The ionic compositions of the intra- and extracellular phases are very different, and these differences can account approximately for the resting potential difference across the cell membrane (inside negative relative to outside), on assuming that the cell membrane at rest is a potassium electrode. However, even at rest the membrane is far from being a barrier to other ions. The resting potential therefore cannot be entirely explained by Donnan equilibrium conditions (Grundfest, 1955).†

Maintenance of a steady state of ionic inequalities despite a constant tendency for mixing by diffusion requires the existence of metabolically energized "pumps." Although their mechanisms are also unknown, at least two are recognized. One extrudes Na^+ against a higher external concentration, the other takes in K^+ against a higher internal concentration. They may be coupled in action in squid giant axons (Hodgkin, 1957). However, in the frog nerve the pumps seem to be coupled differently than in the squid axon (cf. Hurlbut, 1961). The pump mechanisms are probably electroneutral in squid axons (Hodgkin, 1957), but it is conceivable that in other systems their activity may itself contribute an emf (Grundfest, 1955).

Electrogenesis. The ion specific properties of the resting cell membrane probably also form the basis of the electrogenic responses to excitation. According to the ionic theory (Hodgkin, 1951, 1957) and to its various secondary modifications (Eccles *et al.*, 1954; Fatt and Katz, 1951, 1953*a*; Grundfest, 1957*a*) the electrogenesis is caused by changes in membrane permeability for one or another, or for all 3 of the major ionic species present in the living system (Na^+, K^+ and/or Cl^-; TABLE 1), but participation of other ions (for example Ca^{++}, Mg^{++}) is not ruled out. Other theories of electrogenesis have also been put forward (Lorente de Nó, 1947; Tasaki, 1959*a*; Teorell, 1959), but the range of their applicability is far narrower than is that of the ionic theory.

---

* Hodgkin (1957) has modestly described this remarkable achievement as "empirical." In view of the theoretical acumen and boldness that led to the hypothesis, its application to squid axons should more justly be termed semiempirical (Grundfest, 1955).

† For alternative theories of the membrane potential (cf. Lorente de Nó (1947) and Ling (1960)). The view adopted in the present paper is that the resting potential is a diffusion potential based on the unequal distributions of different ions, but primarily of K^+; that the distributions are set by Donnan conditions within the framework of metabolically driven pumps; that it is necessary to take into account the relative permeabilities of all the principal ions, K^+, Cl^-, and Na^+. When appropriately applied, the constant field equation (Hodgkin and Katz, 1949) can account for a wide variety of deviations that result from nonequilibrium conditions that usually prevail in bioelectric measurements (Girardier *et al.*, 1961).

The presence or absence of changes in permeability in response to stimuli distinguishes electrogenically reactive from electrogenically inert membrane components. The latter may be unreactive with respect to all ions, behaving essentially as does an inanimate semipermeable membrane. This type is

TABLE 1
CLASSIFICATION OF ELECTROGENIC SYSTEMS

Electrogenesis	Depolarizing	Polarizing
Transducer actions for:	Na + K and/or Cl	K and/or Cl
Electrically inexcitable activity	Depolarizing receptor potentials	Hyperpolarizing receptor potentials
	Generator potentials	
	Excitatory p.s.p.s	Inhibitory p.s.p.s
	Depolarizing secretory potentials	Hyperpolarizing secretory potentials
Electrically excitable activity	Graded responses	Rectifying conductance increase
	Spikes	(May develop small de- or hyperpolarizations)
	Negative afterpotentials	Positive afterpotentials

Electrogenesis. The overt response to appropriate stimuli, manifested as a change in membrane potential from its value in the unstimulated cell. Depolarization is a decrease in the inside-negative resting potential which in the spike goes as far as to make the membrane temporarily inside-positive; polarization, hyperpolarization or repolarization represent the opposite, a tendency to increase the negativity or to maintain it in the face of depolarization.

Transducer action. The fundamental, as yet unknown, change in membrane properties in response to stimulation. Frequently, but not necessarily always, it causes electrogenesis. The ionic theory holds that the transducer actions produce electrogenesis by causing changes in permeability of the membrane to specific ions.

Electrically inexcitable activity. Reaction of membranes that do not respond to electrical stimuli. It is evoked by specific stimuli such as chemical agents, thermal, mechanical or photic energy.

Electrically excitable activity. This activity may be evoked by specific stimuli but is also initiated by changes in membrane potential. These may be depolarizing or the opposite. Propagation of activity is possible, since once electrogenesis is initiated it can evoke further activity by local circuit action.

Receptor potential. Electrogenesis of a sensory cell that does not have an axon.

Generator potential. Electrogenesis in the receptor portion of a sensory cell which has an axon.

Postsynaptic potential. Response initiated in a neuron or effector cell by activity of a presynaptic fiber.

Secretory potential. Electrogenesis associated with activity of gland or neurosecretory cells.

Spikes. All-or-none responses of electrically excitable membrane, which at their peak usually reverse the membrane potential to inside-positivity. They are capable of decrementless propagation.

Graded responses. Electrogenesis that varies in amplitude depending upon the stimulus strength and is decrementally propagated.

Afterpotentials. Smaller, more labile potentials that may follow the spike or graded response, outlast the spike somewhat, or may be considerably longer and are not all-or-none.

Rectifying conductance changes. Membrane reactions that cause deviations in the linear relation between applied current and membrane potential. They may cause electrogenesis of either sign, or none.

exemplified by the membrane of the rostral, uninnervated surface of eel electroplaques (FIGURE 12). Membranes may also be unreactive only with respect to one or several ion species. Thus, the distribution of Cl^- is a passive phenomenon in many cells, determined by the electrochemical conditions set by a reactive component that changes the K-conductance (Boyle and Conway, 1941). However, in muscle fibers of decapod crustaceans such a passive membrane component for Cl^- (Girardier *et al.*, 1961) exists in parallel with the reactive but electrically inexcitable Cl-conductance membrane of the inhibitory synapses (Boistel and Fatt, 1958; Grundfest *et al.*, 1959). In the uninnervated membrane of Rajid electroplaques there is an electrogenically reactive electrically excitable Cl-conductance component while a reactive K-component is absent (Bennett, 1961; Cohen *et al.*, 1961).

The change of permeability toward one or several ion species alters the electrode properties of the membrane. During activity the membrane passes a high current, since the resistance of the active membrane becomes low for specific ions which have high concentration gradients. A net current density of 10 mAmp./cm^2 is probably a fairly common value, and densities of the order of 50–100 mAmp./cm^2 are found (Grundfest and Bennett, 1961). The latter values probably approach the capacities of high-output primary cells and of storage batteries. Electrochemical theory in general does not cope with systems involving the ion and current conditions of bioelectrogenic activity and it therefore need not be surprising if quantitatively adequate theoretical explanations are not as yet forthcoming for all bioelectric data.

Varieties of Electrogenic Actions

Electrogenic manifestations of excitable membranes. Where the transducer actions are electrically inexcitable, the electrogenic behavior of the active membrane is a relatively simple function of the ions involved and of the electrochemical conditions, and is manifested as depolarizing and polarizing (or hyperpolarizing) potentials of several types (TABLE 1). In electrically excitable membranes, however, the transducer actions are evoked initially by an electrical stimulus and may be further modified as the membrane potential changes. Thus there may be regeneration. Like the manifestations of electrically inexcitable membrane these effects may tend to increase the initial electrogenesis, to restore the resting state, or to increase the internal negativity beyond its resting value. The regenerative feature of electrically excitable activity is usually regarded as a property of depolarizing electrogenesis, but it may also be manifested by processes that exert repolarizing or hyperpolarizing electrogenic influence.

The most conspicuous and commonly recognized electrogenic activities are increases in membrane conductance which are initiated by depolarizing stimuli (that is, those that decrease the resting potential) and themselves cause net additional depolarization. These activities lead to production of graded responses or of all-or-none spikes. However, depolarizing stimuli may also produce increased membrane conductance, which is associated with only minor or with no electrogenic manifestations. Increased membrane conductance, likewise with relatively minor electrogenesis, can also be produced by, or as an aftermath of, electrical stimuli that hyperpolarize the membrane. Furthermore, both depolarizing and hyperpolarizing stimuli can lead to decreases in membrane conductance. These various electrically excitable membrane processes may involve one or more ion species. They may occur in different proportions in different cells and the proportions may vary even in different parts of the same cell.

The occurrence of two parallel systems of electrogenic membranes, in which the ion valving processes appear in basically similar combinations (TABLE 1) but are differently excitable, has numerous theoretical implications and consequences (Grundfest, 1957*b*, 1957*c*, 1958*a*, 1958*b*, 1959*a*, 1959*b*, 1961*a*, 1961*b*). It seems likely that temporary distortions of the molecular arrangements of the membrane, by key chemical agents or by other specific stimuli in one type of membrane, or by the potential across the membrane itself in the other, lead to "opening" of passages for specific ions (Mullins, 1960, and in these pages).

Electrically inexcitable membranes. Among synaptic, electrically inexcitable membranes it is easy to recognize the several varieties of electrogenic activity, largely because the potentials are graded and nonpropagating (Grundfest, 1957*b*, 1959*a*). One and the same neuron (Eccles, 1957) or muscle fiber (Boistel and Fatt, 1958; Fatt and Katz, 1953*a*; Grundfest *et al.*, 1959) may develop depolarizing excitatory and hyperpolarizing inhibitory postsynaptic potentials (e.p.s.p.s and i.p.s.p.s respectively). Sensory neurons develop generator potentials which are electrically inexcitable, as well as spikes (Grundfest, 1961*b*). Some also develop p.s.p.s.

Evidence for electrical inexcitability of a given membrane component may be *direct*; that is, that the electrogenesis cannot be initiated by an electrical stimulus, or *indirect*, on the basis of a constellation of properties that distinguish electrically inexcitable activity from the electrically excitable (Grundfest, 1957*b*, 1959*a*; Grundfest and Bennett, 1961). The direct evidence is most readily obtained in particularly favorable tissues, such as those cells in which the electrically inexcitable and excitable membranes occupy distinctly different regions (such as eccentric cell of *Limulus*; cardiac ganglion neurons of lobster; Pacinian corpuscles; olfactory receptors) or in which an electrically excitable membrane of the spike generating variety is absent (for example, electroplaques of marine electric fish; frog slow muscle fibers). However, direct data can also be obtained even when the two types of membranes are intermingled, but the responses have distinctive characteristics (for example, electroplaques; insect and crustacean muscle fibers). Special devices can also provide direct evidence,* as in the frog muscle endplate (Werman, 1960).

The most explicit criticism of the hypothesis that there are two fundamentally different types of excitable electrogenic membranes is that of Eccles (1960). Its core is the following statement: ". . . there is evidence that some cells activated by chemical transmitters are devoid of the sodium permeability mechanism that is responsible for the spike, as for example the tonic fibres of amphibian muscle and the electric organs of *Torpedo* and *Raia*. However, it may be questioned if it is justifiable to argue by analogy that other chemical receptive membranes are also electrically inexcitable, particularly when some cardiac and crustacean muscle fibres combine a diffuse transmitter sensitivity with electrical excitability. Furthermore, denervated mammalian muscle fibres develop along their whole length a sensitivity to acetylcholine equivalent to that at a normal end-plate, and yet retain their electrical excitability."

---

* It is instructive to note that preoccupation with electrically excitable phenomena may tend to restrict conceptual and experimental approaches. Thus several authors have stated that it would be difficult to apply "rigorous" tests for the electrical inexcitability of synaptic membranes such as that of the muscle endplate, because electrical stimuli cannot be confined to areas as small as those of the synaptic contacts (Pringle, 1960; Spyropoulos and Tasaki, 1960). This is, indeed, a correct statement in so far as tests by electrical stimulation are concerned, but there are other ways of carrying out the tests. Thus recording with external microelectrodes can be confined to small foci (del Castillo and Katz, 1956), and the absence of inward current is then an index of electrical inexcitability (Freygang, 1958). These findings were the basis of the direct tests in the muscle endplate (Werman, 1960).

There are two types of argument by analogy. Simple analogy derives from the basic assumption of general physiology, that functionally homologous parts of various cells tend to have the same properties. Electrophysiology has contributed much of the classical data validating that assumption, as well as examples of its limitations. Categorical resort to simple analogy occurs at three points of the above-cited statement. However, it is only partially correct and requires modification: (1) A sodium permeability mechanism is *probably* responsible for electrically excitable spikes and graded responses, and for electrically inexcitable e.p.s.p.s of all animal cells, but some investigators (Koketsu, 1961; Spyropoulos and Tasaki, 1960) question the role of Na^+ in spike electrogenesis. In at least one plant cell the spike may involve only a chloride permeability mechanism (Gaffey and Mullins, 1958). (2) The three examples of "cells activated by chemical transmitters" do, indeed, provide direct evidence of neurally evoked responses which cannot be produced by electrical stimuli (Grundfest, 1959*a*; Grundfest and Bennett, 1961). However, no direct evidence is now available that these responses are chemically mediated. (3) The direct evidence for chemical transmission, if any exists, is slim indeed, applying perhaps to cardiac muscle (Loewi, 1945; Grundfest and Bennett, 1961). However, nothing is known about the possible transmitters for the excitatory and inhibitory synapses of crustacean muscle fibers. Thus, they cannot be classed among "other chemical receptive membranes" that "combine a diffuse transmitter sensitivity with electrical excitability" unless the evidence that their synaptic membranes are electrically inexcitable (Grundfest *et al.*, 1959) is accepted.

Of the 3 examples given by Eccles as cells which "are devoid of the sodium permeability mechanism that is responsible for the spike" only the Torpedine electroplaques are normally electrically inexcitable (Bennett and Grundfest, 1961*b*; Bennett *et al.*, 1961). The others, although also "devoid of the sodium permeability mechanism" are, nevertheless, normally electrically excitable. Both frog slow muscle fibers (Burke and Ginsborg, 1956; Kuffler and Vaughan-Williams, 1953) and Rajid electroplaques (Bennett, 1961; Bennett and Grundfest, 1961*d*; and Cohen *et al.*, 1961) respond to depolarizing stimuli with increased membrane conductance. The reaction of the electrically excitable component of the muscle fibers is a K-activation (Belton and Grundfest, unpublished). That of Rajid electroplaques is a Cl-activation which under appropriate experimental conditions may result in a "spike" (Cohen *et al.*, 1961). Both electrically excitable membrane transducer actions may be eliminated by experimental procedures. The cells then remain reactive only to neural or chemical stimuli, thus becoming truly electrically inexcitable electrogenic cells.

The second type of analogical argument is based on the analysis of dynamic properties (or transient responses (Pringle, 1960)) of the system under investigation. Of particular interest and challenge is the case where two components with different properties coexist and interact. It may then be difficult to devise direct tests of the hypothesis. However, dynamic analysis of the properties of each component and of their interactions can provide a wealth of indirect evidence, by demonstrating the degree of congruence of the system with the hypothesis or model. This is the case in electroplaques of eel or *Gymnotus carapo*, or muscle fibers and neurons, in which the two types of excitable membranes are intermingled (Grundfest, 1957*b*, 1959*a*). Indeed, Eccles' final example provides a remarkably good affirmation of the validity of the hypothesis. The chemosensitized membrane of denervated muscle fibers develops the electrophysiological characteristics of electrically inexcitable membrane (FIGURE 5) which is intermingled with the electrically excitable membrane. The properties that differentiate electrically excitable spike-generating and electrically inexcitable synaptic membranes are listed in TABLE 2.

The ionic events in production of e.p.s.p.s are still unclear. Originally it had been assumed (Fatt and Katz, 1951) that the active membrane becomes permeable to all ions, as Bernstein had postulated (1912). It now seems likely that the frog fast (Takeuchi and Takeuchi, 1960) and slow (Belton and Grundfest, unpublished) muscle fibers, and *Raia* electroplaques (Cohen *et al.*, 1961), generate e.p.s.p.s by increased permeability for Na^+ and K^+ only. Three distinct varieties of activity respectively involving conductance changes for K^+ and/or Cl^- can all produce the hyperpolarizing or repolarizing electrogenesis of i.p.s.p.s.

Degrees of differences in the chemical responsiveness of membrane of the same electrogenic species in different cells are common. Differences within the same cell are particularly striking in the case of taste buds (FIGURE 1), which are receptor cells without axons (Grundfest, 1961*b*) and are probably electrically inexcitable. Each of the 12 cells included in FIGURE 1 responded with depolarization to at least 2 of 4 different chemical agents causing the sensations of salt, sweet, bitter and acid in man. Most of the cells responded to 3 of the 4 and one to all 4. The patterns of the degree of responsiveness were different in all the cells. It may be reasonably assumed that each of the chemical agents—salt, sugar, quinine, and acid—probably acted upon more or less specific molecular components of the membrane structure. Thus it seems likely that each of the 12 cells had a different combination of these different depolarizing components.

There is no evidence available at present that the repolarizing conductance components of e.p.s.p.s can be modified differently from the depolarizing Na-conductance component. However, this may signify only that current methods for study and analysis of the mechanisms of action of the electrically inexcitable membranes are still too crude (Grundfest, 1961*c*). The conductance components of hyperpolarizing synapses that involve only one or two polarizing ion species certainly can be modified by pharmacological agents which do not affect the depolarizing synapses (Grundfest, 1957*c*, 1958*b*).

Electrically excitable membranes. The electrically inexcitable nature of the electrogenesis of synaptic or receptor membranes emphasizes the chemical sensitivity of these membranes and of their components. The electrically excitable membranes also have chemical sensitivities, although they are not as readily recognized (Grundfest, 1957*a*; Shanes, 1958). These actions are particularly striking in some tissues, notably in the change of normally gradedly responding muscle fibers to produce all-or-none responses (FIGURE 2). These actions may appear related to or independent of the effects of the same pharmacological agents on synaptic membrane in the same cell. Related actions are exemplified by D-tubocurarine and prostigmine, which block or inactivate excitatory synaptic membrane of eel electroplaques (Altamirano *et al.*, 1955*b*). Their effect on the electrically excitable membrane of the electroplaques is to alter its all-or-none response to graded activity (FIGURE 3). It may be similarly regarded as due to some type of "inactivation" (Grundfest, 1957*d*, 1959*a*), but the details require further analysis.

TABLE 2*

CHARACTERISTICS AND PROPERTIES OF DIFFERENTLY EXCITABLE ELECTROGENIC MEMBRANE

Spike (electrically excitable)	P.S.P.s (electrically inexcitable)
A. Characteristics	
Transducer action: (1) Sequential increase of Na$^+$ and K$^+$ conductances and Na$^+$ inactivation	Two types: (*a*) Increased conductances for all ions (*b*) Specific increase in K$^+$ and/or Cl$^-$ conductances
(2) Rates determined by membrane potential	Rates not determined by membrane potential
Electrical response: (1) Begins with graded depolarization, develops overshoot	Two types: (*a*) Depolarizing (*b*) Hyperpolarizing
(2) All-or-none response	Graded response
B. Direct Evidence for Characteristic Differences	
(1) Spike absent (2) Spike present	Developed only by neural or chemical stimuli
C. Consequences of Characteristic Differences	
(1) Always in depolarizing direction	Of either sign, electrochemically reversible
(2) Hindered or blocked by hyperpolarization	Electrochemical gradation
(3) Excited, then blocked by depolarization	Electrochemical gradation
(4) Pulsatile, relatively fixed duration, independent of stimulus	May be prolonged, sustained while stimulus lasts
(5) Vanishingly brief latency	Appreciable, irreducible latency
(6) Relatively inert to chemicals	Sensitive in two ways: response may be (*a*) Evoked by synapse activators; (*b*) Depressed or blocked by inactivators
(7) Decrementless propagation	Nonpropagated, 'standing' potential

* From Grundfest, 1959*a*. Reproduced by permission of the American Physiological Society.

Interactions of the differently excitable components. Examples of different actions of a drug on the two components are shown in FIGURE 4. Serotonin augments somewhat the excitatory p.s.p.s of lobster muscle fibers, though not their inhibitory p.s.p.s. It also can convert the normally graded responsiveness to electrogenesis of spikes. In contrast to these last actions, substitution of Cs^+ for K^+ increases enormously both the excitatory and inhibitory p.s.p.s of lobster muscle fibers, but the normal graded responsiveness of the electrically excitable membrane is retained.

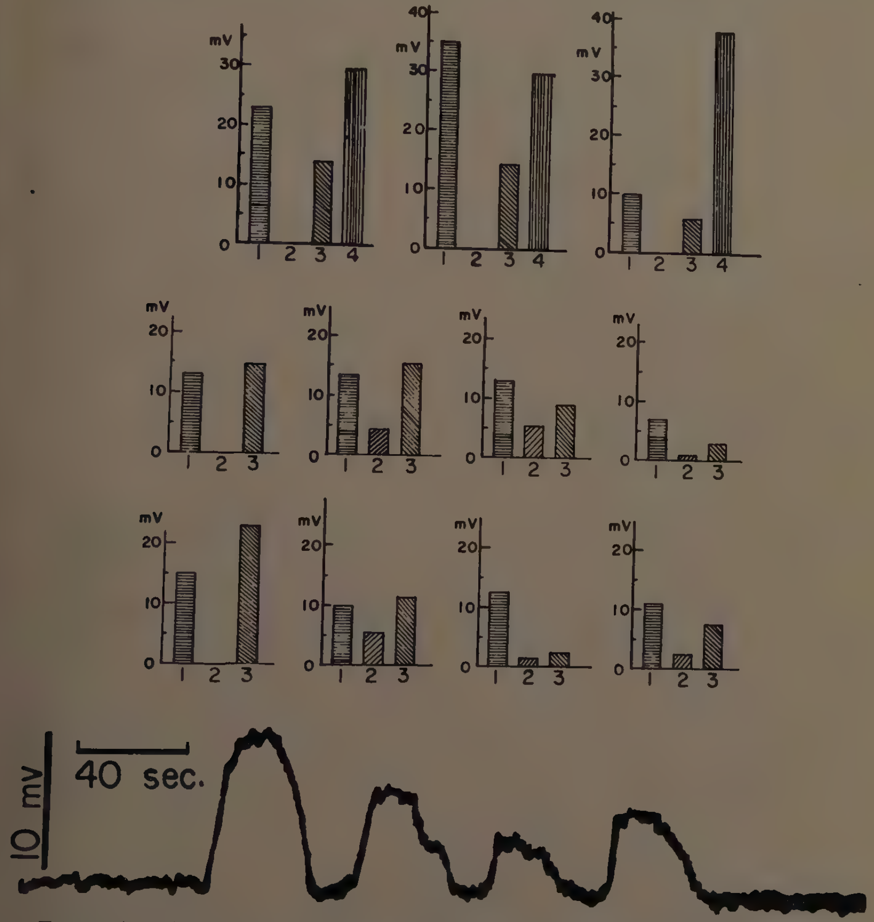

FIGURE 1. Electrical activity in taste buds produced by four standardized stimuli: (1) salt, (2) sweet, (3) bitter, and (4) acid. (*Below*) Records of potentials evoked by the four substances acting on a single taste bud. (*Above*) Different patterns of responses in different cells. Unpublished data of Beidler and Kimura, courtesy of Lloyd M. Beidler.

Evolutionary relations among membranes. The different electrogenic membranes probably derive from some common precursor (Grundfest, 1959*a*, 1960*a*, and 1961*a*). The variously related chemical affinities of synaptic membranes (Grundfest, 1958*b*) and of these with electrically excitable membranes probably derive from that evolutionary relation (Grundfest, 1959*b*). There is also a labile functional interrelation as is evidenced by the pharmacological and electrophysiological changes that occur during maturation of muscle (Diamond and Miledi, 1959; Purpura *et al.*, 1960*a*) and neurons (Purpura *et al.*, 1960*b*) or on their denervation and reinnervation (Axelsson and Thesleff, 1959; Miledi, 1960*a*, 1960*b*; Purpura, this monograph). The change in denervated muscle fibers is particularly instructive (FIGURE 5), since the membrane that has become cholinoceptive in the muscle fiber also appears to be electrically inexcitable (Grundfest, 1961*a*), thus taking on this characteristic of the endplate membrane as well as its chemical sensitivity.*

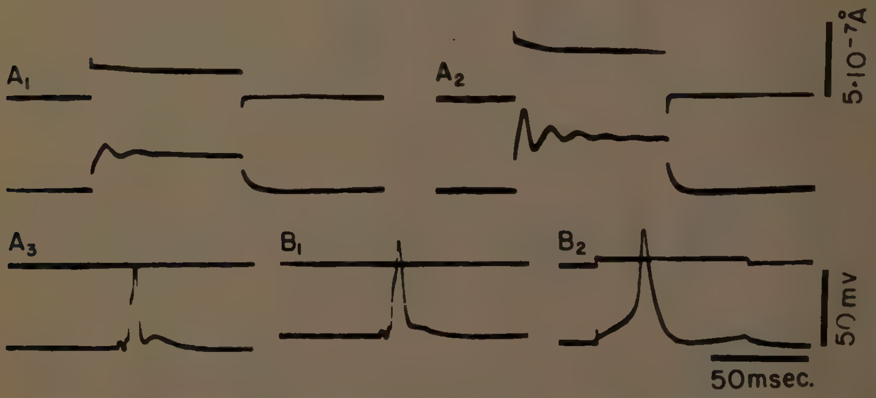

FIGURE 2. Conversion of graded electrically excitable activity to all-or-none responsiveness in muscle fiber of the grasshopper *Romalea microptera*. A_1, A_2 : weak and supramaximal intracellularly applied depolarizing stimuli (current monitored on upper trace of each record). The maximal response was a small, oscillatory graded response. A_3 : the large excitatory postsynaptic potential (e.p.s.p.) evoked in the muscle fiber by stimulating the "fast" axon caused a maximal response of the electrically excitable membrane, the combined potentials having the appearance of a spike. B_1 : the neurally evoked response after treating the preparation with $BaCl_2$ was a slightly increased e.p.s.p. and an all-or-none spike. The latter was now also produced (B_2) by a weak intracellularly applied current. Note the slow change of the membrane potential, which reflects the increase in membrane resistance after applying Ba^{++}. From Werman *et al.* (1961). Reproduced by permission of the *Jour. of Gen. Physiology.*

Electrogenic components. Thus, the electrogenic components of both electrically inexcitable and electrically excitable membranes may have distinctive chemical and pharmacological properties. The effects of these properties may be differently manifested in the two categories of membrane and may thus give rise to overall effects that are not entirely obvious from the effects on individual components. One further example (FIGURE 6) illustrates specifically the main thesis of this paper,* that the electrically excitable membrane possesses a number of relatively independent action components whose different properties need to be taken into account. Their participation to different degrees in a given activity results in the specific characteristics of electrogenic responses in different cells, or in the same cell at different sites, or under different conditions (Grundfest, 1957*a*, 1961*c*).

---

* The newly differentiated cholinoceptive membrane responds not only to various cholinomimetic drugs; like that of cholinergic synapses it is also inactivated by D-tubocurarine (Axelsson and Thesleff, 1959). Its responses are not affected, however, by applying anticholinesterase drugs, while the activity of the denervated endplate membrane continues to be affected by them. This difference appears to be linked to the presence or absence of esterase activity. In denervated muscle fibers esterase activity remains confined to its original sites at the endplate region (Couteaux, 1955). Therefore the chemosensitivity of the electrically inexcitable membrane to acetylcholine may be unrelated to the presence or absence of cholinesterase.

Components of Electrically Excitable Activity

The different varieties of transducer actions and their electrogenic effects. The voltage clamp data of FIGURE 6 describe only two of the action components of electrically excitable membranes. One component, that of initial inward flux of current which, according to the ionic theory (Hodgkin and Huxley, 1952), is associated with increased membrane conductance for Na^+ (Na-activation) was selectively diminished by poisoning the neuron with urethane. This effect was paralleled by a change of the electrical response from a spike to a small graded response. While the later component, associated with increased outward flux of K^+ (K-activation) was not affected by urethane, exposure of the neuron to tetraethylammonium ion (TEA) diminished the potassium outflux much more than it affected the sodium influx. The change in the electrical response associated with this effect was to prolong the spike, as had been predicted on theoretical grounds (Grundfest, 1957*a*, 1960*b*; Hodgkin, 1957; Shanes, 1958). Consideration of only 3 action components (Na- and K-activation, and Na^+-inactivation) was adequate to account, with a high degree of accuracy, for many phenomena manifested by squid axons (Hodgkin and Huxley, 1952) and other cells (Shanes, 1958).

As more types of electrically excitable cells have come to be studied, other components of electrogenic activity of or membrane reactions to depolarizing and hyperpolarizing currents have come to light. Activation of K-conductance or even of a Cl-conductance in the absence of an electrically excited Na-activation has been observed in the "delayed rectification" of frog slow muscle fibers (Kuffler and Vaughan-Williams, 1953; Burke and Ginsborg, 1956; Belton and Grundfest, unpublished) and *Raia* electroplaques (Grundfest and Bennett, 1961; Cohen *et al.*, 1961; Bennett, elsewhere in these pages). These cells produce electrically inexcitable neurally evoked depolarizing p.s.p.s, but are also "electrically excitable" in the sense that they undergo a considerable increase in conductance (or delayed rectification) in response to depolarizing electrical stimuli, but this develops little electrogenic activity (FIGURE 7). However, an electrically excitable plant cell, *Chara*, produces a spike as a result of Cl-activation (Gaffey and Mullins, 1958).

An additional factor that is probably of rather widespread occurrence is that of K-inactivation produced by depolarizing stimuli (Grundfest, 1957*a*, 1957*d*). The stimulus for depolarizing K-inactivation may even be the depolarization produced by the spike itself. More recently hyperpolarizing responses have

---

* A parallel account of current data on electrically inexcitable membranes will appear elsewhere (Grundfest, 1961*c*).

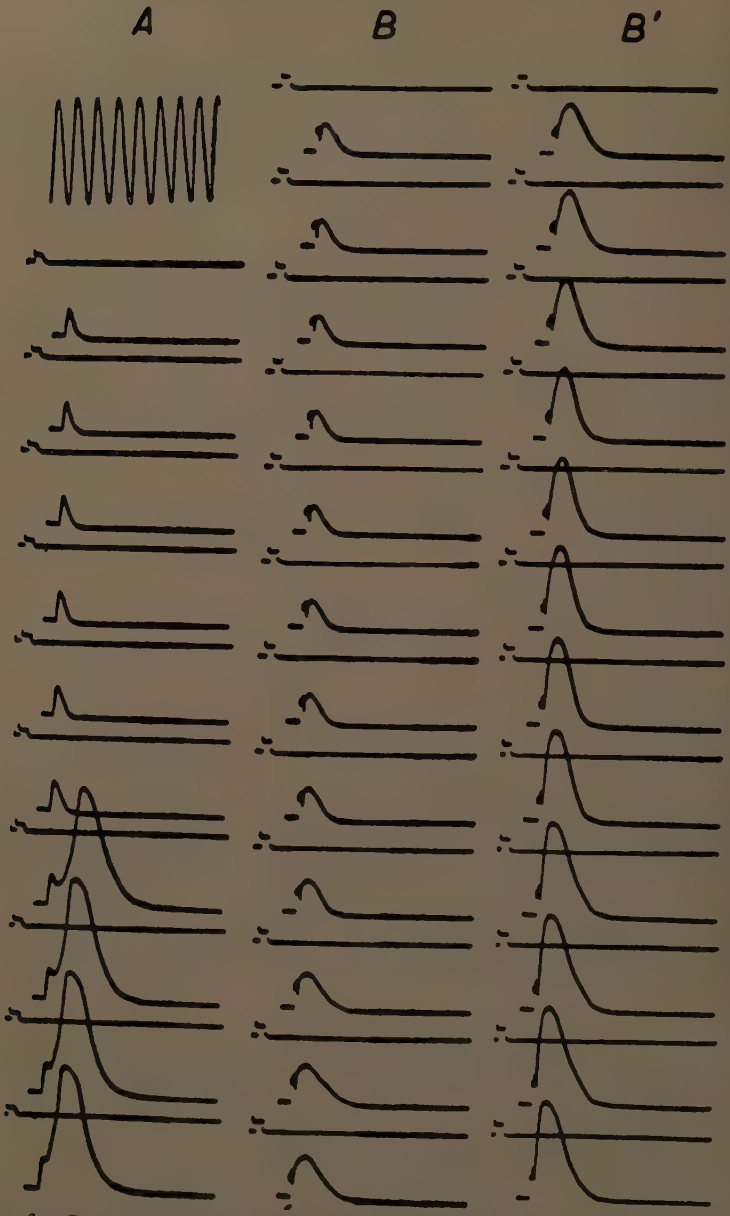

Figure 3. Conversion of all-or-none responsiveness to graded activity in eel electroplaque. Two traces are recorded simultaneously, repeated at the rate of 5 per sec. The upper, longer trace of each set is the zero base line for an internal microelectrode. It also carries the monitoring signal of a stimulus applied to the cell and shows that the stimulus strength remained constant in each of the two series. The lower trace of each set is that of the potential recorded with the microelectrode. The distance between the two represents the resting potential, about 70 mv. The weak stimulus in *A*, before the cell was treated with drug, at first produced only a subthreshold electrotonic depolarization. The seventh

disclosed a K-inactivation due to hyperpolarizing currents, as well as increased conductances produced by such currents. The various complications caused by the interplay of these additional factors will form the major part of the remainder of this paper.

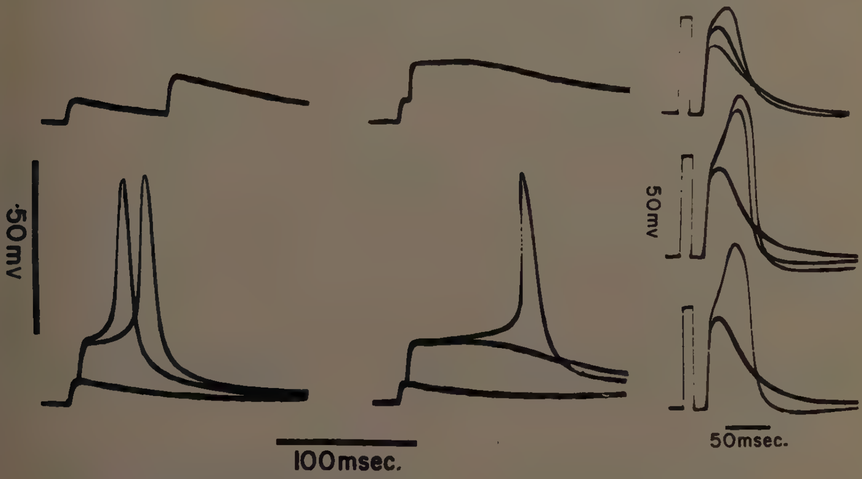

FIGURE 4. Manifestations of different types of responses produced by different combinations of electrically inexcitable and electrically excitable activities. (*Left*) Lobster neuromuscular preparation treated with serotonin and picrotoxin. The amplitude of the individual e.p.s.p.s in response to stimulating the exciter axon increased somewhat over the e.p.s.p.s in untreated preparations, and the e.p.s.p.s were greatly prolonged. Two e.p.s.p.s summating to about 20 mv depolarization developed a small graded response out of which developed the all-or-none spikes seen in the superimposed records below. (*Right*) Another lobster neuromuscular preparation soaked for 10 hours in a Ringer's solution in which 7.5 mmole K was substituted for by Cs^+. The amplitude of the e.p.s.p.s of this preparation ranged from about 30 to 45 mv. Superimposed traces show the facilitation produced by repetitive stimulation. Facilitated e.p.s.p.s about 50 mv in amplitude evoked only graded responses of the electrically excitable membrane. From Grundfest and Reuben, 1961. Reproduced by permission of *Pergamon Press.*

A generalized schema of the electrogenic components in terms of their ionic transducer actions which applies to both electrically excitable and electrically inexcitable membranes is shown in FIGURE 8. Depolarizing electrogenic activity, manifested by excitatory p.s.p.s, spikes, and graded responses, involves

---

FIGURE 3—*continued.*

repetition of the stimulus was followed by a spike. The shorter latency at which successive spikes then developed indicates continued growth of excitability and its persistence through the 200-msec. intervals between stimuli. The resting potential remained unchanged. *B* and *B'*: the sequence of growth in response in the cell after 84-min. exposure to 500 μg. per ml. of physostigmine. The resting potential was not affected by the drug, which eliminated synaptic excitability and converted the all-or-none response of the electrically excitable membrane component to graded responsiveness. The testing stimulus was slightly stronger than before applying the drug, and the first trace seen (upper set of *B*) evoked a distinct although small, graded response. During the course of repetitive stimulation at 5 per sec. the response grew, at first gradually and then more rapidly, indicating that the rise of excitability is nonlinear. The series illustrated ended before the response could grow to an amplitude as large as that of the spike, but in other experiments this was observed. (From Altamirano *et al.*, 1955*b*). Reproduced by permission of *Biochimica et Biophysica Acta.*

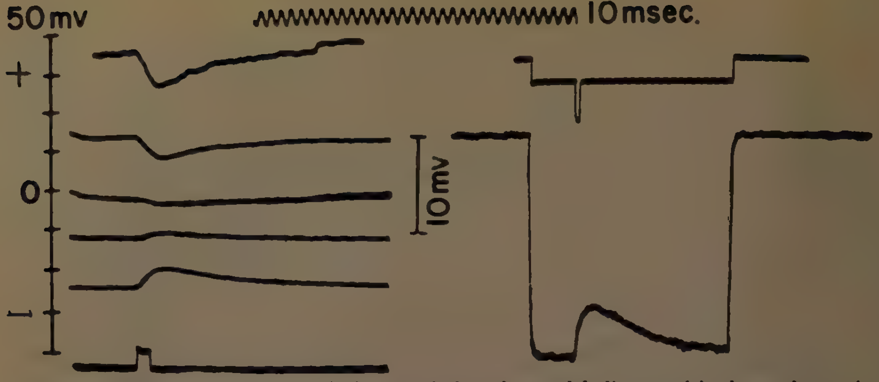

FIGURE 5. Electrophysiological characteristics of acetylcholine-sensitized membrane in denervated muscle fiber of rat. (*Left*) Reversal of potential on changing membrane polarization. Depolarizing response to a jet of acetylcholine (application signaled on lowest trace) was diminished in amplitude when the membrane was depolarized and at about −10 mv depolarization it seemed to disappear. It reappeared in reversed sign when the membrane was polarized inside-positive. (*Right*) Persistence of activity of chemically excitable membrane component in fully depolarized muscle fiber. The preparation was soaked in isotonic K_2SO_4, which depolarized and inactivated the electrically excitable membrane component. A brief pulse was applied to the muscle to restore an inside-negativity of about 20 mv. During the pulse a testing jet of acetylcholine was applied (signaled by a brief deflection on the upper trace, which monitored the polarizing current). The chemical stimulus evoked a response showing that the sensitized membrane of the denervated muscle fiber is electrically inexcitable. Modified from Axelsson and Thesleff, 1959.

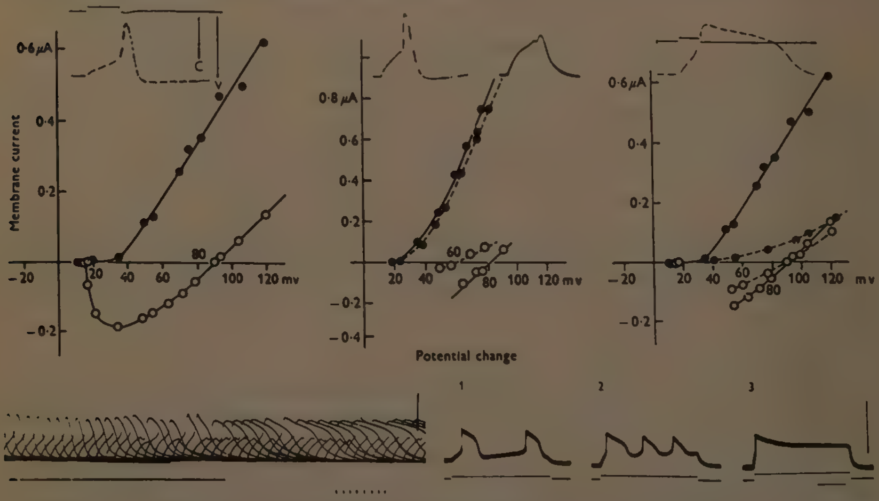

FIGURE 6. Differential elimination of Na-activation and K-activation in *Onchidium* neurons. Voltage clamp experiments show the initial inward current (*circles*) and late outward current (*dots*) as functions of the membrane potential. Solid lines connect control data; broken lines, after treatment with drugs. Insets show the responses to brief stimuli. (*Left*) Control series, blanking of potential trace at 5-msec. intervals; calibration 100 mv and 5×10^{-7} *A*. (*Center*) Neuron in a preparation treated with 2 per cent urethane. Note that the inward (Na^+) current was markedly diminished, while the outward (K^+) current was unaffected. The spike of the cell was changed to a small graded potential. Blanking intervals, 2 msec. (*Right*) From an experiment in which the preparation had been exposed to tetraethylammonium ions (TEA). The K^+-current was diminished much more than was the Na^+-current, and the response of the cell became prolonged. Blanking signals at 5-msec. intervals. (*Below, left*) Development of the prolonged response on applying TEA during a mixing interval indicated by bar line, lower left. Multiple sweeps at 1 sec., each registering a response evoked by a direct stimulus. Calibration for each sweep 100 mv and 5-msec. intervals. (*Right*) Sample records of responses to prolonged applied currents. Calibrations 100 mv and 100 msec. Lower traces show the stimulating currents. Modified from Hagiwara and Saito, 1959.

activity in membranes that have the transducer capacities to permit influx of Na+. This conductance change for a depolarizing ion is countered by repolarizing actions due to increased conductance for K+ and/or Cl−. The relative proportions and kinetics of each component presumably determine various characteristic properties of the electrical responses and of their pharmacological reactions.

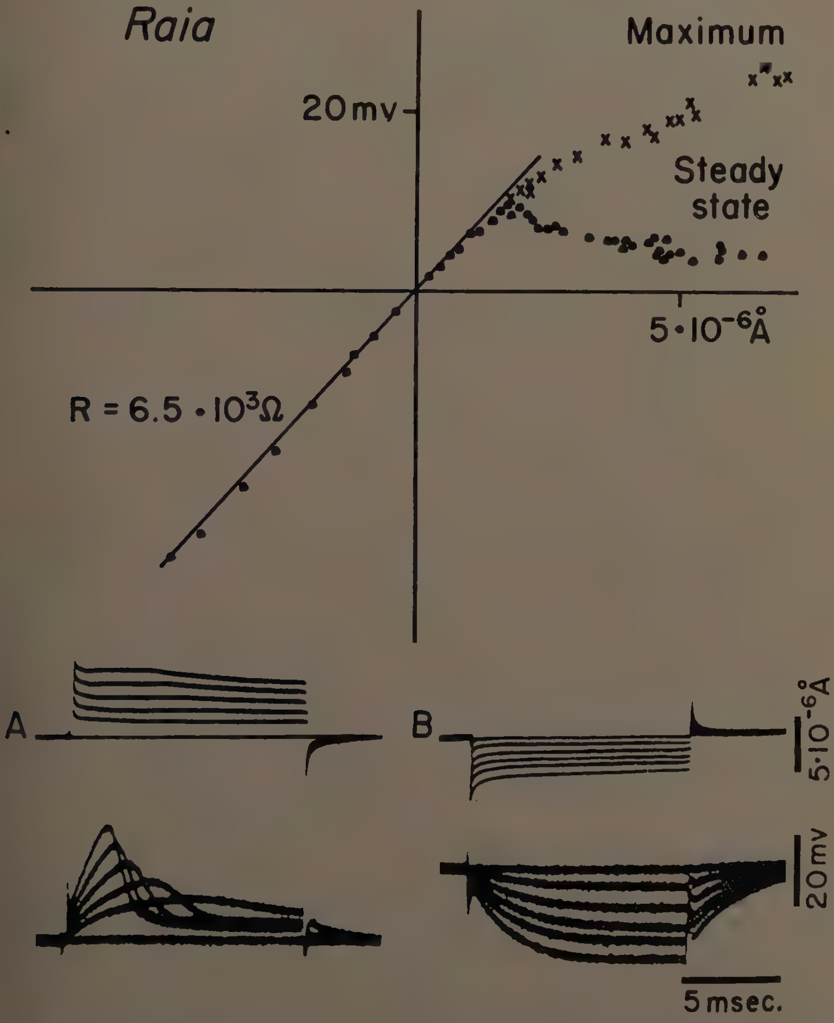

Figure 7. Voltage-current relation in single electroplaque of *Raia ocellata*. Hyperpolarizing currents (*B*) produced proportional changes in membrane potential as seen in graph above. Depolarizing currents (*A*) at first caused large changes in membrane potential, although not proportional to the higher values of currents (*crosses in graph*). During the applied current the membrane potential declined to a low value (*dots in graph*). Note that onset of the decline was more rapid with stronger currents. From Grundfest and Bennett, 1961. Reproduced by permission of the Elsevier Publishing Company.

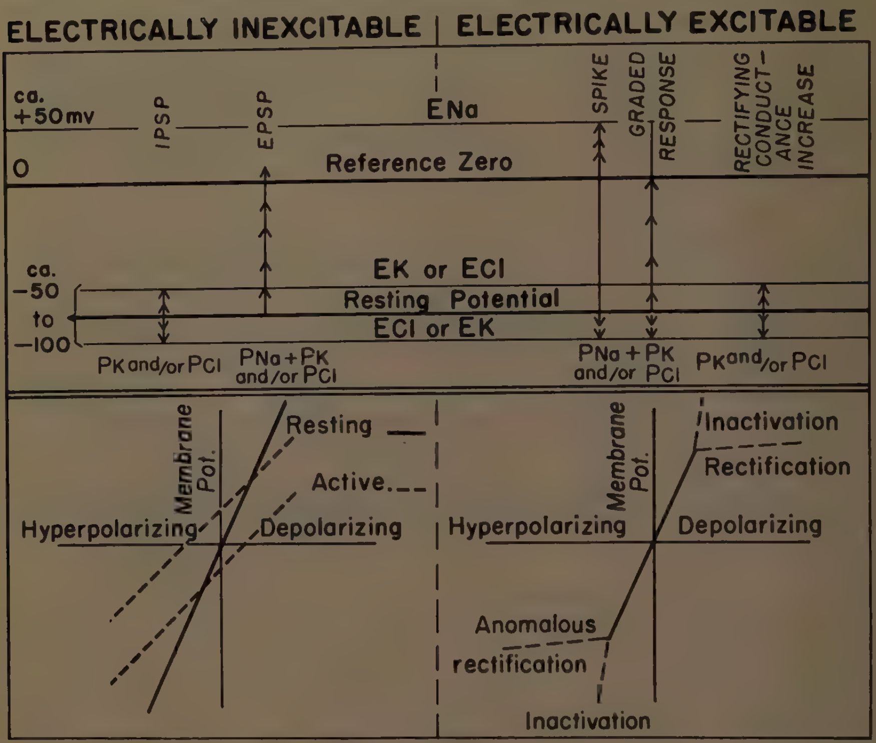

FIGURE 8. Diagrammatic summary of the components of activity of electrogenic membranes. (*Upper part*) The different varieties of electrogenesis and their probable ionic mechanisms. The resting potential is represented as lying between E_K and E_{Cl} the electrode potentials for K and Cl respectively. The electrode potential for Na (E_{Na}) is about 50 mv positive to the reference zero. The membrane reaction (transducer action) to an appropriate stimulus can change its permeability to one or to several ionic species. In electrically excitable as well as electrically inexcitable membrane, increase in permeability toward K or Cl, or both ions, leads to a small electrical effect, its sign depending on the relation of the resting potential to the electrode potential(s) of the relevant ion(s). The graded nature of the electrogenic processes is indicated by the multiple arrowheads. The excitatory synaptic membrane also produces a graded response, but depolarizing by virtue of a component for increased Na-conductance. The e.p.s.p. conceivably may overshoot the reference zero. Depolarizing graded responses can also be produced by electrically excitable membrane and, if P_K and/or P_{Cl} outlast P_{Na} and stand in appropriate electrochemical relation to the resting potential, the activity may also develop an "undershoot." Membrane capable of all-or-none responses may also develop an undershoot after the depolarizing conductance component has subsided. (*Lower part*) Current-voltage relations of the membranes disclose further features. (*Left*) The electrically inexcitable membrane has a linear I-E curve (*solid line*). When the membrane is excited by an appropriate stimulus the slope decreases, reflecting the increased conductance described above. The e.p.s.p. displaces the I-E curve (*broken line*) in a positive direction. The i.p.s.p. is shown as hyperpolarizing. The values at which each active line crosses the resting is the reversal point of the p.s.p.; on depolarization for the e.p.s.p. and on hyperpolarization of the hyperpolarizing i.p.s.p. (*Right*) The I-E relations of electrically excitable membrane show various nonlinearities. Changes causing increased conductance to depolarizing and hyperpolarizing currents are termed rectification and "anomalous" rectification respectively. Membrane reactions that result in increased resistance are termed depolarizing and hyperpolarizing inactivation. See FIGURE 10 for a complex curve showing a number of the components. FIGURE 9 shows another effect, pharmacological K-inactivation denoted by increase in resting resistance, while the associated loss of K-electrode property is seen in FIGURE 11.

The voltage-current relations of excitable membranes reveal further details of the action components. The I-E relation is ohmic, and rectification or nonlinearities of other types are absent, in electrically inexcitable membranes, such as those of electroplaques of marine electric fishes (Bennett *et al.*, 1961; Bennett and Grundfest, 1961*b*, 1961*c*; Grundfest and Bennett, 1961). In electrically excitable membranes rectification may be manifested by decreased conductance as well as by its increase, and both may be caused by hyperpolarizing as well as by depolarizing currents. These effects will be discussed in some detail below.

Pharmacological differences of homologous components in different tissues. Some other distinctive properties are also recognizable by the different behaviors of various cells which are treated with the same agent. Block of K-activation in *Onchidium* neurons by TEA (FIGURE 6) does not affect the resting resistance of the cell (Hagiwara and Saito, 1959). Furthermore, the resistance during the plateau of the prolonged spike is about like that of the resting membrane, or somewhat lowered, in contrast to the increased membrane resistance during the plateau of spikes in cardiac muscle (Weidmann, 1956), or to the markedly decreased resistance during prolonged spikes in insect (Werman *et al.*, 1961) and lobster muscles (Werman and Grundfest, 1961; Reuben *et al.*, 1960*a*). The effect of TEA on *Onchidium* neurons is thus similar to its action on squid giant axons (Tasaki and Hagiwara, 1957; Tasaki, 1959*a*). However, while in the neurons the drug is effective when externally applied, it must be injected into squid axons in order to prolong their spikes.

In contrast to its action on *Onchidium* neurons and squid giant axons, TEA increases the resting membrane resistance in arthropod muscle fibers (Belton and Grundfest, 1961; Werman and Grundfest, 1961) due to pharmacological K-inactivation. This action, which is associated with conversion of the normally gradedly responsive electrically excitable membrane to one producing spikes, is also shared (FIGURE 9) by the alkali earth ions (Grundfest *et al.*, 1959; Fatt and Ginsborg, 1958; Fatt and Katz, 1953*b*; Werman *et al.*, 1961; Werman and Grundfest, 1961). However, conversion of graded responsiveness to all-or-none excitability can be independent of the effect on the resting membrane resistance, as demonstrated (FIGURE 10) by the action of procaine on crustacean muscle fibers (Reuben and Grundfest, 1960; Girardier, Reuben, and Grundfest, unpublished).

Although crayfish-muscle fibers have many properties in common with the muscle fibers of lobster (FIGURE 10), in other respects, however, they differ profoundly. One manifestation is provided by the different reactions of the muscle fibers to high Ca^{++}. In lobster preparations this ion has the same action as does Ba^{++} or Sr^{++}, on both kinds of muscle fibers (Fatt and Ginsborg, 1958; Werman and Grundfest, 1961) increasing their resting membrane resistance. In crayfish, however, the application of Ca^{++} to the muscle fiber decreases their resistance to hyperpolarizing currents and increases the resistance to depolarizing currents (Girardier *et al.*, unpublished). Another difference, already noted, is the absence of a hyperpolarizing response in crayfish muscle fibers, whereas this is a common feature in lobster muscle fibers (cf. below).

K-electrode property. When the resting membrane acts as a K-electrode the resting potential is diminished by about 58 mv for a 10-fold increase of external

K$^+$ according to the Nernst relation $E = 58$ mv $\log K^+_i/K^+_0$. Lobster muscle fibers normally exhibit an average slope of 54 mv/decade (K^+_0), but when treated with alkali-earth or onium ions (FIGURE 11) their sensitivity to external K$^+$ diminishes markedly (Werman and Grundfest, 1961) as a manifestation of pharmacological K-inactivation. TEA likewise "protects" toad nerve fibers (Tasaki, 1959*a*) as well as frog axons (Lüttgau, 1960) against depolarization by high external K$^+$ (FIGURE 11). The role of alkali-earth ions is also emphasized in the effects of external Ca^{++} on the K$^+$-sensitivity of eel electroplaques (FIGURE 12). When the uninnervated surface of the electroplaque is exposed to high K$^+$ the resting potential changes by 35 mv/decade (K^+_0) which indicates that this membrane is an effective K-electrode, since the opposite surface remains at its normal electrochemical condition. The electrode property is exhibited even in the presence of 12 mmole/l. Ca^{++}, twice the normal concentration. The innervated surface, however, fails to respond to a 100-fold change in external K$^+$, when the bathing solution contains the normal concentration of

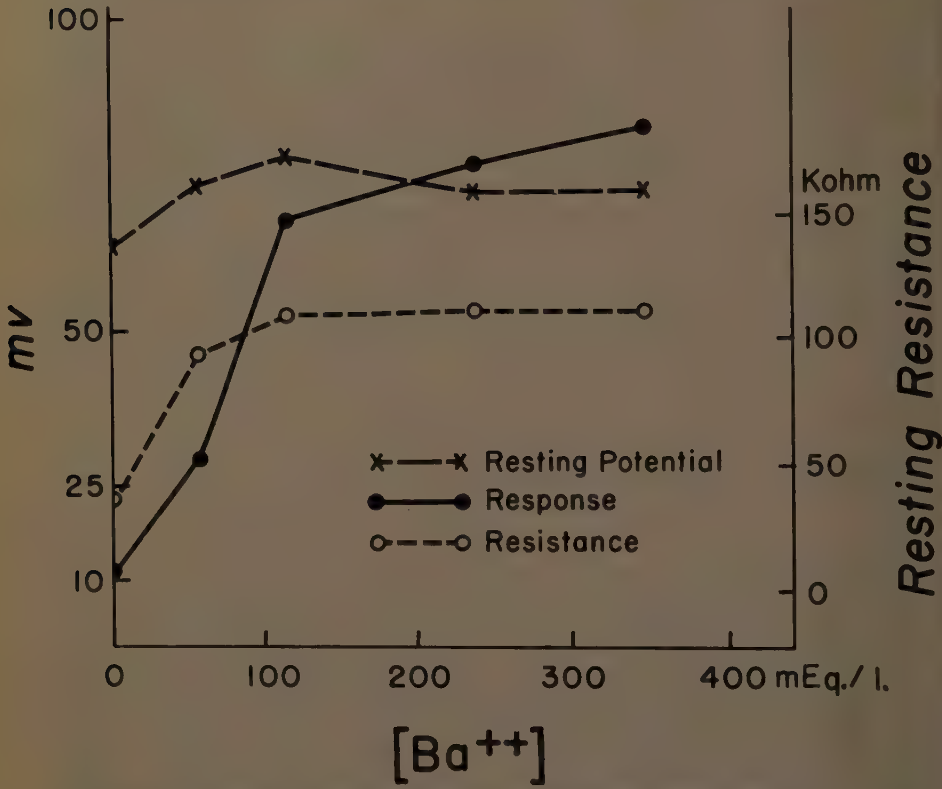

FIGURE 9. Changes in various membrane properties caused by applying Ba^{++} to muscle fibers of lobster. The resting potential increased as did the membrane resistance and response amplitude. The response became all-or-none in the presence of 100 mEq./l. Ba^{++}, and developed an overshoot with the application of higher concentrations of Ba^{++}. From Werman and Grundfest, 1961. Reproduced by permission of the *Jour. of Gen. Physiology.*

Ca^{++}. When the Ca^{++} is decreased to 1 mmole/l. the innervated membrane then also becomes an effective K-electrode. Thus different surfaces of a single cell may have different sensitivities for pharmacological K-inactivation.

The nodal membrane of frog nerve fibers appears to vary in its K-electrode properties (Stämpfli, 1959). In fibers considered to be in the best condition, the resting membrane resistance is high. The fiber depolarizes only slowly when the external K^+ is increased markedly (FIGURE 13), and application of a small inward current to a depolarized axon reverses the depolarization. Thus the presence or absence of K-electrode capacity in the excitable membrane is time dependent as well as a function of the membrane potential.

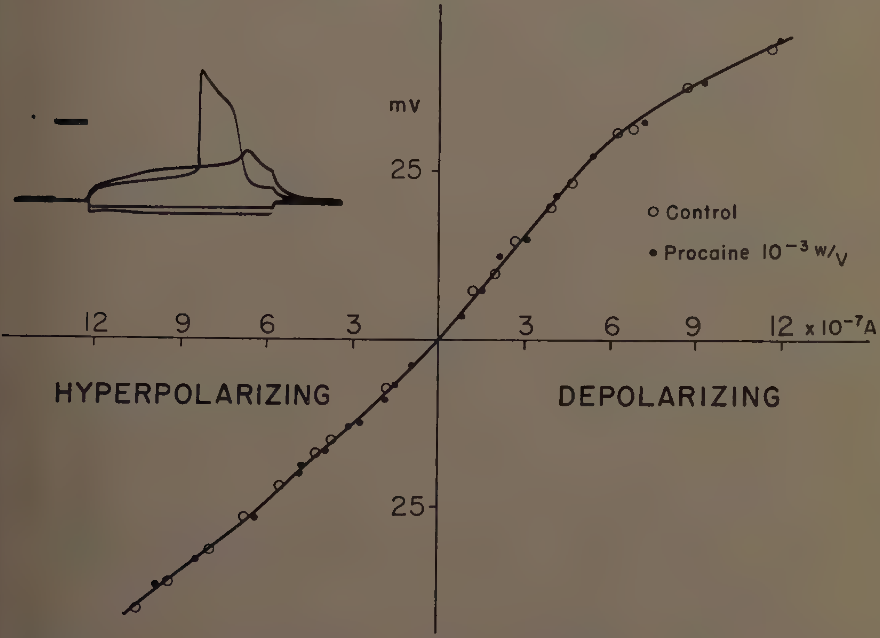

FIGURE 10. Conversion of graded to all-or-none responsiveness without alteration of membrane resistance or resting potential. Crayfish muscle fiber. (*Inset*) Superimposed records of intracellularly applied depolarizing currents (*two traces; downward deflections*) and of the resulting responses (*traces with upward deflection*). Before applying procaine, the larger current evoked a small late potential that was the maximal graded response of the fiber. After applying procaine, the weak stimulus evoked a spike that had a characteristic long time course and plateau. Calibration 50 mv and 100 msec. The graph shows that the complex I-E relation of the same muscle fiber was not affected by procaine (Girardier, Reuben, and Grundfest, unpublished).

Crayfish muscle fibers also exhibit a curious relation of membrane potential to external K^+ (Girardier *et al.*, 1961). The initial phase of insensitivity to K^+, also seen in many other tissues whether the concentration of the ion is increased externally (Hodgkin, 1951) or internally (Grundfest *et al.*, 1954) is followed in crayfish muscle fibers by a phase in which the slope is about 100 mv/decade K^+ (FIGURE 14). The data indicate therefore that the membrane acts as an electrode for at least two ions. It seems likely from a number of findings that cannot be discussed here that the high resistance membrane of crayfish muscle fibers is normally a Cl-electrode, shifting to one for K+ on soaking with high K+ solutions. The membrane conductance increases concomitantly with the depolarization. To some extent therefore, crayfish muscle fibers resemble frog axons in their electrical properties (Hodgkin and Horowitz, 1959).

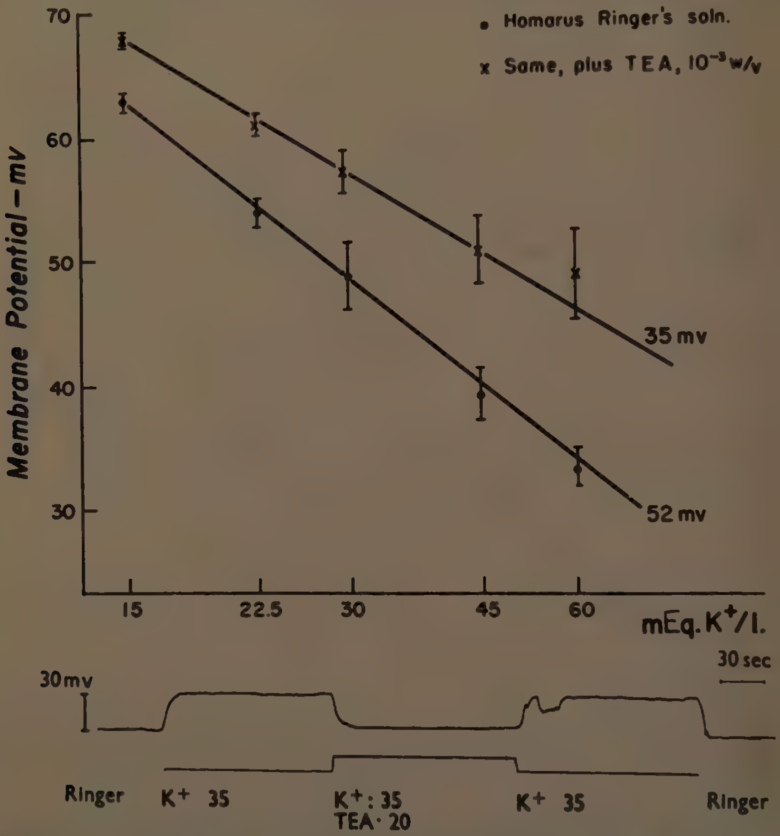

FIGURE 11. Change in K-electrode properties on applying TEA. (*Graph*) A lobster muscle fiber became less responsive to increased external K+, the slope changing from 52 mv to 35 mv/decade change of K_0 (modified from Werman and Grundfest, 1961, and Tasaki, 1959*a*). Reproduced by permission of the Journal of General Physiology. (*Records below*) A toad axon depolarized by 35 mEq./l. K+ was repolarized on changing the solution to one also containing 20 mEq./l. TEA. From Tasaki, 1959*a*.

Delayed rectification. In most types of electrically excitable membranes there is, of course, an initial increase in conductance caused by Na-activation, which is followed by a more slowly rising, more persistent high-conductance phase due to K-activation (Hodgkin and Huxley, 1952). This effect is believed to be responsible for "delayed rectification" (Cole, 1941), the persistent increased conductance during applied depolarizing currents.

As already noted, depolarizing conductance increases also occur in "electrically inexcitable" cells that do not have a Na-conductance component, and the response may be due not only to K-activation but to Cl⁻-activation as well. K-activation appears to be operative in frog slow muscle fibers (Belton and Grundfest, unpublished). The conductance increase, which may be generated by an e.p.s.p. or by applied currents, outlasts the stimulus by as much as 500 msec. (FIGURE 15), and this phase is associated with hyperpolarization. The potential becomes larger when the preparation is bathed in K-free Ringer's solution, and may be eliminated in a high K⁺ medium. It is not affected by removing the external Cl⁻.

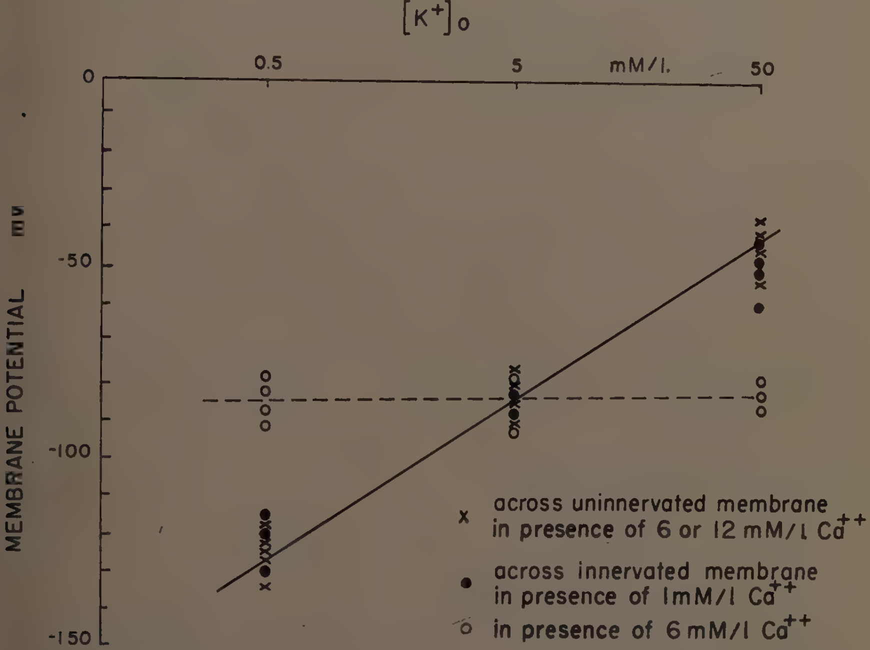

FIGURE 12. Different electrode properties of innervated and uninnervated membranes of eel electroplaque. In the presence of normal concentration of Ca^{++} (6 mmole/l.) the potential of the innervated surface did not change when K^+_0 was changed 100-fold, but the membrane became a K-electrode on decreasing the Ca^{++} to 1 mmole/l. The uninnervated membrane was a K-electrode even in 12 mmole/l. Ca^{++}. Modified from Schoffeniels, 1959.

In *Raia* electroplaques, however, the conductance increase (FIGURE 7) is associated with a slight afterdepolarization, which is unaffected by changing the external K-concentration. The depolarization increases in a Cl-free medium and, to such an extent indeed, that the conductance increase may become regenerative, giving rise to a small all-or-none "spike" (Bennett, elsewhere in these pages). It therefore seems likely that the conductance increase in *Raia* electroplaques is due to Cl-activation (Cohen *et al.*, 1961).

The rectifying phenomena of the muscle fibers and *Raia* electroplaques are the electrically excitable counterparts of the electrically inexcitable responses of inhibitory synapses, both being characterized by the absence of a conductance change for a depolarizing ion (FIGURE 8). The occurrence of K- or Cl-activation independently of Na-activation indicates that in the electrically excitable membranes, as well as in those electrically inexcitable, the processes involving different ion conductance systems may have come to assort randomly in the process of evolution.

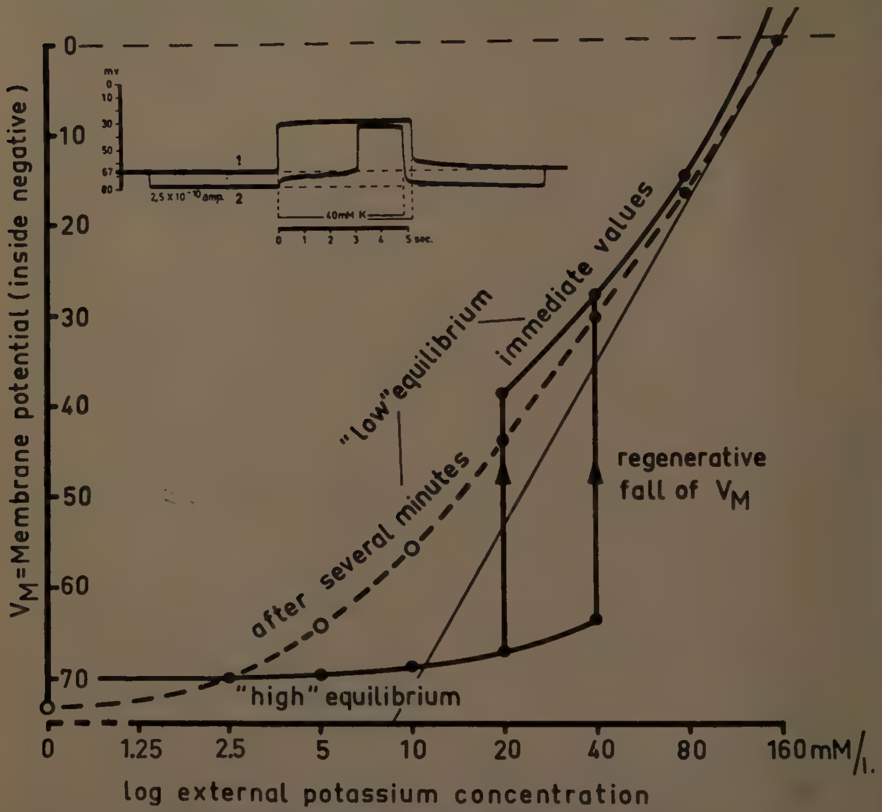

FIGURE 13. K-electrode property of frog axon. (*Inset*) Depolarization was rapid on applying 40 mmole/l. K (record 1), but developed slowly and then rapidly (regeneratively) when the axon was hyperpolarized (record 2). (*Graph*) The dots and heavy solid line shows the membrane potentials during the first minute or so after applying solutions high in K^+. In the range of 20 to 40 mmole/l. K^+ the potential decreased gradually to the "low" equilibrium but could be reversed to the "high" state by hyperpolarizing currents. The circles and broken line show the potential some minutes after the membrane had been exposed to the changed external K^+. The thin line has a slope of 58 mv/decade change in K^+_0. Modified from Stämpfli, 1959.

A pharmacological distinction has been observed between the repolarizing transducer actions of synaptic and electrically excitable membranes. Delayed rectification is eliminated in frog slow muscle fibers (Belton and Grundfest,

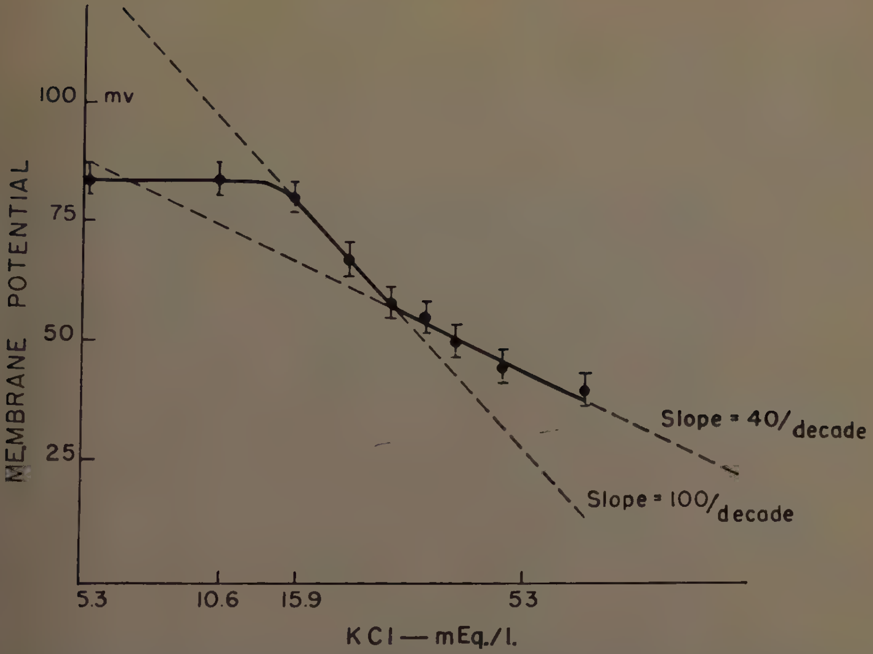

FIGURE 14. Changing electrode properties of crayfish muscle fiber. Continuous line describes the membrane potential (average of 10 fibers) as the external K^+ was increased. The concentration of K in the standard crayfish Ringer's solution was 5.3 mEq./l. The membrane was insensitive to a 4-fold increase in external K^+, then depolarized rapidly (slope = 100 mv/decade increase of K^+) and subsequently more slowly (slope = 40 mv/decade increase of K^+). The broken line with the lower slope also shows the relation which obtains when the preparation is first soaked in high K^+. The bars represent twice the standard deviation of the mean (Girardier, Reuben, and Grundfest, unpublished).

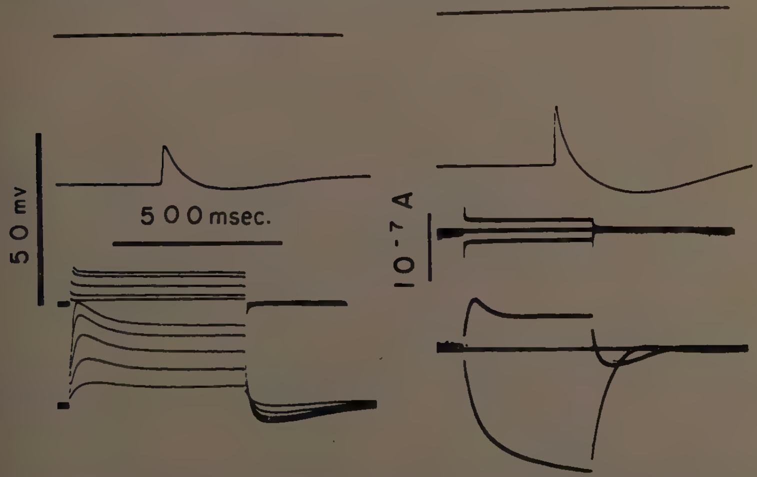

FIGURE 15. Delayed rectification of frog slow muscle fiber. (*Left*) Preparation in norma saline containing 2 mmole/l. K^+. (*Right*) In saline with zero external K^+. (*Upper records*) The e.p.s.p. was increased in the K^+-free solution because of the increased membrane resistance of the muscle fiber. It was shortened by the larger amount of undershoot resulting from electrogenesis associated with the conductance increase of delayed rectification. (*Below*) The hyperpolarizing undershoot following depolarizing pulses was also considerably larger in the K^+-free than in the normal medium. The depolarizing rectification was initiated at a very low depolarizing voltage, as is denoted by the difference between the potential developed on applying the current in either direction. From Belton and Grundfest, unpublished.

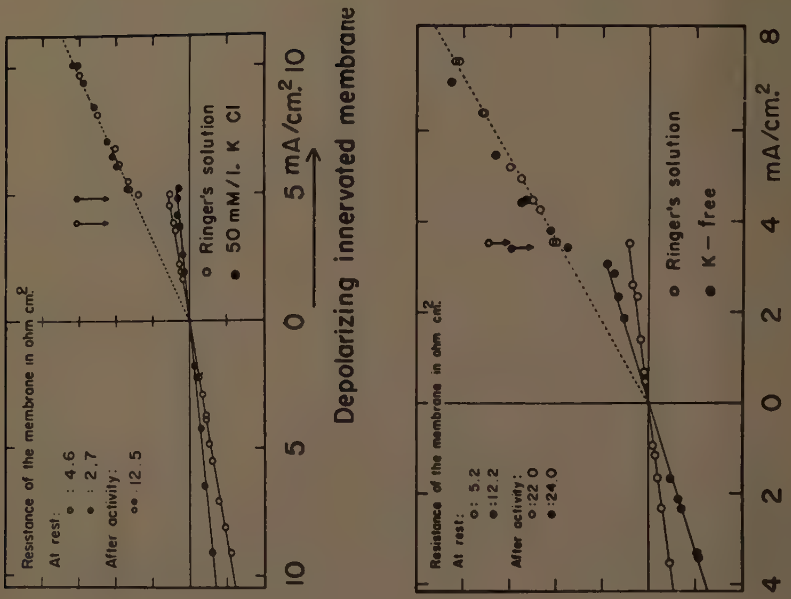
Resistance of the membrane in ohm cm²
At rest:
○ : 4.6
● : 2.7
After activity:
○● : 12.5
○ Ringer's solution
● 50 mM/l. K Cl
10
5
0
5 mA/cm² 10
Depolarizing innervated membrane
Resistance of the membrane in ohm cm²
At rest:
○: 5.2
●: 12.2
After activity:
○: 22.0
●: 24.0
○ Ringer's solution
● K – free
4
2
0
2
4 mA/cm² 8

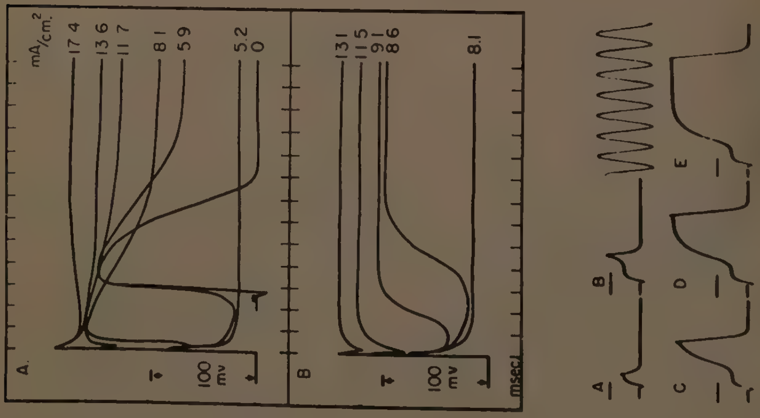
A
mA/cm²
17.4
13.6
11.7
8.1
5.9
5.2
0
100 mv
B
13.1
11.5
9.1
8.6
8.1
100 mv
msec
A
B
C
D
E

FIGURE 16. Depolarizing K-inactivation in eel electroplaques. (*Left*) Potentials across innervated membrane of a single cell recorded during one of the experiments. (*A*) A brief pulse (marked O) evoked a spike. The latter was also produced on applying a current of 5.9 mAmp./cm.^{2} to depolarize the innervated membrane. Note, however, that the terminal depolarization was much larger than with a subthreshold stimulus (5.2 mAmp./cm.^{2}). Stronger currents evoked the spike earlier and caused proportionately larger terminal depolarizations. The strongest current (17.4 mAmp./cm.^{2}) caused depolarization which exceeded E_{Na}, the potential showing a temporary reversal. (*B*) A similar series of experiments after the preparation had been placed in 50 mmole/l. K^+. Spikes were no longer evoked, and the rise in membrane potential, signifying increased membrane resistance, developed slowly. The early large deflections in both sets of records are due to capacitative artifacts. (*Below*, *A* to *E*) Time course of the delayed rise in potential shown by applying successively longer pulses at constant amplitude. (*Right*, *upper graphs*) An experiment like that of *A* and *B* on the left. The arrows indicate the threshold current for the spikes in the control saline solution and for the delayed inactivation process in the high K-solution. (*Lower graphs*) A similar experiment in the standard saline and in a K-free solution. Modified from Altamirano and Coates, 1957.

unpublished) and in *Ràia* electroplaques (Cohen *et al.*, 1961) when the cells are treated with Ba^{++}. The activity of the synaptic membranes is not affected, however, the cells continuing to respond to neural stimuli or to electrophoretic applications of acetylcholine. The transducer actions of the e.p.s.p.s in insect (Werman *et al.*, 1961) and lobster (Werman and Grundfest, 1961) muscle fibers are also unaffected by the alkali earth ions (FIGURE 2), while the electrically excitable components are modified considerably, as described below.

The existence of electrically excitable repolarizing conductance changes without a depolarizing Na-conductance component is clearly demonstrated in the "electrically inexcitable" frog slow muscle fibers and *Raia* electroplaques. However, there seems to be no reason to exclude the possibility that both types of electrically excitable membrane might exist side by side, just as do the excitatory and inhibitory synaptic membranes. This would result in an excess of repolarizing conductance change over the depolarizing and might account for some types of normally gradedly responsive cells, such as many invertebrate muscle fibers. In the absence of a depolarizing electrogenic component the repolarizing electrically excitable membrane can have only a limited role. By diminishing depolarizing e.p.s.p.s (Belton and Grundfest, unpublished) it might have an inhibitory effect on contraction of various muscle fibers, and might be the agent for "supplemental" inhibition described in crustacean muscle (Wiersma, 1961). In *Raia* electric organ, however, the conductance change has an "excitatory" effect in that it tends to maximize the external current (Bennett, elsewhere in these pages).

Depolarizing K-inactivation. Depolarization may also increase membrane resistance (FIGURE 8). This is a process of K-inactivation (Grundfest, 1957*d*) that is observed during application of depolarizing currents to eel electroplaques (FIGURE 16), even after Na-inactivation by depolarization had blocked spike activity (Altamirano and Coates, 1957). The increased membrane resistance is time and voltage dependent over only a small range of initial values and may develop as a result of the depolarization produced by the spikes itself (Altamirano, 1955).

Depolarizing K-inactivation probably also occurs in other cells. Interference with K-activation by pharmacological agents as well as depolarizing K-inactivation should both be manifested by prolongation of the falling phase of the spike. However, the two processes may be differentiated by the membrane resistance during the spike. In TEA-treated *Onchidium* neurons (FIGURE 6) the membrane resistance during the plateau of the prolonged spikes must have been lower than in the resting cell, since K-activation was only partially blocked, while Na-activation was affected even less. If TEA also increased the resting resistance as it does in arthropod muscle fibers (Werman and Grundfest, 1961), the prolonged spikes might conceivably also have a high resistance plateau.* Depolarizing K-inactivation, however, does increase the membrane resistance beyond its resting value. In eel electroplaques the rise occurs (FIGURE 16) to the same extent in cells initially depolarized by high K^+ and therefore are in a low resistance "state," or hyperpolarized and put into a high resistance state by removal of K$^+$. Since the time constant of eel electroplaques is small (Grundfest, 1957*d*), even passive decay of the spike potential is rapid and the spike is relatively brief.

---

* The effects of TEA and alkali earth ions in lobster muscle fibers are more complex and will be described below.

It is theoretically conceivable that different cells may differ in the relative kinetics of Na- and K-activation and inactivation, and these differences would then give rise to various grades of phenomena affecting the spike duration as well as the conductance changes during the spike. However, as with all the manifestations of the more complicated behavior of electrically excitable membrane the study of these possible manifestations is still in a rudimentary stage. Differences in kinetics of K-activation and inactivation may perhaps help to resolve a conflict of experimental findings in amphibian myelinated axons. Impedance measurements (Tasaki and Freygang, 1955) indicated that the falling phase of the spike does not have the high conductance that would result from K-activation. Voltage clamp experiments (Dodge and Frankenhaeuser, 1958), however, indicated presence of this factor. Since frog axons may occur in "high" and "low" resistance states, the former associated with low K-conductance (Stämpfli, 1959), a delay or absence of K-activation in some preparations and its presence in others might be expected.

Only the rising phase and a part of the falling phase of the spikes of electroplaques of *Sternopygus* and *Eigenmannia* are accompanied by increased membrane conductance (Bennett, elsewhere in this publication). These data indicate that the transducer actions of their electrically excitable membrane involve rapid Na-inactivation, a phase of depolarizing K-inactivation, and a much delayed K-activation. A slightly different kinetic sequence can account for the prolonged spikes of cardiac muscle fibers (Grundfest, 1957*a*). There is probably a prolonged phase of heightened Na-conductance, as well as depolarizing K-inactivation, and a later K-activation that terminates the potential (FIGURE 17).*

Another example may be observed from FIGURE 16. Depolarization by excess external K$^+$ presumably caused some increased K-conductance, since the depolarized electroplaques have a low resistance. The relation of this conductance increase to the decrease caused by further depolarization remains to be studied, but the data suggest some threshold for the depolarizing K-inactivation.

Hyperpolarizing K-inactivation. In some cells a threshold for hyperpolarizing K-inactivation does exist and gives rise to hyperpolarizing responses. These occur only on prior depolarization of squid (Segal, 1958; Moore, 1959; Tasaki, 1959*a*), frog (Mueller, 1958; Stämpfli, 1959; Lüttgau, 1960), or toad

---

* The shortening of the cardiac spike by acetylcholine (Cranefield and Hoffman, 1958) may be a corollary effect (Grundfest, 1957*a*). Cardiac muscle has many areas that, although uninnervated, nevertheless exhibit high esterase activity (Ravin *et al.*, 1953). Presumably these regions represent cholinoceptive membrane whose activation would account for the high K-flux caused by this substance in cardiac muscle (Hutter, 1961). The chemically excited conductance increase probably occurs in an electrically inexcitable membrane component, as it does in denervated muscles (FIGURE 5), and thus would not be subject to depolarizing K-inactivation. The increased conductance accordingly would decrease the membrane time constant and shorten the falling phase of the spike. Acetylcholine has somewhat different degrees of effects on different parts of the heart muscle and this may reflect different relative densities of chemosensitive areas of membrane in the various regions of the muscle mass. The occurrence of uninnervated membrane was first suggested by Langley (1905).

(Tasaki, 1959*a*) axons. In lobster muscle fibers hyperpolarizing responses are manifested (FIGURE 18), starting from the normal resting potential of the membrane (Reuben *et al.*, 1959; Reuben *et al.*, 1960*a*), and the analysis of the events is thereby easier than in the other tissues. Hyperpolarizing responses without prior depolarization are observed in several kinds of electroplaques (Bennett and Grundfest, unpublished; Cohen *et al.*, 1961). They may also occur in *Noctiluca*, in which no resting potential has been observed (Chang, 1960).

In lobster muscle fibers the threshold is clearly recorded as a sudden change in the effective resistance of the membrane (FIGURE 19), and the magnitude of the resistance change is large, some 8- to 10-fold (FIGURE 20). The hyperpolarizing response is not affected by removing external Cl^-, nor is the equilibrium potential for the i.p.s.p. of lobster muscle fiber altered during hyperpolarizing responses. Thus the response probably does not involve a change of the membrane conductance for Cl^-. However, the hyperpolarizing response is eliminated in the presence of alkali earth or onium ions, the membrane resistance of the resting cell rising to the value it would have attained during the peak of the hyperpolarizing response (FIGURE 19). All these data therefore indicate that the increased membrane resistance is due to decreased conductance for K^+, a manifestation of hyperpolarizing K-inactivation (FIGURE 8).

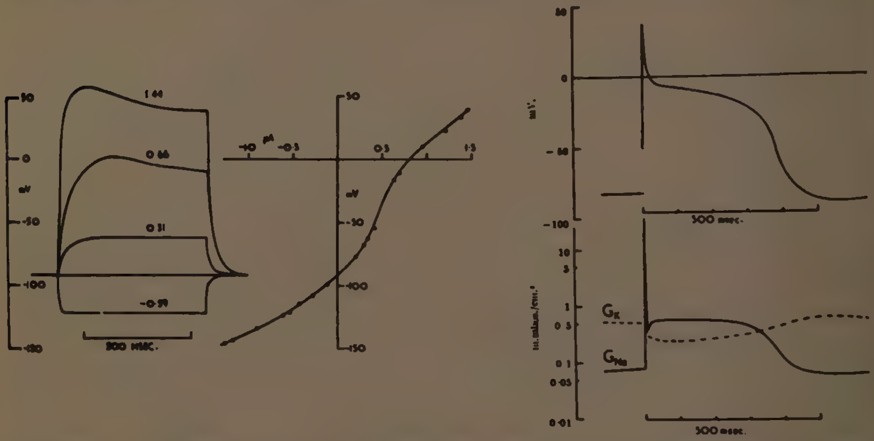

FIGURE 17. K-inactivation and prolonged response of Purkinje fibers of sheep. (*Left*) Records and graph of current-voltage relation in Na^+-free saline solution. Note that depolarizing K-inactivation in medium range of depolarizing current is more extreme than that in the crayfish muscle fiber of FIGURE 10. (*Right*) Cardiac spike calculated on basis of Hodgkin-Huxley equations modified to include continued Na-influx (G_{Na}) and a diminished K-conductance (G_k) followed by delayed increase. Modified from Hutter and Noble, 1960, and Noble, 1961.

The pulse phase of the hyperpolarizing response can be initiated by a small brief hyperpolarizing pulse superimposed on a background hyperpolarization not itself strong enough to evoke the response. It then demonstrates further complexities in the effects of hyperpolarizing currents (FIGURE 21). The different time courses of the onset and subsidence of the pulse and the relative depolarization after the pulses are then clearly evident. These features and the relative refractoriness of the membrane after a conditioning hyperpolarizing response may seem to justify the interpretation (Spyropoulos and Tasaki, 1960; Tasaki, 1959*a*) that the nature of the membrane generator changes when the response occurs. A change does occur, but probably as a complex series

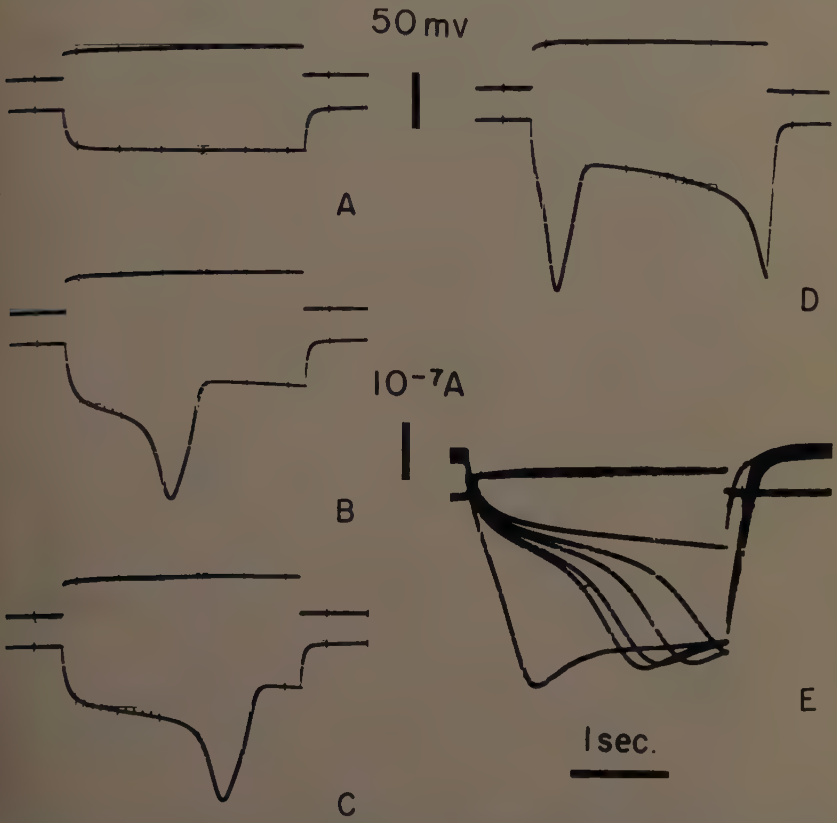

FIGURE 18. Hyperpolarizing responses in lobster muscle fiber. (*Upper trace*) Monitor of intracellularly applied hyperpolarizing current. (*Lower trace*) Membrane potential. (*A*) Current subthreshold for response. (*B* and *C*) Hyperpolarizing responses at threshold show first a slow increase in negativity, then a regenerative rise, and its subsidence to a value less negative than at the start of the hyperpolarizing response. (*D*) A stronger current caused earlier onset of the pulse phase and a second pulse developed before the current was terminated. (*E*) Six superimposed records showing variations of responses (Reuben, Werman, and Grundfest, unpublished).

of effects leading to a marked decrease in K-conductance. This change may be an electrogenic activity under appropriate conditions (FIGURE 28). In the hyperpolarizing response of lobster muscle fibers and probably of several other tissues the change manifests itself electrically as a change in membrane polarization due to an increased IR drop across the membrane during an applied current.

The hyperpolarizing response of frog nodes may also be ascribed to a similar effect. However, while the normal lobster muscle fiber has a K-electrode membrane, that of the axon is relatively ineffective in that respect, but becomes a K-electrode on depolarization with prolonged applications of high K$^+$

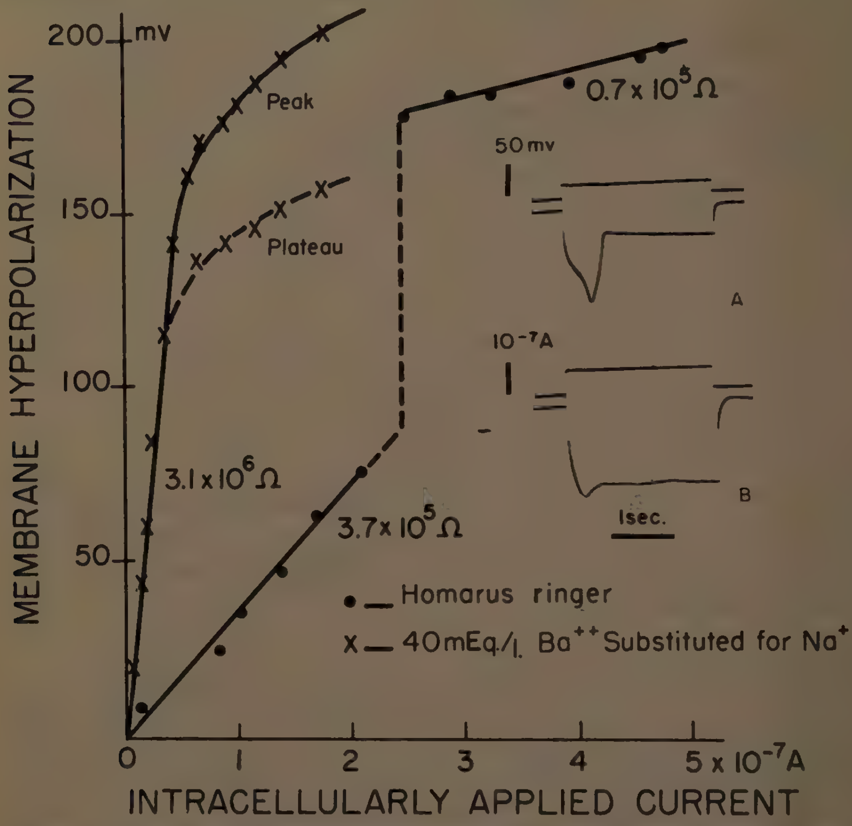

FIGURE 19. Abolition of hyperpolarizing responses of lobster muscle fibers by alkali-earth ions. (*Inset*) Records of hyperpolarizing response in *Homarus* saline (*above*) and its absence in a high-Ca^{++} medium. (*Graphs*) Current-voltage curves for another muscle fiber in the normal Ringer's medium (*dots*) and in a high Ba^{++}-medium (*crosses*). Development of a hyperpolarizing response in the Ringer's solution is denoted by the sudden rise of the peak membrane hyperpolarization when the applied current exceeded about 2.5×10^{-7} A. Note that higher currents caused relatively little further change in the peak potential, indicating a low dynamic resistance. On applying Ba^{++} the effective resistance increased nearly ninefold, and a hyperpolarizing response did not develop. Higher currents produced lower additional hyperpolarizations both in the early peak and in the plateau, indicating that the hyperpolarizing conductance increase was still present (Reuben, Werman, and Grundfest, unpublished).

(FIGURE 13). The latter is the condition under which hyperpolarizing responses are elicited in frog nodes (FIGURE 22). The depolarized membrane is shifted back from its state of low resistance to its initial electrode state and high resistance condition when high inward currents are applied. It is interesting to note in this connection that crayfish muscle fibers, which have a high resting resistance in contrast to lobster muscle fibers, and poor responsiveness as K-electrodes (FIGURE 14) do not exhibit a hyperpolarizing response.

Increased conductance during and after hyperpolarization. "Anomalous rectification" (Katz, 1949) and "anodal breakdown" (Hodgkin, 1947) reflect an increased membrane conductance that occurs under various conditions in many cells when they are hyperpolarized. The increase occurs during and after hyperpolarizing responses of *Noctiluca* (Chang, 1960), squid axons (Tasaki, 1959*a*), frog nodes (Lüttgau, 1960, his FIGURE 2), and of lobster muscle fibers (FIGURE 23). In the latter the increase is manifested even when the response

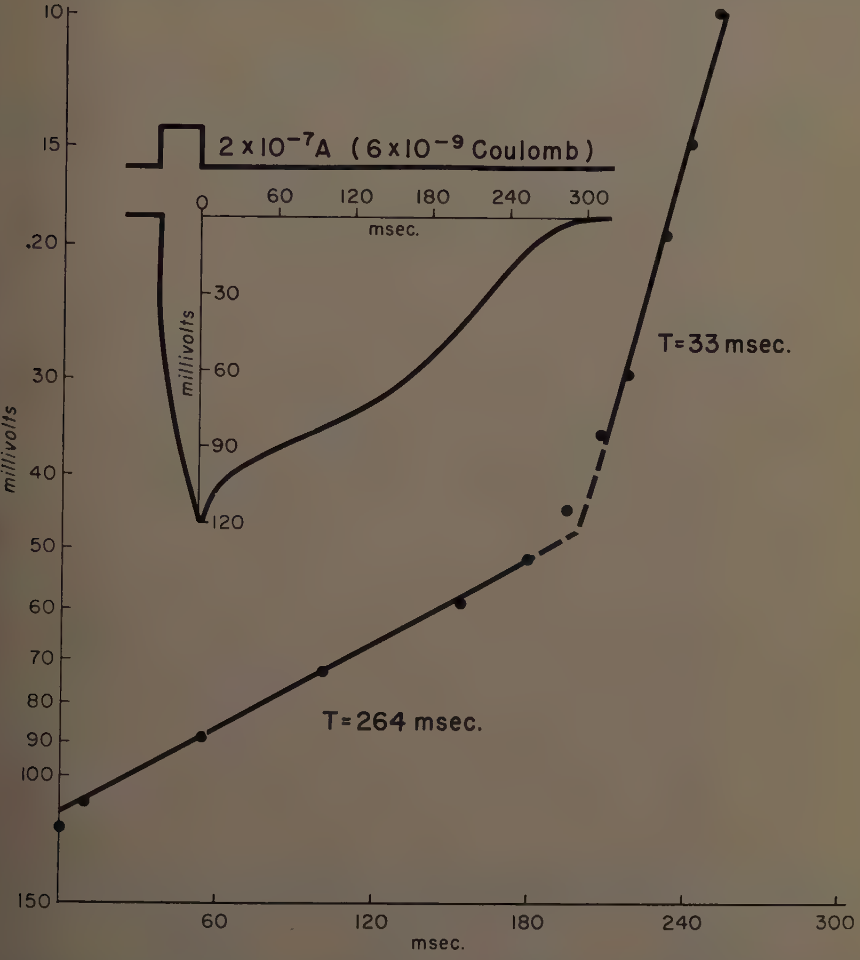

FIGURE 20. Magnitude of increase in membrane resistance during the peak of a hyperpolarizing response. The latter (*inset record*) was evoked by a brief pulse. The time constant of the passive decay of the potential initially was eight times higher than in the the later phase, indicating that the membrane resistance was at least eightfold higher during the initiation of the hyperpolarizing response (Reuben, Werman and Grundfest, unpublished).

is abolished by alkali-earth ions (FIGURE 19). It is time-dependent to some extent, so that the hyperpolarization has an early peak and a less negative plateau. It also occurs in crayfish muscle fibers, which do not produce hyperpolarizing responses (Girardier *et al.*, unpublished).

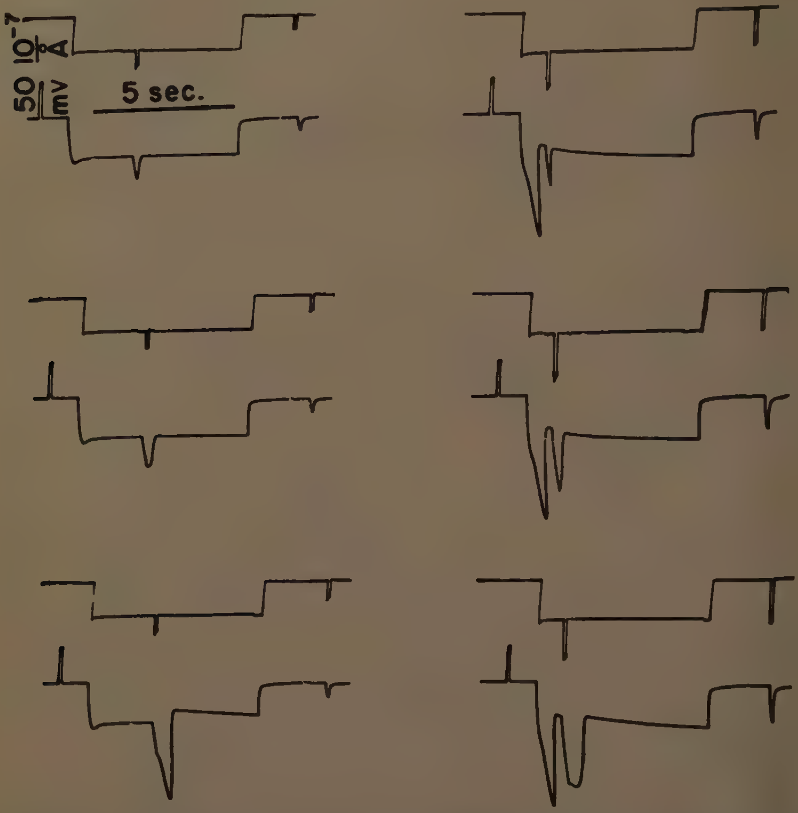

FIGURE 21. Regenerative development of hyperpolarizing response and subsequent graded changes. Ink writer records, upper trace of current; lower of membrane potential. (*Left*) A brief hyperpolarizing pulse was applied during a weak longer-lasting current. Note (*middle record*) a graded response indicated by the prolonged duration of the brief hyperpolarization. A slightly stronger pulse (*lower record*) evoked a full hyperpolarizing response. Its pulse phase was succeeded by a marked decrease in membrane negativity. (*Right*) A stronger prolonged current evoked a hyperpolarizing response. Testing pulses evoked various degrees of graded responses (Reuben, Werman and Grundfest, unpublished).

The amount and duration of the conductance increase that persists after withdrawal of the current is dependent on the applied current, indicating that the change is voltage operated, like the Na- and K-conductance changes during the spike, or the conductance decreases of K-inactivation. Strong hyperpolarizing currents cause a change that persists for more than a minute (FIGURE 23). The change occurs (FIGURE 19) independently of and superimposed on the K-inactivation, which initiates the hyperpolarizing response. The combination of the two factors therefore can give rise to the pulselike form of the latter, as well as to the tendency to oscillatory hyperpolarizing responses.

The relative depolarization that occurs when the pulse of a hyperpolarizing response terminates during an applied current (FIGURES 18 and 21) has its parallel as an absolute depolarization after prolonged hyperpolarizing currents (FIGURE 23). Since the conductance change is very large at this time, depolarization due to Na-activation might be expected to drive the membrane into a regenerative activity. However, the changes are not due to increased Cl-conductance, since the E_{IPSP} in these fibers is usually hyperpolarizing to the resting potential. It is perhaps possible that simultaneous conductance increases

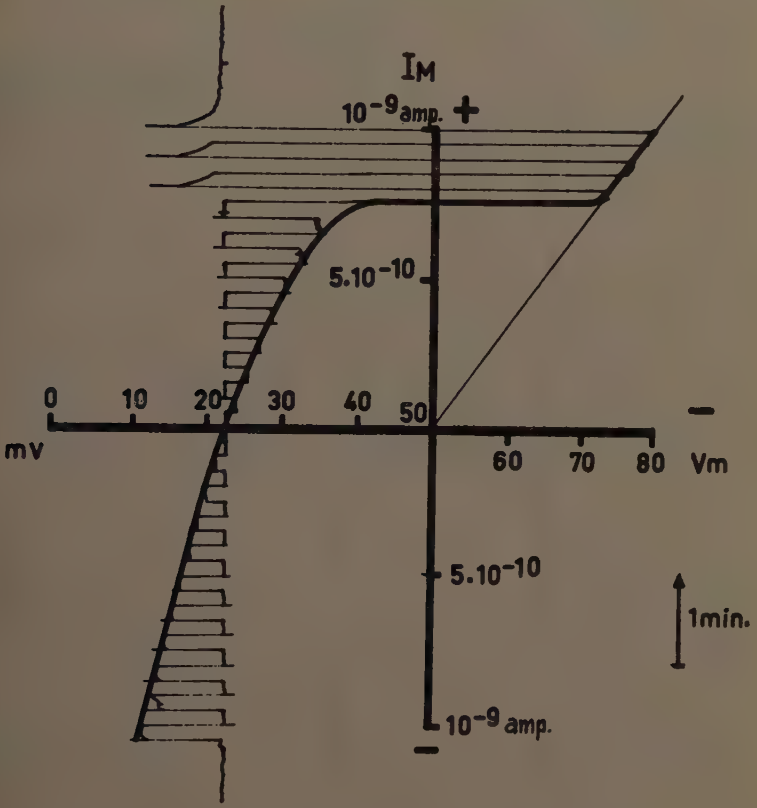

FIGURE 22. Hyperpolarizing responses in frog axon. The origin of the graph is the measured membrane potential in the absence of polarizing currents, that is, a fraction of the true resting potential. The fiber was depolarized in 40 mmole/l. K^+. Beginning with strong depolarizing current at the bottom of the graph, currents were applied at regular intervals (time in upward direction). The heavy line connects the value of the membrane potential. When hyperpolarizing currents exceeded about 5×10^{-10} A there was at first a gradual then a sudden increase in membrane polarization. The thin line connects the experimental values during the peak of the hyperpolarizing responses evoked by currents of above 8×10^{-10} A. The line extrapolates approximately to the initial resting potential. Modified from Stämpfli, 1959.

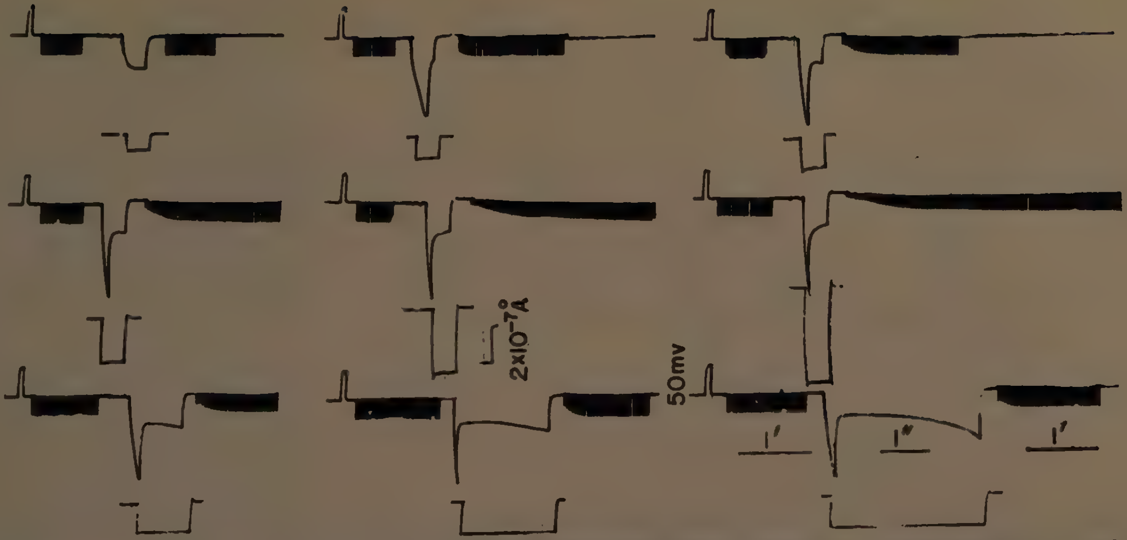

Figure 23. Increased membrane conductance after hyperpolarizing responses of a lobster muscle fiber. Ink-writer records. Each trace registered at two sequences of chart speeds. (*Initial fast*) Calibrating pulse of 50 mv; *slow*, a series of brief hyperpolarizing testing pulses of constant strength; *fast*, during which a hyperpolarizing current was applied; *slow*, during which the testing hyperpolarizing pulses were again applied. Below each of the recordings is also shown the monitoring record of the applied current. After a hyperpolarizing response was evoked (*middle record*, *upper row*) the membrane resistance remained lowered. As the stimulating current was increased the pulse of the hyperpolarizing response became shorter, the membrane resistance subsequently decreased further and remained low for longer times. The conductance change lasted more than 1 min. with the highest currents used (*middle row*). Note the small degree of after-depolarization associated with relatively large conductance changes. During prolonged hyperpolarizing currents (*lower row*) the membrane resistance began to rise, but after the current was withdrawn the membrane resistance fell below its resting value (Reuben, Werman and Grundfest, unpublished).

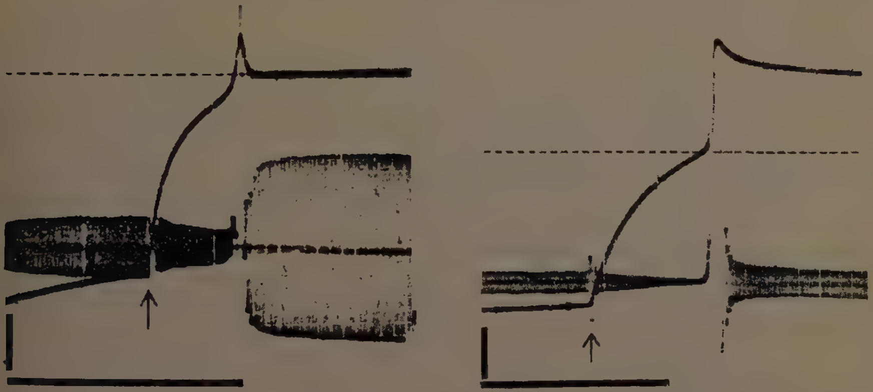

FIGURE 24. Changes in potential and conductance in squid axons after termination of hyperpolarizing currents. Simultaneous recordings of membrane potential and of imbalance of an AC bridge. (*Left*) Axon depolarized in 40 mmole/l. K^+. Record shows the termination of a hyperpolarizing current (*arrow*). The membrane potential returned with a brief depolarizing excursion during which the resistance fell greatly. The resistance continued low after the potential returned to its initial depolarized value (indicated by broken line). (*Right*) Another axon, injected with TEA. The depolarizing excursion after the hyperpolarizing current ended was much larger, developing an overshoot and a prolonged spike, characteristic of the TEA-treated axon. The membrane resistance during the plateau of this spike increased moderately after the initial large change associated with the rising phase. Calibrations 50 mv and 5 msec. Modified from Tasaki, 1959*a*.

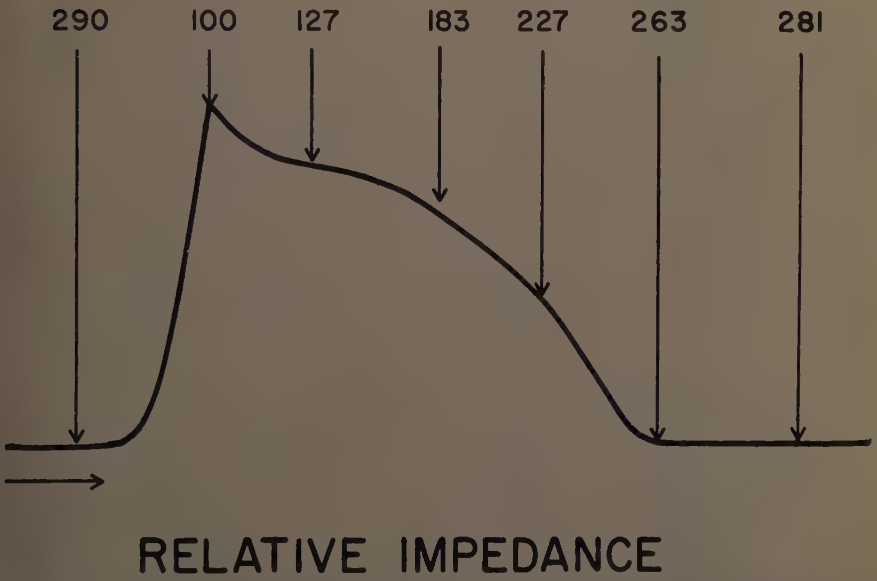

FIGURE 25. Resistance during prolonged spikes of Ba^{++}-treated lobster muscle fibers. Effective resistances are approximate, particularly at peak of spike when the length constant of the fiber is markedly decreased. The figure represents an average of 10 experiments with spikes of different durations. (Werman and Grundfest, 1961). Reproduced by permission of the *Journal of General Physiology.*

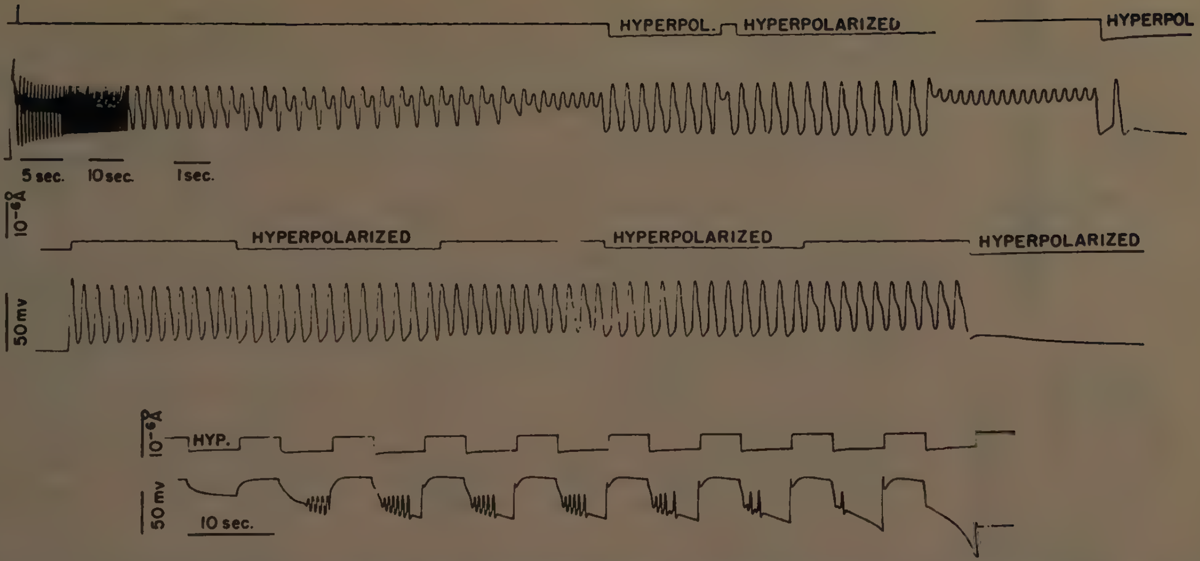

FIGURE 26. Spontaneous and induced oscillations during prolonged responses of lobster muscle fibers. Two experiments: ink-writer records; upper trace of intracellularly applied currents. (*Upper set*) A continuous sequence after a response had been evoked by a brief shock. The frequency of the spontaneous oscillations was slowed by hyperpolarizing currents. (*Lower set*) Impalement of the fiber caused a prolonged spike. The resting potential is seen at end of the train. In the course of the response hyperpolarizing currents caused changes in membrane potential which became progressively larger. Oscillations that developed during the applied currents ended as the membrane potential approached the resting value. Termination of the pulses led to break responses (as in FIGURE 24), but the long-term changes were in the direction of decreasing membrane conductance, so that hyperpolarizing responses tended to develop and one eventually terminated the sequence (Reuben, Werman and Grundfest, unpublished).

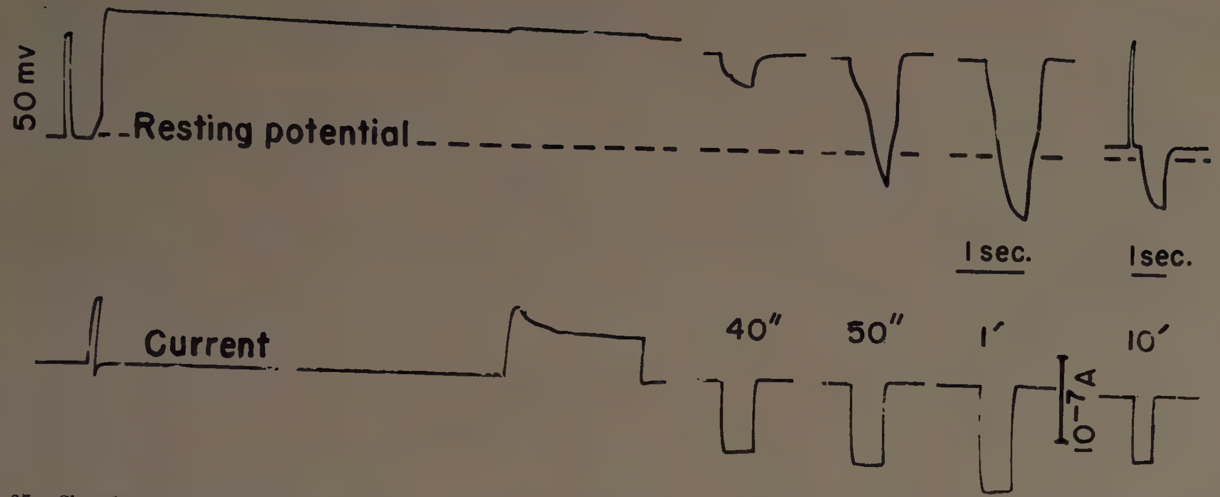

FIGURE 27. Slow decrease in membrane conductance during a prolonged response in a lobster muscle fiber. A large depolarizing current early during the response caused little change in membrane potential. Later the membrane resistance increased considerably, giving rise to augmenting hyperpolarizations which resemble hyperpolarizing responses. The "break-response" at the terminations of the current brought the potential to a slightly greater depolarization than before the pulses (Reuben, Werman, and Grundfest, unpublished).

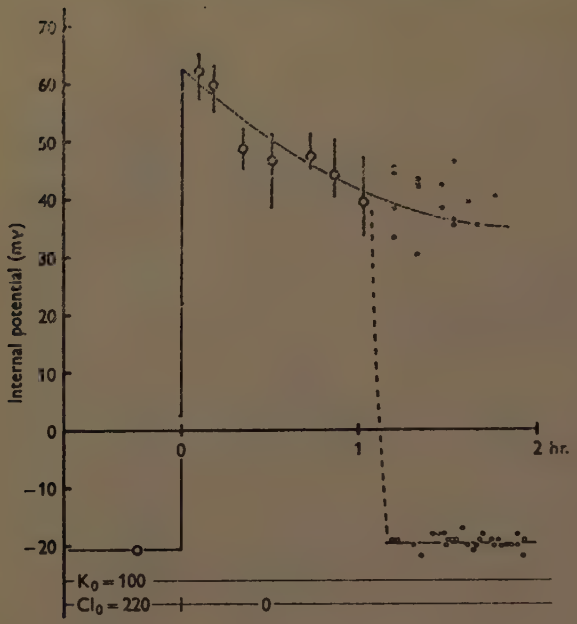

No. of fibres	Solution	Internal potential (mv, approx.)	λ (mm)	τ_m (msec)	r_m (Ωcm)	c_m (μF/cm)
9	Ringer's	−90	2·01	22·3	$12{\cdot}7 \times 10^4$	0·18
3	Solution F (100 mM-K, 0 mM-Cl, sulphate)	+40	3·37	32·6	$28{\cdot}7 \times 10^4$	0·11
3		−20	1·18	3·7	$3{\cdot}0 \times 10^4$	0·12

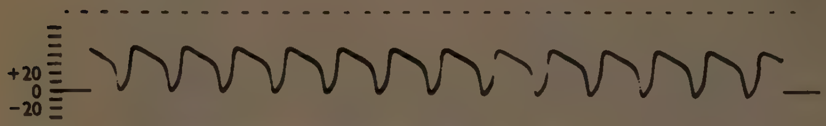

FIGURE 28. "Upside-down" responses and electrode changes in frog muscle fibers. At the beginning of the graph the preparation, soaked in a high K, high Cl medium had a resting potential of −20 mv. On changing to a Cl-free, high K medium the membrane potential became inside positive and acted as a Cl-electrode, reflecting the larger internal Cl$^-$. This was associated with a large rise in membrane resistance (TABLE 1) indicating that its K-conductance was greatly diminished. A change between low and high K-conductance which was correlated with "upside-down" oscillatory potentials (records) took place subsequently. Note changes in length constant (λ) and time constant (τ_m) that are associated with changes in membrane resistance (r_m) while the membrane capacity (c_m) remains nearly constant. Modified from Adrian, 1960.

for both Na^+ and Cl^-, or for Na^+ and K^+ are involved. These could give rise to a large net increase in conductance and only a small depolarization (Grundfest, 1957*d*).

The terminations of the hyperpolarizing responses in squid and toad axons (Tasaki, 1959*a*) appear to have somewhat different properties from those in lobster muscle fibers and the events in the two axons also differ one from the other. However, these differences probably arise from different kinetics of the components in the complex sequence of conductance changes. The depolarizing overshoot in the squid axon is large but brief (FIGURE 24, left), although the conductance increase also outlasts the potential as in lobster muscle fibers. The anodal break response of the depolarized squid axon probably reflects competitive electrogenic effects of two increasing ionic conductances. The depolarizing electrogenesis caused by the Na-conductance increase is quickly counteracted as high K-conductance due to the depolarization of the axon by the external K^+ is restored. The conductance increase therefore continues to be manifested while the electrogenesis terminates. In a TEA-treated axon, however, the K-conductance may be expected to be low (FIGURE 6) and the anodal break response develops into a prolonged spike (FIGURE 24, right) with which is also associated some degree of increased conductance. There is a period of sustained hyperpolarization after the hyperpolarizing current is withdrawn in depolarized toad axons, but the membrane conductance during this phase is not known (Tasaki, 1959*a*).

Prolonged spikes and conversion of graded responses to spikes. The occurrence of different combinations of transducer actions with different kinetics accounts for numerous recent findings that spikes can be prolonged under various experimental conditions (for references cf. Chang and Schmidt, 1960; Spyropoulos and Tasaki, 1960; Werman and Grundfest, 1961), or may occur spontaneously (Bennett *et al.*, 1959). Basically, prolonged spikes result from changed relations between magnitudes and time courses of the depolarizing transducer action (Na-activation) and of the repolarizing (K- and/or Cl-activation), with a relative increase of the former over the latter. However, there are overall differences. The change may involve only block or delay of K-activation which appears to be the major effect in *Onchidium* neurons (FIGURE 6), or that action may be combined also with prolonged Na-activation, as probably occurs in squid giant axons (FIGURE 24), frog dorsal root ganglion cells (Tasaki, 1959*b*), cockroach giant axons (Narahashi and Yamasaki, 1960) and probably also in puffer supramedullary neurons (Bennett, unpublished data). The conductance during the plateau of these prolonged spikes is high relative to that of the resting membrane.

The membrane conductance becomes lower during the plateau of cardiac spikes in comparison with the "resting" (diastolic) resistance (Weidmann, 1956). Thus, while there is probably a small component of enhanced Na-conductance (FIGURE 17), there must also be a depolarizing K-inactivation which increases the membrane resistance. The latter effect also occurs during the spike of eel electroplaques (FIGURE 16), but there is probably also an early Na-inactivation. The normal spike then is "prolonged" but the total duration is brief, since the time constant of the cell is small.

Block of K-activation relative to Na-activation probably accounts for the conversion of graded responses of various arthropod muscles to spikes by procaine (FIGURE 10). Crayfish muscle fibers are much more sensitive to procaine than are lobster muscle fibers (Girardier *et al.*, unpublished), and can develop extremely prolonged responses in procaine. In lobster muscle fibers the spikes are brief, but addition of small quantities of other agents (for example, serotonin and alkali-earth ions) results in spikes that may last for many minutes (Reuben and Grundfest, 1960). This effect is associated with increase in the resting membrane resistance, which also occurs on treating the muscle fibers with TEA or alkali-earth ions (FIGURE 9). Thus pharmacological K-inactivation, superimposed on an increase in Na-activation can lead to very prolonged spikes (Reuben and Grundfest, 1960; Werman and Grundfest, 1961) during the plateau of which the membrane resistance is lower than in the resting fiber (FIGURE 25).

Fatt and Ginsborg (1958) suggested that Ca^{++} is the ion carrying inward positive charge during the graded response of crayfish muscle fibers, and that conversion of graded to all-or-none activity in the presence of Ba^{++} or Sr^{++} is due to the greater permeability of these ions. However, arthropod muscle fibers that give all-or-none responses in Ba^{++} or Sr^{++} also have a very high resting resistance (FIGURE 9). This finding and other data (Werman and Grundfest, 1961) have led to a different explanation, in which Na^+ plays its normal role, although it can be substituted by alkali-earth or onium ions. These agents cause diminution of K-conductance by pharmacological K-inactivation and a concomitant block of Na-inactivation. These effects, which in other cells change brief to prolonged spikes, have a more dramatic effect in the normally gradedly responsive arthropod muscle fibers, since they convert small graded responses to prolonged spikes (FIGURE 2).

Factors that affect the different conductance processes, either diminishing or increasing them, may each operate independently and thus can give rise to many "spontaneous" or induced irregularities in the prolonged responses (FIGURE 26). Thus the spikes may develop oscillations under various conditions and may vary considerably in duration, presumably terminating when the conductance of the repolarizing ion flux exceeds that of the depolarizing. Prolonged spikes with very high plateau conductance can tolerate very large hyperpolarizations (Werman *et al.*, 1960), perhaps because anode break Na-activation is then enhanced (FIGURE 27). However, a fuller analysis of the different varieties of prolonged spikes that have already been observed will require elaboration of still further data.

"Upside down" responses of frog muscle fibers. Superficially this type of change in membrane potential (FIGURE 28) resembles the spontaneous oscillations during prolonged spikes of lobster muscle fibers (FIGURE 29). This probably is due to the analogous causative agents, alternations between two electrode states of the membrane. The electrode states of the "upside-down" responses, however, are for Cl^- and K^+. The muscle fiber membrane apparently becomes predominantly a Cl-electrode under some conditions and in the experimental conditions of FIGURE 28 (0 Cl^- outside), the membrane potential assumes an inside-positive value. This is associated with high membrane re-

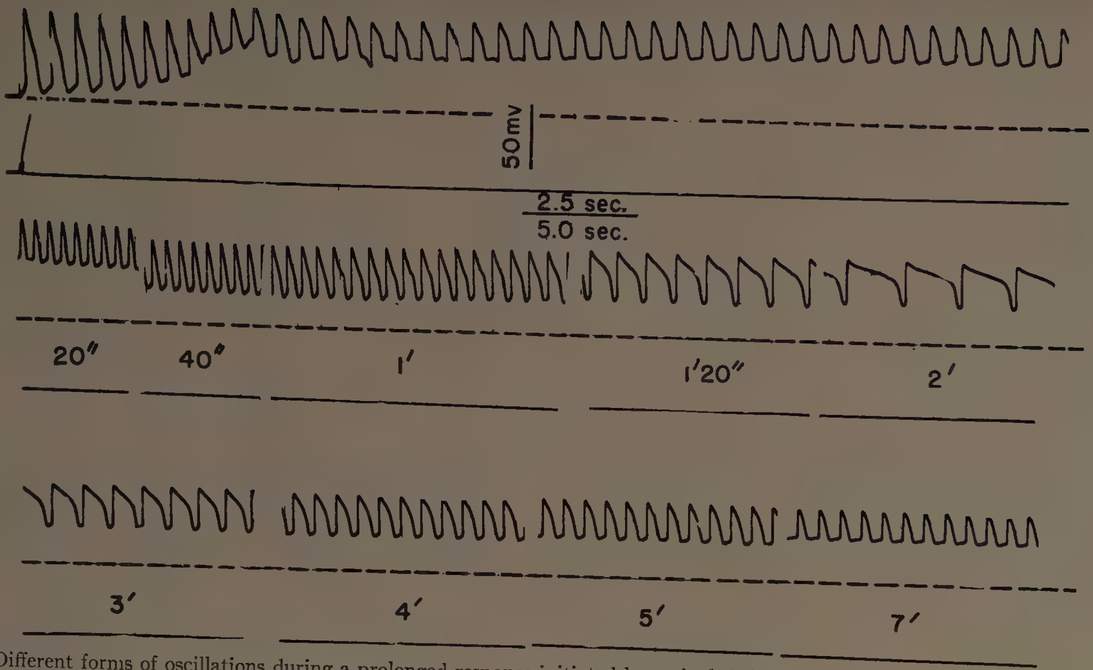

FIGURE 29. Different forms of oscillations during a prolonged response initiated by a single brief direct stimulus to a lobster muscle fiber. Broken line shows the resting potential. (From Reuben, Werman and Grundfest, unpublished.)

sistance, indicating that Cl^- has a lower permeability than K^+ but that K-conductance of the normal fiber is blocked. As is also the case for the oscillatory activity of prolonged spikes, the conductance shifts for some unknown reason. The muscle fiber membrane now becomes again more permeable to K^+, the membrane resistance decreases, and the potential tends toward the equilibrium for K^+, inside negative. The K-conductance decreases again and the membrane resistance and potential return to their earlier values. The oscillations have the form of hyperpolarizing responses if the more positive potential is regarded as the initial level. If the most negative level is taken as the baseline, the oscillations take the appearance of prolonged spikes.

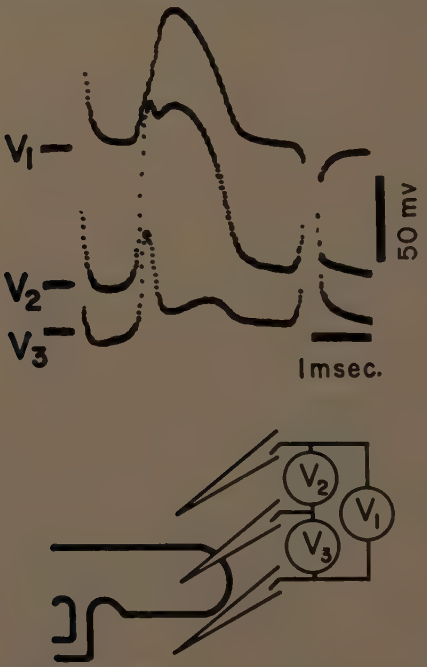

FIGURE 30. Spikes of different form and amplitude generated by the two surfaces of an electroplaque of *Malapterurus*. The response was evoked by an electrical stimulus lasting about 4 msec. (on and off artifacts occurred before and after the spikes). V_1 : recording across the electroplaque. V_2 and V_3 : differential recordings respectively across the anterior and posterior faces of the cell, as shown in the diagram. The caudal face developed a briefer, smaller spike than did the rostral face. (From Bennett, Keynes, and Grundfest, unpublished.)

Regional differences in electrically excitable membranes. The conductile capacity of electrically excitable membrane tends to obscure regional differences, which in synaptic membranes are exemplified not only by electrogenesis of different signs, but also by different degrees of responses to one or another kind of innervation. Nevertheless microelectrophysiological studies do disclose differences in electrical threshold, in accommodation or in the form of the spike and after-potentials, as for example, between the axon and soma of a neuron, or between different parts of an electroplaque (FIGURE 30). Some of these differences are undoubtedly due to electrophysiological properties, such as different kinetics of the different action components (for further discussion cf. Grundfest, 1961*a*).

However, other regional differences may be caused by structural factors. Thus the distribution of currents generated by an extended fiber such as the myelinated vertebrate axon may be expected to differ from that in the approximately spherical unmyelinated cell body. The presence or absence of dendritic branches may also affect the shape and size of an action potential. If parts of the cell body and dendrites are electrically inexcitable they will present a load to the electrically excitable membrane. Dendritic branches that have electrically excitable membrane may have different electrical properties depending upon their dimension, as well as different thresholds and conduction velocities.

Some General Conclusions

The components of ionic transducer actions as populations. The foregoing has described, and to some extent analyzed, the various types of conductance changes that may occur singly or in different combinations and may give rise to various manifestations in electrogenic cells. It is obvious that the occurrence of processes that may involve increase or decrease of conductances for at least three and perhaps for more ionic species of different sign and different concentration gradients can lead to very many types of complications in electrogenesis. No attempt can be made now to treat the phenomena more analytically, since kinetic data for all of the participating processes would have to be available. At present, however, we lack even the methods for characterizing some of these processes precisely.

It is likely, also, that much more sophisticated mathematical models will be required than the semiempirical formulations built on rates of reactions. The peculiar but similar forms of hyperpolarizing responses, "upside-down" responses, and the oscillations during prolonged spikes suggest that population statistics based on irreversible thermodynamics (Grundfest, 1955, 1957*d*; Tasaki, 1959*a*) may be more suitable for building such models. One indication to this effect already exists (Grundfest, 1957*d*). Eel electroplaques treated so as to respond only with graded responses (Altamirano *et al.*, 1955*b*), when excited by localized stimuli, respond with what appears to be all-or-none spikes when threshold stimuli are applied to the whole area of the excitable surface (Altamirano, 1956). This has been interpreted (Grundfest, 1957*a*, 1957*d*) as indicating existence of unit areas with specific distributions of a population of valving elements with different thresholds. Tasaki (Spyropoulos and Tasaki, 1960) has also adopted this view.

The population would be homogeneous with respect to the involved ion in membranes that operate only by K- or Cl-valving. In the other types there may be two populations (for example, for Na^+ and K^+ in membranes with depolarizing electrogenesis and for K^+ and Cl^- in some with hyperpolarizing activity), or three if Na^+, K^+ and Cl^- are all involved. In these cases the total number of valves might be fixed, but the proportions may vary at different times (Mullins, this publication), or they might be independent in number and action. Data now available are inadequate to decide for every case, although the independent modification of Na- and K-activation (FIGURE 6) indicates that the different populations may be independent at least in some cells.*

The independence is also suggested by the fact that some membranes have only an electrically excitable K-conductance or Cl-conductance. Since these valving mechanisms can exist without that for Na^+, perhaps their simultaneous occurrence in other membranes is only a manifestation of random assortment, but one whose occurrence is made more probable by evolutionary pressure. The presence of only the repolarizing valving mechanisms is essentially useless for electrically excitable activity which is initiated by depolarizing stimuli. They might then exist as vestigial elements in cells whose functional purposes are fulfilled by an electrically inexcitable electrogenesis. For conductile purposes the electrically excitable membrane has also evolved a depolarizing ion-valving in addition.

Further complications may also be envisaged. The two interfaces of the membrane with the different internal and external media may cause asymmetries in the energy requirements for penetration of a given ion species in one direction or the other. The interface components of the membrane might also have different structures which would add considerably to the asymmetry. Thus squid axons behave differently to application of ions (Grundfest *et al.*, 1954) or drugs (Tasaki and Hagiwara, 1957) to the two faces of the membrane. It is likely, also, that some cells have membranes whose properties are inverted with respect to each other. This might account for the requirement that TEA be injected into squid axon (Tasaki and Hagiwara, 1957) while it need be applied superficially in others. The thickness of the membrane relative to the size of the penetrating ions can also produce complications that have been shown experimentally in squid axons (Hodgkin and Keynes, 1955) and have been treated theoretically in a recent extension of the Teorell-Meyer and Sievers theory (Teorell, 1953).

Electrode properties. While it is generally assumed that the resting membrane is a K-electrode, considerable recent evidence indicates that many membranes are relatively "poor" K-electrodes, to the extent that they are insensitive to very considerable changes in internal or external K^+. The electrode properties of membranes toward a specific ion apparently depend not only on the absolute value of the permeability of that ion, but also on the relative permeabilities of other ions. Thus the membrane of crayfish muscle fibers even in moderately high concentrations of K^+ act essentially as a Cl-electrode. While the permeability to Cl^- appears to be very low, it nevertheless is probably high relative to that of K^+. When the K-permeability is increased, the membrane becomes a K-electrode. The membrane of frog muscle fibers can also behave as a Cl-electrode. The membrane resistance is then high relative to the resting resistance, but the resistance falls as the membrane again becomes a K-electrode.

The different relations between membrane potential and K^+_0 in lobster and crayfish muscle fibers (FIGURES 11 and 14) can be calculated with remarkable accuracy (Girardier *et al.*, 1961) by inserting appropriate, though very different values of P_K and P_{Cl} in the constant field equation (Hodgkin and Katz, 1949). Cl^- moves passively, as it also does in frog muscle fibers (Hodgkin and Horowicz, 1959). Although the redistribution of total Cl^- takes many hours in frog muscle (Adrian, 1960), the shift in membrane potential due to a change in K^+_i/K^+_0 occurs rapidly (Hodgkin and Horowicz, 1959), indicating rapid redistribution of Cl^- across the membrane. In crustacean muscle fibers, however, the change in membrane potential is also very slow, indicating that the permeability of their membranes for Cl^- is low, with the result that the gradient across the membrane changes only slowly (Girardier *et al.*, 1961).

---

* Electrically excited Cl-conductance of *Raia* electroplaques may be eliminated without affecting K-permeability (Cohen *et al.*, 1961). The resting Cl-permeability of crustaceans (Girardier, Reuben, and Grundfest, unpublished) and frog (Belton and Grundfest, unpublished) muscle fibers may be diminished without affecting K-permeability.

Pharmacological K-inactivation by the alkali-earth and onium ions is clearly evidenced by the loss of the K-electrode property. This should be accompanied by an increase in membrane resistance, and the latter effect has been demonstrated in muscle fibers of various arthropods. A small increase in membrane resistance also occurs in frog axons (Lüttgau, 1960). A related effect of pharmacological K-inactivation is the abolition or diminution of delayed rectification. This is found in arthropod muscle fibers (Werman and Grundfest, 1961), frog slow muscle fibers (Belton and Grundfest, unpublished) and *Raia* electroplaques (Cohen *et al.*, 1961). It also is evidenced in frog nodes treated with TEA (Lüttgau, 1960, figure 8).

Different degrees of pharmacological K-inactivation are produced in a given cell by different agents, or by the same agent in different cells. In some cases the amount of K-inactivation appears to be independent of the amount of the agent, when the latter is greater than a rather small threshold quantity. With other agents and in some cells, however, there is a more extended relation (FIGURE 9). In pharmacological terms, the difference indicates different dose-effect curves. Pharmacological inactivation may also occur in electrogenically inert membrane components. Thus, the passive membrane component for Cl-permeability in frog skeletal muscle fibers (Hodgkin and Horowicz, 1959) and in crustacean fibers (Girardier *et al.*, 1961) may be blocked, as noted above, by appropriate pharmacological agents.

The various relatively ion-specific glass electrodes are best known among nonliving systems. However, even in the case of glass electrodes the mechanisms of electrode processes are still dimly understood (Ling, 1960). In the case of the living membranes, electrode properties selectively for K^+, Na^+, or Cl^- are manifested in spite of very heterogeneous media on both sides of the membrane electrode and under conditions of high ionic strength, and sometimes in the face of large ion fluxes. It is thus not surprising that under certain conditions some membranes do not act as "good" electrodes. What is more surprising, indeed, is that they can behave as ion-specific electrodes at all under these complex circumstances.

Prolonged spikes. In eel electroplaques Na- and K-inactivation come into play as the peak of the spike develops, so that the membrane resistance during the falling phase becomes higher than in the resting cell. Impedance measurements and other data to establish the exact time course of these changes are as yet unavailable. However, in the electroplaques of *Eigenmannia* and *Sternopygus*, Na-inactivation probably develops on the rising phase of the spike, and K-inactivation is brief. Thus at the peak of the spike the resistance is somewhat higher than in the resting cell (Bennett, elsewhere in this volume), but in the falling phase K-activation occurs and the resistance falls. In cardiac muscle, K-inactivation is probably very large even though there is continued Na-activation. Thus while the spike is prolonged the plateau has a higher resistance than does the resting membrane. In *Onchidium* neurons, as in squid axons, depolarizing K-inactivation appears to be insignificant. The outward flux due to K-activation in these cells causes a steeper falling phase than would have occurred if decay of the potential had been passive. The spikes become prolonged, but since depolarizing K-inactivation is absent, the resistance during the plateau is lower than in the resting cell.

Thus the interplay of four conductance factors is adequate to account for the different varieties of spikes that are encountered in various animal cells. Transducer actions for Cl^-, such as appear to be responsible for the spike of *Chara* (Gaffey and Mullins, 1958) need not be taken into account at present although, as indicated by the delayed rectification of *Raia* electroplaques, components of Cl-activation and inactivation may become important in other cases.

Graded responses. The possible role of an excess of polarizing electrogenic components over the depolarizing Na-valving in causing graded responsiveness has been noted above. Although quantitative data on the kinetics of their electrogenic processes are not as yet available, the major factors in graded responses of arthropod muscles appear to be the same as those that operate in the production of spikes.

Evidence on the nature of graded responsiveness of arthropod muscle fibers derives from their conversion to all-or-none spikes by agents known to affect the electrogenic components of spike-generating membranes. As in the latter, so also in the gradedly responsive membrane, various degrees of change are produced depending on the effects of the pharmacological agents on the different components. Conversion of graded responses to spikes can arise by diminution or block of K-activation; by K-inactivation, by enhanced Na-activation, by diminution or block of Na-inactivation, or by various combinations of these. Thus there may occur spikes that are brief or prolonged but develop without a change in resting resistance; others are prolonged and have varying degrees of conductance increase during the plateau.

Oscillatory potentials. Even during the very prolonged spikes of lobster muscle fibers the conductance during the plateau rises only some 3- to 10-fold in comparison with the resting conductance, and frequently the change is much smaller. Thus the excess of depolarizing inward flux of positive charges over fluxes of repolarizing ions may be very small. The net excess inward flux need be only marginal to maintain the membrane in its depolarized state. This marginal character is revealed, however, by instabilities that cause oscillations during prolonged responses. An instability, leading to oscillations of similar appearance, but due to different causes, also is responsible for the "upside-down" responses of depolarized Cl-loaded frog muscle fibers. It is likely that instabilities due to marginal excess of one electrogenic component over another also occur naturally, arising as the "profiles" of ionic distributions (Teorell, 1953) in the membrane change. These instabilities probably account for the variations in spike duration of puffer neurons, variations that are more pronounced in neurons of immature fish. They may also be the cause of pacemaker activity in various types of neurons and of the slow oscillations that have been observed in other neurons, as exemplified by the photodynamically activated oscillatory behavior in giant neurons of *Aplysia* (Arvanitaki and Chalazonitis, 1960).

Hyperpolarizing responses. In lobster muscle fibers hyperpolarizing K-inactivation is readily manifested by the production of the hyperpolarizing responses. That such a transducer action is involved is shown by the increased membrane resistance and by the elimination of hyperpolarizing responses on inducing pharmacological K-inactivation by alkali-earth ions.

The relative ease with which hyperpolarizing responses are produced in lobster muscle fibers is probably related to the high resting K-permeability of the fibers. In squid or vertebrate axons the K-permeability must first be increased by depolarizing the cells. In crayfish muscle fibers the K-permeability is very low and they ordinarily show only anomalous rectification. However, a type of hyperpolarizing response may develop by reinstituting K-inactivation when the K-conductance is first increased under various experimental conditions (unpublished data).

The slow onset of the K-inactivation during hyperpolarizing responses and the subsequent rapid shift of membrane potential indicate that the kinetics of the inactivation process are complicated. Probably they involve, at first, a gradual increase in the number of inactivated K-valves, followed by an explosive regenerative increase. A striking feature is the resemblance of the forms of various oscillatory potentials to the hyperpolarizing response of lobster. This suggests a common general type of action that might be related to similar kinetics of changes in the ionic profiles of the membrane, albeit for different ions.

A conductance increase is evidenced particularly at the end of the anodal current pulse that generates the hyperpolarizing response. It occurs, however, also during the applied current and is manifested by the subsidence of the hyperpolarizing pulse and the decline of the membrane negativity to values below the threshold at which the response had begun. Also manifesting the occurrence of the increased conductance is the lowered dynamic resistance of the membrane to the applied currents. Similar findings have been observed in *Noctiluca*, mammalian heart muscle and axons. However, the occurrence of oscillatory hyperpolarizing responses indicates that the conductance increase may be counteracted by concurrent K-inactivation. The conductance increase is probably a manifestation of anomalous rectification or "anodal breakdown." Several ions are probably involved and are presumably Na^+ and K^+. However, the details of these transducer actions are not as yet clear. It is conceivable that appropriate combinations of the latter account for anodal break responses.

Several alternative explanations for hyperpolarizing responses that have been referred to in the text rest upon the changes of electrode properties or of electrode "states" of the membrane. An explanation somewhat related to that presented here is given by Lüttgau (1960).

The role of Na. Spikes, or large depolarizing graded responses, can be evoked in the absence of Na^+ in many varieties of cells. Indeed, when Na^+ is completely substituted by alkali earth or onium ions, normally gradedly responsive invertebrate muscle fibers can develop larger potentials and even spikes. The numerous findings on the "dispensability" of Na^+ have been interpreted as disproving the ionic theory of spike electrogenesis (Koketsu, 1961; Spyropoulos and Tasaki, 1960).

It must be admitted that some of the recent data do not as yet have a ready explanation in terms of the ionic theory. Particularly is this true of experiments in which spikes have been produced in tissues bathed in ion-free media. However, at least in some of these cases the tissue had to be soaked for considerable periods of time in some particular organic substance (Koketsu, 1961; Laramendi *et al.*, 1956; Lorente de Nó, 1949; Lorente de Nó *et al.*, 1957). Lobster muscle fibers previously treated with procaine or some other substance can develop prolonged spikes in an urea or sucrose medium (Werman *et al.*, 1960). However, when the procedures were reversed, adding procaine to a muscle already bathed in the nonionic media did not lead to spikes.

It is possible, however, to explain most of the data in terms of the ionic theory that they purport to contradict. Thus the prolonged spikes caused in many tissues by alkali-earth or onium ions can be ascribed to the effects of the experimental agents on the different components of the membrane transducer actions (Werman and Grundfest, 1961). For example, in lobster muscle fibers Ba^{++} and TEA apparently cause pharmacological block of K-activation and Na-inactivation, and are capable, as well, of replacing Na^+ as the ion carrying inward positive charge. As described above, these effects may be differentiated from the action of TEA on squid axons or *Onchidium* neurons. The different pharmacological properties of membranes are further emphasized by the effects of Ba^{++} on squid axons. Applied externally this ion has no effect on the axons. When injected in very small quantities into the axon, Ba^{++} destroys electrogenic responsiveness and depolarizes the membrane.

The implications drawn from the "dispensability" of Na^+ lose their meaning in the face of evidence that certain electrically excitable electrogenic membranes operate without Na-valving (FIGURE 8). The fact that the electrical responses of these membranes and of their electrically inexcitable counterparts are predictable from the electrochemical and physiological postulates of the ionic theory give additional support for that hypothesis. Indeed, as noted in the introductory section and as illustrated in the body of this paper, the ionic theory provides a reasonable basis to account for electrogenic activities of both electrically excitable and electrically inexcitable membranes, whereas alternative explanations appear to have only limited applicability.

Summary

Electrically excitable membranes exhibit a number of transducer actions in addition to those of K-activation, Na-activation, and inactivation. These effects, which must be incorporated in an extended ionic hypothesis, include Cl-activation and inactivation as well as K-inactivation by pharmacological agents and by depolarizing and hyperpolarizing currents. Hyperpolarizing currents can also activate increased membrane conductance effects. The vari-

ous membrane reactions may be demonstrated by: modifications of electrogenic activity; altered electrode properties; nonlinear voltage-current relations; oscillatory behavior of the membrane potential, including hyperpolarizing and "upside-down" responses; and various conductance changes. The range of phenomena accounted for on the basis of the extended ionic hypothesis is thus greatly increased, adding support for the theory that changes in ionic permeabilities of the membrane constitute the basic mode of operation of electrogenic tissues.

Acknowledgments

Many of the data incorporated here represent work still unpublished. I thank my colleagues P. Belton, M. V. L. Bennett, B. Cohen, H. Gainer, L. Girardier, J. P. Reuben, and R. Werman for permitting use of their material and for many fruitful discussions. The responsibility for any errors of interpretation are mine, however.

References

Adrian, R. H. 1960. Potassium chloride movement and the membrane potential of frog muscle. J. Physiol. (London). **151:** 154–185.

Altamirano, M. 1955. Electric properties of the innervated membrane of the electroplax of electric eel. J. Cellular Comp. Physiol. **46:** 249–278.

Altamirano, M. 1956. Local response in an excitable membrane. Federation Proc. **15:** 2.

Altamirano, M. & C. W. Coates. 1957. Effect of potassium on electroplax of *Electrophorus electricus*. J. Cellular Comp. Physiol. **49:** 69–102.

Altamirano, M., C. W. Coates & H. Grundfest. 1955*a*. Mechanisms of direct and neural excitability in electroplaques of electric eel. J. Gen. Physiol. **38:** 319–360.

Altamirano, M., C. W. Coates, H. Grundfest & D. Nachmansohn. 1955*b*. Electric activity in electric tissue. III. Modification of electrical activity of acetylcholine and related compounds. Biochim. et Biophys. Acta. **16:** 449–462.

Altamirano, M. & H. Grundfest. 1954. Three excitable systems of the synaptic unit in the innervated electroplaque preparation. Trans. Am. Neurol. Assoc. **79:** 79.

Arvanitaki, A. & N. Chalazonitis. 1960. Photopotentiels d'excitation et d'inhibition de différents somata identifiables (*Aplysia*) Activations monochromatiques. Bull. Inst. Océanographique, No. **1164:** 1–82.

Axelsson, J. & S. Thesleff. 1959. A study of supersensitivity in denervated mammalian skeletal muscle. J. Physiol. (London). **147:** 178–193.

Belton, P. & H. Grundfest. 1961. Comparative effects of drugs on graded responses of insect muscle fibers. Federation Proc. **20:** 339.

Bennett, M. V. L. 1961. Modes of operation of electric organs. Ann. N. Y. Acad. Sci., this volume.

Bennett, M. V. L., S. M. Crain & H. Grundfest. 1959. Electrophysiology of supramedullary neurons in *Spheroides maculatus*. J. Gen. Physiol. **43:** 159–250.

Bennett, M. V. L. & H. Grundfest. 1961*a*. Studies on morphology and electrophysiology of electric organs. III. Electrophysiology of electric organs in Mormyrids. *In* Bioelectrogenesis. C. Chagas & A. Paes-de-Carvalho, Eds. Elsevier. Amsterdam, Holland. In press.

Bennett, M. V. L. & H. Grundfest. 1961*b*. The electrophysiology of electric organs of marine electric fishes. II. The electroplaques of the main and accessory organ of *Narcine brasiliensis*. J. Gen. Physiol. **44:** 805–818.

Bennett, M. V. L. & H. Grundfest. 1961*c*. The electrophysiology of electric organs of marine electric fishes. III. The electroplaques of the Stargazer, *Astroscopus y-graecum*. J. Gen. Physiol. **44:** 819–843.

Bennett, M. V. L. & H. Grundfest. 1961*d*. Structure and function in Rajid electroplaques. Fed. Proc. **20:** 339.

Bennett, M. V. L., M. Wurzel & H. Grundfest. 1961. The electrophysiology of electric organs of marine electric fishes. I. Properties of electroplaques of *Torpedo nobiliana*. J. Gen. Physiol. **44:** 757–804.

Bernstein, J. 1912. Electrobiologie. Braunschweig, Fr. Vieweg.

Boistel, J. & P. Fatt. 1958. Membrane permeability change during inhibitory transmitter action in crustacean muscle. J. Physiol. (London). **144:** 176–191.

Boyle, P. J. & E. J. Conway. 1941. Potassium accumulation in muscle and associated changes. J. Physiol. (London). **100:** 1–63.

Burke, W. & B. L. Ginsborg. 1956. The electrical properties of the slow muscle fibre membrane. J. Physiol. (London). **132:** 586–598.

del Castillo, J. & B. Katz. 1956. Biophysical aspects of neuromuscular transmission. *In* Progress in Biophysics. **6:** 121–170. Pergamon. London, England.

Cerf, J. A., H. Grundfest, G. Hoyle & F. V. McCann. 1959. The mechanism of dual responsiveness in muscle fibers of the grasshopper *Romalea microptera*. J. Gen. Physiol. **43:** 377–395.

Chang, J. J. 1960. Electrophysiological studies of nonluminescent form of a dinoflagellate, *Noctiluca miliaris*. J. Cellular Comp. Physiol. **56:** 33–42.

Chang, J. J. & R. F. Schmidt. 1960. Prolonged action potentials and regenerative hyperpolarizing responses in Purkinje fibers of mammalian heart. Pflüger's Arch. ges Physiol. **272:** 127–141.

Cohen, B., M. V. L. Bennett & H. Grundfest. 1961. Electrically excitable responses in *Raia erinacea* electroplaques. Federation Proc. **20:** 339.

Cole, K. S. 1941. Rectification and inductance in the squid giant axon. J. Gen. Physiol. **25:** 29–51.

Couteaux, R. 1955. Localization of cholinesterase at neuromuscular junctions. Intern. Rev. Cytol. **IV:** 335–375.

Cranefield, P. F. & B. F. Hoffman. 1958. Electrophysiology of single cardiac cells. Physiol. Revs. **38:** 41–76.

Diamond, J. & R. Miledi. 1959. The sensitivity of foetal and newborn rat muscle to acetylcholine. J. Physiol. (London). **149:** 50p.

Dodge, F. A. & B. Frankenhaeuser. 1958. Membrane currents in isolated frog nerve fibre under voltage clamp conditions. J. Physiol. (London). **143:** 76–90.

Eccles, J. C. 1957. The Physiology of Nerve Cells. Johns Hopkins Press. Baltimore, Md.

Eccles, J. C. 1960. The properties of the dendrites. *In* Structure and Function of the Cerebral Cortex. : 192–203. D. B. Tower and J. P. Schadé, Eds. Elsevier. Amsterdam, Holland.

Eccles, J. C., P. Fatt & K. Koketsu. 1954. Cholinergic and inhibitory synapses in a pathway from motor-axon collaterals to motoneurones. J. Physiol. (London). **126:** 524–562.

Fatt, P. & B. L. Ginsborg. 1958. The ionic requirements for the production of action potentials in crustacean muscle fibres. J. Physiol. (London). **142:** 516–543.

Fatt, P. & B. Katz. 1951. An analysis of the end-plate potential recorded with an intracellular electrode. J. Physiol. (London). **115:** 320–370.

Fatt, P. & B. Katz. 1953*a*. The effect of inhibitory nerve impulses on crustacean muscle fibre. J. Physiol. (London). **121:** 374–389.

Fatt, P. & B. Katz. 1953*b*. The electrical properties of crustacean muscle fibres. J. Physiol. (London). **120:** 171–204.

Freygang, W. H., Jr. 1958. An analysis of extracellular potentials from single neurons in the lateral geniculate nucleus of the cat. J. Gen. Physiol. **41:** 543–564.

Gaffey, C. T. & L. J. Mullins. 1958. Ion fluxes during the action potential in *Chara*. J. Physiol. (London). **144:** 505–524.

Girardier, L., J. P. Reuben & H. Grundfest. 1961. Differences in membrane conductance components of crayfish and lobster muscle fibers . Federation Proc. **20:** 339.

Grundfest, H. 1940. Bioelectric potentials. Ann. Rev. Physiol. **2:** 213–242.

Grundfest, H. 1955. The nature of the electrochemical potentials of bioelectric tissues. *In* Electrochemistry in Biology and Medicine. : 141–166. T. Shedlovsky, Ed. Wiley. New York, N. Y.

Grundfest, H. 1957*a*. Excitation triggers in post-junctional cells. *In* Physiological Triggers. T. H. Bullock, Ed. Am. Physiol. Soc. : 119–151.

Grundfest, H. 1957b. Electrical inexcitability of synapses and some of its consequences in the central nervous system. Physiol. Revs. **37:** 337–361.

Grundfest, H. 1957*c*. General problems of drug action on bioelectric phenomena. Ann. N. Y. Acad. Sci. **66**(3): 537–591.

Grundfest, H. 1957*d*. The mechanisms of discharge of the electric organs in relation to general and comparative electrophysiology. *In* Progress in Biophysics. **7:** 1–85. Pergamon. London, England.

Grundfest, H. 1958*a*. Electrophysiology and pharmacology of dendrites. Electroencephalog. J. Suppl. **10:** 22–41.

Grundfest, H. 1958*b*. An electrophysiological basis for neuropharmacology. Federation Proc. **17:** 1006–1018.

Grundfest, H. 1959*a*. Synaptic and ephaptic transmission. *In* Handbook of Physiology, Neurophysiology I. J. Field, Ed. Am. Physiol. Soc. : 147–197.

Grundfest, H. 1959*b*. Evolution of conduction in the nervous system. *In* Evolution of Nervous Control. Allan D. Bass, Ed. Am. Assoc. Advancement Sci. Publ. No. **52:** 43–86.

Grundfest, H. 1960*a*. Biochemical and physiological approaches to the functioning of neurons. *In* Inhibition in the Nervous System and Gamma-Aminobutyric Acid. : 344–352. E. Roberts, Ed. Pergamon. London, England.

Grundfest, H. 1960*b*. A four-factor ionic hypothesis of spike electrogenesis. Biol. Bull. **119:** 284.

Grundfest, H. 1961*a*. Functional specifications for membranes in excitable cells. *In* The Regional Chemistry, Physiology and Pharmacology of the Nervous System. : 378–402. S. Kety, Ed. Pergamon. London, England.

Grundfest, H. 1961*b*. Excitation by hyperpolarizing potentials. A general theory of receptor activities. *In* Nervous Inhibition. E. Florey, Ed. Pergamon. London, England. In press.

Grundfest, H. 1961*c*. General physiology and pharmacology of junctional transmission. *In* Biophysics of Physiological and Pharmacological Actions. A. M. Shanes, Ed. Am. Assoc. Advancement Sci. Symposium. In press.

Grundfest, H. & M. V. L. Bennett. 1961. Studies on morphology and electrophysiology of electric organs. I. Electrophysiology of marine electric fishes. *In* Bioelectrogenesis. C. Chagas & A. Paes-de-Carvalho, Ed. Elsevier. Amsterdam, Holland. In press.

Grundfest, H., C. Y. Kao & M. Altamirano. 1954. Bioelectric effects of ions microinjected into the giant axon of *Loligo*. J. Gen. Physiol. **38:** 245–282.

Grundfest, H. & J. P. Reuben. 1961. Neuromuscular synaptic activity in lobster. *In* Nervous Inhibition. E. Florey, Ed. : 92–104. Pergamon. London, England.

Grundfest, H., J. P. Reuben & W. H. Rickles, Jr. 1959. The electrophysiology and pharmacology of lobster neuromuscular synapses. J. Gen. Physiol. **42:** 1301–1323.

Hagiwara, S. & N. Saito. 1959. Voltage-current relations in nerve cell membrane of *Onchidium verruculatum*. J. Physiol. (London). **148:** 161–179.

Hodgkin, A. L. 1947. The membrane resistance of a non-medullated nerve fibre. J. Physiol. (London). **106:** 305–318.

Hodgkin, A. L. 1951. The ionic basis of electrical activity in nerve and muscle. Biol. Revs. **26:** 339–407.

Hodgkin, A. L. 1957. The Croonian Lecture. Ionic movements and electrical activity in giant nerve fibres. Proc. Roy. Soc. London. **B148:** 1–37.

Hodgkin, A. L. & A. F. Huxley. 1952. A quantitative description of membrane current and its application to conduction and excitation in nerve. J. Physiol. (London). **117:** 500–544.

Hodgkin, A. L. & P. Horowicz. 1959. The influence of potassium and chloride ions on the membrane potential of single muscle fibres. J. Physiol. (London). **148:** 127–160.

Hodgkin, A. L. & B. Katz. 1949. The effect of sodium ions on the electrical activity of the giant axon of the squid. J. Physiol. (London). **108:** 37–77.

Hodgkin, A. L. & R. D. Keynes. 1955. The potassium permeability of a giant nerve fibre. J. Physiol. (London). **128:** 61–88.

Hurlbut, W. P. 1961. Ionic movements in nerve fibers at rest and during recovery. *In* Biophysics of Physiological and Pharmacological Actions. A. M. Shanes, Ed. Am. Assoc. Advancement Sci. Symposium. In press.

Hutter, O. 1961. Ionic movements during vagus inhibition of the heart. *In* Nervous Inhibition. E. Florey, Ed. Pergamon. London, England. In press.

Hutter, O. F. & D. Noble. 1960. Rectifying properties of heart muscle. Nature. **188:** 495.

Katz, B. 1949. Les constants électriques de la membrane du muscle. Arch. Sci. Physiol. **3:** 285–300.

Keynes, R. D., M. V. L. Bennett & H. Grundfest. 1961. Studies on morphology and electrophysiology of electric organs. II. Electrophysiology of electric organ of *Malapterurus electricus*. *In* Bioelectrogenesis. C. Chagas and A. Paes-de-Carvalho, Eds. Elsevier. Amsterdam, the Netherlands. In press.

Koketsu, K. 1961. A concept of the mechanism of active depolarization. (Dispensability of sodium.) *In* Biophysics of Physiological and Pharmacological Actions. A. M. Shanes, Ed. Am. Assoc. Advancement Sci. Symposium. In press.

Kuffler, S. W. & E. M. Vaughan-Williams. 1953. Properties of the "slow" skeletal muscle fibers of the frog. J. Physiol. (London). **121:** 318–340.

Langley, J. N. 1905. On the reactions of cells and nerve-endings to certain poisons, chiefly as regards the reactions of striated muscle to nicotine and curare. J. Physiol. (London). **33:** 374–413.

Larramendi, L. M. H., R. Lorente de Nó & F. Vidal. 1956. Restoration of sodium deficient nerve fibres by an isotonic solution of guanidinium chloride. Nature. **178:** 316.

Ling, G. N. 1960. The interpretation of selective ionic permeability and cellular potentials in terms of the fixed charged-induction hypothesis. J. Gen. Physiol. **43:** 149–174.

Loewi, O. 1945. Aspects of transmission of the nervous impulse; theoretical and clinical implications. (The Edward Gamaliel Janeway Lecture.) J. Mt. Sinai Hospital. **12:** 851–865.

Lorente de Nó, R. 1947. A Study of Nerve Physiology. Rockefeller Inst. Med. Research. 131–132.

Lorente de Nó, R. 1949. On the effects of certain quaternary ammonium ions upon frog nerve. J. Cellular Comp. Physiol. **33:** 1–231.

Lorente de Nó, R., F. Vidal & L. M. H. Larramendi. 1957. Restoration of sodium-deficient frog nerve fibres by onium ions. Nature. **179:** 737.

Lüttgau, H. C. 1960. Das Kalium-Transportsystem am Ranvier-Knoten isolierter markhaltiger Nervenfasern. Pflüger's Arch. ges. Physiol. **271:** 613–633.

Miledi, R. 1960*a*. The acetylcholine sensitivity of frog muscle fibres after complete or partial denervation. J. Physiol. (London). **151:** 1–23.

Miledi, R. 1960*b*. Junctional and extra-junctional acetylcholine receptors in skeletal muscle fibres. J. Physiol. (London). **151:** 24–30.

Moore, J. W. 1959. Excitation of squid axon membrane in isosmotic KCl. Nature. **183:** 265.

Mueller, P. 1958. Prolonged action potentials from single nodes of Ranvier. J. Gen. Physiol. **42:** 137–162.

Mullins, L. J. 1960. An analysis of pore size in excitable membranes. J. Gen. Physiol. **43**. Suppl. : 105–117.

Mullins, L. J. 1961. Macromolecular properties of excitable membranes. Ann. N. Y. Acad. Sci., this volume.

Narahashi, T. & T. Yamasaki. 1960. Behavior of membrane potential in the cockroach giant axon poisoned by D.D.T. J. Cellular Comp. Physiol. **55:** 131–142.

Noble, D. 1960. Cardiac action and pacemaker potentials based on the Hodgkin-Huxley equations. Nature. **188:** 495–497.

Pringle, J. W. S. 1960. Models of Muscle. Symposium Soc. Exptl. Biol. **16:** 41–68.

Purpura, D. P. 1961. Analysis of cortical axodendritic synaptic organization. Ann. N. Y. Acad. Sci., this volume.

Purpura, D. P., M. W. Carmichael & E. M. Housepian. 1960*a*. Succinylcholine-induced contractures in skeletal muscles of newborn cat. Proc. Soc. Exptl. Biol. Med. **103:** 336–338.

Purpura, D. P., M. W. Carmichael & E. M. Housepian. 1960*b*. Physiological and anatomical studies of development of superficial axodendritic synaptic pathways in neocortex. Expl. Neurol. **2:** 324–347.

Ravin, H. A., S. I. Zachs & A. M. Seligman. 1953. The histochemical localization of acetylcholine esterase in nervous tissue. J. Pharmacol. Exptl. Therapeut. **107:** 37–53.

Reuben, J. P. & H. Grundfest. 1960. Further analysis of conversion of graded to all-or-none responsiveness in the electrically excitable membrane of lobster muscle fibers. Biol. Bull. **119:** 335.

Reuben, J. P., R. Werman & H. Grundfest. 1959. Anomalous current-voltage relation induced by hyperpolarization of lobster muscle fibers. Biol. Bull. **117:** 424.

Reuben, J. P., R. Werman & H. Grundfest. 1960*a*. Oscillatory hyperpolarizing responses in lobster muscle fibers. Federation Proc. **19:** 298.

Reuben, J. P., R. Werman & H. Grundfest. 1960*b*. Properties of indefinitely prolonged spikes of lobster muscle fibers. Biol. Bull. **119:** 336.

Ruch, T. C. & J. F. Fulton (Eds.). 1960. Medical Physiology and Biophysics. Howell's Textbook of Physiology. 18th ed. Saunders. Philadelphia, Pa.

Schoffeniels, E. 1959. Ion movements studied with single isolated electroplax. Ann. N. Y. Acad. Sci. **81**(2): 285–306.

Segal, J. 1958. An anodal threshold phenomenon in the squid giant axon. Nature. **182:** 1370–1372.

Shanes, A. M. 1958. Electrochemical aspects of physiological and pharmacological actions in excitable cells. Pharmacol. Revs. **10:** 59–273.

Spyropoulos, C. S. & I. Tasaki. 1960. Nerve excitation and synaptic transmission. Ann. Rev. Physiol. **22:** 407.

Stämpfli, R. 1959. Is the resting potential of Ranvier nodes a potassium potential? Ann. N. Y. Acad. Sci. **81**(2): 265–284.

Takeuchi, A. & N. Takeuchi. 1960. On the permeability of end-plate membrane during the action of transmitter. J. Physiol. (London). **154:** 52-67.

Tasaki, I. 1959*a*. Demonstration of two stable states of the nerve membrane in potassium-rich media. J. Physiol. (London). **148:** 306–331.

Tasaki, I. 1959*b*. Resting and action potentials of reversed polarity in frog nerve cells. Nature. **184:** 1574.

Tasaki, I. 1960. Thermodynamic treatment of radio-tracer movements across biological membranes. Science. **132:** 1661.

Tasaki, I. & W. H. Freygang, Jr. 1955. The parallelism between the action potential active current and membrane resistance at a node of Ranvier. J. Gen. Physiol. **39:** 211–224.

Tasaki, I. & S. Hagiwara. 1957. Demonstration of two stable potential states in the squid giant axon under tetraethylammonium chloride. J. Gen. Physiol. **40:** 859–885.

Teorell, T. 1953. Transport processes and electrical phenomena in ionic membrane. *In* Progress in Biophysics. **3:** 305–367. Academic Press. New York, N. Y.

Teorell, T. 1959. Electrokinetic membrane processes in relation to properties of excitable tissues. J. Gen. Physiol. **42:** 831–863.

Weidmann, S. 1956. Electrophysiologie der Herzmuskelfaser. Hans Huber. Bern, Switzerland.

Werman, R. 1960. Electrical inexcitability of the synaptic membrane in the frog skeletal muscle fibre. Nature. **188:** 149–150.

Werman, R. & H. Grundfest. 1961. Graded and all-or-none electrogenesis in arthropod muscle. II. The effect of alkali-earth and onium ions on lobster muscle fibers. J. Gen. Physiol. In press.

Werman, R., F. V. McCann & H. Grundfest. 1961. Graded and all-or-none electrogenesis in arthropod muscle. I. The effects of alkali-earth cations on the neuromuscular system of *Romalea microptera*. J. Gen. Physiol. In press.

Werman, R., J. P. Reuben & H. Grundfest. 1960. Effects of environmental changes on indefinitely prolonged action potentials of lobster muscle fibers. Biol. Bull. **119:** 347.

Wiersma, C. A. G. 1961. The neuromuscular system. *In* The Physiology of Crustacea. **II:** 191–240. T. H. Waterman, Ed. Academic Press. New York, N. Y.

MODES OF OPERATION OF ELECTRIC ORGANS*

Michael V. L. Bennett†

Department of Neurology, College of Physicians and Surgeons, Columbia University, New York, N.Y.; and Marine Biological Laboratory, Woods Hole, Mass.

INTRODUCTION

Electric fish are characterized by specialized organs that generate external fields large compared to those produced by other electrogenic tissue: nerve, muscle, or gland. These organs have evolved in at least six different lines and are a remarkable example of convergence. The similarities are more fundamental than the generation of electricity suggesting, in the evolutionary process, common features that may have involved the material transformable by natural selection as well as the environmental pressures. The importance of the starting material is emphasized by the presence of electric organs only in fish.

Bernstein (1912) early made an insightful suggestion as to the mode of operation of electric organs. He proposed that the two opposed membranes of the specialized generating cells, the electroplaques, develop at rest equal inside-negative potentials. During a response the innervated one of the membranes would become depolarized to near-zero potential. The other membrane would be inexcitable and tend to maintain its resting potential; current would flow along the axis of the cell as a result. This theory accounts for the large potentials generated by electric organs as the result of two factors: limitation of the discharge to one face, and series-parallel arrangement of many cells.

The Bernstein hypothesis very closely fits the electroplaques of electric rays (Torpedinidae) and stargazers (Astroscopidae). It must be added that the cells produce only postsynaptic potentials that are electrically inexcitable (Bennett and Grundfest, 1961*a* and *b*; Bennett *et al.*, 1961). The electroplaques of the eel, *Electrophorus*, are also closely fitted by the theory. An important modification, however, is that in addition to p.s.p.s the innervated face generates a spike that overshoots the resting potential to make the inside positive (Altamirano *et al.*, 1955*a*; Keynes and Martins-Ferreira, 1953).

Recently a number of additional species of electric fish have been investigated, revealing great variety among them (Bennett and Grundfest, 1959*a* and *b*, 1961*c*; Grundfest and Bennett, 1961; Keynes *et al.*, 1961). On the Bernstein mechanism a number of variants occur. The general picture of opposed membranes generating different potentials remains correct, but both faces of cell may become active and in different ways. In this paper new data on skates (Rajidae) and knifefish (Gymnotidae) will be used to illustrate these findings.

Several functional considerations may be helpful in understanding the electrophysiological data. First, it is obvious that generation of external currents requires low membrane resistance during activity. On the other hand,

---

* This work was supported in part by grants to Harry Grundfest from the Muscular Dystrophy Associations of America, New York, N.Y.; the National Institute of Neurological Diseases and Blindness, Public Health Service, Bethesda, Md.; the National Science Foundation, Washington, D.C.; and the United Cerebral Palsy Research Foundation, New York, N.Y.

† Fellow, National Neurological Research Foundation, Washington, D.C.

little would be gained by making the membrane resistance much lower than that of the current path in the intra- and extracellular material and, to minimize ionic fluxes, membrane resistance should be kept as high as possible, both at rest and during activity. The operation of an electric organ thus represents a compromise between efficiency and peak output. Excitable membranes of nerve and muscle possess a property that would be of advantage in an electric organ; their resistance greatly decreases during activity. In these tissues, however, this property is probably important in increasing the safety factor and velocity of propagation rather than in generating external current (Hodgkin and Huxley, 1952*b*; Yamagiwa, 1956).

A second characteristic may be derived from the same assumptions. During activity, opposing membranes should have more or less the same resistance; that is, there should be a kind of impedance matching. This characteristic does occur in electric organs. In those cells where only one face becomes active in the Bernstein pattern, for example, in *Electrophorus*, Torpedinidae, and Astroscopidae, this face decreases its resistance during activity, and its resting resistance is high compared to that of the opposed face (Altamirano *et al.*, 1955*a*; Bennett and Grundfest, 1961*b*; Bennett *et al.*, 1961; and Keynes and Martins-Ferreira, 1953). The low-resting resistance of the inactive (and inexcitable) face is correlated with a greatly increased surface (Altamirano *et al.*, 1955*a*; Keynes and Martins-Ferreira, 1953; and Mathewson *et al.*, 1961). Where both faces become active, they may both decrease their resistance during activity, and the resting resistances are about equal. In these cells the faces have similar surface areas. The response of the uninnervated face is always electrically excitable since it is initiated by depolarization generated in the innervated face.

METHODS

Preparation of tissue. In all species of *Raja* studied, segments of tail were removed, and the lengths of electric organ therein were dissected free from the surrounding muscle and connective tissue. The organ was studied, placed in a bath of ray Ringer's solution (Brock and Eccles, 1958), and microelectrodes were placed in the superficial electroplaques under direct vision. In both *Hypopomus* and *Sternopygus*, electroplaques were studied *in situ*. The fish were fastened to an inclined plane of paraffin with the head down and extending into an aerated water pool. The electroplaques were exposed by stripping away overlying tissue and were kept moist with a drip of *Electrophorus* Ringer's solution (Altamirano *et al.*, 1953). Where desired, organ discharge was blocked by spinal section.

Recording. Standard microelectrode techniques, as applied in this laboratory, were used for all intracellular stimulation and recording (Bennett *et al.*, 1959*a*). Neural stimulation was provided by paired 125-μ silver wires, Teflon insulated except at the tips and placed close to the nerve to be stimulated.

A. C. impedance measurements were made with isolated lengths of organ (*Raja*) or along the tip of the tail (*Sternopygus*). The preparations were placed in a moist chamber and contacted by large Ag-AgCl electrodes covered with Ringer-saturated gauze. A Wheatstone bridge circuit was used with the preparation, and contacting electrodes as one arm (FIGURE 1). Imbalance due to polarization of the contacting electrodes was negligible. The fixed resistors were selected so that A. C. balance was obtained with all the resistances approximately equal. The alternating currents were applied through a shielded isolation transformer, and polarizing and stimulating pulses through a Schmitt-type R.F. isolation unit. In order to avoid interactions due to transformer saturation and changes of impedance in the rectifiers of the R.F. isolation unit, these components were isolated by high- and low-pass RC filters. The bridge signal was displayed directly after moderate amplification, or led through an electronic variable band-pass filter (Krohnhite 310 AB), and greatly amplified before display.

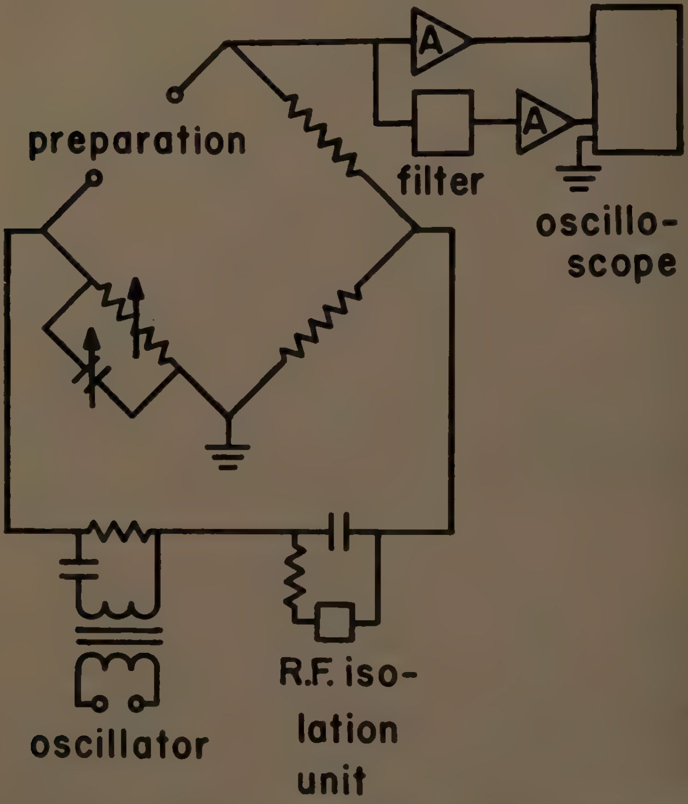

FIGURE 1. Circuit diagram for A. C. impedance measurements. See text for description.

Recording conventions. In all figures monopolar recordings are shown positive deflections upward. Differential recordings across cell membranes are shown intracellular positivity upward. In differential recordings between electrodes external to the two faces of an electroplaque, positivity external to the uninnervated face gives upward deflections. Outward, or anodal currents, through monopolar stimulating electrodes are shown as upward deflections.

RAJIDAE

Results

The electric organs of the skates, Rajidae, show a possible evolutionary sequence, and there are probably enough species to elucidate the graduated steps in the refinement of the organs. At one extreme the cells are like those of other marine electric fish. The excitable membrane is in the innervated face and generates only p.s.p.s. The inexcitable uninnervated face is low resistance correlated with a greatly increased surface. At the other extreme the cells have an additional response component that is similar to delayed rectification (Hodgkin, 1951). This response, largely restricted to the uninnervated face, increases the membrane's conductance when it is depolarized by p.s.p.s generated in the innervated face. The two faces have about the same surface area and, at rest, have about equal resistances. Following activation of the conductance increase in the uninnervated face, the electrical conditions are the same as in the other type of electroplaques, and p.s.p.s produce larger external currents than before.

Anatomy. The electric organs of the Rajids are in the tail, one on each side of the spinal cord, and their development from tail muscles has been quite well described (Ewart, 1892). The electroplaques are flattened in the anterior-posterior direction (FIGURE 2) and profusely innervated over their anterior faces. The posterior surfaces often have a short process or stalk (*s*), a remnant of the muscle fiber from which the cells develop. As in two other groups, Mormyridae (Szabo, 1958, 1961*a*), and Astroscopidae (Mathewson *et al.*, 1961), striated material is present in a more or less central area (FIGURE 2*C* and *D*). The striations are single and, even under examination with the electron microscope, there is none of the additional banding that occurs in muscle (Mathewson and Wachtel, personal communication). Two types of electroplaque, cup and disc, have been described (Ewart, 1892; Ishiyama, 1958). In the cup form, both the anterior and posterior surfaces are quite smooth (FIGURE 2*A* and *C*), and these are the cells in which both faces become active. The term "cup" is used because the cells are often somewhat concave, the centers of the flattened cells lying more posteriorly than the margins. In the disc form, the anterior surface is smooth, but the posterior is highly digitate or vacuolate, thus having an increased surface area (FIGURE 2*B* and *D*). There is little activity in the posterior faces of these cells. The term "disc" is used because the cells tend to be flatter than the cup-type. Often they too are concave, but in the opposite direction. In all species except those with the most primitive cups, the electric organs are divided by connective tissue into chambers, each containing one electroplaque. Cup-type cells lie with their caudal surfaces close to the caudal walls of their chambers. Disc-type cells lie more anteriorly, somewhat rostral to the chambers' centers.

In the species used in this study, the distinction in form between cup and disc was not absolute. Many cups had some digitation on their caudal surfaces (FIGURE 2*A*, lower right), and many discs had some smooth areas (FIGURE 2*B*, lower left). However, the differentiation by position in the connective tissue chambers always held.

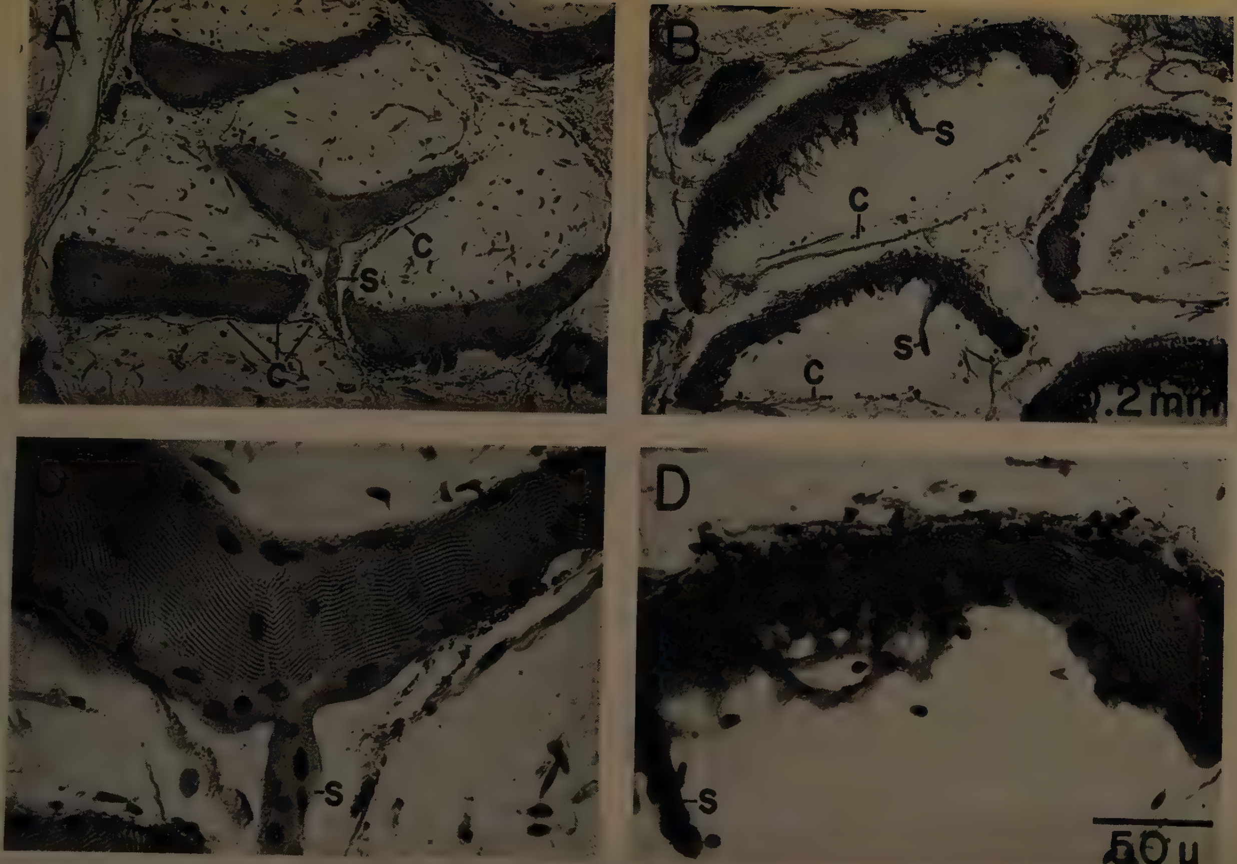

Figure 2. Anatomy of Rajid electroplaques. Longitudinal sections of electric organ from *R. erinacea*, which has cup-type cells (*A*, *C*), and from *R. eglantaria*, which has disc-type cells (*B*, *D*). Rostral surface up, hematoxylin and eosin stain, *A*, *B*, low power, *C*, *D*, high power. Cup-type cells are usually smooth on both surfaces (*A*), although there may be some digitation of the caudal face in some cells (*A*, *lower right*). The cells lie against the caudal walls of the connective tissue chambers (*c*) that contain them. The caudal face of disc-type cells usually is highly digitate or vacuolate (*B*), although in some cells it may be relatively smooth (*B*, *lower right*). The cells lie anteriorly in their connective tissue chambers (*c*). Both types

Organ discharge. The organ discharge of the Rajidae is the most primitive known, and was indistinguishable in organs with cups or discs. It could be elicited only by rather violent manipulation, and then not in every individual. It was long-lasting and irregular in amplitude and duration (FIGURE 3). Corresponding to the rostral innervation the discharge was entirely head-negative. From the irregularity of form, the firing of single elements appears to have been asynchronous and, probably, was repetitive.

The discharge in air was usually so small as to be useless as a weapon, and it was much smaller in sea water (FIGURE 3*D*). It was probably still large enough, however, to affect the ampullae of Lorenzini that are sensitive to voltage gradients of 1 to 2 mv/cm. (Murray, 1960). Possibly, therefore, the organ is functional in some electrical guidance system (cf. Lissmann, 1958).

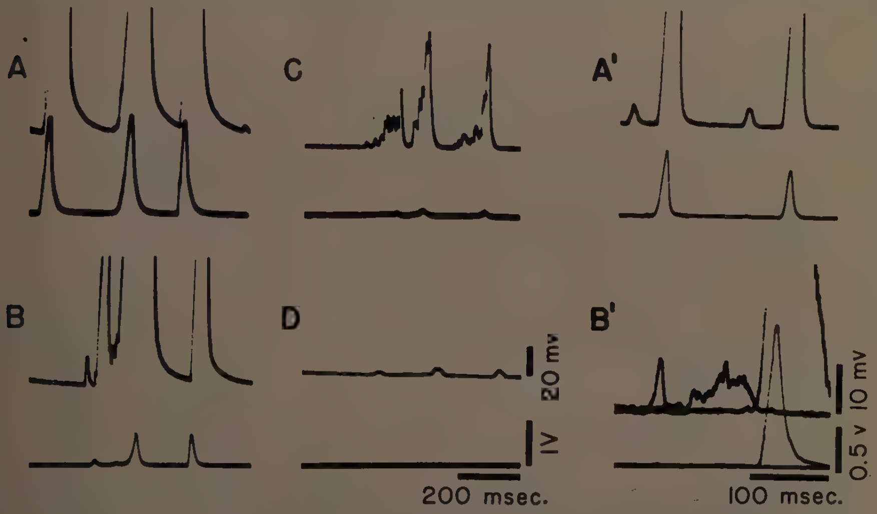

FIGURE 3. Discharge of Rajid electric organs. *A* to *D*: *R. erinacea,* which has cup-type electroplaques. *A′*, *B′*: *R. eglantaria,* which has disc-type electroplaques. Discharges were evoked by vigorous prodding and recorded differentially between tip and base of tail, caudal positivity up. Upper trace, higher gain. In both forms, discharge was asynchronous and very variable in amplitude and duration. All records were in air except *D*, for which the animal was immersed in sea water while regularly responding as in *B*. The discharge was greatly reduced.

The difficulty of eliciting the organ discharge suggests that the responses obtained may not have been normal. The amplitude and frequency are so low that probably no one has looked for the normal discharge with adequate techniques.

Intracellular stimulation of cups. The response of cups to depolarization, increase in conductance similar to delayed rectification, is illustrated in FIGURES 4 and 5. There was no indication of inward current such as occurs in spike generation. Two microelectrodes were placed in the electroplaque; polarizing currents were passed through one, and the resulting voltage was recorded with the other. For hyperpolarizing currents the resistance was linear over 20 to 40 mv (left part of graph and *B* in FIGURE 4). The final voltage was reached approximately exponentially with a time constant of 3 to 5 msec. For small depolarizing currents (right part of graph) the resistance was also linear, but for larger currents an early peak was followed by a falling-off (*A*). If the peaks (*x*s) were plotted against current, they were seen to fall somewhat below what

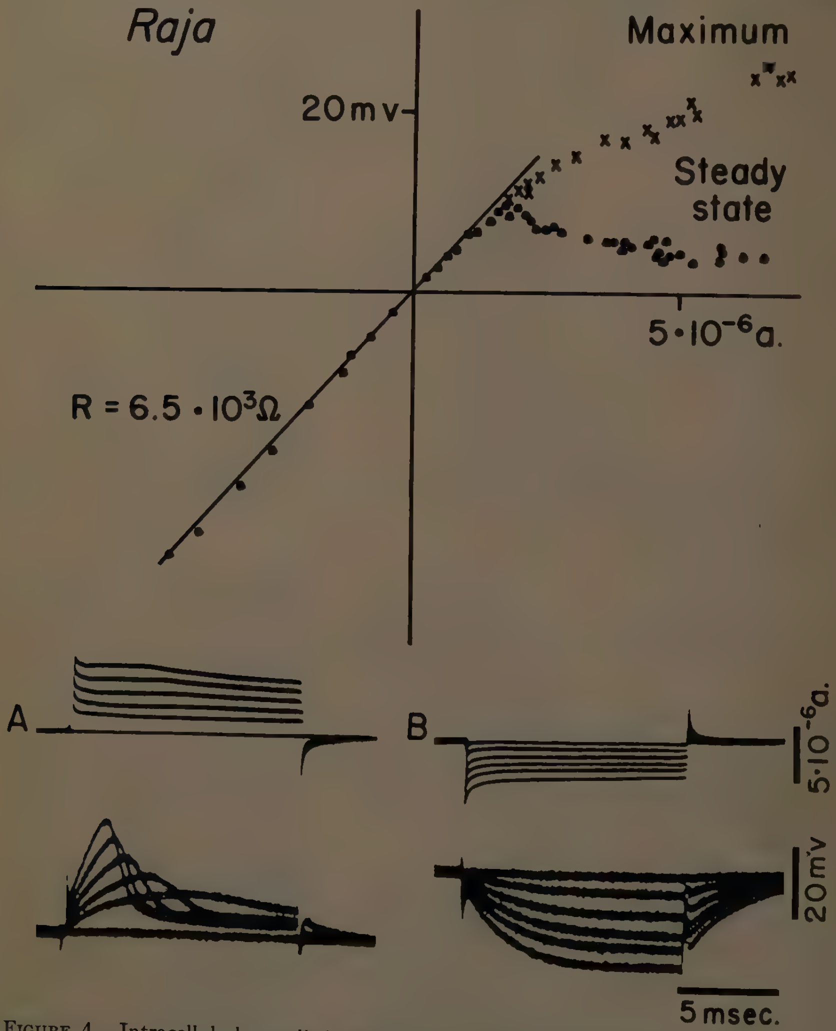

FIGURE 4. Intracellularly applied polarization of cup electroplaques. *R. erinacea*. *A:* superimposed records of responses (*lower traces*) to depolarizing currents (*upper traces*). For larger currents, the voltage reached an initial peak, then fell to a much lower steady value. *B:* records as in *A* to hyperpolarizing currents. The voltage change increased approximately exponentially toward a steady level. Graph: voltage-current relation for the same cell as *A* and *B*, but using additional data. The relation was linear for hyperpolarizing current. For depolarizing current, the initial peaks fell somewhat below what they would have reached if the cell had had the same resistance as for hyperpolarizing current. The steady levels of potential were much lower and continued to decrease as further current was applied. Reproduced by permission of *Elsevier*, Amsterdam, Holland.

would have been expected if the cell had remained passive with the same resistance as for hyperpolarization. If the depolarizing pulses were shortened to various points near the peaks, the voltage always began to decay toward the resting value immediately on cessation of the pulse (FIGURE 5). In this experiment the nonexponential decay is due to appreciable electrotonic decrement along the cell (Hodgkin and Rushton, 1946). Following activation of the conductance increase the rate of decay of the pulses was greatly increased (*D* in FIGURE 5). As the polarizing currents in FIGURE 4 were increased, the final voltage continued to decrease, indicating that the maximum conductance change had not yet been produced.

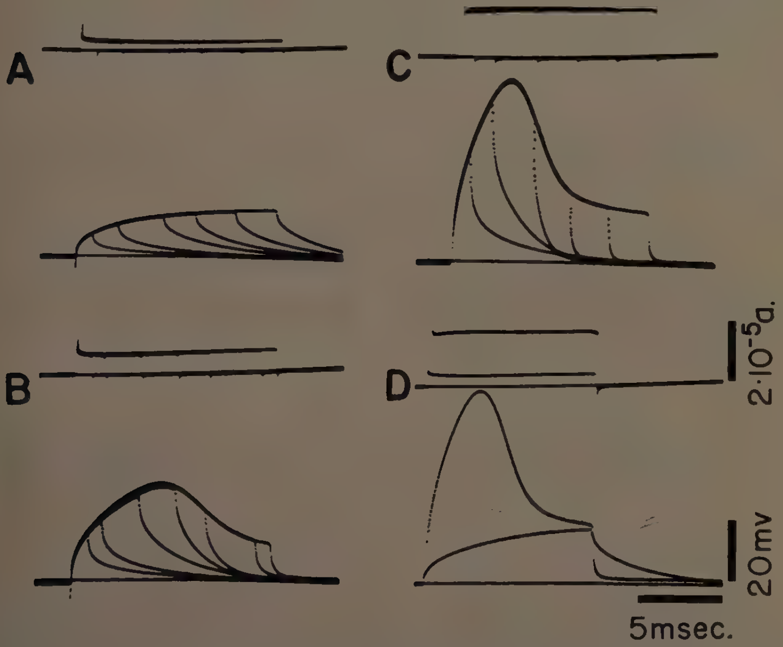

FIGURE 5. Responses of cup electroplaques to depolarizing pulses of different strengths and durations. *R. erinacea.* Lower trace: intracellular voltage. Upper trace: current applied through second intracellular electrode. *A* to *C*: superimposed records of constant current pulses of different lengths, magnitude increasing from *A* to *C*. *D:* superimposed records of a large and a small pulse of the same length; the traces cross following the end of the pulses. Whatever the current strength or duration, the voltage started to decrease immediately on cessation of the current. Following the peaks, the voltages decreased more rapidly than if the pulses were stopped before them. The time course of the decrease was not exponential since the cells were not isopotential. In *D* a small depolarization is seen to be maintained following the larger stimulus.

The duration of the conductance increase, as well as its magnitude, depended on stimulus strength and could approach one-half sec. (FIGURE 6). Rather than the hyperpolarization that is associated with delayed rectification in most tissues, there was a depolarization of a few millivolts (FIGURES 5*D* and 6*D*).

The observed magnitudes of the conductance increase were 5 to 10 times, but the absolute magnitude was difficult to evaluate. There was electrotonic decrement along the cells that are not of a shape for which solutions to the cable equation are convenient. The minimum conductance from FIGURE 5 was about 700Ω, an appreciable fraction of which must have been coupling resistance due to voltage drops in the intra- and extracellular electrolytes. Both nonisopotentiality and coupling resistance lead to underestimation of the change. Probably the membrane conductance becomes so low that the electrolytes are a significant part of the internal resistance of the organ.

Localization of the conductance increase. The conductance increase is of advantage to the skate since it occurs predominantly in the uninnervated surfaces of the electroplaques. It thus increases the current flowing along the axis of a cell, due to generation of p.s.p.s in its innervated face. Indeed to the extent that it occurs in the innervated face, it is disadvantageous, since it tends to "short-circuit" the p.s.p.-generating membrane and thereby reduce axial current.

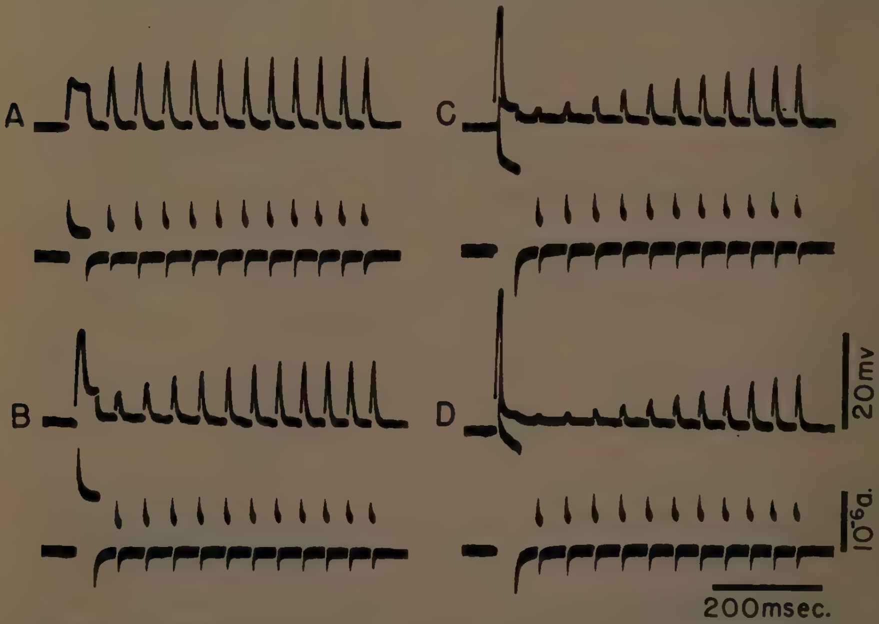

FIGURE 6. Duration of the conductance increase in a cup electroplaque. *R. erinacea* Upper trace: intracellular voltage; lower trace: current applied through a second intracellular electrode. The first, longer pulse, of increasing strength from *A* to *D*, activated the conductance increase. The train of brief testing pulses shows the time course of the return to resting conductance. When near maximally activated (*D*), the conductance increase lasted over 400 msec., and was associated with a small depolarization that decayed as the conductance returned to normal. Reproduced by permission of *Elsevier*, Amsterdam, Holland.

The localization of the conductance increase was established by stimulating with an external electrode. Because the two faces of an electroplaque are opposed, stimulating currents applied along the axis of the cell act oppositely on its faces. Thus to some extent separation of their properties may be obtained, and this technique has proved very useful in the study of electroplaques (Altamirano *et al.*, 1955*a*; Bennett and Grundfest, 1959*a*; and Keynes *et al.*, 1961). The method, as applied here, may best be understood with reference to the equivalent circuit in FIGURE 7. Current was applied through a monopolar electrode, external to the uninnervated face. Current inward through

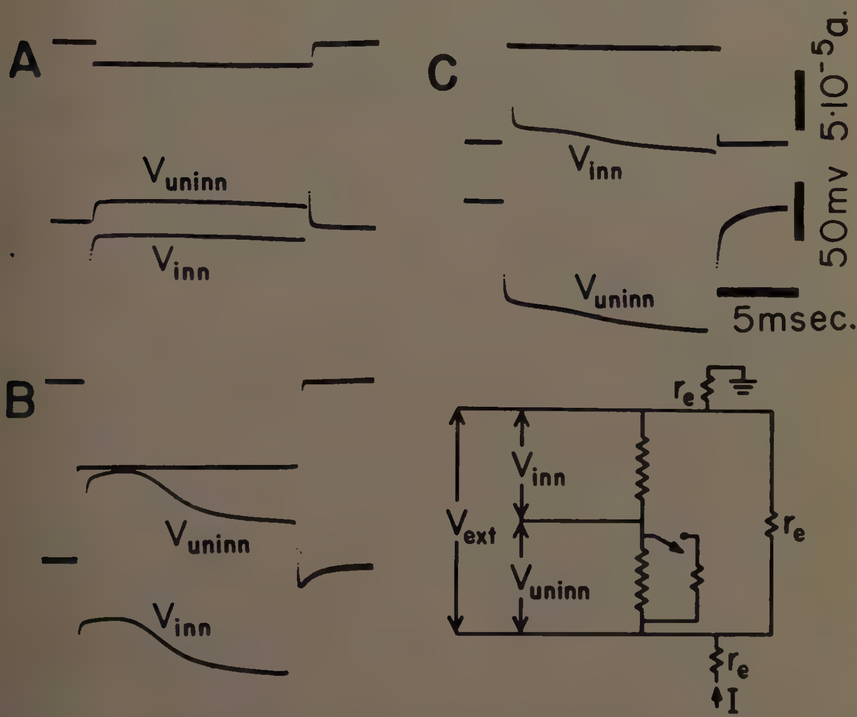

FIGURE 7. Predominance of the conductance increase in the uninnervated face as indicated by externally applied currents. Cup electroplaques of *R. erinacea*. A large Ringer-filled capillary-stimulating electrode was placed external to the uninnervated face. Three electrodes, one external to each face and one intracellular, differentially recorded the voltages across the faces (cf. Diagram in FIGURE 8). The equivalent circuit is shown in the inset where the r_e's represent the low resistances in the extracellular material; the larger resistances represent the resting resistances of the two faces; and the switched shunt across the uninnervated face represents the conductance increase. Upper trace: polarizing current. Lower traces: potential across innervated (V_{inn}) and uninnervated (V_{uninn}) faces, superimposed at the beginning of the records. The potentials across the faces were changed in opposite directions by the applied currents. During a weak stimulus the voltages across the faces remained constant (*A*) and were about equal, showing the similar resistances of the two faces. When a stimulus was applied that depolarized the uninnervated face above threshold for the conductance increase, the potential across this face decreased during the pulse (*B*). Simultaneously the hyperpolarization of the innervated face increased, since the low external resistance tended to maintain the potential across the cell constant. When a stimulus depolarized the innervated face there was much less decrease in potential (*C*), indicating that there was less conductance increase in this face (this direction of current indicated by arrow in diagram).

the electrode; that is, cathodal, would depolarize the uninnervated face and hyperpolarize the innervated. Activation of the conductance increase in the uninnervated face (closing the switch) would reduce the potential across this face. The resistance through the cell would still be high compared to the extracellular resistances, as the innervated face would be hyperpolarized and therefore unchanged in resistance (FIGURE 4). Thus the potential across the cell (V_{ext}) should remain approximately constant and, if the depolarization of the uninnervated face decreased, the hyperpolarization of the innervated face should become greater.

The records in FIGURE 7 show a typical result. For negative pulses that did not depolarize the uninnervated face up to threshold for the conductance increase, the voltages across the faces remained constant (*A*) and were about equal, indicating the similar resistances of the membranes. For stimuli above threshold, the voltage across the uninnervated face decreased during the pulse and simultaneously the voltage across the innervated face increased (*B*). There was some conductance increase in the innervated face also, as was shown by oppositely directed currents (*C*). However, the response was much smaller. In a few cells the magnitude of the conductance increase was very nearly equal in both faces (cf. FIGURE 9), but it was never found to be much larger in the innervated face. Whatever embryological mechanism has evolved to localize the conductance increase to the uninnervated face, it is not completely effective.

Neural responses and the conductance increase. Augmentation of the external currents produced by p.s.p.s following activation of the conductance increase is shown in FIGURE 8. However, the externally recorded response had a peculiar form that illustrates the importance of passive as well as active membrane properties. On neural stimulation of a cell in which the conductance was at the resting value, the external voltage had two peaks, although the voltages across the cell membranes were monophasic (FIGURE 8*A*). The second peak was due to the increased current that flowed as a result of activation of the conductance increase. This peak disappeared when the cell was sufficiently hyperpolarized to block the increase (*B*), and was absent when the p.s.p.s were below its threshold (*C*). The early peak contained a large component of current charging the capacity of the caudal membrane since it preceded the maximum potential recorded across this membrane (Freygang, 1958; Freygang and Frank, 1959). Also when the conductance increase was activated just before a neural response was evoked (*D*) there was only a single peak. In this situation the cell time constant was very brief (FIGURE 5), and the transmembrane and externally recorded responses had the same time course. The peak of the external response was slightly later than when the conductance increase had not been activated. The amplitudes of the transmembrane responses were greatly reduced, but that across the uninnervated face more so. Correspondingly the external voltage was increased. The latter part of the responses in *D* coincided, since the conductance increase was activated in both instances.

The capacitative current did not produce any diphasicity in the external potential (*B*). The criterion for a monophasic voltage applied across the inactive membrane to produce a diphasic current through it is that the voltage should decrease more rapidly than the inactive membrane time constant (Freygang and Frank, 1959). If the two faces had the same time constant there would be no diphasicity for small p.s.p.s, since they decay at a rate as slow as or slower than the membrane time constant. Activation of the conductance increase would reduce the uninnervated membrane's time constant as much as or more than it reduced that of the innervated membrane (FIGURE 7), and again no diphasicity would be expected.

Demonstration of the properties of p.s.p.s, for example, their gradation and reversal by applied currents, may be difficult in cells where there are electrically

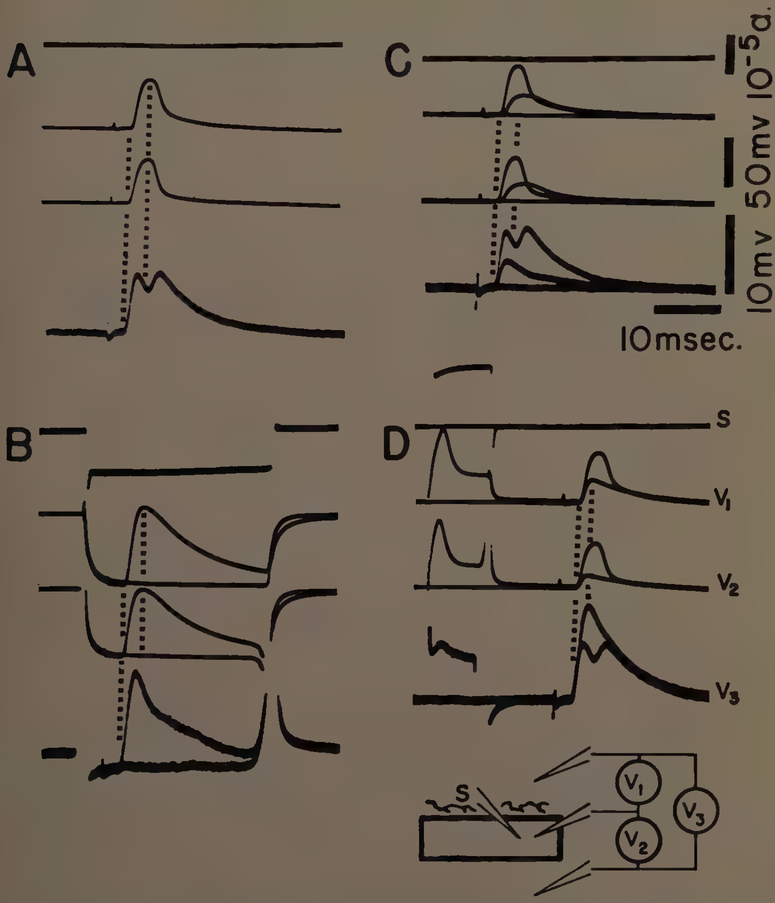

FIGURE 8. Effect of the conductance increase on neural responses. *R. erinacea.* Recording and stimulating as in diagram except that nerve stimulating electrodes are omitted. Upper trace: intracellular stimulating current. Second trace: potential across innervated face (V_1). Third trace: potential across uninnervated face (V_2). Fourth trace: potential across cell, caudal positivity up (V_3). A large neurally evoked response produced a caudal positive external potential that had two peaks (*A*). The second peak was blocked when the conductance increase was prevented by hyperpolarization (*B*) that also prolonged and increased the height of the response. Small neurally evoked responses that did not activate the conductance increase also produced external potentials with a single peak (*C*, superimposed traces of large and small responses). When a neurally evoked response was preceded by activation of the conductance increase, the potentials recorded across the faces were both reduced, but that across the uninnervated more so, and the external potential was therefore enlarged (*D*, superimposed responses with and without applied depolarizing pulse). The cell time constant was greatly reduced so that all the potentials had the same time course. The peak of the external potential occurred later when the conductance increase had been activated.

excitable responses, and in *Raja* electroplaques the conductance increase was a complicating factor. While the p.s.p.s showed increase on hyperpolarization with intracellularly applied currents (FIGURE 8*B*), it was difficult to obtain reversal because of the conductance increase. However, utilizing the larger currents that may be passed through an external polarizing electrode, it was possible to do so (FIGURE 9). Depolarization reduced the response height and then reversed it (*D* to *F*). The value of the reversal potential in this experiment was about 70 mv positive to the resting potential, that is, about zero membrane potential. The response height was not linearly related to the membrane potential or to the polarizing current, which was probably due to the

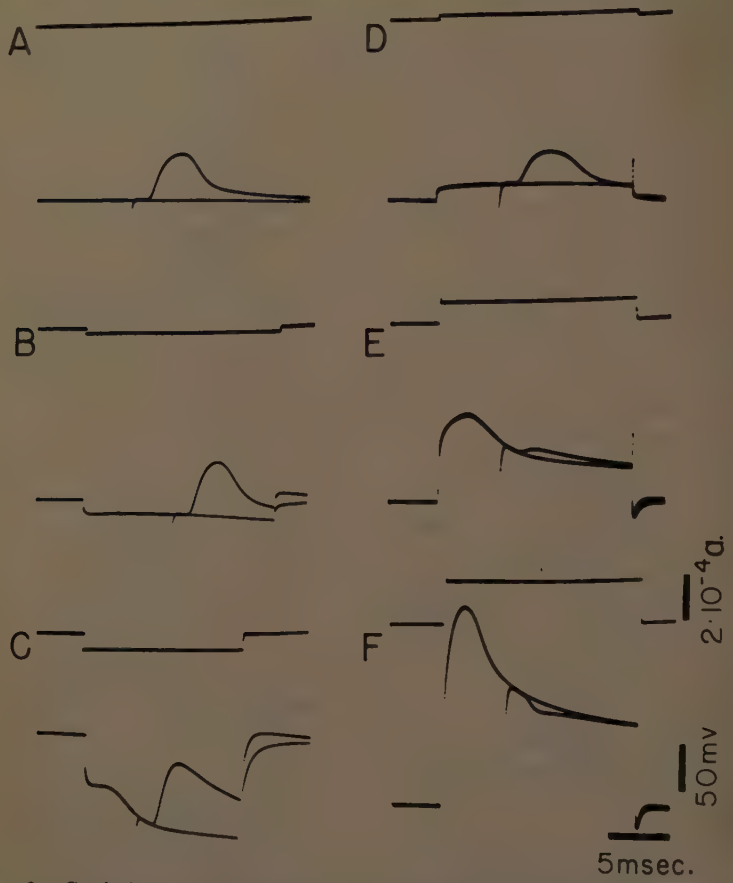

FIGURE 9. Gradation and reversal of the p.s.p. by applied currents. *R. erinacea*. Upper trace: externally applied polarizing current as in FIGURE 7. Lower trace: potential differentially recorded across the innervated face. Nerve stimulation by closely applied wire electrodes. A neurally evoked response (*A*) was augmented and slowed by currents inward through the innervated face (*B*, *C*). Outward currents reduced and reversed the response (*D* to *F*). The reversal potential was about 70 mv. There was considerable conductance increase in the innervated face (cf. FIGURE 7), and the response height was not linearly related to membrane potential.

conductance changes that occurred even in the absence of the p.s.p. In this cell the magnitude of the conductance increase in the innervated face was large. Hyperpolarization of this face augmented the p.s.p. (*B* and *C*) and prolonged it since the conductance increase was prevented.

Neural responses in trains showed changes similar to those recorded in FIGURE 8*D*. The external voltage produced by the first neural response in a train had 2 peaks (FIGURE 10*A*, trains of 1, 2, and 3 responses superimposed), but the later responses had only 1 peak and were increased in size. The potential across the uninnervated face was correspondingly decreased more than that across the innervated face. In *A* the third response was not appreciably increased in size over the second, but its peak was higher since it summed with the preceding activity. In longer trains the summation was very pronounced, and the response across the innervated face must have been close to the reversal potential for the p.s.p.s. Correspondingly, later p.s.p.s each contributed less additional potential. The external voltage reached 25 mv (*B*).

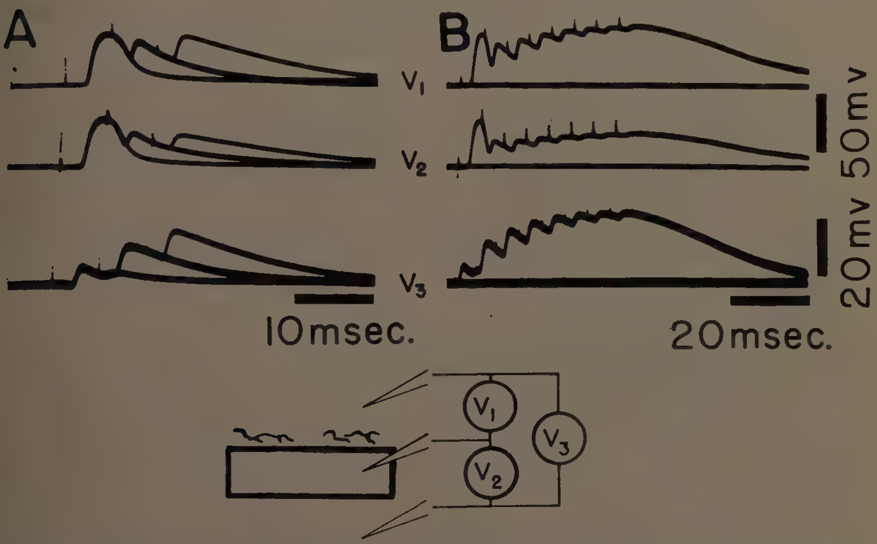

FIGURE 10. Trains of neurally evoked responses. *R. erinacea*. Recording as in diagram; nerve-stimulating electrodes omitted. *A*: superimposed trains of responses to one, two, and three stimuli at ca. 170/sec. *B*: a longer train. The first externally recorded response in a train had two peaks. Later responses had only one peak, and summed with earlier responses. In a long train the potential across the innervated face approached the reversal potential for the p.s.p.s, and the additional potentials contributed by the later p.s.p.s were smaller.

Measurements on segments of organ. The validity of measurements on single cells may be checked using segments of electric organ involving large numbers of cells. This approach is particularly important when, as in *Raja*, there is variability among the cells. Also, new information may often be gained because of technical simplification. Electric organs are particularly suitable for study en masse because of their ordered arrangement (Albe-Fessard, 1951;

Albe-Fessard *et al.*, 1951; Altamirano *et al.*, 1953; Bennett and Grundfest, 1961*a*; and Bennett *et al.*, 1961). However, the analysis using intracellular recording may well be necessary to interpret the potentials produced by the tissue as a whole.

An experiment with a piece of electric organ involving about 90 elements in series and 8 in parallel is shown in FIGURE 11. This tissue was placed in the bridge circuit described above under METHODS. A brief pulse evoked a neural response that, as in FIGURE 8*A*, had 2 peaks. The A. C. bridge imbalance had an initial peak slightly later than the first potential peak, then fell a little, then increased again, and lasted over 100 msec. (FIGURE 16*B*). The long-lasting imbalance must have been due to the conductance increase. Further information was gained by superimposing polarizing pulses on the neural response (FIGURE 11*B* to *F*). Pulses such as to hyperpolarize the uninnervated membrane and depolarize the innervated had several effects. The neural response was first decreased in amplitude and then reversed. As it decreased, the second peak was reduced and finally disappeared and, simultaneously, the long-lasting imbalance was greatly reduced. The simultaneous loss of the second peak and of the long-lasting imbalance with this direction of polarizing current indicates that the conductance increase did indeed predominate in the uninnervated face of most cells. Both the hyperpolarization of the uninnervated face and the reduction of the p.s.p. height would reduce activation of the conductance increase in the uninnervated face, but the pulse alone should produce it if it occurred in the innervated face.

Currents in the opposite direction augmented the response height, but did not greatly affect the bridge imbalance (*F*). With this direction of current the pulse itself should produce the long-lasting imbalance even if there were no neural response.

When a response was evoked during the long-lasting imbalance produced by a preceding response, that is, during the conductance increase, it had no second peak (*G*; cf. FIGURE 10). Block of the conductance increase due to the first response by polarizing as in *D* caused a second peak to appear in the following response that then produced a long-lasting imbalance (*H*).

The initial peak of bridge imbalance was only slightly reduced by the polarizing currents in *A* to *E*, although the evoked potential became larger, smaller, or reversed. This finding indicates that the conductance change associated with the p.s.p. was independent of the membrane potential. The small changes that did occur were probably due to block of impulses in the nerves or to early activation of the conductance increase. The additional imbalance produced by a second response was about equal to the early imbalance (*G* and *H*). However, since the two conductance changes were occuring in different membranes, strict additivity of the bridge imbalance would not necessarily be expected.

Ionic environment and the conductance increase. Because of the similarity of the conductance increase to delayed rectification in other tissues, it is of interest to investigate the effect of changing the ionic environment. As noted earlier, the conductance increase is unlike delayed rectification in muscle in that it is associated with a depolarization rather than a hyperpolarization. Replacement of external Na^+ by choline had no effect, and removal of external K^+

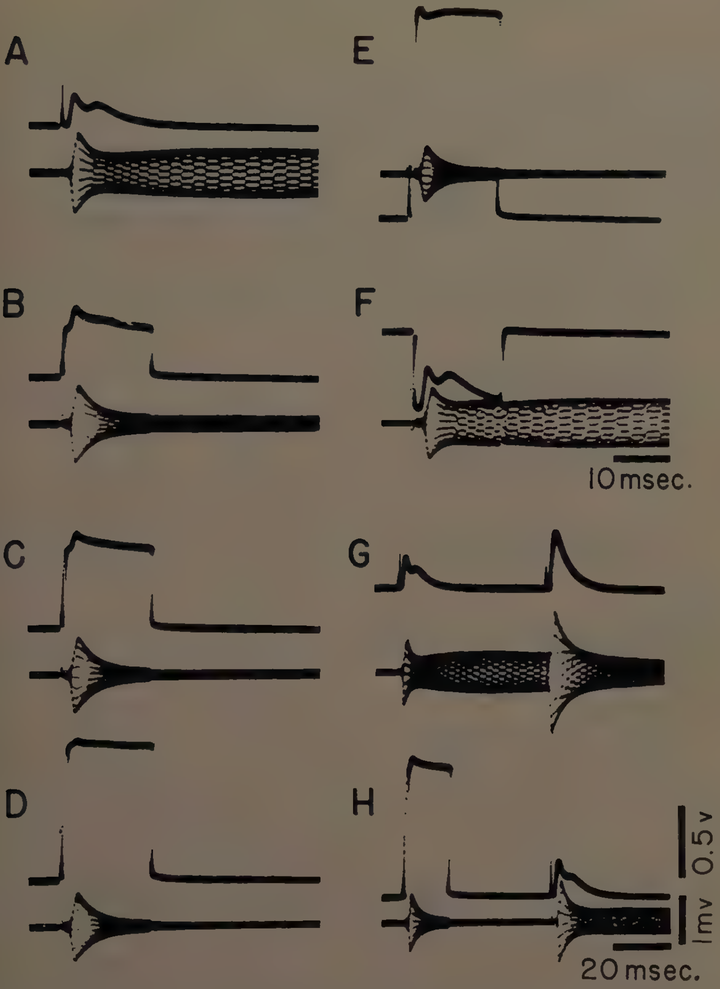

Figure 11. Response of a segment of electric organ and impedance changes. *R. erinacea* Bridge circuit is described under the heading Methods. The preparation contained about 90 electroplaques in series, and 8 columns in parallel. Upper trace: direct display of bridge output. Lower trace: bridge output after filtering out low frequencies and further amplification. Frequency and amplitude of A. C. input, 10 kc. and 0.35 v. The response to a brief stimulus had 2 peaks like the neurally evoked response of single cells. The resulting A. C. imbalance had an initial peak slightly later than the first potential peak and then a slowly developing imbalance that long outlasted the potential change. When polarizing pulses of increasing strength were passed during the neurally evoked response in order to hyperpolarize the uninnervated faces and depolarize the innervated, the response was decreased in amplitude, lost its second peak, and finally became inverted (*B* to *E*). Concomitantly the long-lasting imbalance was greatly decreased, but the initial imbalance was only slightly changed. Oppositely directed currents increased the response height without greatly changing its form or the resulting bridge imbalance (*F*). When a response was evoked during the long-lasting imbalance produced by an earlier response, it had only a single peak (*G*). When polarization was applied during the first response to prevent the long-lasting bridge imbalance, the second response had 2 peaks and was itself followed by a long-lasting imbalance (*H*).

caused only a small hyperpolarization. However, when Cl^- was replaced by acetate, there was an increase in the resting resistance and a marked augmentation of the depolarization associated with the conductance increase. The depolarization became greater than the threshold for activating the conductance increase and, consequently, the response was regenerative. When near-threshold pulses were given, graded subthreshold responses might be seen, or the response might continue to rise following the pulse up to a value 20 to 40 mv positive to the resting potential (FIGURE 12). Corresponding to the slower development of the conductance increase near threshold (FIGURE 5), the rising phase was slow, requiring 20 to 30 msec. for threshold pulses. The response lasted several seconds (*C* to *E*), the conductance remaining high throughout (*E*). The relative refractory period was much longer, particularly when measured by decrease in duration (Cohen *et al.*, 1961).

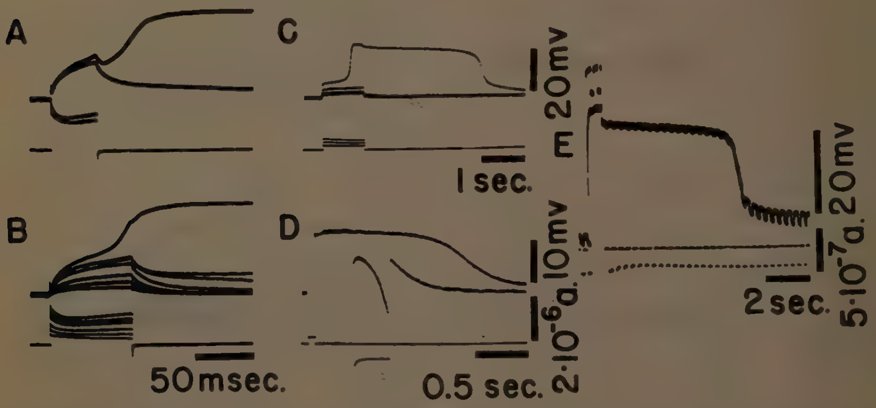

FIGURE 12. All-or-none responses produced by the conductance increase when Cl^- was replaced by acetate. *R. erinacea.* Upper trace: intracellular potentials. Lower trace: polarizing current. *A*, *B*, same cell; *C* to *F*, from different cells. Just suprathreshold pulses evoked a response that continued to rise following cessation of the pulse to a value 20 to 40 mv positive to the resting potential (*A*, *B*). The response could last several seconds (*C* to *E*) with some slow fall-off and then a relatively rapid return to near the base line followed by a further slow repolarization. The conductance was high throughout the response (*E*). The response could be shortened by sufficiently large hyperpolarizing pulses (*D*, superimposed traces with and without hyperpolarizing pulse).

It seems most probable that the conductance increase had been converted into a depolarizing response rather than that the depolarization represented an additional response of the cell. If so, there would be no response component analogous to delayed rectification to terminate the action potential, once it was initiated. The falling phase would therefore necessarily have been due to a turning off of the conductance increase. Initially the turning off probably involved inactivation, since there was marked refractoriness following a response. However, the falling phase would have become regenerative when the potential fell below threshold for the conductance increase. In spite of regeneration, the rate of fall was quite slow. The turning off required several hundred msec. near the resting potential in the normal preparation (FIGURE 6), and probably a similar time in acetate since the subthreshold responses were about this long.

The preceding argument may be extended to predict premature termination or abolition of the response by hyperpolarizing currents (Fitzhugh, 1960; Huxley, 1959; and Tasaki, 1956). If during a response the potential were lowered to below the threshold, the conductance would return to normal more rapidly than if the cell remained depolarized. A stimulus that lowered the membrane potential to near the resting level for sufficiently long did cause the response to be terminated (*D*).

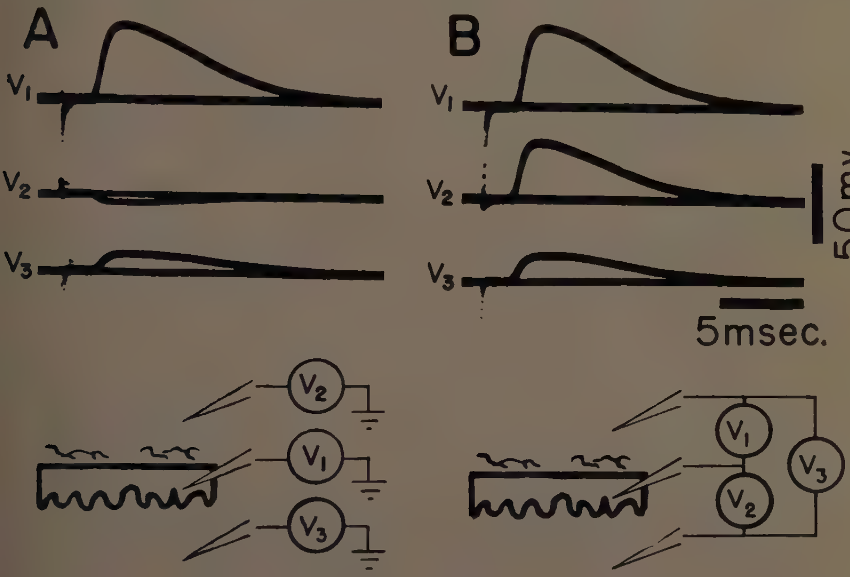

FIGURE 13. Neurally evoked responses of disc-type electroplaques. *R. eglantaria.* Recording as in diagrams except that nerve-stimulating electrodes are omitted. *A*, monopolar recordings; *B*, differential recordings. The responses had slower falling phases than those of cup-type cells. The external potentials had nearly the same time course as the intracellular potentials and were larger than those from cup electroplaques.

The only obvious ionic flow that would result in depolarization when acetate replaces Cl^- is Cl^- leaving the cell. However, the response is maintained for at least 48 hr. in Cl^--free solution. Direct analyses will be required to show whether adequate Cl^- remains to account for the large conductance during the response. Possibly some other internal anion may be involved.

Responses of disc-type electroplaques to neural and direct stimulation. The responses of disc-type electroplaques were simpler than those of the cup-type cells in that there was less of the conductance increase. The anatomical correlation of inactivity of a face with relatively increased surface area was thus confirmed although there was, as in the cup-type, considerable variation from cell to cell. Typical neurally evoked responses of discs are shown in FIGURE 13, recorded monopolarly and differentially. These responses were in several aspects distinctly different from those of the cups. Most obviously the externally recorded responses were larger and had but a single peak (B, V_3). The falling phase of the response recorded both intra- and extracellularly was much slower, and the extracellular records had nearly the same time course as the intracellular ones. These differences suggest that discs differ from cups in that there is less conductance increase produced by depolarization, in having a lower resistance uninnervated surface, and in having a briefer time constant.

The resting resistance of the uninnervated face must have been lower, since the resistance in the extracellular current paths around the cells would be about the same in cup and disc types, and a larger portion of the potential generated in the innervated face appeared across the extracellular resistance (FIGURE 13*B*). The other differences were directly demonstrated with intracellular stimulation. There was less fall-off from the initial peak during a large depolarizing pulse (FIGURE 14*A*; cf. FIGURE 4), and the reduction in a subsequent test pulse or neural response was also smaller (*C*, *D* and *F*). The p.s.p. was inverted when it was superimposed on the initial peak of a depolarizing pulse (*E*). Some discs had even less conductance increase than the cell illustrated in FIGURE 14. The time constant was briefer than in cups (*B*, the slow rise during depolarization was partly due to slow rise of the current pulse).

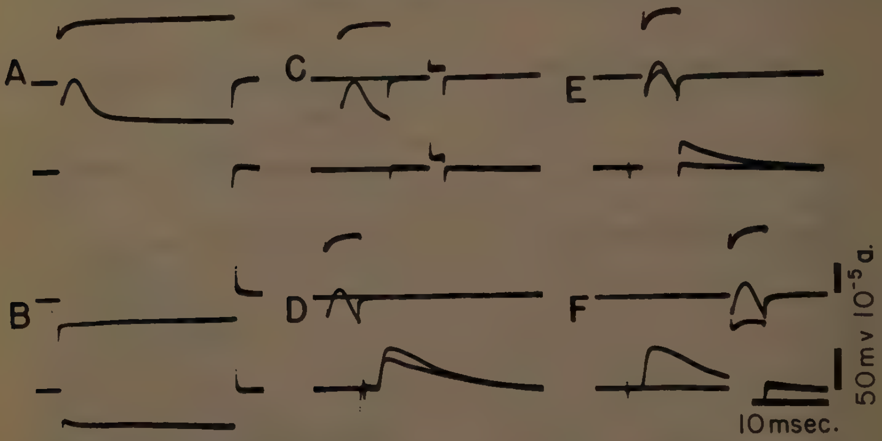

FIGURE 14. Intracellular stimulation of disc-type electroplaques. *R. laevis.* Upper trace: polarizing current. Lower trace: intracellular potential. Neurally evoked responses were elicited in *D* to *F* by external electrodes. The response to depolarizing current showed only a little fall-off during the pulse (*A*). The time constant was brief, as shown by hyperpolarizing pulses (*B*). Following a large depolarizing pulse, a testing pulse and a neurally evoked response were only slightly reduced (*C*, *D*, superimposed traces with and without initial depolarizing pulse). A large, neurally evoked response only slightly reduced the amplitude of a succeeding depolarizing pulse (*F*, with and without neural response). A neurally evoked response evoked during the initial peak of a large depolarization reduced its height, indicating that the depolarization exceeded the reversal potential for the p.s.p. (*E*, with and without neural response).

The limited conductance increase that occurs in discs is predominantly in the uninnervated face and, during a train of neural responses, the external potential was augmented as in cups (FIGURE 15*A* to *C*). Summation was also present, but usually to a smaller extent than in cups, since the initial responses were larger. In some cells there was little alteration of the response indicating the absence of much conductance increase (*D*). Probably the conductance change producing the initial p.s.p. in a train was larger in discs, since there appeared to be less reduction in response due to loading of the generating membrane. However, during a train the additional summation in cups would make the responses about equal (FIGURE 10*B*).

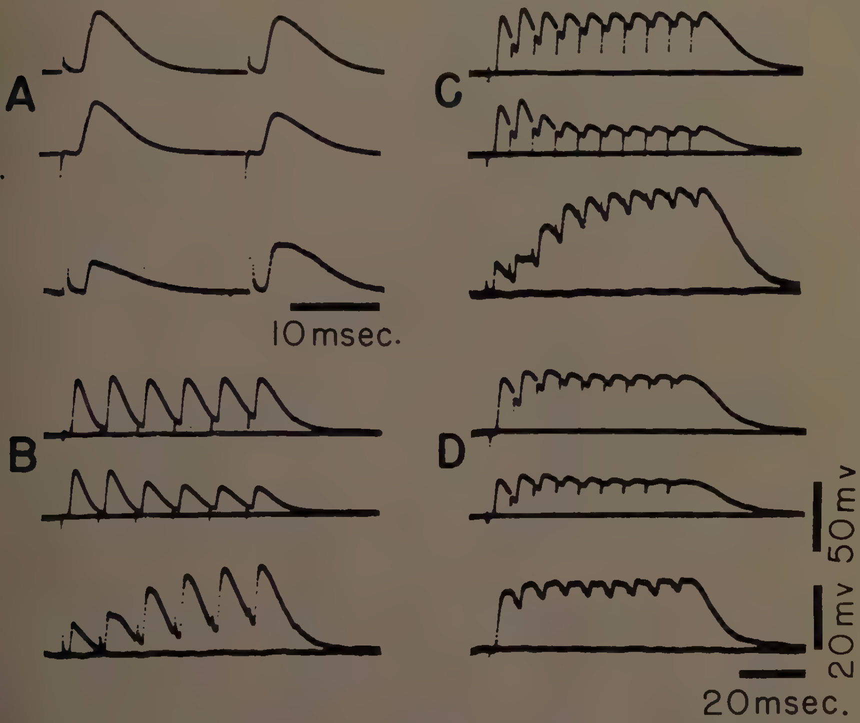

FIGURE 15. Trains of neurally evoked responses. *R. eglantaria*. Recording and stimulating as in FIGURE 10. *A* to *C*: trains of stimuli to one cell of increasing frequency. *D*, another cell. The conductance increase developed slowly and the potential recorded across the uninnervated face decreased while that across the innervated face showed little change in amplitude (*A* to *C*). Correspondingly the external potential increased. There was little conductance increase in the cell of *D*, and the external potential showed little change in amplitude during the train. The potentials across the innervated face were large and probably near the reversal potential. They showed little augmentation in height during the train, but the falling phase was slowed, probably due to summation (*C*, *D*).

Comparison of segments of organ containing cup- and disc-type cells. The relative magnitude of the conductance increase was also tested by measuring A.C. impedance of segments of electric organ. In FIGURE 16, responses of organ segments containing cup- or disc-type cells in approximately equal number in series were recorded with the A.C. imbalance they produced. As in single cells, the external response of the cup-type was smaller, and it was followed by a larger longer-lasting impedance change. The initial imbalance, at the same gain in *A* to *D*, was larger in the disc type, and the long-lasting imbalance was only a small fraction of the initial imbalance (*E*).

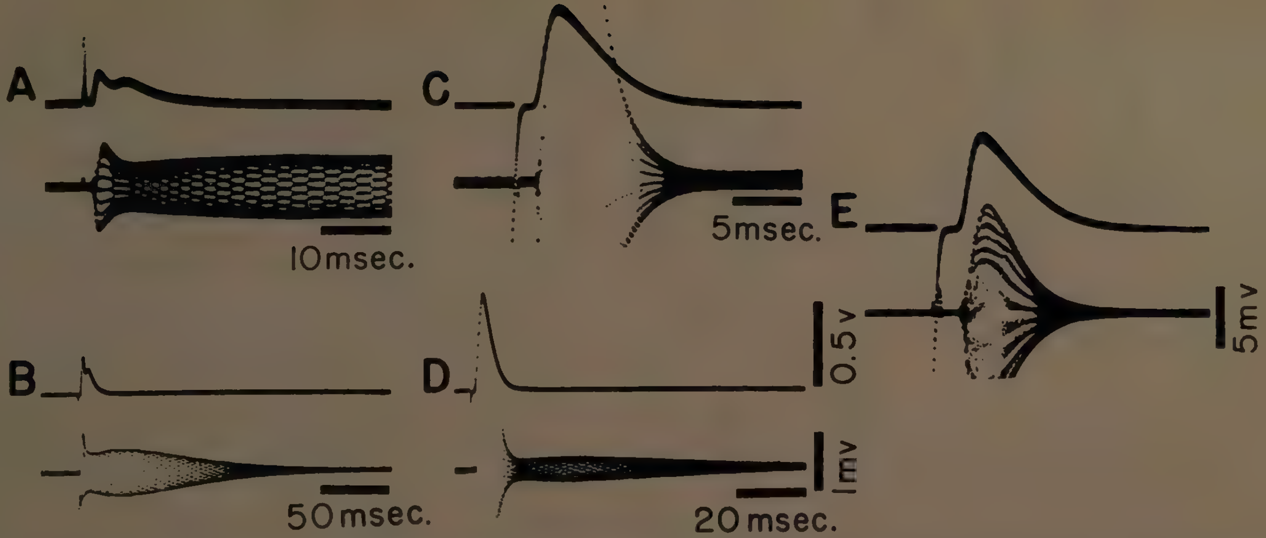

FIGURE 16. Comparison of electrical responses and conductance changes in organ segments containing electroplaques of cup-type (*R. erinacea*) and disc-type (*R. eglantaria*). Displays as in FIGURE 11. Segments of organ of approximately the same size and containing the same number of electroplaques in series were used. The same A. C. signal, 10 kc. and 0.35 v, was applied to both and the gains were the same for *A* to *D*. The bridge imbalance following activity is shown at lower gain in *E*. The response to a brief stimulus of the cup-type organ had 2 peaks and produced a long-lasting bridge imbalance (*A*, *B*). The response of the disc-type organ was larger and produced a smaller long-lasting imbalance (*C*, *D*). The initial imbalance was larger so that the long-lasting imbalance was much smaller proportionately (*E*).

Discussion

Electrically inexcitable and electrically excitable response components. The p.s.p.s in *Raja* electroplaques exhibit most of the properties known of p.s.p.s in other tissues (Grundfest, 1957*b*, 1959). Particularly they show decrease in size and reversal when large enough outward currents are passed through the generating membrane (FIGURE 9). The reversal potential was close to zero membrane potential as in a number of other cells where it has been determined for depolarizing p.s.p.s (del Castillo and Katz, 1954; Eccles, 1957; Grundfest, 1959; and Nishi and Koketsu, 1960). The reversal was more readily demonstrated in segments of organ (FIGURE 11), and the early impedance change producing the p.s.p. was seen to be only slightly changed by the polarizing currents. The changes that did occur may be ascribed to effects on the electrically excitable membranes, either through blocking of impulses in the presynaptic nerve fibers or through activation of the conductance increase. Independence from applied voltage of the p.s.p. impedance change and the potential to which it tends to take the cell, that is, its reversal potential, is the most rigorous definition of electrical inexcitability. Conceivably these aspects of the p.s.p. might be changed by applied fields although the p.s.p. could not be evoked by the fields themselves. These effects would be electrically excitable and probably do occur if sufficiently strong fields are applied. Mechanisms could be similar to the reduction in resistance that occurs with strong hyperpolarizing currents (Bennett *et al.*, 1959*b*; Hodgkin, 1947*a*; and Ito, 1957), or could involve ionophoresis of transmitters (Eccles, 1957).

The constancy of the impedance change producing the p.s.p. has not been carefully determined in electrically excitable cells because of the responses that occur to polarization in the absence of neural stimulation. In the single *Raja* electroplaque the response height was not linearly related to the voltage, implying that the impedance change was not constant, but certainly the conductance increase was at least partially responsible. Although it is difficult to satisfy the constancy criteria in electrically excitable cells, p.s.p.s still show gradation and reversal during and after spikes and other electrically excitable responses involving conductance changes. It is therefore simpler to consider the p.s.p. membrane as separate from the electrically excitable membrane, and as occurring in separate patches be they even of molecular dimensions (Altamirano *et al.*, 1955*a*). It is difficult to conceive of a patch of membrane that when generating a spike would in response to a chemical stimulus stop to generate a p.s.p. tending to take the cell to a different potential from that of the spike. This patch would also have to retain its chemical excitability when it was refractory to further electrical stimuli (del Castillo and Katz, 1954). The separation of spike-generating (or conductance-increase) membrane and p.s.p.-generating membrane would still be attractive even if the p.s.p. were not found to be electrically inexcitable in the precise sense.

The conceptual basis for electrical inexcitability of p.s.p.-generating membrane in electrically excitable cells is quite similar to the Hodgkin and Huxley (1952*b*) suggestion separating areas in axonal membrane responsible for sodium and potassium permeabilities. The work of these investigators provides no direct evidence that a single region might not be permeable to both sodium and potassium and might change with the potential and ionic environment in such a way as to give the observed conductivities. Indeed they state, "an alternative hypothesis (to separate sodium and potassium systems) is that only one system is present but that its selectivity changes soon after the membrane is depolarized." However they note that "this hypothesis cannot be applied in simple form since potassium conductance rises too slowly for a direct conversion from a state of sodium permeability to one of potassium permeability." (Hodgkin and Huxley, 1952*b*, p. 503.)

Additional indications of the separation of p.s.p. and spike-generating membrane are the existence in certain cells of regions that generate p.s.p.s but not spikes, while other regions do generate spikes (Werman, 1960; Hagiwara *et al.*, 1959), and the existence of some electroplaques that produce p.s.p.s but are completely electrically inexcitable (Bennett and Grundfest, 1961*a* and *b*; Bennett *et al.*, 1961). In the cited work on the latter cells the impedance changes during polarization were not measured. However in columns of *T. nobiliana* organ and *Narcine* accessory organ the response height-polarizing current relation is linear up to and beyond the point of reversal. The linearity implies a constant impedance change.

The existence of a reversal potential is strong evidence for chemical transmission, given as the only alternative that postjunctional potentials are generated by electrically excitable prejunctional elements. Reversal would require that the polarization spreading into the prejunctional element from the postjunctional should exceed the reversal potential of the prejunctional response. Conceivably such reversal could be obtained, since the reversal potential of the spike peak can be demonstrated in some isolated electrically excitable cells (Altamirano, 1955; Hodgkin and Huxley, 1952*a*). However, excitation would probably spread throughout the prejunctional cell, reversal could be obtained only at the beginning of a pulse since otherwise the prejunctional structure would be refractory and, depending on the coupling resistance between the pre- and postjunctional structure, particularly if it were rectifying (Furshpan and Potter, 1959), the reversal potential would be very large.

It should be noted that postjunctional potentials of electrotonic junctions (or "ephapses"; Grundfest, 1959) should show over a short range a constant impedance change and gradation of response height, that is, appear electrically inexcitable. These relations would hold as long as the polarization spreading into the prejunctional structure did not affect invasion of the prejunctional impulse into it. However, if the coupling were not close, the impedance change would be small, and the apparent value of the reversal potential obtained by extrapolation would be large (Watanabe *et al.*, 1960).

Absence of reversal potential is not conclusive evidence against chemical transmission. If a transmitter changed the voltage of a membrane without changing its impedance, then no reversal could be demonstrated. A possible example of this kind of response is the secretory potential of the salivary gland (Lundberg, 1958). There is of course pharmacological evidence for chemical transmission in electroplaques (Altamirano *et al.*, 1955*b*; Bennett and Grundfest, 1961*b*; Bennett *et al.*, 1961; Couteaux and Szabo, 1959; Feldberg and

Fessard, 1942; and Szabo, 1961*a*). For example *Raja* electroplaques are depolarized by acetylcholine ionophoretically applied to the innervated face, and the neurally evoked response is blocked by curare and prolonged by prostigmine and eserine (B. Cohen, M. V. L. Bennett and H. Grundfest, unpublished data; Brock and Eccles, 1958).

The electrically excitable component of the *Raja* electroplaque response, that is, the conductance increase on depolarization, appears homologous to delayed rectification in nerve and muscle. The increase is similar to that of the frog slow-muscle fibers (Burke and Ginsborg, 1956) and of twitch fibers (Jenerick, 1959) or squid nerve (Hodgkin and Huxley, 1952*a*) when external sodium is replaced by choline. The natural occurrence of the response in isolation tends to validate the procedure whereby it is isolated experimentally in the latter tissues. The rate constants in the different tissues are different and, what may be more significant, the response in the electroplaques is associated with a depolarization rather than hyperpolarization. In some nerve cells the associated potential also appears to be a depolarization (Bennett *et al.*, 1959*b*; Dalton and Fitzhugh, 1960; Ito, 1957; Kao, 1960; and Kao and Grundfest, 1957).

The nature of the response remains obscure. The tentative identification with Cl^- or perhaps another internal anion does not fit with the data from frog muscle implicating K^+ (Adrian, 1956; Jenerick, 1959). It may be that the muscles from which the electric organs develop are different from frog muscles, or that the electroplaques have changed in the process of evolving. The tail muscles are readily studied with microelectrodes, and it should be relatively easy to resolve this question.

The turning off (or inactivation) of the conductance increase, in spite of continued depolarization (cf. H. Grundfest, this monograph) has not been noted in squid nerve but may occur in motoneurons (Eccles, 1957) and in nodes of Ranvier (Frankenhaeuser and Waltman, 1959). The properties of the all-or-none response in acetate Ringer should be somewhat different from those postulated for other prolonged action potentials (Fitzhugh, 1960; Noble, 1960), and should be investigated further. Only a single conductance change appears to be involved.

Evolution of the Rajidae. In the absence of a demonstrated function the evolution of Rajid electric organs is an open question. Darwin (1959, p. 139) recognized the problem of "by what graduated steps (electric) organs have been developed in each separate group of fishes" in Rajidae, where there was no known function, and in the eel and *Torpedo*, where the first graduated steps would have no value as weapons. The problem has been somewhat clarified by the demonstration of electrical guidance systems in Gymnotidae, Gymnarchidae, and Mormyridae (Bennett and Grundfest, 1959*a*; Grundfest, 1957*a*; Lissmann, 1958; and Lissmann and Machin, 1958). Presumably such systems could develop from the small electric fields produced by muscle (but probably not by nerve), given the already fairly electrically sensitive lateral-line receptors (Regnart, 1931; cf. Lissmann, 1958). In every clear case, electric organs are derived from muscle (Fritsch, 1890; Ewart, 1892; Dahlgren, 1914*a* and *b*; and Szabo, 1960), but in others the precursors do not pass through a stage closely resembling myoblasts (Keynes, 1961; Johnels, 1956). In all cases, however, the pharmacology is similar to that of skeletal muscle. Where known, the electrical receptors appear to be evolved from the lateral-line system (Lissmann, 1958; Bennett and Grundfest, 1959*a*). The involvement of both muscle and lateral line possibly explains the absence of electric organs from invertebrates.

The hypothesis that the evolution was associated with an electrical guidance system is complicated by lack of evidence for any such system in four of the six evolutionary lines. In two of these (Astroscopidae and Malapteruridae) the fish are strongly electric without any sign of a low-voltage system that might be used for location. In Torpedinidae, *Narcine* has an accessory organ producing only small potentials on neural stimulation, but the physiological discharge is completely unknown (Bennett and Grundfest, 1961*a*). In Rajidae also the natural discharge requires investigation.

In the absence of functional data on Rajidae the anatomical and electrophysiological findings may shed some light. Ewart (1888) in considering whether the organs were degenerate concluded rather that they were newly evolving. Histological deterioration is never observed and, in the anatomically simplest form, the organ develops when the fish is almost full grown. Vestigial organs would be expected to develop early and then, possibly, to deteriorate.

The electrophysiological investigations show different degrees of adaptation in cells of a single organ, a characteristic unknown in other electric fish and, possibly, a primitive one or, at least, one suggestive of continuing evolution. The central control also appears to be the least developed in the Rajidae; although in other electric fish synchronization may be exceedingly precise (Bennett and Grundfest, 1959*a*, 1961*c*).

Ewart has suggested that the cup-type cell represents an evolutionary step towards the disc-type. On the other hand Ishiyama (1958), in an extensive study of Japanese skates covering many characters in addition to those of the electroplaques, concluded that there were two divergent evolutionary lines. The present study shows that both forms of electroplaque may be more or less equally effective, at least after the first few responses in the fused tetanus that constitutes the whole discharge. In the cup-type the responses would initially be smaller, but these cells would have the advantage of a lower-resting flux across the uninnervated face. Possibly speed of response is sacrificed to lower resting energy consumption. Before this argument can have much validity, the energy consumption of the two types of organs should be measured, and the importance to organ function of rise time of the response should be evaluated.

The fibers in the muscles from which the electroplaques develop produce spikes (Grundfest and Bennett, 1961), and therefore the disc-type cells may be considered more evolved in having lost more electrically excitable membrane. The presence of the conductance increase in the innervated membrane is clearly nonadaptive. Possibly the discs studied here do produce somewhat larger responses than the cups on the average, although there must be considerable overlap (FIGURES 10 and 15). Ewart (1892) described an intergrade between the cup and disc (*R. fullonica*) and a more primitive cup which was thick, which contained more striated material even extending into the stalk, and which did not lie in a well-formed connective tissue chamber (*R. radiata*). It would be desirable to examine these species electrophysiologically. The variation in cells of a single organ in localization and magnitude of the conductance increase suggests that the anatomical intergrades may also be functional intergrades.*

R. clavata electroplaques, which are of the disc form, were studied by Brock and Eccles (1958). From their data, the uninnervated faces appear to be of lower resistance than in *R. eglantaria* and *R. laevis*, and the external potentials are larger. These cells may represent a more extreme disc type. No direct test for the conductance increase was made, however, and the experimental techniques were sufficiently different that the question should be re-examined. If the cells do have no conductance increase they will be electrophysiologically the same as those in the other families of marine electric fish. Probably one would be justified in considering them more advanced than the *R. eglantaria* cells, although there may be little anatomical differentiation.

Among the more remarkable examples of convergence in electric fish is the absence of spike-generating membrane in all known forms of marine electroplaques (Bennett *et al.*, 1961; Bennett and Grundfest, 1961*a* and *b*), while it occurs in all known fresh-water species. Assuming equal probability of developing electroplaques with and without spike-generating membrane, the probability of segregation of types in the 3 marine and 3 fresh-water lines is about 0.06 (Finney, 1948). In all marine fish the muscles from which the organs evolve have spike-generating membrane, so that a common environmental pressure would appear to be the cause. Most attractive is the high conductivity of sea water in adaptation to which the organs of Torpedinidae and *Astroscopus* are flattened (Grundfest and Bennett, 1961). P.s.p.-generating membrane might be advantageous in generating higher currents per unit area and allowing closer packing of the organ. In fresh water higher voltage would be more important. In view of the small voltages generated by *Narcine* accessory organ and *Raja*, this argument is not strong. Perhaps it is important that the loading of the p.s.p.-generating membrane does not affect the conductance change producing it, and it would be possible to load the organ down to the theoretical maximum power point. Electrically excitable membrane probably could not be loaded down to this extent. However, the electric eel does appear to have an internal resistance independent of load (Cox *et al.*, 1945), and this explanation is probably not valid either.

GYMNOTIDAE

Results

The electroplaques of the Gymnotids are very diverse compared to those of the Rajids, and they take a number of forms with little intergrading between them. The simplest are those of *Electrophorus* in which, as noted already, one face is capable of generating a spike and the other is inexcitable. The electroplaques of *Hypopomus*, which will be discussed here, are more complex. The cells are similar to those of a number of other Gymnotids and also to those of African electric fish (Bennett and Grundfest, 1961*c*; Keynes *et al.*, 1961). Both faces generate spikes but, because of the different properties of the two faces, the spikes are out of phase and a diphasic external potential results. There is also a peculiarity of innervation; it occurs on a short process or stalk from the main part of the electroplaque. The stalk also possesses spike-generating membrane, and the impulse arises in it and propagates to invade the body of the cell.

---

* Ewart examined a specimen with typical cups that he identified as *R. eglantaria*. This identification was probably incorrect, however, since he cited Gunther as stating that *R. eglantaria* was similar to *R. circularis*, while Bigelow and Schroeder (1953) state *R. eglantaria* "is not closely paralleled . . . by any skate so far known from the eastern North Atlantic."

The electroplaques of *Sternopygus*, the other form to be discussed here, produce spikes at only one face as do those of *Electrophorus*. However the other face, when depolarized for some seconds by applied currents, changes its potential in the depolarizing direction. When the applied depolarization ceases the membrane potential gradually returns to the resting level. The result is that, in normal repetitive activity, pulses from firing of the innervated faces are opposed by a steady but smaller potential. The electroplaques have another unusual property: the resistance at the peak of the spike is approximately the same as at rest.

Anatomy. The body types of the Gymnotids are, in contrast to their electroplaques, not very variable, and the same diagram serves adequately for both *Hypopomus* and *Sternopygus* (FIGURE 17). In both, the electric organs run from the tip of the tail to the caudal margin of the head (dots). Caudal to the anal fin, the organs occupy most of the body cross section except for skin and vertebral column (FIGURE 17*A*). Anteriorly the organ lies just dorsal to the anal fin muscles, which have their origin on the overlying fascia. The electroplaques of *Hypopomus* are cylindrical or disc-shaped with their axes in the anterior-posterior direction. In a 15-cm. fish the cells are 300 to 500 μ in diameter and about 200 μ thick. In smaller fish the cells are somewhat less flattened (FIGURE 17*B*). Both faces are smooth except that from the caudal face there is a short stalk (*S*) on which the innervation (*N*) occurs. In the posterior part of the body there are 4 or 5 columns of cells on each side and the number of columns becomes reduced anteriorly. There is 1 electroplaque per column per segment and, consequently, considerable extracellular space between electroplaques.

The electroplaques of *Sternopygus* are rod- or spindle-shaped, and much longer than those of *Hypopomus*. In a 15-cm. fish they are about 1 to 2 mm. in the anterior-posterior direction and 200 μ in diameter. All are innervated at the caudal ends. The cells are tightly packed together, and the extracellular space in the organ is much smaller than in *Hypopomus*. The cells are not regularly arranged in columns, but often the rostral end of one electroplaque will be aligned with the caudal end of another. In these cases the extracellular space between them, 100 to 200 μ along the body axis, is divided by a septum.

Organ discharge of Hypopomus. The external potential produced by *Hypopomus* was diphasic but of opposite polarity at the 2 ends of the body when recorded with respect to a distant electrode (FIGURE 18). Pulses were emitted at about 5/sec. in a resting fish but, reflecting their use in a guidance system, the rate greatly accelerated when the fish was swimming or stimulated. Along

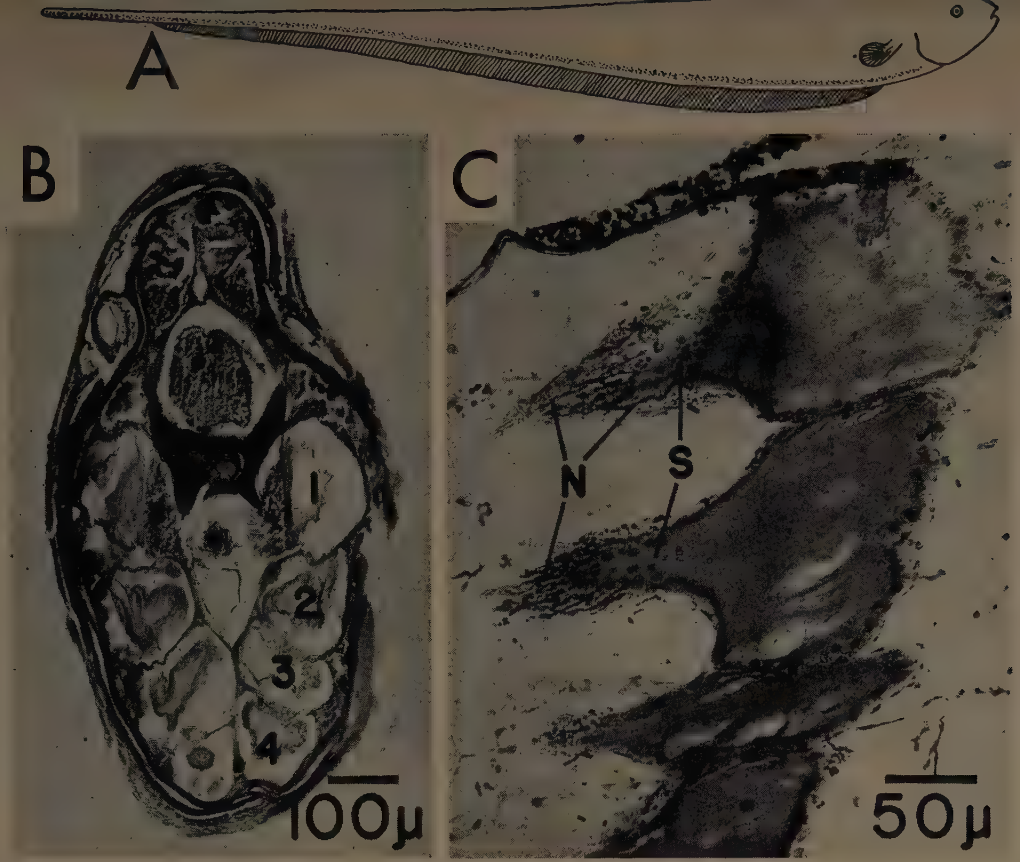

Figure 17. Anatomy of electric organ of *Hypopomus*. *A*, diagram of the fish. *B*, cross section near tip of tail (dorsum up) stained with hematoxylin and eosin. *C*, sagittal section near tip of tail (dorsum up, rostral to the right) stained with silver, Romane's method (5 cm. fish). The electric organ runs from the tip of the tail to just behind the head (*A*, *dots*). Caudally the electroplaques lie 1 above the other in 4 or 5 columns on each side (*B* 1 to 4, *C*). The number becomes reduced anteriorly. The cells are drum-shaped (*B*, *C*) except that they have a short stalk (*S*) emerging from the caudal face. The innervation by a number of nerve fibers (*N*) occurs on the stalk.

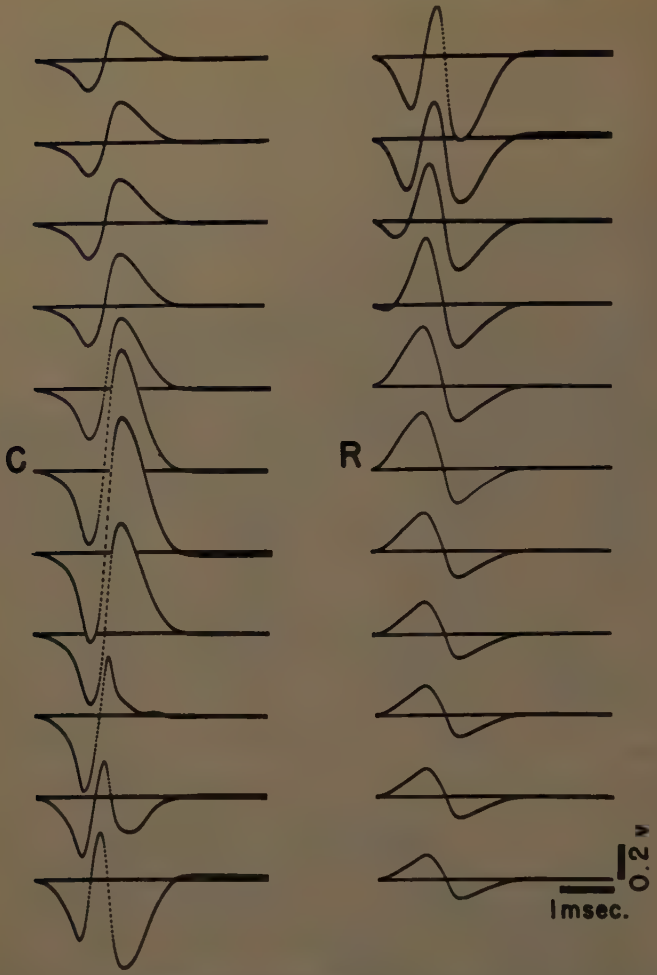

FIGURE 18. Organ discharge of *Hypopomus*. A 16.5-cm. fish was placed in a shallow plastic tray, 45 cm. long by 24 cm. wide by 5 cm. deep, and held by a gauze tube lengthwise against the long side, midway between the surface and bottom. Three electrodes were used. One was fixed at the head, and one was moved at 1.5-cm. intervals along the axis of the fish; these 2 electrodes recorded differentially against an electrode at the mid-point of the opposite side of the tray. The records were therefore somewhat larger but similar in form to what would have been obtained by monopolar recording in a very large volume of water. The brief discharges occurred at about 5/sec. when the fish was unstimulated. The discharge at the rostral-fixed electrode triggered the oscilloscope, and was used to align the records in the figure obtained from the exploring electrode (positivity of this electrode up). At the tip of the tail (*C*) the potential was diphasic and initially tail negative. Moving the electrode farther caudally, it became smaller, but was similar in form (records above *C*). Moving rostrally along the body, the potential became triphasic and then diphasic, initially head-positive, at the tip of the snout (*R*). The potential remained diphasic but decreased as the electrode was farther advanced (records below *R*).

the middle of the fish the discharges were triphasic, probably due to addition of asynchronous diphasic potentials, since all the electroplaques are oriented in the same direction and, as will be seen below, the single cells produce diphasic potentials.

Responses of Hypopomus electroplaques to direct stimulation. The response to intracellular applied depolarizing current is shown in FIGURE 19*A*, recorded monopolarly inside the cell and external to the two faces. The external potentials were equal but opposite, indicating the longitudinal orientation of the cell.

The initial negativity at the caudal (stalk or innervated) face indicates that this face had a lower threshold or a more rapidly rising spike. The ensuing much larger negativity at the rostral face indicates that this face also fired, and that its spike was longer-lasting or larger than that of the caudal face. These characteristics appear more clearly in differential recording (FIGURE 19*B*) where the spikes may be seen more or less separated, although the activity of each face produced some voltage drop across the opposite one. The differential recording between the external electrodes (V_3), rostral positivity up, was twice the size of the monopolar external records, since these were equal but opposite. The spike of the caudal face rose more rapidly than that of the rostral face and consequently there was rostral positivity externally. The caudal spike rapidly subsided, however, while the rostral spike lasted two to three times as long. During this phase there was rostral negativity in the external record. The negativity was large compared to the potential across the caudal face, suggesting increased conductance of the membrane following its spike. The increase would augment the external current produced by the rostral spike. At rest, the two faces had roughly equal resistances (FIGURE 20).

Further characterization of the activity of the two faces was obtained by stimulation with currents running along the cell axis (FIGURE 20; cf. FIGURE 7). When an anode was placed externally to the caudal face, this face was hyperpolarized, and the rostral face was depolarized (*A*). The rostral face was excited first, and there was rostral negativity initially in the external record. This activity then excited the brief discharge of the caudal face and there was a brief rostral positivity externally. The rostral spike outlasted the caudal spike, and the external record became rostral-negative again.

Oppositely directed currents tended to depolarize the caudal face and hyperpolarize the rostral. When the current was strong enough, the rostral face was so hyperpolarized that it was not excited by the caudal spike (*B*). Then the caudal spike was smooth and of short duration without the small longer phase as in *A*. Thus this phase was due to IR drop from activity of the rostral face. In *B* the IR drop produced by the stimulus was smaller following the spike, again indicating an increased conductance. In most cells stimuli threshold for the caudal face blocked excitation of the rostral face. In these cases excitation of the rostral face could be brought about by a little intracellular depolarization, itself subthreshold, but which summed with the caudal spike.

The external record in FIGURE 20*B* is diphasic. The small negative second phase might have been due to discharge of the capacity of the rostral face,

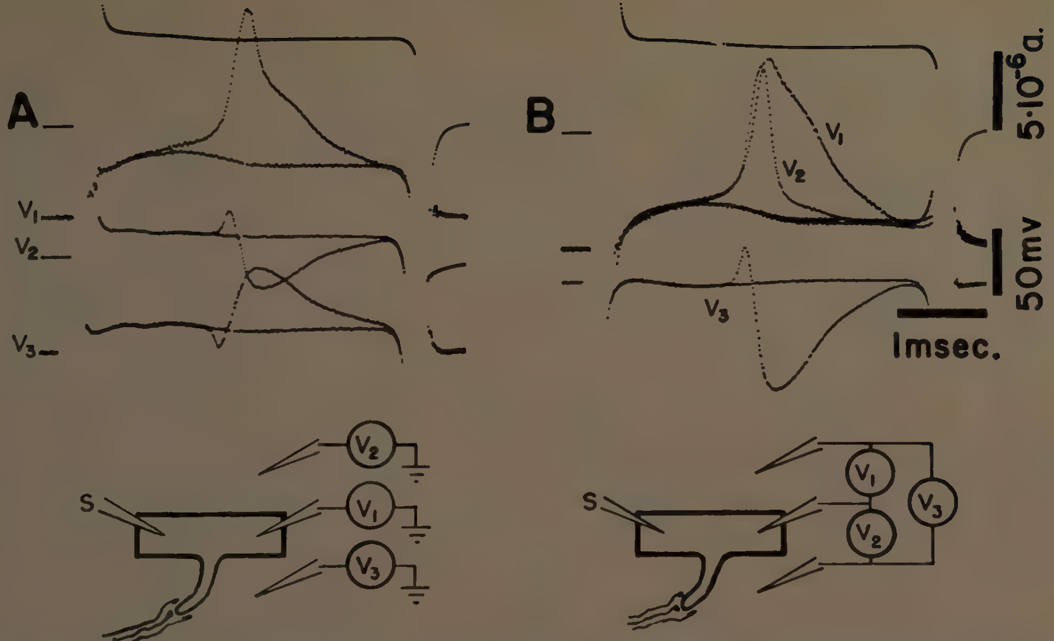

FIGURE 19. Response to intracellularly applied depolarization. *Hypopomus.* Superimposed threshold pulses that did and did not excite the cell. *A*, monopolar recording; *B*, differential recording as in diagrams. Upper trace: stimulating current. The transmembrane potentials in *B* (V_1 and V_2) start from the same level. The external record in *B* (V_3) is shown rostral positivity up. Both faces were excited, the spike of the caudal face was lower threshold or faster rising and initially there was negativity external to this face. The spike of the caudal face was longer-lasting and larger, and there was a longer-lasting negativity external to this face. These characteristics of the spikes are more clearly seen from the differential recordings (*B*). The external records in *A* are mirror images, showing the longitudinal orientation of the cell.

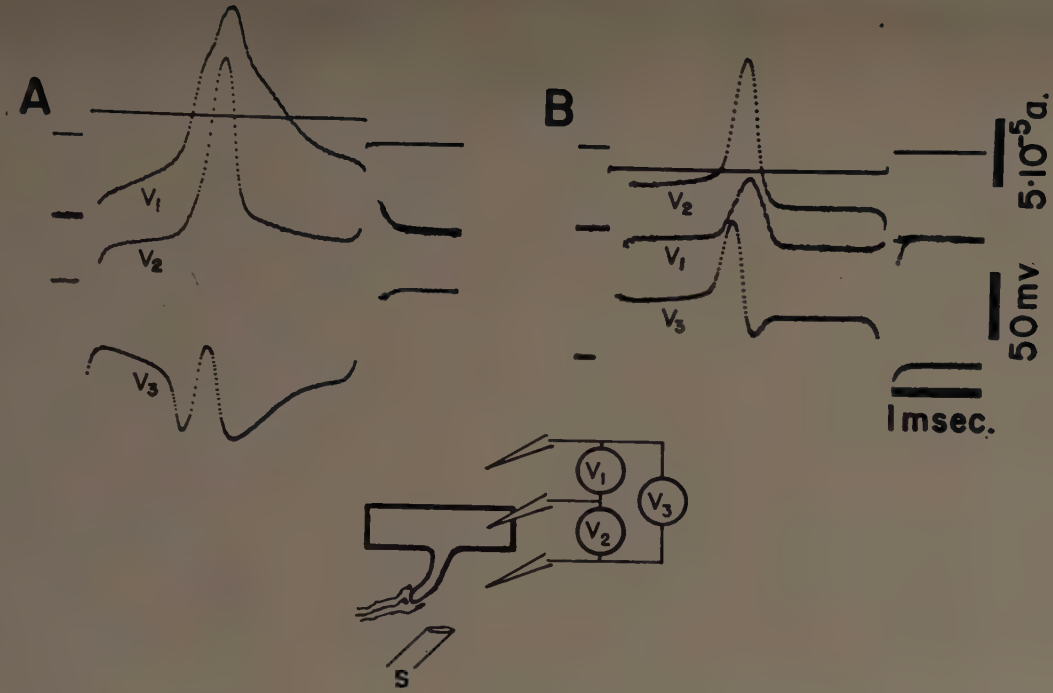

FIGURE 20. Stimulation of an electroplaque by externally applied currents. *Hypopomus*, same cell as FIGURE 19. Stimulation and recording as in diagram. Upper trace: stimulating current. Middle traces (V_1 and V_2): potentials across the two faces starting from the same level. Lower trace: potential between the external electrodes, rostral positivity up. When anodal current was passed (*A*), the caudal face was hyperpolarized and the rostral depolarized. The rostral face was excited first as indicated by initial rostral negativity externally. This activity excited the brief caudal spike which produced a rostral-positive phase in the external record which then became rostral-negative again. Oppositely directed currents (*B*) excited the caudal face first. The caudal spike failed to fire the rostral face, which was hyperpolarized by the stimulus. Only a small rostral negativity occurred in the external record. The potential drop in the current path around the cell, that is, the external potential, was greater than that across the rostral face.

when the caudal spike subsided (Freygang, 1958; Freygang and Frank, 1959). Alternatively it might have been due to a subthreshold response, since the rostral face can produce a spike. These two possibilities are readily distinguished in the electroplaque. Not only was the time constant too brief to give the observed diphasicity, but the negative phase was blocked by stronger stimuli that further hyperpolarized the rostral membrane.

Activation of only the spike of the rostral face analogous to FIGURE 20*B* could not be obtained by the strongest available anodal currents. However by similar stimulation in the refractory period there was no difficulty in obtaining the rostral spike in isolation. This spike was then seen to be as smooth in shape as that of the caudal face in isolation (FIGURE 20*B*). Thus the caudal activity must have been responsible for the inflections in the differential recordings of the rostral spike (FIGURES 19*B* and 20*A*).

Neural activation. The responses of *Hypopomus* electroplaques to stimulation of their nerve supply differed somewhat from those to intracellularly applied depolarization. Principally there was a larger rostral positivity externally indicating greater delay in firing of the rostral face (FIGURE 21*A* and *B*), and the potentials were thus more like the organ discharge. The difference was due to the caudal face in *A* exciting the rostral when it was already somewhat depolarized by the applied stimulus. The neurally activated membrane in the caudal face was more effective in exciting this face since the current flowing through it had a shorter and lower resistance path than that through the opposite face. As may be seen from FIGURE 20*B*, current generated by the caudal spike that flowed through the rostral face produced more potential drop across the extracellular material than across the rostral membrane.

When a neurally activated cell was slightly hyperpolarized, firing of the rostral face was delayed and there was a still larger external rostral positivity (FIGURE 20*C*). Stronger hyperpolarization first blocked firing of the rostral face and the external rostral negativity it produced, and then reduced the height of the remaining response (*D* to *G*). In *D* there was little or no rostral negativity remaining, but there must have been a subthreshold response of the rostral face since the potential across it was different in shape from that across the caudal face in contrast to *E* to *G*. Thus a membrane may be active although it is passing largely outward currents (Bennett *et al.*, 1959*b*).

The small potential remaining (*E* to *G*) does not appear to have been a p.s.p. since it was not increased by hyperpolarization (cf. FIGURES 8 and 9; Grundfest, 1957*b*). Also it was all-or-none with stimulus strength (*E*), which would not be expected in view of the multiple innervation (FIGURE 17). These data suggest that the response was mainly spike activity in the stalk that was initiated by p.s.p.s but failed to invade the body of the electroplaque.

Direct demonstration of neural excitation by way of the stalk was obtained through simultaneous recording from the stalk and body (FIGURE 22). Spikes were generated in the stalk and, during physiological discharge, they started earlier than the spikes in the body. Simultaneously with the peak of the spike across the caudal face there was a hump or second peak on the falling phase of the stalk spike. This phase disappeared when the body was sufficiently hyperpolarized to prevent invasion by the stalk impulse (*B*). When the body failed to fire, there was a corresponding loss of positivity in the potential external to its caudal face.

The duration of the stalk spike exceeded that of the caudal face, but was about the same as that of the rostral face. No definite evidence of p.s.p.s is

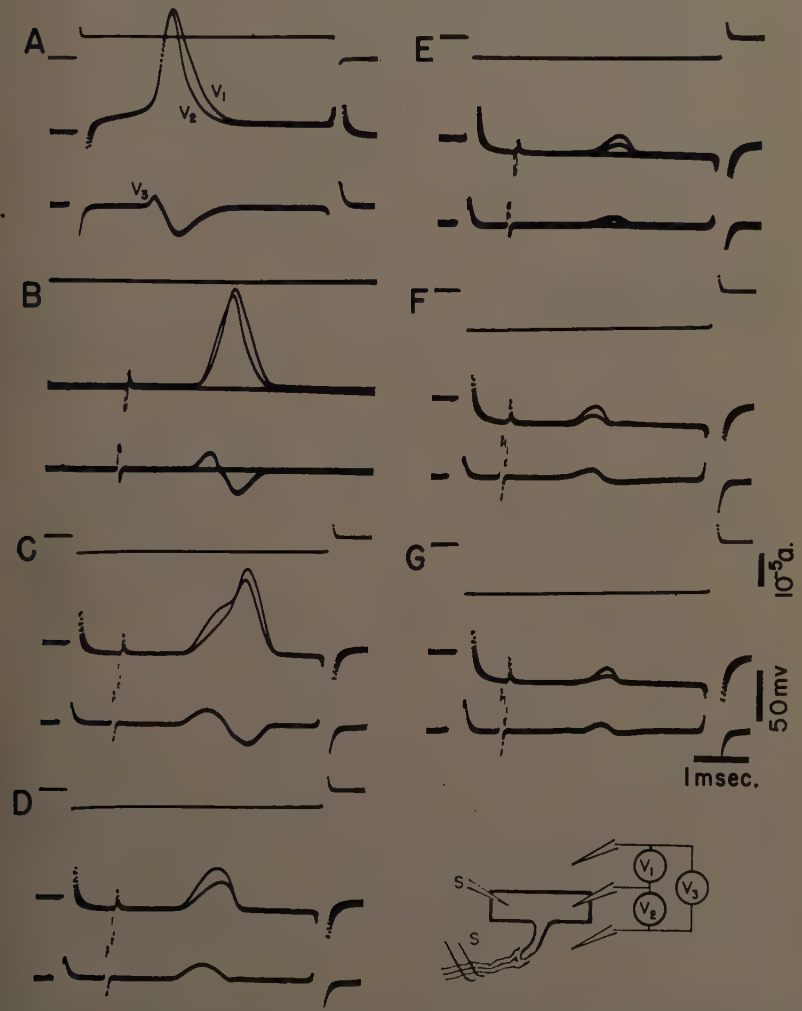

FIGURE 21. Neural activation. *Hypopomus* electroplaque. Stimulation and recording as in diagram. Upper trace: intracellular current. Middle traces (V_1 and V_2): potentials across the two faces starting from the same level. Lower trace: external potential, rostral positivity up. Control response to intracellular depolarization in *A*. Neural stimulation in *B* produced an external potential with a larger rostral positivity. With gradually increasing hyperpolarization, excitation of the rostral face was delayed (*C*) and blocked (*D*, *E*), as indicated by failure of rostral negativity to develop externally. A subthreshold response of the rostral face occurred in *D*, since the potential across it did not have the same time course as that across the caudal face. Further hyperpolarization reduced the remaining potential (*F*, *G*). The response was all-or-none, as was shown by carefully varying the strength of the neural stimulus near threshold in *B* and *E*.

seen in the records of FIGURE 22. However they should be revealed by hyperpolarization applied in the stalk or by using small neural volleys instead of the physiological discharge.

Organ discharge of Sternopygus. The external potential produced by *Sternopygus* was approximately sinusoidal. Although the discharge is also used in a guidance system, the frequency and phase were not affected by very strong stimuli (Bennett, 1961; cf. Grundfest, 1957*a*). In FIGURE 23*A* the discharge is shown as recorded along a portion of the tail, rostral positivity upward, and zero level given by the horizontal line. The rostral end was positive about one half the time and negative about one half the time. The head-negative phase had a somewhat flattened maximum. The section of the spinal cord above the recording site caused an immediate cessation of pulses. However a head-negative potential remained that decayed over a minute or two.

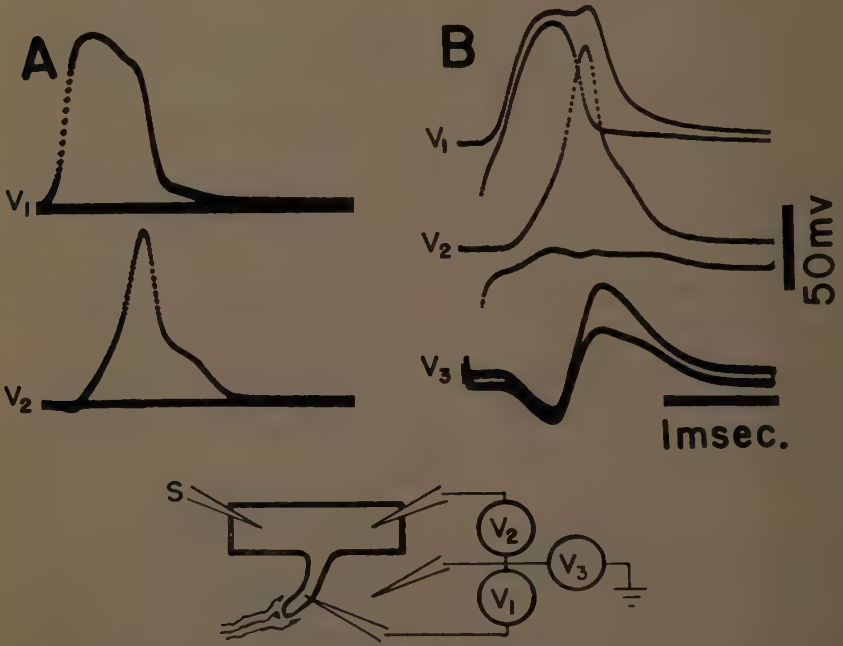

FIGURE 22. Spikes in the stalk and body of the electroplaque. *Hypopomus.* Different cells in *A* and *B*. Recording as in diagram, normal organ discharge. Oscilloscope sweep triggered by potential recorded in the stalk. The spike in the stalk started before that in the body and was longer in duration than that recorded across the caudal face. It had an inflection on the falling phase simultaneously with the peak of the caudal spike and which disappeared when invasion of the body was blocked by hyperpolarization (superimposed traces in *B*). When invasion failed there was a corresponding loss of caudal negativity in the external record. The remaining external potential was mainly due to the discharge of other electroplaques.

The inactive organ could be stimulated by shocks to the spinal cord or by current pulses along the organ tending to depolarize the caudal faces. In FIGURE 23*B* the segment of tail from which recordings were being made was stimulated by separate electrodes. Brief D.C. pulses were passed through a condenser so there was no D.C. component in the stimulus. The monophasic response of the organ appeared superimposed on the diphasic stimulating pulse.

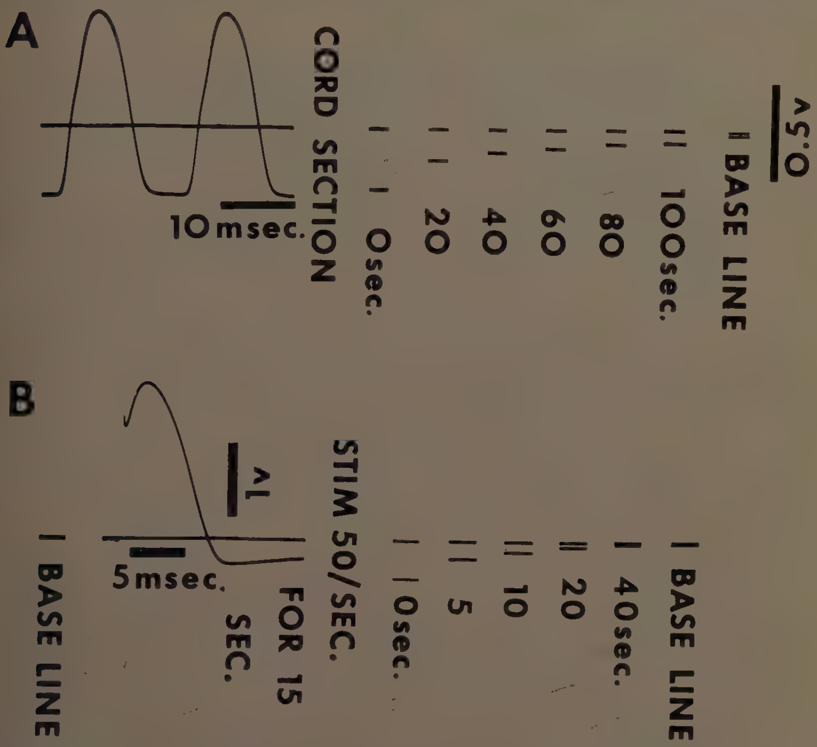

FIGURE 23. Organ discharge of *Sternopygus*, effect of spinal section and repetitive stimulation. Potential recorded differentially along caudal portion of tail, rostral positivity up, zero level indicated by horizontal line and base-line traces. Two preparations. *A*, two complete normal discharge cycles are shown on the left. The potential was head-positive and head-negative for approximately equal times. There was a small inflection during the transition from head negativity to positivity. The head-negative phase had a somewhat flattened maximum. Spinal section abolished the pulses but a head-negative potential about equal to that during regular organ discharge remained (*lower line* at time 0). This potential decayed over approximately 2 min. (*right*). *B*, stimulation of organ inactivated by spinal section. Separate stimulating and recording electrodes, head positivity up. Brief pulses were passed through a condenser to give diphasic stimuli with no direct current component. The pulse was oriented so that the initial brief phase excited the innervated faces. Their response appeared superimposed on the slow opposite phase (*left*). Repetitive stimulation at 50/sec. for 15 sec. developed a head-negative potential that on cessation of stimulation decayed over 15 to 20 sec. (*right*). Reproduced by permission of *Elsevier*, Amsterdam, Holland.

Repetitive stimulation at 50/sec. caused a gradual restoration of the steady head-negative potential on which were superimposed the pulse responses. When stimulation was stopped, the head-negative potential decreased to zero again over about 20 sec. (FIGURE 23*B*, right). This cycle of restoration and disappearance of the head-negative potential could be repeated many times. These results indicate that the organ discharge of *Sternopygus* consisted of 2 components; head-positive pulses superimposed on a steady head-negative potential.

Response of single cells. Microelectrode penetration of single electroplaques showed that each cell produced a spike during each pulse of the organ discharge.

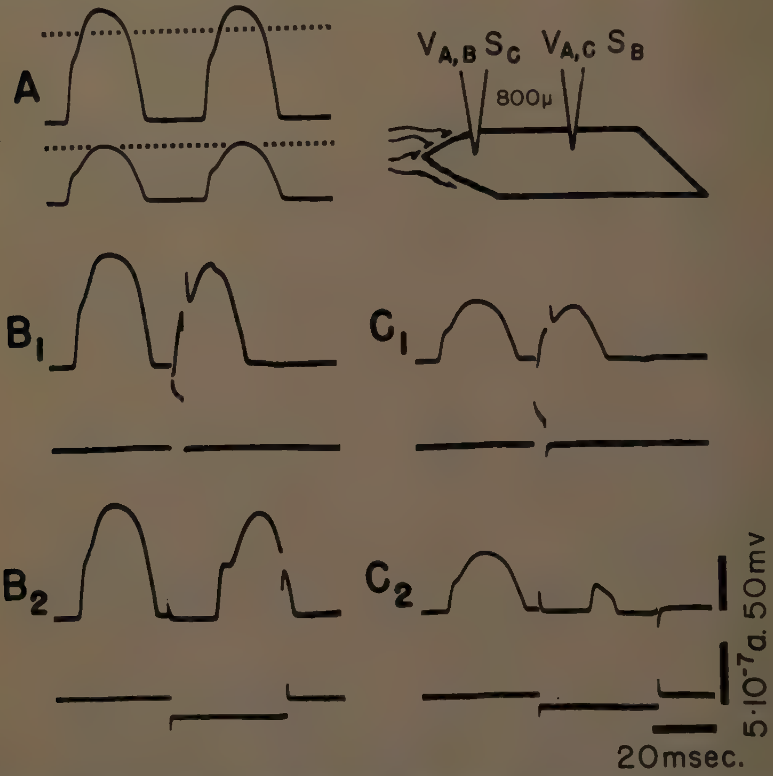

FIGURE 24. Restriction of spike-generating membrane to the caudal end of the electroplaques. *Sternopygus.* Normal organ discharge. Two intracellular electrodes were used 800 μ apart. To minimize pickup from other cells, recording was differential against a closely applied external electrode. During normal discharge the caudal electrode (*A*, *upper trace*) recorded a larger spike and resting potential (*dotted line*) than did the rostral electrode (*A*, *lower trace* and *dotted line*). When stimulating through the caudal electrode (B_1) a larger current was required to excite the cell than when stimulating through the rostral electrode (C_1, both near threshold pulses). The p.s.p. was inverted when it occurred near the peak of the spike in B_1. A larger current had to be passed through the rostral electrode to affect the physiological discharge (B_2, near threshold) while a smaller current through the caudal electrode (C_2) was adequate to block the spike, the p.s.p. and some subthreshold response remaining.

The spikes were about as long-lasting as the time between spikes, and were identical in form to the pulses of the organ discharge (FIGURE 24). At the caudal end of the cells the spikes were usually overshooting and always larger than at the rostral end. During most of a spike the potential at the caudal end was positive to that at the rostral and, consequently, current would flow to make the head of the fish positive. The potential between spikes was more negative at the caudal end of the cell, and between spikes current would flow to make the head of the fish more negative. Thus it appears that each cell generated both components of the organ discharge.

The membrane generating spikes is probably restricted to the caudal end of the cells. Not only was the spike much smaller at the rostral end but, with a polarizing electrode at this end, the currents required to excite the cell and to block the physiological discharge were both larger (FIGURE 24). The firing levels for direct and neural stimulation were approximately equal only at the caudal part of the cell. Polarizing more rostrally the cell had to be more depolarized to elicit a spike and more hyperpolarized to block a neurally evoked spike. P.s.p.s produced at the site of innervation decremented down the cell at the same rate as the spike (FIGURE 26).

Each cell discharge was initiated by a separate p.s.p. When a spike was directly evoked just before a neural response would have occurred, the p.s.p. was inverted on the spike peak (FIGURE $24B_1$).

In organs that were inactive due to spinal section the electroplaques had the same resting potentials at both ends. Repetitive stimulation caused a depolarization to develop that was greater at the rostral end of the cell (FIGURE 25). This depolarization built up and decayed at about the same rate as the head-negative potential of the whole organ. Net current through the stimulating electrode was not necessary to produce the slow depolarization since it was not prevented by hyperpolarizing pulses given between spikes and equal in amplitude to the depolarizing stimulus. There was little resistance change during the slow depolarization.

As is implied by the smaller resting potential at the rostral ends of physiologically discharging cells, slow depolarization greater at this end was also produced by neural discharges. When the normal discharge (*A*) of the cell of FIGURE 26 was blocked for some seconds by repetitive hyperpolarizing pulses, the slow depolarization was reduced until both ends of the cell had the same somewhat larger resting potential (*B*). The p.s.p.s were then mostly below the firing level of the cell. A small number of the p.s.p.s did manage to fire the cell, however, and the fraction gradually increased until the cell returned to the condition in *A*. Probably the slow depolarization summed with the p.s.p.s to fire the cell, and the initial few discharges when the cell was as in *B* caused some depolarization that aided in the production of further discharges.

The extent of membrane generating the slow depolarization was not determined. Considering the decrement moving caudally along the cell, it is probably restricted to the more rostral part.

Resistance during spikes. A surprising finding was that the resistance at the peak of the spike was slightly greater than at rest or between spikes during normal discharge. One kind of evidence is shown in FIGURE 27. Brief pulses (2 msec.) were applied between spikes (*D*) and superimposed on the peaks of the spikes (*B* and *C*). The graphs show the displacement of voltage at the end of the pulse plotted against the current. Between spikes the slope for hyperpolarizing currents was linear for the range of pulses used. The time constant was very short compared to the pulse length (*E*). For depolarizing currents, the slope rapidly increased indicating subthreshold response, and finally there was firing. For pulses at the peak of the spike the converse picture was obtained. For outward currents the slope was approximately linear, but it increased with the strength of inward currents. It is clear from the records that the response was being prematurely terminated by the inward currents (FIGURE 16*C*). Larger pulses could completely abolish the spike. Actually outward currents produced some prolongation of the response (*B*) so that the slope for these currents may be slightly too large. The true resistance is probably given more accurately by the slope of the last four points, for all of which the potential appeared to be constant during the later part of the pulse. Resistance measurements obtained during, before, and after directly evoked spikes gave similar results.

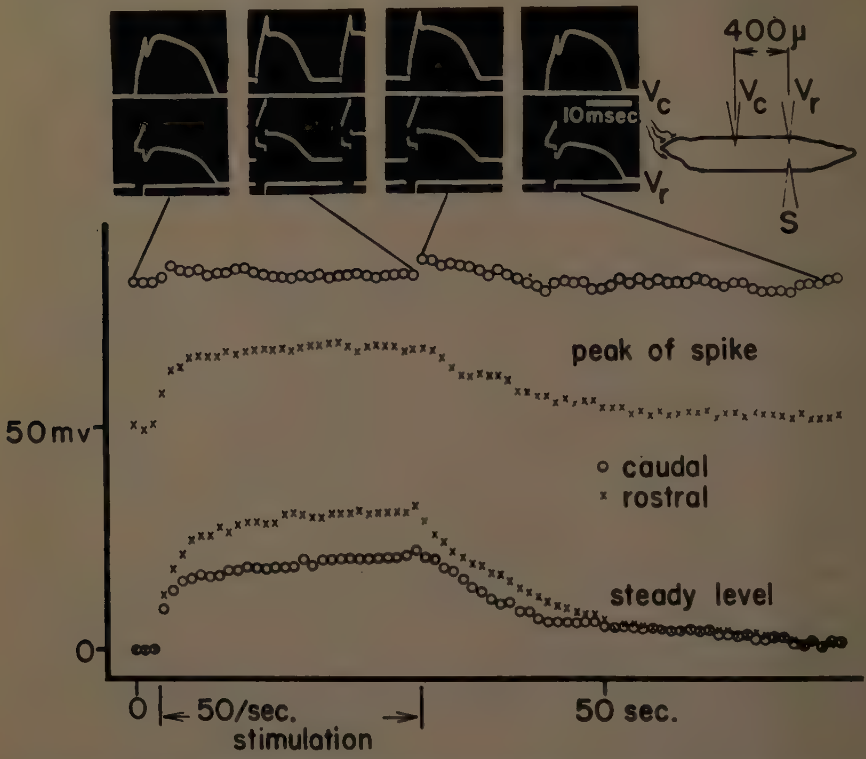

FIGURE 25. Development and decay of slow depolarization produced by repetitive direct stimulation of a single cell. *Sternopygus*. Organ inactivated by spinal section. Three electrodes were used as in diagram. Brief pulses adequate to excite the cell were applied at 1/sec. and 50/sec. Sample records are shown above graph with the connecting lines to the latter indicating when they were taken. Upper traces: caudal potential and base line. Lower traces: rostral potential and stimulating current serving also as base line. Graph: data of complete experiment, resting potentials at the beginning taken as 0. Resting potentials determined at the end of the experiment were 64 mv at the rostral electrode, and 67 mv at the caudal electrode. Repetitive stimulation at 50/sec. caused a steady level of depolarization to develop, which was greater at the rostral end of the cell. On return to stimulation at 1/sec. the depolarization subsided in about 20 sec.

Several criticisms may be made of this kind of experiment. The cells are not isopotential, and perhaps the spike was being generated too far from the electrodes to measure any conductance change. The objection does not appear valid, however, since the spike was large (85 mv in FIGURE 27). If the hypothetical generating membrane had a reversal potential of even 150 mv, a halving of resistance should have been detected. Also the recording electrode must have been close to the generating membrane since the firing level was the same as that at which the p.s.p.s initiated the spikes (*D* and *E*). Placement of the current electrode at some distance from the recording electrode should not have affected the sensitivity of the resistance measurement, as will be discussed more fully in another publication. Indeed if the spike-generating membrane extended to between the recording and polarizing electrodes the sensitivity should have been increased. Finally, a change in resistance was detected, but in the direction of increased resistance at the peak of the spike.

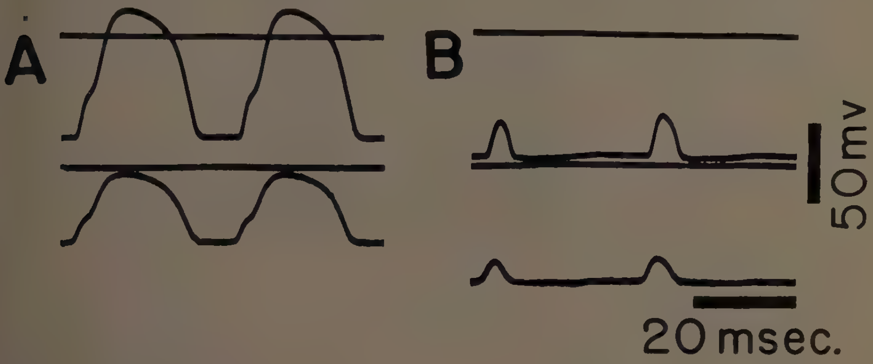

FIGURE 26. Slow depolarization as a result of neural activation. *Sternopygus.* Two intracellular recording electrodes were used, one 700 μ rostral to the other. Both recorded differentially against a closely applied external electrode to minimize pickup from other cells. The second trace gives the potential at the caudal electrode with the upper trace as its zero level. The fourth trace gives the potential at the rostral electrode with the third trace showing its zero level. When the cell was firing regularly, as in *A*, the spikes and the potential between spikes were greater at the caudal end. Repeated hyperpolarizing pulses were passed through a third intracellular electrode in order to block the spikes and, after some seconds, the records became as in *B*. The resting potential was equal at the two ends of the cell and only p.s.p.s were produced, which were larger at the caudal end.

Further evidence on the resistance changes during activity was obtained measuring A.C. impedance of a length of the intact fish. To maximize sensitivity only a small caudal portion of the tail was used where there was a minimum of tissue other than the electric organ.

It was found that the bridge might simultaneously be very near balanced for the peaks of the spikes and for the periods between spikes (FIGURE 28*A*). However on the rising and falling phases there appeared large imbalances, always somewhat larger on the falling phase. When the bridge was balanced for the falling phase (*B*), the bridge was slightly more imbalanced at the spike peaks than between spikes, but approached balance during the rising phase. If the bridge were balanced to the rising phase (*D*, first organ pulse) two other balance points occurred near the beginning and end of the falling phase.

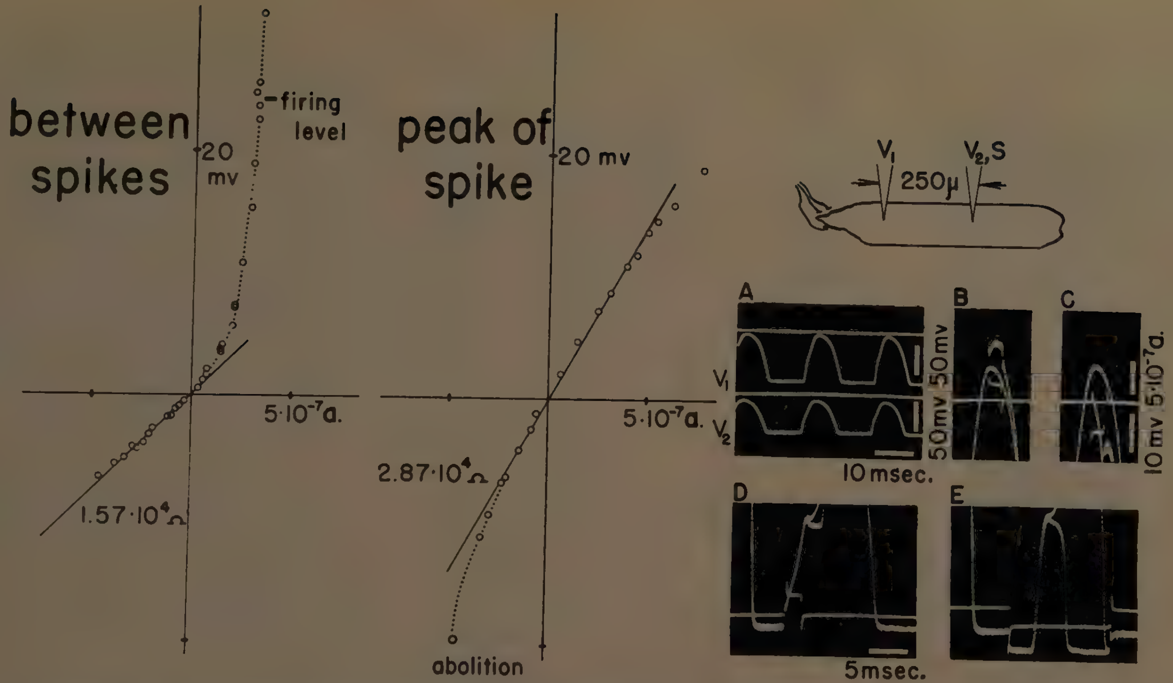

FIGURE 27. Resistance at the peak of the spike and between spikes. *Sternopygus.* Normal organ discharge. Stimulatin and recording as in diagram, except that to minimize pickup from other cells recording was differential against a closely-applied external electrode. The spikes and resting potentials were larger at the caudal end of the cell (*A*). Two-msec. polarizing pulses were applied through the rostral electrode, just before the spikes (*D*), and on the peaks of the spikes (*B*, *C*). The potential at the end of the pulses is plotted against polarizing current. The time constant was short compared to 2 msec. (*E*). The resistance was linear over the range of hyperpolarization (inward current) used for pulses preceding the spike, but depolarizing (outward) pulses excited the cell and produced subthreshold responses so that the potential increased disproportionately. Outward currents during the peak of the spike slightly prolonged the spike (*B*), but the resistance was about linear and somewhat greater than that for hyperpolarizing currents between spikes. Inward currents tended to terminate the response, and the apparent resistance increased. The caudal electrode was close to the spike-generating membrane, since the firing level was the same for direct stimulation (*D*) and neural activation (*E*, *superimposed traces*).

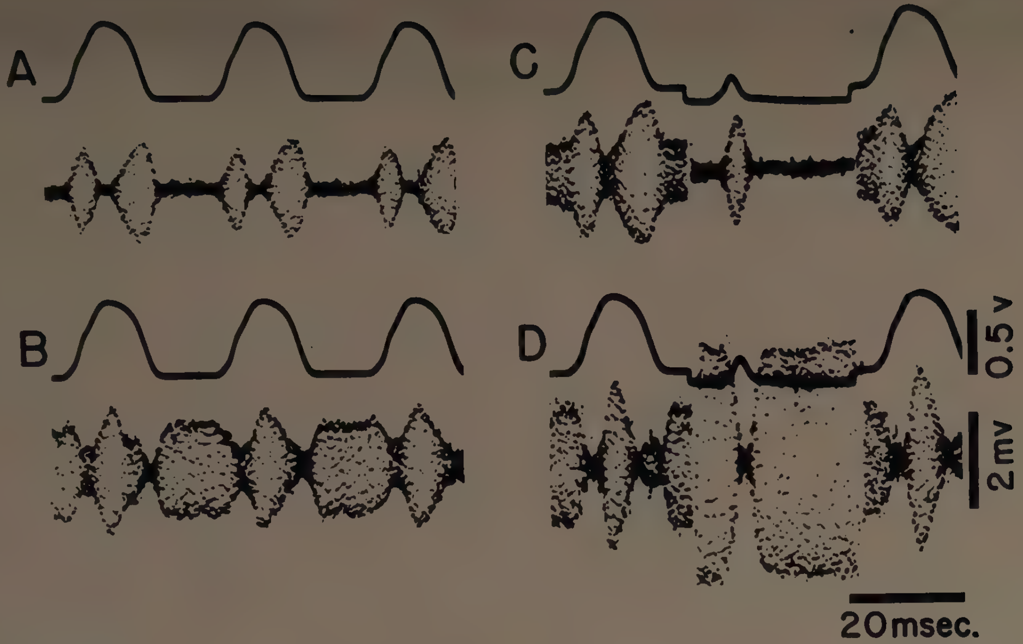

Figure 28. Impedance changes during organ discharge. *Sternopygus.* The tip of the tail was placed in the bridge circuit described under the heading Methods. Upper trace: bridge signal after moderate amplification. Lower trace: after filtering out low frequencies and much greater amplification. Amplitude and frequency of A. C. input 0.5 v and 5 kc. The bridge could be approximately balanced for both spike peaks and between spikes (*A*), but large imbalances occurred on the rising and falling phases. When the bridge was balanced for the falling phase (*B*), the imbalance at the spike peaks was somewhat greater than between spikes, and balance was approached during the rising phase. When the bridge was balanced for the rising phase, balance points occurred near the beginning and end of the falling phase (first pulse in *D*). *C* and *D*: currents hyperpolarizing the innervated faces were passed so that only the p.s.p.s and possibly some subthreshold response remained. The pulse changed the balance between spikes, but when the bridge was balanced during the part of the pulse where there was no p.s.p., balance was approached during the spike peak (*C*). The imbalance produced by the p.s.p. (*C*) was in the same direction as that during the rising and falling phases, since balance could be obtained simultaneously at the peak of the p.s.p. and at the rising phase (*D*).

These data confirm that the impedance at the peak of the spike is close to that between spikes. The alternative possibility that two membrane components are different so that balance is obtained at both times is unlikely in view of data obtained with pulses in single cells.

The direction of the impedance changes on the rising and falling phases is not clear from these data. Functionally a reduction in resistance would facilitate the voltage changes occurring during these times. The resting time constant is short, however, and a reduction might not be necessary.

To reveal the contribution of the p.s.p.s, current pulses hyperpolarizing the innervated faces sufficiently to block spike generation were passed (FIGURE 28*C* and *D*). The hyperpolarizing pulses increased the imbalance between spikes in the same direction as the spike-peak imbalance differed from the falling-phase imbalance. An appreciable imbalance was produced by the p.s.p., although some of it may have been due to subthreshold response. The impedance change was in the same direction as that produced by the rising and falling phases since the bridge could be simultaneously balanced for the peak of the p.s.p. and the rising phase (*D*). If it may be assumed that the p.s.p. was associated with a decrease in resistance, then there was a decreased resistance during the rising and falling phases. A decrease in resistance during the p.s.p. is indicated by its inversion when it occurs on the peak of the spike (FIGURE 24B_1). Resolution of these questions should be advanced by measuring the A. C. impedance at different frequencies (cf. Cole and Curtis, 1939).

Discussion

Electroplaques with both faces generating spikes. The electroplaques of *Hypopomus* are in many ways similar to those of *G. carapo*, *Malapterurus*, and the Mormyridae (Bennett and Grundfest, 1959*a*; Bennett and Grundfest, 1961*c*; and Keynes *et al.*, 1961). In all, both faces have about the same surface areas and both produce spikes during the discharge. In *G. carapo* and some Mormyrids the external potentials are diphasic with each phase approximately equal. From *Hypopomus* through *Mormyrus* to *Malapterurus*, the spike of one face is progressively shorter until in the last the discharge is virtually monophasic. The different properties of the faces with the additional differences in the stalks where they occur provide the most dramatic examples of spike-generating membrane of different properties in different regions of a single cell (cf. Bennett *et al.*, 1959*b*).

The electroplaques of *G. carapo* also differ from those of *Hypopomus* in not having stalks and in being innervated some on their rostral and some on their caudal faces. Opposite diphasic potentials are produced by the differently innervated cells and these are so timed that a triphasic potential results. The other Gymnotids, *Steatogenys* and *Gymnorhamphychthys*, have electroplaques similar in appearance to those of *Hypopomus*. Since their organ discharges are triphasic or somewhat more complicated, most of the cells are probably diphasically responding and, as in *G. carapo*, oriented in different directions. However in the submental filament of *Steatogenys* (Lowry, 1913) the discharges appear to be monophasic (unpublished data).

The significance of having both membranes generate spikes cannot be the same in every case since the potentials produced vary from monophasic at least to triphasic. All strongly electric fish produce monophasic discharges, and possibly direct current pulses are more effective as weapons than are polyphasic pulses. In *Malapterurus*, which is strongly electric, the activity of both faces is so arranged as to result in impedance matching. At rest, the two membranes have about equal resistance. The rostral face produces a long-lasting spike during which the conductance is increased, but the caudal face produces only a brief spike before a conductance increase occurs similar to that in *Raja*. The brief spike in the caudal face is probably important in propagation of the impulse from the single central stalk across the large face of the cell. Perhaps also related to propagation, the conductance increase is much briefer than in *Raja*, about as long as the rostral spike, and repetitive impulses may be produced at over 200/sec. (cf. Keynes *et al.*, 1961).

Polyphasic discharges are the most common forms among fish known to have electrical guidance systems. In *Mormyrus*, however, the discharge is very nearly monophasic (Bennett and Grundfest, 1961*c*), and in *Raja* and in *Narcine* accessory organ, where a guidance use seems possible, the discharges are also monophasic (Bennett and Grundfest, 1961*a*). The significance of polyphasic discharges is unknown. Possibly their function is related to the operation of the guidance system. Another aspect is that most of the discharges have little D. C. component, which may be important in maintaining ionic equilibria. Probably in all forms the spike in the earlier firing face is followed by an increased conductance, as in *Malapterurus*. Where the earlier firing face produces appreciable external current a large fraction of it may flow to charge the capacity of the later-firing face. A large capacity of the later-firing face would increase the external current due to the first activity. In *Raja*, current charging the capacity of the uninnervated face is a significant portion of the initial current, but no opposite phase follows as it does in cells where this face generates a spike.

Electroplaques with a slow depolarization. The electroplaques of *Sternopygus* have two characteristics that are peculiar. These probably are also found in *Eigenmannia* electroplaques, which appear to operate identically to those of *Sternopygus* except that they are on a more rapid time scale, the discharge frequency being 250 to 500/sec. There is a steady potential in both species on which pulses are superimposed, and the resistance is about the same at the peak of spikes and between spikes. Functionally these two properties may be interrelated. Since the organ develops equal but opposite voltages during and between spikes, each phase may be equally important, and the generating membrane during each should have an equally low resistance. If the resistances were the same and the discharge were loaded down by an external load, equal currents would flow during both phases. If the resistances were different, there would be a direct-current component that might be disadvantageous. In fact there appears to be a balancing mechanism that decreases any D. C. component. In individuals where the time between spikes is longer relative to the spike duration, the steady head-negative level between pulses is smaller than in individuals where the firing is relatively more rapid. In repetitive direct stimulation the final level of the slow depolarization is dependent on frequency and, in the whole organ, it is approximately the level that gives no net current.

The cause of the slow depolarization is unknown as yet. One possibility is that current flowing rostrally through the cell accumulates K^+ outside the rostral surface, which thereby becomes depolarized. The septum between this surface and the next cell might be impermeable to K^+, or the abutting caudal face might have this property, since it has been shown in the eel that the caudal face is less sensitive than the rostral to K^+ depolarization (Schoffeniels, 1959). The hypothesis of accumulation in an extracellular chamber is also suggested by the close packing of the cells. The intracellular material is greatly increased at the expense of the extracellular when compared to *G. carapo* and *Hypopomus.*

Depletion of the K^+ accumulated in the extracellular chamber would cause decay of the slow depolarization. The loss could be due to leakage into the circulatory system and surrounding tissue, or due to pumping back into the electroplaques (cf. Hodgkin, 1951). If K^+ carried the current in both directions across the rostral face and there were no other entry or leakage out of the space, then the concentration would remain about constant if there were no D. C. component in the cell discharge. Equal amounts would pass in and out with each organ cycle. Any net current flowing would cause accumulation or depletion until the net current flowing again became zero. If K^+ accumulation causes the slow depolarization, the conductance should be increased during it (Hodgkin, 1947*b*). If such a change occurs it is small.

The mechanisms of spike generation in *Sternopygus* also require further investigation. As has been suggested for the heart (Grundfest, 1957*c*; Hutter and Noble, 1960; and Noble, 1960), potassium conductance may decrease with depolarization, a form of K^+ inactivation (cf. H. Grundfest, elsewhere in these pages). The increased resistance could allow a sodium conductance less than the total resting conductance to generate an overshooting spike. In *Sternopygus* there is no indication of decrease in steady-state resistance below the firing level so that any decrease must occur above this value. K^+ activation or an analogous process would also occur since the conductance probably increases on the falling phase. By assuming suitable rate constants for sodium and potassium activation and inactivation, no doubt an action potential with the observed impedance changes could be calculated.

Innervation on stalks. In addition to *Hypopomus*, innervation on stalks occurs in *Malapterurus* and in the Mormyridae in which it is the exclusive mode of innervation (Bennett and Grundfest, 1961*c*; Keynes *et al.*, 1961; and Szabo, 1958, 1961*a*). In the former, the stalk is single, longer than in *Hypopomus*, and innervated at its tip by the single nerve fiber that supplies all of the electroplaques on one side of the fish. In the Mormyridae there are many stalks coming from one surface of the electroplaque that repeatedly fuse before being innervated at one or at a number of sites.

In those Mormyridae in which the spikes of the faces are of different duration and in *Malapterurus*, as well as *Hypopomus*, the spikes in the faces opposite the stalks are the longer-lasting ones. In the Mormyridae, as in *Hypopomus*, the spike in the stalk is long-lasting compared to that of the stalk face, but it has not been recorded in *Malapterurus.* The significance of the longer spike in the stalk is not known. It probably facilitates impulse initiation by the p.s.p.s and invasion of the electroplaque body by the stalk impulse; it may also increase conduction velocity, which is high in some Mormyrid stalks.

In the Mormyrids, where there is a single site of innervation, the stalks synchronize the firing of the entire stalk face, which in these forms may be several centimeters long. They may also play a role in synchronizing the firing in different cells, as has been suggested for *Malapterurus.* In *Malapterurus* organ there is but a single innervating fiber on each side of the body, and no central delays are possible to compensate for conduction time. There is more delay when stimulating a nerve fiber branch close to a rostral portion of the organ than one close to a caudal portion, and the difference is just sufficient to compensate for the conduction time in the main nerve branch along the organ (Keynes *et al.*, 1961). Possibly, therefore, the stalks serve as variable delay lines: longer rostrally, and shorter caudally. However, stalk length and diameter are very variable and no consistent anatomical differences have been observed between rostral and caudal parts of the organ. Some Mormyrids have single electroplaques that produce triphasic responses; the additional phase is due to activity of the stalks, which are specially oriented (Bennett and Grundfest, 1961*c*).

The stalks may represent a way of reducing transmitter, since the larger effective resistance of a stalk would require a smaller synaptic area to excite it. Conduction along the spike-generating membrane of the stalk would then amplify the depolarization until it was able to invade the body of the electroplaque. In some muscles the synapses are located at the ends of the fibers, which would reduce the required synaptic membrane per synapse by doubling the effective resistance (Mackay *et al.*, 1960). Probably, however, most of these fibers are innervated at both ends. Whatever the functional advantages of stalks, they are clearly not essential, since p.s.p.s without spikes at all are responsible for the activity of marine electric organs, and diffuse innervation occurs in a number of fresh-water forms, the organs of which contain spike-generating membrane (*Electrophorus*, *G. carapo*, and *Gymnarchus*).

Discharge frequency and duty cycle. An important aspect of spike generation is the ratio of recovery time to spike duration. Although in *Sternopygus* the spikes are produced at only 50/sec., the time between spikes is about equal to the spike duration. To use an engineering term, the "duty cycle" is about one half. In *Eigenmannia* the rate is higher but the duty cycle is the same.

The nerve cells innervating the electroplaques and probably every synapse in the central control system discharge at the full organ frequency (Bennett, 1961). There are still faster-firing Gymnotids, the Sternarchidae, which discharge constantly at frequencies that may exceed 1500/sec. While the electrophysiology of their electroplaques is not known in detail, both these cells and the controlling neurons fire at the full rate.

In heart, the duty cycle can be quite large, but the increased conductance phases during the rise and fall occupy a much shorter fraction (Weidmann, 1956). The peak frequencies in electric organs are not greatly different from those recorded in the mammalian central nervous system. The Renshaw cell can discharge at 1400/sec. (Eccles *et al.*, 1954; Frank and Fuortes, 1956; and Renshaw, 1946), and neurons in the sensory path sometimes produce bursts at about 1000/sec. (Grundfest and Campbell, 1942; Rose and Mountcastle, 1954). However these activities are transient. In the constantly firing electric fish, the cells must be in a steady state since the discharge can be produced for years. Although the metabolic systems involved are as yet completely unknown, they should be extremely developed compared to those in other neurons (cf. Grundfest and Bennett, 1961).

Discharge pattern and organ function. The adaptive values in the Gymnotids of the different forms of discharge and repetition pattern remain obscure. Two groups may be defined (Grundfest, 1957*a*): those that emit pulses at variable frequencies, and those where the frequency is constant. Probably all are able to detect very small changes in the environment's conductivity (Bennett and Grundfest, 1959*a*; Grundfest, 1957*a*; and Lissmann, 1958), but there does not appear to be any relation between the discharge and mode of life (cf. Lissmann, 1961). In the variable frequency group is *Electrophorus*, the monophasic discharges of which can stop altogether. Apparently the Sachs organ is used in location, and the main organ in offense and defense (Keynes and Martins-Ferreira, 1953; Coates, 1950). Also in this group are *Hypopomus*, *G. carapo*, *Steatogenys*, and *Gymnorhamphychthys*. All the latter forms fire continuously, but the resting rate varies from about 2 to over 100/sec. and, during stimulation or activity, the rate increases.

In the constant frequency group are *Sternopygus*, *Eigenmannia*, and the Sternarchidae. *Sternopygus* and the Sternarchidae are solitary dwellers, as are the variable frequency emitters *G. carapo* and *Gymnorhamphychthys*. *Eigenmannia* is social, as are *Steatogenys* and *Hypopomus*. The central control mechanisms (Szabo, 1957, 1961*b*) and probably also the electrosensory systems are different in the constant and variable frequency groups. Understanding of these mechanisms may give some functional significance to the differences in pulse shape and pattern of discharge.

It is interesting that both constant and variable frequency forms have evolved in African waters also. These are *Gymnarchus* and the Mormyrids respectively. The Mormyrids emit at frequencies that are dependent on activity and stimulation but that can stop altogether. Pulse forms also vary from nearly monophasic to diphasic and triphasic (Bennett and Grundfest, 1961*c*). *Gymnarchus* emits at a constant frequency, although under certain conditions the discharge may cease (Lissmann, 1958). The discharge appears similar to that of *Sternopygus* and *Eigenmannia*. However, recordings with directly coupled amplifiers have not been made, and there may or may not be a direct-current component.

CONCLUSIONS

Fish have evolved a number of ways to develop electric current outside their bodies. The electroplaques show a wide range of properties, but the basic cause of external current is universal. During a discharge the potentials across opposed membranes become different because of their different responsiveness. The electroplaque that is most simple electrophysiologically has but a single responsive membrane that generates p.s.p.s only. In the next stage of complexity a cell may have, in addition to membrane-generating p.s.p.s, that which shows a conductance increase similar to delayed rectification. In a still more complex cell, spike-generating membrane of one, two, or three different kinds may occur, and there may be membranes showing a slowly developing and long-lasting depolarization. The electrophysiologically simplest are probably not the least evolved, since the muscles of origin produce spikes. Some of the more complex cells are clearly also highly modified from muscle. In many but not all instances the specializations may be understood in terms of maximizing current production and efficiency. However the evolutionary picture is far from complete from lack of both functional data and, in most groups, of intermediate forms.

Of particular interest for further study are the isolated membranes showing p.s.p.s or the conductance increase like delayed rectification, since these response components are not readily available in other tissues. Also, in several species the spike-generating membranes are of interest for their unusual properties including the high frequencies at which they respond. Evolution appears in the electric fish to have provided the electrophysiologist with much valuable experimental material.

Summary

(1) Electrophysiological data are presented on two anatomical types of electroplaques of Rajidae, cup and disc, and on electroplaques of two species of Gymnotids, *Hypopomus*, and *Sternopygus*. These data are used to illustrate the general modes of operation of electric organs. Where possible the specializations that occur are interpreted in terms of functional significance.

(2) When cup-type electroplaques were depolarized, a conductance increase similar to delayed rectification occurred, but associated with a small depolarization. There was no indication of a regenerative response. The conductance increase was graded and could exceed a fivefold change; its duration was about one-half sec.

(3) In most cup-type cells, the conductance increase was mainly localized in the uninnervated face, and served to increase the external current flow produced by p.s.p.s in the innervated face. The externally recorded response of a cell before activation of the conductance increase had two peaks. The first was due to a surge of current to charge the capacity of the uninnervated face; the second was due to activation of the conductance increase.

(4) The p.s.p.s of the cup-type electroplaques reversed at about zero membrane potential. In segments of organ the impedance change associated with the p.s.p. was little affected by the membrane potential, even to the point where the p.s.p.s were inverted.

(5) When Cl^- Ringer bathing cup-type electroplaques were replaced by acetate Ringer, the depolarization associated with the conductance increase became 20 to 40 mv positive to the resting potential and exceeded the threshold for its production. Thus a regenerative all-or-none response could be evoked. This response lasted several seconds and apparently was terminated by inactivation of the conductance increase.

(6) Rajid electroplaques of the disc-type had a lower-resistance uninnervated face correlated with an increased surface area and correspondingly less of the conductance increase. To the extent to which the conductance increase did occur it predominated in the uninnervated faces and augmented the external currents produced by the p.s.p.s.

(7) Both faces of the electroplaques of *Hypopomus* generated spikes. The discharges occurred out of phase and a diphasic external potential resulted. The spike of the caudal face was briefer than that of the rostral face.

(8) The innervation in *Hypopomus* electroplaques occurred on a stalk from the caudal face. The p.s.p.s initiated a spike in the stalk which propagated to invade the body of the cell. The duration of the stalk spike was about the same as that of the rostral face, and longer than that of the caudal face.

(9) The electroplaques of *Sternopygus* have spike-generating membrane only in their caudal, innervated faces. However, repetitive firing depolarized the rostral ends of the cells. The normal organ discharge thus consisted of two components; rostral-positive pulses superimposed on a steady rostral-negative potential. The time between pulses was about equal to the pulse duration, and the steady level was such that there was little net current flow.

(10) The resistance at the peaks of spikes in the *Sternopygus* cells was about equal to that at rest. On the rising and falling phases, the resistance appeared to be decreased.

ACKNOWLEDGMENTS

Preliminary reports have appeared on some of the work on Rajidae (Bennett and Grundfest, 1961*d*; Cohen *et al.*, 1961; and Grundfest and Bennett, 1961). FIGURES 4 and 6 are from the latter paper. FIGURE 12 is from unpublished work by B. Cohen, M. V. L. Bennett, and H. Grundfest. A preliminary report on the work on *Sternopygus* has also appeared (Bennett and Grundfest, 1959*b*) and FIGURE 23, from that work, was published in Bennett (1961). All other figures are from unpublished work by Bennett and Grundfest. I am greatly indebted to Cohen and Grundfest for permission to use these data.

REFERENCES

ADRIAN, R. H. 1956. The effect of internal and external potassium concentration on the membrane potential of frog muscle. J. Physiol. **133:** 631–658.

ALBE-FESSARD, D. 1951. Modifications de l'activité des organes électriques par des courants d'origine extérieure. Arch. Sci. Physiol. **5:** 45–73.

ALBE-FESSARD, D., C. CHAGAS & H. MARTINS-FERREIRA. 1951. Sur l'existence d'un systeme effecteur de la décharge électrique chez *Electrophorus electricus*. Ann. Acad. Brasil Cienc. **23:** 327–332.

ALTAMIRANO, M. 1955. Electrical properties of the innervated membrane of the electroplax of electric eel. J. Comp. Cell. Physiol. **46:** 249–278.

ALTAMIRANO, M., C. W. COATES, H. GRUNDFEST & D. NACHMANSOHN. 1953. Mechanisms of bioelectric activity in electric tissue. I. The response to indirect and direct stimulation of electroplax of *Electrophorus electricus*. J. Gen. Physiol. **37:** 91–110.

ALTAMIRANO, M., C. W. COATES & H. GRUNDFEST. 1955*a*. Mechanisms of direct and neural excitability in electroplaques of electric eel. J. Gen. Physiol. **38:** 319–360.

ALTAMIRANO, M., C. W. COATES, H. GRUNDFEST & D. NACHMANSOHN. 1955*b*. Electric activity in electric tissue. III. Modification of electrical activity of acetylcholine and related compounds. Biochem. Biophys. Acta. **16:** 449–463.

BENNETT, M. V. L. 1961. Discussion. *In* Bioelectrogenesis. C. Chagas & A. Paes-de-Carvalho, Eds. Elsevier. Amsterdam, Holland.

BENNETT, M. V. L., S. M. CRAIN & H. GRUNDFEST. 1959*a*. Electrophysiology of supramedullary neurons. I. Orthodromic and antidromic responses. J. Gen. Physiol. **43:** 159–188.

BENNETT, M. V. L., S. M. CRAIN & H. GRUNDFEST. 1959*b*. Electrophysiology of supramedullary neurons. II. Properties of the electrically excitable membrane. J. Gen. Physiol. **43:** 189–219.

BENNETT, M. V. L. & H. GRUNDFEST. 1959*a*. Electrophysiology of electric organ in *Gymnotus carapo*. J. Gen. Physiol. **42:** 1067–1104.

BENNETT, M. V. L. & H. GRUNDFEST. 1959*b*. Electrophysiology of *Sternopygus* electric organ. XXI Intern. Physiol. Congr. **35.**

BENNETT, M. V. L. & H. GRUNDFEST. 1961*a*. The electrophysiology of electric organs of marine electric fishes. II. The electroplaques of the main and accessory organ of *Narcine brasiliensis*. J. Gen. Physiol. **44:** 805–818.

BENNETT, M. V. L. & H. GRUNDFEST. 1961*b*. The electrophysiology of electric organs of marine electric fishes. III. The electroplaques of the Stargazer, *Astroscopus y-graecum*. J. Gen. Physiol. **44:** 819–843.

BENNETT, M. V. L. & H. GRUNDFEST. 1961*c*. Studies on morphology and electrophysiology of electric organs. III. Electrophysiology of electric organs in Mormyrids. *In* Bioelectrogenesis. C. Chagas & A. Paes-de-Carvalho, Eds. Elsevier. Amsterdam, Holland.

BENNETT, M. V. L. & H. GRUNDFEST. 1961*d*. Structure and function in rajid electroplaques. Federation Proc. **20:** 339.

BENNETT, M. V. L., M. WURZEL & H. GRUNDFEST. 1961. The electrophysiology of electric organs of marine electric fishes. I. Properties of electroplaques of *Torpedo nobiliana*. J. Gen. Physiol. **44:** 757–804.

BERNSTEIN, J. 1912. Electrobiologie. Braunschweiz, Fr. Vieweg.

BIGELOW, H. B. & W. C. SCHROEDER. 1953. Fishes of the Western North Atlantic, No. 1, part 2. New Haven; Sears Foundation for Marine Research. Yale University. New Haven, Conn.

BROCK, L. G. & R. M. ECCLES. 1958. The membrane potentials during rest and activity of the ray electroplate. J. Physiol. **142:** 251–274.

BURKE, W. & B. L. GINSBORG. 1956. The action of the neuromuscular transmitter on the slow fibre membrane. J. Physiol. **132:** 599–610.

DEL CASTILLO, J. & B. KATZ. 1954. The membrane changes produced by the neuromuscular transmitter. J. Physiol. **125:** 546–565.

COATES, C. W. 1950. Electric fishes. Elect. Eng. N.Y. **69:** 47–50.

COHEN, B., M. V. L. BENNETT & H. GRUNDFEST. 1961. Electrically excitable responses in *Raia erinacea* electroplaques. Federation Proc. **20:** 339.

COLE, K. S. & H. J. CURTIS. 1939. Electric impedance of the squid giant axon during activity. J. Gen. Physiol. **22:** 649–670.

COUTEAUX, R. & T. SZABO. 1959. Siège de la jonction nerf-électroplaque dans les organes électriques a électroplaques pédiculées. Compt. rend. acad. sci. **248:** 457–470.

COX, R. I., C. W. COATES & M. V. BROWN. 1945. Electric tissue. Relation between the structure, electrical characteristics, and chemical processes of electric tissue. J. Gen. Physiol. **28:** 187–212.

ECCLES, J. C. 1957. The Physiology of Nerve Cells. The Johns Hopkins Press. Baltimore, Md.

ECCLES, J. C., P. FATT & K. KOKETSU. 1954. Cholinergic and inhibitory synapses in a pathway from motor-axon collaterals to motoneurones. J. Physiol. **126:** 524–562.

DAHLGREN, U. 1914*a*. The origin of the electric tissues of *Gymnarchus niloticus*. *In* Papers From The Tortugas Laboratory. Carnegie Inst. Wash., VI, 159–194.

DAHLGREN, U. 1914*b*. The habits of *Astroscopus* and the development of its electric organs. Carnegie Inst. Wash. Year Book No. **13:** 201–203.

DALTON, J. C. & R. FITZHUGH. 1960. Applicability of Hodgkin-Huxley model to experimental data from the giant axon of the lobster. Science. **131:** 1533.

DARWIN, C. 1959. The Origin of Species and The Descent of Man. : 159.0 Modern Library Edition. Random House. New York, N. Y.

EWART, J. C. 1888. The electric organ of the skate. The electric organ of *Raia radiata*. Phil. Trans. Roy. Soc. **B.** : 399–416.

EWART, J. C. 1892. The electric organ of the skate. Observations on the structure, relations, progressive development, and growth of the electric organ of the skate. Phil. Trans. Roy. Soc. **B.** : 389–420.

FELDBERG, W. & A. FESSARD. 1942. Cholinergic nature of the nerves to the electric organ of the *Torpedo*. J. Physiol. (London). **101:** 300.

FINNEY, D. J. 1948. Fisher-Yates test of significance in 2 x 2 contingency tables. Biometrika. **35:** 145.

Fitzhugh, R. 1960. Thresholds and plateaus in the Hodgkin-Huxley nerve equations. J. Gen. Physiol. **43:** 867–896.

Frank, K. & M. G. F. Fuortes. 1956. Unitary activity of spinal interneurones of cats. J. Physiol. (London). **131:** 424–435.

Frankenhaeuser, B. & B. Waltman. 1959. Membrane resistance and conduction velocity of large myelinated nerve fibres from *Xenopus laevis*. J. Physiol. (London). **148:** 677–682.

Freygang, W. H., Jr. 1958. An analysis of extracellular potentials from single neurons in the lateral geniculate nucleus of the cat. J. Gen. Physiol. **41:** 543–564.

Freygang, W. H., Jr. & K. Frank. 1959. Extracellular potentials from single spinal motoneurons. J. Gen. Physiol. **42:** 749–760.

Fritsch, G. 1890. Die elektrischen Fische. II. Die Torpedineen. Leipzig, Germany.

Furshpan, E. J. & D. D. Potter. 1959. Transmission at the giant motor synapses of the crayfish. J. Physiol. (London). **145:** 289–325.

Grundfest, H. 1957*a*. The mechanisms of discharge of the electric organs in relation to general and comparative electrophysiology. *In* Progress in Biophysics. **7:** 1–85. Pergamon Press. London, England.

Grundfest, H. 1957*b*. Electrical inexcitability of synapses and some of its consequences in the central nervous system. Physiol. Revs. **37:** 337–361.

Grundfest, H. 1957*c*. Excitation triggers in post-junctional cells. *In* Physiological Triggers. T. H. Bullock, Ed. Am. Physiol. Soc. : 119–151.

Grundfest, H. 1959. Synaptic and ephaptic transmission. *In* Handbook of Physiology. Section I, Neurophysiology I. Am. Physiol. Soc. : 147–197.

Grundfest, H. & M. V. L. Bennett. 1961. Studies on morphology and electrophysiology of electric organs. I. Electrophysiology of marine electric fishes. *In* Bioelectrogenesis. C. Chagas & A. Paes-de-Carvalho, Eds. Elsevier. Amsterdam, Holland.

Grundfest, H. & B. Campbell. 1942. Origin, conduction and termination of impulses in the dorsal spinocerebellar tract of cats. J. Neurophysiol. **5:** 275–294.

Hagiwara, S., A. Watanabe & N. Saito. 1959. Potential changes in syncytial neurons of lobster cardiac ganglion. J. Neurophysiol. **22:** 554–572.

Hodgkin, A. L. 1947*a*. The membrane resistance of a non-medullated nerve fibre. J. Physiol. (London). **106:** 305–318.

Hodgkin, A. L. 1947*b*. The effect of potassium on the surface membrane of an isolated axon. J. Physiol. (London). **106:** 319–340.

Hodgkin, A. L. 1951. The ionic basis of electrical activity in nerve and muscle. Biol. Revs. **26:** 339–407.

Hodgkin, A. L. & A. F. Huxley. 1952*a*. Currents carried by sodium and potassium ions through the membrane of the giant axon of *Loligo*. J. Physiol. (London). **116:** 449–472.

Hodgkin, A. L. & A. F. Huxley. 1952*b*. A quantitative description of membrane current and its application to conductance and excitation in nerve. J. Physiol. (London). **117:** 500–544.

Hodgkin, A. L. & W. A. H. Rushton. 1946. The electrical constants of a crustacean nerve fibre. Proc. Roy. Soc. **B133:** 444–479.

Hutter, O. F. & D. Noble. 1960. Rectifying properties of heart muscle. Nature. **188:** 495.

Huxley, A. F. 1959. Ion movements during nerve activity. Ann. N.Y. Acad. Sci. **81**(2): 221–246.

Ishiyama, R. 1958. Studies on the rajid fishes (Rajidae) found in the waters around Japan. J. Shimonoseki College of Fisheries. **7:** 189–394.

Ito, M. 1957. The electrical activity of spinal ganglion cells investigated with intracellular microelectrodes. Japan. J. Physiol. **7:** 297–323.

Jenerick, H. 1959. The control of membrane ionic currents by the membrane potential of muscle. J. Gen. Physiol. **42:** 923–930.

Johnels, A. G. 1956. On the origin of the electric organ in *Malapterurus electricus*. Quart. J. Microscop. Sci. **97:** 455–464.

Kao, C. Y. 1960. Postsynaptic electrogenesis in septate giant axons. II. Comparison of medial and lateral giant axons of crayfish. J. Neurophysiol. **23:** 618–635.

Kao, C. Y. & H. Grundfest. 1957. Postsynaptic electrogenesis in septate giant axons. I. Earthworm median giant axon. J. Neurophysiol. **20:** 553–573.

Keynes, R. D. 1961. The development of the electric organ in *Electrophorus electricus*. *In* Bioelectrogenesis. C. Chagas & A. Paes-de-Carvalho, Eds. Elsevier. Amsterdam, Holland.

Keynes, R. D., M. V. L. Bennett & H. Grundfest. 1961. Studies on morphology and electrophysiology of electric organs. II. Electrophysiology of electric organ of *Malapterurus electricus*. *In* Bioelectrogenesis. C. Chagas & A. Paes-de-Carvalho, Eds. Elsevier. Amsterdam, Holland.

Keynes, R. D. & H. Martins-Ferreira. 1953. Membrane potentials in the electroplates of the electric eel. J. Physiol. (London). **119:** 315–351.

Lissmann, H. W. 1961. Ecological studies on gymnotids. *In* Bioelectrogenesis. C. Chagas & A. Paes-de-Carvalho, Eds. Elsevier. Amsterdam, Holland.

Lissmann, H. W. 1958. On the function and evolution of electric organs in fish. J. Exptl. Biol. **35:** 156–191.

Lissmann, H. W. & K. E. Machin. 1958. The mechanism of object location in *Gymnarchus niloticus* and similar fish. J. Exptl. Biol. **35:** 451–486.

Lowrey, A. 1913. A study of submental filaments considered as probable electric organ in the gymnotid eel (*Steatogenys elegans*). M.A. Thesis. Univ. Colo. Boulder, Colo.

Lundberg, A. 1958. Electrophysiology of salivary glands. Physiol. Revs. **38:** 21–40.

Mackay, B., A. R. Muir & A. Peter. 1960. Observations on the terminal innervation of segmental muscle fibres in amphibia. Acta Anat. **40:** 1–12.

Mathewson, R. F., A. Wachtel & H. Grundfest. 1961. Comparative study of fine structure in electroplaques. *In* Bioelectrogenesis. C. Chagas & A. Paes-de-Carvalho, Eds. Elsevier. Amsterdam, Holland.

Murray, R. W. 1960. Electrical sensitivity of the ampullae of Lorenzini. Nature. **187:** 957.

Nishi, S. & K. Koketsu. 1960. Electrical properties and activities of single sympathetic neurons in frogs. J. Cell. Comp. Physiol. **55:** 15–30.

Noble, D. 1960. Cardiac action and pacemaker potentials based on the Hodgkin-Huxley equations. Nature. **188:** 495–497.

Regnart, H. C. 1931. On the lower limits of perception of electrical currents by fish. J. Marine Biol. Assoc. (U.K.). **8:** 13–32.

Renshaw, B. 1946. Central effects of centripetal impulses in axons of spinal ventral roots. J. Neurophysiol. **9:** 191–204.

Rose, J. E. & V. B. Mountcastle. 1954. Activity of single neurons in the tactile thalamic region of the cat in response to a transient peripheral stimulus. Bull. Johns Hopkins Hosp. **94:** 238.

Schoffeniels, E. 1959. Ion movements studied with single isolated electroplax. Ann. N.Y. Acad. Sci. **81**(2): 295–306.

Szabo, T. 1957. Un noyau particulier dans la formation réticulée bulbaire de quatre Poissons électriques appartenant á la famille des Gymnotidae. Compt. rend. acad. sci. **244:** 1957–1959.

Szabo, T. 1958. Structure intime de l'organe électrique de trois Mormyrides. Z. Zellforsch. Bd. **49:** 33–45.

Szabo, T. 1960. Development of the electric organ of Mormyridae. Nature. **188:** 760–762.

Szabo, T. 1961*a*. Histologie des organes électriques de quelques Mormyrides. *In* Bioelectrogenesis. C. Chagas & A. Paes-de-Carvalho, Eds. Elsevier. Amsterdam, Holland.

Szabo, T. 1961*b*. Anatomo-physiologie des centres nerveux specifiques de quelques organes électriques. *In* Bioelectrogenesis. C. Chagas & A. Paes-de-Carvalho, Eds. Elsevier. Amsterdam, Holland.

Tasaki, I. 1956. Initiation and abolition of the action potential of a single node of Ranvier. J. Gen. Physiol. **39:** 377–396.

Watanabe, A., T. G. Smith & H. Grundfest. 1960. Segmental and crossed ephaptic transmission in crayfish lateral giant axons. Federation Proc. **19:** 298.

Weidmann, S. 1956. Electrophysiologie der Herzmuskelfaser. Huber. Bern, Switzerland.

Werman, R. 1960. Electrical inexcitability of the synaptic membrane in the frog skeletal muscle fibre. Nature. **188:** 149.

Yamagiwa, K. 1956. Active and resting membrane resistances and safety factor co-operating for conduction. Japan. J. Physiol. **6:** 167–174.

EXCITATION AND INACTIVATION IN A RECEPTOR MEMBRANE*

Werner R. Loewenstein
Department of Physiology, College of Physicians and Surgeons, Columbia University, New York, N.Y.

Introduction

The nonmyelinated nerve ending of Pacinian corpuscles offers the opportunity for studying mechanisms of excitation at the receptor-membrane level. It has the unusual length of 600 to 800 μ of receptor membrane accessible for recording and stimulation. It can be freed by dissection from other tissues of the corpuscle and can be kept alive in isolation for several hours (Loewenstein and Rathkamp, 1958 FIGURE 1). Its membrane appears to be the receptor proper: any part of it responds with a nonregenerative transfer of charge to mechanical stimulation. This paper deals with some of the properties of such a membrane.

Activation

Membrane Area and Charge Transfer

Local excitation. When a spot of the receptor membrane is stimulated mechanically, excitation is restricted to this spot without spreading to other parts of the receptor membrane. This property is illustrated by the experiment of FIGURES 2 and 3. A small region of receptor membrane is stimulated mechanically, and the resulting generator potential is recorded at various distances from the stimulated region. The region is stimulated with constant mechanical pulses delivered by a stylus of about 20 μ diameter, while a microelectrode scans the surface of the remaining 800 μ length of receptor membrane. There is considerable scatter of values of generator potential, as may be expected in surface recording. But if one discards the extreme values that almost certainly are due to bad electrode contact, it becomes clear that the amplitude of the generator potential decreases exponentially with distance.

This result reveals that excitation in the receptor membrane is a local affair. Excitation appears to be localized at and confined to the mechanically stimulated region. This stands in striking contrast to the propagated nature of excitation of a typical nerve or skeletal muscle fibre membrane. The peculiarity here—and this merely describes the result of FIGURE 3 without providing its mechanism—is that there is no local circuit excitation in the receptor membrane. Excitation appears to be produced by the adequate stimulus alone—the mechanical stimulus in this case—but not by the local flow of current (for a comparison with other excitable structures, see Grundfest, 1957 and 1959).

Charge transfer as a function of membrane area: spatial summation. The preceding experiment showed that, within the same receptor membrane,

---

* The work reported in this paper was supported in part by the National Science Foundation, Washington, D.C.; the National Institute of Neurological Diseases and Blindness, Public Health Service, Bethesda, Md. (Grant B-1466); and the National Cystic Fibrosis Research Foundation, Philadelphia, Pa.

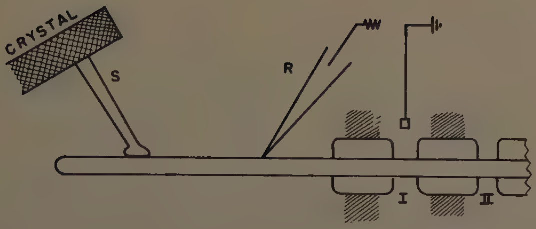

FIGURE 1. Diagram of preparation and setup. The lamellae of a Pacinian corpuscle (cat mesentery) are progressively removed by microdissection, leaving a fairly clean non-myelinated nerve ending accessible for stimulation and for microelectrode recording (see Loewenstein and Rathkamp, 1958, for a description of technique). The membrane of the ending, the receptor membrane proper, is stimulated with variable mechanical pulses of a piezoelectric crystal. The pulses are applied to the receptor membrane by a glass stylus (*S*), and the resulting generator potentials are recorded with a microelectrode (*R*) from the surface of the receptor membrane or, alternatively, between the first (I) and second (II) nodes of Ranvier by electrotonic spread. The mechanical pulses are monitored photoelectrically.

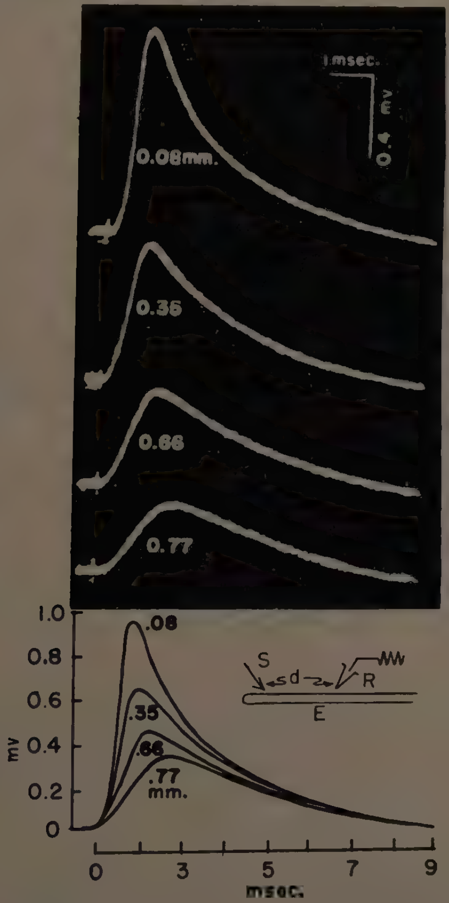

FIGURE 2. Local excitation. A small region of receptor membrane is stimulated with equal mechanical pulses from a stylus (*S*) of approximately 20 μ diameter, while the surface of the receptor membrane is scanned with a microelectrode. Four (selected) samples of generator potential (complete set of values is given in FIGURE 3) recorded at 4 different distances (*d*) from the stimulated site are shown, and their tracings superimposed below.

charge transfer can be excited in a given region of membrane independently of a neighboring one. The only coupling agent in the excitation process along the membrane appears to be the mechanical stimulus. One may expect, therefore, the total amount of charge transfer to increase in a gradual manner with the area of mechanically excited membrane. The following experiment shows that this in fact is the case: if two separate regions of the receptor membrane are stimulated independently, the resulting generator potentials sum (FIGURE 4; Loewenstein, 1959*b*). The quantitative relationship between membrane area and generator potential can be studied experimentally, and the remainder of this section will be devoted chiefly to describing the results. As a preliminary, however, some general aspects of the relationship will be analyzed.

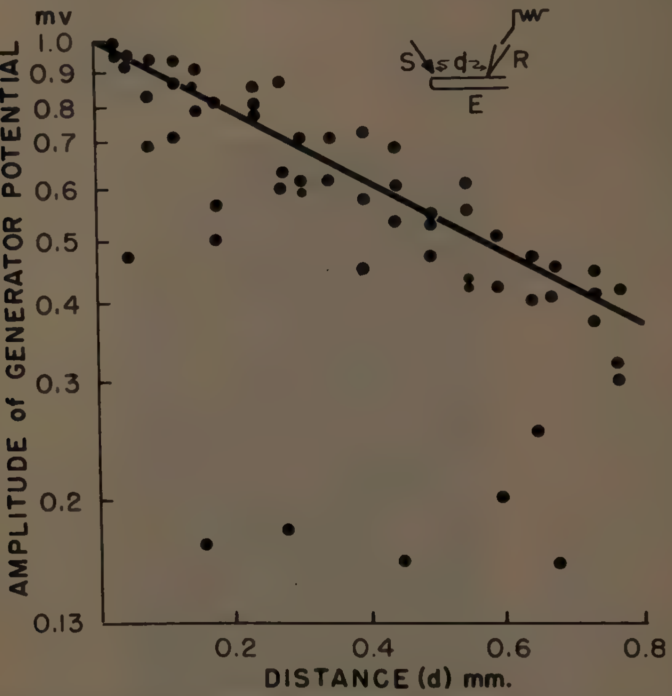

FIGURE 3. Local excitation. A spot of membrane is stimulated as described in FIGURE 2, and the resulting generator potentials (logarithmic scale) are recorded at varying distances (*d*) from the stimulated spot (the average length constant is approximately 0.8 mm.).

Analysis. The receptor membrane and associated myelinated axon can be represented by a network, as shown in FIGURE 5. Capacitance C and transmembrane resistance r_1 are uniformly distributed over the membrane. Each unit U represents a fractional value of the total membrane capacitance and conductance. It is thus merely an analytical element and not necessarily a real structural element of membrane as is, for example, a piece of mosaic structure. The feature of local excitation is represented by a local drop in transmembrane resistance r. To simplify the analysis, it will be assumed that the drop in resistance at each U-element is all-or-nothing with respect to mechanical stimulus strength. Shunt resistor r_2 performs this, so that the local resting potential E of the corresponding U-elements drops proportionally with the

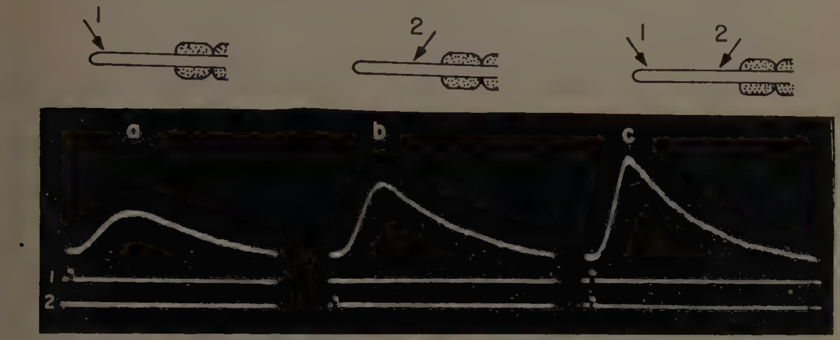

FIGURE 4. Spatial summation in the receptor membrane. Styli *1* (about 30 μ diameter) and *2* (about 20 μ diameter) belong to independent crystals that stimulate 2 membrane spots about 400 μ apart. Generator potentials (*upper beam*) in response to a mechanical pulse applied in *a*, to spot 1; in *b*, to spot 2; and in *c* to both spots simultaneously. *Lower beam* signals pulses of styli. Calibration: 1 msec.; 50 μV.

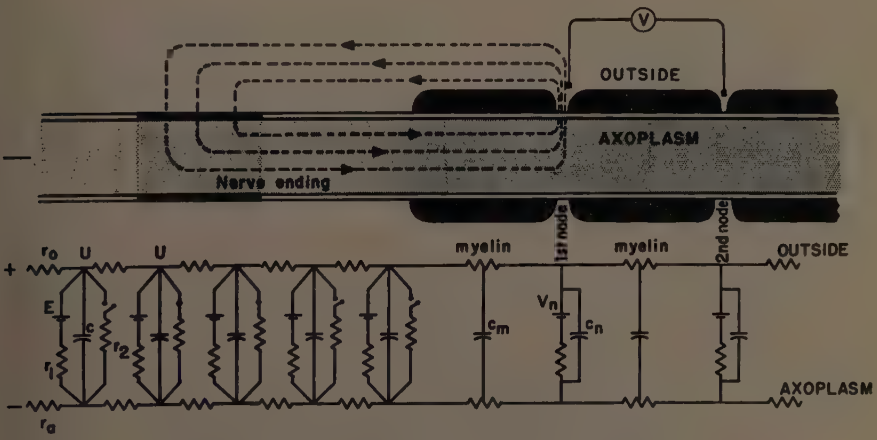

FIGURE 5. Receptor analog. Description in the text.

resistance. The generator potential V (rising phase), recorded extracellularly from the axon, is then given approximately by equation

$$V = k\,\frac{Ebx}{1 + bx}\,(1 - e^{-t/R_1C}). \qquad (1)$$

Where x is the fraction of U-units excited, that is, the ratio of excited area to total excitable area of receptor membrane; E, the resting potential; $1 + b$, the ratio between resting potential and the final value to which the membrane potential drops in the excited membrane regions due to a mechanical stimulus of unlimited strength; R_1, the parallel combination of (distributed) transmembrane resistance of the entire receptor membrane in parallel with that of the excited membrane; C, the lumped capacitance of the entire membrane; and k, a constant whose value depends on the location of the recording electrodes (Loewenstein, 1959*a*).

To simplify the equation, the nodal capacitance C_n has not been taken into account; and the relatively small resistances of the extracellular fluid around the ending r_0 and of its axoplasm r_a have been neglected. The omission of C_n affects the rate of rise (Loewenstein, 1959*a*, Equation **2**) but not the peak amplitude with which we are concerned here. The neglect of r_0 and r_a introduces an error in the calculation of the peak generator potential. If r_0 and r_a are considered, as has now been done by S. J. Socolar of this laboratory with the aid of an analog computer, the peak values still can be fitted to an equation of Form **1** with maximum discrepancy not exceeding 10 per cent for shunts uniformly distributed along the ending (in this approximation, the best fit for b becomes slightly dependent on placement of the recording "electrodes," and k, in turn, on the value of b).

It is clear from Equation **1** that the generator potential reaches its peak value at $t = \infty$. However, the values of R_1 and C are so small that the generator potential approaches within 10^{-6} per cent of its peak value already within 1 msec. (Loewenstein, 1959*a*).

The graph of Equation **1** for the case of a drop of r to $\frac{1}{10}$ of its resting value at $t = \infty$ is given in FIGURE 6. It describes a function in which *the peak values of the generator potential* (V) *increase progressively with area* (x) *of excited membrane, and in which the increments in generator potential for successive equal increments of area become progressively smaller.*

Experiments on the area-charge transfer relation. An approximate area-generator potential curve can be obtained in the actual receptor membrane. A convenient procedure is to stimulate the denuded nerve ending with interchangeable styli of different diameters. In this manner, varying areas of receptor membrane can be excited at equal strength, and the corresponding generator potentials recorded. The experimental generator potential is then found to increase with the area of excited membrane (FIGURE 7).

An attempt has been made in FIGURE 7 to fit the theoretical curve of Equation **1** to the experimental values of generator potential. The fair agreement between the experimental values of generator potential and Equation **1** (solid line of FIGURE 7) is encouraging. However, it seems unwise at present to assign undue quantitative significance to it. The result will be stated therefore merely in descriptive terms: *the generator current increases nonlinearly at a diminishing rate with area of membrane excited.*

The diameter of the ending (3 to 5 μ) is small compared to that of the stimulating stylus. Thus, as the diameter of the styli increases, the area of excited membrane grows essentially by an increase in length. The experimental abscissae values in FIGURE 7 correspond to areas of ending, that is, to elliptical cylinders of lengths equal to the corresponding stylus diameter. The actual boundaries, of course, are not so sharply defined. However, since the diameter of the ending is much smaller than that of the styli, the fringe zone of excitation spread should be roughly equal for different lengths of ending stimulated.

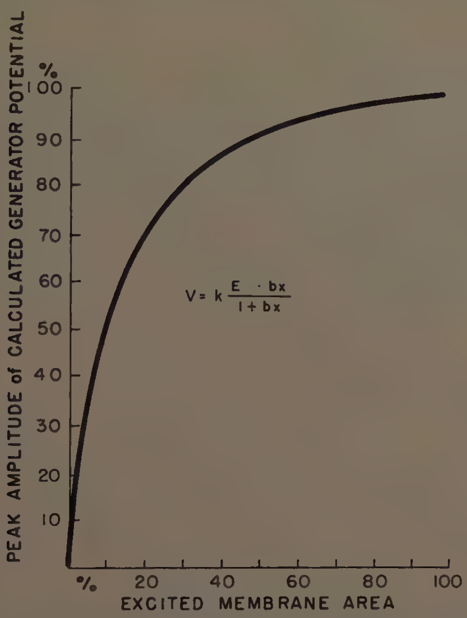

FIGURE 6. The calculated generator potential as a function of excited membrane area. Graph of Equation **1** for $r_2 = \frac{1}{9} r_1$ (see FIGURE 5), that is, for a drop in resistance in the excited membrane to $\frac{1}{10}$ of the inexcited value. The normalized peak generator potential is plotted against $100x$, the per cent excited membrane area.

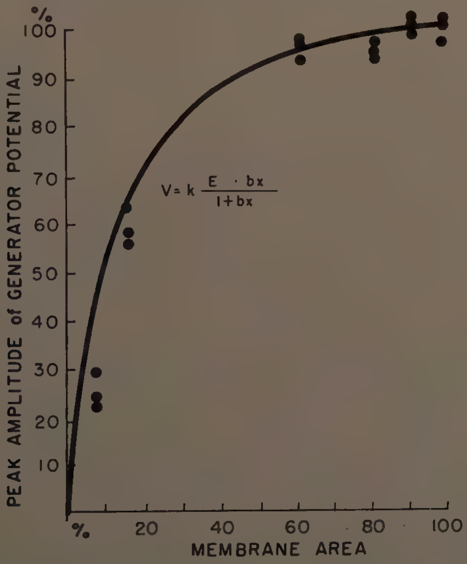

FIGURE 7. The observed generator potential as a function of excited membrane area. An increasing area of receptor membrane is excited with styli of increasing diameter, and the resulting generator potential is recorded by electrotonic spread from the nerve fibre. The area that produces the maximal generator potential equals 100 per cent area. The solid line gives the theoretical curve as calculated from Equation **1** (see FIGURE 6).

The normalized generator potential-"true" area curve thus should be essentially the same as that of FIGURE 7.

Stimulus strength and excited membrane area. When an intact Pacinian corpuscle is stimulated with mechanical pulses of progressively increasing amplitude (hereafter referred to as *stimulus strength*), the resulting generator potentials are of progressively increasing amplitude (Álvarez-Buylla and de Arellano, 1953; Gray and Sato, 1953). FIGURE 8*B* illustrates a typical stimulus strength-generator potential curve obtained with a stimulating stylus of diameter about one third that of the nerve ending. Except for its initial portion, the shape resembles in general that of an area-generator potential curve (FIGURE 8*A*). This suggests the possibility that in both cases the increments in generator potential may be caused by the same mechanism, namely, by an increase in area of excited receptor membrane.

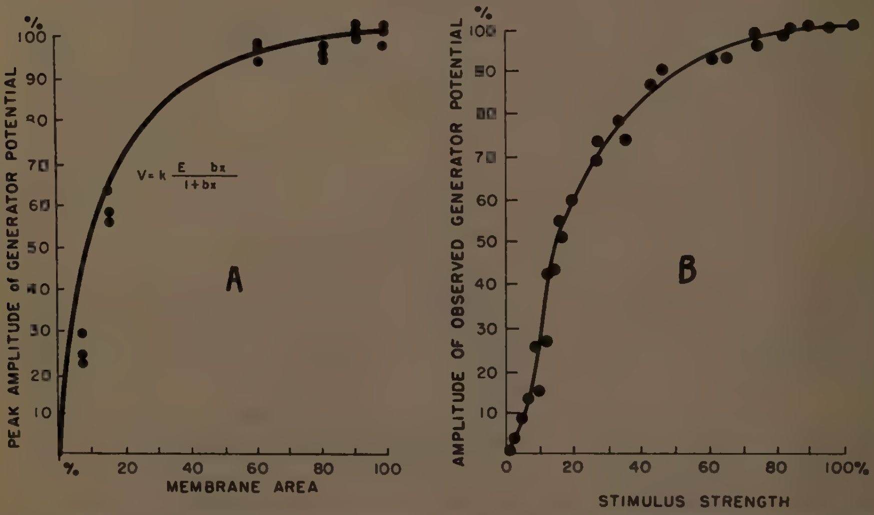

FIGURE 8. *B*, the generator potential as a function of stimulus strength. An intact corpuscle is stimulated with mechanical pulses of increasing amplitude (stimulus strength) and the resulting generator potential is recorded by electrotonic spread from the nerve fibre. The first and second nodes of Ranvier have been blocked with procaine to prevent firing of nerve impulses. *A*, for comparison, the area-generator potential relation of FIGURE 7 is here reproduced.

The nerve ending of the Pacinian corpuscle is wrapped in many connective tissue-like lamellae that form a multilayered fluid-filled parcel around it. It is therefore quite possible that when mechanical pulses of increasing strengths are applied to such a mechanically coupled system (for example, with a stylus smaller than the length of ending), the resulting deformation spreads over an increasing area of receptor membrane. The question is, then, whether the increase in generator potential that results from an increase in stimulus strength can be accounted for by an increase in excited area alone. There seem to be only two plausible mechanisms to account for such a change in generator potential: (1) an increase in specific membrane conductance at the point of excitation, and/or (2) an increase in lumped membrane conductance, that is, in area of membrane excited (a possible change in membrane capacitance would be far too small to account for the observed change in generator potential). The following experiment is an attempt to see which of the mechanisms operates.

It is possible to crush the terminal piece of nerve ending so that the remaining stump continues to produce generator potentials for some time (Loewenstein and Rathkamp, 1958). The strength-generator potential relation thus can be studied in varying lengths of ending. This method helps one to distinguish between two alternative mechanisms. If an increase in stimulus strength were to increase the charge transfer by way of an increase in area of excited receptor membrane, one might expect the range of strength in which the corresponding maximal generator potential is attained to increase with length. If, on the other hand, an increase in stimulus strength were to operate through the alternative mode, through an increase in specific membrane conductance without an increase in the membrane area, the maximal generator potential and the strength range at which the latter is attained should be independent of length.

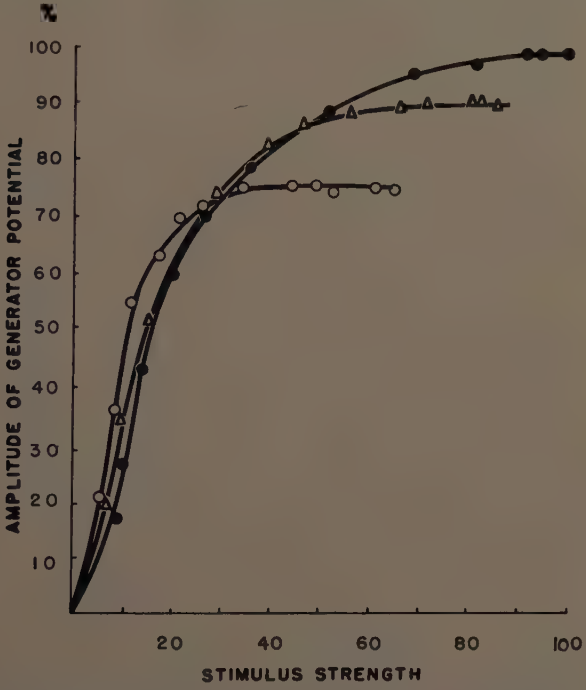

FIGURE 9. Excited membrane area and the generator potential-stimulus strength relationship. The generator potential-stimulus strength relation is studied in a piece of ending of about ○, one third; △, two thirds; and ●, full length. Ordinates, per cent amplitude of maximal generator potential at full length of ending.

The contention of an increase in area is borne out by the experiment illustrated in FIGURE 9. The stimulus strength-generator potential relation is studied in the intact ending, and in stumps of about two thirds and one half the intact length respectively (the point of stimulus application and stylus diameter is the same throughout). It is seen that the longer the piece of ending, the greater is the amplitude of the maximal generator potential and—of more significance here—the higher the strength range at which the maximal generator potential is attained.

This result is due to a change in length of ending and not to a change in its resting potential. As may be expected, the resting potential of the injured ending diminishes eventually. However, with proper precautions, the time constants of fall in resting potential are from 40 to 70 min., whereas the entire experiment of FIGURE 9 lasts only 1 to 2 min. Thus only a small part of the diminution in maximal generator potential can be due to a decrease in resting potential. A simple way to show this is to cut off the tip of the ending. The area and the initial generator response are thereby practically unchanged. The generator potential in response to a given stimulus is then found to decline with the previously indicated time constants; or, if a longer piece of ending (for example one-half length) is crushed, the decline has about the same time constant.

In conclusion it may be stated that *a change in stimulus strength brings about a change in charge transfer by changing the area of excited receptor membrane.* As the area of excited membrane increases, a progressively increasing area of membrane is shunted, that is, the total membrane conductance increases. Thus, one way by which charge transfer is varied under physiological conditions in the sense organ is by changing the area of excited membrane, that is, the (lumped) membrane conductance. Whether this is the only way to increase charge transfer cannot be stated. The question remains whether, in addition to the lumped conductance, also the specific conductance of the excited membrane varies with stimulus strength; or, stated in terms of the receptor model of FIGURE 5, whether in addition to the *number* of shunt resistors r_2, also the *value* of each shunt resistor is continuously variable with stimulus strength. This question, of course, cannot be solved analytically; an output curve of the type illustrated in FIGURE 8 can be accounted for in analytical terms equally well with r_2 as a fixed or as a variable resistor. There is also no direct experimental solution possible at present. The space-resolving power of microelectrodes is far too low. However, the point that is clear here is that charge transfer increases with area of membrane excited, and that one way by which an increase in stimulus strength brings about an increase in charge transfer is through an increase in excited membrane area.

It seems worthwhile at this point to discuss briefly the physiological significance of the area-generator potential relationship. The character of the sensory impulse discharge is determined by the intensity and the rate of rise of the generator current. The frequency, the number of impulses, a good part of the sensory coding depend on the generator current. This is known for a variety of receptors in addition to the Pacinian corpuscle: for muscle spindles (Katz, 1950; Lippold *et al.*, 1960), crustacean stretch receptor nerve cells (Eyzaguirre and Kuffler, 1955; Burkhardt, 1959; Terzuolo and Washizo, 1960), photoreceptors (Hartline *et al.*, 1952; cf. Granit, 1955; Fuortes, 1959; Rushton, 1959; Tomita, 1958), olfactory receptors (Ottoson, 1956), insect hair receptors

(Wolbaruht, 1960) and Lorenzinian ampullae (Loewenstein, 1960). We have seen that in the Pacinian corpuscle the generator current in turn depends on the area of membrane excited. It appears therefore that in the end the impulse message in a given sensory fiber is graded by the area of membrane excited at its receptor terminal.

OTHER FACTORS THAT INFLUENCE CHARGE TRANSFER

Electrical gradients and charge transfer. A plausible way to explain the charge transfer in the receptor membrane is to assume that the membrane separates two media of different ionic concentration, and that the mechanical stimulus elicits an increase in conductance for one or several species of ions. If the ionic distribution is in general similar to that of other excitable nerve membranes, such a conductance change would result in a depolarizing transfer of charges through the mechanically excited membrane by ions moving along their electrochemical gradients. On this basis one would expect the charge transfer of a given area of membrane to increase as a function of resting membrane potential. This is also what the receptor analog of FIGURE 5 describes, and is implicit in Equation **1**, where the relation $V = V(E)$ is specified as one of direct proportionality.

A simple way to study the effect of membrane polarization is to record the generator potential in response to a mechanical stimulus of constant strength, that is, of a constant mean membrane area, while inward or outward currents are passed through the membrane. It is then found that over a wide range of polarizing currents the generator potential increases with membrane polarization (FIGURE 10) (Loewenstein and Ishiko, 1960). Moreover if the generator potential-strength relationship is studied at various levels of membrane polarization, it is found that the effect of membrane polarization is to multiply the generator potential at any given strength by a constant factor (FIGURE 11).

Temperature and charge transfer. Another factor that influences charge transfer in the receptor membrane is temperature. A detailed description of the temperature effects has been given by Inman and Peruzzi (1961) and Ishiko and Loewenstein (1960, 1961*a*). Reference here will be made only to the following:

The rate of rise of the generator potential (FIGURE 12) in response to a constant stimulus increases markedly with temperature ($Q_{10} = 2.5$). Moreover, in addition, the *amplitude* of the generator potential increases ($Q_{10} = 2.0$) while the duration of the falling phase is almost unchanged (FIGURES 12 and 13). This is another feature of the receptor membrane that contrasts with the membrane of the adjacent Ranvier node. The amplitude of the latter's action potential, like that of other membranes with regenerative excitability, remains rather constant over a wide range of temperature, while its duration is markedly increased. These results on the receptor membrane are best explained by assuming that temperature increases the short-circuiting factor during the active phase—that is, the conductance of the excited receptor membrane—and thereby causes the rate of rise and the amplitude of generator potential to increase (Equation **1**).

Temperature has, however, merely a modulatory effect. A change in temperature appears to modify the conductance during the active phase in the *mechanically* excited membrane, but does not initiate the conductance change. The conductance change, namely excitation, is initiated only by the mechanical stimulus (Loewenstein, 1961). In this sense, the receptor membrane is rather specifically sensitive to mechanical stimuli.

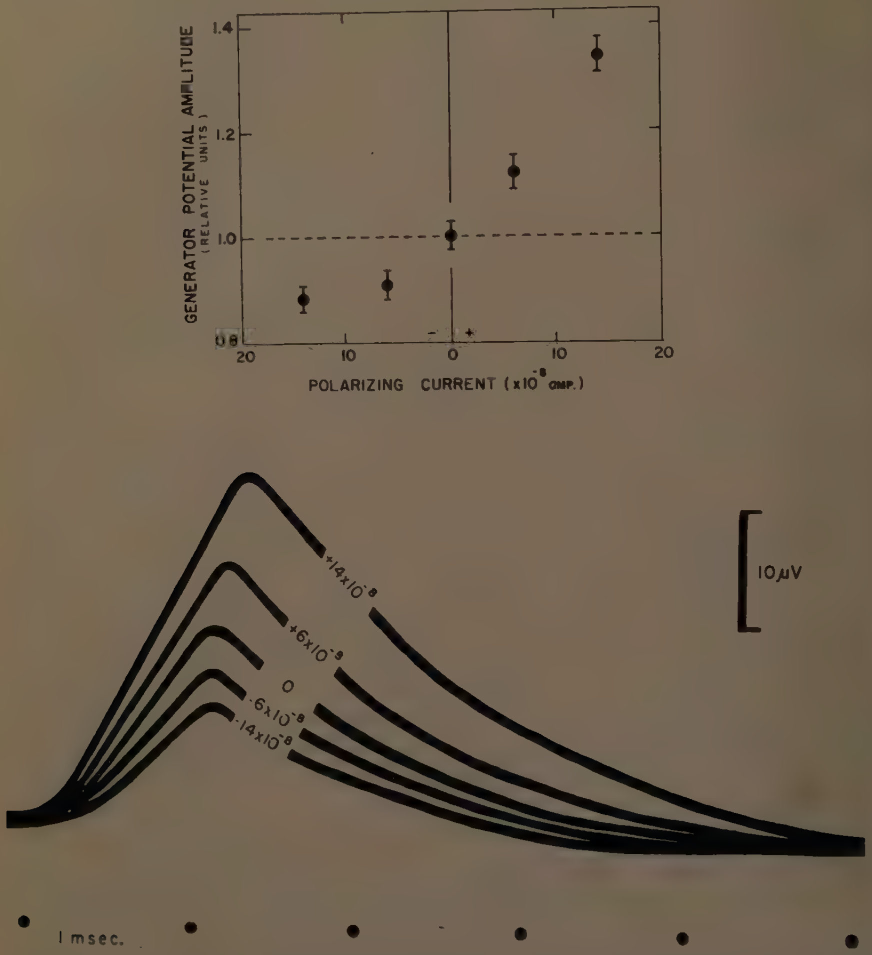

FIGURE 10. Generator potential at various levels of receptor membrane polarization. The receptor membrane is stimulated with equal mechanical stimuli while being hyperpolarized or depolarized with, respectively, inward (+) or outward currents (−). Vertical bars subtend the standard error of the mean of 50 potentials (from Loewenstein and Ishiko, 1960). Reproduced by permission of the *Journal of General Physiology.*

STATISTICAL EXCITATION

When equal mechanical stimuli are applied to the receptor membrane, the resulting generator potentials fluctuate statistically (FIGURE 14) (Loewenstein and Altamirano-Orrego, 1958; Ishiko and Loewenstein, 1959). The fluctuations are at random and follow an approximately symmetric distribution (FIGURE 15; Ishiko and Loewenstein, 1961*b*). The fluctuations are large; much larger than the usual fluctuations of action potential in nerve or muscle fibre membranes. For example the standard deviation of a submaximal generator potential may be as high as 8 per cent of the mean amplitude. A typical case appears in FIGURE 17. The receptor is stimulated with equal mechanical pulses, and the statistical fluctuations of the resulting generator potential are determined for various strength values of the pulses. The constancy of the mechanical pulses is controlled photoelectrically within 0.5 per cent. Two hundred generator potentials (V) were recorded at each strength and the variance (σ_V^2) determined. The variance was obtained by subtracting the base-line variance, which includes all fluctuations of our amplifier and recording systems, from the recorded generator potential variance. The variance so

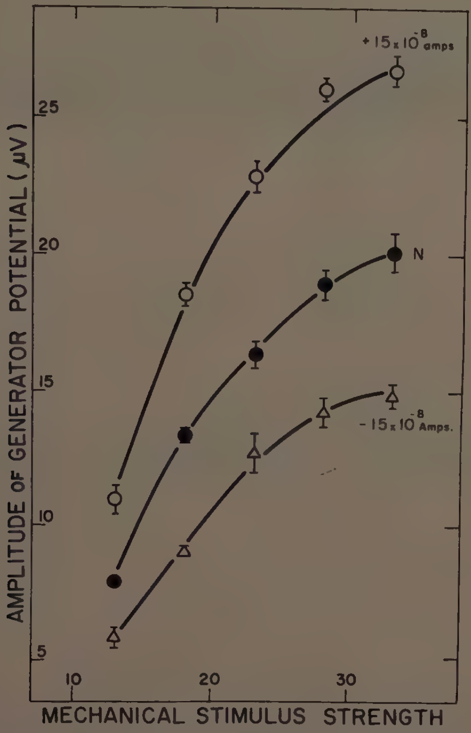

FIGURE 11. The transducer relation of the receptor membrane at various levels of polarization. The generator potential-stimulus strength function is determined in the receptor membrane at normal resting potential (●); in the receptor membrane depolarized (△) by a constant outward current; and hyperpolarized (○) by a constant inward current of 15 × 10^{-8} amp. The values of generator potential obtained in the depolarized and hyperpolarized membrane fall on curves that respectively multiply the corresponding normal generator potential curve by factors of 0.73 and 1.35. Bars subtend the standard error of the mean of 50 potentials (from Loewenstein and Ishiko, 1960).
Reproduced by permission of the *Journal of General Physiology.*

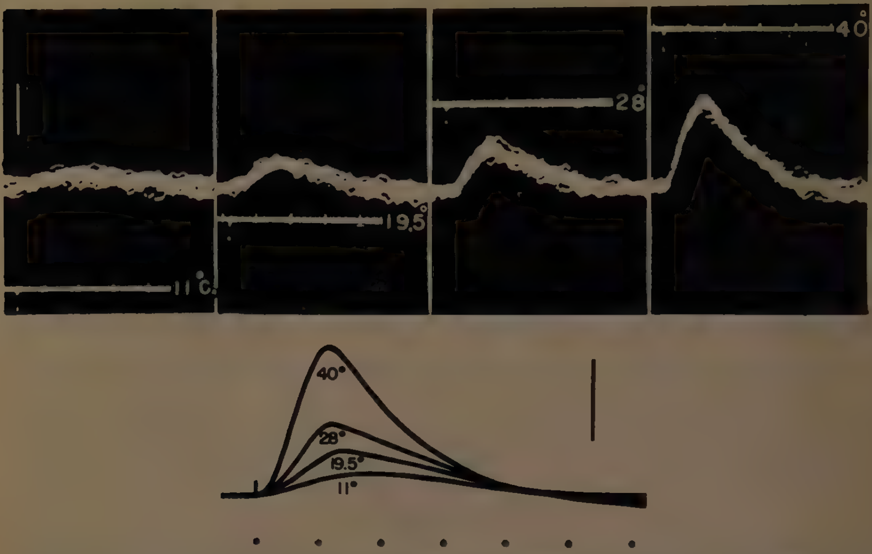

FIGURE 12. *Upper row.* Effect of temperature on generator potential. The receptor is stimulated with equal mechanical stimuli and the resulting generator potentials are recorded at different temperatures. Seven successive oscilloscope sweeps are superimposed on each photograph. The second beam records the thermistor reading of temperature. *Lower row.* Tracings of upper records slightly enlarged. Calibration: 25 μV; 1 msec. (from Ishiko and Loewenstein, 1961*b*).

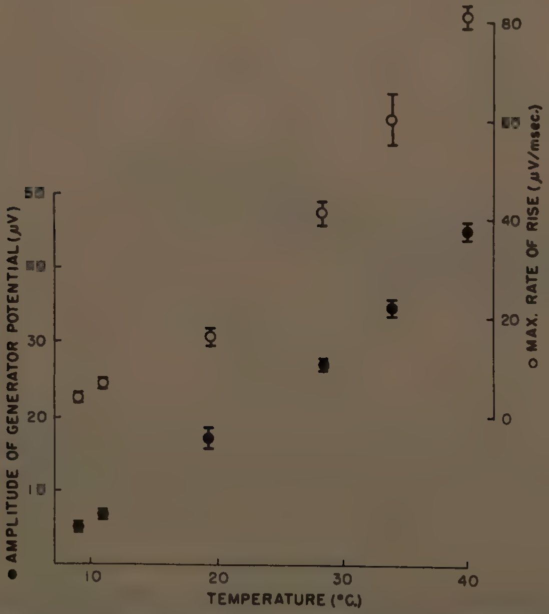

FIGURE 13. Effect of temperature on the amplitude and rate of rise of generator potential. *Abscissa:* temperature of the receptor. *Ordinates:* ●, mean value of amplitude, and ○, of maximal rate of rise of 35 to 50 generator potentials. Bars subtend standard error of the mean (from Ishiko and Loewenstein, 1961*b*).

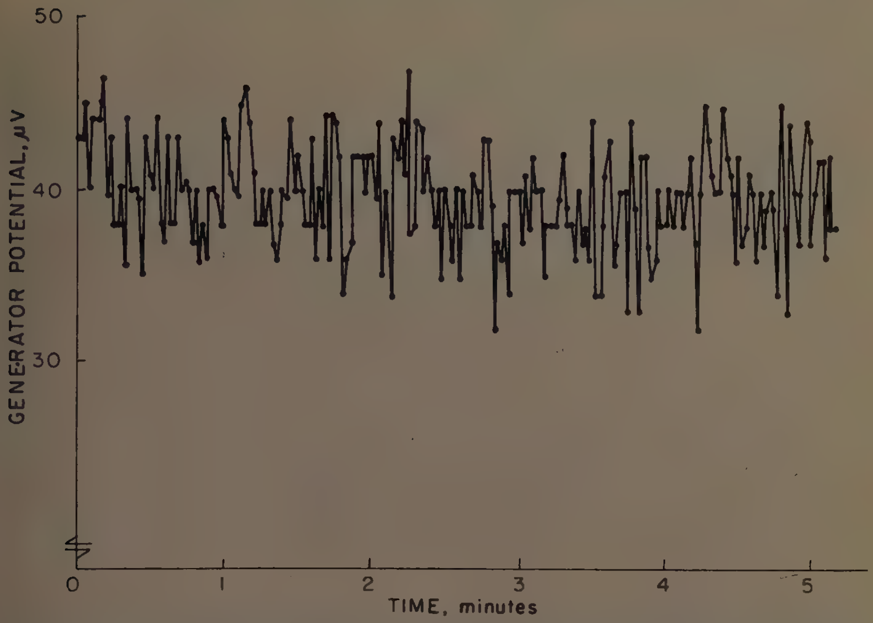

FIGURE 14. Fluctuations in generator potential. A series of generator potentials in response to equal mechanical stimuli. The stimuli are monitored photoelectrically within 0.5 per cent (from Ishiko and Loewenstein, 1961*b*).

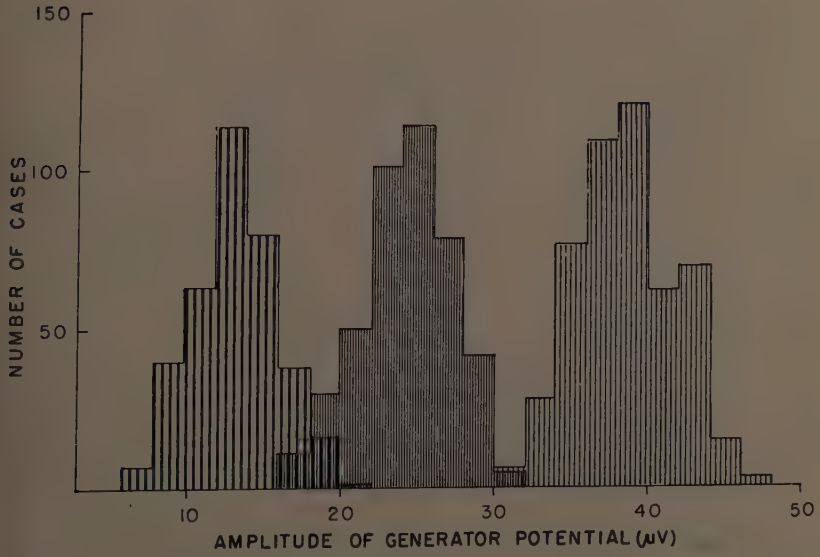

FIGURE 15. Amplitude distribution of generator potential at three stimulus strengths.

determined represents very nearly the true fluctuation in the excitation process of the receptor membrane, contributions of fluctuations in mechanical stimulus being negligible (Ishiko and Loewenstein, 1959; Ishiko and Loewenstein, 1961*b*). It is seen that as the stimulus strength increases, the fluctuations rise to a maximum and then decline (FIGURE 17).

An attempt may now be made to explain these fluctuations of generator potential as a consequence of the peculiar mode of excitation described in the preceding section. In a typical nerve or muscle fibre membrane where charge transfer is regenerated at full size by local current excitation along the entire membrane, and where the amount of charge transferred is independent of the stimulus, fluctuations in charge transfer of successive excitations may be rather small. In the receptor membrane, on the other hand, where there is no electrical coupling in the excitation process nor coupling of any kind other than mechanical, one may expect a marked statistical play in excitation. In such a membrane that forms part of a system with elastic and nonelastic elements (a long nerve ending encased in many tissue layers), the accessibility for excitation by mechanical stimulation is necessarily unequal for different regions of membrane. This alone should introduce considerable fluctuation in the charge transfer and should account for the larger part of the observed fluctuation in generator potential.* Further contributions to the fluctuations, probably of much lesser magnitude, may arise from statistical play in the charge-transfer process proper.

Membrane area and statistical fluctuation. To visualize what is meant here by statistical excitation it may be helpful to give a hypothetical scheme of possible spatial distribution patterns of excited membrane area. One may picture the excitation as occurring in subareas of membrane following two patterns: (1) subareas randomly scattered over the entire receptor membrane, as shown in FIGURE 16*a*; and (2) subareas distributed at random with radially decreasing density around the zone of stimulation (FIGURE 16*b*). The former pattern is likely to occur under physiological conditions in the intact sense organ, where the capsule tends to distribute the deformation over the ending, or when the denuded ending is stimulated with a large stylus; the latter pattern is likely to correspond to the case in which a small area of denuded membrane is stimulated with a fine stylus. The spatial distribution of membrane area accessible for excitation is assumed to fluctuate at random with time. The division of the membrane into subareas does not imply a mosaic structure, nor structural discontinuities of any other sort in the receptor membrane. In so far as the experimental evidence is concerned, and in so far as the present argument is concerned, the membrane may be continuous. The subdivision into excited and nonexcited subareas is merely a consequence of the local nature of excitation described in the preceding section and of accessibility and inaccessibility for excitation. An excited subarea may be defined as the minimal region of receptor membrane that, at a given time, is excited independently of adjacent regions.

---

* The mechanical stimulation process of such a system possibly could be nonstatistical only if the energy requirement for excitation of the membrane were so low as to make it virtually a triggered system. This is certainly not the case. The fact that the excited area in the experiments of FIGURES 4 and 7 is variable is alone sufficient argument against it.

In the light of the present hypothesis the generator potential is built up by charge transfer through a statistically fluctuating area of receptor membrane; or, more generally, by a statistically fluctuating population of excited subareas. The situation resembles, in a way, that of the motor endplate (Castillo and Katz, 1954). As the stimulus strength increases, a progressively increasing population of subareas is excited; thus the probability for a given stimulus to gain access to (that is, to excite) a membrane area increases with its strength

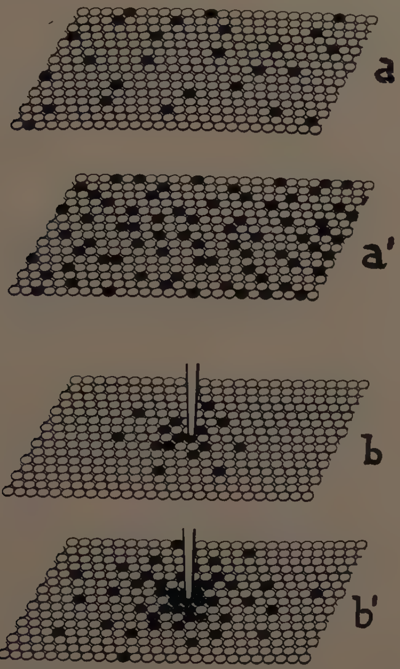

FIGURE 16. Schematic representation of hypothetical distribution patterns of excited membrane area. Key: (*a*) excited subareas (black) randomly scattered among nonexcited areas (white); (*b*) excited subareas randomly distributed with radially decreasing density around the zone of stimulation; and (*a'*, *b'*) the same after increasing the excited area by an increase in stimulus strength.

In either of the two distribution patterns of excited membrane, one may expect the fluctuation of excited area to increase with the excited area (and, hence, also with strength).

It is helpful now to consider again the electrical analog expression for the generator potential given in Equation **1**, as a basis for a quantitative explanation of the fluctuation.* Assume that the excited membrane area (represented in Equation **1** by x) is characterized by a standard deviation σ_x (corresponding to fluctuations of the U elements of the model of FIGURE 5). It follows, then, that the generator potential amplitude fluctuates with a standard deviation given by

---

* The analysis in this paragraph is part of a private communication from S. J. Socolar.

$$\sigma_V = \sigma_x \frac{kEb}{(1 + bx)^2},$$

or, more conveniently,

$$\sigma_V = \frac{\sigma_x}{x} V(1 - V/kE) \qquad (2)$$

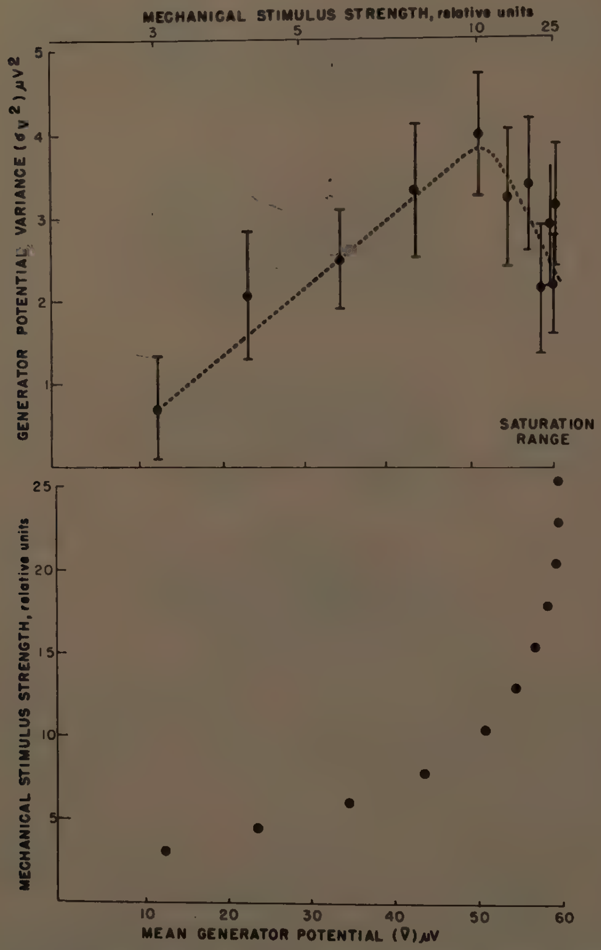

FIGURE 17. Fluctuations of generator potential as a function of mean generator potential (and of stimulus strength). Stimuli of varying strengths are applied to the receptor to produce generator potentials of varying amplitude. Two-hundred generator responses are recorded at each given stimulus strength. In the *lower curve*, the corresponding mean generator potentials (abscissae, standard error of mean smaller than dots) are plotted against stimulus strength (ordinates); in the *upper curve*, the variance of generator potential is given as a function of the mean generator potential (lower abscissae) and stimulus strength (upper abscissae, nonlinear scale). Bars subtend standard error of variance. The dotted line is the theoretical curve as calculated from Equation **1** and the slope of FIGURE 18 (Ishiko and Loewenstein, 1961*b*).

It is useful now to replot the data of FIGURE 17 in the form σ_V/V versus $\overline{V}$, as in FIGURE 18. Clearly Equation **2** is of the right form to account for the fluctuation data that cluster about a descending straight line. Thus if the model represented by Equation **1** is correct, σ_x/x must be constant in the experiment; that is, the mean fluctuation of area is proportional to mean area excited. A least-square fit of a straight line to the data of FIGURE 18 gives the estimate $\sigma_x/x = 0.08$. The corresponding theoretical curve of fluctuation has also been drawn in FIGURE 17 (dotted line). Equation **2** predicts that the peak of generator fluctuation occurs at $V = kE/2$. The agreement with the observed behaviour of the generator potential fluctuations is especially gratifying both because it flows from the description of an electrical analog already made much earlier and because it was possible to apply this model despite the lack of a direct measure of the area factor x.

The qualitative aspects of the fluctuation-generator potential relationships are already intuitively seen from the area-generator potential relationship of FIGURES 6 and 7. Let us suppose that the fluctuations in excited membrane area are proportional to the membrane area excited. Then in the initial quasi-linear range of the area-generator potential curve (FIGURE 6), we should also expect the fluctuations of generator potential to rise quasi-linearly with area excited. However, as the area-generator potential relationship becomes more nonlinear, the increments in generator potential fluctuations for successive equal increments in area fluctuation will become progressively smaller. Eventually, as the relationship between area and generator potential approaches saturation, the slope of the curve becomes small enough so that the generator potential is relatively insensitive to fluctuations on the order of 8 per cent of the total excitable membrane area. Considerable fluctuation in area may thus occur without appreciable concomitant fluctuation in generator potential. The fluctuation of generator potential becomes then small once again as the gener-

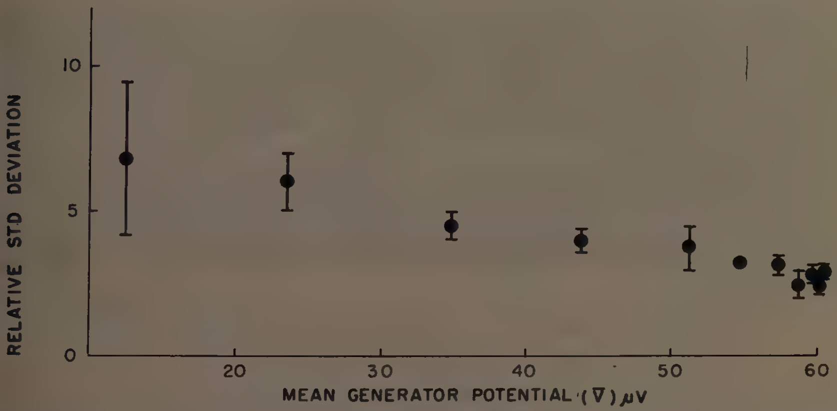

FIGURE 18. Relative fluctuation of generator potential as a function of mean generator potential. *Ordinates*, relative standard deviation of generator potential (ratio of square root of the variance of FIGURE 17 to mean generator potential); bars subtend standard error of relative standard deviation. *Abscissae*, mean generator potential; same data as FIGURE 17.

ator potential approaches its upper limit. The graph of σ_V^2 versus $\bar{V}$ should therefore exhibit a peak (FIGURE 17).

INACTIVATION

Depression of charge transfer. Mechanical stimulation has a dual action on the receptor membrane: it excites it, and inactivates it. The *excitation* manifests itself by a charge transfer that is of a clearly detectable magnitude, even when single stimuli are used. The *inactivation*, on the other hand, is brought out only by repeated stimulation. It then manifests itself by a diminution in the charge transfer. A convenient procedure to show inactivation is to subject the receptor membrane to a train of high-frequency stimulation and to probe its responsiveness before and after the train. The responsiveness is then found to be markedly reduced after the train (Loewenstein and Cohen, 1959*a* and *b*; FIGURE 19). For example, the generator potential in response to a given test stimulus may diminish to 20 per cent of its original value after application of a train of 180 stimuli at 500/sec., or to nought after 10,000 stimuli. The effect of repetitive stimulation is to depress the charge transfer in an apparently cumulative manner, so that upon repetitive stimulation the generator response is driven progressively toward a minimal value (FIGURE 20). The effect is fully reversible, has low energy requirement (stimuli of subthreshold strength will elicit it), and is independent of resting membrane potential. The depression of charge transfer increases with (1) (repetitive) stimulus strength, (2) stimulus frequency, and (3) (train) duration of repetitive stimulation (FIGURES 20 and 22).

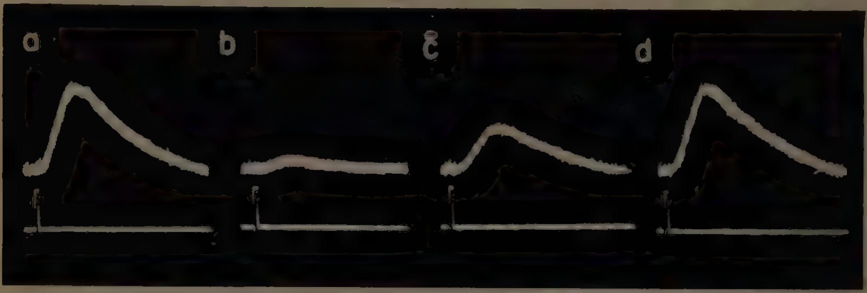

FIGURE 19. Receptor inactivation. A train of repetitive mechanical stimuli at 500/sec. is applied to the receptor for 30 sec., and the responsiveness is tested with a given stimulus. Key: (*a*) before; (*b*) 0.2 sec.; (*c*) 5 sec.; and (*d*) 50 sec. after the end of the train. *Lower beam* signals the mechanical stimulus; *upper beam*, the electrical activity of the receptor. Calibration: 20 μV; 0.5 msec. (from Loewenstein and Cohen, 1959*b*).
Reproduced by permission of the *Journal of General Physiology.*

Local inactivation. The mechanism of the depression of charge transfer is not known. One possible mechanism is that repetitive transfer causes a transient depletion of charges. Such a depletion would seem conceivable here, since the fluid space around the ending is extraordinarily small. Pease and Quilliam's (1957) electronmicrographs show the ending enclosed in tightly packed core lamellae, each representing a strong diffusion barrier (Gray and

Sato, 1955). Except for the polar clefts, the space between the nerve ending and the innermost lamella is of the order of 200 Å. However, a depletion mechanism would require, in addition, a 1:1 ion exchange, to account for the absence of a shift in resting potential during depression; and a time constant of restoration of the order of 0.1 sec. or even several sec. (at about 25° C.) to account for the recovery time of generator potential from depression after prolonged and strong repetitive stimulation.

An alternative mechanism is that of repetitive stimulation actions on a stage in excitation prior to the charge transfer acting, namely, causing inactivation of the membrane processes that lead to the conductance change. The kinetics of the depression of generator potential and those of its restoration are compatible with both a depletion and an inactivation process. However, the two processes may be expected to differ distinctly in their extent of spatial spread. While a depletion should be diffuse over the entire receptor membrane of the ending (the electronmicroscope reveals no transverse barriers in the fluid space around the ending), a membrane inactivation process may be expected to be localized in view of the localized nature of the excitation process shown above.

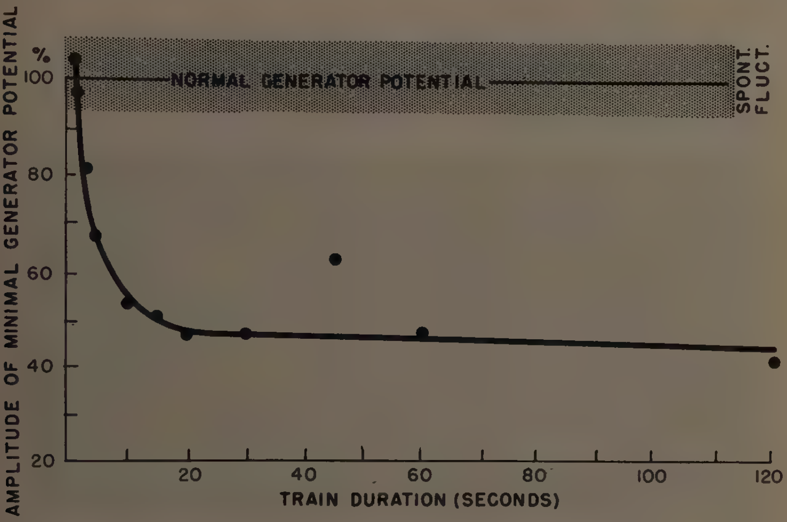

FIGURE 20. Time course of inactivation. *Abscissae:* duration of train of repetitive stimuli (500/sec.). *Ordinates:* amplitude of test generator potential. The shaded area delineates the fluctuation of the normal test generator potential (from Loewenstein and Cohen, 1959*b*).

Reproduced by permission of the *Journal of General Physiology.*

This allows one to test the two possibilities experimentally. Two small membrane regions (*1* and *2*, FIGURE 21) separated by about 500 μ are stimulated with styli driven by 2 independent piezoelectric crystals. A train of high frequency stimuli is applied to region 1, and subsequently the responsiveness is tested at regions *1* and *2*. The responsiveness at region *1* is found to be considerably lowered, while that of region *2* is essentially the same as before repetitive stimulation.

The depression of charge transfer appears thus to reflect an inactivation process in the receptor membrane which, like excitation, is a highly localized process.

A discussion on statistical inactivation. An attempt may now be made to relate inactivation to excitation. Such an attempt is necessarily speculative at present. However, the nature of this symposium, and certainly its title, justify some speculation.

The general assumption will be made here that excitation of a given region of receptor membrane leads to its inactivation. Such an assumption of spatial identity would seem to be a very plausible one in view of the preceding results.

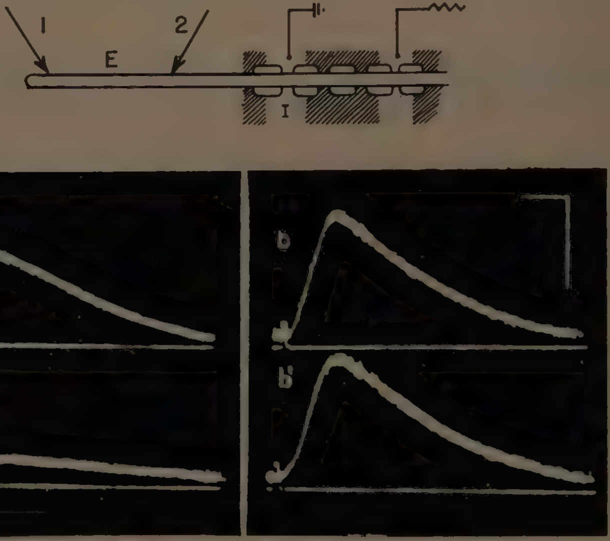

FIGURE 21. Local inactivation. Two regions of membrane (*1* and *2*) separated by about 200 to 250 μ are stimulated with small styli (stylus diameter of region *1* is somewhat larger than that of *2*) of independent piezoelectric crystals. A train of repetitive stimuli (500/sec.; 2 sec. duration) is applied to region *1*. Responsiveness of regions *1* and *2* is tested before and after the train. Key: (*a*) responses at region *1* before the train; (*a'*) after the train; (*b*) responses at region *2* before the train; (*b'*) after the train. Calibration: 100 μV; 1 msec.

The statistical model of excitation may then be applied to inactivation, and one may undertake on this basis to examine the dependence of inactivation on strength, duration, and frequency of repetitive stimulation. For instance the increase in generator potential depression with (repetitive) stimulus strength (FIGURE 22) can then be accounted for by statistical inactivation, even if inactivation in a given subarea were to be all-or-nothing with respect to stimulus strength. Consider for example the case in which inactivation is caused with repetitive stimuli of—in successive runs—progressively increasing strength, delivered to a given application point on the nerve ending, and in which the degree of inactivation is probed with stimuli of a given strength with the same stylus and at the same application point. This is exactly the situation of the experiment of FIGURE 22, and is thought to correspond to the statistical excitation-inactivation scheme of FIGURE 16*b*. The experiment may then be described in the following terms: a progressively increasing population of subareas is inactivated, and the inactivation is probed in a concentric population sample of a given mean size. Since the probability of excitation (hence that of inactivation) within a membrane subarea increases with stimulus strength, as previously mentioned, the area of inactivated membrane in the test area sample will increase with (repetitive) stimulus strength, and its generator potential (namely, the test generator potential) will expectedly decrease. The experiment of FIGURE 22 shows that the test generator potential in fact decreases.

The dependence of generator potential depression on frequency and duration of repetitive stimulation may be similarly explained without any further assumptions, since the element of recovery time is implicit in reversible inactivation.

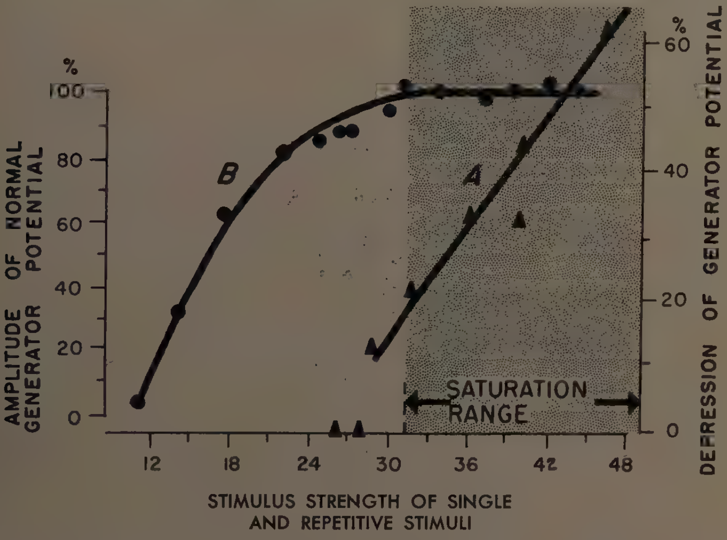

FIGURE 22. Inactivation as a function of stimulus strength of repetitive stimuli. *A:* Depression of generator potential is produced by trains of 700/sec. frequency and 15 sec. duration. The depression is probed with constant test stimuli of submaximal strength (13.5 U. on this abscissa scale). *B:* The transducer relation of the fully rested receptor membrane; the normal generator potential of the fully rested receptor as a function of strength of single stimuli. Note that inactivation does not depend on the charge transfer during repetitive stimulation, but on another factor, related to stimulus strength.

An interesting consequence of the inactivation scheme is that depression of charge transfer should depend on the area of inactivated membrane, that is, on the conditioning excited area, but not on the conditioning amount of charge transfer. The experiment of FIGURE 22 reveals that the generator potential depression is not uniquely determined by the conditioning charge transfer. It shows that the test generator potential diminishes progressively with (repetitive) stimulus strength, even in the strength range (saturation range) where the generator potential no longer increases with stimulus strength. In this range the charge transfer, but not the area, becomes saturated with strength (see FIGURE 8). Consequently, according to the inactivation scheme, the inactivation within the test area sample and the depression of its test generator potential should continue to increase in this range.

This independence of inactivation of charge transfer can also be shown in a slightly different way. If inactivation is produced in a constant mean area (submaximal), and the inactivation is tested in a concentric sample area of progressively increasing size, the measured depression in charge transfer should be progressively diminishing, even within the saturation range of charge transfer. FIGURE 23 illustrates the corresponding experiment in which inactivation is produced with repetitive stimuli of constant strength and tested with stimuli of progressively increasing strength.

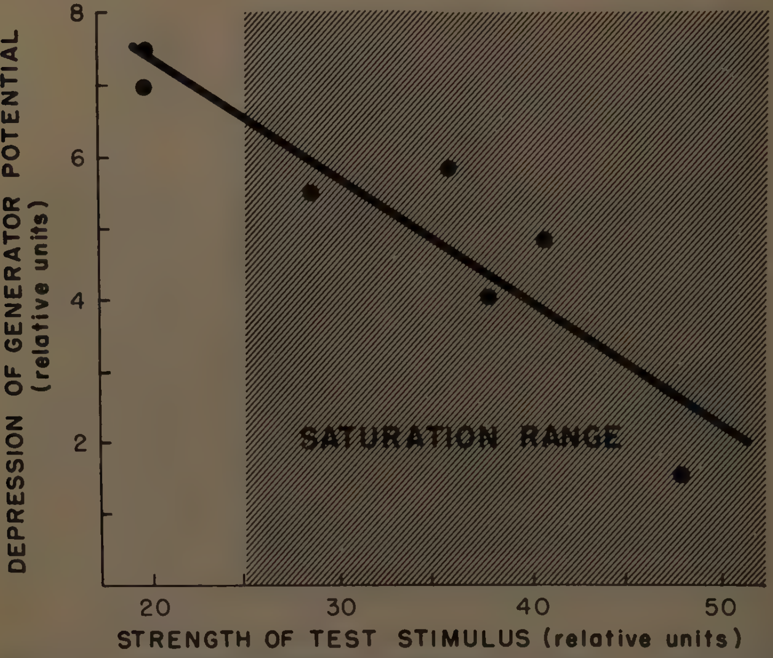

FIGURE 23. Inactivation as a function of test stimulus strength. A variation of the experiment of FIGURE 20. Inactivation is here caused with trains of constant stimulus parameters, and the resulting generator potential depression is probed with test stimuli of varying strength.

CONCLUSIONS

Excitation in the receptor membrane is local. In contrast to the propagated nature of excitation in a typical nerve fibre, excitation in the receptor membrane is localized at and confined to the membrane region that has been stimulated mechanically, and does not spread to adjacent regions within the same membrane by local circuit excitation. The reasons for the failure of local circuit excitation are not known. The electrical response of the membrane to a mechanical stimulus, the generator current, increases as a function of area of excited receptor membrane. The relationship is a nonlinear one, so that the increments in generator current for successive equal increments in area (that is, lumped membrane conductance) become progressively smaller. The well-known progressive increase in generator current that one observes with increase in strength of physiological stimulus is due largely, if not entirely, to a progressive increase in excited membrane area. (In addition, the generator current increases also with temperature and resting membrane potential.)

The generator current appears to be built up by a statistically fluctuating area of excited membrane. As a result, the generator current in response to a given stimulus shows large statistical fluctuations (of the order of 8 per cent). When the stimulus strength and, hence, the area of excited membrane, is progressively increased, the fluctuations of generator current first increase and then decline.

Repetitive excitation leads to a transient inactivation of the receptor membrane. This effect manifests itself as a depression in the generator current. The effect is fully reversible, has low energy requirements, and is independent of resting membrane potential. Like excitation, inactivation of the receptor membrane is a highly localized process.

REFERENCES

ÁLVAREZ-BUYLLA, R. & I. R. DE ARELLANO. 1953. Local responses in Pacinian corpuscles. Am. J. Physiol. **172:** 237–250.

BURKHARDT, D. 1959. Die Erregunsvorgänge vensibler Sanglienzeller in Abhangigkeit von der Temperatur. Biol. Zentralblatt. **78:** 22–62.

CASTILLO, J. DEL & B. KATZ. 1954. Quantal components of the end-plate potential. J. Physiol. (London). **124:** 560–573.

EYZAGUIRRE, C. & S. KUFFLER. 1955. Processes of excitation in the dendrites and in the soma of single isolated sensory nerve cells of the lobster and crayfish. J. Gen. Physiol. **39:** 87–119.

FUORTES, M. G. F. 1959. Initiation of impulses in visual cells of *Limulus*. J. Physiol. (London). **148:** 14–28.

GRANIT, R. 1955. Receptors and Sensory Perception. 369 pp. Yale Univ. Press. New Haven, Conn.

GRAY, J. A. B. & M. SATO. 1953. Properties of the receptor potential in Pacinian corpuscles. J. Physiol. (London). **122:** 610–636.

GRAY, J. A. B. & M. SATO. 1955. The movement of sodium and other ions in Pacinian corpuscles. J. Physiol. (London). **129:** 594–607.

GRUNDFEST, H. 1957. Electrical inexcitability of synapses and some consequences in the central nervous system. Physiol. Rev. **37:** 337–361.

GRUNDFEST, H. 1959. Evolution of conduction in the nervous system. From Evolution of Nervous Control. Am. Assoc. Advancement Sci. **:** 43–86.

HARTLINE, H. K., H. G. WAGNER & E. F. MACNICHOL, JR. 1952. The peripheral origin of nervous activity in the visual system. Cold Spring Harbor Symposia Quant. Biol. **17:** 125–141.

INMAN, D. R. & P. PERUZZI. 1961. The effects of temperature on the responses of the Pacinian corpuscles. J. Physiol. (London). **155:** 280–298.

ISHIKO, N. & W. R. LOEWENSTEIN. 1959. Properties of a receptor membrane: Spontaneous fluctuations in generator potential in a receptor membrane. Nature. **183:** 1724–1726.

ISHIKO, N. & W. R. LOEWENSTEIN. 1960. Temperature and charge transfer in a receptor membrane. Science. **132:** 1841–1842.

ISHIKO, N. & W. R. LOEWENSTEIN. 1961*a*. Effects of temperature on the generator and action potentials of a sense organ. J. Gen. Physiol. **45:** 105.

ISHIKO, N. & W. R. LOEWENSTEIN. 1961*b*. Statistical fluctuation of generator potential. In preparation.

KATZ, B. 1950. Depolarization of sensory terminals and the initiation of impulses in the muscle spindle. J. Physiol. (London). **111:** 261–282.

LIPPOLD, O. C. J., J. G. NICHOLLS & J. W. T. REDFEARN. 1960. Electrical and mechanical factors in the adaptation of a mammalian muscle spindle. J. Physiol. (London). **153:** 209–217.

Loewenstein, W. R. 1959*a*. The generation of electric activity in a nerve ending. Ann. N.Y. Acad. Sci. **81:** 367–387.

Loewenstein, W. R. 1959*b*. Properties of a receptor membrane: Spatial summation of electric activity in a non-myelinated nerve ending. Nature. **183:** 1724–1726.

Loewenstein, W. R. 1960. Mechanisms of nerve impulse initiation in a pressure receptor (Lorenzinian ampulla). Nature. **188:** 1034–1035.

Loewenstein, W. R. 1961. On the 'specificity' of a sensory receptor. J. Neurophysiol. **24:** 150–158.

Loewenstein, W. R. & R. Altamirano-Orrego. 1958. The refractory state of the generator and propagated potentials in a Pacinian corpuscle. J. Gen. Physiol. **41:** 805–824.

Loewenstein, W. R. & R. Rathkamp. 1958. The sites for mechano-electric conversion in a Pacinian corpuscle. J. Gen. Physiol. **41:** 1245–1265.

Loewenstein, W. R. & N. Ishiko. 1960. Effects of polarization of the receptor membrane of the first Ranvier node in a sense organ. J. Gen. Physiol. **43:** 981–998.

Loewenstein, W. R. & S. Cohen. 1959*a*. After-effects of repetitive activity in a nerve ending. J. Gen. Physiol. **43:** 335–345.

Loewenstein, W. R. & S. Cohen. 1959*b*. Post tetanic potentiation and depression of generator potential in a single non-myelinated nerve ending. J. Gen. Physiol. **43:** 347–376.

Ottoson, D. 1956. Analysis of the electrical activity of the olfactory epithelium. Acta Physiol. Scand. Suppl. **122:** 7–83.

Pease, D. C. & T. A. Quilliam. 1957. Electron microscopy of the Pacinian corpuscle. J. Biophys. Biochem. Cytol. **3:** 331–357.

Rushton, W. A. H. 1959. A theoretical treatment of Fuortes's observations upon eccentric cell activity in *Limulus*. J. Physiol. (London). **148:** 29–38.

Terzuolo, C. & Y. Washizo. 1960. A study of the generator potential of the crayfish stretch receptor. Physiologist. **3:** 162.

Tomita, T. 1958. Mechanism of lateral inhibition in the eye of *Limulus*. J. Neurophysiol. **21:** 419–429.

Wobarsht, M. L. 1960. Electrical characteristics of insect mechanoreceptors. J. Gen. Physiol. **44:** 105–122.

NERVOUS CONTROL OF CHEMOSENSITIVITY IN MUSCLE*

S. Thesleff

Department of Pharmacology, University of Lund, Lund, Sweden

Motor innervation influences skeletal muscle in several ways. The best known and most obvious influence is its control of the mechanical activity of muscle. In addition, innervation affects the chemical composition, metabolic reactions, electrical excitability, and the chemosensitivity of muscle. It is this last aspect of nervous control that has been the subject of study in our laboratory. The results have recently been summarized in a review article.[1]

First I shall relate our experimental results and then discuss their chief implications.

Most of the studies done by my associates and myself used isolated mammalian skeletal muscle with electrical micromethods for drug application and recording. With an electric current pulse it is possible to release iontophoretically constant quantities of acetylcholine (ACh) from the tip of a fine micropipette.[2,3] At a sensitive "spot," iontophoretically released ACh produces a transient membrane depolarization, which is recorded by a capillary glass electrode inserted into the muscle fiber close to the point of drug application (the experimental technique is schematically illustrated by FIGURE 1). By moving the drug pipette and the recording electrode to various parts of a muscle fiber it is possible to determine the distribution and relative sensitivity of its ACh receptors.

In an innervated muscle, ACh produces membrane depolarization only when applied to the end-plate region of a muscle fiber. The area sensitive to ACh is small and covers less than one millimeter of the fiber length, as shown in lower records in FIGURES 2, 3, and 4.

Motor Nerve Degeneration

Following motor denervation, the entire muscle membrane becomes sensitive to applied ACh (FIGURE 2 and upper records in FIGURE 3). Four to five days after denervation in the cat and two to three days in the rat, locally released ACh produces depolarizations with a slow time course outside the former end-plate region. The increase in the chemosensitive area starts at the end plate and spreads towards the tendons. After one to two weeks of denervation, the whole surface of the muscle fiber is as sensitive to ACh as the end-plate region, which has maintained its original responsiveness to the drug. A true supersensitivity of end-plate receptors is not observed.[4]

The new ACh receptors formed after denervation have properties identical to those at an innervated end plate. Thus their response to drugs such as ACh, carbachol, and tubocurarine is similar to that in an innervated end plate. Drugs with anticholinesterase activity, however, do not potentiate the effects

---

* The work reported in this paper was supported in part by Grant B-2646 from the National Institute of Neurological Diseases and Blindness, Public Health Service, Bethesda, Md., and by research grants from the Muscular Dystrophy Associations of America, Inc., New York, N.Y. and the United States Air Research and Development Command, Brussels, Belgium.

of ACh in a chronically denervated muscle to the same extent that they do at the normal end plate. Presumably the denervated membrane, despite its high ACh-sensitivity, is in a practical sense devoid of cholinesterase.[4]

Studies on the Cause of Denervation Supersensitivity

Effect of reduced transmitter release. The conversion, following denervation, of the muscle membrane into an ACh-sensitive surface is presumably due to the absence of some influence exerted when the motor innervation is intact. To elucidate whether the chemical transmitter agent provided such an influence, we have used botulinum toxin.

Characteristic of botulinum poisoning is a lack of transmitter release from cholinergic nerves while, otherwise, nerve and muscle are unaffected by the toxin.[6-8] As shown by Katz, quoted by myself,[9] the ultrastructure of motor nerve terminals is not altered by botulinum toxin. Thus degenerative changes in the nerve endings similar to those described during Wallerian degeneration are not observed even after a long-lasting and complete paralysis produced by botulinum toxin.

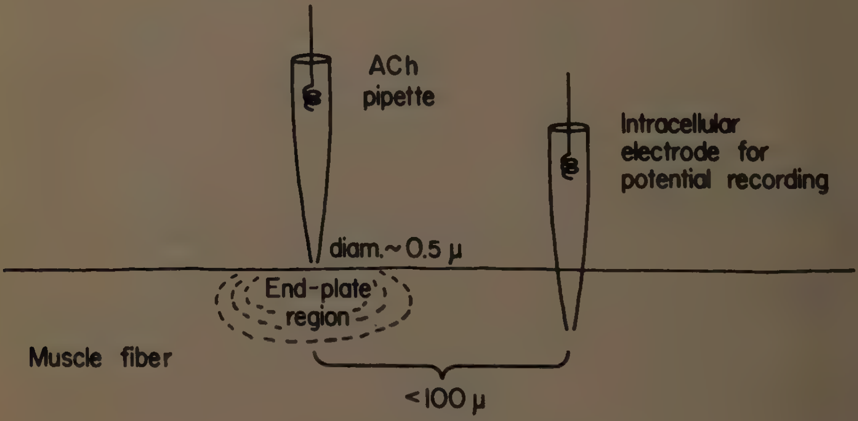

FIGURE 1. A schematic drawing of the position of the ACh pipette and the intracellular electrode at the motor end plate of a single muscle fiber.

When transmitter release is blocked by the toxin, the fibers become sensitive to applied ACh along their entire length. About two weeks after the administration of the toxin, ACh released from the tip of a micropipette produces depolarizations with a rapid time course wherever applied to the muscle membrane (FIGURE 4, *upper* records). The whole surface of the membrane becomes as sensitive to ACh as the end plate, which maintains its original responsiveness to the drug. The uniform chemosensitivity of the muscle membrane in a botulinum-intoxicated muscle is similar to that observed in chronically denervated muscles.[9] Also, the electromyographic findings in chronic botulinum poisoning correspond to those of motor nerve degeneration: typical spontaneous

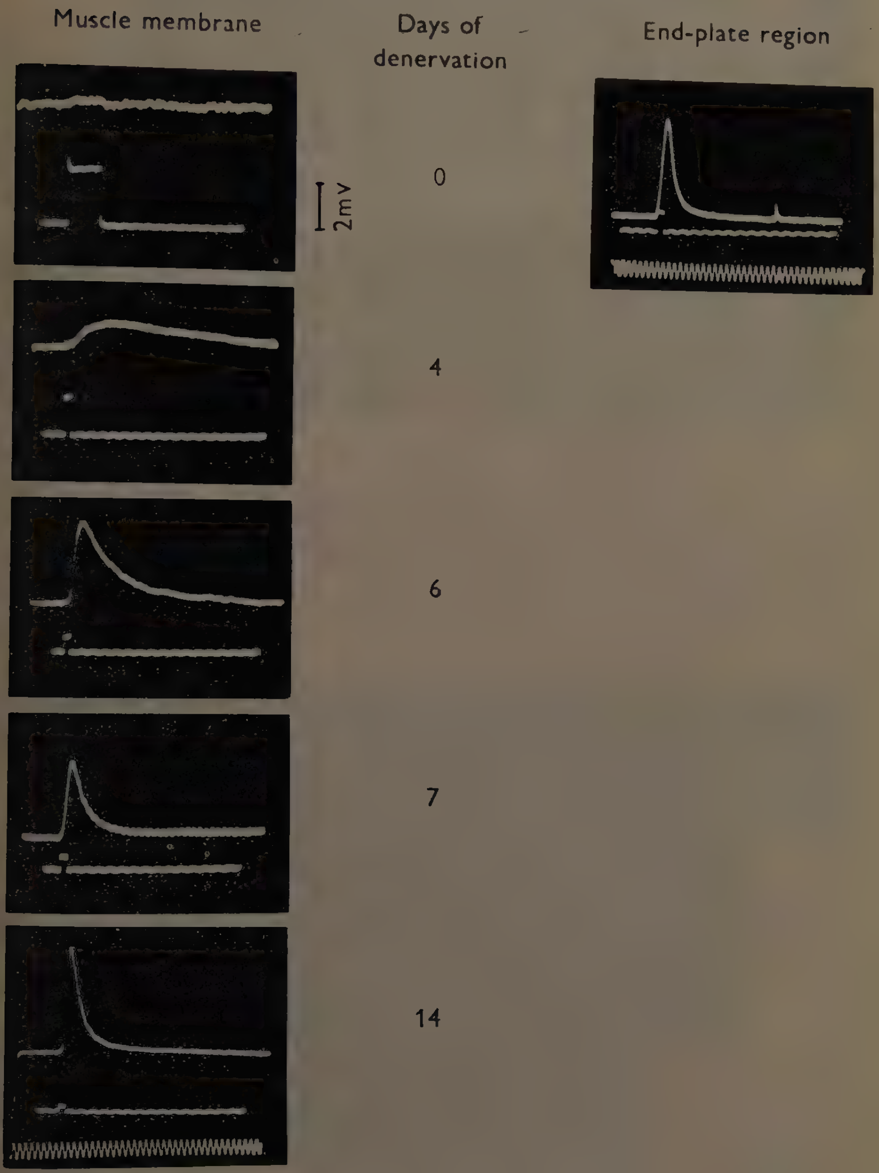

FIGURE 2. The sensitivity of innervated and denervated muscle fibers of the cat tenuissimus to iontophoretically applied ACh. The membrane potential is recorded in the upper tracing and the current passing through the pipette in the lower tracing of each record. In an innervated muscle ACh causes membrane depolarization only when applied to the end-plate region (*upper right record*) but not when released outside this area of the membrane (*upper left record*). After denervation the whole muscle membrane becomes sensitive to ACh that, wherever applied, causes a potential change (subsequent records). Time marker, 100 cps. Reproduced by permission from *The Journal of Physiology.*[4]

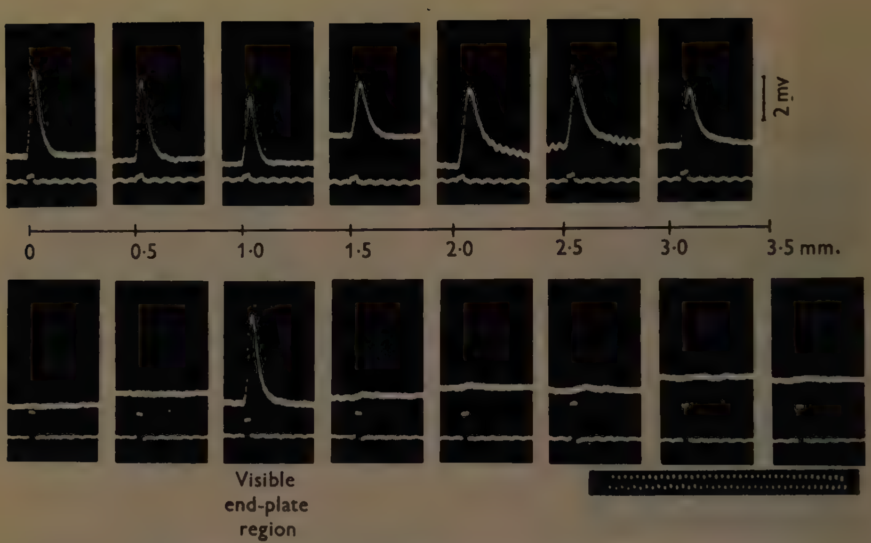

FIGURE 3. The sensitivity of a muscle fiber of the cat tenuissimus to locally applied ACh was tested by moving the tip of an ACh pipette close to the fiber membrane at points separated by distances of about 0.5 mm. In an innervated fiber (*lower records*) only the visible end-plate region was sensitive. In a 14-day denervated fiber a constant pulse of ACh produced a potential change of about equal magnitude at each point of the membrane (*upper records*). Time marker, 100 cps. Reproduced by permission from *The Journal of Physiology*.[4]

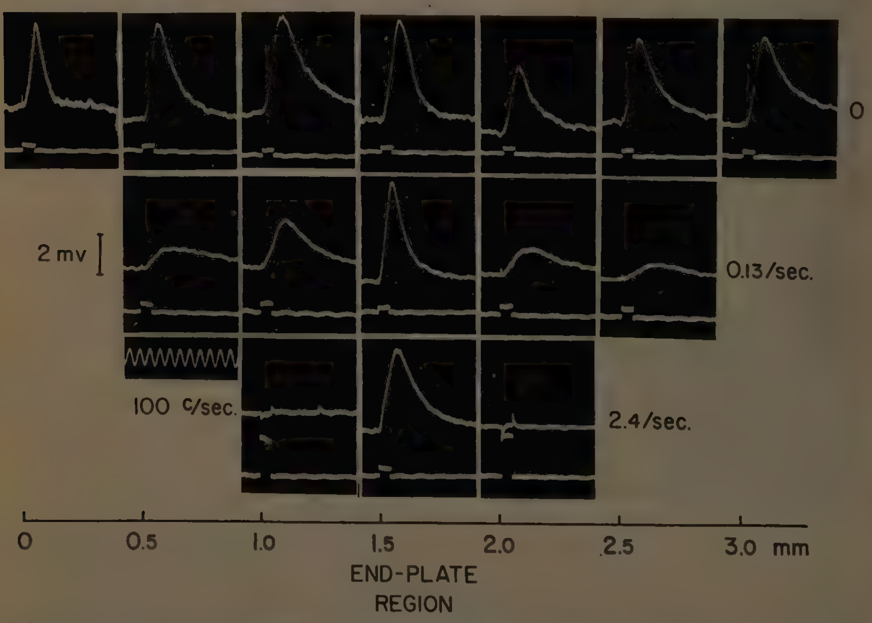

FIGURE 4. In a cat tenuissimus muscle intoxicated 3 weeks earlier with botulinum toxin, muscle fibers were observed in which the ACh-sensitive surface varied in size. The fiber illustrated by upper records was uniformly sensitive to applied ACh over a distance of at least 1.5 mm. at each side of the end plate. The size of the ACh-sensitive surface in two other fibers was smaller (*middle and lower records*). The respective frequency of miniature end-plate potentials is shown by right-hand figures. Reproduced by permission from *The Journal of Physiology*.[9]

fibrillation potentials are recorded 5 to 6 days after the administration of the toxin.[10]

When transmitter release is reduced but not completely suppressed, as shown by the occurrence of spontaneous miniature end-plate potentials at a low frequency, the receptor area is enlarged but does not cover the whole muscle fiber (FIGURE 4 and TABLE 1).

Since, as mentioned, botulinum toxin is without effect on the morphological structure of motor nerve endings, the results suggest that in nerve degeneration the lack of transmitter release is responsible for initiating the process that causes the high and uniform chemosensitivity of chronically denervated muscles.

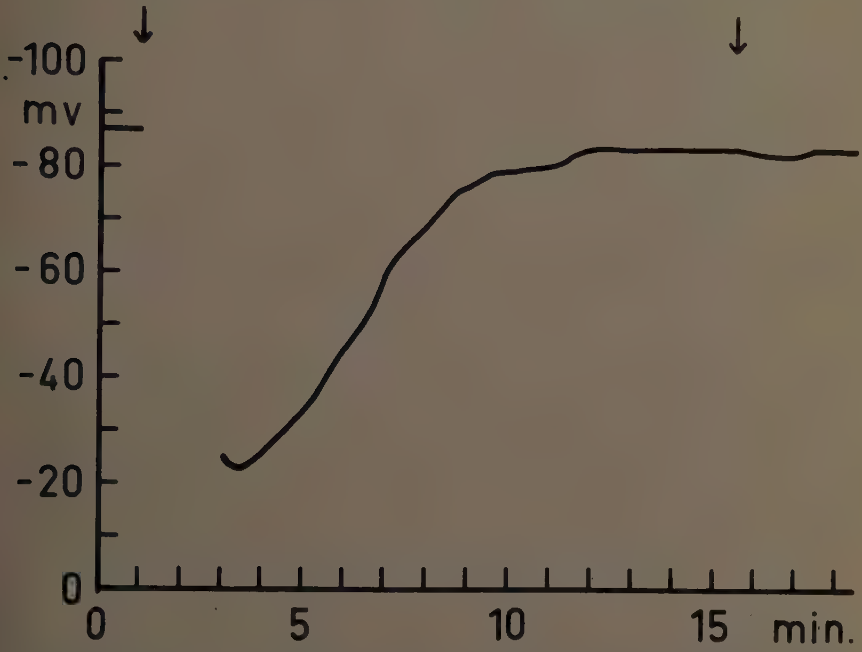

FIGURE 5. Continuous recording of the resting membrane potential at the end-plate region of a single fiber of the frog sartorius muscle. At the arrows, ACh-iodide was added to the muscle bath. Reproduced by permission from *Acta Physiologica Scandinavica*.[20]

Effects of motor inactivation. The possibility that the extension of chemosensitivity following denervation was due to inactivity has been investigated by isolation of the motor mechanism in the cat's spinal cord, as described by Tower.[11,12] The surgical procedure consisted of severance of the dorsal roots below a lower-lumbar cord transection. In such a segment the ventral horn cells are intact but deprived of all ingoing impulses. Spontaneous transmitter release recorded as miniature end-plate potentials is not affected by the operation.[13]

The size of the ACh-sensitive surface in muscle fibers increased somewhat after this type of decentralization but, as long as three weeks after the operation, it usually covered not more than a few millimeters of the fiber length (TABLE 2). Therefore inactivity alone cannot be responsible for extension of the receptor surface after nerve degeneration.[13] Miledi[14] has reached the same conclusion while working with incompletely denervated frog muscle. In sartorius fibers with at least two end plates he observed that section of the nerve to one of them caused a spread of chemosensitivity in the region of the latter end plate, despite the fact that impulse transmission continued through the intact junction.

TABLE 1

THE RELATIONSHIP BETWEEN THE FREQUENCY OF SPONTANEOUS MINIATURE END-PLATE POTENTIALS* AND THE LENGTH OF THE PART OF THE MUSCLE FIBER SENSITIVE TO APPLIED ACH†

Frequency of m.e.p.p./sec.	No. of fibers	Mean length (mm.) of ACh-sensitive area
0.01–0.1	16	2.0 (2.0)
0.1 –1.0	8	1.6 (1.0–2.0)
1.0	26	0.8 (0.3–2.0)

* M.e.p.p.

† The experiments were made on tenuissimus muscles intoxicated 3 to 4 weeks previously with botulinum toxin. Figures within parentheses denote the range of measurements.

TABLE 2

MEAN VALUES AND STANDARD DEVIATIONS FOR THE FREQUENCY OF MINIATURE END-PLATE POTENTIALS* AND THE LENGTH OF THE ACH-SENSITIVE SURFACE IN SINGLE FIBERS OF CAT TENUISSIMUS MUSCLE†

Duration of inactivity (days)	Number of muscles	Number of end plates	Mean frequency of m.e.p.p. (per sec.)	Mean length of receptor surface (mm.)
Control	6	35	14.3 ± 1.18	0.67 0.019
7	6	30	7.4 ± 0.80	0.81 0.027
12–13	6	29	5.3 ± 0.68	(1.16)‡ range 0.5–2.5
18–27	6	24	22.1 ± 3.80	(1.04)‡ range 0.5–2.5

* M.e.p.p.

† The values are recorded according to the duration of the period of muscle inactivity produced by surgical isolation of the motor neurones.

‡ For technical reasons distances longer than 2.5 mm. could not be measured.

Consequently, it is likely that lack of transmitter release per se causes the aforementioned change in chemosensitivity. Isolation of lower motor neurones abolishes synchronous transmitter release by nerve impulses yet leaves the spontaneous transmitter activity intact. The continuous subthreshold transmitter release may be sufficient to maintain the chemosensitivity of the muscle in about its normal area.

The Chemosensitivity of Fetal Muscle

The results presented have shown that, following motor nerve degeneration or lack of transmitter release, the whole muscle membrane is converted into an ACh-sensitive surface. This indicates, as suggested in 1942 by Ginetsinsky and Shamarina[15] and in 1945 by Loewi,[16] that a uniform and high chemosensitivity probably is the original state of the cell and that this is modified upon innervation by the release of the transmitter or some other substance from the motor nerve.

This view is supported by investigations made by Diamond and Miledi.[17] They showed that the fibers in the fetal and newborn rat diaphragm muscle were sensitive to ACh over their whole surface. Shortly after birth, when a functional innervation was established, the chemosensitivity receded, starting from the tendons toward the end plate. We have made similar observations in fetal rabbit and cat diaphragm muscles (unpublished observations). Somewhat similar conclusions have also been reached by Purpura *et al.*,[18] who observed that succinylcholine produced electrically silent contractures in newborn cats up to the 10th to 12th postnatal day and that a general chemosensitivity of muscle fibers could account for the contracture-inducing effect of the drug.

Effects of Applied ACh and of Repetitive Nerve Stimuli

The preceding section dealt with the increase in chemosensitivity observed in muscles deprived of transmitter release. To present a comprehensive picture of the influence of innervation, however, the effects of an excess of transmitter should also be considered.

As shown by Brown *et al.*,[19] close arterial injections of ACh into a normal innervated mammalian muscle produced a depression of its excitability to nerve stimulation. The depressant effect of the drug was confined to the end plate, since the response of the muscle to direct electrical stimulation was unaltered.

The experiment illustrated in FIGURE 5 shows that, in the isolated frog sartorius, diffusely applied ACh produced a reduction of the membrane potential at the end plate from −90 mv to −20 mv, that is, by 70 mv. Without removal of the ACh the depolarization subsided spontaneously, and the membrane potential was restored to about its original value. During the period of depolarization a neuromuscular block developed and persisted despite repolarization of the membrane to the normal level. The muscle remained unresponsive as long as ACh was in the muscle bath and its chemosensitivity was restored only after washing in Ringer's fluid for 15 to 45 min.[20] Qualitatively similar results have been obtained in mammalian muscles.[21,22]

Repetitive motor nerve stimulation also renders the end plate refractory to applied ACh.[23] In the isolated phrenic-diaphragm preparation of the rat, nerve stimulation at a frequency higher than 40/sec. caused a reduction in the response to locally applied ACh and, with stimulation frequencies of 60/sec. or more, the response sometimes was completely abolished (FIGURE 6).

The effect of varying the duration of the period of tetanic stimulation was such that, at stimulation frequencies above 40/sec., a maximum of desensitization occurred within 0.2 sec. of starting the stimulation. The time for complete recovery of the sensitivity of the end plate to ACh was also about 0.2 sec. (FIGURE 7).

Thus an excess of ACh, irrespective of whether it is applied or released by nerve stimulation, will reversibly reduce the chemosensitivity of ACh receptors. In principle this is a phenomenon similar but opposite to that described in the

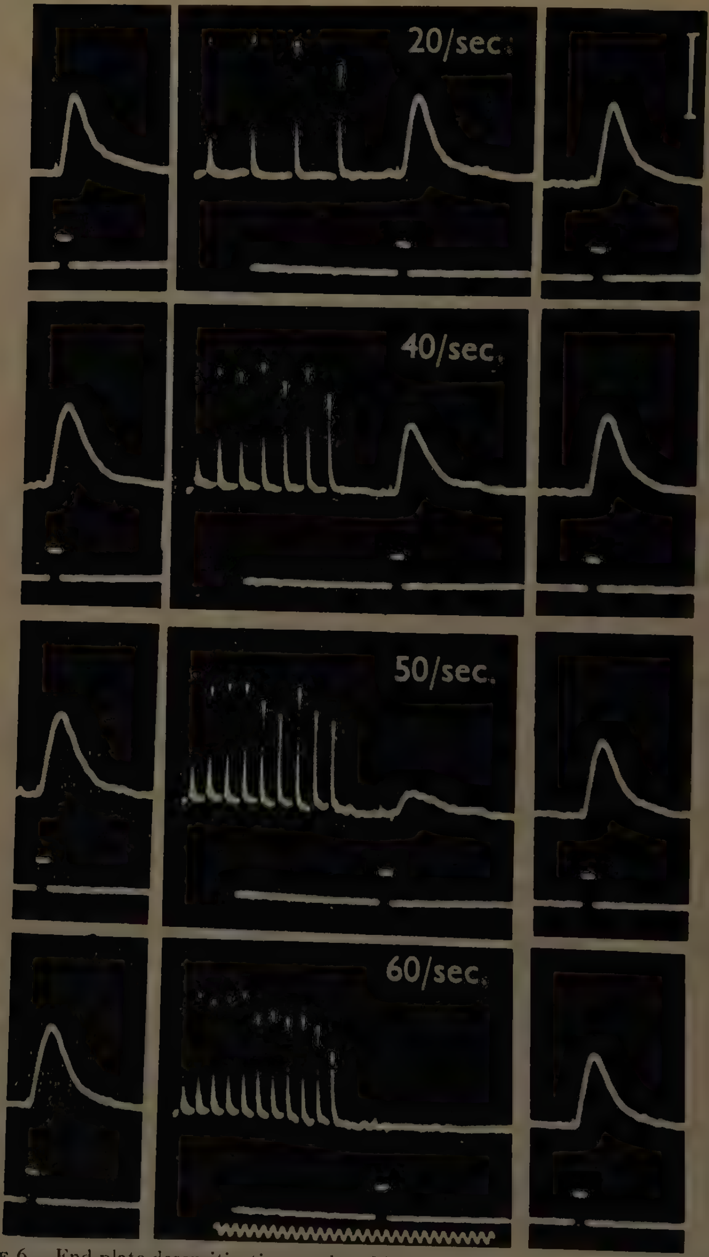

FIGURE 6. End-plate desensitization produced in the rat diaphragm preparation by repetitive nerve stimulation at frequencies of 20, 40, 50, and 60/sec. The entire period of stimulation (150 msec.) is shown in each record. Responses to test pulses of ACh are shown: 5 sec. before nerve stimulation (*left-hand record*); 50 msec. after the end of stimulation (*middle records*); and 5 sec. later (*right-hand records*). Time marker, 100 cps; voltage calibration, 10 mv. Reproduced by permission from *The Journal of Physiology*.[23]

previous section dealing with effects of a diminished transmitter release. Therefore, receptor "desensitization" by ACh is probably related to the process by which the motor nerve controls the size of the receptor area in a muscle fiber. However, the time course of the two phenomena are markedly different:

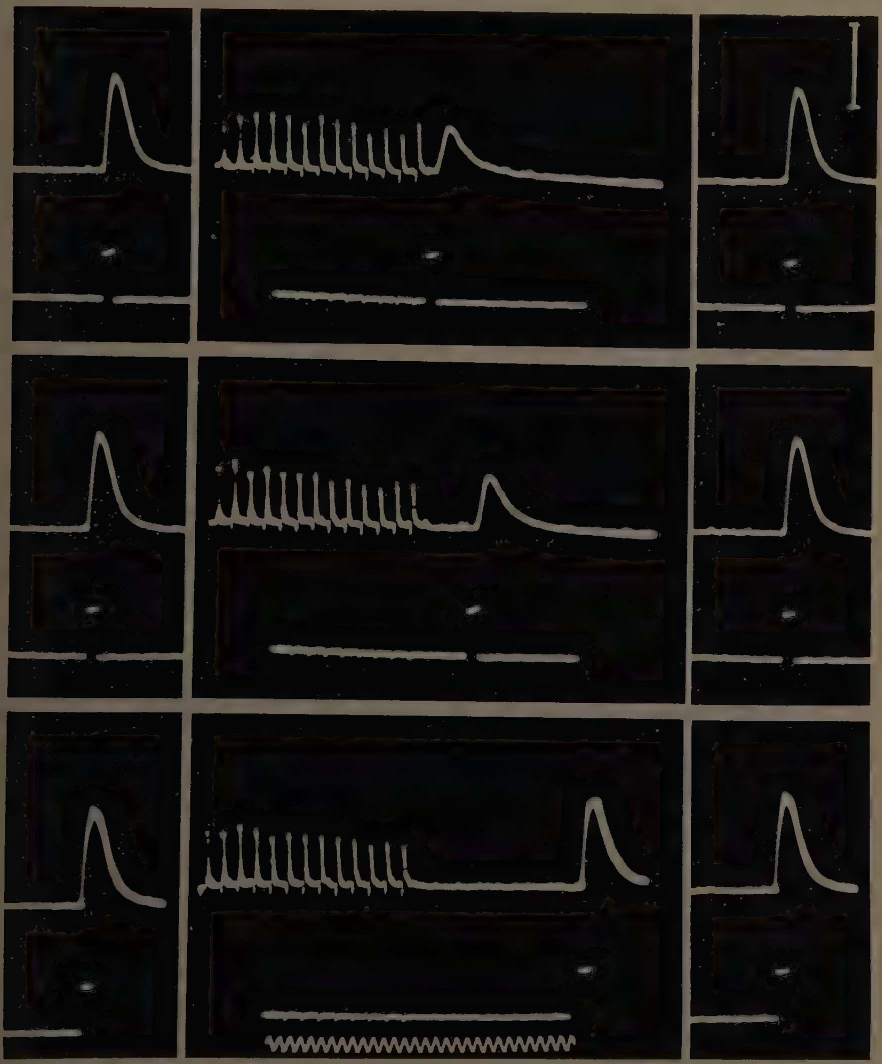

Figure 7. The time course of recovery from desensitization produced in the rat diaphragm by repetitive nerve stimuli at a frequency of 60/sec. The entire period of stimulation is shown in each record. The response to a test pulse of ACh is reduced for a period of about 0.2 sec. after the end of the stimulation. The control response obtained before and after each period of stimulation are shown in left-hand and right-hand records respectively. Time marker, 100 cps; voltage calibration, 10 mv. Reproduced by permission from *The Journal of Physiology*.[23]

receptor "desensitization" occurs in a matter of seconds or less, while the spread of chemosensitivity, following denervation, requires hours to develop.

Discussion

The experimental findings I have presented suggest that the genuine state of a muscle fiber is one with a high uniform sensitivity to ACh, and that upon innervation the chemosensitive area decreases in size until it covers only the end-plate region. According to this view the motor nerve has two functions: first, to initiate mechanical activity in muscle and, second, to control the size of its chemo-receptor surface.

Since inactivity cannot explain the global chemosensitivity of denervated muscle fibers, it is pertinent to assume that lack of some chemical agent released by the nerve is responsible for the extension of the receptor surface. The experiments with botulinum toxin indicate that this substance is either ACh or some unknown agent released simultaneously with the transmitter. At the moment it is not possible to distinguish between these two possibilities. It should, however, be mentioned that spread of chemosensitivity in a denervated muscle is not reversed by prolonged immersion of the muscle in ACh solution.[14] Neither has it been possible to produce changes similar to denervation in the cat tenuissimus muscle by complete curarization of the animal for a period as long as 7 days (unpublished observations). Both experiments, however, have been made under rather unphysiological conditions, and they cannot be held as crucial evidence against the possibility that intermittent bombardment of the membrane by ACh is not normally the determining factor for the size of the receptor area.

The observation that following innervation the chemosensitivity of a muscle fiber is reduced from the tendons toward the end plate suggests that the change in the distribution of ACh receptors is not primarily caused by a substance entering the fiber at the end plate. It is more likely that formation or activation of chemoreceptors require the presence of some substance formed inside the muscle fiber. If, due to transmitter activity from the nerve, such a substance were formed only in the nervous portion of an innervated fiber and then produced everywhere following denervation, the spatial sequence of the receptor change would be obvious. Perhaps the entire muscle membrane is always covered by chemoreceptors, but the ACh-receptor combination causes depolarization only when a substance formed inside the fiber can be utilized in the reaction. An excess of ACh could be expected to deplete the membrane of this substance. The experimentally observed degree and time course of desensitization with locally applied ACh fits such a mechanism,[25] and it can explain the slow recovery following desensitization by "bulk" application of ACh.[20]

The metabolic reactions and the chemical composition of skeletal muscle undergo striking changes following denervation.[26] It seems possible that the increase in the chemosensitivity of the membrane is in some way connected with these processes.

Because of the electric "cable-conductor" properties of a muscle fiber, an increase of its chemosensitive surface makes it supersensitive to drugs. FIGURE

8 is a diagram of a model with electrical properties similar to those of a muscle fiber. A potential difference (for example the membrane potential) between A and B can be reduced by short-circuiting either a fraction, or all, of the parallel resistors r_m. In an innervated fiber only the end plate is affected by ACh, that is, only a small fraction of the total effective resistance between the inside and the external medium is reduced. A relatively larger reduction of the resistance in the end plate is therefore needed, according to Ohm's law, in order to produce a given membrane potential change. From membrane constants obtained for mammalian muscles it can be estimated that the sensitivity to ACh should increase through this mechanism after denervation by a factor of 10 to 500, depending upon whether 100 or 20 μ is taken as the diameter of the active end-plate membrane.[4] The extension of ACh sensitivity, in combination with the lack of cholinesterase and an increased electrical excitability of the membrane, can provide an adequate explanation for the phenomenon known as denervation supersensitivity.

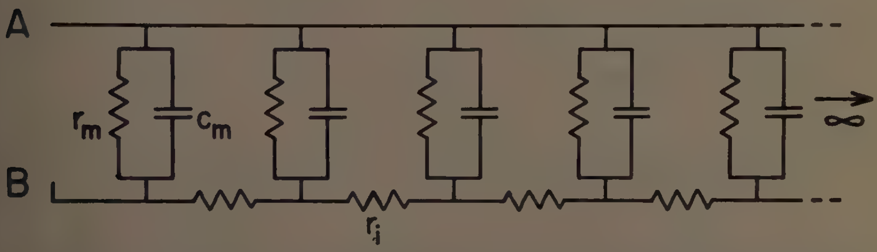

FIGURE 8. A diagram illustrating the electric cable conductor properties of a muscle fiber: r_m = membrane resistance; r_i = longitudinal resistance of myoplasm; c_m = membrane capacitance.

Whether the aforementioned mechanism also offers an explanation for denervation supersensitivity in other organs remains to be shown. Considering the close similarity of this process in various types of tissues,[27] however, it would be rather surprising if the mechanism varied markedly. Particularly attractive is the possibility that presynaptic activity might determine the size of the receptor area in neurons. According to such a hypothesis in neurons of the central nervous system, the postsynaptic receptor area could be confined to the sites of the most frequently activated synaptic knobs, leaving the rest of the membrane relatively insensitive to transmitter action. This might explain plastic changes and an increased synaptic effectiveness with usage.

References

1. THESLEFF, S. 1960. Effects of motor innervation on the chemical sensitivity of skeletal muscle. Physiol. Revs. **40:** 734.
2. NASTUK, W. L. 1953. Membrane potential changes at a single muscle end plate produced by transitory application of acetylcholine with an electrically controlled micro-jet. Federation Proc. **12:** 102.
3. DEL CASTILLO, J. & B. KATZ. 1955. On the localization of acetylcholine receptors. J. Physiol. London. **128:** 157.
4. AXELSSON, J. & S. THESLEFF. 1959. A study of supersensitivity in denervated mammalian skeletal muscle. J. Physiol. London. **147:** 178.

5. Miledi, R. 1960. Junctional and extra-junctional acetylcholine receptors in skeletal muscle fibres. J. Physiol. London. **151:** 24.
6. Wright, G. P. 1955. Neurotoxins of *Clostridium botulinum* and *Clostridium tetani.* Pharmacol. Revs. **7:** 413.
7. Stevenson, J. W. 1958. Bacterial neurotoxins. Am. J. Med. Sci. **235:** 317.
8. Lamanna, C. 1959. The most poisonous poison. Science. **130:** 763.
9. Thesleff, S. 1960. Supersensitivity of skeletal muscle produced by botulinum toxin. J. Physiol. London. **151:** 598.
10. Josefsson, J.-O. & S. Thesleff. Electromyographic findings in experimental botulinum intoxication. Acta Physiol. Scand. In press.
11. Tower, S. S. 1937. Function and structure in chronically isolated lumbo-sacral spinal cord of the dog. J. Comp. Neurol. **67:** 109.
12. Tower, S. S. 1937. Trophic control of nonnervous tissues by the nervous system: a study of muscle and bone innervated from an isolated and quiescent region of spinal cord. J. Comp. Neurol. **67:** 241.
13. Johns, T. R. & S. Thesleff. Effects of motor inactivation on the chemical sensitivity of skeletal muscle. Acta Physiol. Scand. In press.
14. Miledi, R. 1960. The acetylcholine sensitivity of frog muscle fibres after complete or partial denervation. J. Physiol. London. **151:** 1.
15. Ginetsinskii, A. G. & N. M. Shamarina. 1942. Tonomotornyi fenomen v denervirovannoi myshtse: Uspekhi Sovremennoĭ Biol. **15:** 283.
16. Loewi, O. 1945. Aspects on the transmission of the nervous impulse. J. Mt. Sinai Hosp. **12:** 851.
17. Diamond, J. & R. Miledi. 1959. Sensitivity of fetal and newborn rat muscle to acetylcholine. J. Physiol. London. **149:** 50 p.
18. Purpura, D. P., M. W. Carmichael & E. M. Housepian. 1960. Succinylcholine-induced contractures in skeletal muscles of newborn cat. Proc. Soc. Exptl. Biol. Med. **103:** 336.
19. Brown, G. L., H. H. Dale & W. Feldberg. 1936. Reactions of the normal mammalian muscle to acetylcholine and to eserine. J. Physiol. London. **87:** 394.
20. Thesleff, S. 1955. Mode of neuromuscular block caused by acetylcholine, nicotine, decamethonium, and succinylcholine. Acta Physiol. Scand. **34:** 218.
21. Thesleff, S. 1955. Effects of acetylcholine, decamethonium, and succinylcholine on neuromuscular transmission in the rat. Acta Physiol. Scand. **34:** 386.
22. Axelsson, J. & S. Thesleff. 1958. "Desensitizing" effect of acetylcholine on the mammalian motor end-plate. Acta Physiol. Scand. **43:** 15.
23. Thesleff, S. 1959. Motor end-plate "desensitization" by repetitive nerve stimuli. J. Physiol. London. **148:** 659.
24. Miledi, R. 1960. Properties of regenerating neuromuscular synapses in the frog. J. Physiol. London. **154:** 190.
25. Katz, B. & S. Thesleff. 1957. A study of the "desensitization" produced by acetylcholine at the motor end-plate. J. Physiol. London. **138:** 63.
26. Gutmann, E. 1959. Metabolic reactions of denervated and reinnervated muscle. Am. J. Phys. Med. **38:** 104.
27. Cannon, W. B. & A. Rosenblueth. 1949. Supersensitivity of Denervated Structures. Macmillan. New York, N.Y.

AN ANALYSIS OF INTRA- VERSUS EXTRACELLULAR POTENTIAL CHANGES ASSOCIATED WITH ACTIVITY OF SINGLE SPINAL MOTONEURONS*

Carlo A. Terzuolo† and T. Araki‡
Department of Anatomy, University of California at Los Angeles, Calif.

Introduction

The potential field due to activity of a single spinal motoneuron was first investigated by Fatt.[1] Different results were obtained by Freygang and Frank[2] who recorded simultaneously intra- and extracellular potential changes from the cell soma. The interpretations of the extracellular currents proposed by the above authors do not agree with the hypothesis of spike propagation in spinal motoneurons first suggested by Araki and Otani[3] and further elaborated by Fuortes *et al.*[4] and Coombs *et al.*[5,6] According to this hypothesis the first component of the action potential recorded intracellularly from the soma of spinal motoneurons (the IS or A spike) results from activity of the initial segment, while the subsequent invasion of the soma membrane, and possibly of some portion of the dendrites, causes the SD or B spike. This hypothesis is consistent with the results of recent voltage clamp experiments on spinal motoneurons of cat (T. Araki and C. A. Terzuolo, in preparation). In these experiments the membrane whose activity causes the SD spike was localized within the soma-dendrite complex. However, it was not possible to determine which portion of this complex is active when the SD spike is recorded. Therefore the problem of spike propagation in spinal motoneurons was re-examined by recording simultaneously intra- and extracellular potential changes from different regions of the cell membrane.

Methods

The cats were anesthetized with Nembutal, paralyzed with Flaxedil, and artificially ventilated. Bilateral pneumothorax was performed. The lumbar segments of the spinal cord were exposed by laminectomy. The sectioned ventral roots were mounted on platinum electrodes under paraffin oil. The strength of the stimulus applied to the ventral root was adjusted so that the motoneuron under study was activated in approximately 50 per cent of the trials. This procedure was sufficient, in most cases, to minimize in the extracellular records potential changes caused by activity in neurons other than the one being studied. The cell was stimulated directly through the impaling microelectrode to confirm this point.

Microelectrodes. The type of double microelectrode used in these experiments, which might be called "parallel-microelectrodes," is shown in FIGURE 1. It consists of two micropipettes whose tips are completely independent. Par-

---

* The work described in this paper was supported in part by Research Grants B-1143 and B-5260 from the National Institute of Neurological Diseases and Blindness, Public Health Service, Bethesda, Md.

† The research reported in this paper was completed after this author moved to his present address: Department of Physiology, University of Minnesota, Minneapolis, Minn.

‡ Present address: Department of Physiology, University of Kyoto, Kyoto, Japan.

allel-microelectrodes can be obtained in several ways. The method used was the following: the walls of two pieces of pyrex tubing (external diameter 1.2 mm.; wall thickness 0.3 mm.) were joined together for a short distance with a gas flame. The characteristics of the juncture determined the distance between the tips of the electrodes obtained by placing the fused region in a microelectrode puller. The shafts of the two micropipettes were therefore separate; they were joined only by small bridges of glass, located at the region in which the tapering increased sharply. The shafts were enclosed in a girdle of dental cement to avoid separation during handling. Parallel-microelectrodes with tip diameters less than 1 μ, and intertip distances ranging from 3 to 20 μ were used. This distance was subject to change while the electrodes were moving in the cord; usually it increased.

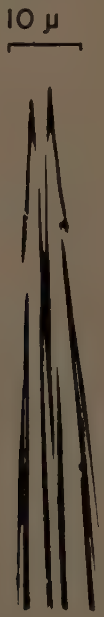

Figure 1. Photomicrograph of a "parallel-microelectrode."

The electrodes were filled with KCl. The coupling capacity and resistance between each pair of micropipettes were of the order of 3 to 8 μμF and 5 to 50 KΩ respectively. This electrical coupling was minimized by cross neutralization, after Tomita.[7] The electrical activities were led from both microelectrodes through cathode follower input stages with grid currents less than 1×10^{-12} amp. The effectiveness of the cross neutralization was continually tested while the microelectrodes were advancing in the cord and after penetration of the cell. The outputs from the decoupling amplifier were displayed, after suitable amplification, on a double beam oscilloscope.

Results

(1) *Potential changes recorded from the outside of the axon and the cell soma.* Records representative of the potential changes observed outside of the axon

and the soma of spinal motoneurons activated antidromically are shown in FIGURE 2. The voltage drop across the membrane of the same region of the cell was simultaneously recorded by the second micropipette (bottom line of each record).

The intracellular action potential shown in A has a steep rising phase and a short duration suggesting that it was recorded from a motor axon.[1,5,8] The potential change recorded simultaneously by the external microelectrode (upper beam) is positive-negative-positive, as recorded from outside a nerve when an impulse is propagating.[9]

In B, C, and D the intracellular records are similar to those ascribed by Coombs *et al.*[5,6] to potential changes from the initial segment of the axon. The evidence supporting this interpretation has been discussed by these authors.

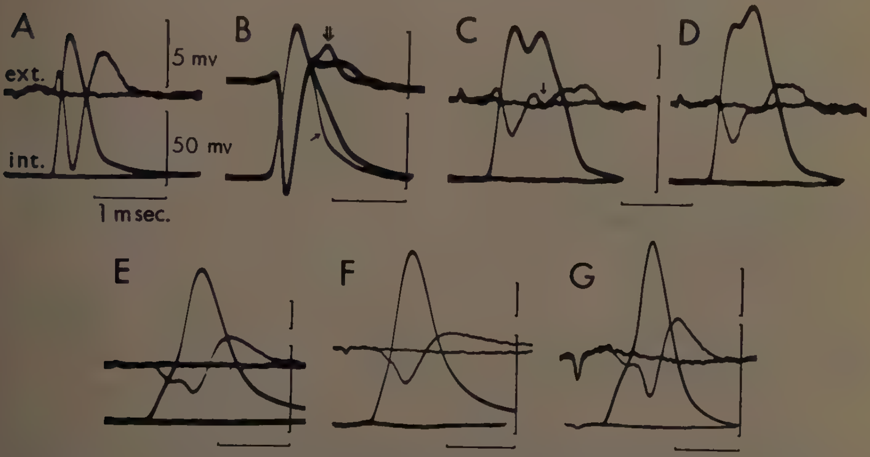

FIGURE 2. Potential changes recorded simultaneously, inside and outside the axon and the soma of spinal motoneurons with parallel-microelectrodes. The records were taken from different cells except for C and D. Two or more sweeps were superimposed in each frame to provide the baseline as recorded from the external microelectrode in the absence of activity in the cell studied. The intensity of stimulation applied to the ventral root was adjusted to activate the cell in approximately 50 per cent of the trials. Full description of the figure is given in the text.

Records C and D were obtained from the same cell; after a slight withdrawal of the "parallel electrodes" the common type of intracellular action potential was recorded from this cell. The hump in the falling phase of the intracellular spike in record B (indicated by the single arrow) disappeared with repetitive stimulation, as expected if the membrane responsible for the SD spike were no longer invaded. In this case the extracellular potential was triphasic, as recorded in A. In the presence of the SD spike, however, the amplitude of the last positive wave (indicated by the double arrow) was decreased while its duration was longer. This observation implies that the external field caused by activity within the soma-dendrite complex was different from that produced in the volume conductor by an action potential propagating along a nerve fiber. An interpretation of this finding will be proposed later.

In record C, the microelectrodes may be assumed to be closer to the cell soma than in B. The potential changes recorded intracellularly had, in fact, two peaks, the first of which was due to activity of the initial segment while the second resulted from the activation of the membrane responsible for the SD spike. The extracellular late positive wave was also decreased in this record, that is, a relative negativity (indicated by the arrow) was induced when the action potential propagated within the soma-dendrite complex. This relative negativity was even more conspicuous in record D in which the extracellular microelectrode may be assumed to be closer to the soma membrane, as indicated by the intracellular record.

Records E, F, and G depict the type of extracellular potential most commonly encountered. Penetration of single motoneurons with both microelectrode occurred almost exclusively, with exceptions to be mentioned later, when th

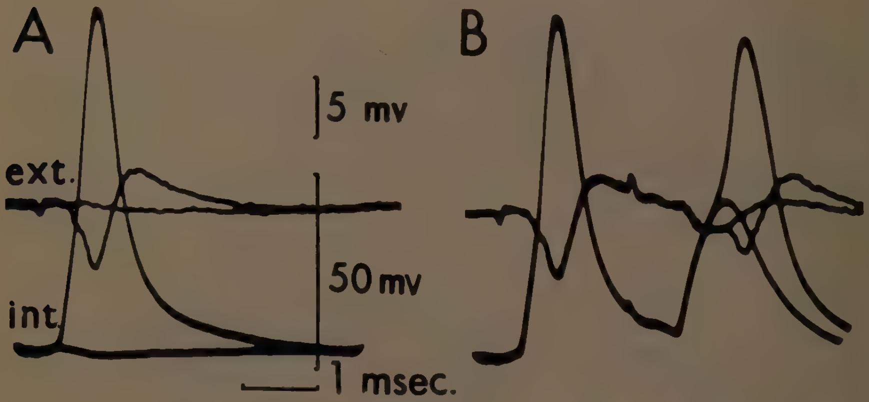

FIGURE 3. Extracellular potentials recorded in the absence of an SD spike. In B two stimuli were applied to the ventral root with a short time interval. In some of the trials the soma-dendrite complex was not invaded. The last positive wave of the extracellular records and the negativity that precedes it were no longer present in this condition.

extracellular potential recorded by the outside electrode was similar to that of records E, F, and G. Because of the distance between the tips of the two microelectrodes and because of the geometry of spinal motoneurons it is quite safe to assume that the extracellular potential changes shown in E, F, and G were recorded from outside of the membrane of the soma and adjacent portions of the dendrites. This region of the cell membrane will be called soma, while the terms dendrite and dendritic membrane will be applied to the dendritic tree after branching has occurred.

The extracellular potentials of records E, F, and G consist of four components (positive, negative, negative, and positive). The initial positive wave is small and frequently difficult to detect in the background noise. The first negative wave may exhibit a plateau when there is a pronounced delay in the invasion of the membrane responsible for the SD spike. The second negative wave always begins in close time relationship with the inflection present in the rising phase of the intracellularly recorded action potential; its peak always precedes the peak of the SD spike, although this time difference is not equal in all cells.

While this point will be discussed later, it is important to emphasize here that the second of the two negative waves and the positivity that followed were recorded only when the SD spike was present. The extracellular potential in the absence of the SD spike is shown in the upper trace of FIGURE 3B.

(2) *Interpretation of extracellular potentials.* The presence of a double negativity outside of the soma membrane, as well as the decrease of the late positivity recorded from the outside of the initial segment previously described, are difficult to understand unless one considers the direction of current flow around the activated motoneuron.

According to Lorente de Nó[10,11] the external fields of current flow caused by activity of single neurons within the central nervous system can be classified in three types: closed field, open field, or a type intermediate between the two. Since most spinal motoneurons of cat have numerous dendritic branches that radiate in nearly all directions away from the soma, a closed-field type of external current flow would be observed while recording from the outside of the great majority of motoneurons. In these cases, the following sequence of events may be postulated to take place during antidromic invasion.

While the action potential propagates along the motor axon, the external field of current flow would be of the open type, the presence of axon collaterals being negligible. An extracellular microelectrode placed near the axonal membrane would therefore record a triphasic potential change (record A of FIGURE 2). This membrane would, in fact, become source, sink, and source. When the impulse invades the initial segment, however, the external field of current would tend to shift from the open-type to the closed-field type if most of the current that flows into the membrane of the initial segment is supplied by the dendrites rather than the soma. Once the impulse has invaded the soma the closed-field type would be established. The zero-isopotential surface of this field is assumed to be located in the dendritic zone and, possibly, to pass through the regions in which the dendrites ramify.[11]

This postulated sequence of events can account for the results thus far presented. The situation to be analyzed first is that of a microelectrode placed outside of the soma during the IS spike. Initially an outward flow of local current from the soma into the sink of the initial segment would cause such an electrode to become positive. In a lineal structure this positivity would last until the potential across the membrane at the point of recording became less than that of the initial segment. However, since the dendrites become the main source of current, a microelectrode located at the center of the closed field would be on the side where the sink is located with respect to the zero-isopotential surface. Because of this field effect the amplitude and the duration of the first positive wave recorded extracellularly from the soma region would be reduced, and this positivity would be quickly replaced by a negativity. Although most of the current for a sink in the initial segment would be supplied by the dendrites, the density of current flowing across the dendritic membrane might be quite small.

It must be stressed that zero isopotential surfaces oriented differently from the one postulated, can also account for the negative potential change recorded outside of the soma region while an outward current flows across the soma membrane. The closed field hypothesis has been selected, however, because it accounts for the observations reported in sections 1 and 3 without disagreeing with those to be presented in section 4.

The second situation to be analyzed is that of an external electrode located near the membrane of the initial segment when the action potential invades the soma-dendrite complex. Such an electrode would be expected to become positive since the repolarized membrane of the initial segment would act as a source for the new sink. However, a microelectrode placed outside the initial segment is not far from the center of the closed field. If the structure at the center of this field becomes active, then the positivity due to the outward flow of current across the membrane of the initial segment will be opposed by the negativity resulting from the closed field. The reduction of the amplitude of the last positive wave, or relative negativity, observed when recording from the outside of the initial segment (records B, C, D of FIGURE 2) can thus be explained, assuming that the membrane of the soma, here considered to be at the center of the closed field, is invaded by the action potential.

The activation of the soma is proved by the time relationship between the extracellular current (the second negative potential change recorded outside of the soma) and the SD spike recorded simultaneously by the intracellular microelectrode. The invasion of the soma membrane, therefore, can be established independently of the interpretations proposed for the observed extracellular potential changes (see under *Discussion*). We must emphasize, however, that the assumption that a closed field of current flow would be established when the soma becomes active is consistent with the results. The argument goes as follows: when the soma becomes active, current will flow radially inward from the dendrites, where the major source is assumed to be located, toward the soma, the zero isopotential surface being located in the dendritic zone. The second negative wave recorded outside of the soma, therefore, may be taken to indicate an inward flow of current across the soma membrane, which is assumed to be at the center of the closed field.

One more potential change remains to be interpreted. This is the late positive wave recorded by a microelectrode located outside of the soma membrane. This positivity indicates a reversal of the sink and source relationship in the region in which the electrode is located, that is, close to the center of the closed field. Such a reversal from sink to source may occur: (1) if the action potential propagates out in the dendrites; or (2) as a consequence of an electrotonic spread to the dendrites of the activity of the soma. In both cases current would, in fact, start to flow outward from the soma when the potential across the dendritic membrane becomes lower than that of the repolarized soma membrane. The first of the two mentioned possibilities is likely to cause a larger and longer lasting positive potential change. It should be noted that the late positivity recorded from the outside of the membrane of the initial segment becomes longer when the action potential propagates to the soma-dendrite complex (FIGURE 2B).

(3) *Dendritic potential.* If the sequence of events postulated is correct, then by recording on the dendritic side of the zero isopotential surface, extracellular potentials different from those previously illustrated should be recorded. A positive potential, indicating an outward flow of current, should be recorded

when the action potential invades the initial segment and the soma. This positive wave or waves should be followed by a negative potential if the dendrites are subsequently invaded. This inwardly directed current would begin to flow after the one observed by recording outside of the soma, and should not be followed by a positive wave since no reversal of sink-source relationship will occur.

Records C of FIGURE 4 fulfills these predictions. Reversal of the outward current to an inward one occurs near the peak of the intracellularly recorded SD spike. The peak of this current is too late to be that which causes the SD spike. This strongly suggests that the action potential is propagated along some portion, at least, of the dendrites. Consistent with this are records A and B of FIGURE 4.

In two instances, of several hundred cells we examined, two action potentials of different time course were simultaneously recorded from the two micropipettes placed inside the same motoneurons. While the micropipette impaling the soma region recorded the ordinary intracellular spike (lower beam) the spike recorded by the second microelectrode had a retarded rising phase and a much slower falling phase. No sign of injury was present in the two cells in question. The membrane always responded to stimulation, and the time course of the two intracellularly recorded action potentials did not change throughout the time of penetration. Moreover, direct stimulation through the impaling microelectrodes was successful in both cells. This fact also proves that both microelectrodes were placed inside the same cell. The amplitude of the two action potentials of record A are about equal (the difference in frequency response between the two channels, as shown by the calibration pulse at the end of the sweep, is too small to produce any appreciable reduction of the amplitude of the potential recorded by the lower beam). However, the time delay between the peaks of the 2 potentials was about 0.3 msec., indicating that the action potential recorded by the upper beam was taken from a structure located far from the soma, that is, a dendrite. It is likely that if the spike recorded by the upper beam resulted from the electrotonic spread of the soma

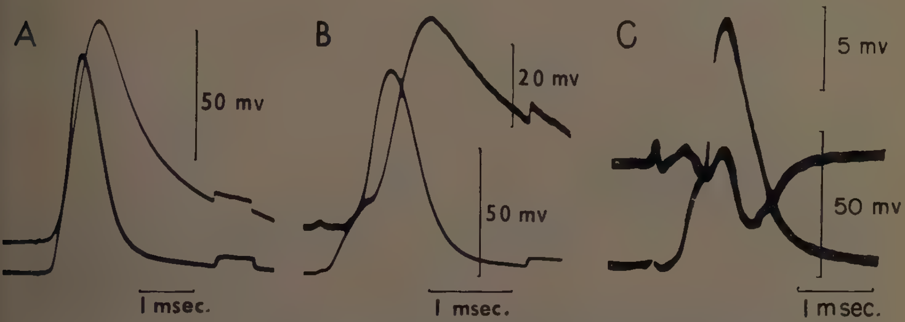

FIGURE 4. Dendritic potentials. In A and B both microelectrodes were placed inside the soma cell. In C the external microelectrode was assumed to record from the dendritic trees. Full explanation in the text.

spike along a dendritic membrane, a large reduction of amplitude would be observed at a point where the peak of this spike was delayed by 0.3 msec. Moreover, in record B the ratio between the amplitude of the electrotonically propagated IS spike recorded in the lower trace and the upper trace is about 4. This ratio seems to indicate that the microelectrode was placed quite far from the soma. On the contrary, the ratio between the total height of the spikes recorded by the two microelectrodes is about 1, 3.

The above considerations preclude the spike potential recorded in the upper trace from being the result of electrotonic spread of the action potential due to activity of the soma membrane. The action potential therefore propagates at least at some distance from the soma. This distance cannot be estimated on the basis of our data.

(4) *Open-field type.* Although the external field of current around the antidromically activated motoneurons was in most cases a closed field, as previously discussed, in a few motoneurons different extracellular potentials were recorded. The extracellular potential recorded during antidromic invasion of these motoneurons was characterized by a relatively large and long lasting initial positive wave, as shown in FIGURE 5. The extracellular potential of record A is positive-negative-positive. The initial positive wave developed while the IS spike was recorded intracellularly from the soma. The inflection between the IS and SD spike of the intracellular record coincided with the start of the negative potential change recorded by the outside electrode. The peak of this negative wave preceded the peak of the SD spike, and was followed by a positive potential change as in the closed-field pattern. In FIGURE 3B the action potential failed to invade the soma, and only the IS spike was present. In this condition, a positive wave with a sharp rising phase was recorded extracellularly. This was followed by a small negativity.

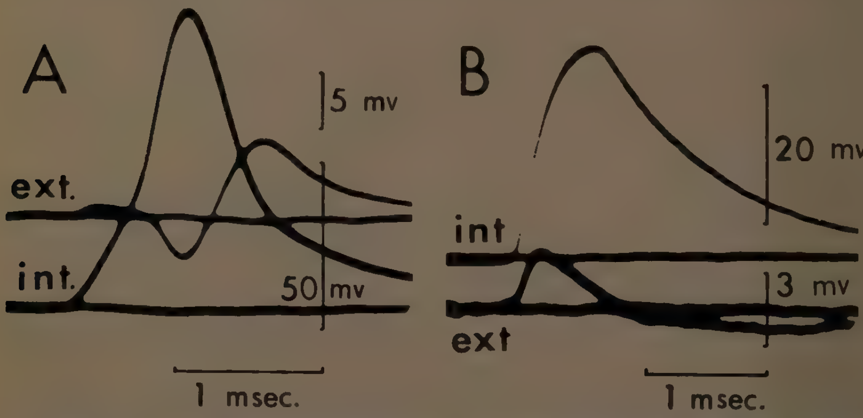

FIGURE 5. Extracellular potentials recorded in motoneurons with an open field of extracellular current flow. Full explanation in the text.

These records can be interpreted by assuming that the cell under study had elongated dendrites concentrated on the side of the soma opposite to the axon.

If so, the soma would be the main source for a sink in the initial segment. Therefore the electrode outside of the soma would record a positivity until the soma itself is activated, the field of external current being an open field as for an action potential propagating along nerve fibers. When the soma became a sink, the source would be located in the dendrites and in the repolarized initial segment. The field in this case would therefore have two zero isopotential surfaces, one near the axon hillock region, the second at the boundary between soma and the elongated dendrites. If so the potential recorded extracellularly from the soma would be negative during activation of this membrane and would become positive when the impulse propagated into the dendrite.

The small negative wave present in the absence of invasion of the soma membrane (record B of FIGURE 4), following the positive one, could be the consequence of the rapid repolarization of the membrane of the initial segment. As suggested by Coombs *et al.*[5,6] a reversal of local current flow between initial segment and soma would take place as soon as the potential across the soma membrane exceeded that of the repolarized initial segment.

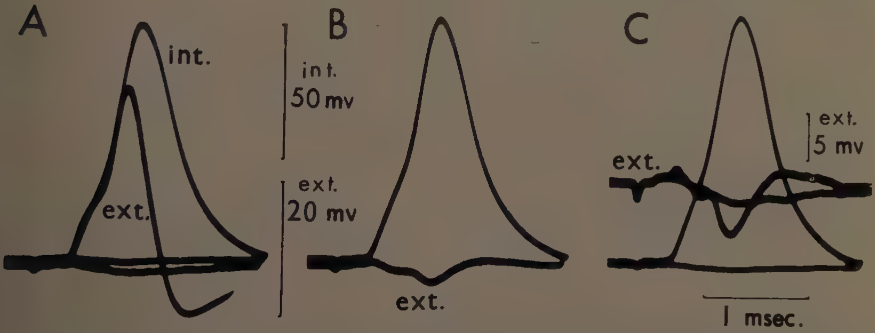

FIGURE 6. Giant extracellular spike. In A the extracellular potential is of the giant type. A slight withdrawal of the parallel microelectrodes between A and B was followed by a change of the extracellular potential which become similar to those of FIGURE 2 E–G. In C the same extracellular potential of B at higher amplification.

(5) *Extracellular giant spike.* On a few occasions extracellular potentials were recorded with a time course and amplitude characteristic of the so-called giant extracellular spike.[2,12,13,14] An example of such an extracellular potential is shown in record A of FIGURE 6. A slight withdrawal of the microelectrode was followed by a dramatic change of both amplitude and time course of this extracellular potential, while the intracellularly recorded action potential showed only a small increase in amplitude (record B). In record C the gain of the extracellular record was increased. This potential is similar to those presented in FIGURES 2E to G. An explanation for the differentiated extracellular spikes recorded outside of spinal motoneurons will be given in the *Discussion.*

Discussion

Lorente de Nó[9] pointed out that the surface action potential recorded from a nerve is proportional to the membrane action current, that is, to the density of the transverse membrane current flowing at the point of recording during the propagation of the nerve impulse. The density of this transverse membrane current is described by the second derivative of the voltage drop across the membrane.[9,15,16,17] In the present investigation, however, the extracellular recording is not strictly a "surface recording" since the external microelectrode was not pressed tightly against the membrane as indicated by the result illustrated in FIGURE 6. Moreover, because of the field effect and because the propagation of an antidromic impulse between the initial segment and the soma is not a continuous process, the extracellular potential recorded around the membrane of spinal motoneurons cannot be expected to be strictly proportional to the density of the transmembrane current nor to fit all the phases of the second derivative of the intracellularly recorded action potential. Only the time course of the last two extracellular potential changes recorded from outside of the soma (the last positivity and the negativity that precedes) bore a close relationship to the second derivative of the intracellularly recorded SD spike. This point can be taken to prove that the soma membrane is active when the SD spike is recorded. It should be mentioned, however, that in most of the cases examined the amplitude and sometimes also the duration of the last positive wave recorded from the outside of the soma region were larger and longer than expected (the ratio of the inward and the outward current of the second derivative of the intracellular spike was bigger than the ratio of the corresponding potential changes recorded from the same cell). This discrepancy might be accounted for on the basis of the field effect as described under *Results*.

Another discrepancy was sometimes observed. The peak of the extracellular negative wave which preceded the last positivity was late, in some cells with a closed field pattern of current flow, in comparison with the corresponding phase of the second derivative of the intracellularly recorded action potential. It is likely that in this case the potential change at the point of extracellular recording followed in time the potential change at the place of intracellular recording. Since the action potential propagates along at least some portion of the dendrites, there are regions producing an action potential with increasing latency.

In the case of motoneurons with an open field pattern the time course and amplitude of the extracellular current recorded from outside of the soma during the development of the IS spike bore a close relationship to the first derivative of the intracellular record. This fact indicates that the soma membrane was passive, as will be further elaborated below. Therefore, the IS spike was due to the electrotonic spread to the soma of activity in the initial segment. This conclusion is inconsistent with the hypothesis that the IS spike is due to activity of the soma membrane as proposed by Fatt.[1]

A passive behavior of the soma membrane also explains the giant extracellular spike, according to the analyses of Freygang[12] and Freygang and Frank.[2] However, only a restricted portion of the soma membrane near to the external microelectrode was passive at the time in which record A of FIGURE 6 was taken. If this were not so, it would be impossible to explain the dramatic change of the extracellular record after slight withdrawal of the microelectrode. In fact, the extracellular potential recorded in B and C of FIGURE 6 is similar to those observed in the case of a closed field indicating that the soma membrane was active. This does not preclude the subsynaptic portions of the soma membrane from being "electrically inexcitable" as defined and postulated by Grundfest.[18] In this case a microelectrode placed close against a cluster of synaptic boutons would record a differentiated spike if the resistance of the leakage pathway between the tip of the microelectrode and the membrane was much higher than the resistance of the membrane itself. As recently pointed out by Wolbarsht,[19] the amplitude of this spike would depend "on the ratio of the resistance of the portion of membrane under the electrode and the leakage pathway."

The passive behavior of the membrane may also result from the mechanical pressure of the microelectrode.[2] This possibility is supported by the results of Murakami *et al.*,[20] who recorded from sartorius muscle fibers using the concentric type of double microelectrode[7] also used by Freygang and Frank[2] in their study of spinal motoneuron. Murakami *et al.*[20] found that the common triphasic extracellular potential recorded by the outside microelectrode sometimes becomes diphasic when the inner microelectrode impales the membrane, although a normal spike with overshoot is recorded intracellularly by this electrode. The time course of the diphasic extracellular potential is similar to the first derivative of the intracellularly recorded action potential, as expected when the passive membrane current becomes preponderant (cf. Expression 1 in the paper of Freygang and Frank[2]). This is also the case for the giant extracellular spike in record A of FIGURE 6. In light of the observation of Murakami *et al.*,[20] it may be concluded that the membrane near to the external electrode was damaged by impalement of the other microelectrode, located close to the external one, or by the mechanical pressure exerted by the external microelectrode itself. It should be emphasized that in the case of spinal motoneurons, extracellular records indicating activation of the soma-dendrite complex were usually observed, while only a few differentiated records were obtained. Although the explanations for this differentiated extracellular recording may be questioned, there is no evidence that experimental interference can cause a passive membrane to become active. It should therefore be concluded that the soma membrane of spinal motoneurons, with the possible exception of the subsynaptic portions, is invaded by the action potential. This is in agreement with the hypothesis stated in the introduction,[3-6] with the results of voltage clamp experiments (T. Araki and C. A. Terzuolo, in preparation) and with the more recent data of Nelson *et al.*[22]

Dendritic potentials with time course similar to those described here have previously been reported by other authors in different neurons.[21] In our case, however, since the action potential was recorded simultaneously from the soma, it is quite safe to exclude the possibility that the recorded dendritic potentials were simply due to electrotonic spread of the action potential of the soma. Our results, however, do not solve the problem of how far in the dendrites the action potential propagates. This point, as well as the question of the speed at which the action potential propagates along dendritic branches can be answered by plotting the external field around a single motoneuron as has been done by Fatt[1] and, more recently, by Nelson *et al.*[22] The results of these authors suggest that the action potential might propagate several hundred microns along the dendrite. The speed of this propagation according to Fatt[1] is about 0.7 to 1 m./sec.

References

1. Fatt, P. 1957. Electrical potentials occurring around a neuron during its antidromic invasion. J. Neurophysiol. **20:** 27–60.
2. Freygang, W. H. & K. Frank. 1959. Extracellular potentials from single spinal motoneurons. J. Gen. Physiol. **42:** 749–760.
3. Araki, T. & T. Otani. 1955. Response of single motoneurons to direct stimulation in toad's spinal cord. J. Neurophysiol. **18:** 472–485.
4. Fuortes, M. G. F., K. Frank & M. C. Becker. 1957. Steps in the production of motoneuron spikes. J. Gen. Physiol. **40:** 735–752.
5. Coombs, J. S., D. R. Curtis & J. C. Eccles. 1957. The interpretation of spike potentials of motoneurons. J. Physiol. **139:** 198–231.
6. Coombs, J. S., D. R. Curtis & J. C. Eccles. 1957. The generation of impulses in motoneurons. J. Physiol. **139:** 232–249.
7. Tomita, T. 1956. The nature of action potentials in the lateral eye of the horseshoe crab as revealed by simultaneous intra- and extracellular recording. Japan. J. Physiol. **6:** 327–340 (and personal communication).
8. Frank, K. & M. G. F. Fuortes. 1955. Potentials recorded from the spinal cord with microelectrodes. J. Physiol. **130:** 625–654.
9. Lorente de Nó, R. 1947. A study of nerve physiology. Stud. Rockefeller Inst. Med. Res. **131, 132:** chapter XVI.
10. Lorente de Nó, R. 1939. Transmission of impulses through cranial motor nuclei. J. Neurophysiol. **2:** 402–464.
11. Lorente de Nó, R. 1953. Conduction of impulses in the neurons of the oculomotor nucleus. The spinal cord. Ciba Foundation Symposium. Little, Brown. Boston, Mass. : 132–173.
12. Freygang, W. H. 1958. An analysis of extracellular potentials from single neurons in the lateral geniculate nucleus of the cat. J. Gen. Physiol. **41:** 543–564.
13. Granit, R. & C. G. Phillips. 1956. Excitatory and inhibitory process acting upon individual Purkinje cell of the cerebellum in cats. J. Physiol. **133:** 520–547.
14. Matthews, P. B. C., C. G. Phillips & G. Rushworth. 1958. Afferent systems converging upon cerebellar Purkinje cells in the frog. Quart. J. Exptl. Physiol. **43:** 38.
15. Hodgkin, A. L. & A. F. Huxley. 1952. A quantitative description of membrane current and its application to conduction and excitation in nerve. J. Physiol. **117:** 500–544.
16. Cremer, M. von. 1929. Erregungsgesetze des nerven. Handb. normal pathol. physiol. **9:** 244–284.
17. Cole, K. C. & H. J. Curtis. 1939. Electric impendance of the squid giant axon during activity. J. Gen. Physiol. **22:** 649–670.
18. Grundfest, H. 1957. Electrical inexcitability of synapses and some of its consequences in the central nervous system. Physiol. Revs. **37:** 337–361.
19. Wolbarsht, M. L. 1960. Electrical characteristics of insects mechanoreceptors. J. Gen. Physiol. **44:** 105–122.
20. Murakami, M., K. Watanabe & T. Tomita. 1961. Effect of impalement with a micropipette on the local cell membrane. Study by simultaneous intra- and extracellular recording from the muscle fiber and giant axon. Japan J. Physiol. **II:** 80–88.
21. Tasaki, I., S. Hagiwara & A. Watanabe. 1954. Action potentials recorded from inside a Mauthner cell of the catfish. Japan. J. Physiol. **4:** 79–90.
22. Nelson, P. G., K. Frank & W. Rall. 1960. Single spinal motoneuron extracellular potential fields. Fed. Proc. **19:** 303.

THE ORGANIZATION OF CORTEX WITH RESPECT TO ITS AFFERENT SUPPLY*

George H. Bishop
Division of Neurology, Washington University School of Medicine, St. Louis, Mo.

It is obvious that the most precise information concerning nervous activity is obtainable from the study of single units or of small aggregations of them, employing arbitrary stimuli for certain accurate controls of the response. The complex activity of nervous *system* behavior often yields equivocal results, and a problem remains as to how the activity of neurones is organized into the more complex patterns of neural behavior. Information concerning the latter, from disciplines such as morphology, physiology, and psychology, is also stated in terminologies so different (each appropriate to its own point of view) that it is difficult to correlate one set of data with another. The following statement attempts to consider the activity of the vertebrate and, particularly, the mammalian nervous system from as many points of view as possible in the space available. Chief attention will be directed toward the cerebral cortex.

Herrick[1] emphasized two general aspects of function, in operational terms, for which he employed the designations *integration* and *analysis*. The former he evidently considered to be the more general or more basic or primitive mode of functioning. Integration consists of the focusing of several paths and their activities on a common pattern, in the simplest case a stereotyped and undifferentiated one. Analysis implies differentiation and, in a sense, the opposite of integration, the separate and distinctive recognition of or reaction to the activities initiated from different sources. Complex patterns obviously involve both. In complex behavior there is a third mode of functioning, the selection of one pattern of response from, or the making of a choice between, two or more possible response patterns. This mode of functioning will be termed here *modulation*, implying the biasing or redirecting of a stream of activity, especially when accomplished by neural activities that do not initiate the overt behavioral response. In some cases this may amount in effect to a subthreshold integration. These three terms, employed in the more general sense, can apply to various kinds of data, with connotations appropriate to different levels or degrees of complexity in the situations at hand.

In terms of a single neurone, the activity of a pyramidal cell of the optic cortex exemplifies these three operations. This cell's most specific activation is via the optic radiation, which projects from a circumscribed locus in the retina to one in the visual cortex. This function is an analytic one, designed to differentiate at the cortical level the details of the peripheral visual field. The apical dendrite of this cell receives impulses from various paths, as indicated by processes such as summation and interference when two such paths as cortico-cortical, thalamocortical, or callosal, are stimulated in appropriate

---

* The work reported in this paper was supported in part by a grant from the Supreme Council, 33rd Scottish Rite, Northern Masonic Jurisdiction, U.S.A. through the National Association for Mental Health, Public Health Service, Bethesda, Md., and by contract between Washington University, St. Louis, Mo. and the Office of Naval Research, Washington, D.C.

time relations.[2,3] It thus serves as an integrative apparatus. The relationship between activity of the apical dendrite and that of the basal portion of the cell is modulatory in the sense that activity in the former facilitates discharge of the latter's impulses, although it appears not to initiate such activity when acting alone at ordinary levels of stimulation.

Herrick described in the brain of Amblystoma two corresponding mechanisms, the basal neuropil surrounding the single layer of neurones (each making synaptic contact with its neighbors), and a superficial alba layer containing fibers to and from distant points and making contact with apical dendrites. Herrick termed the first an integrative mechanism; the second performs analytic functions in the sense of making specific connections from one locus to another. Orrego[4] has confirmed this physiologically in the mature turtle cortex, where the afferent impulses from the olfactory nerve via the bulb mitral cells, and from the other afferent systems via the thalamus, impinge on the apical dendrites of pyramidal cells. This appears to foreshadow a primitive analytic system differential in character, although it may with equal probability comprise a modulatory system acting on bulb and thalamic functions respectively. An associative system of connections ending on the basal regions of cortical neurones spreads activity widely from a stimulated region to surrounding regions of cortex in the manner predicted by Herrick as an integrative process.

Coghill's observations[19,20] on the activity of the amphibian larva (reviewed by Herrick[1]) and Herrick's interpretation of its anatomy indicate that the most primitive system was integrative involving a center for spinal activity in the medulla and one for head and mouthparts activity in the brain stem. Stimuli applied to loci innervated from one of these regions result in a stereotyped response from that level, referred to as a total pattern, and obviously integrative in Herrick's sense. Two developments follow: more specific responses appear, as reflexes or partial patterns differentiating between different stimuli or loci stimulated, a step toward analytic function; and relay connections between the two centers become established with anterior dominance. These connections, in effect, extend the peripheral afferent path upward and the motor path downward. They appear to constitute initial steps in the establishment of afferent and efferent linked paths, anticipating primitive sensory and extrapyramidal motor paths along the neuraxis.

In the mature amphibian such paths, in fact, extend to and from the thalamus by a further linkage, as the optic thalamus becomes a general afferent center for all modalities except possibly olfaction. The next stage in higher animals finds the cortex first acting as a general facilitatory apparatus adjunct to the olfactory bulb. A central region of the pallium thus originated becomes the general or somatic cortex, presumably developing similar relations to and from the thalamus. One may infer that the first stage accomplished a facilitatory or modulating influence on the thalamus, still the dominant afferent center, such as the primitive olfactory pallium exerted on the bulb. In the reptilian cortex Herrick[1] and Johnson[5] recognized some localization of function of visual, auditory, and somaesthetic modalities, which Herrick did not consider to be specific projection areas comparable to those of the mammal. These areas of the general or somatic cortex have been studied physiologically by Orrego[4] in the turtle, where their afferent paths terminate on apical dendrites, as do the bulb mitral cell axons innervating the olfactory cortex. Another link in the afferent path for each modality is thus added with probable efferent connections to the basal ganglia as well as to thalamus.

Several rules seem to have been followed in this evolutionary elaboration of the afferent paths.[1]

(1) There has been a succession of "brains," if a brain can be defined as a centralized collection of neurones whose function is to organize behavior in response to information received from the periphery. This succession has progressed from caudal to cephalic levels.

(2) Each such structure develops by elaboration and extension of the secondary nucleus of one of the main afferent modalities: somaesthetic, visual, and finally olfactory, with an auditory center possibly following visual elaboration at least at the brain-stem level.

(3) The higher levels successively dominate those below, with respect both to afferent coordination and to motor control.

(4) Major stages in this advance in cephalization appear to have been such as to enable the animal to invade at each step a new environment, in the successful occupation of which the one or another special sense was of primary importance. For example, the emergence on land from a water environment and the acquisition of limbs for locomotion is correlated with a demand on the somaesthetic afferent system permitting flexibility and variety of motor activity. The development of the optic thalamus may be related to the increased dependence of the land vertebrate on visual information. The development of a cortex signalizes the dependence on olfaction as a major source of information enabling animals to maneuver in an environment of obscurity.

(5) A new center acquired dominance over the levels below it by two major processes: an increase in competence of an afferent modality by increase in numbers and complexity of organization of the neurones serving it, and the acquisition of similar connections from other afferent systems to be coordinated with the modality from which the center was elaborated.

(6) Two processes have been employed in the extension upward of afferent paths. One, a simple relay of activity from a lower to a next higher level, adds another link to a chain. In the other, parallel paths from the periphery that bypass a given relay station reach the higher level more directly. A corresponding duplication of motor paths occurs, for example, in the pyramidal tract operating in part on the successive levels of the older extrapyramidal system and in part bypassing them to reach the local cord level.

(7) There appears to be a progressive increase of specificity of central coordination and of motor control from lower and more pimitive to higher levels, correlated with the successive addition of parallel paths noted above and also with an increase in the size of the fibers of which they consist. This appears to accomplish a consecutive refinement of analytic function.

(8) The organization of the primate sensory systems bears evidence that even the more primitive and early developed afferent components have been preserved and, in the somaesthetic system at least, still mediate not only afferent but also sensory information. The visual system obviously fails to register in consciousness the activity of certain of its more primitive components which, however, are still present; the mammal is blind after removal of the

visual projection area of the cortex or a section of its path. Further details will be noted in relation to the sensory paths present in mammals.

The Afferent and Sensory Paths in the Mammal

It is well known that the afferent fibers of the peripheral nerves of vertebrates display a wide size distribution, from the unmyelinated (some well below 1 mμ in diameter) to more than 20 mμ in the frog and turtle and nearly 20 in the common laboratory animals and man. This spectrum of fiber sizes shows successive maxima in numbers that have been designated by letters of the Greek and Latin alphabet, but it has become increasingly evident that fibers of one-functional connotation (submodality within the somaesthetic modality) are not strictly confined to one of the narrow ranges so designated. Neither are all the maxima equally distinct. Such facts have raised the question of the appropriateness of using the original nomenclature which was recently emphasized, quite justifiably, by one of its originators.[6] Since the discrepancies noted have led to some confusion in the literature, it is emphasized that the original names to be employed here will be applied to *ranges* in the fiber spectrum. These ranges overlap in functional significance on either side of the observable maxima so extensively that a brief review of the distributions of fiber sizes and of functional significance in the several afferent paths is in order. Mention of other criteria useful in the analysis of this distribution may further elucidate the relations between fiber size and the function mediated. These criteria will also be useful in the analysis of the afferent innervation of thalamus and cortex.

Such criteria have applied primarily to the fibers in peripheral nerves, but measurements of the threshold and latency of response at higher levels to the activation of peripheral nerves indicate that, to a first approximation, the higher segments of relayed paths contain fibers of sizes corresponding to those of the nerve components from which they originate peripherally. A fundamental division, roughly on the basis of size, occurs as the dorsal nerve roots enter the cord. The larger-size components, including alpha and beta peaks, pass up the dorsal column. The larger of these (alpha range) chiefly innervate Clark's column, relaying to the dorsal or neospinocerebellar tract. The smaller (beta) include those that synapse in the gracilis and cuneate nuclei. Others, chiefly in the beta range, terminate along the medullary and brain-stem reticular formation. Relays from the cuneate and gracilis constitute the medial lemniscus projecting to the somaesthetic area of cortex through a relay in the ventral nucleus of the thalamus. This path is not present in vertebrates below the mammals. It mediates vibration sense, touch, joint, and certain proprioceptive impulses in the human subject.

Other nerve fibers, in general smaller, relay in the cord, and their postsynaptic connections ascend the lateral column in the spinal lemniscus. Five components of this bundle can be traced to different destinations by various differential techniques, incidentally giving evidence of fiber size. The extension of the unmyelinated or *C* fiber path separates off in the medulla and projects to certain of its medial nuclei.[7,8] From here it is relayed to the upper brain-stem-medial thalamus region, where it synapses again. How or whether its impulses are relayed to the cortex is not known. Its course, medullary projection, small size of fibers, and other characteristics, suggest that it is the mammalian derivative of the most primitive path of the amphibian spinal system. In the human subject it mediates second or "burning" delayed pain, temperature, and itch; in the cat some of its fibers respond to touch, not detectable as a human sensation.

A second component, corresponding to the nerve afferents of the myelinated gamma-delta range synapses in the cat in the upper brain stem, and its postsynaptic response is apparently in the medial thalamus near the centrum medianum nucleus.[9] This response is present after section of the dorsal cord column but not after section of the lateral column. Its sensory reference is unknown. A third component bypasses this synaptic region and projects to parts of the intralaminar nuclei of the thalamus.[10] It almost certainly mediates pricking pain and temperature, since these are excluded from the remaining divisions of the spinal lemniscus. Its fibers are described as small and, presumably, they correspond to the delta-range of nerve. It is probably the mammalian analogue of the premammalian or paleospinothalamic tract.

A fourth component terminates more laterally, in the posterior group of thalamic nuclei.[11] This region has been explored recently with microelectrodes.[12] Single cells are found there responding to stimuli at widely different loci of the periphery and even to different modalities, in contrast to the cells of the ventral nucleus. These cells and, by implication, this area represent a nonspecific integrative center for afferent, possibly sensory, impulses at the thalamic level. Destruction of the cortex, including but not confined to the secondary sensory area, is followed by degeneration in the posterior nuclei, which implies a relatively nonspecific projection to an association area of cortex. A fifth component of the spinal lemniscus parallels the medial lemniscus as it terminates in the lateroventral nucleus and, in fact, constitutes, with the fourth component, the classic spinothalamic tract of mammals. Like the medial lemniscus, it is not present in premammals. Since it presumably projects to the somaesthetic area, where pain and temperature are not represented, it may tentatively be held responsible for mediation of the lateral-column touch. It is minimally present in lower mammals, even the cat, but becomes increasingly prominent in primates and man,[13] thus offering evidence that this pathway has been established progressively during the evolution of the mammalian sequence.

In addition to these fiber concentrations, many other fibers distribute along the brain-stem reticular tissue, with not more than one fourth of the ascending bundle continuing as the neospinothalamic tract. A fan of fibers whose terminations spread from medulla to ventrolateral thalamus includes these more specific bundles, to certain of which the mediation of sensation can be most definitely assigned. These components show an over-all increase of fiber size to successively higher levels of projection. The lowest path, to the medulla, mediates a full complement of somaesthetic impulses, including touch, pain, itch, and temperature.[14,15] The paleospinothalamic path to the medial thalamus duplicates this range of sensations, including pricking pain, temperature, and touch. The neospinothalamic and medial lemniscus paths to the ventrolateral thalamus duplicate again only the mediation of touch, but include other epicritic sensations concerned chiefly with contact with the physical environment. The inference that may be drawn from these circumstances is that the somaesthetic projection area of the cortex is concerned immediately with only a small fraction of the somaesthetic sensory impulses and their qualitative implications.

From the various lines of evidence can be inferred at least three superimposed systems of afferents, projecting most immediately to three levels of the nervous system and arranged in a phylogenetic sequence. The more primitive in derivation of these systems mediates in human subjects sensations with poor localization and two-point discrimination, characterized by an extreme degree of summation with duration of stimulus and having an intensely penetrating qualitative affect. The second path mediates somewhat similar sensations, but with better localization and discrimination. The most recently acquired system affords the highest degree of discrimination and differentiation, particularly with respect to quantitative dimensions. One may see in this sequence an increasing capacity for differentiation or analysis, with final development of one area of cortex capable of distributing one group of the sensory messages in a most detailed array. This sequence of sensory paths corresponds to a progressive increase of fiber size employed for sensory mediation to levels of consciousness, permitting a surmise that a larger fiber is somehow more appropriate or effective for detailed analysis of the sensory input. A similar distribution[16] of fiber-size components from the retina is afferent to various structures in a phylogenetic sequence, the smallest direct to the brain stem, the next relayed to the thalamus, and the largest to the visual cortex. This again restricts the visual projection area primarily to discrimination of environmental detail. Qualitative aspects of visual sensations, such as those characterizing the smaller fiber paths of the somaesthetic system, appear not to be registered in the consciousness of the human subject.

Stages in the Evolution of Cortex

Four major stages may be recognized in cortical evolution. In the first stage (Amblystoma) the forebrain pallium is related to the olfactory system only. In the second stage (turtle) a general or somatic cortex, still single-layered, acquires similar relations to the dorsal thalamus with cortical regions of response for the main afferent systems presumably already represented in the thalamus. In the third stage there occurs in the mammalian cortex an increase in thickness with many layers, and the cortex also differentiates projection areas primarily related to certain large-fiber afferent paths that, below the mammals, do not reach even the thalamus. This fact, the circumstance that previously acquired paths to the thalamus persist in the mammal, and the fact that some of them still mediate sensations in the human subject, imply the persistence in the mammalian cortex of areas analogous to the regions of sensory reference in the reptilian cortex. These are probably included in the association cortex of mammals adjacent to the specific projection areas and may include the so-called secondary sensory areas. A fourth stage culminates in the pronounced expansion of frontal and temporal lobes and other less well-defined regions. Results of destruction here indicate that certain of such areas are not primarily concerned with memory, with sensory discrimination, or with motor coordination, although their loss modifies behavior significantly in other respects. To the extent that their functioning corresponds to facilitation or modulation of behavior, they might be considered as more sophisticated analogues of the most primitive cortical apparatus of earlier forms, which has a rather nonspecific relation to the olfactory bulb system of the amphibian. Such tentative and problematical speculations seem justifiable in view of the essential conservatism of the vertebrate nervous system, which seems to have progressed by adding new structures or improvements on older ones without losing its most primitive scheme of organization.

The Sizes of Fibers Traversing the White Matter Under Cortex

Study by means of the electron microscope (in progress) of fibers passing to and from the mammalian cortex indicates that almost all are myelinated, although many are of the size of unmyelinated fibers elsewhere. Their myelin is lost near the terminals, particularly the myelin of the many fine fibers reaching the superficial terminations of apical dendrites. The largest fibers (except those below the Betz-cell area) are 12 to 14 μ in diameter. The same distribution is found in the optic nerve and tract. The peak in numbers is just below 1 μ, and most of those found below the cat suprasylvian and visual areas, cat corpus callosum, and human frontal area from biopsies have approximately the same size distribution. In the corpus callosum, fibers in both directions pass equivalently, afferent and efferent, to a given cortex, obviating the distinction between those leaving and entering it. No distinct group maxima are found, although in the cat optic tract two well-defined potentials appear followed by a remainder of lower amplitude. These three ranges are as different in thresholds as in conduction rates. In the corpus callosum, approximately 85 per cent of the total number are below 3 or 4 μ, 12 per cent between this and 6 μ, and 3 per cent over 6 μ. There thus seems to be a general similarity in all distributions to the cortex. In the optic nerve it is estimated that, when the first spike assignable to fibers above 5 or 6 μ is maximally excited, the specific response of the visual cortex is also maximal. Other regions of the thalamus are activated via the second size range, and the superior colliculus and pretectal areas by the smaller range.

These three ranges are similar to and reminiscent of the three major divisions of peripheral nerve afferents (unmyelinated, small myelinated, and large) with corresponding projections of pathways to the medulla, the medial thalamus, and the ventral nucleus relay to the cortex respectively. In the two larger-fiber divisions, the sizes are larger than any fibers innervating the turtle cortex. These conditions in the mammal, as compared to the premammal, might be viewed as an acquisition by the cortex of such larger fiber components as were earlier developed in the peripheral systems. Not only the sensory projection areas but all regions of the cortex show similar distributions. This organization thus seems to constitute a generalized later development, in the most recently evolved central nervous system structure, of fiber-size distribution established much earlier in the more peripheral nervous structures.

The Afferents to Cortex

The mammalian cortex is stratified with respect to its principal cell type, the pyramid cell, with larger cells below and smaller ones superficially. The relative fiber sizes of their axons probably correspond to cell size. Large fibers from the specific sensory nuclei project to the region of the fourth layer, containing larger pyramids. Smaller fibers from the nonspecific thalamic nuclei pass largely to higher levels of cortex where many terminate on apical dendrites. Thus fibers both afferent and efferent, to and from the cortex, show some degree of vertical stratification of fiber-size termination or origin, as well as of cell size. The afferent distribution in the cat is in part similar to the arrangements in the turtle cortex. In the latter a single layer of cells shows only minor size differences but receives terminals of afferents most conspicuously at two levels: near the cell body and on the apical dendrites. These two paths are further characterized in both the reptilian and mammalian cortex by the type of response to stimulation of each.

In the cat, stimulation of the nonspecific thalamic nuclei induces in the cortex two types of response with different latencies presumably indicating different fiber sizes of the pathway. The longer latency response, typically a surface-negative postsynaptic process in apical dendrites, when stimulated at 6 to 10 cps, appears as a recruiting series with a characteristic excitability cycle.[17] A shorter latency response, negative or sometimes initially surface-positive, is more or less decremental and nonrecruiting. Both paths presumably terminate on apical dendrites, the faster-conducting fibers perhaps being lower in the cortex than the slower. In the turtle[4] quite similar paths and responses are found. The longer latency responses are simply surface-negative and show recruitment on repetitive stimulation with a characteristic excitability increase following each response.

The shorter latency responses are diphasic with initial surface positivity, and are decremental at any frequency of stimulation. The plus-minus diphasicity indicates initial deep negativity with propagation upward, and such negativity is found to be maximal at the level of cell bodies. Stimulation of sensory afferents activating the cortex induces the recruiting surface-negative response; stimulation of the interconnections from one cortical region to another induces decremental responses.

In addition to these types of response the mammal has a large-fiber system of afferents to the projective cortical areas. Stimulation of these afferents arouses a series of brief surface-positive spikes, which have been interpreted as activities of pyramidal cells at successively higher levels of the cortex. The spikes are superimposed on a slow wave diphasic potential that appears to register upward conduction along apical dendrites. This system, absent in the turtle, apparently corresponds to the acquisition by the mammal of the new large fiber-afferent system from the dorsal cord columns. With the exception of this system, the responses of the reptilian and mammalian cortices are similar enough to suggest correspondingly similar functional connotations.

The older afferent path to the medial thalamus in the mammal, interpreted above as the analogue of a similar path in the premammal, mediates the lateral column spinal lemniscus impulses from the somaesthetic periphery. Stimulation of the thalamic medial region where this path terminates (and of other so-called diffuse projection nuclei) induces at the cortical level typical recruiting responses[18] that are particularly prominent in the association areas. The afferent paths in the turtle similarly mediate impulses to the cortex that arouse typically surface-negative recruiting responses, as in the mammal. From certain mammalian thalamic nuclei, these stimuli also arouse cortical decremental responses, as well as recruiting responses. The decremental responses are of shorter latency than the recruiting ones. The following relations in the two cortices are suggested by these comparisons.

First, among the recruiting circuits of the thalamocortex of mammals, one may seek the cortical activity induced via the more primitive sensory system of small fibers inherited from the prevertebrates, suggesting that the sensory areas of the cortex of the turtle anticipate some of the association cortex of the mammal. Furthermore, as the mammal has acquired fibers of larger size not only in the large-fiber projection areas but everywhere in the cortex, it may have extended the newer type of cortical activity to other than sensory projection areas, in fact to the whole cortex that has been differentiated in many other respects from the simple, more homogeneous cortex of the earlier forms. If the decremental responses of the mammalian cortex are to be considered analogues of those of the turtle, their surface negativity, even when preceded by surface positivity, may imply that their fibers make contact more distally along apical dendrites from the cell bodies than in the turtle. Or, at the basal regions of the neurones of the mammalian projection areas, the newer large-fiber system may have displaced, at least in part, these older decremental connections to become the specific sensory mediators to these neurones.

It may be significant in this connection that, in other than projection areas, stimulation of white matter below the cortex elicits either very small or no spikes, although an initial positive, diphasic slow potential results, similar to that everywhere present in the turtle. Responses of a locus of the cortex to stimulation of distant cortical points arouses both recruiting and nonrecruiting responses, chiefly surface negative, the nonrecruiting type similar to the cortico-cortical response in the turtle being the more prominent. The functional significance of such cortico-cortical responses cannot be defined at present, beyond suggesting that activity in these circuits performs a modulating function and may contribute to the constant background activity that affects the excitability of sensory cortex to stimulation of its radiations. It can be demonstrated that, during such a cortico-cortical negative response activated by specific electrical stimulation, the excitability of visual cortex to stimulation of its radiation is increased.

Summary

In the foregoing synopsis of different approaches to what is, after all, the same brain, possibilities rather than firm conclusions have been presented, intended to emphasize the fact that the significance of one type of evidence is measured largely by its consistency with another. It is not yet clear to what extent the general operational terms suggested as applicable to various aspects of nervous activity as well as those applicable to activity at different levels of complexity will in fact be terms adequate to advance our understanding of how the brain actually functions.

In such a schematic review of the afferent nervous system, an infinitude of detail complicates to the point of obscurity any simple or general concepts of its over-all behavior. Even if one would grant that a general scheme laid down in the primitive vertebrate brain has persisted as a skeletal framework for the more highly sophisticated apparatus of the mammal, it is apparent that the mammal has acquired not only more brain but more functions and more neurological mechanisms back of them. A first approach appears to be to identify what functions are primitive or inherited from the premammal. We may then hope to identify in more detail what has been added since, and how the additions modify or amplify the more primitive functional patterns.

By making analogies between reptilian and mammalian brains, pending more detailed study, one may infer as to what areas of the mammalian cortex and thalamus the more primitively developed paths are more immediately related; it may even be possible to project what thalamocortical activities they initiate. The paths from the smallest fibers of peripheral nerves, traced upward through the reticular formation, may be expected to relate to brainstem "activating" functions. Medium-sized spinal lemniscus fibers seem to be aimed at what are usually considered to be association areas. The specific projection areas, each innervated chiefly from a large-fiber component, may be looked upon as an extra link in a path whose final target includes the more primitive association areas also innervated by paths earlier established. These three systems of afferents presumably overlap there, and are interrelated in the substrate of consciousness.

In any event, each successively developed brain appears to operate by some of the same general processes, however complicated by adaptive detail, and with increased effectiveness, at the cost of increasing complexity of an organization culminating in cortex and subjective behavior and finally, to some extent, dissociated from motor activity.

References

1. Herrick, C. J. 1948. The Brain of the Tiger Salamander. Univ. Chicago Press' Chicago, Ill.
2. Landau, W. M., G. H. Bishop & M. H. Clare. The interaction of several varieties of evoked response in visual and association cortex of the cat. Electroencephalog. Clin. Neurophysiol. **13**. In press.
3. Bishop, G. H., M. H. Clare & W. M. Landau. The equivalence of augmenting and recruiting phenomena in the visual cortex of the cat. Electroencephalog. Clin. Neurophysiol. **13**. In press.
4. Orrego, F. & D. Lisenby. Electrical activity in turtle cortex. Arch. ital. Biol. In press.
5. Johnston, J. B. 1923. Further contributions to the study of the forebrain. J. Comp. Neurol. **36:** 143–192.
6. Gasser, H. S. 1960. Effect of method of leading on the recording of the nerve fiber spectrum. J. Gen. Physiol. **43:** 927–940.
7. Collins, W. F. & C. T. Randt. 1958. Evoked central nervous system activity relating to peripheral unmyelinated or C fibers in the cat. J. Neurophysiol. **21:** 345–352.
8. Collins, W. F. & C. T. Randt. 1960. Midbrain evoked responses relating to peripheral unmyelinated or C fibers in the cat. J. Neurophysiol. **23:** 47–53.
9. Collins, W. F. & J. L. O'Leary. 1954. Study of a somatic evoked response in midbrain reticular substance. Electroencephalog. Clin. Neurophysiol. **6:** 619–628.
10. Mehler, W. R., M. E. Feferman & W. J. H. Nauta. 1960. Ascending axonal degeneration following antelateral cordotomy. Brain. **83:** 718–750.

11. Harlow, H. F. & C. N. Woolsey. 1958. Cortical connections and functional organization of the thalamic auditory system in the cat. *In* Biological and Biochemical Bases of Behavior. Univ. Wis. Press. Madison, Wis.
12. Poggio, G. F. & V. B. Mountcastle. 1960. A study of the functional contributions of the lemniscal and spinothalamic systems to somatic sensibility. Bull. Johns Hopkins Hosp. **106:** 266–316.
13. Mehler, W. R. 1957. The mammalian pain tract in phylogeny. Anat. Record. **127:** 332.
14. Landau, W. M. & G. H. Bishop. 1953. Pain from dermal, periosteal, and fascial endings and from inflammation. A.M.A. Arch. Neurol. Psychiat. **69:** 490–504.
15. Bishop, G. H. 1959. The relation between nerve fiber size and sensory modality; phylogenetic implications of the afferent innervation of cortex. J. Nerv. Mental Diseases. **128:** 89–114.
16. Bishop, G. H. & M. H. Clare. 1955. Organization and distribution of fibers in the optic nerve of the cat. J. Comp. Neurol. **103:** 269–304.
17. Clare, M. H. & G. H. Bishop. 1956. Potential wave mechanisms in cat cortex. Electroencephalog. Clin. Neurophysiol. **8:** 583–602.
18. Morison, R. S. & E. W. Dempsey. 1942. A study of thalamocortical relations. Am. J. Physiol. **135:** 281–292.
19. Coghill, G. 1943. Flexion spasms and mass reflexes in relation to the ontogentic development of behavior. J. Comp. Neurol. **79:** 463–486.
20. Coghill, G. 1914–1936. Correlated anatomical and physiological studies of the growth of the nervous system of Amphibia. Papers I to XII. J. Comp. Neurol. **24–64.**

ELECTROPHYSIOLOGICAL PROPERTIES OF AN ARCHICORTICAL NEURON

E. R. Kandel* and W. A. Spencer†
Laboratory of Neurophysiology, National Institute of Mental Health, Public Health Service, Bethesda, Md.

The detailed understanding of the electrophysiology of central neurons derives primarily from the extensive intracellular microelectrode studies of the spinal motoneuron.[2,13,14,19,22,39,56] The important model derived from these investigations has already proved applicable to the neurons of a variety of submammalian species: the supramedullary cell of the pufferfish,[4,5] the giant ganglion cell of *Aplysia*,[54,55] and the sensory neuron of the crayfish.[18] By contrast, the test of the motoneuron model in mammals has been largely limited to other nerve cells of the spinal cord (for example, Clarke's column and interneurons).[11,26] In particular there is a paucity of information about cortical neurons. It is indeed difficult to obtain intracellular recordings in the mammalian cortex due, in large part, to the small size of most cortical cells and to brain pulsation.

The present series of investigations received their impetus from Phillips' success in impaling the neocortical Betz cell.[42,43,44] By activating these cells antidromically, Phillips was able to show that the steps in the production of the antidromic spike were similar to those in the spinal motoneuron. He demonstrated further that excitation occurred with depolarization and inhibition with hyperpolarization.

Since the Betz cell is an unusually large-sized and fairly specialized neocortical motor cell, it seemed advantageous to test the motoneuron model on another cell that is both morphologically and functionally different. The hippocampal pyramidal cell was selected for study because it is a more typically correlational neuron, that is, it does not have specific motor or sensory functions and it is part of the archi- rather than the neocortex.

The hippocampus is a particularly favorable cortex for single unit analysis. It is directly accessible following suction removal of the overlying part of the hemisphere. Therefore gross stimulating and recording electrodes can be placed under direct vision on various portions of the exposed archicortex. The absence of pial covering permits multiple electrode penetrations to be made rapidly and easily. The relative simplicity of the cellular architecture and its constancy throughout the mammalian class have traditionally attracted the attention of morphologists. Consequently the anatomy and hodology of the hippocampus are particularly well described.[7,38,40,45,46] The somata of the primary neurons, the pyramidal cells, are clustered in a tightly packed layer (FIGURE 1*a*). These neurons send their axons into alveus, fimbria, and fornix, an outflow tract that is readily accessible for stimulation (FIGURE 1*b*). The pyramidal cell can therefore be activated antidromically and identified electrophysiologically. There are also available two orthodromic pathways to the pyramidal cells and an extensive system of recurrent collaterals.

---

* Present address: Department of Psychiatry, Harvard Medical School, and Massachusetts Mental Health Center, Boston, Mass.

† Present address: Istituto di Fisiologia, Universita di Pisa, Pisa, Italy.

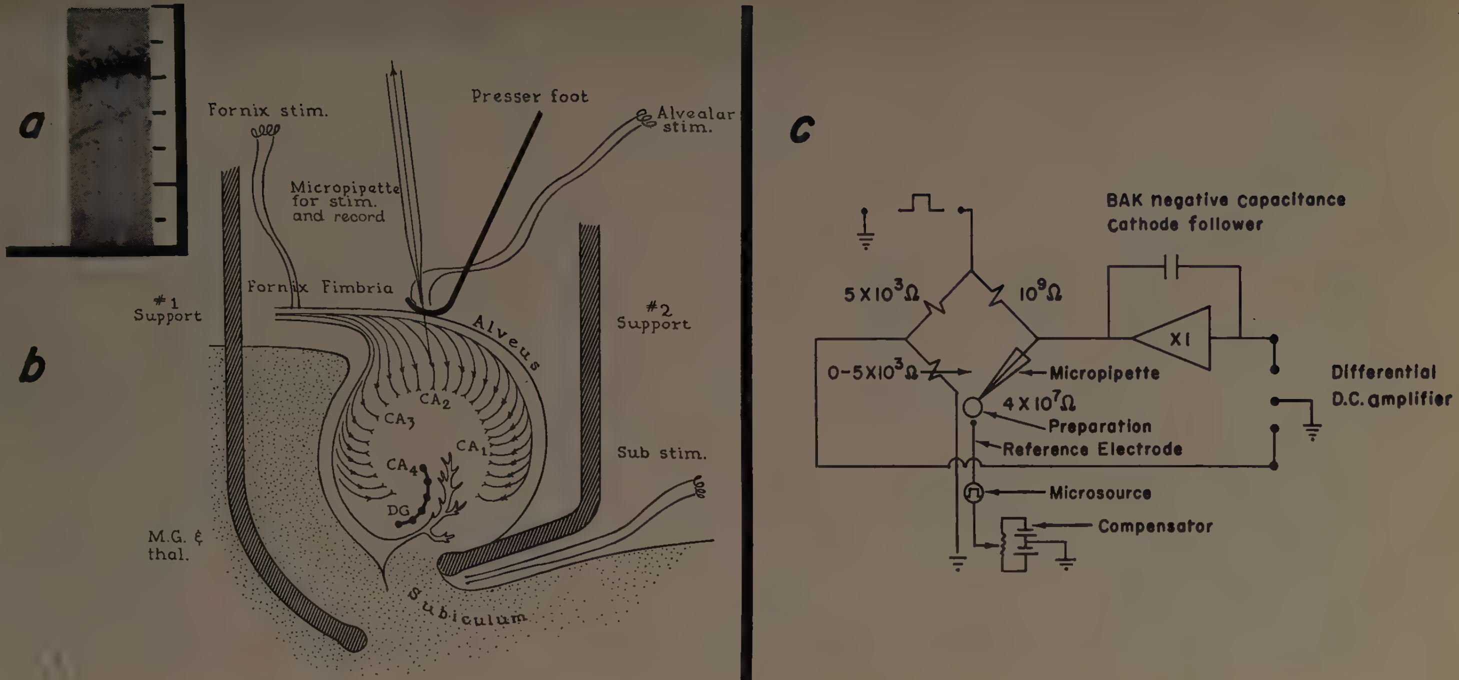

FIGURE 1. (*a*) A Nissl stain of the hippocampus at CA$_2$ (in *b*), to indicate the tightly packed cellular layer. Each calibration bar at the right of the photograph represents a distance of 100 μ. (*b*) A diagram of the experimental arrangement, representing a cross-section through the midportion of the hippocampus. Pulsation control was usually achieved by means of the two supports and, when necessary, with the additional use of the presser foot. Note the placement of the stimulating electrodes on the fornix, the alveus (in the presser foot), and the subiculum. (*c*) A schematic diagram of the bridge circuit for stimulating through the recording electrode.

In addition to the advantages offered by the general organization of the archicortex, the pyramidal neurons possess a certain morphological simplicity. In contrast to spinal and other cortical neurons the pyramidal cell has two discrete and clearly separate dendritic systems: a basilar system that converges upon the axonal pole of the cell body, and an apical system that converges upon a short unbranched dendritic stalk.

In the discussion that follows we shall focus on three areas of investigation. First, we shall describe the relation of excitatory postsynaptic potentials to solitary and repetitive firing and discuss some properties of an extensive intrahippocampal inhibitory system. Next, we shall consider the steps in the production of the pyramidal cell spike. The emphasis here will be on a new finding, a spike generated in a portion of the dendritic tree of these cells that seems to act as a booster mechanism for more remote dendritic synapses. Finally, we shall consider a more specifically cortical problem: how the pyramidal cell behaves during hippocampal seizure.

The experiments were performed on anesthetized (Evipal), paralyzed (succinylcholine or Flaxedil) cats. Intracellular recordings were obtained with ultrafine K^+ citrate electrodes connected to a Bak negative capacitance cathode follower.[3] A wheatstone bridge was used to inject current through the pipette (FIGURE 1*c*). The criteria for the selection of the data and the operative and other experimental details are described elsewhere.[32,50,52] The analysis described below is based upon stable recordings from approximately 100 cells.

Synaptic Excitation and Inhibition

FIGURE 2 shows the transmembrane voltage changes recorded from a pyramidal cell following single shock stimulation of the subiculum. This volley activates the perforant pathway, which is the major afferent tract to the hippocampus. A weak shock gave rise to a small depolarizing, excitatory, postsynaptic potential (uppermost trace). With a slightly stronger shock the synaptic potential was increased in amplitude but was still subthreshold for spike generation (second trace). The long latency and time course of this excitatory postsynaptic potential (EPSP) suggests that it is neither monosynaptic nor synchronous. At slightly greater stimulus strength, the EPSP reached a critical firing level (in this case 5 mv) and an action potential was generated (third trace). When supraliminal or prolonged synaptic depolarization occurred, repetitive firing was initiated. This ranged from double or triple spikes (fourth trace) to more prolonged bursts containing five spikes (fifth trace).

The action potentials of the pyramidal cell were found to range up to 110 mv, with a mean of 70 mv. The average resting potential was 50 mv and the average spike duration was 1.84 msec. The action potential was followed by a depolarizing after potential of approximately 10 mv amplitude and 23 msec. duration. On the basis of their responses to antidromic stimulation, all impaled cells could be categorized into two groups: identified pyramidal and unidentified neurons. Both groups proved to have remarkably similar properties.[32] Two distinctive features of these membrane parameters distinguish the pyramidal from the Betz and motor horn cells: the presence of a significant

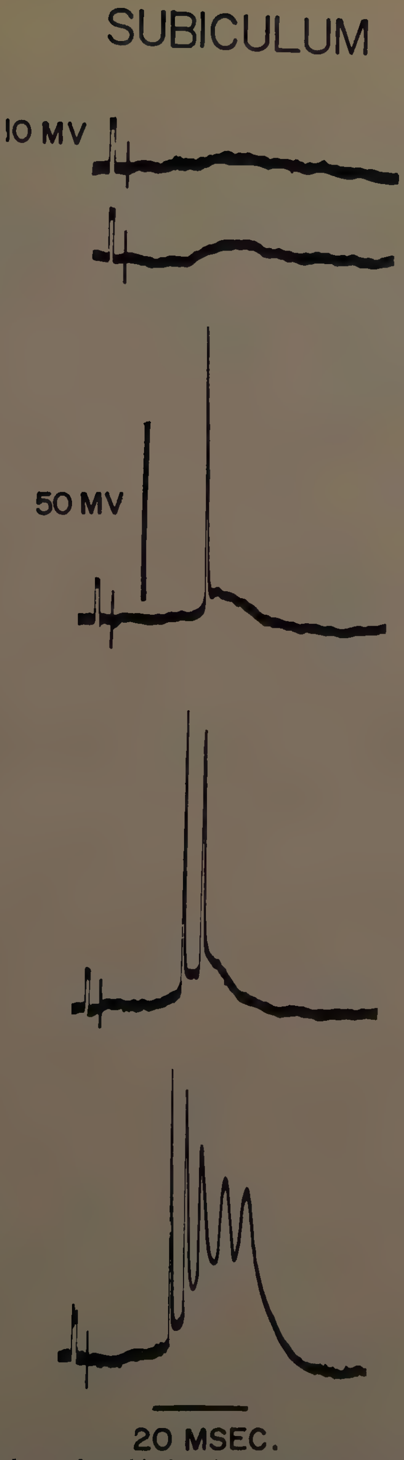

FIGURE 2. Single shocks to the subiculum in an identified pyramidal cell. The uppermost trace shows a very weak shock. A slightly stronger shock is shown in the second trace; note the long latency and time course of the EPSP. A slight increase in stimulus strength (*third trace*) brings the EPSP to the threshold for spike generation. The fourth and fifth traces show supraliminal synaptic depolarization initiating repetitive firing.

depolarizing afterpotential (DAP) and the absence of a hyperpolarizing afterpotential.

The orthodromic patterns evoked by subiculum stimulation are similar to those occurring during the spontaneous firing of the pyramidal cell. FIGURE 3 (upper trace) illustrates the spontaneous firing of a pyramidal cell in a lightly anesthetized preparation. FIGURE 3 (lower trace) is an extracellular recording made under comparable conditions of anesthesia. In both instances the firing pattern consists of solitary and multiple firing.

The existence of these distinctive bursts raised the question of whether this repetitive firing was maintained by unusually large synaptic potentials or whether part of the underlying depolarization could be attributed to the addition of DAPs.

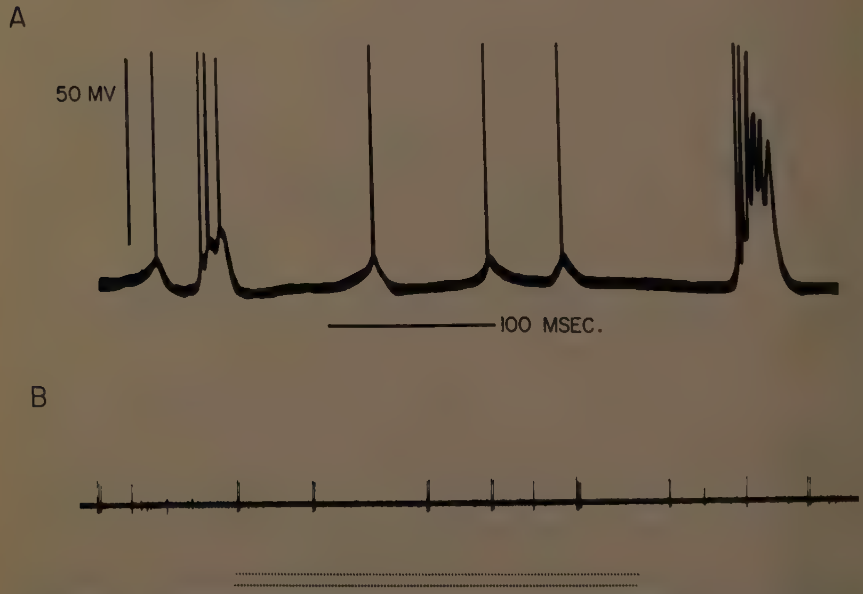

FIGURE 3. A comparison of firing patterns recorded intracellularly (A) and extracellularly (B). The time line for the lower trace is 60 cps. An isotonic NaCl-filled glass pipette, with a diameter of 8 μ, was used to obtain the extracellular record. Negativity in the extracellular record is indicated by an upward deflection.

By passing increasing amounts of current through the microelectrode it proved possible to simulate the entire range of spontaneous firing patterns and to study, in a controlled manner, several of the mechanisms involved in the repetitive firing of the pyramidal cell.[31] FIGURE 4 summarizes the results obtained by direct stimulation under three different conditions. The repetitive firing in FIGURE 4*a* occurred in response to a 250-msec. constant depolarizing current pulse. Upon completion of the burst the membrane repolarized. The potential difference between the bridge unbalance after the burst and the peak of the slow depolarization cannot be accounted for by pipette current. This argument is further supported in situations in which no polarizing current

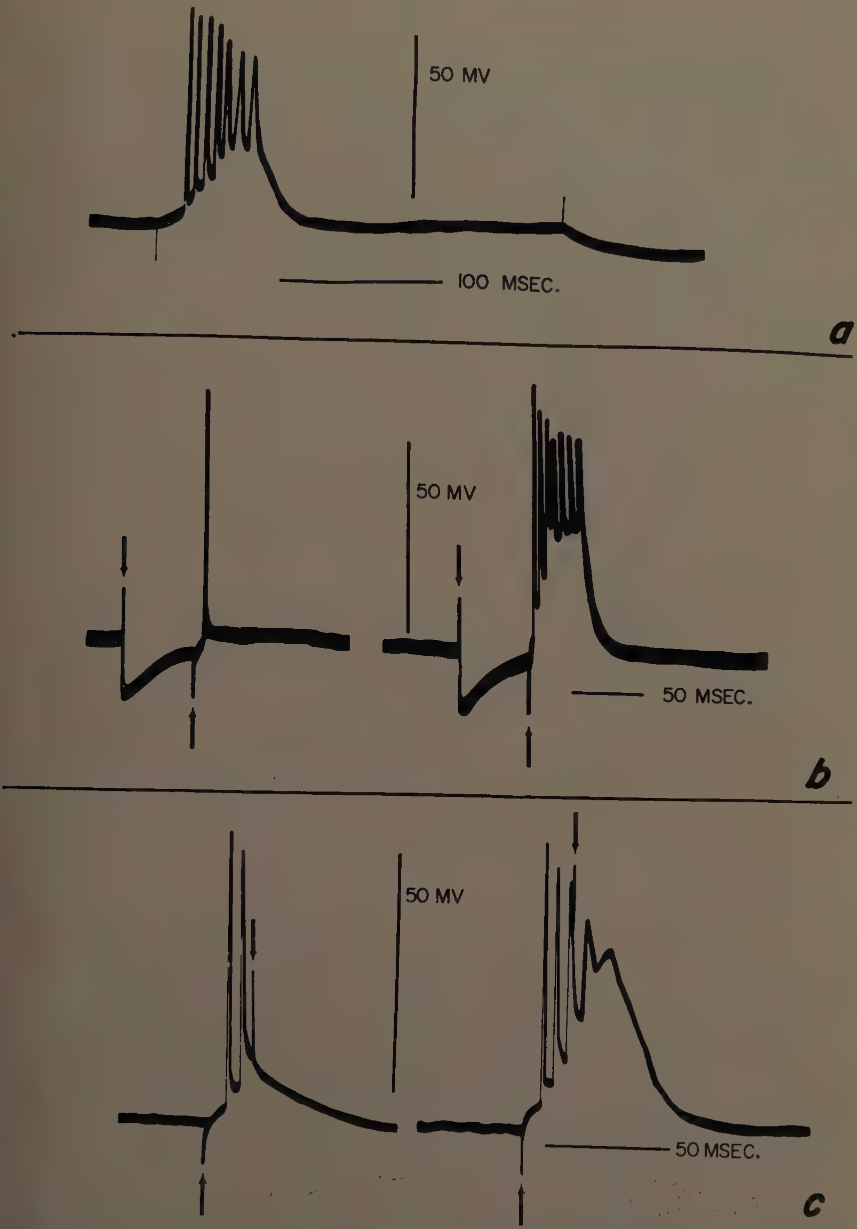

FIGURE 4. (*a*) A burst response to a 250-msec. depolarizing pulse injected through the microelectrode. At the completion of the burst the membrane repolarizes. (*b*) Rebound responses to hyperpolarizing pulses: single-spike rebound (*left*) to a moderate-intensity pulse, and a burst rebound (*right*) to a slight increase in the intensity of the hyperpolarizing pulse. The arrows indicate "on" and "off" artifacts. The time course of the membrane potential change is distorted because of capacitative artifact. (*c*) Continuation of the burst following depolarizing pulses: (*left*) a weak pulse, and (*right*) a slightly stronger pulse. The arrows indicate "on" and "off" artifacts.

is injected by the micropipette. In FIGURE 4*b* (left) a single spike is shown to occur as a rebound to a strong hyperpolarizing pulse. When the intensity of the hyperpolarizing pulse was increased (FIGURE 4*b*, right), a rebound repetitive burst was triggered. FIGURE 4*c* (left) demonstrates a burst in response to a brief depolarizing pulse. When the depolarizing pulse was increased (duration remaining constant), the burst continued for 50 msec. after the "off" (FIGURE 4*c*, right). In both the rebound to hyperpolarizing current and maintenance after cessation of depolarizing current, the underlying depolarization and repetitive firing are maintained in the absence of polarizing current.*

The evidence therefore suggests that the excitatory state underlying repetitive firing in the pyramidal cell can be maintained by the summation of DAPs.[31]

An attempt was also made to analyze the limiting factors in the repetitive firing of the pyramidal cell.[31] The arguments that were advanced favor the concept that the maintained depolarization depresses the spike generator and limits both frequency and duration of the burst, presumably by inactivation of the Na^+ carrier.[25]

The other afferent input to the pyramidal cell employed in these studies was the fornix. Here the situation is more complicated because the fornix is a mixed tract and carries predominantly hippocampal efferent fibers. The voltage changes following single shock stimulation to the fornix are illustrated in FIGURE 5. The top trace in FIGURE 5*a* illustrates the antidromic spike. When the stimulus strength was slightly reduced (second trace), the spike was generated orthodromically. Its latency was then increased by 1 msec. and it was preceded by an EPSP that brought the membrane potential to the firing level. With subthreshold volleys the time course of the EPSP became evident (third trace). A slower sweep (fourth trace) demonstrated a prolonged hyperpolarizing postsynaptic potential following the relatively brief EPSP. In response to single fornix volleys the EPSP was usually small or altogether absent. It could, however, be made evident with repetitive stimuli (FIGURE 19). By contrast, the hyperpolarizing postsynaptic potential was invariant.

The two traces of FIGURE 5*b* summarize some of these characteristics of the synaptic convergence upon a single pyramidal cell. A single subiculum shock gives rise to an EPSP that generates a spike (upper trace); a shock to fornix causes synaptic hyperpolarization that prevents cell firing (lower trace).

Synaptic hyperpolarizations in hippocampal neurons are similar to those of other cells.[14] Following the convention established in the investigation of the motoneuron, these hyperpolarizations will be referred to as inhibitory postsynaptic potentials (IPSPs). As illustrated in FIGURE 6*a*, IPSPs interrupt spontaneous firing. During the peak of the synaptic hyperpolarization the current required for threshold stimulation is increased by a factor of three or

---

* It must be pointed out that membrane events that result from previously injected currents continue after a direct pulse. A passive decay determined by the membrane time constant follows the depolarizing pulse. A depolarizing "overshoot" may follow the cessation of a hyperpolarizing current.[27] It would seem that the magnitude and duration of either decay or "overshoot" account only in small part for the long-lasting and large depolarizations described in FIGURE 4. These small, extrinsically produced membrane depolarizations may trigger the burst; they seem insufficient to explain either the magnitude or the duration of the maintained depolarizations.

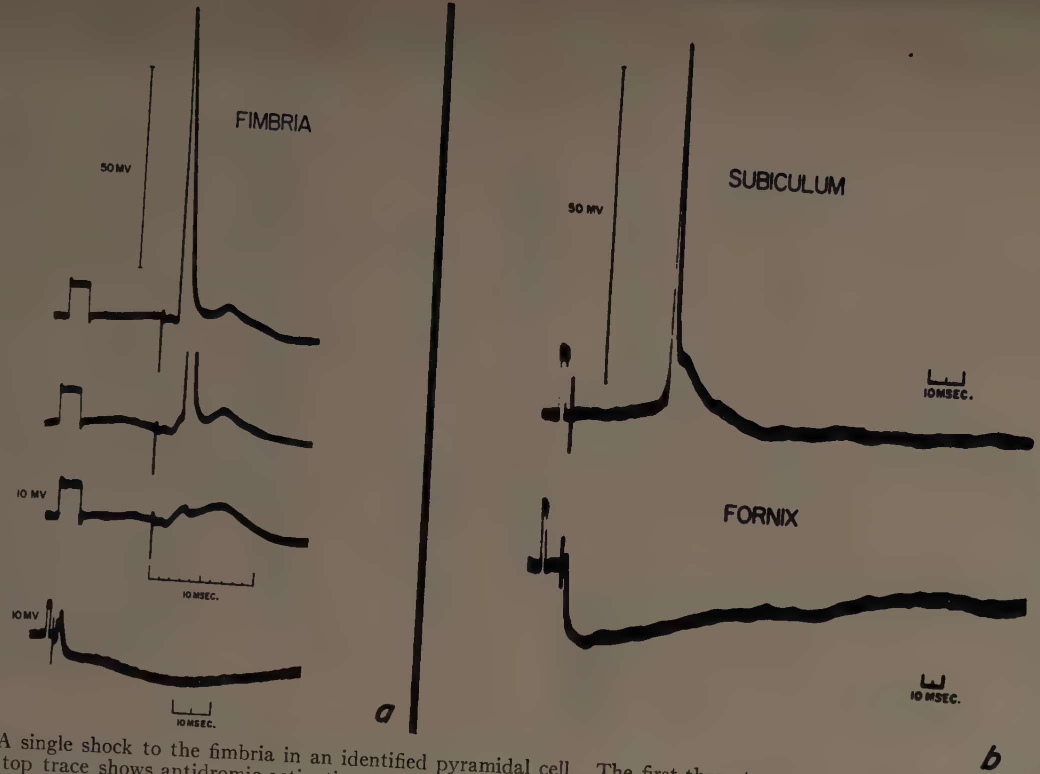

FIGURE 5. (*a*) A single shock to the fimbria in an identified pyramidal cell. The first three traces are arranged in descending order of stimulus strength. The top trace shows antidromic activation and the second trace, with a weaker shock, shows orthodromic activation. Note the increase in latency and EPSP at the foot of the orthodromic spike. The third trace, with a still weaker shock, shows a subthreshold EPSP. The fourth trace has the same PSP as the third, but on a slower sweep to demonstrate that the EPSP is relatively small and brief in comparison to the IPSP. The upper trace in *b* is a single subiculum shock that gives rise to an EPSP generating a spike. In this same cell a fornix volley generates an IPSP. Note that the IPSP is not preceded by an EPSP, which is the more usual finding.

more (from a rheobase of about 3×10^{-10} amp. to one of more than 10×10^{-10} amp.). Hyperpolarizing PSPs were noted to invert to depolarizing PSPs when KCl electrodes were used. FIGURE 6*b* is an example of this effect. Presumably it is due to the diffusion of Cl^- into the cell, since the inversion did not occur when K^+ citrate electrodes were used. This finding has previously been noted for motoneuron[9] and for the cells of Clarke's column.[11] In the latter two groups of cells the generation of IPSPs has been attributed to a transiently increased permeability of the subsynaptic membrane to chloride and other small ions. Our data suggest that similar ionic mechanisms produce the IPSPs of pyramidal cells.

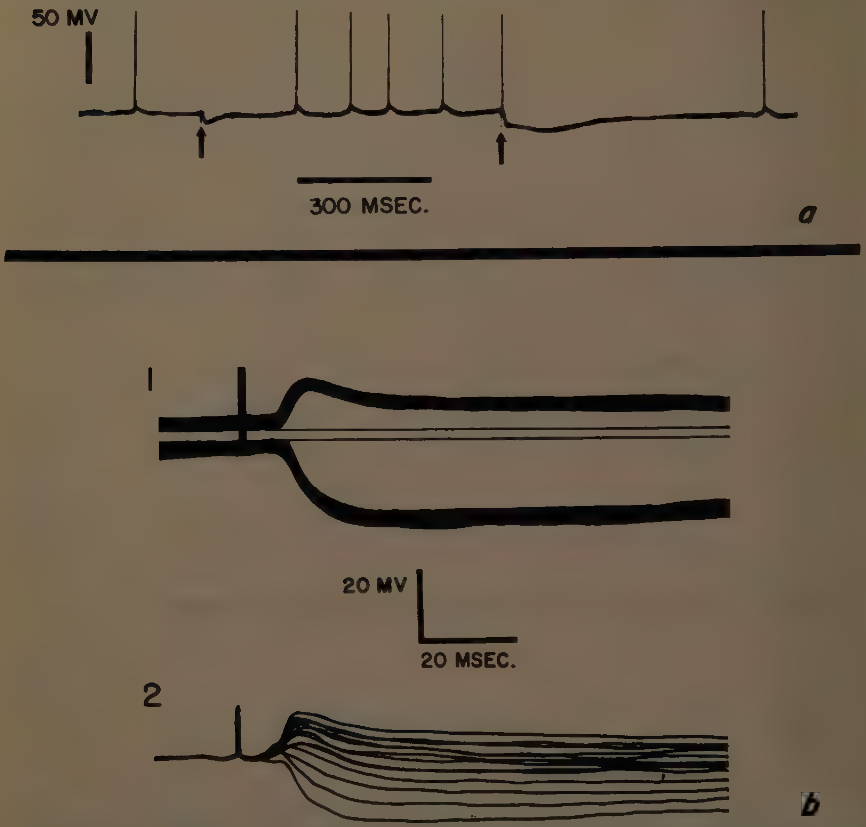

FIGURE 6. IPSPs in an identified pyramidal cell. The spontaneous firing (*a*) of a pyramidal cell is interrupted by a first weak shock to the fornix, which produces a small IPSP. The second, stronger, shock triggers an antidromic spike and a larger and longer-lasting IPSP. The inversion of a hyperpolarizing to a depolarizing PSP, using a KCl electrode, is shown in *b*. Trace 1 indicates the initial PSP before inversion (*lower*) and the final PSP after inversion (*upper*). Trace 2 shows the sequence of inversion with superimposed fine line tracings.

The inversion of the IPSP by the diffusion of Cl^- into the cell is of particular interest because it clearly demonstrates the existence of inhibition by chemical transmission at this pyramidal cell synapse.[14,24]

Since the fornix carries both afferent and efferent fibers (FIGURE 7*a*, top), experiments were performed in animals with deafferented fornices to determine whether the IPSP represents orthodromic (direct) or antidromic (collateral) inhibition. Deafferentiation was accomplished by operative section of the fornix and commissure. Degeneration of the afferent fibers occurred within 10 days. The fornix was then a purely efferent pathway comparable to a

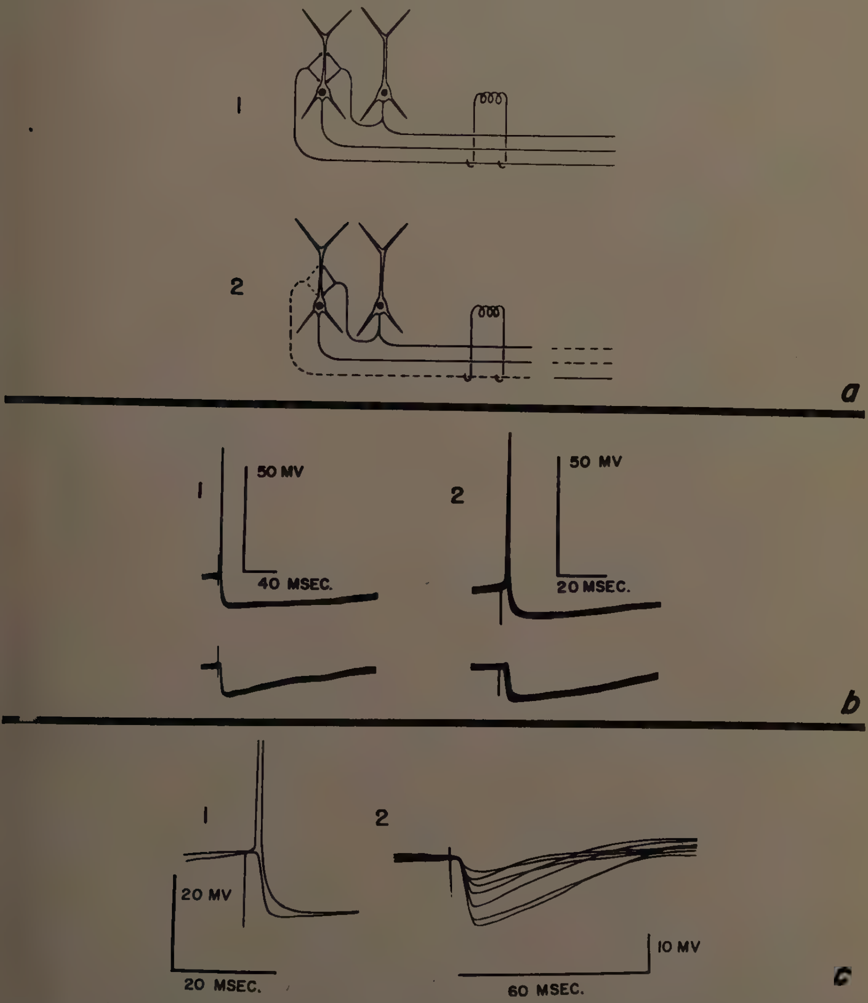

FIGURE 7. Schematic representation (*a*) of the afferent, efferent, and recurrent collateral fibers in the intact (diagram 1) and the deafferented (diagram 2) fornix. In *b* are shown antidromic volleys in the intact (1) and deafferented (2) fornix. The upper traces in 1 and 2 illustrate the antidromic spike and the afterhyperpolarizations. The lower traces, produced in each case by a weaker fornix volley, demonstrate the IPSPs in isolation. The IPSPs following stimulation of the deafferented fornix are shown in *c*. Group 1 is a superimposed tracing of antidromic spike and subthreshold volley to the fornix, illustrating that the onset of the IPSP occurs *during* the antidromic spike. Group 2 is a family of IPSP tracings at different stimulus strengths. Note that latency is relatively independent of stimulus strength.

spinal ventral root (FIGURE 7*a*, bottom). The pyramidal cells are unaffected by fornix deafferentation.[12,45] The details of this procedure and of the anatomical and physiological controls used are described elsewhere.[52]

FIGURES 7*b* (left and right) show an antidromic spike from pyramidal cells in an intact and in a deafferented fornix preparation respectively. In both cases the spike was followed by a hyperpolarization that persisted when the stimulus was reduced below the threshold for the axon of the impaled cell. Since they persist in the absence of a spike, the hyperpolarizations in each case are clearly PSPs and not afterpotentials. Latency, time course, and magnitude of the IPSPs are similar. This indicates that stimulation of the antidromic pathway is capable of activating a powerful system of collateral inhibition.

The latency of the IPSP to stimulation of the deafferented fornix was consistently brief. When preceded by an antidromic spike, the IPSP began during the course of the action potential, thus distorting its descending limb and masking its depolarizing afterpotential (FIGURE 7*c*, left). The latency was relatively independent of stimulus strength. The family of IPSPs traced in FIGURE 7*c* (right) represents responses from the same cell at different stimulus intensities. These latency measurements suggest that the IPSPs represent activity in nearby, rather than remote, collaterals.

When repetitive stimuli at frequencies of 10 to 60 per second were delivered to the deafferented fornix, intracellular recordings consistently showed prolonged and sustained hyperpolarization associated with cessation of spike generation. The hyperpolarization lasted as long as the tetanus was maintained (FIGURE 17, lines 1 and 2).

The early EPSP observed with volleys to the intact fornix was not noted upon either single or repetitive stimulation of the deafferented fornix. This finding suggests that the EPSP is mediated by fornix afferent fibers.

It seems reasonable to ascribe the intracellularly recorded steady voltages, which occur upon repetitive stimulation of the fornix, to the superimposition and summation of individual PSPs. Such summation, which implies the absence of refractoriness, has been seen in a wide variety of preparations[24] and is a mode of neuronal operation closely analogous to that seen in response to natural stimuli. The polarity of this intracellular DC shift depends upon whether EPSPs or IPSPs are superimposed.[52]

These electrophysiological data, which demonstrate the existence of powerful synaptic inhibitory effects due to the selective stimulation of fornix efferent collateral axons, are consistent with the anatomical studies of Cajal[7] and Lorente de Nó.[38] These studies indicate that the fornix carries predominantly efferent fibers and that most of these axons give off recurrent collaterals within the hippocampus. The recurrent collateral axons form two massive systems, the Schaffer (transverse) collaterals that relate the fields of various segments of the hippocampus, and the longitudinal (axial) collaterals that associate different segments of the hippocampus.

While the function of this hippocampal inhibitory feedback system is obscure, its role in both normal and abnormal (*vide infra*) behavior of the hippocampus must be taken into consideration in any theoretical treatment of this structure. The general importance of inhibition in the integrative function of the spinal cord has long been appreciated,[48] and the occurrence of both direct and recurrent inhibition has now been exceedingly well documented.[14] The existence of comparable and perhaps even more powerful inhibitory systems in cortical and subcortical nuclei has only recently become evident.[1,6 35,41,44,47]

Steps in the Production of the Hippocampal Neuron Spike

We shall first consider the pattern of sequential two-step invasion familiar from the study of the motoneuron.[2,14,19,22,39]

Following antidromic, orthodromic, or intracellular stimulation, the spikes of hippocampal neurons manifest an inflection on the rising phase of the action potential similar to that seen in motoneuron spikes. Following the notation introduced by Fuortes *et al.*,[22] the small action potential will be designated as the *A* spike, the large one as the *B* spike, and the total complex as the *AB* spike. Similarly, the areas giving rise to each of these spikes will be denoted *A* and *B* respectively.

This break in the ascending limb of the action potential was most clearly evident when two antidromic shocks were used and the stimulus interval gradually decreased (FIGURE 8). After an interval of 14 msec. the break in the ascending limb was more pronounced in the test than in the conditioning response (uppermost trace). At a critical firing interval of 12 msec., the *B* spike failed to fire and the isolated *A* spike was unmasked (second trace). In order to estimate the contribution of field potentials generated in the volume conductor by activity in neighboring cells, a subthreshold shock was delivered and the "outside" potential recorded (third trace). This potential was then algebraically subtracted from the spikes of the second trace to obtain a more accurate record of their time course (lowest trace).

The *AB* break of the pyramidal cell spike can also be emphasized by differentiating the action potential with respect to time.[19] FIGURE 9 shows the behavior of a cell following antidromic, orthodromic, and direct activation. The simultaneously recorded electrical derivatives appear below the action potentials. All three derivatives show a break marked by the arrow. This is most pronounced in the antidromic record (see also FIGURE 14*b*). Similar breaks were observed in spontaneously occurring spikes.

Sequential invasion with different modes of activation, similar to that seen in the pyramidal cell, has been demonstrated in a variety of neurons.[2,4,5,10,11,14,16-19,27,39,43,44,53,55,56]

The evidence is strong, albeit indirect in the motoneuron,[8,22,55,56] that the *A* area is located in the axon and that its low threshold (10 mv), compared to the *B* area (30 mv), makes it the trigger zone of the neuron.* Eccles has suggested[14] that the *A* area is in the axon hillock and initial segment and the *B* area is in the soma-dendritic membrane; this separation of the trigger zone from soma and dendrites has functional significance; an impulse that could be generated anywhere over the soma-dendritic membrane would favor the action of strategic groupings of excitatory synapses and could lead to a breakdown of the integrative function of the neuron.

* For three particularly elegant documentations of this point in isolated peripheral neurons see Bennett,[4] Edwards and Ottoson,[18] and Tauc.[55]

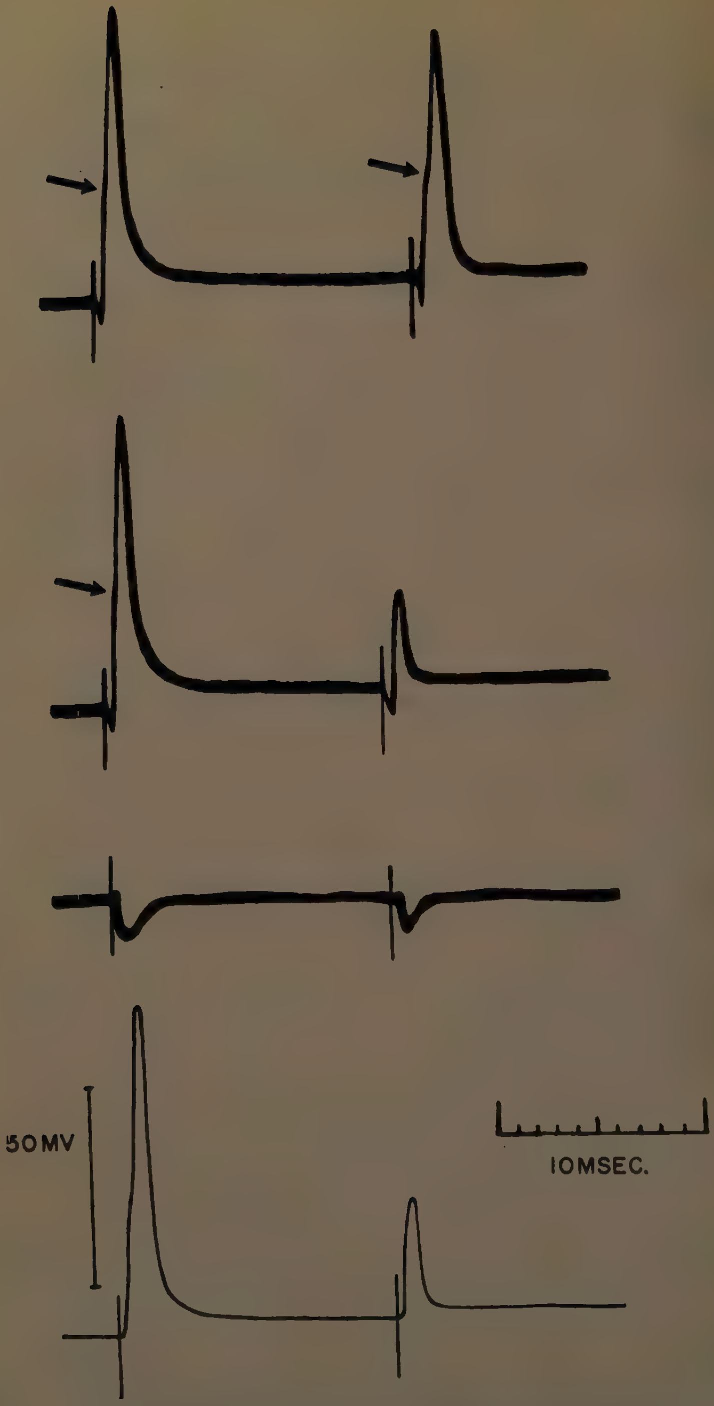

Figure 8. An intracellular recording from a pyramidal cell showing two steps in the production of the antidromic spike, as revealed by the two-shock technique (see text for details). The third tracing shows a recording made when the stimulus intensity was subthreshold for the axon of this cell and represents the contribution of neighboring cells to the recorded potential. The bottom tracing is an algebraic summation of the second and third tracings and reveals more accurately the configuration and time course of the spikes.

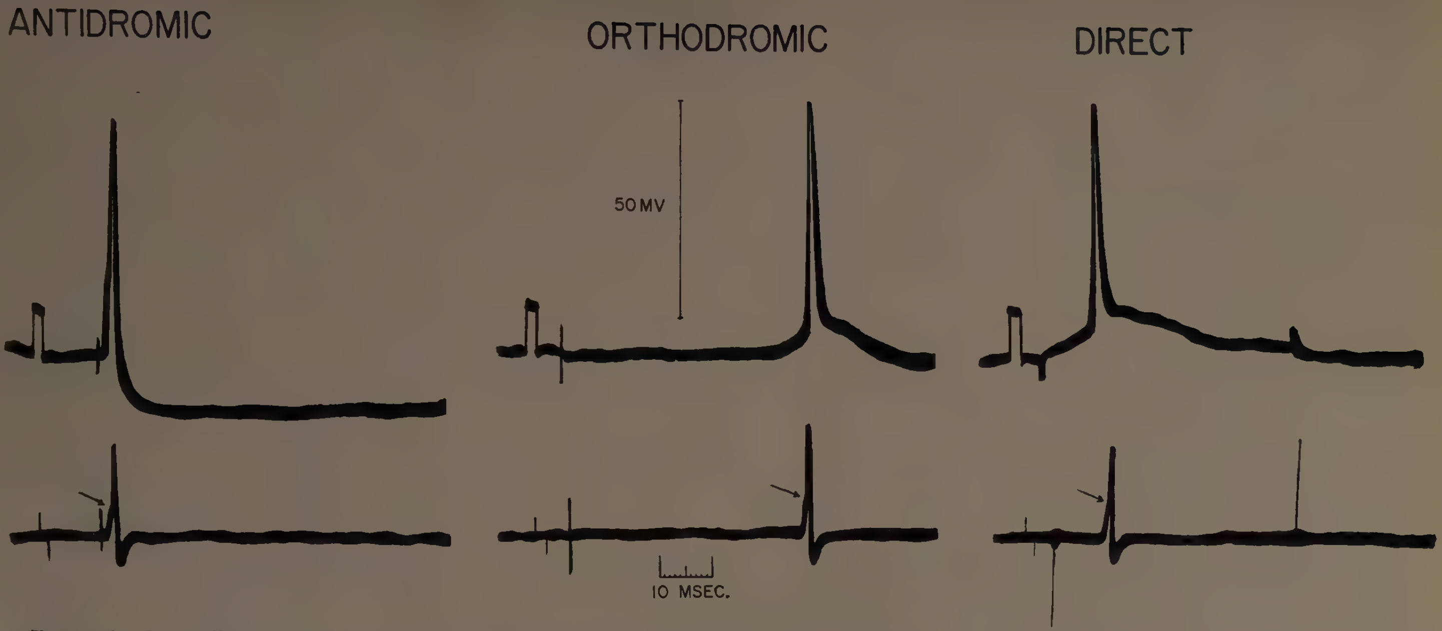

FIGURE 9. Intracellular recording from a hippocampal pyramidal cell activated via three different routes: antidromic (fornix); orthodromic (subiculum); and direct (intracellular stimulation by passing current through a microelectrode). The upper traces are DC recordings of the action potentials; the lower traces are simultaneously registered, electrically differentiated records of each action potential. There is an inflection, indicated by an arrow, on the rising phase of the three differentiated records. The time constant of the differentiating circuit was 1 μsec.

The finding that impulse initiation usually occurs in the *A* area with different modes of activation prompted an investigation of the firing level of hippocampal neurons. If certain generally accepted assumptions* are valid for the pyramidal cell, the firing level should be constant with different modes of activation. This, in fact, was the case in 75 per cent of the units studied.[50] Again, this finding is essentially similar to that presented by Frank and Fuortes[21] and by Eccles[14] for the motoneuron and suggests that in archicortical neurons, as well, impulse initiation occurs when the trigger area membrane is depolarized to a critical firing level. It is therefore unnecessary to postulate any additional mechanisms for impulse initiation.

In 25 per cent of the hippocampal neurons studied, a more complex process underlying impulse initiation occurs that reveals a significant difference from the general pattern described. The unique additional feature is the presence of a third step immediately preceding the development of the *A* spike. This intermediate depolarizing step has been called a fast prepotential (FPP) to distinguish this fast step from the slow graded (synaptic) potentials that usually precede the *A* spike. Evidence will be presented to the effect that this step is an all-or-none spike generated within the dendritic tree of the neuron. This spike represents the activity of another trigger zone that permits the depolarizations generated within the remote dendritic portions of the neuron to affect the *A* area, the final common trigger zone.[51]

FIGURE 10 illustrates spikes showing typical fast prepotentials. The discontinuity between the FPP and the rest of the spike is indicated by arrows. This break is more constant than the level at which the FPP rises out of the graded slow prepotential (FIGURE 10*b*). Note that the FPPs superimpose exactly. The slow prepotentials often appeared in subliminal forms, but the FPPs were always associated with full-blown spikes except in obvious injury discharges. To accentuate the discontinuity between the FPP and the rest of the spike, weak hyperpolarizing currents were passed through the microelectrode during spontaneous activity (FIGURE 10*c*). When a spontaneous discharge occurred during this pulse, it often showed a slightly more pronounced break and occasionally the FPP could, in this manner, be disclosed in isolation (see FIGURE 12). While FPPs frequently became evident during injury, many of the units exhibiting them were among the most stable in our series and least suspect of injury. Although the FPP was constant in its dimensions in a given unit, as shown in the superimposed tracings of part *b* in FIGURE 10, there was considerable variability between different cells. Because of this variability we are making an explicit assumption that the FPP represents qualitatively the same kind of potential change in all cells.

Units that were fired by a FPP frequently were also triggered by a slow prepotential. In these circumstances both the slow and the fast prepotentials reduced the membrane voltage to the same critical firing level (as shown in FIGURE 14*a*).

Attempts were made to determine whether an *AB* inflection also occurred in

---

* The assumptions are as follows: (1) the recording electrode is located in the soma; (2) the recorded soma potential changes reflect potential changes in the *A* area; and (3) impulse generation occurs when the membrane of the *A* area is depolarized to a critical level regardless of the source of the excitatory current.[14,21]

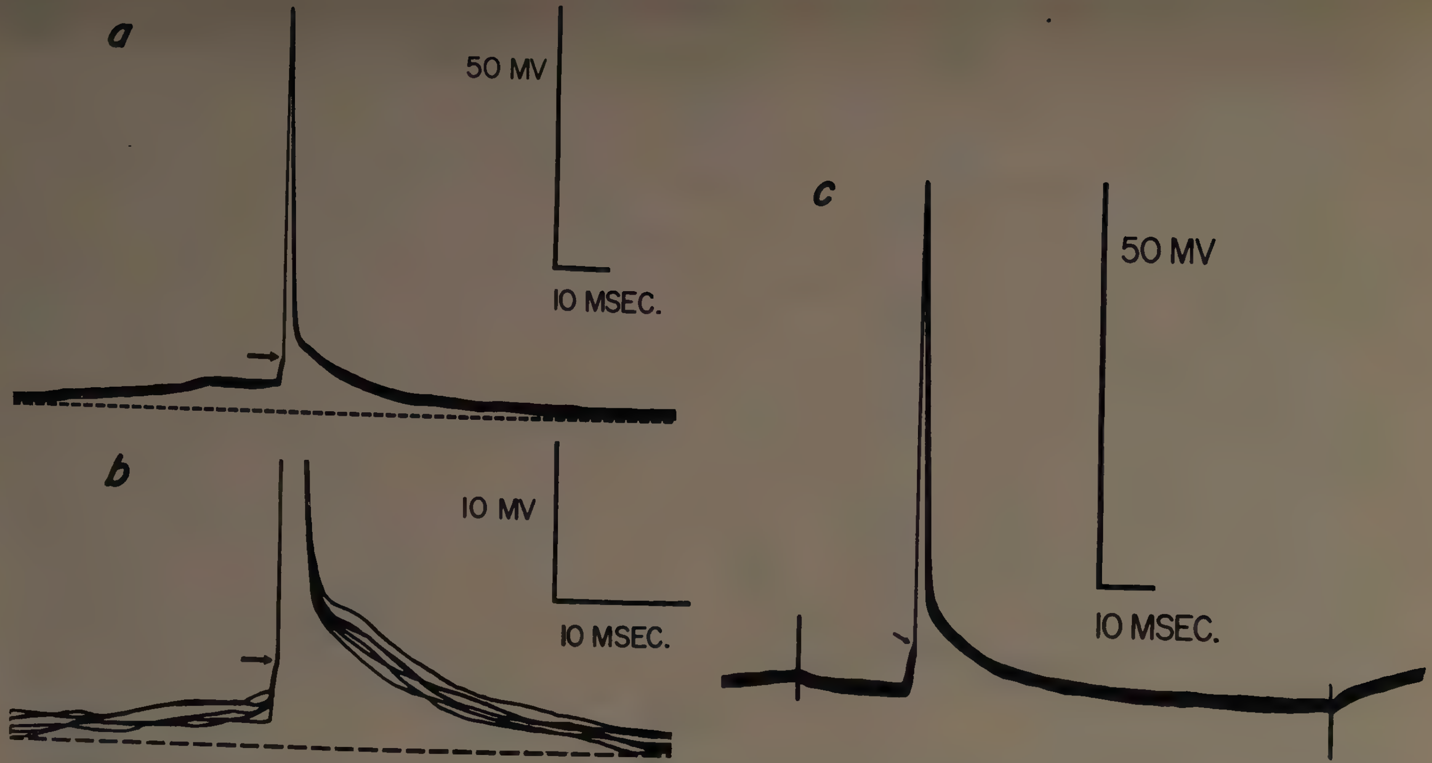

FIGURE 10. Examples of FPPs occurring in spontaneous discharges. Groups *a* and *b* show spikes preceded by slow depolarizations (slow prepotentials) and initiated by abrupt depolarizations called fast prepotentials (FPPs). The break between the latter and the rest of the spike is indicated by an arrow. The superimposed tracings in *b* indicate that the FPPs superimpose exactly but that the slow prepotentials do not. The discontinuity (*c*) between the FPP and the rest of the spike (arrow) is accentuated by a weak hyperpolarizing pulse (1 to 3 × 10^{-10} amp.). Unidentified unit.

those spikes that exhibited a fast prepotential. FIGURE 11 illustrates the existence of such an *AB* break.

FIGURE 12 illustrates FPPs revealed in isolation by passing hyperpolarizing pulses during spontaneous discharges. To the right, the time course of these isolated FPPs is indicated by the solid line with long dashes at the end. The last part of the line is dashed because of the uncertainty in judging the baseline on which these small prepotentials ride. The dotted line in part *c* depicts approximately what the falling phase of the FPP would be if it occurred purely as a passive restitution of membrane potential. This is the average value of the membrane time-constant for this cell, as determined by bridge unbalance. Note that the early falling phase of the FPP is considerably more rapid than purely passive decay, as measured by our technique.*

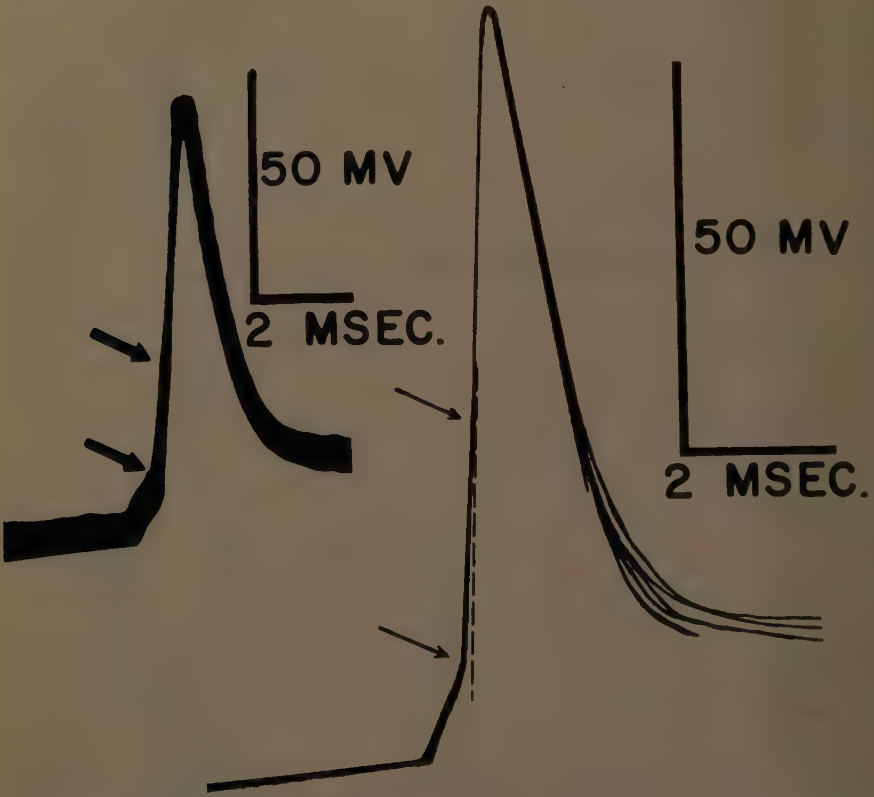

FIGURE 11. Presence of an *AB* break (*upper arrows*) in association with an FPP (*lower arrows*). The baseline (indicated by the dashed line) is diagonal, because this is a record of a horizontal sweep made on moving film. The superimposed tracings are shown to illustrate the change in slope of the rising phase more clearly. Unidentified unit.

---

* This argument is weakened by the fact that the time-constant measurements were made with pulses that lasted longer (4 to 100 msec.) than the FPP (<2 msec.). The passive decay of the potential following a very brief current pulse might indeed be more rapid than indicated

FIGURE 13 shows the same unit discharged both by a depolarizing intracellular pulse (top record in part *a*) and as a rebound to hyperpolarizing pulses (second and third records in part *a*). It was not possible to identify an FPP in either of these two upper responses. In the bottom record, the FPP of a rebound spike is made evident by virtue of the refractoriness engendered by a spontaneous discharge occurring just before the "off" of the pulse. Data such as these suggest that the FPP may sometimes appear in an occult form under conditions that favor rapid development of the full spike without obvious delays. Part *b* of FIGURE 13 illustrates cases in which an FPP was evident in rebound discharges following hyperpolarizing pulses, during which there were no spontaneous discharges. The intensity of the hyperpolarizing current was varied by small increments near the threshold for rebound excitation. Note that the FPP does not appear in any form that is subliminal for full spike generation and that, when elicited, the FPPs have uniform slope and uniform inflection with the rest of the spike.

There are, therefore, several observations that suggest that the FPP is generated by an electrically excitable membrane somewhere within the impaled neuron: (1) FPPs appeared in an all-or-none manner as a rebound to intracellularly applied currents, which are generally assumed to be effective only on the impaled cell[14,21]; (2) FPPs never appeared at amplitudes that were subliminal for spike generation; and (3) FPPs in a given unit always exhibited constant slope and inflection with the rest of the spike.

The location of this responsive membrane now becomes of considerable interest. Experiments using antidromic volleys, an example of which is illustrated in FIGURE 14, gave a partial answer to this question.

The top line of FIGURE 14*a* shows three spikes: (1) a spontaneous discharge; (2) an antidromic spike to stimulation of the fimbria; and (3) a spike arising out of the late phase of the IPSP generated by the fimbrial volley. In the second and third lines, spikes 1 and 3 are progressively enlarged to facilitate comparison between them. Note that spike 1 was generated when the slow prepotential reached the firing level indicated by the horizontal line. Note also that this same firing level was achieved in the initiation of spike 3 but that, in this case, it was accomplished by a fast prepotential. The FPP itself was initiated at a level of depolarization nearly 10 mv below the usual firing level. In part *b* the same unit is displayed in such a way as to reveal the AB break with both direct and antidromic activation. The bottom tracings are corresponding derivative records that accentuate the break. *Note especially that there is nothing corresponding to a fast prepotential in the antidromic spike.* It was impossible to detect a discontinuity suggestive of a fast prepotential on any antidromic spikes using either the two-shock technique or superimposed hyperpolarizing pulses.[14,19,20,22,32,39]

The failure to demonstrate the FPP in response to antidromic volleys makes it unlikely that the FPPs arise from the axon, as does the M spike in the moto-

---

by the dotted line in FIGURE 12. Conversely, spatial considerations tend to strengthen the argument that the early falling phase of the FPP is too rapid to represent a purely passive restitution of the membrane potential, since the FPP is most likely generated some distance from the soma while the current pulse is applied through an intrasomatic electrode (see Spencer and Kandel[50] for detailed discussion).

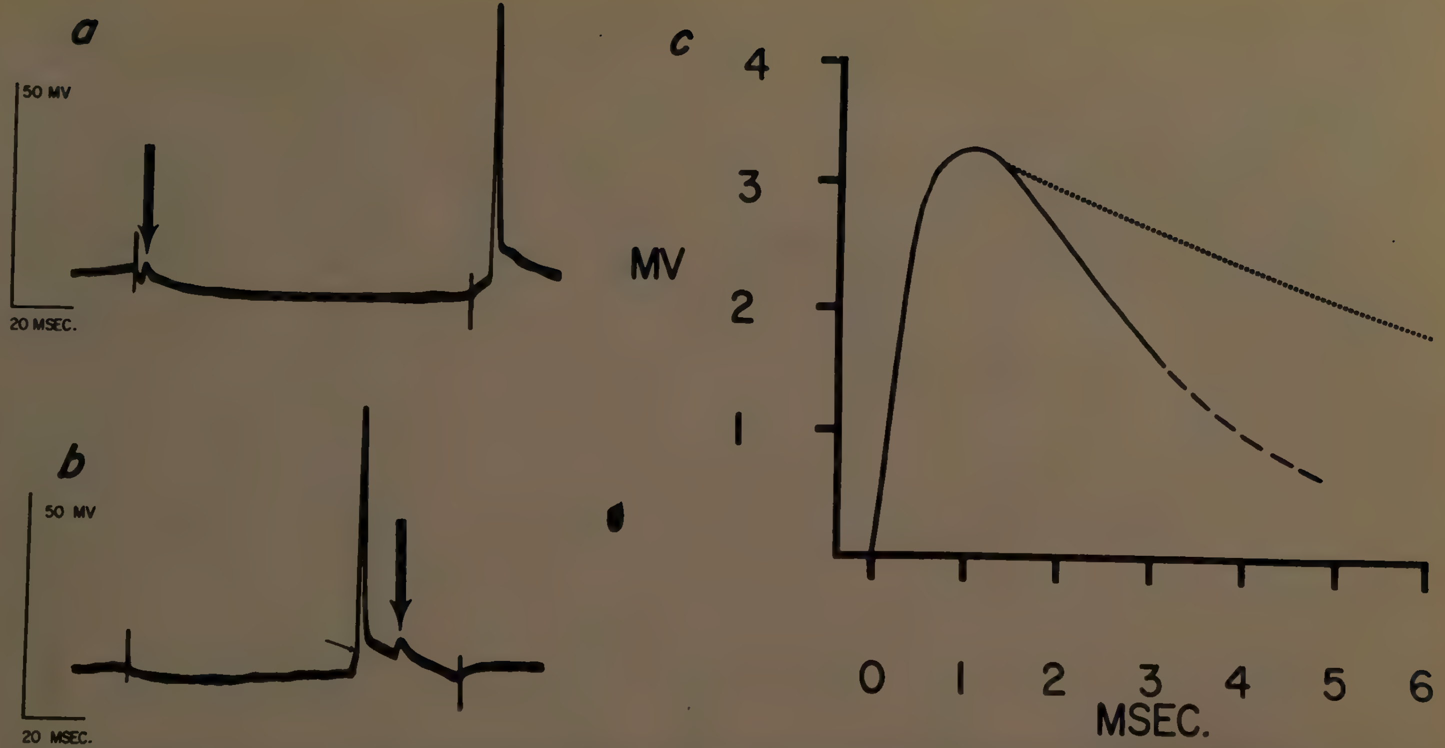

FIGURE 12. Isolated FPPs occurring spontaneously during passage of weak hyperpolarizing currents (approximately 1 to 5 × 10^{-10} amp.). The isolated prepotentials are indicated by large vertical arrows. The FPP associated with the spike in *b* is indicated by the diagonal arrow, while no FPP was evident in the rebound spike (*a*). The graph (*c*) shows the estimated time course of isolated FPP (solid line with long dashes at its end). The dotted line (*above*) shows what the falling phase of the FPP would be if it represented a purely passive restitution of the membrane potential. Unidentified unit.

neuron, for example.[14] Conditions during antidromic activation are, if anything, much more favorable for disclosing an M spike than those that prevail during orthodromic activation, yet the FPP was not seen with the former but was seen with the latter. The small amplitude of the FPP and the fact that it can be generated during soma hyperpolarization (FIGURES 12, 14, and 15) make it unlikely that the FPP arises within the soma. Therefore, by a process of elimination, it appears that the most likely site of origin of the FPP is neither in the axon nor in the soma, but probably at some point within the dendritic tree of these cells. Because of the small amplitude of the FPPs, however, it must also be postulated that these responses block before conducting to the soma.

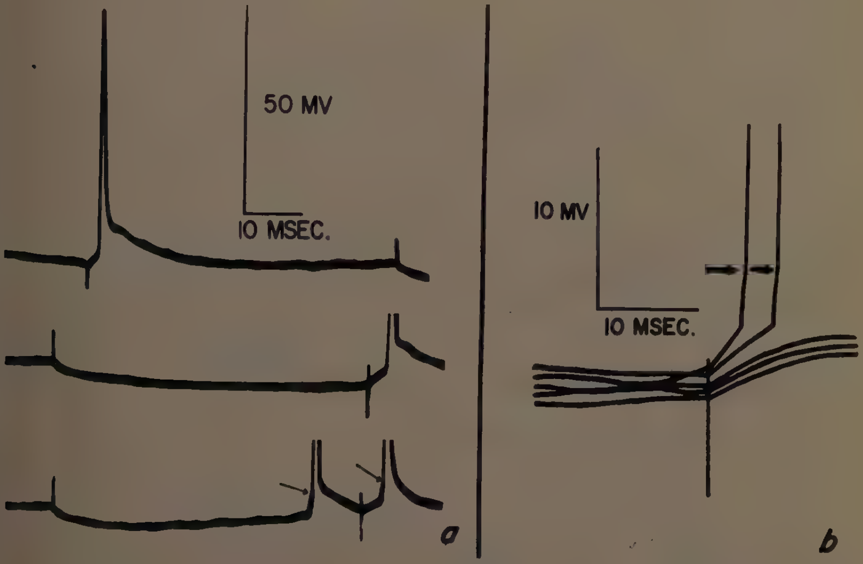

FIGURE 13. (*a*) Spikes generated by a depolarizing intracellular pulse (*top record*) and as a rebound to hyperpolarizing pulses (*lower two records*). The spontaneous discharge occurring during the hyperpolarizing pulse in the third record made the cell partially refractory during the rebound discharge, and this emphasized the break between the FPP and the rest of the spike (indicated by diagonal arrow). The current strength was approximately 3 to 5 × 10^{-10} amp. (*b*) Tracings of the FPPs occurring as a rebound to the hyperpolarizing pulses of "threshold-straddling" intensity. Note the all-or-none characteristics of the FPP. Unidentified unit.

Attempts to localize more precisely the site of generation of the FPPs within the dendritic tree are illustrated in the following series of experiments. FIGURE 15 shows an FPP arising in response to orthodromic subiculum volleys. Part *a* of this figure illustrates orthodromic volleys evoked during the passage of weak hyperpolarizing current. Trace 1 is a complex diphasic synaptic potential elicited by a single shock to the subiculum. In trace 2, a spike produced by a slightly stronger shock is shown. The arrow is directed toward an inflection on the rising phase of the spike. As is evident in the superimposed fine line tracings of trace 3, the level of this inflection is considerably above the crest of the synaptic potential produced by the subliminal shock. It is presumed, therefore, that the inflection indicates the presence of a fast prepotential. It was possible to strengthen this inference by utilizing stronger hyperpolarizing currents and varying the strength of the subiculum shock to elicit the fast prepotential in isolation, as shown in trace 2 of part *b*. The strong hyperpolarizing pulses that were necessary (about 1 × 10^{-9} amp.) produced considerable distortion of the baseline. The prepotential corresponds to the inflection on the full spike indicated by the arrow in trace 3*b* and in the superimposed fine

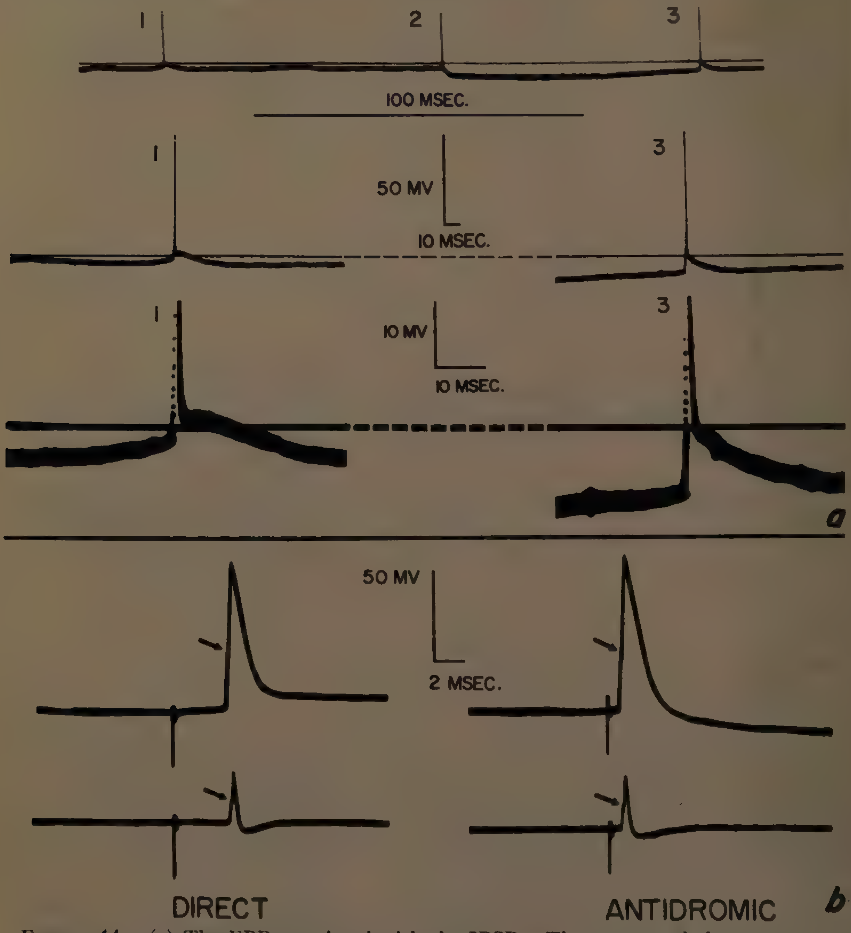

FIGURE 14. (*a*) The FPP associated with the IPSP. The top record shows a sequence of three spikes. The first is a spontaneous discharge not associated with an FPP, the second is an antidromic response to fornix shock, and the third is a discharge occurring during the late phase of the IPSP that follows the antidromic spike. This third discharge is initiated by an FPP. The second and third line in *a* show progressive enlargements of spikes 1 and 3. See the text for further details.

(*b*) Direct (*left*) and antidromic (*right*) responses of the same unit. Note the presence of an *AB* break, but the absence of FPP in both records. Identified unit.

line tracings of trace 4*b*. Note that the fast prepotential isolated in this way exhibits a time course similar to that shown in FIGURE 12.

The fact that subiculum volleys, which presumably would involve activity in the perforant pathway, did evoke short latency FPPs favors the notion that

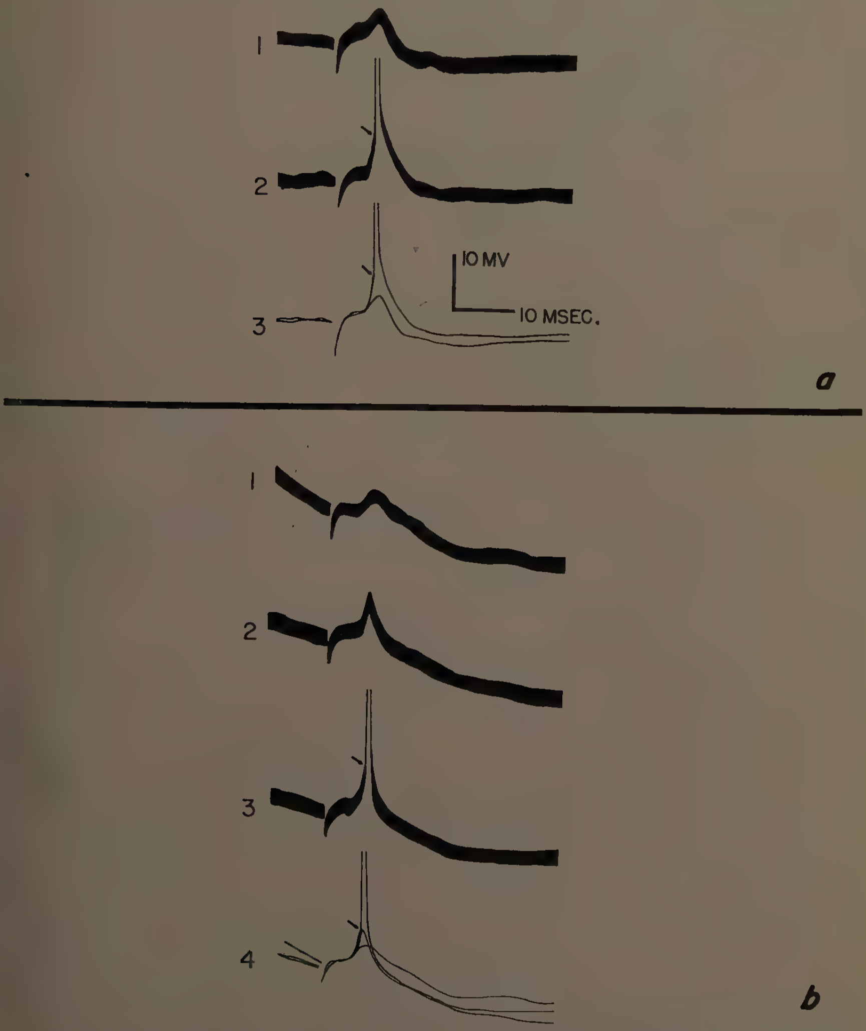

FIGURE 15. Orthodromic production of an FPP following a single shock to the subiculum. Trace 1 in *a* shows the complex diphasic subliminal synaptic potential; trace 2 shows the orthodromic spike with the FPP indicated by the diagonal arrow; and trace 3 shows fine line superimposed tracings of the first two traces. Traces 1 to 4 in *b* show orthodromic responses similar to those in *a*, but produced during passage of strong (approximately 10^{-9} amp.) hyperpolarizing current, which distorts the baseline. Traces 1 and 3 are analogous to traces 1 and 3 in *a*, but trace 2 in *b* shows the FPP riding in isolation on top of the synaptic potential. Trace 4 (*b*) shows the fine line superimposed tracings of the first three lines in *b*. Identified unit.

the FPPs arise within the *apical* dendritic tree, since this is the first point of impingement of this hippocampopetal system.

As may be appreciated by comparing FIGURES 2 and 15, there is a great variability in the latency and configuration of the PSPs generated in response to stimulation of the subiculum. These variations depend upon the site of stimulation and the stimulus parameters. Although all shocks to the subiculum probably excite the perforant pathway, this pathway engages several complex intrahippocampal circuits that, in turn, may produce pyramidal cell discharge.[38] Probably only the shortest latency responses, such as those in FIGURE 15 represent activity produced directly by the perforant pathway upon apical dendrites.

In his studies of dendritic structure in neocortical pyramidal cells, Sholl[49] has treated the apical and basilar dendrites as two separate systems converging upon the main bifurcation of the apical dendrite and soma respectively. Golgi stains of hippocampal pyramidal neurons suggest an even more clear-cut division into two separate dendritic systems.[7,38] It has been suggested by Eccles[14] that the main apical dendritic bifurcation would be a particularly favorable location for dendritic spike production since PSPs generated on the dendritic branches would electrotonically summate at this bifurcation. In suggesting this mechanism for the production of FPPs in hippocampal neurons, it is also necessary to postulate that the spike does not conduct regeneratively all the way down the main dendritic shaft to the soma, since the prepotential is of small amplitude and is not blocked by hyperpolarizing currents sufficient to block the rest of the spike (FIGURE 12). It seems reasonable to suggest that the prepotential represents a spike localized to a rather restricted portion of the dendritic tree at some distance from the soma.

In FIGURE 16 an attempt has been made to represent diagrammatically a possible functional role for the FPP. It is proposed that the neuron have two loci, the *A* area and the main apical dendritic bifurcation, which serve as trigger zones for the basilar and apical dendritic systems respectively. The FPP is presumed to represent the electrical response of the bifurcation trigger zone, which thereby behaves as a booster zone for the more distal dendritic synapses. In this scheme the slow prepotentials that precede the fast prepotential (FIGURE 15) would represent primarily electrotonically propagated apical dendritic PSPs or graded responses, casually antecedent to the FPPs. The FPP would trigger the *A* area, the final common trigger zone, which, in turn, would initiate axon discharge and the retrograde invasion of the *B* area. This would provide a means whereby distant dendritic synapses might cause neuronal discharge even when the soma was hyperpolarized (FIGURES 12, 14, and 15). Since firing level was relatively constant and FPPs were absent in about 75 per cent of hippocampal units studied,[50] the basilar system probably predominates more often under the conditions of our experiments and initiates impulses by critically depolarizing the axon hillock.

In summary, the motoneuron model can be fairly successfully applied to an archicortical neuron, the hippocampal pyramidal cell. As in the motoneuron, excitation occurs by a depolarization to a critical firing level and inhibition by a Cl^- sensitive hyperpolarization. An *AB* break can be demonstrated in the hippocampal neuron with all three modes of activation, suggesting a sequential pattern of spike generation similar to that of the motoneuron. Finally, both neurons engage a system of inhibitory recurrent collaterals. There are, also, several important differences. The DAP and FPP of hippocampal cells have not been encountered in the motoneuron.* The afterpotential contributes importantly to the distinctive repetitive firing pattern of the pyramidal cell. The FPP offers an additional degree of freedom in the sequence of steps that produce the pyramidal cell spike; this further complexity seems well suited to the particular geometry of the archicortical neuron dendritic system.

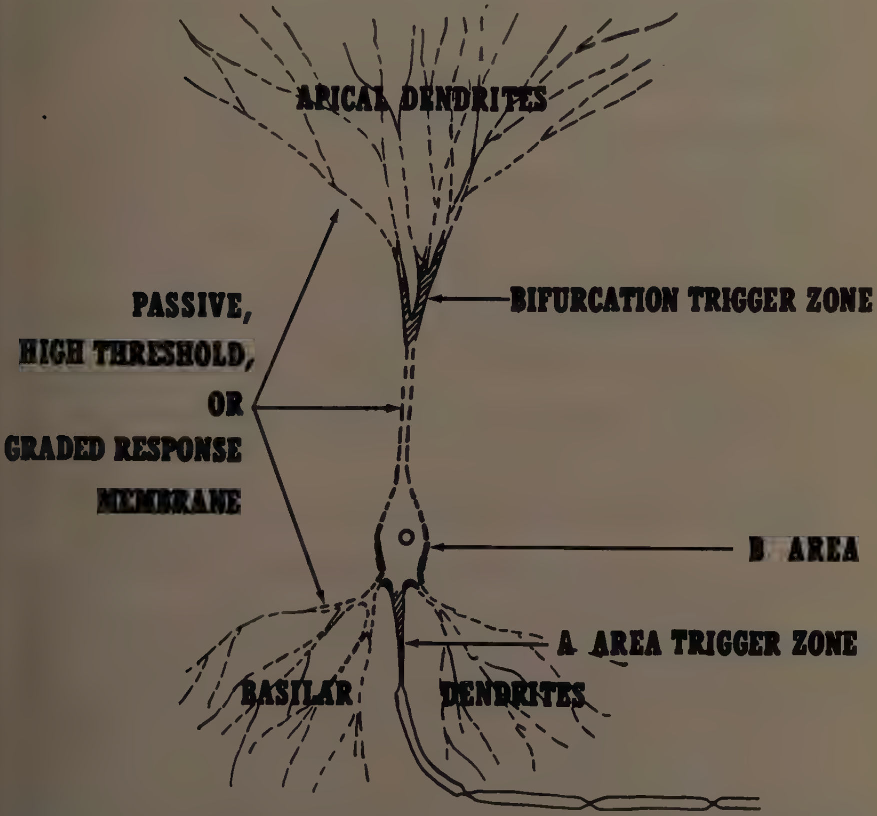

Figure 16. A hypothetical scheme to account for data on the fast prepotential (see text for details).

These studies on synaptic potentials and spike generation will now be used as a baseline from which "abnormal" pyramidal cell function can be viewed.

Pyramidal Cell Activity During Hippocampal Seizure

The tendency toward convulsive activity is one of the most interesting and best documented pathophysiological characteristics of the hippocampus. This

---

* Chromatolytic motoneurons[15] do show a dendritic spike that looks much like the FPP.

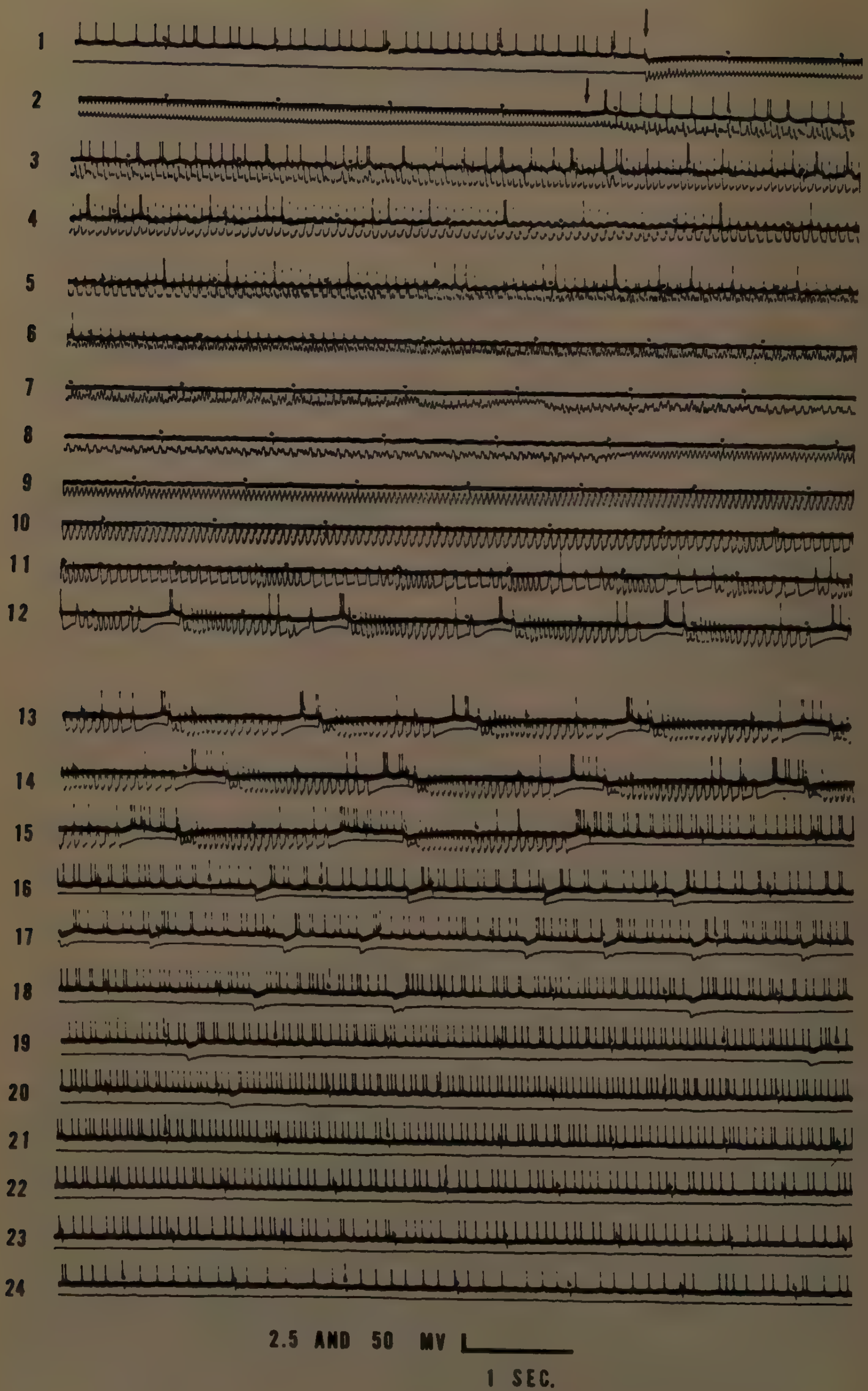
1
2
3
4
5
6
7
8
9
10
11
12
13
14
15
16
17
18
19
20
21
22
23
24
2.5 AND 50 MV
1 SEC.

FIGURE 17.

finding, first demonstrated in the cat,[23,28,29] has now been confirmed in the guinea pig,[37] the dog,[29] the monkey,[33] and man.[36]

Fornix tetanization was used to initiate hippocampal seizure, and pyramidal cell activity was studied in both intact and deafferented fornix preparations. Hippocampal seizure could be produced with equal facility in both preparations. However large differences between these two preparations could be observed at the unit level during seizure.[30]

We shall first consider seizure in the deafferented fornix preparation. FIGURE 17 illustrates a continuous record of one full seizure. The top record in each line is from the intracellular microelectrode, the lower record is from the surface monitor. The calibration pips on the intracellular trace represent a voltage pulse of 10 mv and 20 msec. occurring 1/sec.

A portion of the control record has been included in line 1 to illustrate the spontaneous firing pattern of the pyramidal cell before the seizure. The two arrows, in lines 1 and 2, indicate the "on" and "off" of a 6.4-sec. tetanus. The tetanus produced a membrane hyperpolarization and inhibition of spontaneous firing. Seizure onset was immediately evident in the surface record after the cessation of the tetanus. However, the intracellular record did not, at first, show any significant changes from the control firing of the unit. There was a latency period of several seconds after the end of the tetanus before the membrane potential first began to undergo oscillations that were synchronized with the surface record. These oscillations (lines 3, 4, and 5) were diphasic; their depolarizing peaks occasionally triggered solitary or multiple firing. With the onset of oscillation, the mean membrane potential increased. Unit firing at first decreased and then ceased. For 25 per cent of the total seizure period, the membrane was "clamped" at a hyperpolarized potential that was 10 mv below the critical firing level.

This persistent hyperpolarization was terminated by the appearance of the clonic phase (lines 11 and 12). During this phase every interruption of the surface oscillation was accompanied by a burst of activity in the pyramidal cell.* The cessation of the surface oscillations between clonic bursts became progressively longer and finally persisted. The termination of surface activity, evident in line 15, was associated with a return of steady firing in the pyramidal cell. The occasional interruption of the isoelectric surface record by a negative potential transient (lines 16 to 20) was accompanied by a membrane hyperpolarization with inhibition of spike generation. Firing continued at a higher than control rate for about 30 sec. after the cessation of all surface activity (lines 20 to 23). Finally, in line 24, the unit returned to its resting level.

FIGURE 18 shows several features of this seizure in greater detail. Frames *a* and *b* illustrate the early oscillatory phase of the seizure. Note the good temporal correlation between the surface and the intracellular record. Frame *c*

---

* For variations in the clonic phase, see Kandel and Spencer.[30]

FIGURE 17. The continuous record of a seizure in a deafferented fornix preparation. The top tracing is from the intracellular microelectrode and the bottom record is from the surface monitor. The arrows in lines 1 and 2 indicate the onset and termination of the fornix tetanus. The voltage calibration refers to both the surface (2.5 mv) and the intracellular (50 mv) records. The intracellular record also has a constant-voltage (10 mv) 20-msec. calibration pip that occurs at the rate of 1/sec. See text for details.

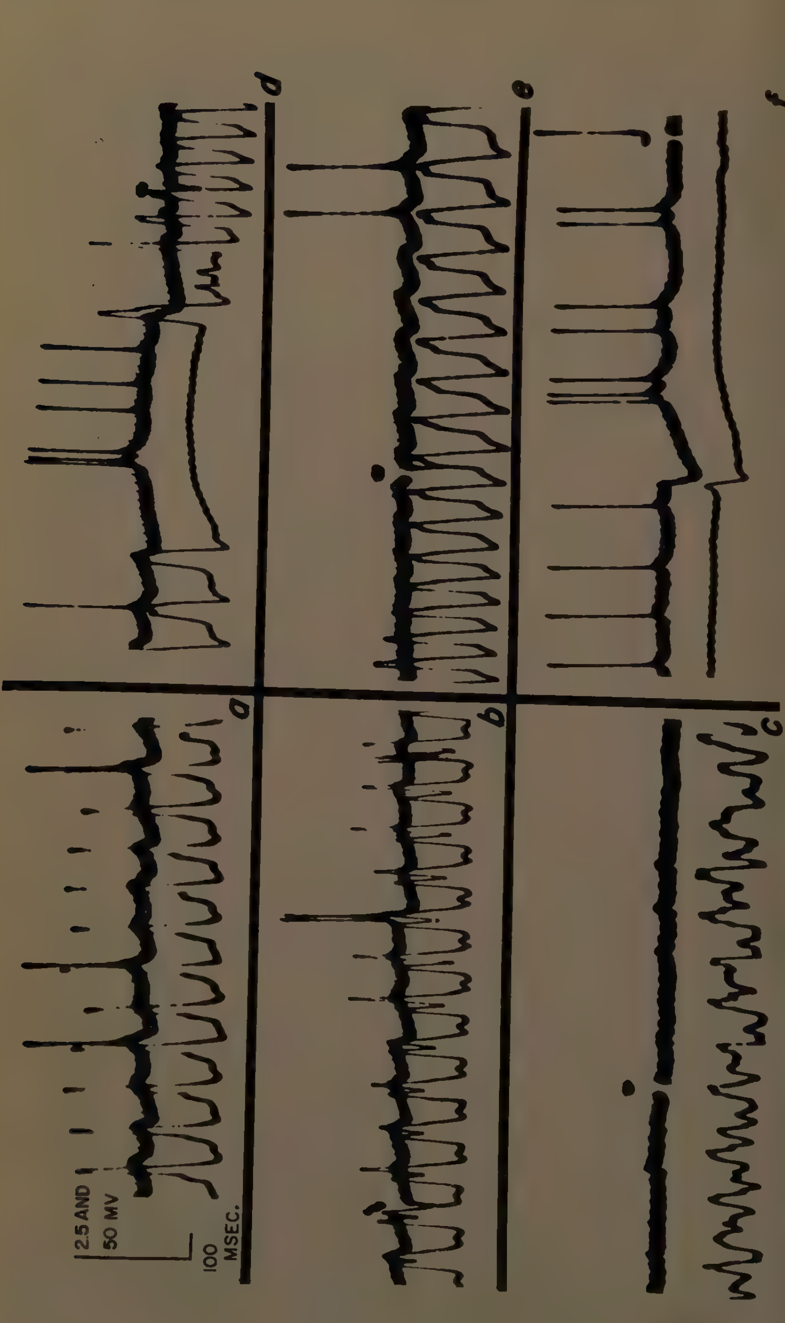

FIGURE 18. Details of the deafferented fornix seizure illustrated in FIGURE 17. Frame *a* is from line 4; *b* is from line 5; *c* is from line 7, *d* and *e* are from line 14 and *f* is from 16.

demonstrates high-frequency surface oscillations and the associated maintained hyperpolarization of the soma membrane. Frames *d* and *e* show a burst and interburst period, respectively, of a clonic phase, and *f* shows the intracellular hyperpolarization that accompanies the surface transient during the final phase of the seizure.

We shall next consider seizure in the *intact* fornix preparation.

Previous experiments have demonstrated that single-shock stimulation of the intact fornix generates an isolated inhibitory postsynaptic potential (IPSP) occasionally preceded by a brief excitatory postsynaptic potential (EPSP). The IPSPs have been attributed to the activity of recurrent collaterals of efferent axons. The early EPSP has been inferred to represent the activity of afferent axons. Although the EPSP is inconstant when single shocks are used, it usually can be demonstrated with tetanic stimulation.

Figure 19 illustrates several of these features. Two rates of tetanic stimulation were used. The first two arrows mark a period of slow tetanization. Each shock gave rise to a brief EPSP and longer-lasting IPSP. The IPSPs added and increased the mean membrane potential. As the slow tetanus continued, the EPSPs increased slightly in amplitude; occasionally they reached the firing level and triggered an action potential. The interval between the second and third arrow indicates a brief tetanus at higher frequency that produced a selective recruitment of EPSPs. The latter, in turn, gave rise to a sustained depolarizing shift that at first plateaued (line 1) and then, after the termination of the tetanus, increased to reach a point 20 mv below the preseizure level (line 3). In addition to this well-sustained depolarization, the membrane began to generate transient depolarizing oscillations immediately following the cessation of the tetanus. The early oscillations produced an occasional clearly recognizable, albeit small, spike. At their peak (line 3) the transient responses depolarized the membrane by another 40 mv, or a total of 60 mv. This summed value of the steady and transient depolarizations approached the amplitude of a full-sized spike. Gradually the oscillations decreased in frequency and, as is evident in line 4, the membrane began to repolarize. As it approached the previous resting level, spike generation was resumed. A period of slight hyperpolarization (lines 4 and 5) followed. Finally, normal spontaneous and evoked responsiveness returned.

As in the deafferented fornix preparation there was good temporal correlation between the surface record and the transmembrane potential. Figure 20 shows a portion of a clonic phase in an intact fornix preparation. R.M.P. represents the mean resting potential (interspike baseline) during the preseizure period. During the later portion of the clonic phase the membrane potential was decreased by 60 mv. Each surface oscillation was accompanied by an intracellular depolarizing transient; each surface interruption of the surface activity was associated with an interruption of the pulsatile transient response of the membrane.

Figure 21 shows selected portions of seizures from two different experiments in the intact fornix preparation. These portions were selected to show the maximum and minimum levels of sustained membrane polarizations achieved during seizures, as well as to illustrate the variations in configuration and amplitude of the transient responses. The latter include three types of responses:

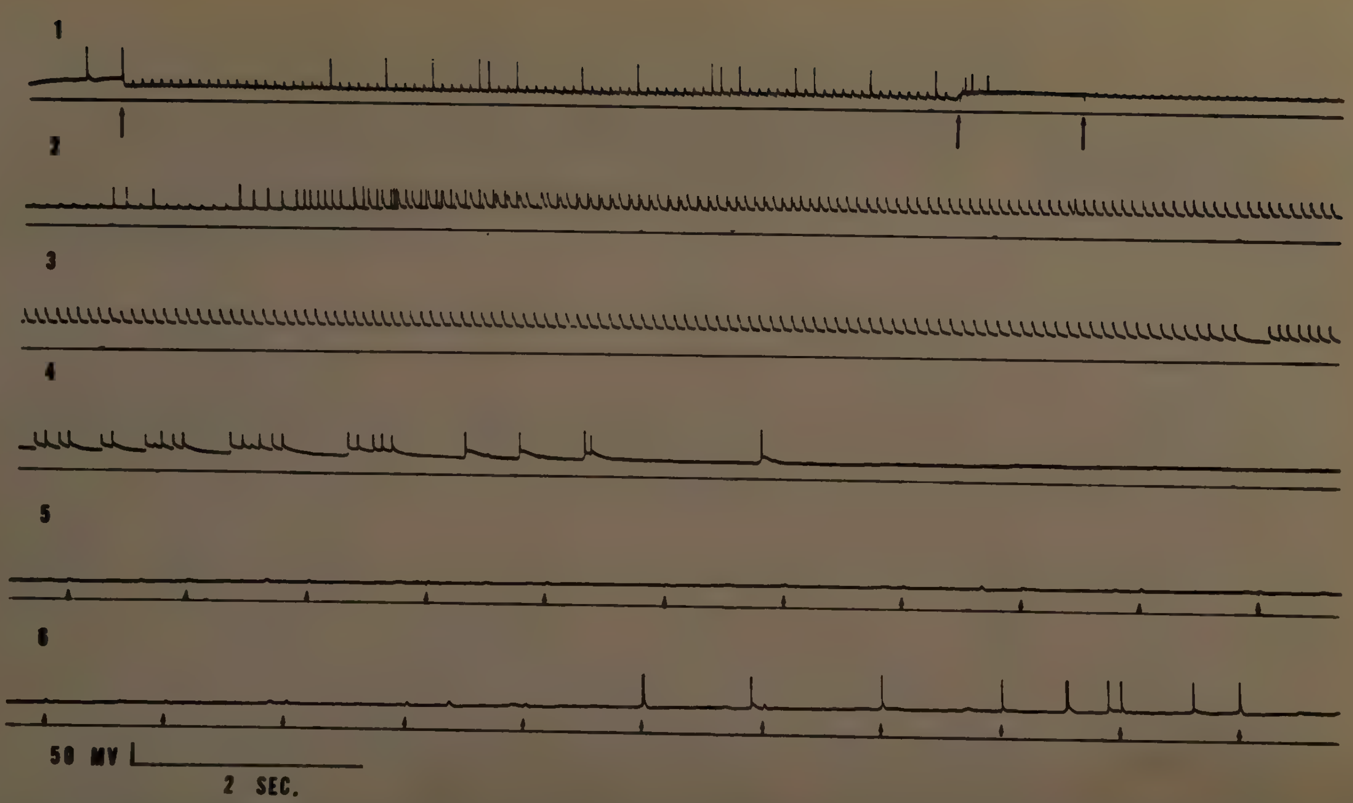

FIGURE 19. Seizure in an intact fornix preparation. The top record in each line is from the intracellular microelectrode and the bottom record is an arbitrary reference baseline. The interval between the first and the second arrows in line 1 indicates the period of slow fornix tetanization, and that between the second and third arrows a period of rapid tetanization. The arrows in lines 5 and 6 indicate single fornix stimuli.

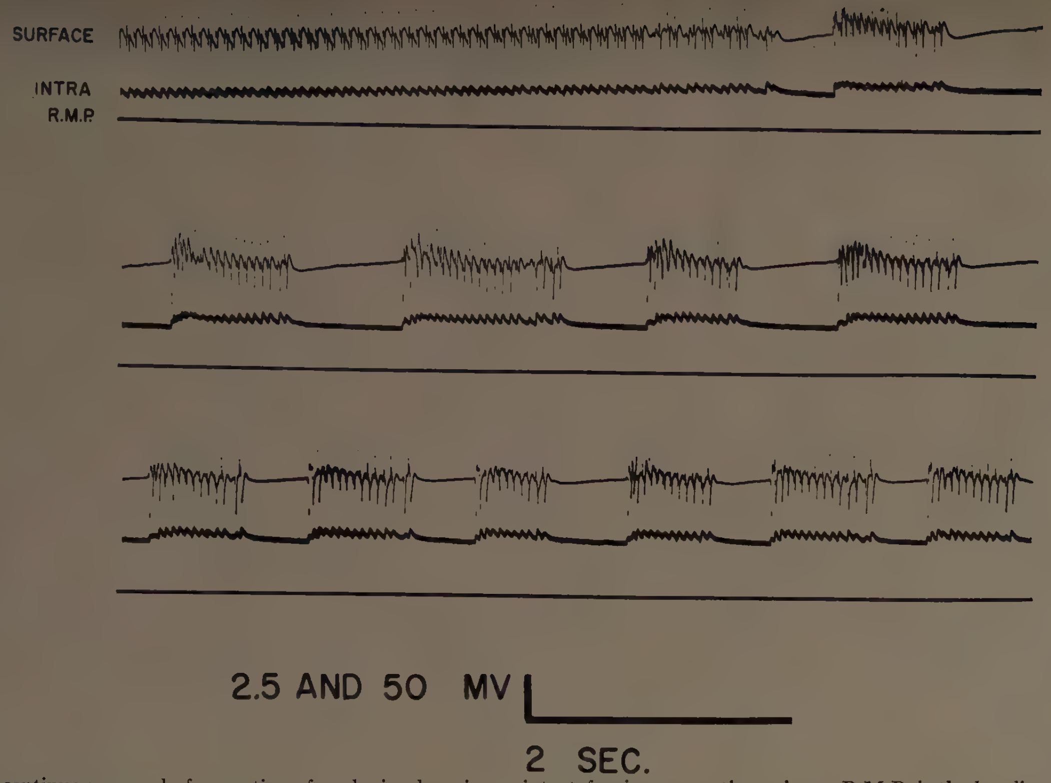

Figure 20. A continuous record of a portion of a clonic phase in an intact fornix preparation seizure. R.M.P. is the baseline value of the membrane potential; this line was drawn by choosing the most constant interspike baseline level in the preseizure trace. Note that during the clonic phase the mean steady potential has been decreased by about 60 mv.

clearly recognizable abortive spikes (*b* in trace 1 and *e* in trace 2); slow, graded, complex oscillations that bear little resemblance to all-or-none action potentials (*d* in trace 2); and intermediate forms that are combinations of these two patterns (*c* in trace 1).

It seems clear that the deafferented and intact fornix preparations produce strikingly different seizures as recorded intracellularly.

The distinctive feature of the seizure in the deafferented fornix preparation is that for most of its duration the seizure involves a hyperpolarization of the pyramidal cell. This hyperpolarization was found to be sensitive to Cl^- and to have the same properties as the inhibitory postsynaptic potentials produced by single fornix volleys in the absence of seizure.

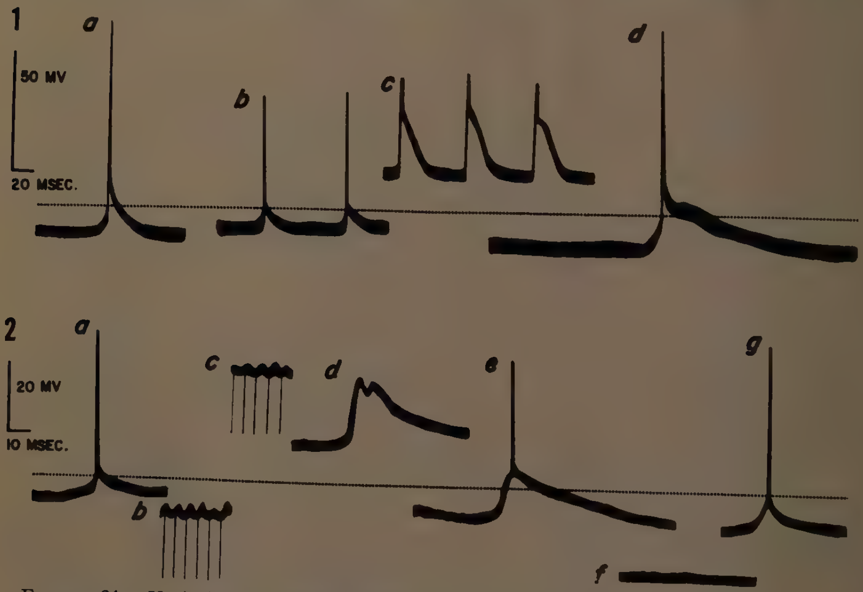

FIGURE 21. Variations in steady membrane potential and transient responses in two different intact fornix preparation seizures. The upper trace shows details of the seizure illustrated in FIGURE 19. A control spike (not indicated in FIGURE 6) is shown at *a*; *b* is from line 2 of FIGURE 19; *c* is from line 3; and *d* is from line 4. The bottom trace shows details from another seizure: *a* is the control spike; *b* is the maximum hyperpolarization during the early phase of the fornix tetanus; *c* is the maximum depolarization during the late phase of the tetanus; *d* and *e* are transient responses during the middle and late phases of the seizure, respectively; *f* is the maximum hyperpolarization during the final phase of the seizure; and *g* is the first spike generated after the membrane has returned from the hyperpolarization indicated in *f*. The dotted lines indicate the preseizure critical firing levels.

The latency period between the onset of the seizure at the surface and its appearance in the intracellular record, the appearance of normal spike generation triggered at a constant firing level, the predominance of inhibition, and the absence of an evident mechanism for starting and ending the seizure suggest that the pyramidal cells sampled do not actively participate in the seizure process. These cells seem rather to act as "follower" neurons whose active pacemaker locus is elsewhere.

In the intact fornix preparation, the unit immediately becomes involved in the generalized seizure. Synaptic bombardment during rapid tetanization is primarily excitatory. The early depolarizing shift is maintained throughout the major portion of the seizure; hyperpolarization occurs only in the final stage of the afterdischarge. Both the maintained and the superimposed transient depolarizations are clearly abnormal. It is these qualitative differences in the membrane behavior of the pyramidal cell that are the distinctive feature of this type of seizure.

Although the nature of these abnormal depolarizations cannot be specified, their effect is clear. They inactivate the spike generator, which then cannot give rise to normal all-or-none action potentials. As described previously, the depressant effect of a maintained depolarization appears to be a prominent limiting mechanism even in normally discharging pyramidal cells.[31] The fact that the recordable *A* and *B* areas spike generators are inactivated does not necessarily mean that the axon is not being fired. It is quite possible that a depolarization of this magnitude (40 to 60 mv), although inactivating soma and initial segment, does in fact fire the first or second node, which now becomes the neuronal trigger zone.[56]

In comparing the seizures in the deafferented and intact fornix preparations, the striking difference is that hyperpolarization predominates in one situation and depolarization in the other. The existence of afferent fibers in the intact fornix preparation is apparently responsible for the development of abnormal responses involving excessive depolarization. The different types of neuronal behavior during seizure in the two preparations appears to result not from a permanent change in the intrinsic properties of the cells but rather from a difference in the synaptic bombardment that initiates seizure in each case.

One final point pertinent to the more general problems of cortical electrophysiology derives from the attempted correlation between the electrocorticogram and the transmembrane voltage. In general, the correlations between surface and intracellular potentials were good with respect to time but variable with respect to sign. Transients in surface and intracellular recordings usually occurred simultaneously, although their shape often differed. Intracellular hyperpolarizing transients would be associated with a surface-positive deflection in one unit and a surface-negative deflection in another. In any given unit, however, the signs of the transient surface-potential change and the intracellular record were usually consistent. Sometimes, however, surface transients were unaccompanied by intracellular changes (FIGURE 19*c*).

In view of the poor correlations generally reported between the electrocorticogram and extracellular unitary recordings,[34,47] it is evident from the data described above that surface activity correlates better with transmembrane events than with spike generation alone. This may be partially attributable to two factors: (1) large intracellular depolarizing transients may fail to trigger spikes when the membrane potential is far below or far above the firing level; and (2) electrical changes associated with the intracellular hyperpolarizations may contribute to the surface record.[47]

References

1. ALBE-FESSARD, D. & P. BUSER. 1955. Activités intracellulaires receuillies dans le cortex sigmoide du chat: participation des neurons pyramidaux au "potentiel évoqué" somesthétique. J. Physiol. **47:** 67–69.

2. Araki, T. & T. Otani. 1955. Response of single motoneurons to direct stimulation in toad's spinal cord. J. Neurophysiol. **18:** 472–485.
3. Bak, A. F. 1958. A unity gain cathode follower. Electroencephalog. Clin. Neurophysiol. **10:** 745–748.
4. Bennett, M. V. L. 1959. Neurite and soma spikes in a monopolar neuron. Federation Proc. **18:** 10.
5. Bennett, M. V. L., S. M. Crain & H. Grundfest. 1959. Electrophysiology of supramedullar neuron. II. Properties of the electrically excitable membrane. J. Gen. Physiol. **43:** 189–219.
6. Branch, C. L. & A. R. Martin. 1958. Inhibition of Betz cell activity by thalamic and cortical stimulation. J. Neurophysiol. **21:** 380–390.
7. Cajal, S. R. 1955. Studies on the cerebral cortex. (*Limbic structures*). Translated by Kraft, M. Lisbeth. Year Book Publishers. Chicago.
8. Coombs, J. S., D. R. Curtis & J. C. Eccles. 1957. The interpretation of spike potentials of motoneurons. J. Physiol. **139:** 198–231.
9. Coombs, J. S., J. C. Eccles & P. Fatt. 1955. The specific ionic conductances and the ionic movements across the motoneuronal membrane that produce the inhibitory post-synaptic potential. J. Physiol. **130:** 326–373.
10. Crain, S. M. 1956. Resting and action potentials of cultured chick embryo spinal ganglion cells. J. Comp. Neurol. **104:** 285–326.
11. Curtis, D. R., J. C. Eccles & A. Lundberg. 1958. Intracellular recording from cells in Clarke's column. Acta physiol. scand. **43:** 303–314.
12. Daitz, H. M. & T. P. S. Powell. 1954. Studies of the connexions of the fornix system. J. Neurol. Neurosurg. & Psychiat. **17:** 75–82.
13. Eccles, J. C. 1953. The Neurophysiological Basis of Mind. Clarendon Press. Oxford, England.
14. Eccles, J. C. 1957. The Physiology of Nerve Cells. Johns Hopkins Press. Baltimore, Md.
15. Eccles, J. C., B. Libet & R. R. Young. 1958. The behavior of chromatolysed motoneurons studied by intracellular recording. J. Physiol. **143:** 11–40.
16. Eccles, R. M. 1955. Intracellular potentials recorded from a mammalian sympathetic ganglion. J. Physiol. **130:** 572–584.
17. Eccles, R. M. 1956. *In* J. C. Eccles, The Physiology of Nerve Cells. : 87. Johns Hopkins Press. Baltimore, Md.
18. Edwards, C. & D. Ottoson. 1958. The site of impulse initiation in a nerve cell of a crustacean stretch receptor. J. Physiol. **143:** 138–148.
19. Fatt, P. 1957. Sequence of events in synaptic activation of motoneuron. J. Neurophysiol. **20:** 61–81.
20. Frank, K. & M. G. F. Fuortes. 1955. Potentials recorded from the spinal cord with microelectrodes. J. Physiol. **130:** 625–654.
21. Frank, K. & M. G. F. Fuortes. 1956. Stimulation of spinal motoneurones with intracellular electrodes. J. Physiol. **134:** 451–470.
22. Fuortes, M. G. F., K. Frank & M. C. Becker. 1957. Steps in the production of motoneuron spikes. J. Gen. Physiol. **40:** 735–752.
23. Gibbs, F. A. & E. L. Gibbs. 1936. The convulsive threshold of various parts of the cat's brain. Arch. Neurol. and Psychiat. **35:** 109–116.
24. Grundfest, H. 1959. "Synaptic and ephaptic transmission". *In* Handbook of Physiology. Chapt. V. Sect. 1: Neurophysiology, **1.** Williams & Wilkins. Baltimore, Md.
25. Hodgkin, A. L. & A. F. Huxley. 1952. The dual effect of membrane potential on sodium conductance in the giant axon of *Loligo*. J. Physiol. **116:** 497–506.
26. Hunt, C. C. & M. Kuno. 1959. Properties of spinal interneurons. J. Physiol. **147:** 346–363.
27. Ito, M. 1957. The electrical activity of spinal ganglion cells investigated with intracellular microelectrodes. Japan. J. Physiol. **7:** 297–323.
28. Jung, R. 1950. Der Electrokrampf in corticalen und subcorticalen Hirngebietten. Demonstration und Diskussion des zentralen Krampfmechanismus. Ber. ges. Physiol. **139:** 211.
29. Kaada, B. R. 1951. Somato-motor, autonomic and electrocorticographic responses to electrical stimulation of rhinencephalic and other structures in primates, cat and dog. Acta physiol. scand. **231:** Suppl. **83:** 1–285.
30. Kandel, E. R. & W. A. Spencer. Excitation and inhibition of single pyramidal cells during hippocampal seizure. J. Exptl. Neurol. To be published.
31. Kandel, E. R. & W. A. Spencer. Electrophysiology of hippocampal neurons. II. Afterpotential and repetitive firing. J. Neurophysiol. In press.

32. Kandel, E. R., W. A. Spencer & F. J. Brinley, Jr. 1961. Electrophysiology of hippocampal neurons. I. Sequential invasion and synaptic organization. J. Neurophysiol. In press.
33. Lennox, M. A., R. H. Dunsmore, J. A. Epstein & K. H. Pribram. 1950. Electrocorticographic effects of stimulation of posterior orbital, temporal and cingulate areas of *Macaca mulatta.* J. Neurophysiol. **13:** 383–388.
34. Li, C. L. & H. Jasper. 1953. Microelectrode studies of electrical activity of the cerebral cortex in the cat. J. Physiol. **121:** 117–140.
35. Li, C. L. & S. N. Chou. 1960. Inhibitory interneurons in the neocortex. *In* Inhibition in the Nervous System and Gamma-Amino Butyric Acid. Pergamon Press. London, England.
36. Liberson, W. T., W. B. Scoville & R. H. Dunsmore. 1951. Stimulation studies of the prefrontal lobe and uncus in man. Electroencephalog. Clin. Neurophysiol. **3:** 1–8.
37. Liberson, W. T. & K. Akert. 1953. Observations on the electrical activity of the hippocampus, thalamus, striatum and cortex under resting conditions and during experimental seizure in guinea pigs. Electroencephalog. Clin. Neurophysiol. **53:** 320.
38. Lorente de Nó, R. 1934. Studies on the structure of the cerebral cortex. II. Continuation of the study of the ammonic system. J. Psychol. u. Neurol. **46:** 113–177.
39. Machne, X., E. Fadiga & J. M. Brookhart. 1959. Antidromic and synaptic activation of frog motor neurones. J. Neurophysiol. **22:** 483–503.
40. Nauta, W. J. H. 1958. Hippocampal projections and related neural pathways to the mid-brain of the cat. Brain. **81:** 319–340.
41. Nelson, P. G. & S. D. Erulkar. 1960. Intracellular recordings from cat inferior colliculus. Physiologist. **3:** 120.
42. Phillips, C. G. 1956. Intracellular records from Betz cells in the cat. Quant. J. Exptl. Physiol. **41:** 58–69.
43. Phillips, C. G. 1956. Cortical motor threshold and the thresholds and distribution of excited Betz cells in the cat. Quant. J. Exptl. Physiol. **41:** 70–84.
44. Phillips, C. G. 1959. Actions of antidromic pyramidal volleys on single Betz cells in the cat. Quant. J. Exptl. Physiol. **44:** 1–25.
45. Powell, T. P. S. 1958. The organization and connections of the hippocampal and intralaminar systems. Recent Progress in Psychiatry. **3:** 54–74.
46. Powell, T. P. S. & W. M. Cowan. 1955. An experimental study of the efferent connexions of the hippocampus. Brain. **78:** 115–132.
47. Purpura, D. P. 1959. Nature of electrocortical potential and synaptic organizations in cerebral and cerebellar cortex. *In* Internal Review of Neurobiology. **1:** 47–163. Academic Press. New York, N.Y.
48. Sherrington, C. B. 1906. The Integrative Action of the Nervous System. Yale Univ. Press. New Haven, Conn.
49. Sholl, D. A. 1953. Dendritic organization in the neurones of the visual and motor cortices of the cat. J. Anat. **87:** 387–406.
50. Spencer, W. A. & E. R. Kandel. 1961. Electrophysiology of hippocampal neurons. III. Firing level and time constant. J. Neurophysiol. In press.
51. Spencer, W. A. & E. R. Kandel. 1961. Electrophysiology of hippocampal neurons. IV. Fast prepotentials. J. Neurophysiol. In press.
52. Spencer, W. A. & E. R. Kandel. Selective activation of axon collaterals of hippocampal neurons. J. Exptl. Neurol. To be published.
53. Svaetichin, G. 1958. Component analysis of action potentials from single neurons. Exptl. Cell Research, Suppl. **5:** 234–261.
54. Tauc, L. 1958. Processus postsynaptiques d'éxcitation et d'inhibition dans le soma neuronique de l'Aplysie et de l'Escargot. Arch. ital. Biol. **96:** 78–110.
55. Tauc, L. 1960. The site of origin of the efferent action potentials in the giant nerve cell of *Aplysia.* J. Physiol. **152:** 36–37.
56. Terzuolo, C. A. & T. Araki. 1960. Federation Proc. **19:** 303.
57. Washizu, Y. & C. A. Terzuolo. 1960. Repetitive firing in the crayfish stretch receptors. Physiologist. **3:** 174.

ANALYSIS OF AXODENDRITIC SYNAPTIC ORGANIZATIONS IN IMMATURE CEREBRAL CORTEX*

Dominick P. Purpura†
Paul Moore Neurosurgical Research Laboratory, College of Physicians and Surgeons, Columbia University, New York, N.Y.

Introduction

Morphological studies of the mammalian cerebral cortex may be classified according to the degree to which they reveal various aspects of its complex organization. Particularly helpful in providing a general view of the basic cytoarchitectonic organization of different areas of cortex are studies of the number, type, and distribution of neurons as seen in Nissl preparations.[1,2] Considerably more valuable in providing some quantitative data on cortical organizations are studies of the distribution of dendrites and axons of various types of neurons that derive, in part, from analyses of Golgi preparations that, fortunately, reveal only 1 to 3% of the total number of neuronal elements in any given region.[3-6] Least important in providing data on the structural organization of cortex but nevertheless indispensible for disclosing details as to the type and distribution of synapses on the soma-dendritic membrane of neurons are electron microscopical studies.[7] Ideally, then, morphological studies of Golgi preparations in combination with suitable electron microscopical observations should provide useful information on the structural organization of a given region of cortex that might be of value in the analysis of its functional activity. Were it possible to limit such analyses to a particular type of cortical organization, it is reasonable to suspect that such information could serve to clarify a number of problems concerning the origin and nature of a variety of electrocortical activities. Clearly the outcome of such an endeavor is strongly dependent on the fortuitous selection of material that is physiologically analyzable, yet sufficiently limited in over-all structural complexity to permit meaningful morphophysiological correlations.

The present report is concerned with an attempt to characterize some overt cortical synaptic activities in terms of their possible morphological substrate. The material selected for examination is immature cortex or, more specifically, the anterior suprasylvian gyrus of the newborn cat. Although a few studies of evoked activities in posterior sigmoid gyrus are described, the primary objective is to define the extent to which the distinctive morphological characteristics of elements in anterior suprasylvian gyrus of the newborn cat can provide important clues to the analysis and interpretation of physiological events of varying complexity that are generated in this restricted region of cortex.

The usefulness of ontogenesis as an analytical tool in the analysis of the functional activities of the brain has long been recognized and need not be

---

* The studies reported in this paper were supported in part by Research Grant B-1312(C3) from the National Institute of Neurological Diseases and Blindness, Public Health Service, Bethesda, Md., by Grant R-133-60 from the United Cerebral Palsy Research and Educational Foundation, New York, N.Y. and by a grant from the Parkinson's Disease Foundation, Inc., New York, N.Y.

† Scholar, Sister Elizabeth Kenny Foundation, New York, N.Y.

commented on further. The particular significance of the present ontogenetic studies derives primarily from the fact that the postnatal development of neocortical neurons is characterized by a relatively early phase of maturation of superficial axodendritic synaptic pathways; then, somewhat later, a prolonged phase during which axodendritic and axosomatic pathways in the cortical depths exhibit their maximum rate of proliferation[8,9] (K. K. Voeller *et al.*, in preparation). Thus, to a large extent, synaptic activities generated in subsurface elements may be expected to contribute relatively little to the production of cortically evoked potentials, at least in the immediate perinatal period. This finding (and others to be detailed below) permits focusing attention on analyses of the composition of superficial axodendritic synaptic organizations involved in different varieties of electrocortical activities. Another advantage is worthy of preliminary consideration, for inasmuch as axodendritic synaptic pathways constituting the deep cortical neuropil are as yet poorly developed in the first postnatal week in the cat, the morphophysiological consequences of altering the normal progression of this development can be elucidated with reasonable precision. It goes without saying that the ontogenetic data surveyed below bear on problems of cortical organization that are not solely referable to the peculiarities of immature cortex.

Methods

The results summarized in this report were obtained in various types of studies carried out over a two-year period on more than 130 kittens. All electrophysiological and pharmacological data were obtained in locally anesthetized-succinylcholine paralyzed kittens. Operative procedures (such as external jugular vein and tracheal cannulation, craniectomy, and cerebellectomy) were performed under ether anesthesia. Neonatal kittens undergoing cerebellectomy for brain stem exposure were transfused with 1 to 2 cc. of packed red cells in order to reverse some of the generalized depression resulting from the operative procedures. No untoward effects of the transfusion were observed in any of the kittens so treated. Studies on chronically isolated cortex were carried out in 4 to 21-day-old kittens. Subpial isolation of cortical slabs was performed transdurally in neonatal (<2-day-old) kittens according to the methods of Echlin *et al.*[10]

Golgi-Cox (DeFano modification) sections (200 μ thick) were prepared from normal and isolated neocortex of kittens employed in physiological studies Electron microscopical studies of the suprasylvian gyrus of the newborn cat were carried out on fresh specimens fixed with 1 per cent osmium tetroxide buffered at *p*H 8.2 with veronal-acetate buffer, dehydrated with graded alcohols, and embedded in either 80 to 20 butyl methyl methacrylate or Epon. Sections were cut with a Porter-Blum microtome and examined in an RCA EMU-3C electron microscope (Voeller *et al.*, in preparation). Details as to stimulating and recording techniques and the preparation and use of ω-amino aliphatic acids in pharmacological studies have been described elsewhere.[9,11-13]

Mode of Generation and Propagation of Superficial Cortical Responses

At least 3 hypothesis have been proposed to account for the production and spread of 10 to 20 msec. surface-negative responses evoked by local stimulation of neocortex.[14] Superficial cortical responses (SCRs) recorded up to 3 to 5 mm. from the site of stimulation have been viewed as conducted action potentials of dendrites,[15] graded decrementally conducting responses of directly and indirectly excited apical dendrites,[16] and as postsynaptic potentials (p.s.p.s) generated in apical dendrites by directly excited pathways of variable trajectory.[12,17,18] SCRs recorded at distances greater than 3 to 5 mm. from the site of stimulation have either been neglected from consideration, viewed as postsynaptic potentials of apical dendrites,[19] or thought to involve elements in pathways with different conduction velocities.[20] A view has also been expressed that SCR is both generated in and conducted along unspecified, randomly oriented nerve processes that stretch across the surface of the brain for about 10 mm.[21]

A detailed analysis of the changes in the physiological and pharmacological properties of SCRs evoked in immature cat cortex has been presented elsewhere.[9,22] For present purposes only a few results of this analysis that permit some decision as to which of aforementioned hypothesis can satisfactorily account for the ontogenetic data need be summarized.

Graded SCRs recorded in neonatal cat cortex under conditions identical to those employed in similar studies in adult animals[12,13,23] are of relatively long duration with respect to those evoked in mature cortex (FIGURE 1). When care is taken to record SCRs in neonatal cortex as close to the site of stimulation as is technically possible, SCRs can be shown to be identical in all respects to those recorded at more distant sites in the neocortex of adult animals (FIGURE 1). Of considerable interest is the observation that although SCRs may be recorded at distances up to 5 to 7 mm. from the site of stimulation in the immediate neonatal period, distant responses are never of greater magnitude than those recorded within 2 mm. from the stimulating electrodes. It should be noted also that in the first postnatal week, SCRs are generated at distant sites after relatively long latencies, indicating involvement of pathways with conduction characteristics of 0.3 to 0.4 m./sec.

The changing characteristics of distant SCRs during the second postnatal week are shown in FIGURE 2. The points of major significance to be noted in this illustration are: (1) SCRs are recorded at greater distances by the end of the second postnatal week than during the immediate neonatal period; (2) SCRs evoked at distant sites may be of greater amplitude than those recorded closer to the locus of stimulation; and (3) linear changes in latency with distance are characteristically observed. Another feature shown in FIGURE 2 (bottom records in C) is worthy of note. Elimination of the SCR evoked close to the site of stimulation (1.5 mm.) by topically applied γ-aminobutyric acid (GABA) does not alter SCRs recorded outside of the GABA-treated area of cortex.

Interpretation of the foregoing electrophysiological data is greatly facilitated by examination of the morphological characteristics of elements in superficial regions of immature neocortex. Golgi-Cox preparations of neonatal cat cortex reveal extraordinarily well-developed apical dendrites of cortical pyramidal neurons (FIGURE 3). In the molecular layer and immediate subjacent regions, wherein the SCR is generated,[12,14,16,23,24] dendrites of underlying pyramidal neurons and Cajal-Retzius cells (FIGURES 3B and C) are densely

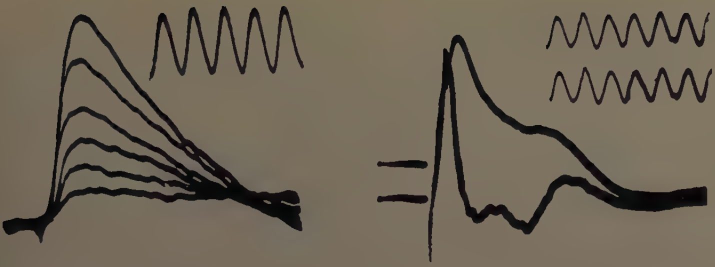

FIGURE 1. (*Left.*) Characteristics of long-duration superficial cortical responses (SCR) recorded 1.5 mm. from stimulating electrodes on suprasylvian gyrus in a near-term fetal kitten. Stimulus frequency 0.5/sec.; 6 superposed responses at different stimulus strengths. Negativity upwards in this and all subsequent figures. (*Right.*) Five-hour-old kitten. Comparison of SCR recorded 0.5 mm. from stimulating electrodes with a large (0.5-mm.) ball-tipped electrode (*upper channel*) and SCR recorded "at the site of stimulation" with 0.1-mm. tip-diameter wire electrode. When recorded with the wire electrode at the site of stimulation, the SCR has characteristics identical to those recorded in the adult animal. Calibrations 100 cps; 0.1 mv.

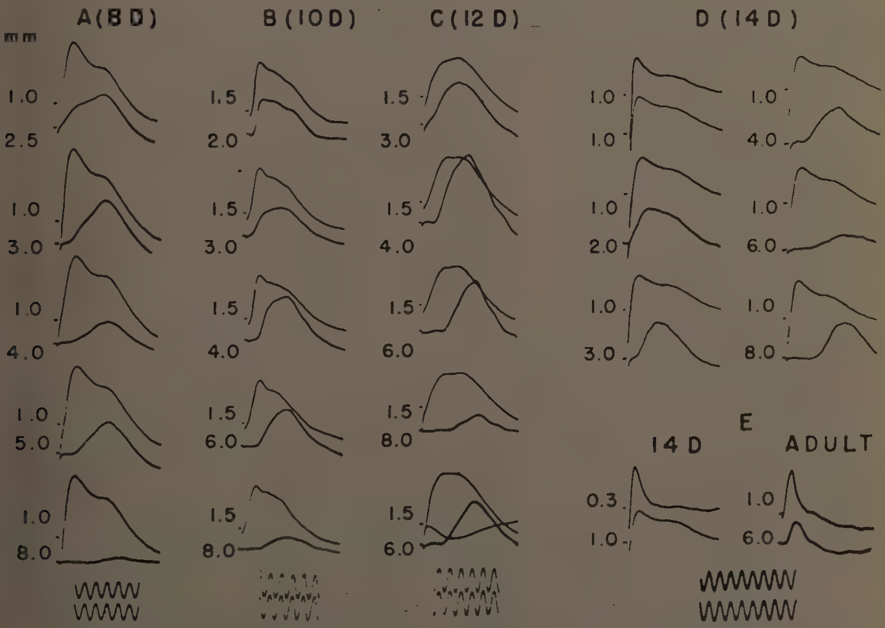

FIGURE 2. Changing characteristics of distant SCRs during second postnatal week (A to D) Relationship between near (*upper channel*) and distant (*lower channel*) responses recorded at distances from stimulating electrodes indicated at left in each series; ages shown above. (A) SCRs at 5 and 3 mm. larger than at 2.5 and 4 mm. (B) Augmented responses at 4 and 6 mm. (C) Note extraordinary magnitude of response at 4 and 6 mm. (D) Reinforced SCR at 8 mm.; latency about 25 msec. In C, records at bottom of column taken before and after topical application of 1 per cent GABA to near electrode site. In this record, upper channel shows abolition of surface negativity and unmasking of surface positivity after GABA; lower channel shows two perfectly superposable distant responses. (E) Comparison of responses at indicated distances in a 14-day-old kitten and adult cat studied under identical conditions. Wire electrode (0.1 mm.) employed to record response at 0.3 mm. in kitten. Compare characteristics of responses at 1 mm. Duration of the distant response in adult preparation is similar to that of near response. Calibrations 100 cps; 0.1 mv in A; 0.3 mv in B to E; that for D shown in E. Reproduced by permission of *Experimental Neurology*.[9]

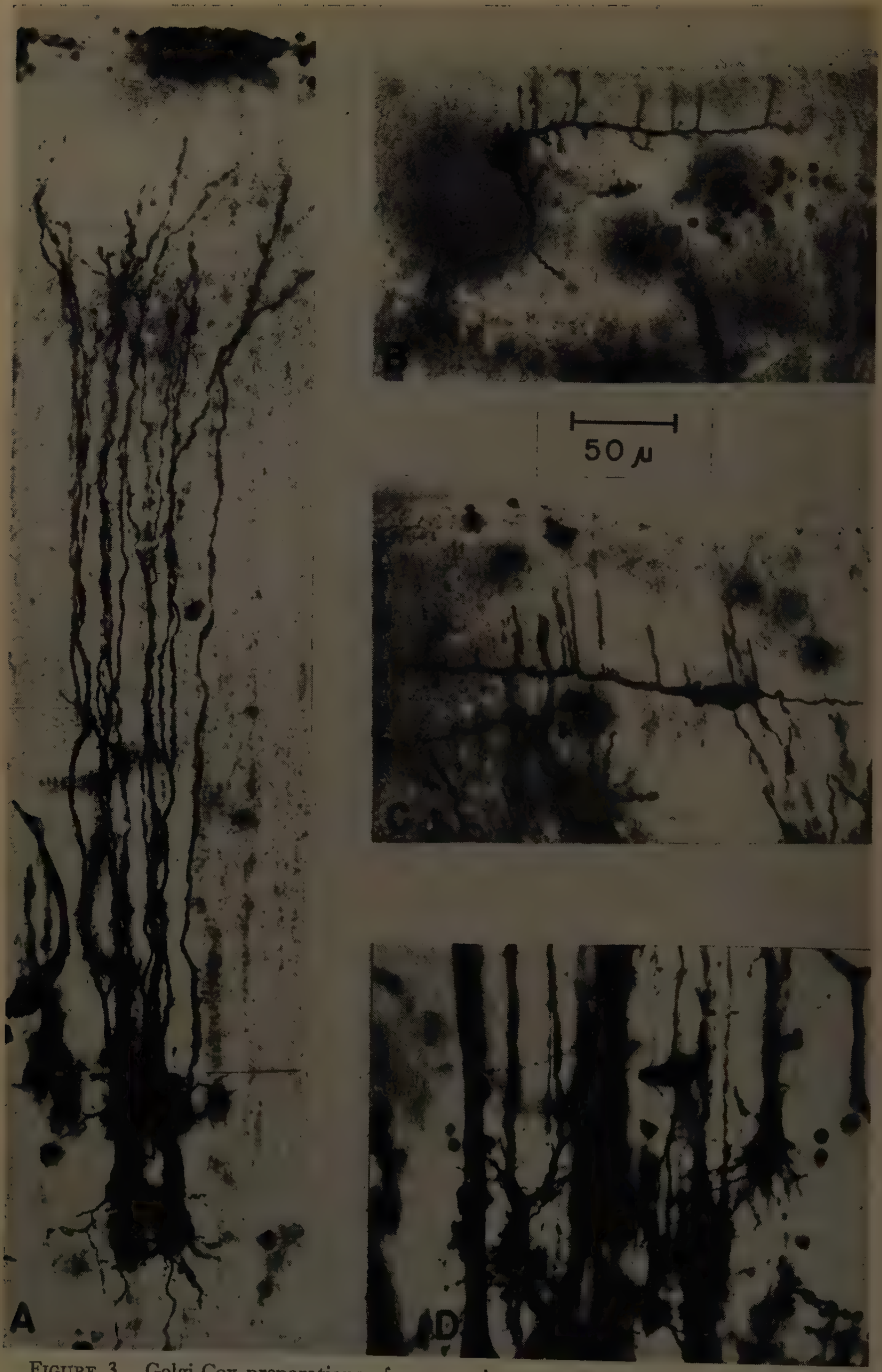

FIGURE 3. Golgi-Cox preparations of neurons in suprasylvian (A and B) and anterior sigmoid gyrus (C and D) of 5-hour-old kitten. (A) Cluster of medium and large pyramidal neurons. Apical dendrites extend to within 25 to 50 μ of pial surface. Note absence of lateral branches. Axons of two neurons clearly shown extending downward. Basilar dendrites at this stage are short, thin processes. (B and C) Embryonic Cajal-Retzius neurons in molecular layer. (D) Giant pyramidal cell in motor cortex with massive apical dendrites, but poorly developed basilar dendritic system. Same magnification throughout. Reproduced by permission of *Experimental Neurology*.[9]

packed. With advancing age, this density decreases due largely to the development of non-neural elements, loss of the elaborate dendritic apparatus of Cajal-Retzius cells, and over-all increases in neuronal volume.[8,25,27] In contrast to apical dendrites, basilar dendrites and axon collaterals of deep lying pyramidal neurons are poorly developed in the immediate neonatal period. Toward the end of the first postnatal week basilar dendrites and axon collaterals begin a rapid phase of growth that extends through the second and third postnatal weeks. By the fourth postnatal week, the basilar dendritic systems of

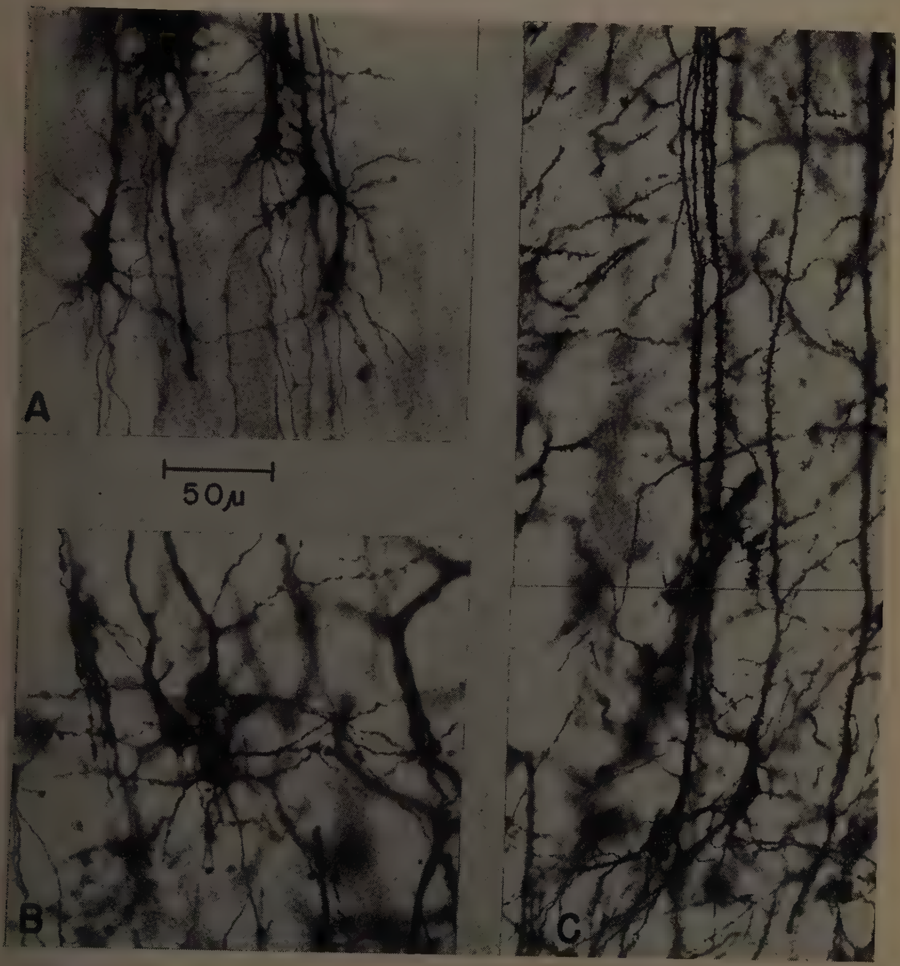

FIGURE 4. Postnatal maturation of basilar dendrites of neocortical pyramidal neurons. (A) Examples of small and medium pyramidal neurons from suprasylvian gyrus of 3-day-old kitten. Basilar dendrites beginning rapid phase of growth. (B) Further elaboration of basilar dendritic system in 8-day-old kitten. (C) Large pyramidal neurons from anterior suprasylvian gyrus of 21-day-old kitten. Note extensively developed basilar dendrites and spines on apical dendrites. Same magnification throughout. Reproduced by permission of *Experimental Neurology*.[9]

neocortical pyramidal neurons have attained their mature characteristics (FIGURE 4).

Further examination of the morphological features of apical dendrites of cortical pyramidal neurons in the immediate perinatal period reveals two additional factors that are particularly relevant to the analysis of the mode of production and propagation of the SCR in immature cortex. Although radially oriented dendritic elements are densely packed in the molecular layer their tangential spread in superficial cortex is extremely limited. Indeed, it is unusual to observe tangential branches of apical dendrites that exceed 100 to 150 μ. In view of the fact that even in adult cat cortex, apical dendrites do not have tangential branches in the molecular layer that are longer than 200 μ,[5] it is concluded that apart from changes in over-all radial length and the later

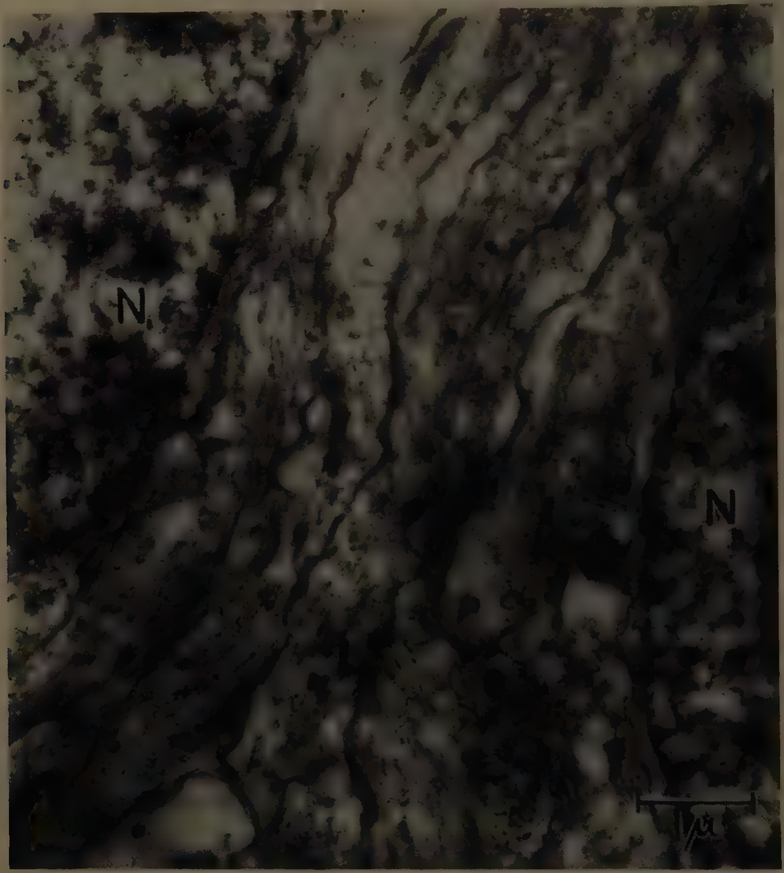

FIGURE 5. Electron micrograph of subsurface neuronal elements in suprasylvian gyrus of 1-day-old kitten. Cell bodies of 2 neurons are shown (*left and right, N*) with the space between them occupied by 5 or 6 apical dendrites from deeper lying pyramidal elements. Note absence of synaptic complexes similar to those shown in FIGURES 6 and 7. (From Voeller *et al.*, in preparation.)

appearance of tangential branches on proximal portions of apical dendrites, the distal segments of dendritic elements in the molecular layer exhibit little alterations *relative* to the postnatal changes observed in basilar dendrites.[8,9] Another characteristic is the late appearance of dendritic spines (thorns or gemmules). These structures, which are clearly detectable on apical dendrites of neocortical pyramidal neurons during the second postnatal week, are either absent or modified in the immediate neonatal period. It is impossible to determine from available Golgi-Cox material whether the small protuberances observed almost exclusively on distal segments of apical dendrites in the newborn kitten are artifacts or modified dendritic spines. However, since it has been shown in electron microscopical studies that dendritic spines represent one variety of axodendritic synapses seen in mature cortex,[7] it is reasonable to suspect that the small protuberances present on distal segments of apical dendrites in Golgi-Cox preparations may be modified axodendritic synapses.

As pointed out elsewhere,[9,22] further definition of the morphological features of elements in the superficial neuropil requires electron microscopical studies of immature neocortex. For this reason, some preliminary electron microscopical data obtained in studies with Kytja K. Voeller and G. D. Pappas may be summarized to indicate wherein they contribute to the present problem.*

With respect to the extraordinary density of apical dendrites in immature cortex, electron microscopical observations completely confirm light microscopical data that indicate close packing of these elements throughout their entire course. In favorable specimens from submolecular regions of neocortex in newborn kittens, as many as 5 to 6 dendrites may be seen between cell bodies of superficial neurons that are 2 to 3 μ apart (FIGURE 5). The presence of clearly definable synapses on cell bodies in the immediate neonatal period has, as yet, not been established. This negative finding, however, may be of considerable importance in view of the fact that axodendritic synapses with characteristics similar to those described for axodendritic synapses in adult rat cortex[7] are detectable on apical dendrites at various sites along their radial trajectory (FIGURE 6).† In some preparations of superficial neuropil, axodendritic synapses may be encountered with relative ease (FIGURE 7) although this is not always the case. The primary objective of the present survey is achieved with the demonstration of axodendritic synapses on closely packed apical dendrites in the immediate neonatal period. It remains to indicate how the aforementioned light and electron microscopical data contribute to the

* The electron microscopical data shown here were obtained by Kytja K. Voeller and are part of a collaborative study on the ultrastructural characteristics of developing neocortex currently in progress in the Department of Anatomy (G. D. Pappas) and the Department of Neurological Surgery (K. K. Voeller *et al.*, in preparation).

† The criteria for identification of synapses in the cerebral cortex are by no means completely established. This is especially true in the case of immature cortex, where it is entirely possible that some of the ultrastructural characteristics described for synapses in adult cortex[7,28] may be considerably modified. For present purposes, however, it is sufficient to point out that the electron microscopical criteria currently regarded as adequate for the identification of synapses in the mature mammalian central nervous system[28-30] are applicable to the problem at hand. In view of this, I can see little value to speculations concerning the possible existence of cortical dendrodendritic junctions based on light microscopical studies of Golgi-Cox preparations.[31] Indeed, although examination of electron microscopical material of immature neocortex reveals that dendrites may be 200 to 300 Å apart, none of the features characteristically observed at axodendritic junctions can be discerned (FIGURE 5).

interpretations of electrophysiological data on the SCR evoked in immature cortex.

As noted previously, the SCR in newborn kittens has a duration similar to that observed in adult animals, but this is true only at sites close to the locus of stimulation. In view of the extraordinary density of dendrites and the presence of axodendritic synapses in neonatal cat cortex, the hypothesis concerning the axodendritic synaptic origin of the SCR is greatly strengthened. Further support for this is provided by the finding that SCRs recorded at various distances from the site of stimulation have similar characteristics but apical dendrites in the immediate neonatal period are devoid of tangential branches in their proximal segments and do not have a tangential spread in the molecular layer which exceeds 100 to 200 μ. The hypothesis that the SCR is a conducted action potential of tangential dendrites[15] would thus appear to be inconsistent with the known structural features of these elements in immature

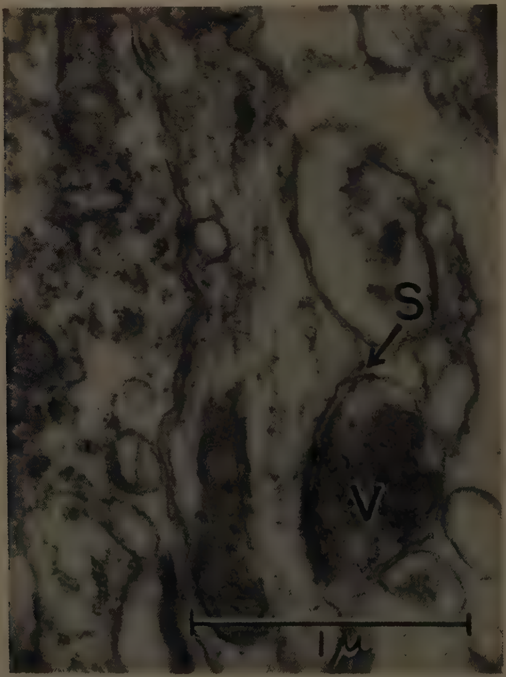

FIGURE 6. Electron micrograph of an axodendritic synapse (S) in suprasylvian gyrus of a 1-day-old kitten. An axonal terminal is shown on the right in synaptic relation to an apical dendrite. The terminal contains a large number of vesicles (V) that are densely clustered near the thickened presynaptic membrane. The other immediately adjacent process is apparently devoid of vesicles and does not show thickening of appositional membranes. Its identity is not established. To the left of the vertically oriented apical dendrite in this micrograph the cytoplasm of a neuron containing ribosomes and mitochondria is seen. Although the cell body and dendrite are separated by a 200 Å space as are the dendrite and axonal terminal (S), no specialized processes are discernible along the course of the cell body-dendrite appositional membranes. (From Voeller *et al.*, in preparation.)

cortex. That a single species of conductors is involved in the production and spread of the SCR is also made unlikely by the finding that elimination of near SCRs does not alter distant SCRs and that SCRs at different distances may vary considerably in amplitude in duration. Thus the morphophysiological data on the SCR in immature cortex outlined above, and presented in more detail elsewhere,[9,22] are entirely consistent with the view that SCRs are axodendritic p.s.p.s generated in different populations of dendrites by conductile pathways both tangential and more circuitous in their trajectory.[12,32]

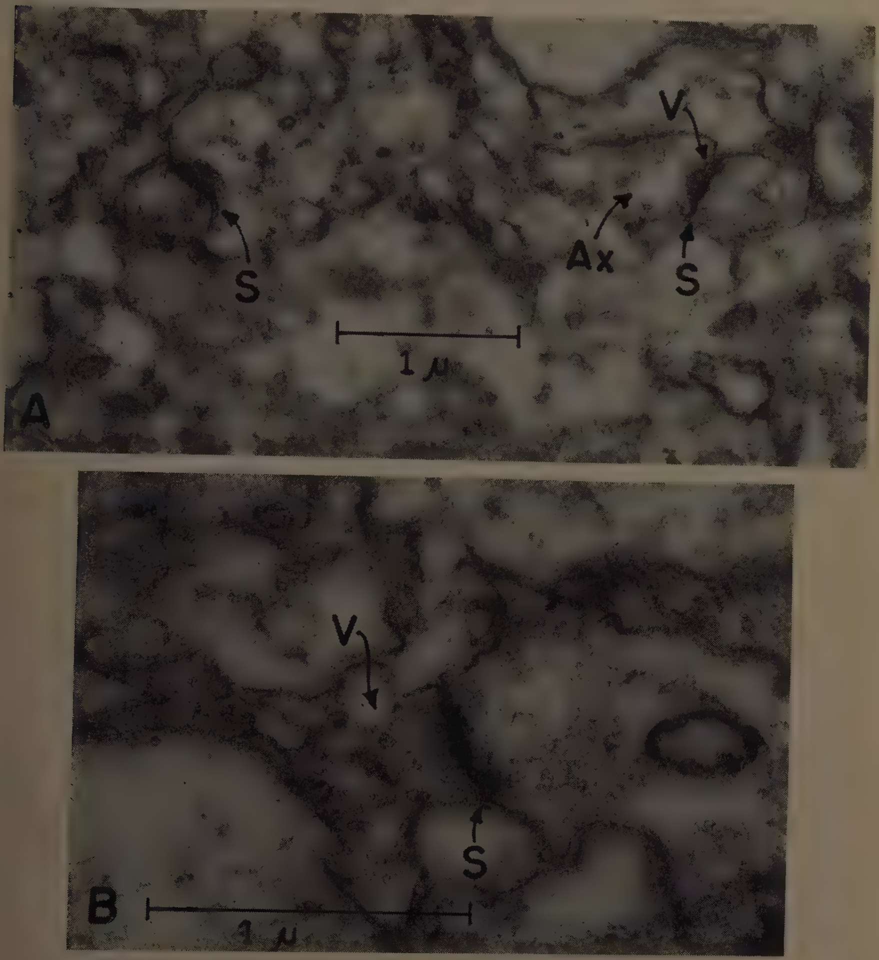

FIGURE 7. Electron micrographs of axodendritic synaptic complexes in superficial neocortical neuropil of newborn cat.

(A) Two synapses (S) are shown at arrows. Axon (Ax) readily identified by presence of synaptic vesicles (V), some of which are concentrated at presynaptic membrane.

(B) Higher magnification of another axodendritic synaptic complex to show details of synaptic vesicles and characteristics of thickened appositional membranes. (From Voeller *et al.*, in preparation.)

At this juncture it is to be noted that although morphological data of the type presented above have been useful in clarifying the interpretation of the origin and nature of the SCR, it cannot be expected that further clues to the internal composition of the axodendritic synaptic pathways involved in this overt response will be forthcoming from currently available anatomical data. The reason for this becomes immediately apparent when it is recognized that there are as yet no criteria for distinguishing excitatory and inhibitory elements on the basis of their overt or ultrastructural characteristics. Whether a particular neuron exerts an excitatory or inhibitory synaptic action on other elements is dependent on differences in ionic permeability changes produced in postsynaptic membrane by transmitter action.[33-35] This being the case, attempts to "dissect" complex axodendritic synaptic pathways into their excitatory and inhibitory components are best directed towards analyses of the alterations in the response of such pathways produced by pharmacological agents capable of blocking one or the other variety of synaptic activity in responses that are composites of excitatory and inhibitory p.s.p.s.[11] Such an operational approach has already greatly facilitated the analysis of a relatively large series of surface and focally recorded evoked responses in neocortex,[12,23,36] hippocampus,[11,37] and cerebellar cortex[38] of adult animals. When pharmacological agents are employed in combination with ontogenetic analyses of axodendritic synaptic pathways, the results thus obtained serve to characterize further the synaptic composition of these pathways and to provide additional information as to their probable morphological substrate.

The usefulness of the aforementioned combined analytical methods in studying the properties of axodendritic synaptic pathways in superficial cortex is clearly illustrated in the different effects produced by 'convulsant' ω-amino acids on SCRs during the postnatal ontogenesis of neocortex.[22,39] In adult animals, SCRs recorded close to the locus of stimulation are markedly augmented within a few seconds after topical application of long chain ω-amino acids (ϵ-amino caproic, C_6, or ω-amino caprylic, C_8) to the site of registration. This effect has been ascribed to the blocking action of the long chain ω-amino acids on axodendritic inhibitory p.s.p.s.[13] In sharp contrast to the effects observed in mature cortex, topically applied long chain ω-amino acids do not augment SCRs evoked in the neocortex of kittens prior to the third postnatal week (FIGURES 8 and 9). During the first postnatal week, depression of SCRs is characteristically observed despite the fact that some changes may be detectable in late components of SCRs and, in the background, spontaneous electrocortical activity (FIGURE 8). During the second postnatal week, augmentation of spontaneous electrocortical activity is readily detectable in cortex treated with convulsant ω-amino acids, but only after the third postnatal week do all components of the SCR increase in amplitude within a few seconds after topical application of these compounds. Of considerable interest is the finding that at a time when SCRs recorded 1 to 3 mm. from the site of stimulation are augmented by convulsant ω-amino acids, no effects are observed on SCRs recorded at more distant sites that have been similarly treated (FIGURE 9). This finding, revealed for the first time in ontogenetic studies, was subsequently shown to represent a final maturational event.[22] Thus when "near" and "distant" sites of SCR registration were treated with ϵ-amino caproic acid only

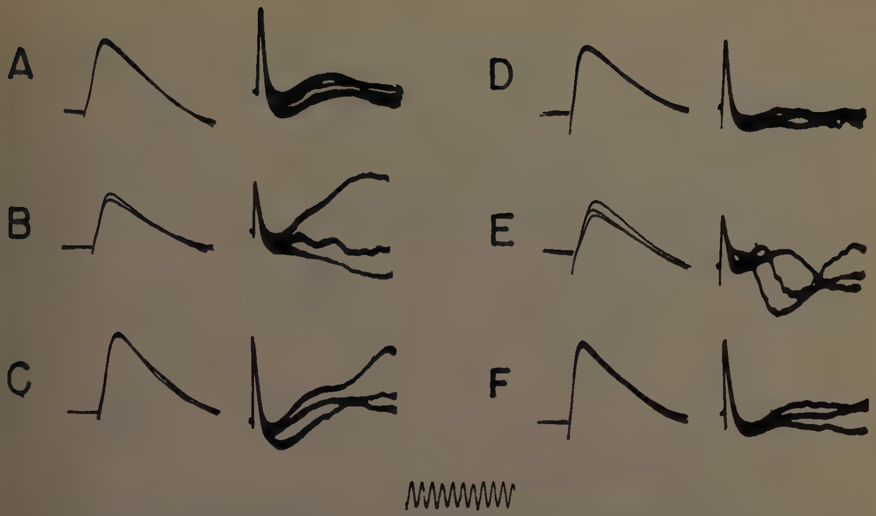

FIGURE 8. Five-hour-old kitten. Effects of topical ϵ-amino caproic acid (C_6) and ω-amino caprylic acid (C_8) on SCRs and succeeding long duration responses. SCRs recorded 1.5 mm. from site of stimulation. Left column, fast sweep (Cal. 100 cps); right column, slow sweep (Calibrations 10 cps).

(A) Control SCRs, note later positive-negative sequences in slow sweep records; (B) 1 min. after C_6; (C) recovery of SCR 10 min. after flushing cortex with Ringer's solution; (D) 20 min. after C, control prior to C_8 application; (E) 2 min. after C_8; (F) recovery 20 min. after removal of C_8. Reproduced by permission from Pergamon Press.[22]

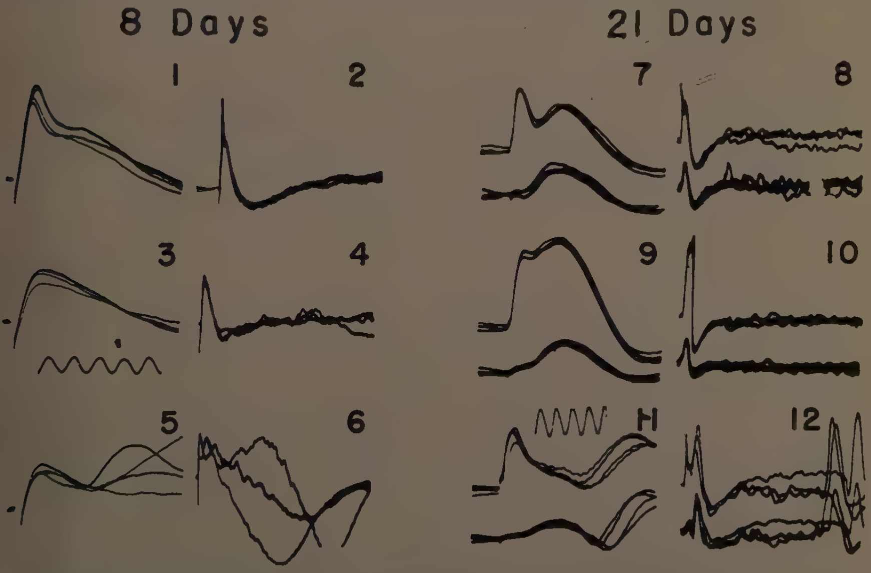

FIGURE 9. Comparative effects of C_6 on SCRs in 8- and 21-day-old litter mates. Sweeps and calibrations as in FIGURE 8. (*1* and *2*) Control SCRs recorded 1.0 mm. from site of stimulation; (*3* and *4*) 2 min. after topical C_6; (*5* and *6*) after complete recovery from depressant effects of C_6, and 2 min. after C_8. Differences in the action of C_6 and C_8 are apparent; note, in particular, changes in late components of SCR after C_8; (*7* and *8*) control near (*upper channel*) and 4 mm. distant SCRs (*lower channel*); (*9* and *10*) immediate effects of C_6; rapid augmentation of early and late components of near SCR with more pronounced action on late components; distant response unaffected; (*11* and *12*) onset of C_6-induced convulsant activity. Reproduced by permission of Pergamon Press.[22]

near responses were immediately augmented. Changes in late components of distant SCRs occurred after propagation of augmented late components of near SCRs (FIGURE 10).

Additional details of the different effects of ω-amino acids on different components of the SCR have been described elsewhere.[22] It is sufficient here to emphasize one interpretation of the data illustrated in FIGURES 8 to 10 that is particularly relevant to the analysis of axodendritic synaptic pathways. If, as has been proposed elsewhere,[11,13] ω-amino acids exert their convulsant effects through elimination of inhibitory axodendritic p.s.p.s, then it follows that failure to observe augmentation of SCRs prior to the third postnatal week must be ascribed either to unresponsiveness of inhibitory axodendritic synapses in superficial neuropil to long chain ω-amino acids, or the relative absence of these synapses on elements involved in the production of the SCR. Of the

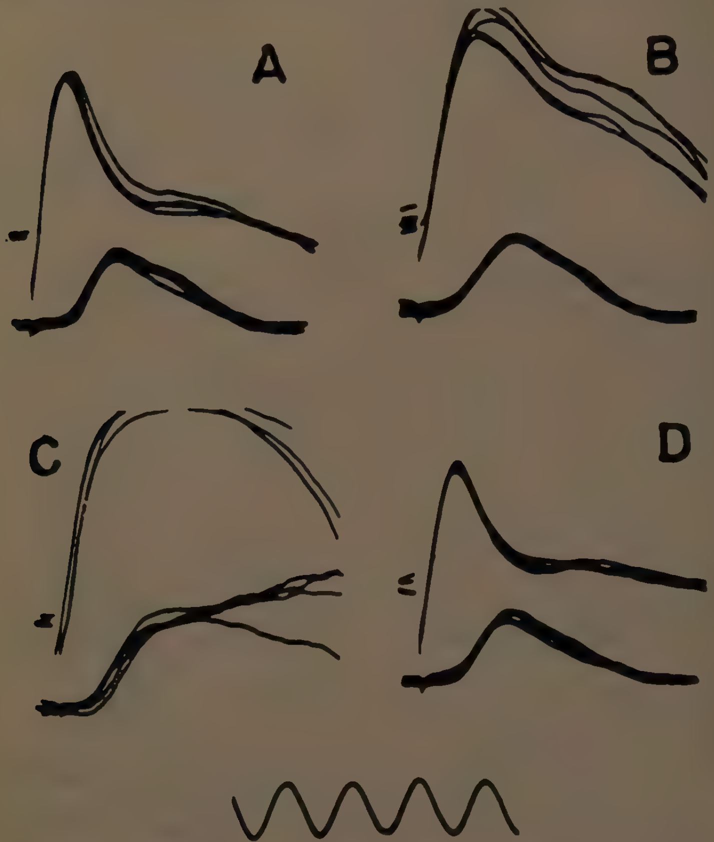

FIGURE 10. (A) Near (1.5 mm., in lower channel, and distant 6.0 mm.) SCRs evoked in suprasylvian gyrus of adult cat with stimuli at threshold for late negative component; (B) 20 sec. after application of C_6 to both recording sites; (C) 40 sec. after B; (D) recovery after rinsing cortex with Ringer's solution. Calibrations 100 cps; 0.1 mv. Reproduced by permission of Pergamon Press.[22]

two possibilities, the second would appear to be more reasonable in view of the fact that electrocortical activities other than the SCR are affected by convulsant ω-amino acids when the SCR is unaffected or depressed by these compounds. Effects entirely similar to those produced by long chain ω-amino acids (FIGURES 8 to 10) are observed with topically applied strychnine, a drug that initiates paroxysmal activity through blockade of inhibitory synapses.[33,36,40] These and other data[22] thus permit the tentative conclusion that during the postnatal development of axodendritic synaptic organizations in superficial cortex excitatory pathways involved in the production and spread of the SCR mature earlier than the pathways which generate inhibitory p.s.p.s in apical dendrites. Furthermore, when fully developed, superficial inhibitory pathways activated by surface stimulation would appear to exert their effects on apical dendrites at relatively close range.[33]

It is not to be inferred from the foregoing analysis that inhibitory synaptic activities generated in apical dendrites are not detectable with appropriate pharmacological agents in the immediate neonatal period. The point of emphasis here is that excitatory and inhibitory axodendritic synaptic pathways involved in the SCR appear to exhibit different rates of functional maturation. Inasmuch as a weak stimulus to the neocortical surface activates only a limited population of conductile elements synaptically related to apical dendrites, no information is provided by such studies concerning the developmental status of axodendritic synaptic organizations activated via other afferent pathways. That axodendritic synaptic organizations involved in different varieties of cortical activities evoked in newborn kittens appear to contain large proportions of inhibitory elements has been indicated elsewhere.[22] In view of this, it becomes necessary to extend the present inquiry to include consideration of the manner in which these synaptic organizations participate in the elaboration of more complex electrocortical events detectable in immature neocortex.

Contribution of Axodendritic Synaptic Activities to Evoked Responses of Immature Neocortex

The remarkable differential development of superficial axodendritic synaptic pathways in the neocortex of newborn kittens is reflected in part in the prominence of surface-negative components in a variety of evoked responses. This is especially true for specific responses evoked in somesthetic[41] and visual cortex[42-44] and to a lesser extent for primary responses in auditory cortex, although studies on the latter system have not been carried out in kittens in the immediate perinatal period.[42,45]

Low-frequency electrical stimulation of ventrolateral thalamic nuclei in newborn kittens evokes responses over wide areas of sensorimotor cortex. These responses may evolve with little or no initial surface-positivity in contrast to responses commonly observed in mature animals.[32] Apart from the relatively long latency of such responses, which is probably referable to delayed conduction in elements constituting the presynaptic pathway,[46] specific thalamocortical evoked responses in neonatal cat cortex exhibit prolonged periods of postactivation depression (FIGURE 11). This is particularly evident at stimulus frequencies as low as 2 to 5/sec.; almost complete failure of such responses occurring at 10/sec. stimulation. At the latter stimulus frequency the prominent surface negativity is shown to be compounded of early and late components (FIGURE 11D). Thus despite the apparent simplicity of the surface negativity of the specific evoked response in the newborn kitten, more than one species of axodendritic synaptic pathways appears to be involved in its production. It is not to be assumed that because specific evoked responses are almost exclusively surface-negative in overt configuration, prior surface positivity is absent in the immediate perinatal period. When thalamocortical radiations to posterior sigmoid gyrus are stimulated at various sites along their trajectory to cortex, diphasic positive-negative potential sequences may be readily detectable (FIGURE 12). Under these conditions both phases of the overt surface response are similarly depressed during low-frequency radiation stimulation. Surface-positive components, reflecting synaptic activation of deep lying cortical elements, are also revealed after GABA blockade of superficial axodendritic synapses contributing to the surface negativity.[22,47] The singular characteristics of specific evoked responses in the immediate neonatal period, that is, their prominent surface negativity and absent or small initial surface positivity are probably not due to fundamental differences in the mode of engagement of superficial and deep elements by specific thalamocortical afferents in the immature animal, but rather to differences in the degree of maturation of the synaptic pathways involving these elements. In view of the relatively poor development of basilar dendritic systems of cortical pyramidal neurons and stellate cells in the newborn kitten, the electrophysiological data would appear to indicate activation of superficial dendritic plexuses by a slowly conducting group of 'specific' thalamocortical afferents and another faster conducting group terminating in relation to late-maturing elements in the cortical depths. Thus the overt configuration of specific thalamocortical responses revealed in the immediate neonatal period may be accountable for by the prominent synaptic activity in superficial dendritic elements which is sufficiently intense to swamp out the relatively weak synaptic activity initiated in the cortical depths.

The hypothesis that thalamocortical pathways in immature animals evoke potent synaptic activities in superficial axodendritic synaptic organizations is strengthened by data on the characteristics of surface responses evoked in fundamentally different types of neocortex by stimulation at different sites in the anterolateral nuclear complex of the thalamus of newborn kittens. Analysis of these response patterns introduces additional features of the properties of axodendritic synaptic pathways that have not been sufficiently clarified thus far, that is, the degree to which different organizations participate in the elaboration of complex electrocortical events and the possible nature of the differences in the responsiveness of these organizations to corticipetal volleys.

The fact that vertically oriented stimulating electrodes in the thalamus of adult animals may evoke a variety of surface activities when the exploring electrodes activate different nuclear groups is too well known to require further comment.[32] When similar stimulating procedures are carried out in the newborn kitten and stimulation is limited to single or paired shocks repeated every two seconds, a constellation of different responses may be evoked from different cortical regions. Here discussion may be focused on responses simultaneously evoked in somatic sensory cortex (posterior sigmoid gyrus)

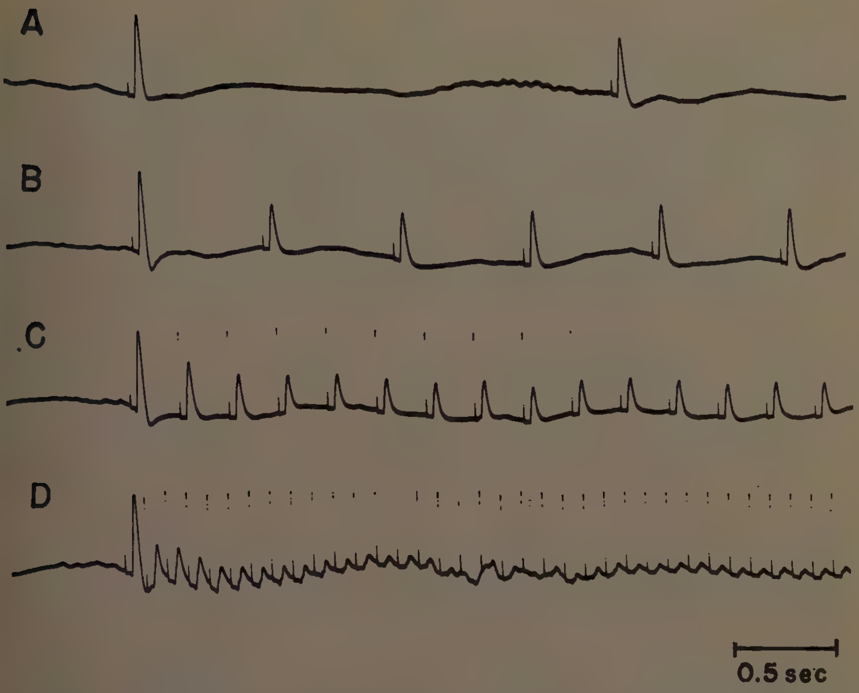

FIGURE 11. Predominantly surface-negative specific responses evoked in posterior sigmoid gyrus following stimulation of ventrolateral thalamic nuclei and their projections in an 8-hour-old kitten. Stimulus frequency as follows: (A) 0.5/sec.; (B) 2/sec.; (C) 5/sec.; (D) 10/sec. Depression of response is evident during 0.5/sec. stimulation and profound during 10/sec. stimulation. Note increased duration of surface negativity in second to fifth responses in D and tendency for these responses to exhibit initial rapid and later slow components prior to almost complete blockade. Reproduced from *Annals of The New York Academy of Sciences*, Vol. 92, Art. 2.[55]

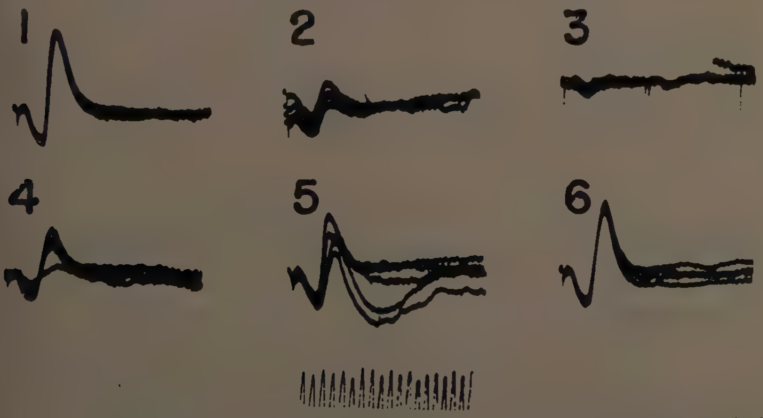

FIGURE 12. Specific responses in posterior sigmoid gyrus evoked by stimulation of thalamocortical radiations (8-hour-old kitten). (*1*) Superposed responses during 0.5/sec. stimulation. (*2* and *3*) Depression of responses during 5 and 10/sec. stimulation respectively. (*4* and *5*) Recovery of 0.5/sec. evoked responses. Note delayed recovery of surface negativity. (*6*) One min. after *5*. Some depression of surface negativity still evident. Time calibrations 100 cps.

and 'association' cortex (anterior and middle suprasylvian gyrus). A commonly observed series of responses evoked from these cortical regions during vertical displacement of stimulating electrodes through anteroventral thalamic region is shown in FIGURE 13. Short-interval paired-shock stimulation of dorsal parts of the rostral thalamus evoked 30 to 40 msec. latency surface-negative responses in posterior sigmoid gyrus and surface-positive responses in anterior suprasylvian gyrus (FIGURE 13A). With progressive downward displacement of the stimulating electrodes posterior sigmoid gyrus responses were attenuated and those in association cortex were augmented (FIGURES 13B to D). At these sites of stimulation, the testing response of the pair exhibited a markedly facilitated late negativity that was strictly confined to anterior suprasylvian gyrus (13D). Stimulation in ventral regions of the anterolateral thalamus resulted in attenuation of anterior suprasylvian gyrus responses and reappearance of 30 to 40 msec. latency activity in posterior sigmoid gyrus (13E and F). The latter responses were unrelated to the posterior sigmoid responses recorded during stimulation of more dorsal thalamic sites. Because of their strict localization to posterior sigmoid gyrus, involvement of components of a specific pathway terminating in subsurface synaptic organizations is not un-

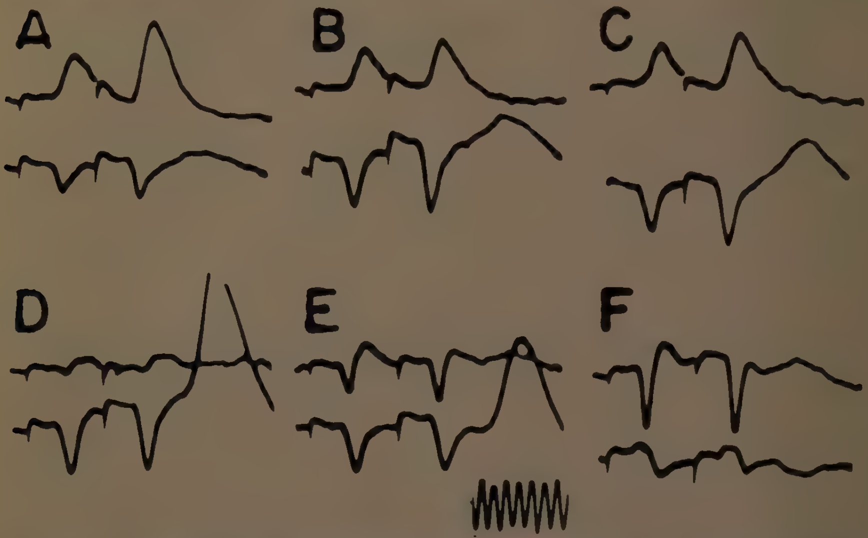

FIGURE 13. Changing characteristics of surface evoked responses in posterior sigmoid gyrus (*upper channel*) and anterior suprasylvian gyrus (*lower channel*) during progressive downward displacement of vertically oriented stimulating electrodes in anterolateral thalamus of a 2-day-old kitten. Paired shocks (70 msec. intervals) of equal strength employed throughout. Responses evoked by stimulation of dorsal regions of thalamus shown in A, those from the ventral aspects of anterolateral thalamus in F. The total vertical excursion of the stimulating electrodes was 4 mm. The changes in evoked responses shown in A to F were obtained during 0.6 to 0.8 mm. displacements. Note appearance of long-latency facilitated surface negativity in anterior suprasylvian gyrus (C to D) obtained during considerable downward movement of stimulating electrodes through thalamic regions containing elements that induce different polarity responses in posterior sigmoid gyrus. Further explanation in text. Calibrations 100 cps; 0.1 mv.

likely. As to the nature of the responses evoked in anterior suprasylvian gyrus, involvement of superficial axodendritic synaptic organizations with different activity cycle characteristics than those present in specific projection cortex is clearly indicated. Identification of such response patterns in anterior suprasylvian gyrus of newborn kittens as nonspecific activities appears justified in view of the fact that they are also obtainable from stimulation of mid-line thalamic structures and, in somewhat modified form, from stimulation of medial pontomesencephalic reticular regions. Neglecting for the moment any consideration as to the validity of this identification, it is highly instructive to examine further the characteristics of these association cortex activities in the newborn animal.

.The activity cycle of these responses as revealed by paired conditioning and testing stimuli (FIGURE 13C) is particularly interesting. In the wake of a weak conditioning activity, a period of facilitation occurs that is reflected in markedly augmented surface negativity. When, instead of utilizing paired stimuli to anterolateral thalamic nuclei, repetitive stimulation of medial pontomesencephalic regions is carried out, progressive build-up of late negativity is prominent (FIGURE 14) at low stimulus frequencies (5/sec.), whereas entirely new responses are elicited at higher frequencies (>10/sec.). Following brief periods of 25 to 50/sec. stimulation prolonged facilitation of surface negativity is detectable. Such facilitation, however, is never seen in simultaneously evoked surface-negative responses in posterior sigmoid gyrus.

Bearing in mind the remarkable morphological development of superficial axodendritic synaptic pathways in the suprasylvian gyrus of the newborn cat (FIGURES 3 to 7), it is not surprising that repetitive stimulation of these synaptic systems should result in profound changes in surface evoked activity. What is of particular interest, therefore, is not the demonstration that complex evoked activities can be registered in nonspecific projection cortex in the newborn cat but that such activities are generated predominantly in pathways involving apical dendrites, since the latter elements account for almost all of the surface area of cortical pyramidal neurons available for synaptic contacts in the immediate neonatal period. This is not to say that the surface negativity of potentiated responses shown in FIGURES 13 and 14 represents synaptic activity confined to the distal portions of apical dendrites, nor for that matter, that interneurons do not participate in some fashion in the production of the overt response. Although major components of the surface negativity are synaptically generated in distal portions of apical dendrites, during the phase of postactivation facilitation of this surface negativity, participation of activated synapses along the entire vertical course of apical dendrites is demonstrable. Also of interest is the finding that activation of different synaptic loci on apical dendrites presumably via different interneuronal organizations is independent of synaptic events initiated in more distal dendritic segments. Data supporting these statements are shown in FIGURES 15 and 16.

When a microelectrode is located in the cortical depths (0.4 mm.) at a locus where the initial surface positivity of nonspecific evoked responses is markedly attenuated, focal negativity is recorded that is of somewhat longer latency than the negativity registered from the cortical surface (FIGURE 15A). Following a brief tetanization both the focal and surface negativities were selectively potentiated. Attenuation of delayed focal negativity was observed after further downward displacement of the exploring microelectrode to a depth where the initial surface positivity was reflected in a brief subsurface

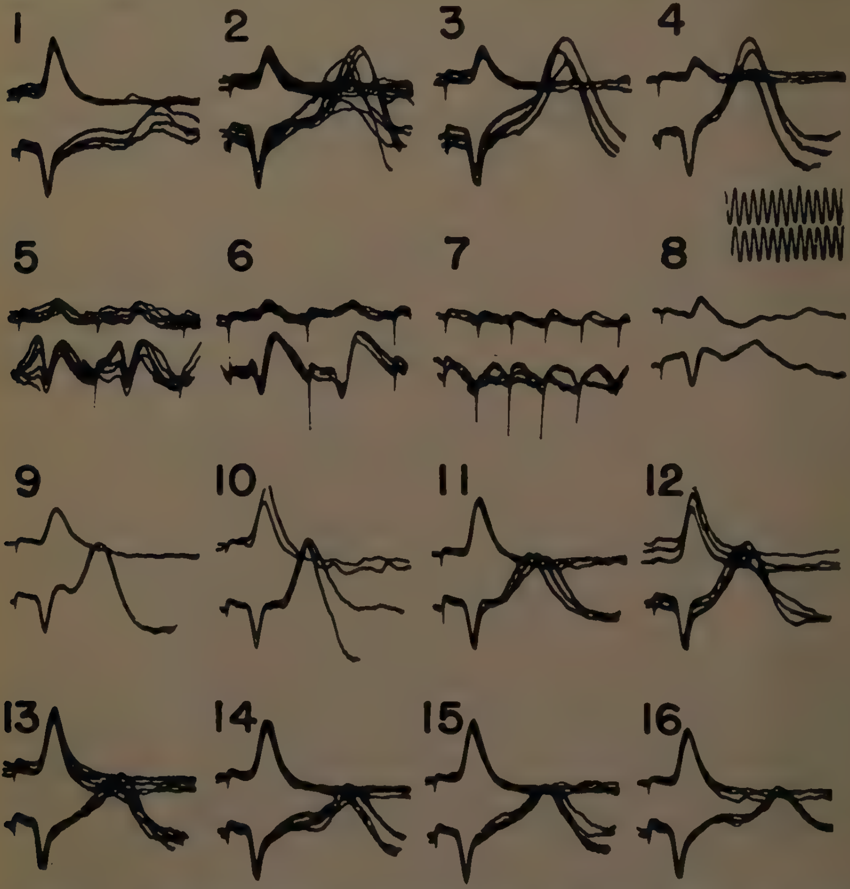

FIGURE 14. Responses evoked in posterior sigmoid gyrus (*upper channel*) and anterior suprasylvian gyrus (*lower channel*) by stimulation of anterolateral thalamus in a 2-day-old kitten. (*1*) One half/sec. stimulation. Surface-negative response in specific projection cortex is associated with a shorter duration surface-positive response in nonspecific cortex. A long-latency (120 msec.) variable, surface-negative response in anterior suprasylvian gyrus is barely detectable at 0.5/sec. stimulation. During 5/sec. stimulation (*2* to *4*) specific evoked responses are depressed. The surface-positive component in nonspecific cortex is unaffected, but the succeeding negativity is markedly augmented in amplitude and develops with a shorter latency (60 msec.). With 10/sec. stimulation (*5* to *6*) depression of specific responses increases and responses evoked in anterior suprasylvian gyrus exhibit further changes consisting of abolition of late negativity and conversion of prior surface positivity into a diphasic positive-negative sequence. Stimulation at 25/sec. eliminates all components except a small positivity in anterior suprasylvian gyrus (*7*). Following this, responses evoked at 0.5/sec. frequency (*8* to *16*) show an initial 2- to 4-sec. phase of depression. After recovery of specific responses, facilitation of the long-latency surface negativity in nonspecific cortex persists for over 2 min. The superposed responses in *13* to *16* are samples of a continuous series of records during the 2-min. period of postactivation facilitation. Calibrations 100 cps; 0.1 mv. Reproduced from *Annals of The New York Academy of Sciences*, Vol. 92, Art. 2.[55]

negativity (FIGURE 15B). Finally, at the lower limits of cortex (0.8 mm.), the initial surface positivity was associated with a prominent focal negativity and the late surface negativity was reflected in a brief focal positivity that was essentially unchanged in the immediate postactivation period (FIGURE 15C). It should be noted that discharges of cortical neurons are most prominent in focal recordings from the cortical depths (15C). It is clear from these results

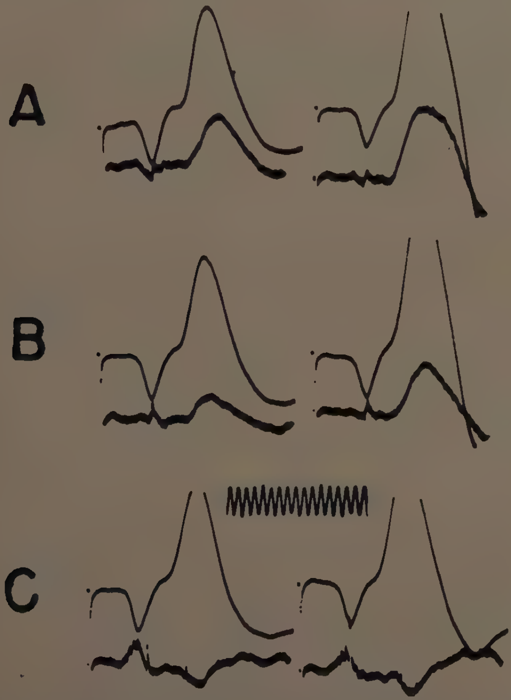

FIGURE 15. Comparison of surface responses (*upper channel*) evoked by stimulation of medial mesencephalic region, and focal responses recorded at various intracortical depths with an exploring microelectrode in anterior suprasylvian gyrus of a 2-day-old kitten. Responses were recorded before (*left column*) and after (*right column*) brief tetanization (25/sec.) of pontomesencephalic sites with same stimulating electrodes. (A) Focally evoked responses recorded with the microelectrode located 0.4 mm. below pial surface. In B and C, subsurface responses recorded at 0.6 and 0.8 mm. respectively. At the lower depths the late surface negativity is reflected in a minor focal positivity, whereas the initial surface positivity is associated with a prominent subsurface negativity upon which brief discharges of cortical units are barely detectable. Further explanation in text. Calibrations 100 cps; 0.1 mv.

that the positive-negative components of the surface evoked responses have different spatial distributions in neonatal cortex and that, although the negativity is relatively diffusely distributed in depth, it is not reflected in a significant subsurface focal positivity.

The independent nature of the surface and focal negativities is provided by a comparison of their characteristics at various times after a sustained tetanus (FIGURE 16A). Then the subsurface negativity may undergo changes in amplitude and duration that are not at all reflected in surface responses. FIGURE 16B illustrates still another point relevant to the interpretation of the surface and focal negativities. In this experiment advantage was taken of previous findings on the lability of the blood-brain barrier of newborn animals to systemically administered γ-aminobutyric acid[47] to demonstrate that when injected GABA blocks superficial axodendritic depolarizing synapses, thus eliminating the surface negativity of responses evoked prior to tetanization (cf. *1* and *3* in FIGURE 16B), during the phase of postactivation facilitation the potentiated surface negativity is 'reversed' in polarity, but the polarity of the focal response is unchanged (4 in FIGURE 16B). Failure to detect a significant focal positivity during registration of the surface negativity in evoked responses prior to GABA (FIGURES 15 and 16A) would appear to be inconsistent with

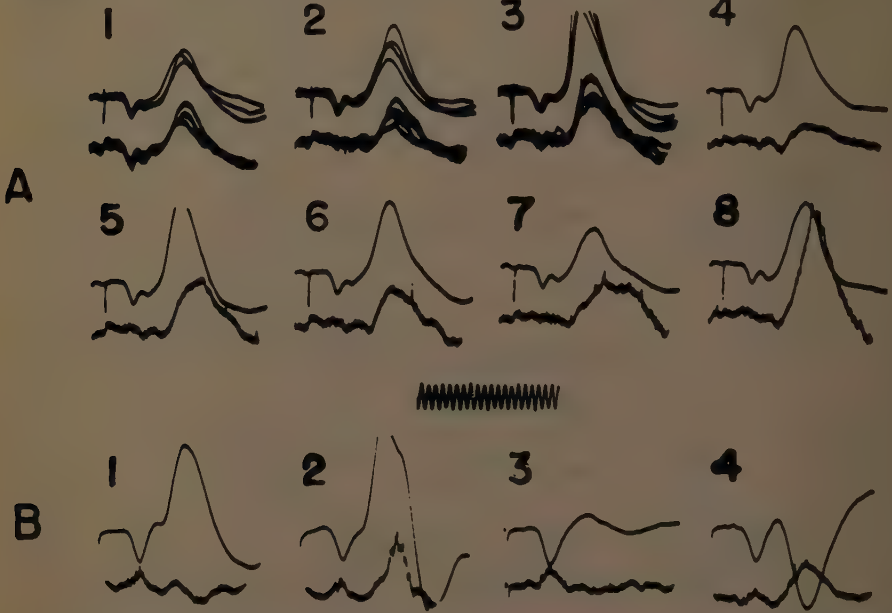

FIGURE 16. Postactivation facilitation of evoked responses in nonspecific cortex (suprasylvian gyrus) in a 2-day-old kitten. Stimulation in medial portion of lower mesencephalon.

A. (*1*) Evoked responses recorded from the cortical surface with a ball-tipped electrode (*upper channel*) and an adjacent saline-filled micropipette (*lower channel*). (*2*) Two minutes after microelectrode placed in position 0.4 mm. below cortical surface. Stimulation in *1* and *2* at 0.5/sec. During 5/sec. stimulation (*3*) responses recorded at surface and subsurface sites are enhanced. Between *3* and *4*, stimulus frequency increased to 25/sec. for 4 sec. Responses in *4* to *8* were obtained with 0.5/sec. stimulation during postactivation period. Dissociation of effects recorded at surface and subsurface sites is clearly seen, especially in *4* and *8*. Further explanation in text.

B. Same experiment as in A, but stimulation in more rostral mid-brain regions. (*1*) Microelectrode (*lower channel records*) in position 0.55 mm. below cortical surface. At this site, phase reversal of initial surface positivity is complete and late surface negativity is reflected in a small subsurface focal positivity. (*2*) During the early phase of postactivation facilitation as in A (*5*). (*3*) 30 sec. after intravenous injection of 100 mg./kg. GABA. Long-latency surface negativity is abolished. (*4*) During GABA action, long-latency surface positivity is unmasked in the postactivation period, but polarity of focal responses is similar to that recorded prior to the action of the ω-amino acid. Calibrations 100 cps; 0.1 mv. Reproduced from *Annals of The New York Academy of Sciences*, Vol. 92, Art. 2.[55]

the view that appearance of surface positivity after GABA is due to some obscure alteration in "source-sink" relations.[48] Rather it seems more likely that the appearance of surface positivity after GABA blockade of superficial axodendritic depolarizing synapses represents an 'unmasking' of hyperpolarizing axodendritic p.s.p.s that, like depolarizing p.s.p.s, are focally generated in distal dendritic segments. Failure of systemically administered GABA to alter subsurface negativity may be explainable on the basis of a limited passage of the amino acid across capillary-glial membranes in the cortical depths that have not been altered as a consequence of cortical exposure in the newborn kitten.[47] The possibility must also be considered that the focal subsurface negativity is compounded of aoxdendritic p.s.p.s and p.s.p.s generated axosomatically in interneurons. If such is the case, the contribution of axosomatic p.s.p.s to the focal response would be unaffected by GABA since the amino acid does not appear to alter transmission at axosomatic excitatory synapses in cerebral cortex.[11,13,23,38,49]

Further speculation concerning the interpretation of the GABA effects shown in FIGURE 16B must await acquisition of additional data. Information already at hand indicates the fiction of assuming that the elaboration of highly complex electrocortical events must of necessity require participation of synaptic activities distributed in basilar, as well as apical dendritic systems of cortical neurons. For while it is obvious that the rapid, but delayed, development of basilar dendritic systems of cortical pyramidal elements must be a major factor contributing to the ultimate morphophysiological complexity of the mammalian cerebral cortex, synaptic organizations involving apical dendrites and their related interneurons would appear to be sufficient for the production of a wide variety of electrocortical activities, at least in the immediate neonatal period. Further examination of these activities in newborn animals permits consideration of a number of problems concerning the manner in which axodendritic synaptic pathways in the neocortical neuropil may participate in response patterns of the most complex nature.

A detailed analysis of evoked response patterns in 'association' cortex of newborn kittens is made possible by the relative absence of organized spontaneous electrocortical activity in the immediate perinatal period. This is not to say, however, that the neocortex is electrically quiescent in the intact newborn kitten. What is meant here is that even when the greatest care is taken in preparing locally anesthetized, paralyzed kittens for such experimentation as multiple cortical surface and subsurface recordings and brain stem stimulation some generalized depression of activity cannot be avoided. Consequently, background spontaneous electrocortical activity is negligible largely because of obscure factors related to "immaturity" and, secondarily, because of the operational procedures required for the analysis. These preliminary remarks aside, a few examples of the effects of repetitive stimulation of nonspecific projection pathways on association cortex evoked responses may be noted.

One of the most interesting results observed in the perinatal period during repetitive stimulation of intralaminar nuclei concerns the characteristics of evoked responses in anterior suprasylvian gyrus. Unlike responses recorded in mature cortex during low-frequency stimulation of nonspecific thalamic

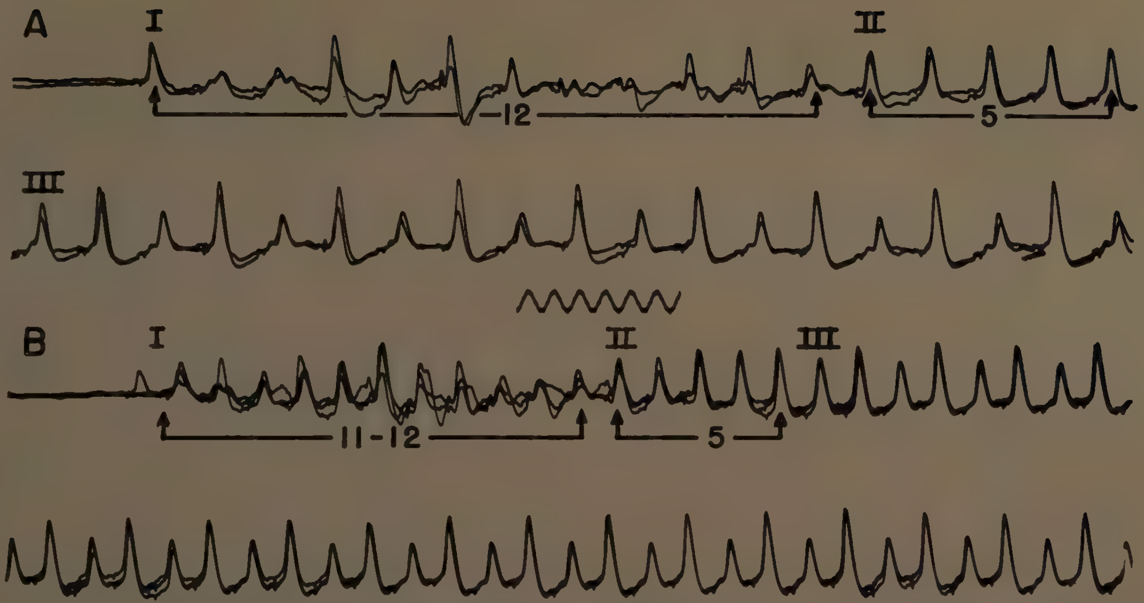

FIGURE 17. Characteristics of repetitively evoked responses in anterior suprasylvian gyrus of 1-day-old kitten during stimulation of intralaminar thalamic nuclei. Stimulus frequencies in A, 5/sec.; that in B, 10/sec. Two superposed sequences of continuous records shown in A and 3 superposed sequences shown in B. For convenience, the 3 phases of the alteration in evoked responses are labeled I to III. At 5/sec. stimulation, the phases evolve with remarkable regularity to the point of response alternation (III). In the continuous records shown in B, superposition of all 3 traces was accomplished by eliminating the first response in one of the series. Particularly noteworthy in these records is the complex but orderly evolution of the various phases at different stimulus frequencies. Further discussion in text. Calibration 10 cps; 0.1 mv.

nuclei[50,51] the first of a sequence of repetitively evoked responses in the newborn kitten is well developed, whereas the second, third, and sometimes the fourth responses in the series are attenuated (FIGURE 17). A similar phenomenon has been described recently in the newborn rabbit.[52] If 5/sec. stimulation is extended beyond the period of initial attenuation, there occurs first a phase during which evoked responses maintain a constant high-amplitude then another phase in which responses alternate in amplitude. For analytical purposes, the various phases thus outlined can be thought of as representing three stages of activation; the first encompassing 12 responses; the second, 5, and the third all subsequent alternating responses. It is to be noted in FIGURE 17A, that this response pattern may be so stereotyped as to permit superposition of successively evoked trains of responses, if a recovery time of 20 to 30 sec. is allowed between trains. Of particular significance is the fact that the development of the various stages proceeds similarly at 5/sec. and 10/sec. stimulation (FIGURE 17B). Demonstrated here is a complex sequence of electrocortical events of the most orderly character in which the transition from one synaptic event to another is apparently governed by the number of corticipetal volleys, whatever their composition, and not their frequency, at least within the low limits specified. At higher stimulus frequencies (> 10/sec.) orderly transitions from one event to the other may not be detectable. For at higher frequencies, additional synaptic events are introduced which profoundly alter transmission in the axodendritic synaptic pathways involved in nonspecific evoked responses.

Some understanding of the nature of the alterations in responses evoked in rostral suprasylvian gyrus of newborn kittens by high-frequency intralaminar thalamic stimulation is provided by re-examination of the activity cycle characteristics of these responses (cf. FIGURE 13). It has been noted that with paired conditioning-testing stimuli of equal strength marked facilitation of surface negativity occurred at stimulus intervals of 30 to 60 msec. In FIGURE 18A, facilitation of surface negativity produced by paired intralaminar conditioning-testing stimuli of equal strength is shown when the stimulus interval is 50 msec. and paired stimuli are repeated at 0.5/sec. frequency. The continuous records B to F in FIGURE 18 illustrate initial stabilization, then some alternation of 10/sec. evoked responses to the conditioning stimulus and the pronounced augmentation of 10/sec. activity when the testing stimulus follows the conditioning stimulus by 50 msec. Thus at repetition rates of 10/sec. each conditioning response appears to leave in its wake a prolonged phase of augmented excitability in superficial axodendritic synaptic organizations. This phase attains maximal intensity 40-60 msec. after the conditioning stimulus and is reflected in facilitation of testing responses when the latter are interpolated during the peak of the alteration in excitability. From this it might be expected that sustained 'driving' of high-amplitude 10 to 14/sec. evoked responses would result from employing stimulus repetition rates of 25/sec. Unfortunately, the situation that obtains when such stimulus frequencies are employed is far removed from expectation. For although the second stimulus in a 25/sec. train evokes a facilitated response, this is followed by a prolonged phase of apparent depression during which surface negativity is abolished (FIGURE 19A). With continued 25/sec. stimulation this phase passes over into another during which high-amplitude 10 to 12/sec. surface negativity reappears and persists for several seconds (FIGURE 19A). Then, interpolation of a 50/sec. stimulus produces little effect other than a slight increase of response frequency (FIGURE 19C). Resumption of the 25/sec. stimulus results in progressive attenuation, then disappearance of evoked activity, but interpolation of the 50/sec. stimulus immediately induces reappearance of 10/sec. responses (FIGURES 19D to F).

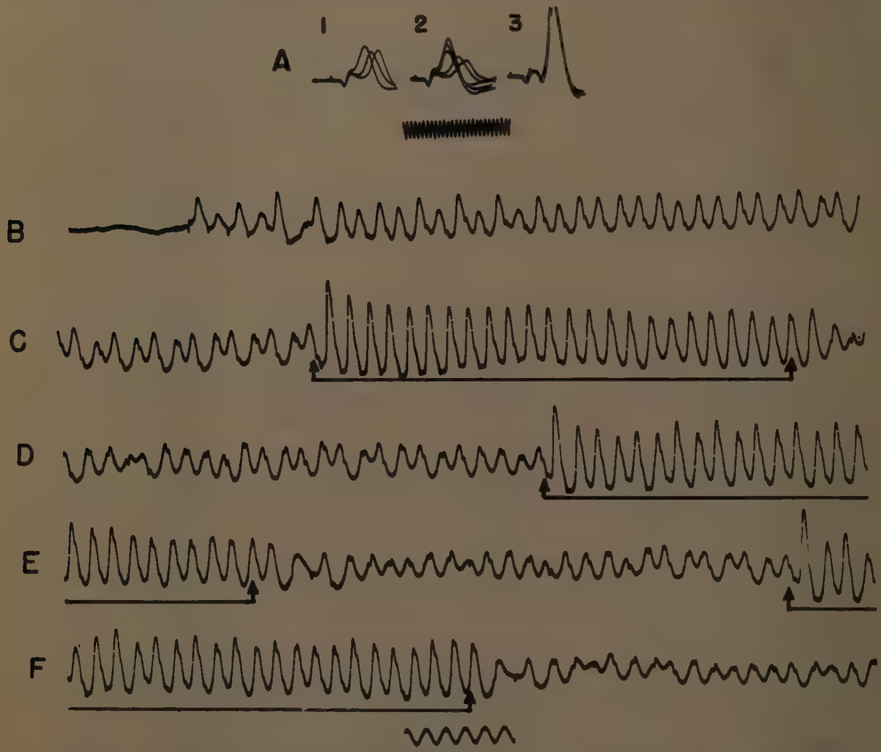

FIGURE 18. Facilitation of repetitively evoked responses in anterior suprasylvian gyrus of a 2-day-old kitten during short-interval, paired-shock, 10/sec. stimulation of intralaminar thalamic regions (histologically verified). A. Conditioning (*1*), and testing (*2*) responses evoked by 0.5/sec. stimuli exhibit considerable variability, but this is only seen in surface-negative component of response. With paired-stimulation (*3*), (showing 30 to 40 msec. stimulus-intervals), surface negativity of 0.5/sec. evoked responses is markedly facilitated. Continuous records (B to F) show effects of introducing second stimulus during continuous 10/sec. stimulation. Interval during 30 msec. paired-stimulation is indicated by arrows. Facilitation is maintained during the entire period of double-shock stimulation. Calibrations 10 cps; 0.1 mv.

The foregoing results indicate that as the frequency of stimulation of nonspecific thalamocortical pathways is increased from 10/sec. to 25/sec. and again from 25/sec. to 50/sec., the responsiveness of axodendritic synaptic organizations in nonspecific projection cortex of the newborn cat fluctuates over relatively wide ranges, but the frequency of driven evoked electrocortical activity remains "fixed" at 10 to 14/sec. This is significant in providing information on the origin of certain brain wave patterns, but far more significant is it that changes in the frequency of corticipetal volleys or, for that matter, long-continued stimulation at a constant frequency should set into operation additional synaptic processes that contribute to facilitation or suppression of the 10 to 14/sec. evoked activity characteristic of axodendritic synaptic organizations in some regions of immature neocortex.

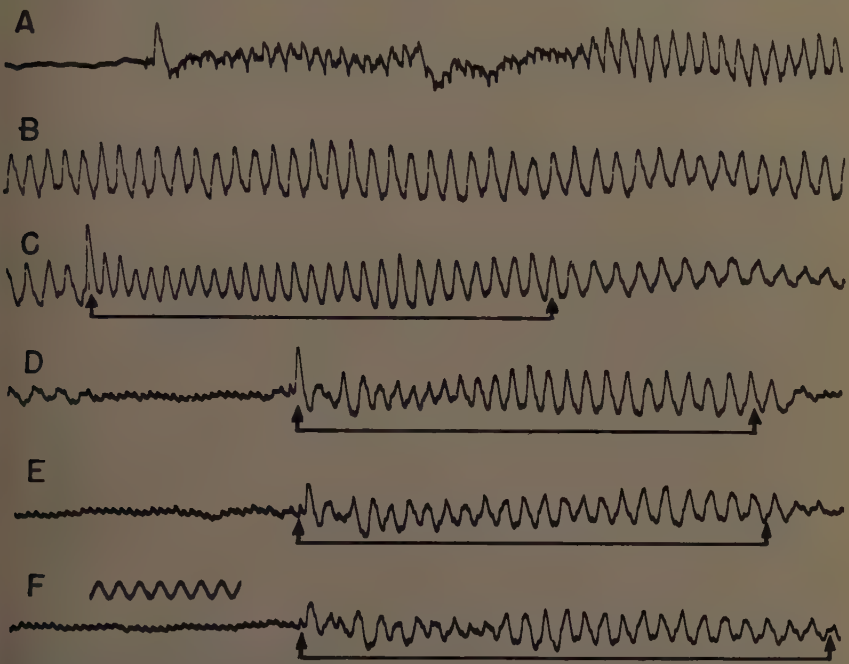

FIGURE 19. Alterations in evoked electrocortical activity in nonspecific projection cortex (anterior suprasylvian gyrus) following high-frequency intralaminar thalamic stimulation in a 2-day-old kitten. Spontaneous electrocortical activity absent in this preparation at the time of stimulation. (A to F) Continuous record. Intralaminar stimulation (25/sec.) initiated in A. High-amplitude evoked potential is followed by a phase of depressed responsiveness, then progressive build-up of 10/sec. waves driven by 25/sec. stimulation (B). In C, the stimulus frequency is changed to 50/sec. (for period indicated by arrows) then reduced again to 25/sec. In D to F, stimulus frequency changes from 25 to 50/sec. are similarly indicated. Note blockade of 10/sec. waves during continued 25/sec. stimulation and reappearance during 50/sec. stimulation. Calibrations (*lower left, above record F*) 100 cps; 0.1 mv. Reproduced from *Annals of The New York Academy of Sciences*, Vol. 92, Art. 2.[55]

The contributions of various subcortical organizations to the overt effects of different stimulus frequencies on axodendritic synaptic pathways involved in the production of evoked 10 to 14/sec. responses in nonspecific projection cortex cannot be assessed from available data. That a considerable degree of involvement of different subcortical, as well as cortical organizations, in these effects does occur seems likely from other studies.[23,53,54] In this respect it is of interest to note that similar prolonged suppression or facilitation of nonspecific evoked responses in immature cortex can be observed following stimulation of medial pontomesencephalic reticular regions at different frequencies. Under these conditions sustained synaptic processes are revealed that, although they are not reflected in overt cortical surface potentials, are nevertheless clearly demonstrable by the effects they exert on pathways involved in the production of non-specific evoked activities.

Some of the data supporting these conclusions are displayed in three different ways in FIGURES 20 to 22 in order to illustrate different aspects of the complexity of the underlying synaptic processes. The characteristics of driven 10 to 14/sec. activity evoked in suprasylvian gyrus by 25 and 50/sec. stimulation of pontomesencephalic reticular regions in a 2-day-old kitten is shown in FIGURE 20A. Emphasis is placed on the magnitude of the initial "facilitated" response, the brief phase of suppression and the later phase of evoked rhythmical activity that persists after cessation of the high-frequency stimulus. In FIGURE 20C, the last response (marked by black dot) of a long series evoked by 0.5/sec. stimulation is shown prior to a period of 10/sec. stimulation. At the end of the 10/sec. stimulation, 0.5/sec. stimulation is resumed but no significant change in the evoked response is detectable. Entirely different effects on 0.5/sec.-evoked responses are observed after interpolation of a period of 25 and 50/sec. stimulation (20D and E). Then profound facilitation of 0.5/sec. evoked activity occurs which may persist for many seconds.

The sequence of alterations in 0.5/sec.-evoked responses occurring before and after interpolation of brief 25/sec. stimulation is shown in greater detail in FIGURE 21. Three events are of particular interest: (1) the progressive fall-off and virtual disappearance of 0.5/sec.-evoked responses in the series (21A *1* to *12*) prior to a 25/sec. burst (S-S) lasting 4 seconds; (2) build-up and persisting facilitation of subsequent 0.5/sec.-evoked response; (3) the gradual dissipation of the facilitation and stabilization of evoked responses at a low level prior to another period of 25/sec. stimulation. Graphical representation of data similar to that in FIGURE 21 is shown in FIGURE 22 from another series obtained in the same preparation. In this series, the initial response evoked after a long "rest" period was of considerable amplitude, but over a 2-minute period of continuous 0.5/sec. stimulation surface-evoked activity almost completely disappeared. After a 4-sec. tetanization (25/sec., arrow *1* in FIGURE 22) 0.5/sec.-evoked responses were markedly facilitated for about 30 sec. then gradually fell to a low amplitude. Each time this occurred, restoration of activity was effected by a brief 4-sec. tetanization (at 25/sec., arrows *2* to *6*), but the magnitude of this facilitation progressively diminished with each tetanization. Interpolation of a new stimulus pattern (50/sec., arrow *7*) restored the initial facilitation almost to full magnitude and, when this was again dissipated, 25/sec.-tetanization (arrow *8*) produced a period of facilitation that was of greater intensity than that observed before the 50/sec. stimulus.

An attempt to explain the electrocortical event illustrated in FIGURES 20 to 22 in terms of the morphophysiological characteristics of different synaptic organizations in the immature brain is obviously impossible since nothing is known concerning the manner in which synaptic pathways other than those in superficial neocortex participate in the elaboration of these complex activities. Despite this, some of the processes presumably involved in these events may be considered briefly.

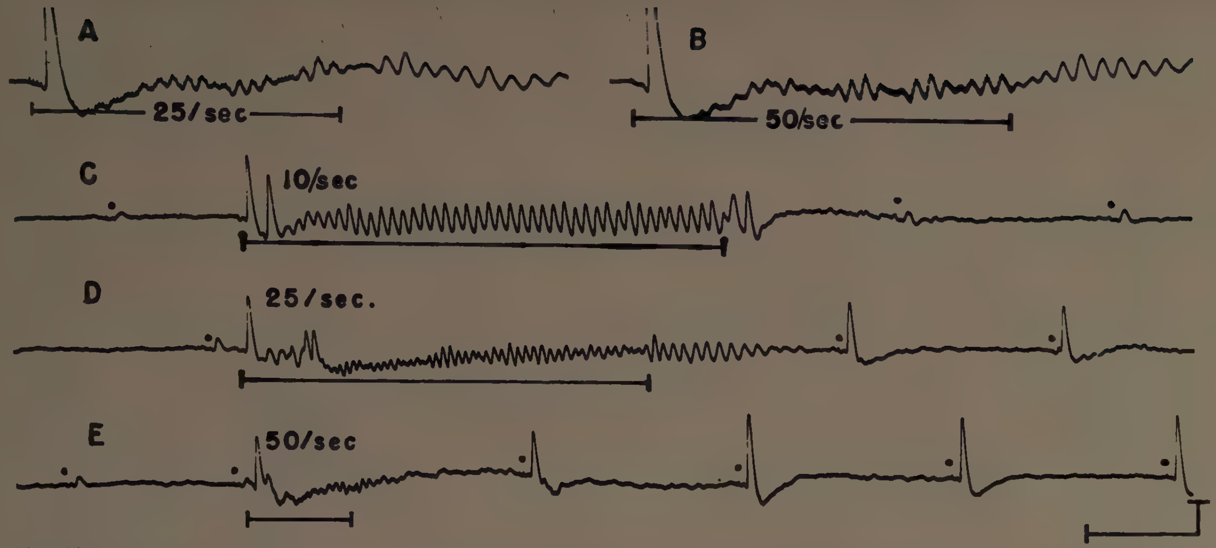

FIGURE 20. Alterations in surface-evoked responses in anterior suprasylvian gyrus during and after medial pontomesencephalic stimulation in a 2-day-old kitten. Note prominent evoked potential, then 10 to 14/sec. waves persisting after 25/sec. (A), and 50/sec. (B) stimulation. C. A low-amplitude response evoked by 0.5/sec. stimulation is shown (*black dot*) prior to change in stimulus frequency to 10/sec. After cessation of 10/sec.-driving, minimal change occurs in 0.5/sec.-evoked responses. D and E same as in C, but stimulus changed from 0.5/sec. to 25/sec. in D, and 50/sec. in E, as indicated. Note profound postactivation facilitation especially after short 50/sec. burst. Time calibration lower right; A and B, 0.5/sec.; C to E, 1 sec. Reproduced from *Annals of The New York Academy of Sciences*, Vol. 92, Art. 2.[55]

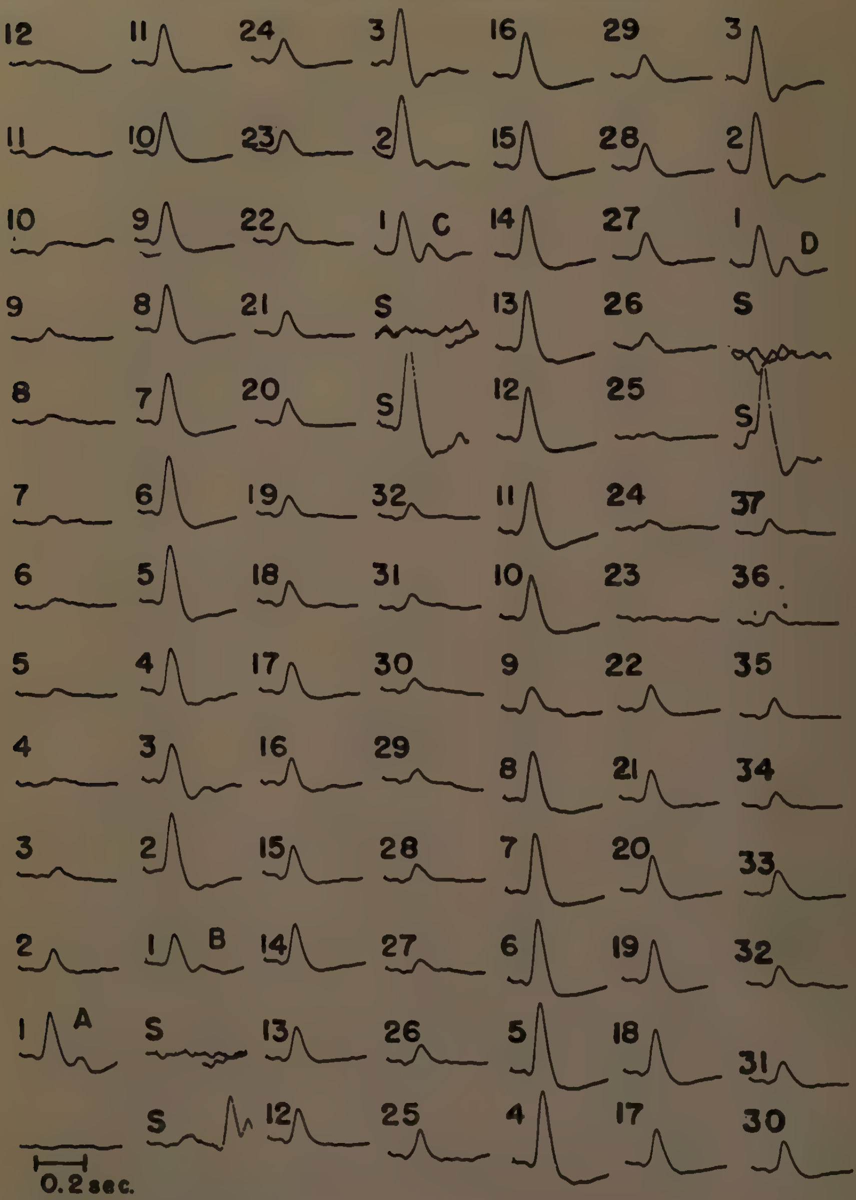

FIGURE 21. Continuous series of surface responses in anterior suprasylvian gyrus evoked by 0.5/sec. brain stem stimulation for 3 min. Figure to be read from lower left to upper right. First series (A, *1* to *12*) was initiated after a 30-min. rest period. Note rapid disappearance of response during 0.5/sec. stimulation and facilitation after 4 sec. bursts of 25/sec. stimulation (S to S). Series B shows a 1-min. period of postactivation facilitation. Cyclic changes in responsiveness occasionally observed during postactivation facilitation is shown in series C, *1* to *37*. Reproduced from *Annals of The New York Academy of Sciences*, Vol. 92, Art. 2.[55]

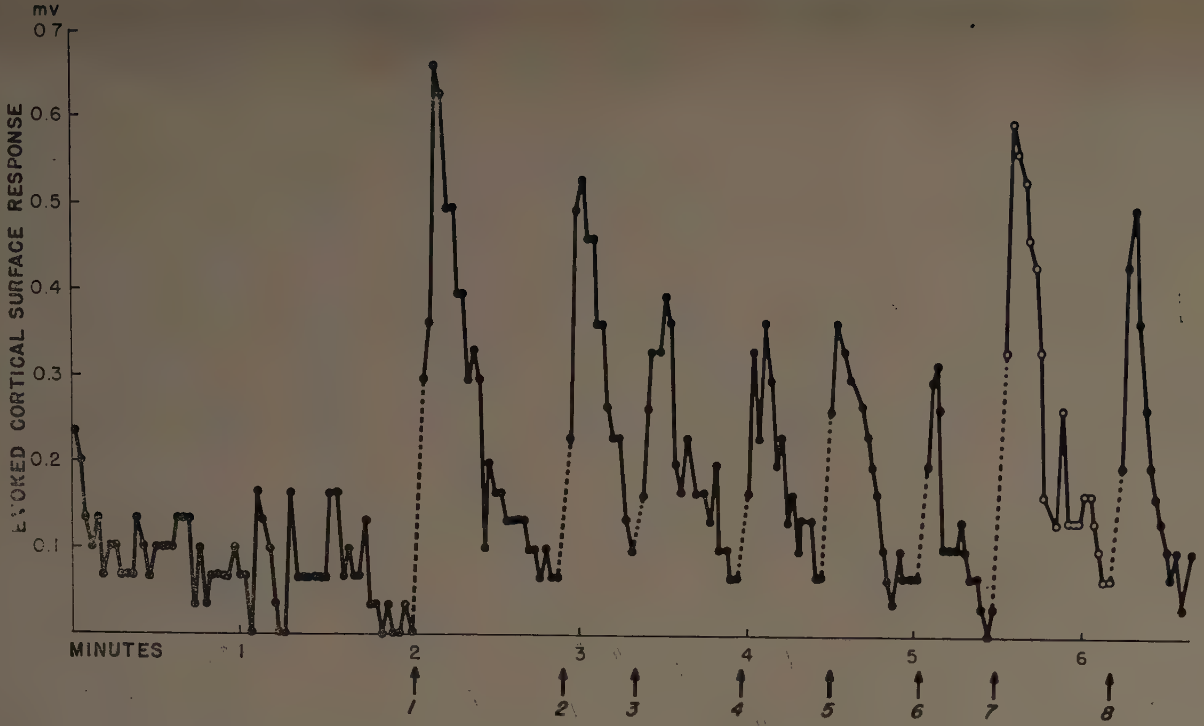

FIGURE 22. Graphical representation of data similar to that shown in FIGURE 21 but from another continuous series lasting more than 6 min. Amplitude of 0.5/sec. evoked responses in anterior suprasylvian gyrus rapidly decreases over 2-min. period. At first arrow, stimulus frequency abruptly changed to 25/sec. for 4 sec. (*dotted portion of curve*). Postactivation facilitation of 0.5/sec. evoked response is profound initially, but during continued presentation of 25/sec. stimulation (*arrows 2 to 6*) the latter becomes less effective. The magnitude of the postactivation facilitation is partially restored after 50/sec. stimulation (*arrow 7, series with open circles*), and again with 25/sec. stimulation (*arrow 8*). Reproduced from *Annals of The New York Academy of Sciences*, Vol. 92, Art. 2.[55]

The initial progressive attenuation of evoked responses observed during prolonged low-frequency (0.5/sec.) stimulation of pontomesencephalic pathways is surely not explainable on the basis of accumulation of "refractoriness" in the pathways involved in the evoked activity. Nor can it be inferred that the increasing ineffectiveness of tetanizing stimuli of the same pontomesencephalic regions at a particular frequency is a reflection of some obscure alteration in the degree to which high-frequency corticipetal volleys are capable of mobilizing facilitatory synaptic activities. One alternative explanation is that the suppression of 0.5/sec.-evoked responses and the suppression of the facilitating effect of repeated 25/sec. stimuli may be consequences of the build-up of inhibition in parallel pathways activated by the brain stem stimulation. Viewed in this way the effectiveness of these inhibitory processes distributed in neocortical organizations involved in evoked responses might be augmented during monotonous repetition of a particular stimulus pattern. The necessity of invoking the operation of excitatory and inhibitory synaptic activities that differ in proportion, magnitude, and time course in explaining the alterations in evoked responses shown in FIGURES 20 to 22 seems no less plausible in this situation than in others in which complex alterations in cortically evoked potentials have been analyzed in greater detail.[23,38,53,54] Neglecting any further consideration of the possible mechanisms that may provide a more satisfactory explanation of the foregoing observations, the fact that complex electrocortical events involving predominantly superficial axodendritic synaptic pathways are demonstrable in the immediate neonatal period is sufficient to suggest the important role these organizations play in the elaboration of different varieties of "higher nervous activity" in the immature, as well as the mature animal.[55]

Reorganization of Axodendritic Synaptic Pathways in Isolated Immature Neocortex

In previous sections attempts have been made to define the contribution of superficial axodendritic synaptic pathways to different varieties of activities evoked in the neocortex of the newborn cat. In these studies, carried out for the most part in kittens less than 2 to 3 days old, emphasis was placed on the morphological features of neocortical pyramidal neurons in the immediate perinatal period in order to provide data on the origin and nature of surface-negative components of different evoked responses. The origin of surface-positive components in some varieties of evoked responses in the newborn cat has not, as yet, been detailed although some evidence has been noted suggesting an axosomatic and/or proximal apical dendritic origin of some synaptically evoked activities. In this section an additional analytical approach to the study of synaptic organizations in immature neocortex is introduced, that is, one that permits some conclusions concerning the transmission of activities in recurrent axodendritic excitatory synaptic pathways in the cortical depths.

It is to be recalled that axon-collaterals of neocortical pyramidal neurons are relatively poorly developed in the immediate neonatal period. Indeed, it is not until the second postnatal week that these elements, basilar dendrites and stellate cells attain their maximal rate of growth. Attempts to define the morphophysiological characteristics of axodendritic synaptic pathways constituting the deep cortical neuropil in 2- and 3-week-old kittens are likely to be frustrated by the overwhelming complexity of this elaborate neuronal network.

Consider now the consequences of isolating a slab of neocortex in the immediate neonatal period.[56] When care is taken to insure maintenance of an adequate blood supply in such isolated slabs, cortical pyramidal neurons whose descending axons have been interrupted below the origin of their intracortical collaterals are not only completely preserved, but continue to elaborate their basilar dendritic systems. In response to the loss of descending axons, pyramidal neurons in the isolated cortical slab immediately undergo a phase of intense axon-collateral proliferation which, as Cajal[57] first pointed out, converts Type I neurons with descending axons into Type II neurons whose axons ramify entirely within cortex. Suffice it to say that the observations of Cajal[57] on the morphological changes occurring in immature cortex after cuts in the subcortical white matter have been thoroughly confirmed.[56] To Cajal's observations and speculations concerning the possible physiological implications of this reorganization can now be added details of the morphophysiological characteristics of "Type II pyramidal neurons" in 4- to 10-day-old kittens. The data summarized here were obtained 2 to 9 days after complete isolation of approximately 1.5 sq. cm. of neocortex including the anterior and middle suprasylvian gyrus and portions of the marginal and ectosylvian gyri.

A Golgi-Cox preparation of a chronically isolated cortical slab in a 10-day-old kitten is shown in FIGURE 23A. The 200-μ section is taken through a small corner of the slab prepared on the first postnatal day, in order to demonstrate its complete isolation from the subjacent white matter and surrounding cortex. The microphotographs below this (FIGURES 23B and C) are of deep pyramidal neurons whose descending axons were interrupted at the line of section passing from the left downward toward the right in B and, in C, a short distance below the lower limits of the field photographed. FIGURE 23B is from the same preparation as in A, whereas FIGURE 23C is from a 7-day-old-kitten whose cortex was isolated on the third postnatal day. No trace of the segment of descending axon below the first collaterals is seen in either of the preparations. At the point of origin of the initial collaterals 2 or 3 of the latter are shown, some of which (B) assume a recurrent trajectory. Further details of the relationship between these collaterals and adjacent pyramidal neurons is shown in FIGURES 24 and 25. Of particular importance is the profound proliferation of recurrent axon collaterals.

Some idea of the localized nature of the repetitive activities generated in isolated slabs of immature cortex by weak surface stimulation is obtained by a comparison of the surface activities recorded 1.5 and 3.5 mm. from the site of stimulation (FIGURE 26) in a 10-day-old kitten whose cortex was isolated on the third postnatal day. The near (1.5 mm.) and distant (3.5 mm.) SCRs in this series are followed by additional surface negativities of variable duration and latency. These terminate in a slow positivity after which a repetitive sequence of predominantly surface-positive responses is recorded largely in the immediate vicinity of the site of stimulation (FIGURE 26C). The variable delay between the time of stimulation and the appearance of repetitive activity is particularly noteworthy.

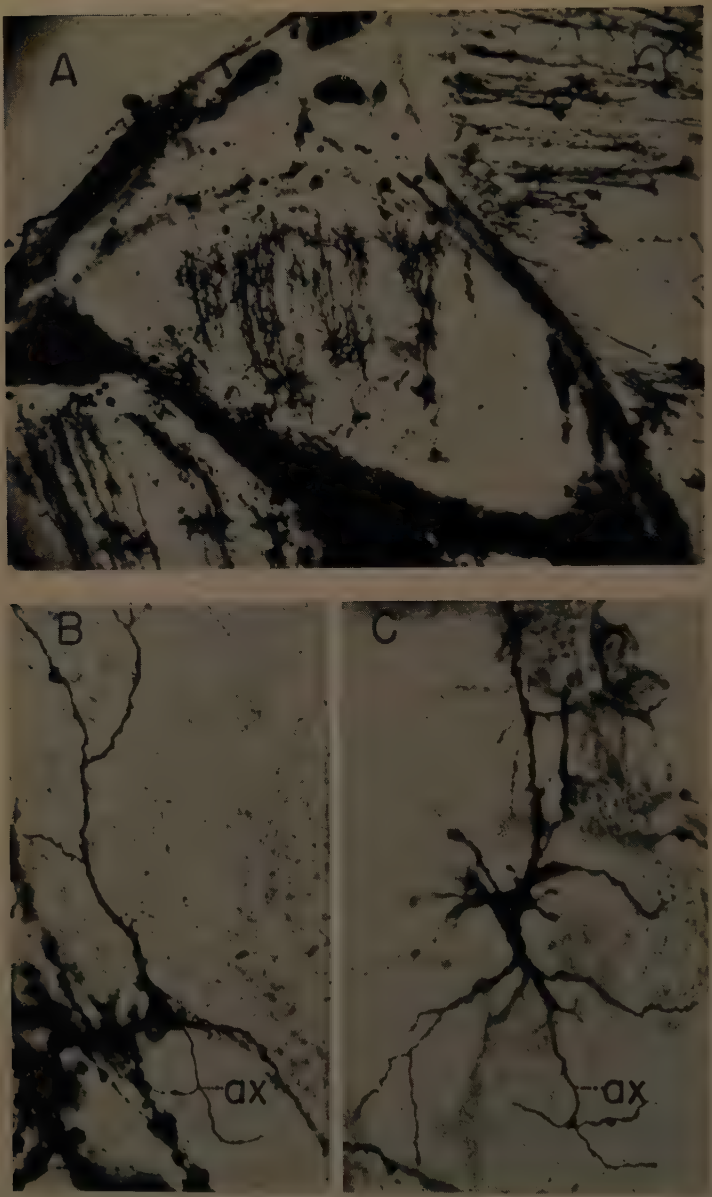

Figure 23. (A) Low power (Golgi-Cox) microphotograph of a portion of isolated cortex in a 10-day-old kitten 9 days after preparation of the slab. The section is taken through a small corner of the slab to show the completeness of the surgical procedure. (B) Large pyramidal neuron near the margin of section (*passing from middle-left to lower-right*) from the same preparation as that shown in A, but from another site in slab. The axon (Ax) is shown giving off two recurrent collaterals, but no segment below the collaterals is seen. (C) Large pyramidal neuron with axon giving off three recurrent collaterals: 7-day-old kitten, 4 days postcortical isolation. Magnification in A, ×25. In B and C, about ×300.

The lack of a temporal relationship between stimuli and the development of repetitive activity is also shown in FIGURE 27 in records taken from a 5-day-old kitten in which a cortical slab was isolated on the second postnatal day. In FIGURE 27A, the SCR and a high-amplitude surface positivity was evoked with one stimulus, whereas a second stimulus, delivered 3/sec. later, evoked an SCR and a repetitive sequence of 8 to 10/sec. diphasic positive-negative responses.

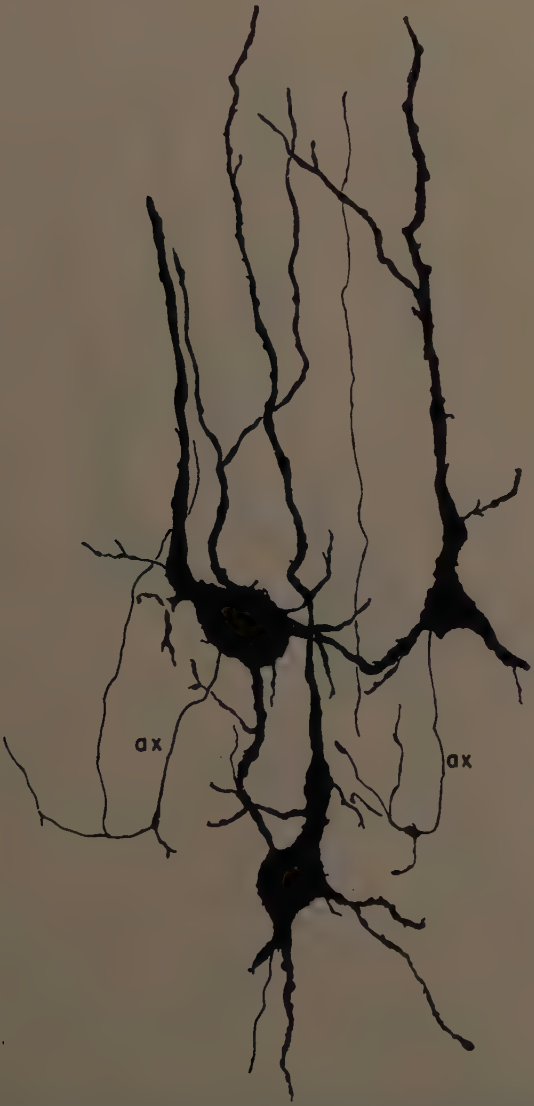

FIGURE 24. Drawing of pyramidal neurons in a single high-power field near the margin of section in an isolated slab of cortex in a 7-day-old kitten, 6 days postisolation.
Note axons (Ax) and proliferation of axon-collaterals, as well as their recurrent trajectory.

The continuous records (FIGURES 27B to E) illustrate 2 further points; (1) failure of weak repetitive surface stimuli to 'drive' the paroxysmal discharges in the isolated slab; and (2) the prolonged depression of pathways involved in the SCR when the latter are evoked on the late negative components of the discharges or up to 0.8 to 1 sec. thereafter.

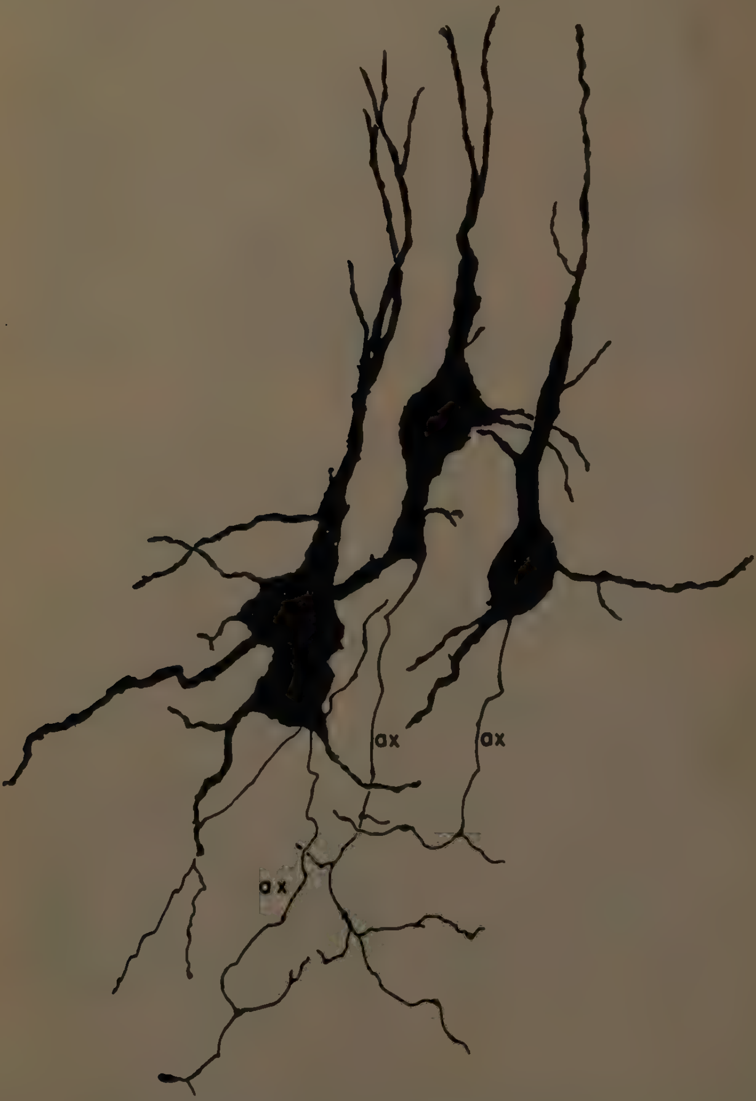

FIGURE 25. Deep-lying pyramidal neurons in a single high-power field from an isolated cortical slab in an 8-day-old kitten, 7 days postisolation. Axons (Ax) exhibit features similar to those shown in FIGURE 24. The descending axonal segment below the origin of the collaterals is not preserved.

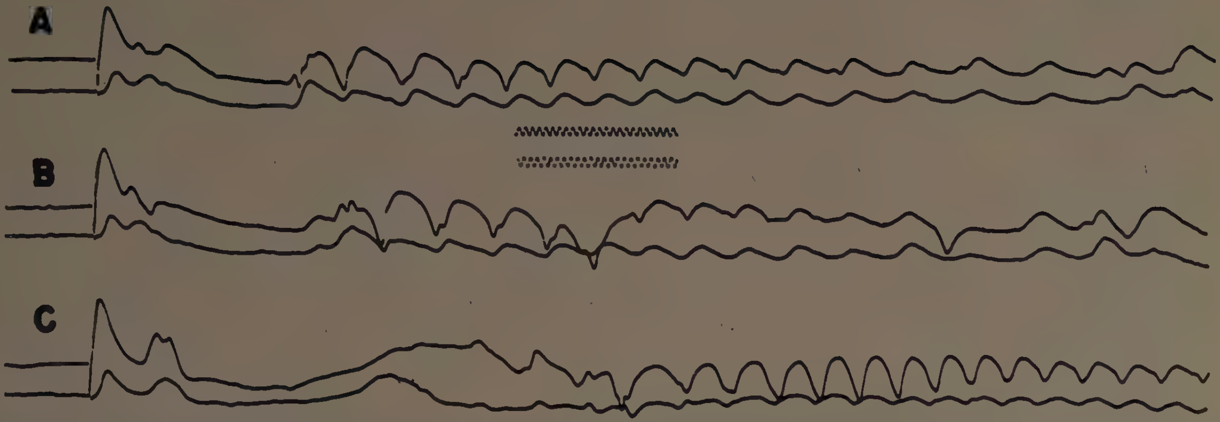

FIGURE 26. Superficial cortical responses and repetitive activity initiated by weak surface stimulation in isolated cortex of a 10-day-old kitten, 7 days postisolation. Upper channel responses recorded 1.5 mm. from the site of stimulation; lower channel responses recorded 3.5 mm. from the site of stimulation. Note localized nature of repetitive activity, especially in B and C, as well as the lack of temporal relationship between SCR and repetitive sequence. Further explanation in text. Calibration 100 cps; 0.1 mv.

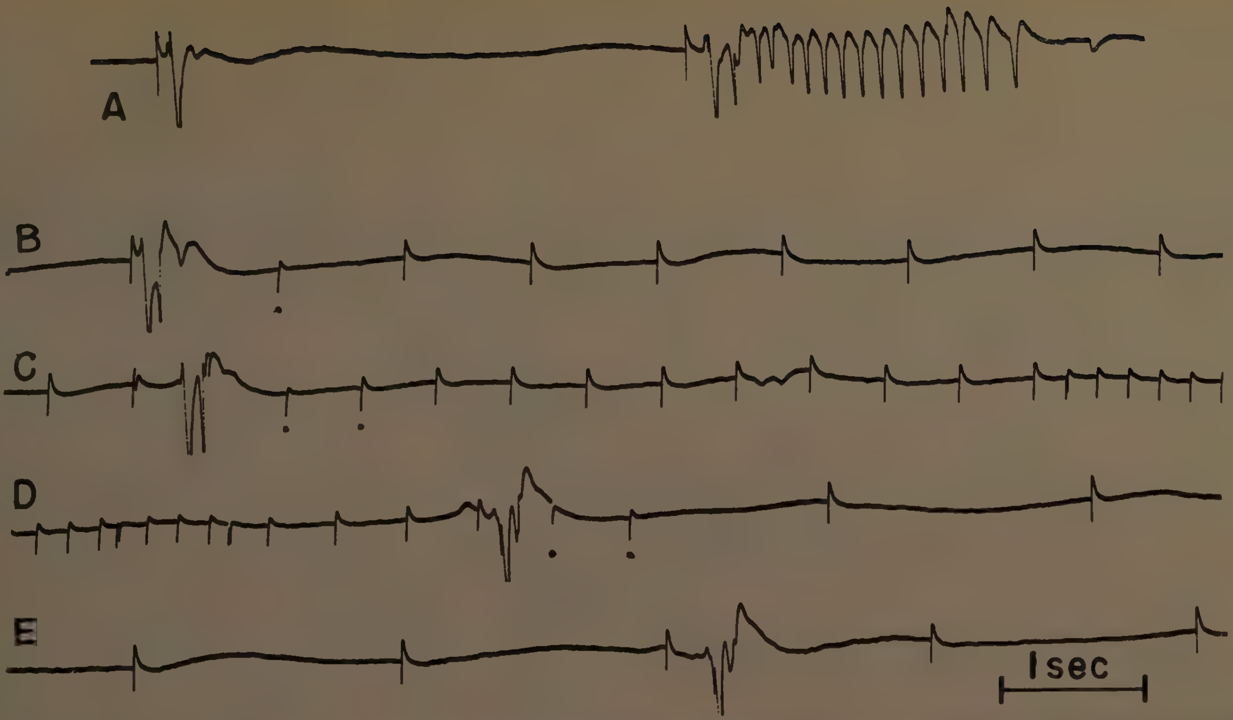

FIGURE 27. SCRs and repetitive activity evoked in an isolated cortical slab in a 5-day-old kitten (3 days postcortical isolation). Recording electrode 1 mm. from site of stimulation.

(A) A weak stimulus to the cortical surface evokes an SCR and a multiphasic discharge, whereas a second stimulus delivered 3/sec. later evokes an SCR and a repetitive 8–10/sec. train of surface-positive-negative responses.

(B to E) Continuous record in which frequency of surface stimulus is increased from 0.5/sec. to 5/sec., then decreased to 0.5/sec. Multiphasic discharges develop erratically, but when stimuli (indicated by black dots under stimulus artifacts) are superposed on descending phases of surface-negative components of paroxysmal discharges or 0.5 to 1/sec. thereafter, evoked SCRs are markedly attenuated. Further explanation in text.

In preparations exhibiting only occasional repetitive 8 to 10/sec. discharges in response to low frequency (0.5/sec.) surface stimulation, fluctuations in the over-all excitability of the cortical slab might be of such magnitude and duration that ordinarily ineffective surface stimuli were capable of activating subsurface organizations involved in paroxysmal discharges (FIGURES 28A to F) for relatively long periods. When this occurred, surface-positive activity was evoked with short latency (G to I); then, during the decaying phases of the period of "hyperexcitability," latency was progressively increased until paroxysmal discharges were no longer obtained (J to M). When short-latency activity was evoked in the cortical depths by weak surface stimuli, SCRs appeared to be swamped by the development of subsurface activity (G to I). That this was more apparent than real is indicated by the fact that with increasing latency of subsurface activity, evoked SCRs were reduced in amplitude and remained "depressed" for many seconds after the phase of augmented excitability. FIGURE 28 illustrates another finding to be emphasized. When repetitive stimulation at low frequency (0.5/sec.) initiated paroxysmal activity the complex patterns of evoked responses so obtained were remarkably constant in overt configuration for many seconds. Although the period during which such complex, but orderly, evoked response sequences could be elicited was found to vary in different preparations (and in the same preparations from one area of the isolated slab to another) in the most favorable preparations complex response patterns were evoked with remarkable regularity. Under these

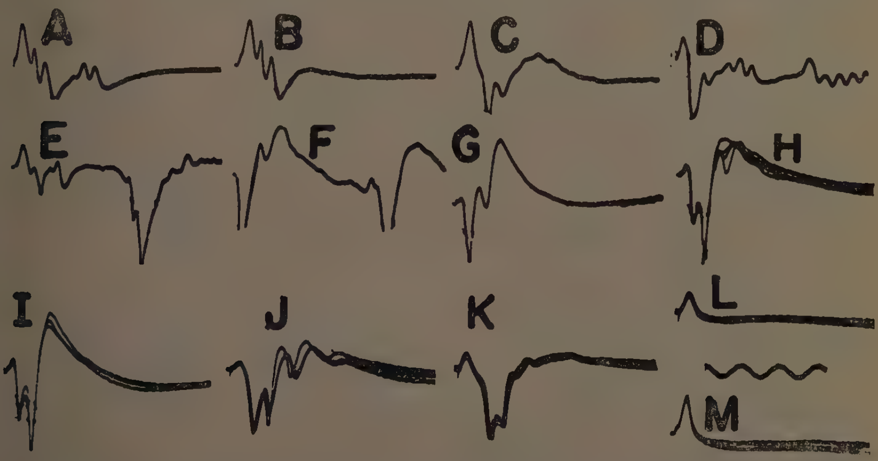

FIGURE 28. Progressive changes in surface responses evoked by weak stimuli (0.5/sec frequency) during a phase of augmented excitability in an isolated cortical slab in a 6-day-old kitten (5 days postisolation).

(A to D) Successive responses evoked at 0.5/sec. frequency showing rapid development of surface positivity. (E to F) Various stages of paroxysmal discharge. (H and I) Later stages of stabilization during which weak stimulus initiates stereotyped discharge. (J and K) Decaying phase of excitability indicated by increasing latency of discharge and reappearance of SCR. (L) Superposed SCRs depressed for 30 sec. after cessation of paroxysmal activity. (M) Recovery of 'normal' SCR excitability prior to another phase of augmented activity in the slab. Calibrations 10 cps; 0.1 mv.

conditions, some idea of the nature of the subsurface organizations involved in the repetitive discharges was forthcoming by noting the effects of topically applied ω-amino acids and strychnine.

The regularity of the complex surface activity evoked by 0.5/sec. stimulation of an area of isolated cortex in a 5-day-old kitten (3 days postisolation) is shown in superposed traces in FIGURE 29A. A few seconds after topical application of 1 per cent GABA the initial SCR was reduced in amplitude and some late components of the repetitive response were eliminated (29B). Still later, after abolition of the SCR, surface positivity of the initial components of the repetitive sequence was augmented, the latency of first positivity was increased, and the number of discharges in the repetitive train decreased (29C to E). At this stage all evoked activity was eliminated (F) but gradually returned after removal of GABA (G to H). A phase of augmented excitability after recovery from GABA, similar to that described previously in adult animals[13] was characteristically observed (H). After recovery towards 'normal' excitability (I), ε-amino caproic acid was topically applied. This resulted in depression of

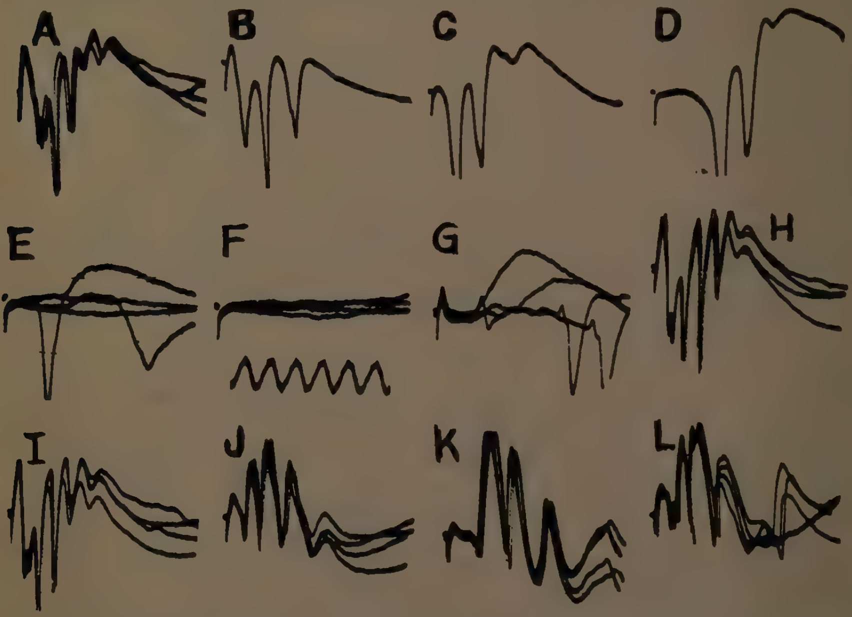

FIGURE 29. Effects of topically applied GABA and ε-amino caproic acid on SCRs and stereotyped repetitive discharges evoked from isolated cortical slab in a 5-day-old kitten (3 days postcortical isolation). (A) Control, superposed 0.5/sec. evoked surface responses recorded 1.5 mm. from site of stimulation exhibit a remarkable orderliness. (B to F) Various phases of alterations induced by topically applied GABA. (B) Early recovery after rinsing cortex with warm Ringer's solution. (H) Phase of post-GABA augmentation of evoked activity. (I) Control prior to application of ε-amino caproic acid (C_6). (J and K) Early and late stages, respectively of C_6 action. Note depression of SCR and gradual negative shift of repetitive responses. The latter were reduced in magnitude after K (not shown). (L) Early recovery from C_6 action. Calibrations 10 cps; 0.1 mv.

the SCR (cf. FIGURES 8 and 9), a progressive negative shift of all components in the repetitive response, then increase in latency of the first component of the repetitive sequence (29J–K).

In an attempt to characterize further the origin of the repetitive sequence in isolated immature neocortex, micropipettes were inserted into the cortex and the cortex stimulated at various depths with weak shocks delivered through a pair of fine stimulating electrodes located 3 mm. from the extracellularly located microelectrodes. 'Low' threshold sites for eliciting repetitive sequences were found at a cortical depth corresponding to the lower limits of the isolated slab.

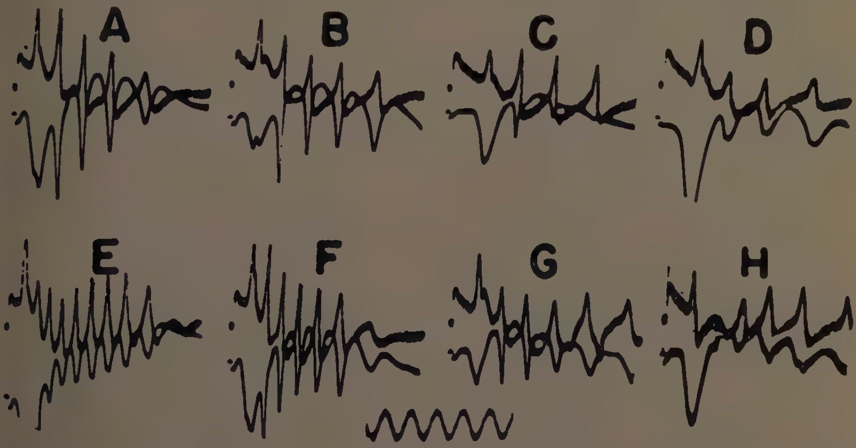

FIGURE 30. Evoked repetitive responses in same preparation as described in FIGURE 29 but recorded from another site in the cortical slab. Stimulating wire electrodes located at a depth of 0.8 mm. Surface responses (*lower channel*) recorded 3 mm. from the site of stimulation; focally evoked responses (*upper channel*) simultaneously recorded with a microelectrode in the cortical depths (0.5 mm). (A) Control. (B) Three min. after topical application of ε-amino caproic acid (C_6). Note depression of surface and focally recorded responses. (C) A few seconds after addition of GABA to C_6. (D) One min. after C. Lack of relationship between surface and focal responses is especially noteworthy in C. (E) Phase of augmentation during recovery from GABA action. (F) Control. (G) Maximum effect produced by topically applied strychnine sulphate (1:1000). (H) A few seconds after addition of GABA during strychnine action. Calibrations 10 cps; 0.1 mv.

Weak stimulation (0.5/sec.) evoked predominantly surface-positive repetitive responses that were reflected in focal negativities of maximum amplitude 0.5 to 0.6 mm. below the cortical surface (FIGURE 30A). Topically applied ε-amino caproic acid reduced the initial surface positivity but did not significantly alter the focal negativities (30B). Immediately after application of GABA the initial surface positivity augmented, and subsequent surface and focal responses exhibited little relationship (C). Further augmentation of initial surface positivity produced little change in the initial focal negativity although late components in the repetitive sequence were attenuated during the reappearance of late surface positivity. After removal of GABA and ε-amino caproic acid, some residual hyperexcitability was detectable in the form of an increased frequency of repetitive activity (E). The effects of topically applied strychnine (1:1000) were similar to those of ε-amino caproic (cf. G and C).

Topical GABA after strychnine (H) produced changes not unlike those seen when the amino acid was added to cortex previously treated with ϵ-amino caproic acid (D).

The foregoing studies on isolated immature cortex are as yet in their most preliminary stages and for this reason only a few remarks concerning their general significance can be made at this time. To view these data in a proper perspective, it is sufficient to emphasize that in a relatively large series of experiments involving electrical stimulation of *intact* immature neocortex at no time has it been possible to evoke repetitive discharges of the type illustrated in FIGURES 26 to 30 with stimulating techniques and parameters similar to those employed in the experiments on isolated immature neocortex.* As to the factors responsible for the 'hyperexcitability' of isolated immature cortex, it seems reasonable to attribute them to an over-all increase in excitatory synaptic activities subsequent to the rapid proliferation of axon collaterals of pyramidal neurons whose descending axons have been interrupted during the isolation procedures. The problem of establishing the nature of the synaptic contacts made by such axon collaterals on adjacent pyramidal neurons (and presumably also stellate cells) is somewhat simplified by the demonstration that repetitive activity evoked by subsurface stimuli is abolished by GABA. It has been demonstrated that GABA exerts its major, if not exclusive, action in cortex by blocking excitatory synaptic activities generated in dendritic elements.[11,13,23,38,58] In view of this it appears likely that this action might also adequately explain the effects observed in isolated immature neocortex. Thus while the details of the complex alterations in surface and subsurface activities seen in immature cortex after GABA and, for that matter, after topically applied ϵ-amino caproic acid and strychnine, are as yet incompletely known, it may be tentatively concluded that the repetititve discharges of isolated immature neocortex result from recurrent excitation in relatively closed axodendritic synaptic pathways. One corollary to this should also be noted. For inasmuch as the excitatory axodendritic synaptic bombardment on pyramidal neurons must be effective in discharging elements it would appear that newly formed axon-collaterals establish synaptic relations with pyramidal neurons on the most proximal segments of their apical dendrites and, perhaps, to a lesser extent on their cell bodies. It is thus seen from this how a strategic grouping of exclusively excitatory synapses formed by axon collaterals of Type I pyramidal neurons that have been converted into Type II elements is capable, in the absence of counteracting inhibitory synaptic bombardment, of effecting the discharge of adjacent pyramidal neurons. A presentation of these data would be incomplete without noting the course of the excitatory axodendritic synaptic pathways envisioned by Cajal[57] in his discussion of the consequences of axon-

---

* Acutely isolated cortical slabs have been studied in 5- to 10-day-old kittens in a manner similar to that described above. Within a few hours after preparation of these slabs, strong surface stimulation evokes an SCR that is succeeded by a prominent surface positivity. During repetitive stimulation, facilitation of surface positivity is observed that generally persists for many seconds after cessation of the repetitive stimulus. Similar effects are observed during subsurface stimulation, but it is impossible to elicit the repetitive sequence shown in FIGURES 26 to 30, even 6 hours after preparation of the slab. Thus, although the acutely isolated neocortex of 5- to 10-day-old animals may exhibit a minimal increase in excitability, the alterations seen in acute preparations are fundamentally different from those observed 2 to 7 days after preparation of isolated cortical slabs in newborn kittens.

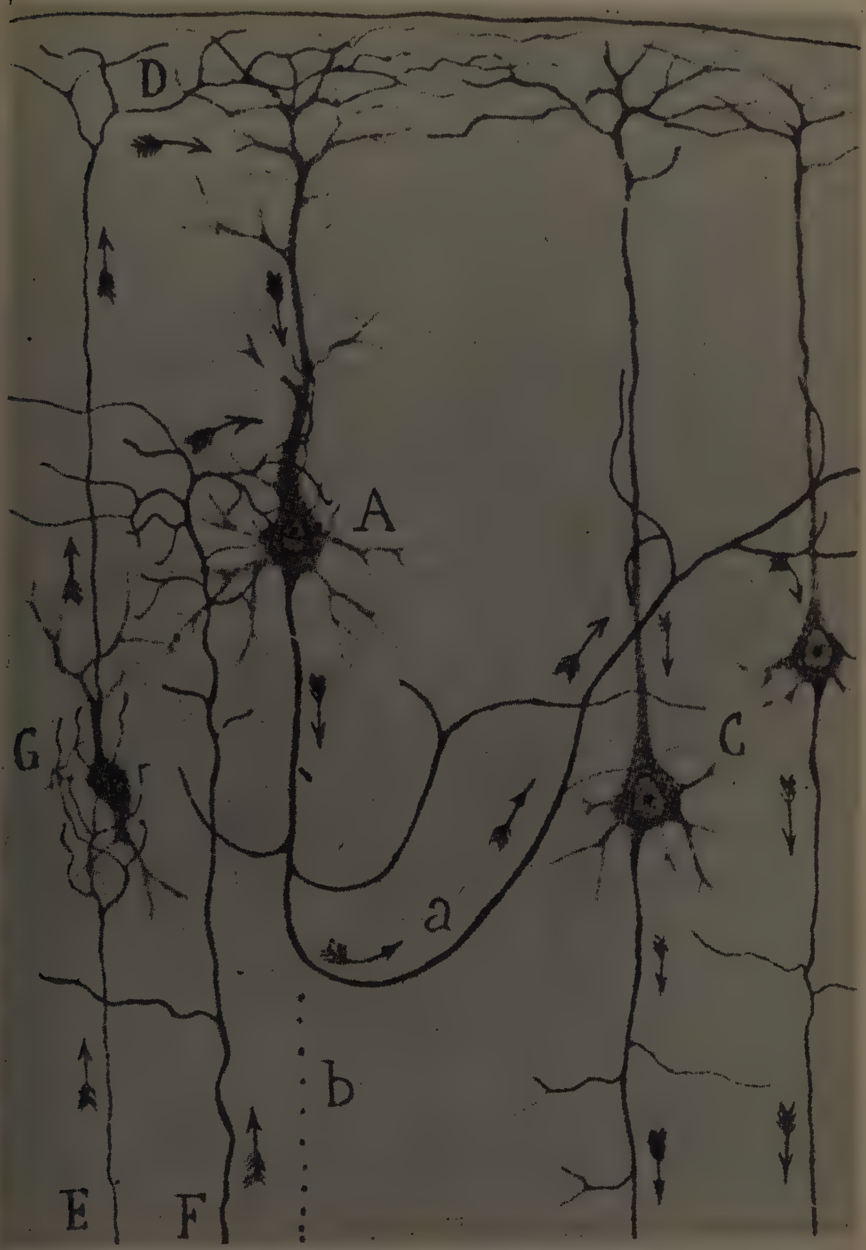

FIGURE 31. Cajal's representation of the possible consequences of the proliferation of axon collaterals of a pyramidal neuron after its main stem axon has been interrupted below the origin of initial intracortical collaterals. The original description of this figure follows: "Schematic drawing showing the possible tract of the currents across the arciform pyramidal cells. (A) Arciform pyramidal cell; (C) normal pyramidal cells; (D) plexiform layer; (E, F) afferent fibres; (G) cell with an ascending axon, called Martinotti's cell; (*a*) hypertrophic collateral; (*b*) part of the axon that has disappeared." Reproduced by permission of the Hafner Publishing Co., Inc.[57]

collateral proliferation of neocortical pyramidal neurons after interruption of the descending axons (FIGURE 31). The case in point testifies to the remarkable acuity of this great morphologist in looking well beyond the resolving power of his optical instruments.

Comment

The foregoing results amply illustrate the usefulness of a multioperational approach to the analysis of different synaptic organizations in immature neocortex. Still to be considered is the problem of how these data may contribute to a further understanding of the nature and origin of different varieties of electrocortical activities[32] and how they may provide clues to the interpretation of some complex synaptic events that have been described in the mature mammalian central nervous system under fundamentally different situations.

Particular emphasis has been placed in these ontogenetic studies on the morphophysiological and pharmacological evidence indicating that evoked electrocortical activities are generated predominantly in superficial axodendritic synaptic organizations in the immediate neonatal period. These activities, ranging from the relatively simple responses initiated by local cortical surface stimulation to the complex responses evoked by nonspecific thalamic and lower brain stem stimulation, reflect differences in the degree to which excitatory and inhibitory pathways in superficial neuropil participate in the elaboration of evoked potentials in immature neocortex.

Various kinds of data have been presented in support of the hypothesis that SCRs are axodendritic p.s.p.s generated in superficial neuropil by conductile pathways activated by surface stimulation.[12,17,18,32] Of these data, the least impressive to some electrophysiologists might be the electron microscopical demonstration of relatively large numbers of axodendritic synapses in superficial cortical regions in the immediate neonatal period. Why then have these data been introduced? They have been introduced primarily to provide a firm basis for the electrophysiological interpretations. Were it impossible with currently available electron microscopical techniques to demonstrate axodendritic synapses in immature cortex at a developmental stage when SCRs are readily obtainable, the hypothesis concerning the postsynaptic origin of these responses might be seriously embarrassed. As it turns out the electron microscopical observations, taken together with the morphological data on the gross characteristics of superficially located dendrites compel rejection of some alternative interpretations of the nature and origin of the SCR, especially those based on an incomplete knowledge of its neuronal substrate. This is not to say that as a consequence of a relatively few series of morphological studies all the electrophysiological data on the SCR have become readily interpretable. What is emphasized here is the usefulness of incorporating data obtained from anatomical (and for that matter pharmacological studies) in the analysis of some electrophysiological events. In the case of the SCR the results of employing a multioperational approach have been sufficiently encouraging to warrant its continued application to problems still unclarified. Of the latter, the most difficult remains the problem of defining the composition of the pathways which initiate p.s.p.s in dendrites remote from the site of stimulation. On this point comparative pharmacological studies have proved to be valuable in suggesting differences in the proportion of excitatory and inhibitory elements in these pathways at various sites along their trajectory. Nothing, however, can be inferred from the present studies concerning the intracortical distribution of these pathways. Until evidence to the contrary is forthcoming, it must be allowed that subsurface, as well as superficial circuits may play a role in carrying impulses to distant dendritic elements.[32]

In considering electrocortical activities evoked in immature neocortex by stimulation of various corticipetal pathways, attention has been focused on the characteristics of responses initiated in dendritic elements at synaptic sites other than those giving rise to the SCR. These studies provide information on the internal composition of different intracortical pathways to apical dendrites and permit an appraisal of the degree to which different organizations in immature cortex participate in the elaboration of enduring synaptic activities. Fundamental differences in these organizations are indicated, in part, by differences in their responsiveness to repetitive stimulation of corticipetal afferents and, more importantly, in the differences in their "excitability" observed subsequent to brief periods of high-frequency activation.

The rapid and sustained depression of evoked responses in specific projection cortex (postsigmoid gyrus) following repetitive stimulation of ventrolateral thalamus or thalamocortical radiations is in sharp contrast to the changes in responses evoked in association cortex during repetitive stimulation of nonspecific projection pathways. Although these differences are qualitatively similar to those encountered in mature animals,[59] repetitively evoked responses in nonspecific cortex in the newborn animal undergo a series of alterations that appear to be peculiar to immature cortex. Particularly significant in this respect is the finding that the first of a repetitive sequence of nonspecific evoked responses is ordinarily well developed, whereas the subsequent 4 to 5 responses in the series are depressed. In other words, typical recruitment of the type characteristically observed in mature animals during 6 to 10/sec. stimulation of nonspecific thalamic nuclei[50] is not detectable in the immediate neonatal period. Rather, the initial depression of evoked responses passes over into a number of phases that eventually terminate in response alternation, a phenomenon originally described in connection with recruiting responses in the adult animal.[50] The mechanisms underlying such differences in the overt characteristics of repetitively evoked nonspecific responses in the immature animal are as yet entirely obscure, but in the search for adequate explanations, some clues may also be forthcoming concerning the synaptic processes operating in recruiting responses in the adult animal. Indeed, since the first stimulus of a repetitive train of stimuli to nonspecific thalamic nuclei appears to "lose its effectiveness" with advancing age, it is not unlikely that the small evoked response initiated by a single stimulus to nonspecific nuclei in the adult animal is a reflection both of the relatively large proportion of inhibitory activity generated by single stimuli, as well as the degree to which elements contributing to the fully developed recruiting response participate in other varieties of on-going activity.[32]

The fact that high-amplitude 10 to 14/sec. predominantly surface-negative responses can be evoked in restricted regions of association cortex following high-frequency stimulation of nonspecific thalamic nuclei or medial pontomesencephalic regions in the newborn cat is of interest from the standpoint of the ontogenesis of certain spontaneous and evoked electrocortical rhythms. The subcortical structures capable of generating this 10 to 14/sec. rhythm in superficial axodendritic organizations are, presumably, the same as those that participate in the elaboration of high-frequency low-amplitude electrocortical activation patterns in mature animals.[60] In view of this the question arises of whether the electrographic pattern observed in the newborn animal may represent a rudimentary form of electrocortical activation whose cortical distribution and overt characteristics are reflections of the differential rate of maturation of superficial and deep synaptic organizations in fundamentally different types of cortex. To answer this question obviously requires considerably more information on the postnatal changes in responses to high-frequency stimulation of nonspecific thalamic brain stem stimulation than is now available. Until then there would appear to be little serious objection to the conception that the distinctive electrographic characteristics of brain waves in immature-born animals at birth and newborn human infants are not so much a reflection of global immaturity of the brain, but rather a consequence of the differential rate of development of superficial axodendritic pathways in the immediate neonatal period. Activity in superficial organizations evoked by high-frequency corticipetal volleys dominates that initiated in subsurface cortical organizations in the newborn animal. The evoked 10 to 14/sec. electrographic patterns may thus be considered the physiological expression of activity in superficial axodendritic synaptic organization at a developmental stage when cortical organizations other than those in the superficial neuropil have yet to exert their complex effects in modifying this activity. In considering the nature of the differences in the type of electrocortical activity evoked by brain-stem stimulation in neonatal and mature animals, the possibility that the electrocortical events evoked in neonatal preparations may be a reflection of the activity of reticulocortical pathways subserving synchronization of EEG activity in mature animals[61] should also be explored. Were such a relationship to be established, the data so obtained might further serve to clarify the physiological role of reticular organizations involved in EEG synchronization.

Closely allied to the problem of defining the synaptic processes underlying the activity cycle characteristic of superficial axodendritic patterns in the newborn animal are those concerning the mechanisms responsible for the alterations in nonspecific evoked responses subsequent to prolonged repetition at very low stimulation frequencies. Some of the factors underlying these and other alterations have been noted above. The remarkable similarity is to be noted in the alterations shown in FIGURES 20 to 22 and those described in cortical and subcortical organizations during certain types of electrophysiological studies of complex behavioral activities.[62] Particularly interesting in this respect are the findings that the first of a series of stimuli delivered every 2 sec. to medial pontomesencephalic regions evokes a prominent response in association cortex, whereas all subsequent responses are progressively attenuated until surface-evoked activity is virtually abolished. The extraordinary rapidity with which this cortically evoked response is 'extinguished' calls to mind changes observed in a large variety of responses recorded at different neuraxial sites in adult animals subjected to repeated presentation of indifferent signals.[63] As is well known, attenuation of some responses evoked in cerebral cortex may occur with surprising rapidity. This phenomenon, considered to be an electrophysiological correlate of "habituation,"[62] may be eliminated by relatively minor changes in the characteristics of the indifferent stimulus or pairing the indifferent stimulus with another signal of considerably more significance to the animal. Under these conditions, augmentation of evoked responses may be observed ('dishabituation').[63,64] It is not to be inferred from this that the synaptic processes associated with 'habituation or dishabituation' of evoked activities recorded during certain changes in behavior are the same as those that underlie the changes in nonspecific evoked responses in newborn animals. The point of emphasis is that repetition of an indifferent stimulus in the newborn animal (electrical stimulation of medial brain stem) sets into operation a complex sequence of synaptic events in restricted regions of superficial neocortex that culminates in elimination of evoked responses, whereas a change in stimulus pattern results in prolonged facilitation of responses. Of importance is the fact that in the newborn kitten these events appear to be confined entirely to synaptic organizations subserving the mediation of nonspecific evoked activities. May it not be, then, that these events represent elementary patterns of activity of reticulocortical synaptic organizations? If such is the case, the question may also be raised as to what possible role these organizations could play in the postnatal development of those synaptic processes that underly different varieties of 'higher nervous activity'? For inasmuch as reticulocortical organizations have been shown here to be potentially capable of elaborating electrocortical events of the utmost complexity in the immediate neonatal period, it would be surprising indeed if the relatively early maturation of these pathways were of little functional significance to the newborn animal.

A few remarks concerning the reorganization of intracortical excitatory synaptic pathways in isolated immature neocortex would appear necessary to indicate their relevance to the general problem of the analysis of cortical synaptic organizations. Hyperexcitability of neuronally isolated cortex has been repeatedly demonstrated in adult animals,[10,65] but the mechanisms responsible for the augmentation in excitability have not been entirely elucidated. The contribution of Burns and his associates[21] to the problem are especially noteworthy, as are those of Echlin on the hyperexcitability of chronically isolated cortex.[66] In the studies of Burns[21] emphasis has been placed on the role of self-re-exciting networks of pyramidal neurons in the production of surface-positive burst responses of isolated immature cortex. Although the present studies support this hypothesis, the data obtained in the chronically isolated immature cortex are at variance with those derived from studies on acutely isolated slabs of mature cortex in a number of respects. In isolated mature cortex surface-positive burst responses may be initiated shortly after preparation of the slab. Bursts evoked by relatively strong stimuli spread in an all-or-none fashion throughout the entire slab, but according to Burns,[22] page 10, "the same stimulus delivered periodically to the same cortical point never produces the same pattern of potential change twice at a remote point on the brain's surface (from which bursts responses are being recorded)." The bursts observed in acutely isolated mature cortex presumably reflect the activity of complex neuronal networks whose intrinsic activity has been so altered by the isolation procedure as to permit demonstration of responses that are never observed in intact mature cortex.[32] In immature chronically isolated cortex, "bursts" may be localized to within a few millimeters of cortex surrounding the site of stimulation and, at different sites of stimulation, different burst patterns may be observed. What is particularly important, however, is the fact that in favorable preparations of isolated immature neocortex a remarkably stereotyped pattern of paroxysmal activity may be evoked from a localized region during prolonged periods of stimulation. Thus while isolation of mature cortex appears rapidly to 'unmask' the activities of neuronal networks that are ordinarily influenced by a variety of excitatory and inhibitory influences emanating from without the slab,[32] in immature cortex the isolation procedure sets into operation a rapid reorganization of axodendritic (and probably some axosomatic) synaptic pathways. In other words, the burst phenomenon of acutely isolated mature cortex seems to be a manifestation of the modified activity of pre-existing neuronal organizations, whereas in the immature chronically isolated cortex the paroxysmal responses result from the rapid development of entirely new synaptic connections. As to whether in *chronically* isolated mature cortex (partially or completely isolated) a similar reorganization of excitatory synaptic pathways may also occur, one can with certainty only point out the differences noted in the activity of acutely and chronically isolated mature cortex[66] and emphasize once more the findings of Cajal,[57] which strongly suggest that such may be the case. The problem of elucidating the mechanisms responsible for changes in cortical excitability following traumatic lesions that interrupt connections between cortex and white matter is of no little importance. Needless to say, from the adequate solution of this problem may come an answer to the enigmatic problem of the origin of focal paroxysmal activity in traumatized areas of neocortex.

The data on the immature isolated cortex may be particularly useful in permitting some decision as to the validity of attributing the hyperexcitability of chronically isolated cortex to "denervation sensitivity."[67] For since these data indicate that the collaterals of interrupted pyramidal axons can rapidly proliferate and seek out loci for excitatory synaptic contacts at available sites on adjacent elements, it would appear that "hyperinnervation" rather than "denervation sensitivity" is more likely the underlying factor responsible for the hyperexcitability of chronically isolated cortex. Viewed in this fashion, much of the data on the properties of chronically isolated cortex, including suggestions as to the increased concentration of cholinesterase in partially denervated cortical areas,[68] may become explainable on the basis of a net increase in the number of excitatory synaptic contacts on pyramidal neurons, an increase that is a consequence of the interruption of main-stem axons below the origin of their intracortical collaterals. Until evidence is presented to the contrary, there is no reason to assume that the reorganization of axon-collateral synaptic pathways that occurs secondary to severance of pyramidal neuron axons may not be a major factor in altering synaptic organizations in other types of cerebral cortex after interruption of pyramidal axons (Kandel and Spencer, this monograph).

Summary

The present report surveys recent morphophysiological studies on the neocortex of the newborn cat primarily designed to elucidate further the role of axodendritic synaptic organizations in the production of a wide variety of evoked electrocortical events.

Particular emphasis is placed on morphophysiological data obtained by light (Golgi-Cox material) and electron microscopical studies indicating that superficial axodendritic synaptic pathways are developed to a remarkable degree in the immediate neonatal period. The differential maturation of superficial neuropil is reflected, in part, in the prominent surface-negative responses evoked by local cortical surface stimulation, stimulation of different corticipetal projection pathways, and in the extraordinary complexity of axodendritic synaptic activities demonstrable in fundamentally different types of cortex.

Data on superficial cortical responses (SCRs) in perinatal kittens are entirely consistent with the hypothesis that these responses are largely p.s.p.s of apical dendrites. Pharmacological evidence is presented indicating that maturation of inhibitory components in pathways generating SCRs in superficial dendritic elements is delayed with respect to the development of excitatory pathways. Inhibitory p.s.p.s are generated, however, in superficial organizations by corticipetal pathways from thalamic and pontomesencephalic regions in the newborn animal.

The characteristics of surface- and subsurface-evoked activities in anterior suprasylvian gyrus (association cortex) contrast sharply with those evoked in posterior sigmoid gyrus (somatic sensory cortex) in the immediate neonatal period. The latter responses are markedly depressed during repetitive thalamic or radiation stimulation and never exhibit phases of postactivation facilitation. Association cortex responses evoked by stimulation of nonspecific pathways exhibit prominent delayed surface negativity and show complex, but orderly, transitions in amplitude during repetitive stimulation. Synaptic activation of elements in superficial neuropil by high-frequency (25 to 50/sec.) stimulation of nonspecific projection pathways in newborn animals results in the production of 10 to 14/sec. high-amplitude predominantly surface-negative potentials. These persist for a variable period after cessation of the stimulus and are associated with the onset of a prolonged phase of postactivation facilitation of evoked responses.

Experiments are illustrated on 'habituation' and 'dishabituation' of nonspecific evoked responses involving predominantly superficial axodendritic pathways. These findings are discussed in terms of the possible mode of operation of reticulocortical pathways in the elaboration of complex electrocortical activities in the immature animal.

Preliminary studies on the morphophysiological characteristics of subsurface axodendritic excitatory synaptic pathways in slabs of "chronically" isolated immature neocortex are described to emphasize the analytical value of at-

tempts to alter the normal course of postnatal ontogenesis of different cortical synaptic organizations. Pyramidal neurons whose axons are interrupted below the origin of their intracortical collaterals are rapidly converted to Type II elements that activate, via their proliferating axon collaterals, large numbers of adjacent elements. One consequence of this is the establishment of powerful recurrent axodendritic excitatory synaptic pathways capable of supporting repetitive paroxysmal discharges of extraordinary magnitude.

Acknowledgments

The physiological data summarized in this paper were obtained in various collaborative studies carried out with E. M. Housepian, a Parkinson's Disease Foundation Fellow, and M. W. Carmichael. I am indebted to both of these colleagues, and to Kytja K. Voeller, and G. Pappas of the Department of Anatomy of the College of Physicians and Surgeons, Columbia University, for kindly permitting publication of electron microscopical data obtained in joint studies.

References

1. BRODMANN, K. 1909. Vergleichende Lokalisation der Grosshirnrinde. Leipzig, Germany.
2. ECONOMO, C. VON & G. N. KOSKINAS. 1925. Die Cytoarchitektonik der Hirnrinde. Oxford Univ. Press. Oxford, England.
3. BOK, S. T. 1959. Histonomy of the Cerebral Cortex. Elsevier. Amsterdam, Holland.
4. SARKISOV, S. A. 1960. The functional interpretation of certain morphological structures of cortex of the brain in the evolutionary aspect. *In* Structure and Function of the Cerebral Cortex. Elsevier. Amsterdam, Holland.
5. SHOLL, D. A. 1956. The Organization of the Cerebral Cortex. Methuen. London, England.
6. SHOLL, D. A. 1960. Anatomical heterogeneity in the cerebral cortex. *In* Structure and Function of the Cerebral Cortex. Elsevier. Amsterdam, Holland.
7. GRAY, E. G. 1959. Axo-somatic and axo-dendritic synapses of the cerebral cortex: An electron microscope study. J. Anat. **93:** 420.
8. NOBACK, C. R. & D. P. PURPURA. Postnatal ontogenesis of cat neocortex. J. Comp. Neurol. In press.
9. PURPURA, D. P., M. W. CARMICHAEL & E. M. HOUSEPIAN. 1960. Physiological and anatomical studies of development of superfical axodendritic synaptic pathways in neocortex. Exptl. Neurol. **2:** 34.
10. ECHLIN, F. A., V. ARNETT & J. ZOLL. 1952. Paroxysmal high voltage discharges from isolated and partially isolated human and animal cerebral cortex. Electroencephalog. Clin. Neurophysiol. **4:** 147.
11. PURPURA, D. P. 1960. Pharmacological actions of ω-amino acid drugs on different cortical synaptic organizations. *In* Inhibition in the Nervous System and γ-Aminobutyric Acid Pergamon Press. New York, N.Y.
12. PURPURA, D. P. & H. GRUNDFEST. 1956. Nature of dendritic potentials and synaptic mechanisms in cat cerebral cortex. J. Neurophysiol. **19:** 573.
13. PURPURA, D. P., M. GIRADO, T. G. SMITH, D. A. CALLAN & H. GRUNDFEST. 1959. Structure-activity determinants of pharmacological effects of amino acid and related compounds on central synapses. J. Neurochem. **3:** 238.
14. ADRIAN, E. D. 1936. The spread of activity in the cerebral cortex. J. Physiol. (London). **88:** 127.
15. CHANG, H.-T. 1951. Dendritic potential of cortical neurones as produced by direct stimulation of the cerebral cortex. J. Neurophysiol. **14:** 1.
16. CLARE, M. H. & G. H. BISHOP. 1955. Properties of dendrites; apical dendrites of the cat cortex. Electroencephalog. Clin. Neurophysiol. **7:** 85.
17. ECCLES, J. C. 1951. Interpretation of action potentials evoked in the cerebral cortex. Electroencephalog. Clin. Neurophysiol. **3:** 449.

18. Grundfest, H. 1958. Electrophysiology and pharmacology of dendrites. Electroencephalog. Clin. Neurophysiol. Suppl. **10:** 22.
19. Fan, S.-F. & T. P. Feng. 1957. Concerning conduction and electrical excitability in the terminal portions of the apical dendrites of the pyramidal neurons. Acta physiol. Sinica (Shanghai). **21:** 423.
20. Brooks, V. B. & P. S. Enger. 1959. Spread of directly evoked activity in the cat's cerebral cortex. J. Gen. Physiol. **42:** 761.
21. Burns, B. D. 1958. The Mammalian Cerebral Cortex. Edward Arnold. London, England.
22. Purpura, D. P. 1961. Ontogenetic analysis of some evoked synaptic activities in superficial neocortical neuropil. *In* Nervous Inhibition. Pergamon. London, England. In press.
23. Purpura, D. P., M. Girado & H. Grundfest. 1960. Components of evoked potentials in cerebral cortex. Electroencephalog. Clin. Neurophysiol. **12:** 95.
24. Suzuki, H. & N. Taira. 1958. Regional difference of the direct cortical response. Japan. J. Physiol. **8:** 365.
25. Eayrs, J. T. & B. Goodhead. 1959. Postnatal development of the cerebral cortex in the rat. J. Anat. **93:** 385.
26. Haug, H. 1960. Die quantitativen Zellvolumenverhältnisse der Hirnrinde. *In* Structure and Function of the Cerebral Cortex. Elsevier. Amsterdam, Holland.
27. Schadé, J. P. & C. F. Baxter. 1960. Changes during growth in the volume and surface area of cortical neurons in the rabbit. Exptl. Neurol. **2:** 158.
28. Palay, S. L. 1956. Synapses in the central nervous system. J. Biophys. Biochem. Cytol. Suppl. **2:** 193.
29. Fernandez-Morán, H. 1957. Electron microscopy of nervous tissue. *In* Metabolism of the Nervous System. Pergamon. London, England.
30. DeRobertis, E. & H. S. D. Bennett. 1955. Some features of the submicroscopic morphology of synapses in frog and earthworm. J. Biophys. Biochem. Cytol. **1:** 47.
31. Van der Loos, H. 1960. On dendro-dendritic junctions in the cerebral cortex. *In* Structure and Function of the Cerebral Cortex. Elsevier. Amsterdam, Holland.
32. Purpura, D. P. 1959. Nature of electrocortical potentals and synaptic organizations in cerebral and cerebellar cortex. Intern. Rev. Neurobiol. **1:** 47.
33. Eccles, J. C. 1957. The Physiology of Nerve Cells. Johns Hopkins Press. Baltimore, Md.
34. Grundfest, H. 1957. Electrical inexcitability of synapses. Physiol. Revs. **37:** 337.
35. Grundfest, H. 1959. Synaptic and ephaptic transmission. Chap. V. *In* Handbook of Physiology. Neurophysiology I. J. Field, Ed. Am. Physiol. Soc. Washington, D.C.
36. Purpura, D. P. & H. Grundfest. 1957. Physiological and pharmacological consequences of different synaptic organizations in cerebral and cerebellar cortex of cat. J. Neurophysiol. **20:** 494.
37. Purpura, D. P. & H. Grundfest. 1959. Comparative pharmacological analysis of different hippocampal synaptic organizations (cat). Federation Proc. **18:** 123.
38. Purpura, D. P., M. Girado & H. Grundfest. 1959. Synaptic components of cerebellar electrocortical activity evoked by various afferent pathways. J. Gen. Physiol. **42:** 1037.
39. Carmichael, M. W., E. M. Housepian & D. P. Purpura. 1960. Effects of 'convulsant' ω-amino acids during cortical maturation (cat). Federation Proc. **19:** 267.
40. Kuno, M. 1957. Strychnine on intracellular potentials of spinal motoneurones of the toad. Japan. J. Physiol. **7:** 42.
41. Scherrer, J. & D. Oeconomos. 1955. Résponses évoquées corticales somesthéseques des mammiféres adulte et nouveau-né. *In* Les Grandes Activites du Lobe Temporal. Mason. Paris, France.
42. Ellingson, R. J. & R. C. Wilcott. 1960. Development of evoked responses in visual and auditory cortices of kittens. J. Neurophysiol. **23:** 363.
43. Hunt, W. E. & S. Goldring. 1951. Maturation of evoked response of the visual cortex in the postnatal rabbit. Electroencephalog. Clin. Neurophysiol. **3:** 465.
44. Marty, R., F. Contamin & J. Scherrer. 1958. Cortical response to photic stimulation in a new-born cat. Electroencephalog. Clin. Neurophysiol. **10:** 761.
45. Grossman, C. 1955. Electro-ontogenesis of cerebral activity. Forms of neonatal responses and their recurrence in epileptic discharges. Arch. Neurol. Psychiat. Chicago. **74:** 186.
46. Housepian, E. M., C. R. Noback & D. P. Purpura. 1961. Ontogenetic changes in evoked activity in pyramidal and 'extrapyramidal' pathways (cat). Federation Proc. **20:** 325.

47. Purpura, D. P. & M. W. Carmichael. 1960. Characteristics of the blood-brain barrier to γ-aminobutyric acid in neonatal cat. Science. **131:** 410.

48. Goldring, S., J. L. O'Leary & S. H. Huang. 1958. Experimental modification of dendritic and recruiting processes and their DC after-effects. Electroencephalog. Clin. Neurophysiol. **10:** 663.

49. Iwama, K. & H. H. Jasper. 1957. The action of gamma-aminobutyric acid upon cortical electrical activity. J. Physiol. **138:** 365.

50. Dempsey, E. W. & R. S. Morison. 1942. The production of rhythmically recurrent cortical potential after localized thalamic stimulation. Am. J. Physiol. **135:** 293.

51. Jasper, H. H. 1949. Diffuse projection systems: the integrative action of the thalamic reticular system. Electroencephalog. Clin. Neurophysiol. **1:** 405.

52. DoCarmo, R. J. 1960. Direct cortical and recruiting responses in postnatal rabbit. J. Neurophysiol. **23:** 496.

53. Purpura, D. P. 1958. Organization of excitatory and inhibitory synaptic electrogenesis in the cerebral cortex. *In* Symposium on Reticular Formation of Brain. : 435. L. C. Proctor, R. S. Knighton, H. H. Jasper, W. C. Noshay and R. T. Costello, Eds. Little, Brown. Boston, Mass.

54. Purpura, D. P., E. M. Housepian & H. Grundfest. 1958. Analysis of caudate-cortical connections in neuraxially intact and telencephale isole cats. Arch. ital. Biol. **96:** 145.

55. Purpura, D. P. Morphophysiological basis of elementary evoked response patterns in neocortex of newborn cat. Pavlovian Conference, Higher Nervous Activity. Ann. N.Y. Acad. Sci. In press.

56. Purpura, D. P. & E. M. Housepian. 1961. Physiological consequences of axon-collateral proliferation in isolated immature neocortex. Federation Proc. **20:** 333.

57. Ramón y Cajal, S. 1959. Degeneration and Regeneration of the Nervous System. II. Translated by R. M. May. Hafner. New York, N.Y.

58. Purpura, D. P. & E. M. Housepian. Alterations in corticospinal neuron activity associated with thalamocortical recruiting responses. Electroencephalog. Clin. Neurophysiol. In press.

59. Clare, M. H. & G. H. Bishop. 1956. Potential wave mechanism in cat cortex. Electroencephalog. Clin. Neurophysiol. **8:** 583.

60. Moruzzi, G. & H. W. Magoun. 1949. Brain stem reticular formation and activation of the EEG. Electroencephalog. Clin. Neurophysiol. **1:** 455.

61. Moruzzi, G. 1960. Synchronizing influences of the brain stem and the inhibitory mechanisms underlying the production of sleep by sensory stimulation. Colloquium on Electroencephalography of Higher Nervous Activity, Moscow. Electroencephalog. Clin. Neurophysiol. Suppl. **13:** 231.

62. Jasper, H. H. & G. D. Smirnov, (Eds.). 1960. Colloquium on Electroencephalography of Higher Nervous Activity, Moscow. Electroencephalog. Clin. Neurophysiol. Suppl. **13.**

63. Hernández-Peon, R. 1960. Neurophysiological correlates of habituation and other manifestations of plastic inhibition (internal inhibition). Colloquium on Electroencephalography ofl Higher Nervous Activity. Moscow. Electroencephalog. Clin. Neurophysiol. Supp. **13:** 101.

64. Hernández-Peon, R., H. Brust-Carmona, J. Peñaloza-Rojas, G. Bach-y-Rita. 1961. The efferent control of afferent signals entering the central nervous system. Ann. N.Y. Acad. Sci. **85:** 866.

65. Kristiansen, K. & G. Courtois. 1949. Rhythmic electrical activity from isolated cerebral cortex. Electroencephalog. Clin. Neurophysiol. **1:** 265.

66. Echlin, F. A. 1959. The supersensitivity of chronically "isolated" cerebral cortex as a mechanism in focal epilepsy. Electroencephalog. Clin. Neurophysiol. **11:** 697.

67. Cannon, W. B. 1939. A law of denervation. Am. J. Med. Sci. **198:** 737.

68. Krech, D., M. R. Rosenzweig & E. L. Bennett. 1960. Interhemispheric effects of cortical lesions on brain biochemistry. Science. **132:** 352.

Printed in the United States of America